Demonstration Project to Test a New Interdisciplinary Approach to Rehabilitating Salmon Spawning Habitat in the Central Valley

Final Report

for

Cooperative Agreement DCN# 113322G003

Prepared by:

Gregory B. Pasternack

Professor of Watershed Hydrology

University of California at Davis
Department of Land, Air and Water Resources

http://shira.lawr.ucdavis.edu

Copies of this final report, all quarterly progress reports, and all other publications stemming from this project may be found on the internet at

http://shira.lawr.ucdavis.edu/publications.htm

Executive Summary

Gravel augmentation is being implemented in the Central Valley in accordance with established CALFED Ecosystem Restoration Program priorities to enhance anadromous salmon spawning habitat and restore in-stream geomorphic processes. Prior to the study reported here, few objective criteria existed for designing and placing geomorphological features into regulated gravel/cobble channels that are heavily used for salmon spawning. Project failure often results from poor understanding of geomorphology and from designs based on aesthetics and intuition rather than scientific principles of ecology, geomorphology, and hydraulics. Working together 1999-2002, UC Davis and East Bay Municipal Utility District (EBMUD) developed an integrated approach to designing and implementing in-stream spawning gravel rehabilitation projects. While the approach employs empirical scientific knowledge from ecology, hydrology, and geomorphology to guide design of project alternatives that promote improved natural geomorphic evolution, it also uses computer-aided-design and a 2D mechanistic hydrodynamic model to quantify fine-scale channel hydraulics, geomorphic complexity, sediment mobility, and physical spawning habitat quality. Recognizing that the spawning life stage of anadromous salmon is a sensitive indicator of overall river conditions, the name of the interdisciplinary framework developed was chosen to be the Spawning Habitat Integrated Rehabilitation Approach (SHIRA).

The purpose of this demonstration project was to test, evaluate, and adaptively improve SHIRA by applying it to a series of three annual river-rehabilitation projects on the lower Mokelumne River, a regulated Sierran stream flowing into the Sacramento-San Joaquin Delta of central California. In accordance with the project proposal, SHIRA was used collaboratively by UC Davis and EBMUD with agency oversight by USFWS and CDFG in 2003, 2004, and 2005 to design, construct, and monitor river-rehabilitation projects on the lower Mokelumne River. With additional funding from EBMUD, three more SHIRA applications were done in 2001, 2002, and 2006, bringing the total number to 6. These 6 SHIRA projects were compared against the two reference non-SHIRA projects implemented by EBMUD in 1999 and 2000 on an *ad hoc* basis as well as pre-existing riffle remnants in the stream.

Overall, the eight projects 1999-2006 placed 23,484 metric tons of gravel and cobble in the river, representing about half of the long-term gravel deficit for the first kilometer below Camanche Dam. Focusing on the 2003-2005 demonstration projects implemented in this study, biological monitoring revealed that even though the number of spawners in the river each fall declined by 50% due to increased hatchery take, the number of redds observed in the rehabilitated area increased by 160%. Further, only 7 % of spawners in the total run used the project area before rehabilitation, but after each stage that percentage increased so that in 2005 22 % of them chose it. This demonstrates a population-scale benefit of the rehabilitation actions over a relatively small area. Beyond increasing the amount of spawning in the project area, an egg-tube study revealed a 35% increase in survival of incubating embryos to the fry stage in rehabilitated sites as compared to un-enhanced riffle sites. The overall conclusion of the 3-year evaluation is that the SHIRA demonstration projects have yielded measurable improvements in hydraulic, geomorphic, and ecological functioning of the lower Mokelumne River, as detailed in the subsections of this report that cover the diverse aspects of a large, interdisciplinary study. Independent scientific review of most subsections of this report has vetted the conclusions.

Acknowledgements

This project involved the effort of a large number of individuals and institutions. Financial support beyond that provided through this contract with CALFED helped leverage the breadth and depth of the project, and came from East Bay Municipal Utility District, the University of California, the U.S. Fish and Wildlife Service, the Ticho Foundation, and Professor Greg Pasternack. Graduate students Joe Merz, Joe Wheaton, Eve Elkins, Marisa Escobar, Chien Wang, and Rocko Brown all contributed to designing, implementing, and monitoring the demonstration projects as part of their graduate educations. We thank the undergraduate students Andy Tranmer, April Sawyer, Carlos Alvarado, Dave Van Herrick, Evan Buckland, Kashaul Parikh, Mike Bezemek, Chris Flower, Aaron Fulton, and Mike Bounrisavong for help with field work, modeling, and data analysis. Professors Jeff Mount, Peter Moyle, Joe Cech, and Mark Grismer served on graduate thesis committees, providing valuable critique and input. Postdoctoral researchers Hamish Moir, Peng Gao, and Joshua Wyrick also provided critical thinking about the project. Professor Jeff Mount, Ellen Mantalica, and Diana Cummings at the UC Davis Center for Watershed Sciences provided valuable administrative and project-management support. Kimberly Lamar in the UCD Office of the Vice Chancellor for Research provided contract and grant support. At EBMUD, Joe Merz served as the primary contact and collaborator, with many others contributing to this project, including but not limited to Jim Smith, Russell Taylor, Michelle Workman, Jose Setka, Lee Ochikubo Chan, Bert Mulchaey, Robyn Bilski, Jason Shillam, Matt Saldat, Charles Hunter, Brian kong, James Burke, Warren Yung, and Sabrina Taaning. The editors and reviewers of several scientific journals reviewed many subsections of this report and provided valuable feedback, criticism, and input.

Table of Contents

Section 1
What is SHIRA?

Introduction

The Spawning Habitat Integrated Rehabilitation Approach (SHIRA) is a new framework for rehabilitating gravel-bed regulated rivers that has been thoroughly vetted through the academic peer-review process. In creating it, we poured through extensive scientific literature on how gravel-bed rivers are thought to function as well as the literature on problems and opportunities in river restoration. We considered what everyone had to say and then made our best professional judgment to prioritize conceptual models and rehabilitation tools for the special case of regulated gravel-bed rivers. We also focused on those concepts and tools that are practicable in contrast to many academic "oughts" that are not feasible at this time, but are helpful to motivate further scientific advancement.

Based on input from many different sources, we concluded that any river-rehabilitation framework needs to 1) have a transparent procedure that is documented in the open literature, 2) use the hypothesis-driven scientific method, 3) make specific, testable predictions over a range of scales relevant to natural processes, 4) provide for long-term monitoring and adaptive management, and 5) incorporate ecological linkages. As you read the material in this report, you should judge for yourself whether SHIRA meets these criteria; we think it does. We have done our best to hold to these ideals through all phases of implementing SHIRA-based river rehabilitation demonstration projects at our testbed stream, the lower Mokelumne River, CA.

The purpose of this section of the final report is to thoroughly describe the concepts and tools that were incorporated into SHIRA during this demonstration project. Such concepts and tools are modular, and can be improved or replaced as needed without disrupting the overall structure of the system. The following subsections of this section are composed of the 2 peer-reviewed journal articles that lay out the foundation of SHIRA. The first subsection describes the concepts behind SHIRA. The second subsection illustrates how SHIRA may be used to design project alternatives and evaluate them using design hypothesis testing.

When viewed within its proper context, SHIRA is not a universal cure-all for decades of river degradation due to flow regulation, water quality degradation, overharvesting of biota, and channel manipulation on all streams across America. Addressing these systemic challenges requires significant political will and economic investment as well as more scientific advancement. Instead, SHIRA is a very helpful guide that can significantly reduce the uncertainty regarding the likely ecological and hydrogeomorphic outcomes of physical river rehabilitation on regulated gravel-bed rivers.

Intl. J. River Basin Management Vol. 2, No. 1 (2004), pp. 3–20

Spawning habitat rehabilitation – I. Conceptual approach and methods

JOSEPH M. WHEATON, *Department of Land, Air, and Water Resources, University of California at Davis, One Shields Avenue, Davis, CA 95616*
Corresponding Author: School of Geography, University of Southampton, Highfield, Southampton SO17 1BJ. E-mail: Joe.Wheaton@soton.ac.uk

GREGORY B. PASTERNACK, *Department of Land, Air, and Water Resources, University of California at Davis, One Shields Avenue, Davis, CA 95616*

JOSEPH E. MERZ, *East Bay Municipal Utility District, 1 Winemasters Way, Lodi, CA 95240*

Department of Wildlife, Fish and Conservation Biology, University of California at Davis, One Shields Avenue, Davis, CA 95616

ABSTRACT
Altered sediment and flow regimes in regulated rivers limit available spawning habitat for many fishes, especially salmonids. Mitigation efforts include spawning habitat rehabilitation and dam-removal, but often neglect conceptual or predictive models of hydrogeomorphic and ecological processes. Complete restoration of processes necessary for maintaining spawning habitat is often unrealistic in regulated rivers. However, we present a framework for spawning habitat rehabilitation based on the premise that certain ecologic functions and geomorphic processes can be restored in a manner that facilitates testing of underlying scientific theories. SHIRA (Spawning Habitat Integrated Rehabilitation Approach) provides a science-based, systematic framework for reach-scale rehabilitation of salmonid spawning habitat in regulated rivers. This approach is driven by a mix of field data, conceptual models and numerical models to provide predictive and explanatory insight into the rehabilitation process. Conceptual models are advocated for developing multiple design scenarios and explicit hypotheses about hydrogeomorphic processes and ecologic functions provided by said designs. Hydrodynamic, habitat suitability and sediment entrainment models that test the potential validity of design hypotheses prior to construction are reviewed. It is presumed that the added insight would improve the outcome of rehabilitation projects and test underlying scientific theories against the rigors of real-world uncertainties.

Keywords: River restoration; gravel augmentation; spawning gravels; habitat enhancement; salmonid spawning beds; restoration design.

1 Introduction

Throughout the Northern Hemisphere, rivers that once sustained robust anadromous salmon and trout runs are now regulated, harnessed, or otherwise impacted by dams, diversions, chanelisation and instream gravel mining (Graf, 2001; Marmulla, 2001). The decline of salmonids in regulated rivers has been linked to many perturbations including over-harvest and inaccessibility, degradation and reduction of spawning habitat for these fish (Moyle and Randall, 1998; Nehlsen *et al.*, 1991; Yoshiyama *et al.*, 1998). For three decades, efforts in North America and Europe to restore the health of salmon fisheries have included spawning habitat rehabilitation (SHR) projects (Brookes, 1996) (Figure 1). Most SHR projects lack science-based designs (NRC, 1992), and instead attempt to mimic the form of analogue reaches based on local knowledge and an ad hoc implementation (Kondolf, 2000b). Hydrogeomorphic processes are frequently neglected and monitoring is often inadequate (Sear, 1994). Project failure is not uncommon (NRC, 1992) and success can be difficult to assess accurately due to inadequate monitoring and unclear objectives (Downs and Kondolf, 2002). SHR is based on the ecological concept of indicator species (Willson and Halupka, 1995). The concept suggests that there exist species whose needs are similar to and reflect the needs of a broader group of species, and whose abundance is an indicator of ecosystem health. Thus, SHR focuses on improving spawning habitat, because such improvements can also yield benefits to fish during multiple life stages, macroinvertebrates and the entire food web (Merz, in press). Despite uncertainty in using indicator species as the basis for river rehabilitation (Anderson *et al.*, 2003), single-species recovery of socially and economically important fish is a political and funding reality for agencies, practitioners and river managers (Brookes *et al.*, 1996). Furthermore, SHR is commonly required for dam re-licensing (e.g. FERC, 1998) and will likely continue for some time until broader ecosystem restoration approaches might prevail. Our premise for this paper is, in the interim much

Received and accepted on February 18, 2004. Open for discussion until December 31, 2004.

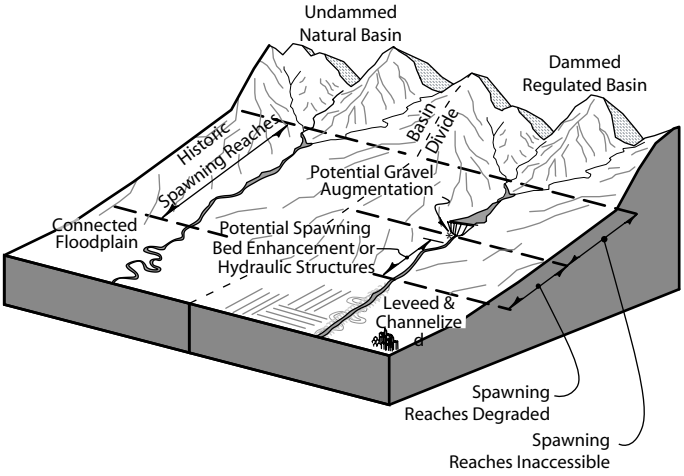

Figure 1 Context of spawning habitat rehabilitation. Regulated rivers alter basin-scale hydrogeomorphic processes, block access to historic spawning habitat upstream of dams and degrade historic spawning habitat downstream of dams. Hypothetical locations of three types of spawning habitat rehabilitation activities downstream of a dam are shown in the regulated basin.

can be learnt from SHR and incremental improvements in practice are realistic.

No clear consensus emerges from the literature on the definition of river restoration much less SHR (e.g. Boon, 1998; Sear, 1994; Shields *et al.*, 2003). Here, SHR is segregated into three categories: (1) gravel augmentation, (2) hydraulic structure placement and (3) spawning bed enhancement. Gravel augmentation (also known as gravel injection, infusion or replenishment) involves dumping clean spawning gravels into piles along the edges of a river (usually just downstream of a dam). For this approach to yield usable spawning habitat, practitioners must assume that high flows occur in the near future, that augmented gravels entrain during high flows, and that gravels do not fill mining holes or pools but instead deposit as bars or riffles. Hydraulic structure placement entails placement of large woody debris (LWD), boulder clusters, v-dams or similar structures to alter hydrodynamics in such a way that spawning gravels are deposited in the vicinity of the structures (Brookes *et al.*, 1996). The technique relies on an adequate supply of gravel from upstream and an active bedload transport regime to deliver it. Such structures may also be intended to provide refugia, cover and add habitat heterogeneity (Van-Zyll-De-Jong *et al.*, 1997). Spawning bed enhancement is the direct modification of the bed to provide immediate spawning habitat (e.g. riffle construction, bed ripping and riffle cleansing). Although bed enhancement may quickly provide usable spawning habitat, limited project lifespan may result without adequate consideration of geomorphic processes or regular gravel replenishment (Kondolf, 2000b). In summary, SHR projects are typically reach-scale restoration activities sometimes, but not necessarily, nested within a larger, long-term, basin-scale management plan (e.g. McBain and Trush, 1997).

SHR lacks a comprehensive design and implementation approach published in the peer-reviewed literature. Generalized outlines for stream restoration (FISRWG, 1998), and more specific guidelines incorporating fluvial geomorphology (Brookes and Sear, 1996; Gilvear, 1999; Sear, 1994), ecosystem theory (Stanford *et al.*, 1996) and design procedures (Hey *et al.*, 1994; Miller *et al.*, 2001; Shields *et al.*, 2003; Soar and Thorne, 2001) have been put forth in both the peer-reviewed and grey literature. It appears Kondolf (2000b) is one of the few authors to offer some fundamental considerations for SHR. The scattered examples of technical reports and grey literature, which mention SHR design rely on fairly basic, non-process based, best-management-practice recommendations (e.g. Slaney and Zaldokas, 1997). Only occasional pre and post-project assessments of SHR have been reported (e.g. Harper *et al.*, 1998; Kondolf *et al.*, 1996) and overviews of common practices are sparse (e.g. Brookes *et al.*, 1996). Where more sophisticated analyses of SHR based on hydrodynamic and habitat modelling have been performed, they provide little design insight (e.g. Hardy and Addley, 2001; Lacey and Millar, 2001). The problems with applying the plethora of existing published restoration approaches to SHR is they focus on what to do as opposed to how to do it; and they are not actively used by SHR practitioners (something this paper does not address). We presume the later is due to a combination of lack of specific implementation directions and the reality that most approaches are published in scientific journals, not easily accessible to practitioners, or in grey literature reports that are often difficult to find.

Several themes in the river restoration literature point towards some methodological consensus. Similar to Hildén (2000), we hypothesize that if restoration science and practice are to proceed collaboratively, a design approach drawing on scientific concepts and tools from multiple disciplines should be used (i.e. the familiar but vague buzzwords: adaptive, holistic and integrated still apply). In reality, this hypothesis is virtually impossible to test and the transferability of results from case studies to other projects can only hint at its validity or falseness. For practitioners, such a design approach should provide mechanistic understanding and predictive capability to the hydrogeomorphic and ecological underpinnings of SHR (Annable, 1999). For scientists, the designs should put our underlying theories about the interaction of hydrogeomorphic processes and ecologic functions to the test. Most agree that a "process-based" approach is superior to "form mimicry" (Kondolf, 1995b), but considerable discrepancies arise when one labels another's approach as "form mimicry" (Wilcock, 1997). Part of the confusion stems from both the difficulty and appropriateness in selecting an analogue condition (either from historical evidence or a present day location). In referring to an analogue condition, does one mimic the desired form or the desired process? Alternatively, analogue conditions can be abandoned and process focused on exclusively. The restoration literature generally supports the model of adaptive management (Clark, 2002). However, Walters (1997) astutely highlights four reasons why there has been such poor success in implementing adaptive management policies in restoration practice and river basin management: (1) over-reliance and faith in modelling to provide "best use" policies; (2) effective experiments are too expensive; (3) strong institutional opposition to

experimental policies and breaking status-quo; and (4) deep environmental value conflicts within management. Finally, there is widespread recognition of the importance of adopting a watershed or catchment approach to restoration (Pess *et al.*, 2003), but confusion over whether this means: (a) restore the entire catchment (Frissell *et al.*, 1993); (b) use watershed assessments to nest reach scale restoration in a catchment context (Bohn and Kershner, 2002; Walker *et al.*, 2002); or (c) undertake a range of management and restoration activities across various spatial scales but nested within a catchment context (Roni *et al.*, 2002).

Two areas where fundamental methodological differences arise in restoration is with respect to passive versus active approaches (Edmonds *et al.*, 2003; Wissmar and Beschta, 1998). Referring to our three types of SHR as an example, gravel augmentation is a passive approach that relies on the river to do the work. By contrast, spawning bed enhancement and hydraulic structure placement are active approaches, which intervene because natural or passive recovery may take an unacceptably long time (Montgomery and Bolton, 2003). The choice of passive versus active will depend very much on the specific social, political, economic and environmental context of specific river basins (Wissmar *et al.*, 2003). In some cases, it may be appropriate to employ passive approaches like gravel augmentation in concert with active approaches like spawning bed enhancement.

In this paper, we review the application of a variety of existing science-based tools and concepts to design and analyze SHR projects in regulated rivers and suggest a framework within which those tools may be employed. To draw on the terminology above, the proposed framework is by choice interdisciplinary, process-based and adaptive; but by default it is active. That is, because the approach provides guidelines for spawning bed enhancement and hydraulic structure placement forms of SHR it is active. Our proposed framework is based primarily on our own attempts at SHR on the Mokelumne River, California and synthesis of the restoration literature. In a companion paper (Wheaton *et al.*, 2004), we present partial results of hypothesis testing during design using a case study on the Mokelumne River. More assessments across a broad range of biological, engineering, and geomorphic criteria are underway and will be reported subsequently.

2 Spawning Habitat Integrated Rehabilitation Approach

We did not formalize the concepts presented in this paper into the Spawning Habitat Integrated Rehabilitation Approach (SHIRA) to provide a step-by-step laundry list for practitioners. Much of SHIRA is intuitive and based on concepts and tools already well established in the literature and to a lesser extent in practice. Instead, we target a perceived gap between restoration science, which produces approaches detailing what restoration should be doing or assessments of what has been done wrong, and restoration practitioners charged with the daunting task of figuring out how to do it. Wilcock (1997) argues, it is not that the critiques and suggested approaches of science are faulty, but that they are ineffective. To this end, practitioners looking for guidance in how to design SHR projects might find SHIRA useful. Whereas, scientists or academics interested in testing the application of their theories in restoration might use SHIRA as a concise review of SHR. Although we know of no such approach for SHR in the peer-reviewed literature, we humbly acknowledge the parallels in structure SHIRA has with existing restoration approaches and guidelines (e.g. Brookes and Shields, 1996; FISRWG, 1998; NRC, 1992; Waal *et al.*, 1998). As with most approaches, SHIRA advocates comprehensive pre-project assessment, planning and design phases followed by construction, post-project assessment, monitoring and hopefully adaptive management. During each of seven *phases,* four primary *modes* are used iteratively to collect and analyze data on which flexible and informed decisions can be based (Figure 2). In Section 4.2, extra emphasis is provided on the design development stage, which is largely underdeveloped in SHR. Specific methods that are well established in the literature are only referenced for brevity.

Recall that SHR is typically reach-scale in implementation and SHIRA is focused on application in regulated rivers. Hence, how can practitioners carry out reach scale projects, while being mindful of basin scale processes? In any river system, the means to carry out "basin-scale management" are ambiguous and challenged with uncertainties due to variable socio-political drivers

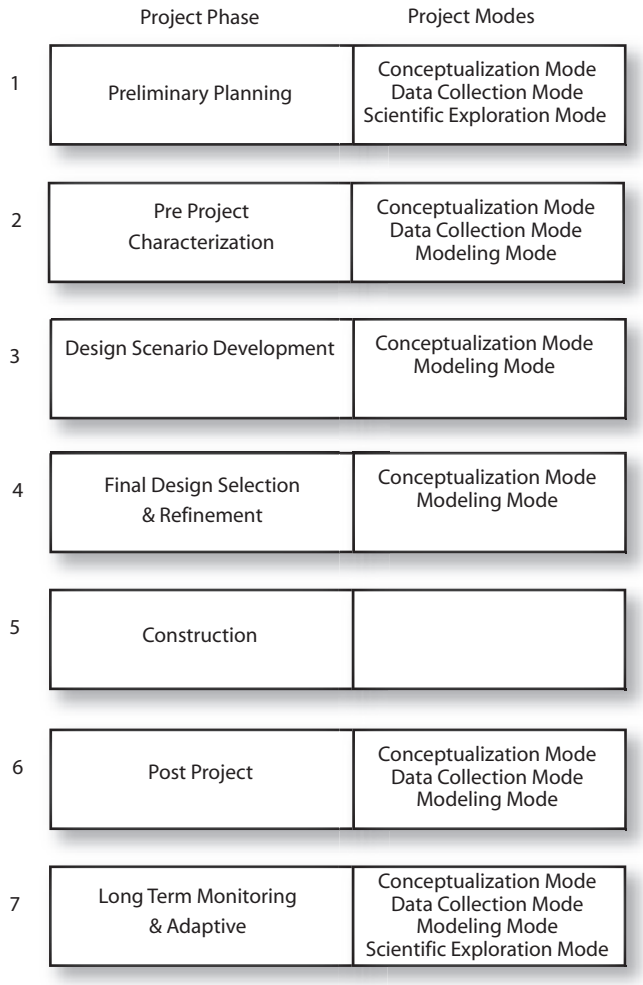

Figure 2 SHIRA Framework. Four modes (right hand side) are used to perform analyses and guide the decision making process in seven distinct phases (left hand side).

as well as lack of scientific knowledge (Anderson *et al.*, 2003). One conciliation of SHR in regulated rivers is that the basin context is dramatically simplified due to a phenomenon Stanford *et al.* (1996) term the serial discontinuity concept. That is, the ecological and geomorphic consequences of dams are largely predictable, and hence simplify consideration of basin scale drivers (Kondolf, 1997; Ligon *et al.*, 1995). Especially when SHR is carried out downstream of major dams (Figure 1), the uncertainty in flow regime is constrained by dam operations and the uncertainty in sediment supply from the upper basin is negligible because the dam is incapable of passing it. Thus, we assume and advocate that SHR under SHIRA is nested within a broader basin-scale management and assessment scheme (e.g. Montgomery *et al.*, 1995), but take advantage of the simplifications due to flow regulation.

3 SHIRA modes: Tools to encourage objective designs

3.1 Conceptualization mode

Design includes a creative process that enumerates multiple potential solutions. Preferably, those solutions are then analyzed to support a transparent decision to either proceed with a final design or not continue with the project (Clark and Richards, 2002). Because rivers are open systems, the design process will always have multiple "correct" solutions. Ideally, quantitative modelling and systems optimization might be used to create and select design alternatives, but there are many reasons why this cannot work. For example, the degrees of freedom that a computer would need to evaluate far exceed possibilities for the foreseeable future (Pasternack *et al.*, in press). Furthermore, mathematical models for many processes relevant to SHR do not exist and their uncertainties are poorly understood. A wealth of qualitative and empirical scientific conceptual models exist among ecology, hydrology, geomorphology and engineering (Table 1). On a site-by-site basis, conceptual models help designers plan and analyze projects. Rigid guidelines for applying conceptual models to design processes is inappropriate as the concepts for each project should be carefully chosen by a multidisciplinary team of local experts familiar with local conditions.

The design team may develop its own conceptual model(s) to explicitly and transparently document their understanding of how the specific river system functions. For example, a conceptual salmonid spawning habitat model was prepared to guide SHIRA on the Mokelumne River (Figure 3). This conceptual model asserts that where a female chooses to construct a redd is controlled by a mixture of ecological, geomorphic and hydrologic factors. At the basin scale, inherent factors (geology, topography, soils, climate, vegetation and human activities) yield river discharge and constituent loadings. Discharge and loadings are independent driving forces imposed on a reach to yield local flow and substrate conditions that interact to create physical habitat, which influences spawning site selection. Habitat heterogeneity, including hydraulic structures, proximity to refuge, patch size and patch mosaic variability, is an important feature of spawning conditions at the sub-reach scale. Redd construction itself alters

Table 1 Some potential conceptual models and their sources for use in the conceptualization mode.

Conceptual model	Source
Ecology	
Salmonid redd development	Chapman, 1988
Physical habitat assessments	Maddock, 1999
River continuum concept	Mishnall *et al.*, 1985
Primary controlling variables and biophysical interactions of river ecosystems	Stanford *et al.*, 1996
Conceptualization of riparian and hydrarch successional diversity in dynamic and regulated rivers	Ward *et al.*, 2001
Hydrogeomorphology	
Secondary flow cells	Booker *et al*., 2001
Geomorphic thresholds	Church, 2002
Hydraulic geometry	Leopold and Maddock, 1953
Sediment transport (Chapter 4)	Knighton, 1998
The sediment supply system	Sear, 1996a; Sear, 1994
Sediment transport processes in pool-riffle sequences	Sear, 1996b
Revised velocity reversal hypothesis as pool maintenance mechanism	Thompson and Hoffman, 2001; Thompson *et al.*, 1999
Effective discharge	Wolman and Miller, 1960
Bankfull discharge	Wolman and Leopold, 1957
Integrated/Restoration	
Conceptualized continuum of regulated and unregulated rivers	Stanford *et al.*, 1996
River styles	Brierley and Fryirs, 2000; Thomson *et al.*, 2001
Living river strategy	Pedroli *et al.*, 2002
Disturbance regimes in riverine landscape	Poudevigne *et al.*, 2002
Spatial and temporal scales in river restoration	Sear, 1994
Five dimensions of river restoration	Boon, 1998
Potential influences of human activities on riverine attributes and processes	Wissmar and Beschta, 1998

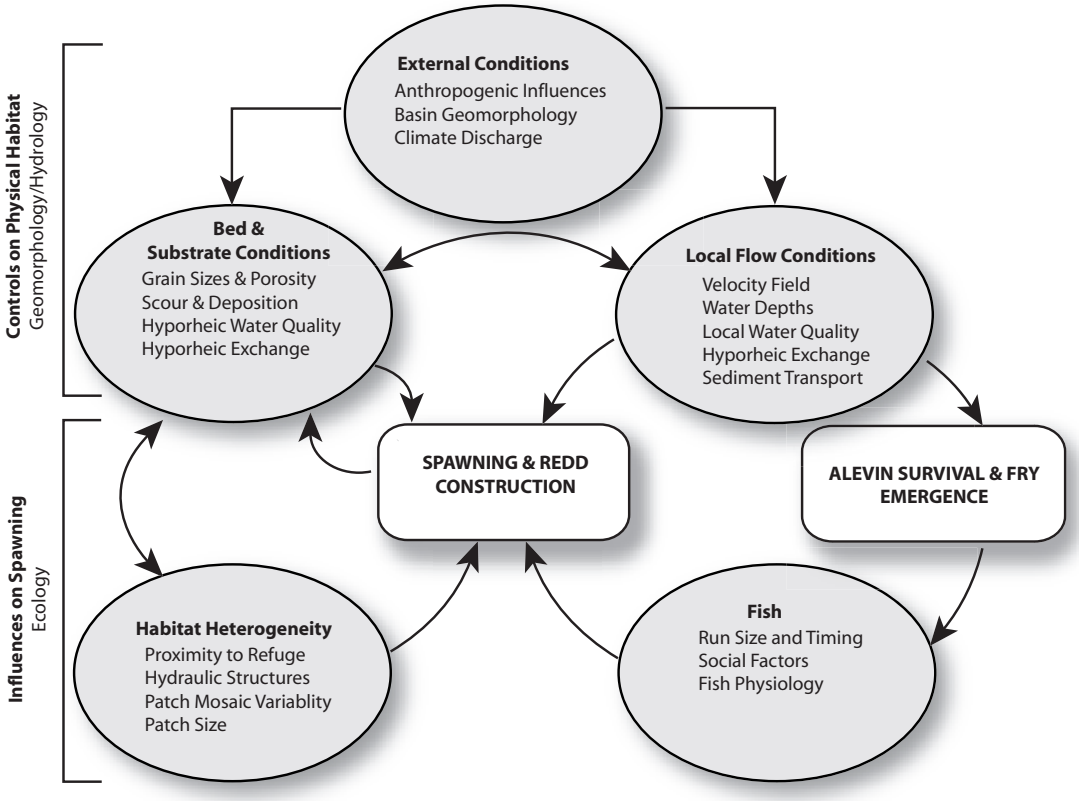

Figure 3 Conceptual spawning habitat model. The arrows indicate influences, the circles represent processes and characteristics, and the boxes are the outcomes. A combination of hydrogeomorphic processes spanning a range of scales combine to create physical habitat. Physical habitat is chosen by females for redd construction based on the ecologic functions provided by physical habitat and ecologic factors including habitat heterogeneity, run size, timing, social factors and physiology. The survival of alevins and ultimate emergence of fry is then primarily controlled by the substrate and local flow conditions during the incubation period.

local bed and flow conditions. In addition to physical factors, there are a host of ecological influences on spawning habitat utilization, including run size, run timing, competition, predation, hatchery management, harvest, social and physiological factors. The success of egg development and the ultimate emergence of fry are controlled by local flow and substrate conditions throughout the incubation period. For example, flood disturbance may produce local scour to egg burial depth or deposition of fines that infiltrates pores and prevent flushing of metabolic wastes (Lisle and Lewis, 1992).

A conceptual understanding of channel form and the primary process controls, which create, maintain, modify or destroy spawning habitat is essential. Four components comprise geomorphic analysis in the conceptualization mode: (1) geomorphic mapping, (2) empirical geomorphic analysis, (3) sediment budget and (4) geomorphic process inventory. First, a multi-scalar geomorphic classification scheme should be used to map morphology so that process inferences can be made across multiple scales (e.g. Maddock, 1999; Sear *et al.*, 1995; Thomson *et al.*, 2001). Second, an empirical geomorphic analysis of hydraulic geometry data derived from topography and flow records explains how flow and channel shape respond to changes in discharge (refer to: Leopold and Maddock, 1953). Third, sediment budgets quantify sediment supply, storage, and export (e.g. McLean and Church, 1999; Reid and Dunne, 1996). Because river regulation alters the sediment budget and flow regime, a sediment budget is needed at the basin-scale to characterize the distribution of aggradation versus degradation. Finally, a process inventory helps pinpoint problems and potential solutions. For example, if spawning substrate quality deteriorates due to an intrusion of fines, is it the result of fine-sediment production from land use changes or a flow regime incapable of flushing fines? The process inventory can be conceptual (i.e. field reconnaissance) or more quantitative, involving detailed process measurements (Thorne, 1998).

3.2 Modelling mode

SHIRA draws on quantitative modelling tools to make specific predictions about hydrogeomorphic and ecological processes. Empirical concepts used in river restoration employ a best-fit line to identify design specifications at cross-sections (e.g. Rosgen, 1996). However, acceptable errors in log-log trends for first-order science far exceed that for practical, sustainable design. Individual reaches have unique processes and morphologies that defy empirical prediction (Kondolf, 1995b). In contrast, high-resolution numerical models can simulate and predict unique river features, thereby making such models useful for design and analysis.

3.2.1 Digital elevation modelling

High quality digital elevation models (DEMs) and derived topographic maps are invaluable for planning, design and analysis,

and critical to the success of predictive 2D hydrodynamic models (French and Clifford, 2000). A number of methods and software applications are available to create DEMs from topographic survey point data (e.g. ACAD™, ARC™, MATLAB™, Surfer™). The spatial distribution of these points (e.g. random, grid, irregular, stratified) help determine which interpolation method is most appropriate to create a DEM. For highly irregularly distributed data sets, simple linear interpolation algorithms that use triangular irregular networks (TINs) tend to produce the most realistic DEMs (McCullagh, 1981). Although many hydrodynamic model interfaces provide basic DEM development tools, computer assisted drafting provides more powerful DEM editing, refinement and management capabilities in design contexts. French and Clifford (2000) suggest that DEM development consists of four iterative stages that are repeated until DEM quality is satisfactory: (1) visualization, (2) editing, (3) augmentation and (4) interpolation.

3.2.2 Hydrodynamic modelling

Hydrodynamic modelling is an accessible tool for understanding river flow dynamics and processes at the same scale as experienced by fish. In SHR projects, two-dimensional (2D) hydrodynamic modelling allows testing of numerous design scenarios thereby reducing implementation uncertainty (Pasternack *et al.*, in press). Past SHR analyses typically employed one-dimensional (1D) models, such as PHABSIM, HEC2 or MIKE11. While 1D models have fewer data needs, they do not capture habitat patterns at reach and sub-reach scales (Crowder and Diplas, 2000). Alternatively, 2D and 3D models make spatially distributed velocity (depth-averaged for 2D) and depth predictions. Many examples of public 2D hydrodynamic models now exist: FESWMS (Froehlich, 1989), RMA2 (Donnell *et al.*, 2001), TELEMAC (Galland *et al.*, 1991; Hervouet, 2000; Hervouet and Bates, 2000) and RIVER2D (Steffler and Blackburn, 2002). A code capable of modelling subcritical-supercritical transitions, wetting and drying and steady and unsteady flows is suggested. Academic (e.g. SSIIM: Olsen, 2003) and commercial 3D models exist, but they are very costly to field validate and remain largely untested in restoration practice (with a few exceptions, e.g. Swindale, 1999). In gravel-bed rivers, 3D models are frequently being used in scientific geomorphic investigations (Lane *et al.*, 1999; Parsons, 2002) and may in the future be suitable for application in restoration practice. However, a number of methodological issues, including assessing credibility of model simulations (Hardy *et al.*, 2003), accurately specifying model boundary conditions and handling complex bed topography variations (Lane *et al.*, 1999) suggest their application in restoration may be premature.

A realistic discretization of the model domain is critical to achieving accurate model results (French and Clifford, 2000). Discretization of the modelling domain is typically done by creating a computational mesh in place of the DEM. The quality of a mesh is highly dependent on two factors: (1) DEM quality and (2) mesh resolution. DEM quality is controlled in DEM development; whereas mesh resolution is controlled by node spacing and element size. Models allowing irregular node spacing permit finer-scale mesh discretization (i.e. tight node spacing $\approx$0.20 m to 0.75 m) around topographically complex areas and coarse-scale mesh discretization (relaxed node spacing $\approx$0.75 m to 5.0 m) around less complex topography. Tighter mesh resolution can more accurately represent the bathymetry and produce better hydrodynamic model results. However, as node spacing decreases, mesh resolution and computing time increase (refer to: Hardy *et al.*, 1999). Model results should be validated with field data before their use in designs (Bates *et al.*, 1998). Though, field observations have their own sources of error that should also be evaluated.

3.2.3 Sediment entrainment modelling

The longevity of a SHR project depends in large part on the fate of spawning gravels. A channel bed which remains immobile over time typically leads to deteriorated spawning habitat as organics and fines fill interstitial pore-spaces and dissolved oxygen and permeability decline (Chapman, 1988). Even though redd construction itself can clean and mobilize bed material locally (Hassan *et al.*, 2002), gravel movement during peak flows is invaluable to flush fines from spawning beds, replenish spawning gravels and maintain substrate suitability for spawning (Gilvear, 1999). Hence, at least some analysis of the flow conditions under which to expect sediment entrainment is warranted.

A well-accepted approach to predicting sediment entrainment is to compare model-predicted shear stresses to the critical shear stress for entrainment of specified gravel grain sizes. From 2D hydrodynamic model results depth averaged velocity can be used to calculate shear stress on a node by node basis (Wilcock, 1996). Critical shear stress can be estimated using field data, Shields' incipient motion criterion (Garde and Raju, 1985), and Einstein's log velocity profile equation (see Pasternack *et al.*, in press for detail). The ratio of model predicted velocity to critical velocity defines a sediment mobility index (SMI). Sediment entrainment prediction alone is a meaningful indicator of local scour. A variety of more sophisticated techniques for estimating entrainment and transport rates exist; however, sediment transport estimates can vary over orders of magnitude depending on formulae employed and boundary conditions assumed (Gomez and Church, 1989). Wilcock (2001) proposed a "practical" method (that could have utility in SHR) for estimating transport rates that relies on minimizing such errors by calibrating transport formulae against a limited number of observations. Unfortunately, sediment transport observations are frequently nonexistent for SHR projects. The few examples of mobile bed hydrodynamic models (i.e. bed adjusted iteratively in relationship to predicted transport rates) that do exist are still in developmental stages and are primarily only suitable for sand-bedded rivers (e.g. CH3D-SED: Gessler *et al.*, 1999).

3.2.4 Habitat suitability modelling

A quantitative prediction of habitat quality is a key design and assessment tool and readily available for SHR. The most widely employed conceptual model used to explain abiotic-biotic linkages and habitat suitability is the instream flow incremental

methodology (IFIM), which employs the PHABSIM 1D model (Bovee, 1996). PHABSIM relies on cross-sectionally and reach-averaged estimates of velocities and depth to assess usable habitat area, but not at a scale relevant to individual fish (Leclerc *et al.*, 1994). Leclerc *et al.* (1995a) introduced a 2D version that resolves predictions of habitat quality at the scale that fish experience it. Pasternack *et al.* (in press) and Wheaton *et al.* (2004) employed a similar approach to assess a SHR project for two separate projects on the Mokelumne River, California. All of the above methods rely on habitat suitability curves (HSC), which are commonly used in aquatic biology (Armour and Taylor, 1991). In such an approach, normalized habitat suitability curves for water depth, velocity and substrate size are developed (refer to Section 3.3.2). The HSCs are then combined into a single global habitat suitability index (GHSI). GHSI can be computed on a node-by-node basis from 2D model results to predict patterns of spawning habitat quality for use in assessment or design. GHSI values range from 0 to 1, with 1 representing the most optimal spawning habitat and 0 indicating non-habitat. GHSI is further subjectively classed as poor (0–0.1), low (0.1–0.4), medium (0.4–0.7) and high (0.7–1.0) quality habitat (Leclerc *et al.*, 1995b).

3.3 Data collection mode

The data collection mode includes a combination of desk-top studies, field campaigns and data analyses. For convenience, we segregate data collection activities into mapping, habitat, bed material and flow.

3.3.1 Mapping data collection

The conceptualization and modelling modes each have specific mapping requirements across a variety of scales. A coarse-scale map (e.g. 1 : 250,000) and DEM (5–30 m contours) of the catchment quantifies basin area, total relief, longitudinal profile, valley type, and channel network pattern. Landscape-scale maps (e.g. 1 : 24,000 or 1 : 63,000) should be used to segregate sub basins into landscape units (e.g. floodplain, hillslope, alluvial fan, valley), identify land use, soils, geology, vegetative cover and assess the role of valley confinement on fluvial processes. Longitudinal profiles of channel thalweg and water surface elevation surveyed throughout the entire length of spawning reaches are invaluable for choosing project reaches (Figure 4). Finally, the hydrodynamic modelling sub-mode requires, a

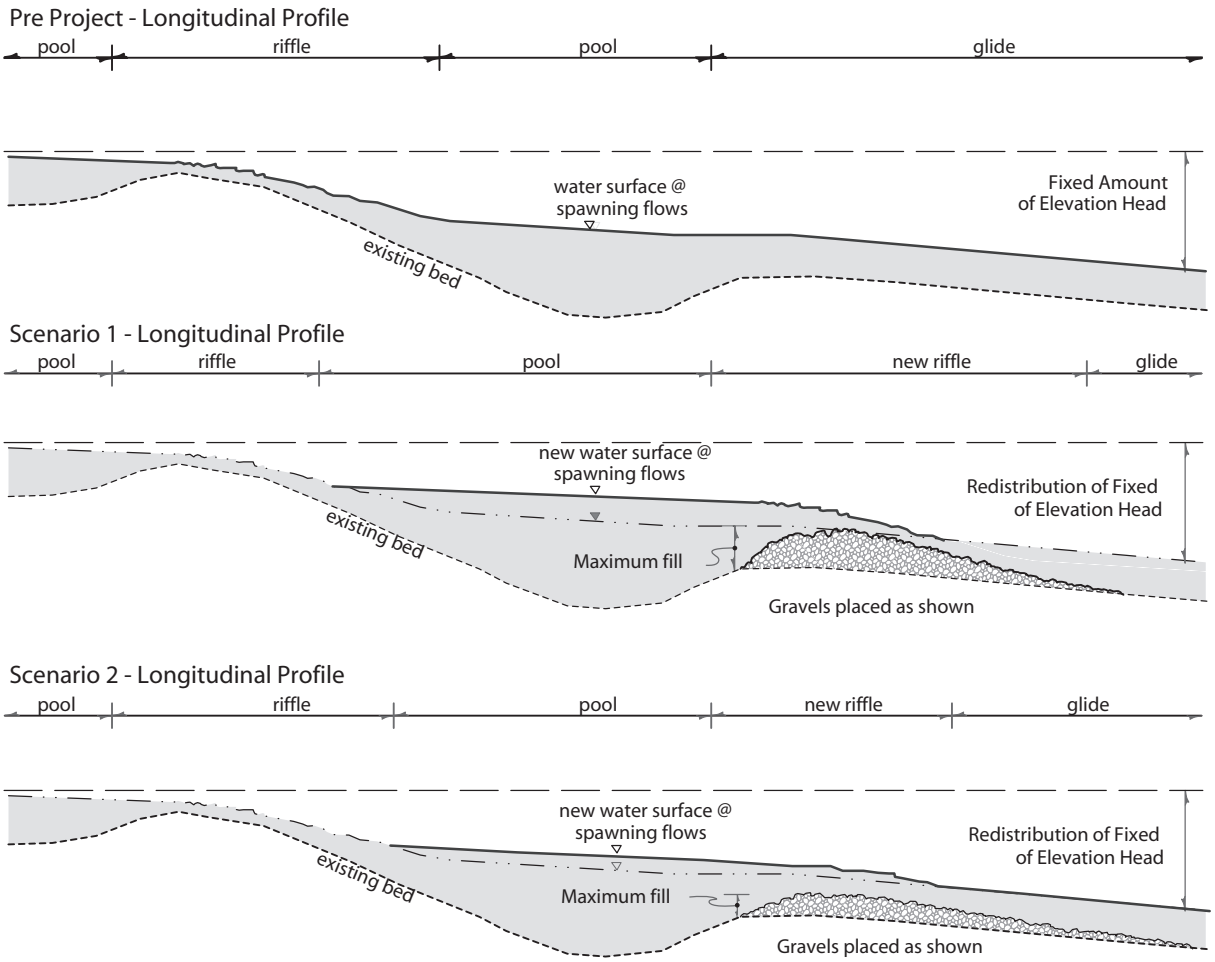

Figure 4 Concept of finite elevation head. The maximum fill depth at the upstream end of a spawning bed enhancement project is the critical control for how much new spawning habitat is created and how much existing spawning habitat is deteriorated upstream from backwater effects. In the pre-project condition, the existing upstream riffle provides high quality spawning habitat but the glide downstream provides poor quality spawning habitat. In scenario one, gravel is placed in the glide to decrease depths and increase velocities; thereby creating optimal spawning habitat over much of the old glide but also inducing a backwater effect on the upstream riffle and deteriorating spawning habitat quality. In scenario two, the maximum fill depth is lower and the trade-off between backwater effect on the upstream riffle and creation of high quality spawning habitat is optimized.

detailed topographic survey (>0.75 point per m^2) using a total station or real-time kinematic Global Positioning System (rtkGPS) and control network tied to a known coordinate system. Lidar technology (refer to: French, 2003) and aerial or close range photogrammetric methods (refer to: Lane *et al.*, 2000) are becoming increasingly popular. If Lidar or photogrammetric methods can produce topographic data of similar resolution, they may be appropriate. However, in a comparison to high resolution rtkGPS and digital aerial photogrammetric surveys of the same reaches, Brasington *et al.* (2003) concluded that data precision and accuracy were lower than traditional ground topographic surveys.

Detailed topographic surveying provides abundantly more useful data than standard cross sections and longitudinal profiles alone. In-channel features should be surveyed with adequate resolution to capture grade breaks and bedforms comprising roughness elements. Stratified point spacing (as opposed to random or uniform) in quasi-systematic manner can be used to obtain high quality data (Brasington *et al.*, 2000). High point density (>3 points per m^2) is used in topographically complex areas (bedrock outcroppings, channel margins) and relaxed point density (>0.5 points per m^2) is used in topographically uniform areas (floodplain, plane bed). At the reach scale, a 15-cm contour interval, 1 : 250 scale mapping, can serve as a "rule of thumb" for resolving geomorphic units, which could have significant influence on two dimensional flow paths. For high-flow modelling, it is helpful to extend surveying out of the channel to include the inundation area of at least over-bank flows with decadal recurrence intervals. Surveying of trees, hardscape, fencing, travel paths, drainage features and utilities is also useful for design purposes. Topographic surveys are often misperceived as too expensive for restoration projects. Once control networks are established, simple reach surveys can be performed by two persons in one day and even complicated reaches rarely take more than a week (Brasington *et al.*, 2000).

3.3.2 Habitat data collection

Physical habitat data collection includes (1) habitat mapping (2) redd surveys and (3) habitat suitability curve (HSC) development. General habitat mapping can be performed by drawing field sketches over topographic surveys, which segregate the channel corridor into habitat types (e.g. riffles, pools, backwaters, glides, etc.). A multi-scalar, geomorphic based approach to mapping habitat is recommended and many exist (e.g. Frothingham *et al.*, 2002; Newson *et al.*, 1998; Thomson *et al.*, 2001). Weekly redd surveys are conducted throughout the duration of the spawning season. Merz and Setka (in press) suggest surveying location by dGPS and measuring depths, velocities, grain sizes, dissolved oxygen content and temperatures at redds soon after spawning and during flow conditions similar to those present at the onset of spawning.

Although many physical, physiological and ecological factors influence spawning site selection, those shown to account for much of the variability include depth, velocity, water temperature, and substrate quality (Knapp and Preisler, 1999). HSCs should be constructed from the distributions of these data for the particular species of interest and preferably from the specific river where SHR is proposed (Hardy and Addley, 2001). Since these measurements are made after redd construction, they are not a true measure of those present when the female selected the site for spawning, so measurements can either be averaged over a range of points in and around the nest or taken at a point just upstream of the nest thought to be characteristic of the pre-redd hydraulic conditions (Merz and Setka, in press). Redd surveys can be overlaid on GHSI model results (Section 3.2.4) to test the predictive capability of HSC. Where HSCs are inadequate to explain variability in spawning patterns, other methods such as Kondolf's (2000a) nine-step method for assessing spawning gravel quality may be used.

3.3.3 Bed material data collection

Habitat quality, sediment entrainment and hydrodynamics are all dependent on the composition and arrangement of substrate. Modelling hydrodynamics relies on estimates of roughness, which are related to substrate composition and bedform shape (Lane *et al.*, 1999). A surface grain size distribution obtained by Wolman pebble counts quantifies percentile classes if such distributions are approximately normal (Bunte and Abt, 2001). If further spatial segregation of bed sediments is deemed necessary, facies maps can be drawn in concert with Wolman pebble counts stratified by substrate class (facies). Frozen sediment core samples can be obtained at random locations within specific sediment facies to characterize subsurface sediments (Bunte and Abt, 2001). If a sediment budget is being prepared, bedload and suspended load measurements over a range of discharges are desirable (McLean and Church, 1999). For monitoring, gravel tracer studies can be used to track the fate of placed spawning gravels (Wilcock *et al.*, 1996).

3.3.4 Flow data collection

Three types of flow data are needed for SHR projects. First, historical flow records characterize flow regime, with particular attention towards spawning and flood flows. If pre-regulation flow records exist, insightful comparisons of pre- and post-regulation flow regimes can help illuminate the impacts of flow regulation on hydrologic and geomorphic processes (e.g. Richter *et al.*, 1996). Second, rating curves of stage versus discharge spanning minimum releases to flood flows are needed at the downstream boundary of each hydrodynamic modelling reach. Finally, measurements of water depth and velocity are needed to validate hydrodynamic model results (Pasternack *et al.*, in press), estimate bed shear stresses (Dietrich and Whiting, 1989), verify discharges against gage readings, estimate hydrodynamic model parameters such as eddy viscosity (Fischer *et al.*, 1979) and assess appropriate spawning velocities for target species (Section 3.3.2). As hydrodynamic processes vary in time and space, careful consideration should be given to the spatial and temporal resolution at which such measurements are performed (Lane *et al.*, 1998).

3.4 Scientific exploration mode

Given that SHIRA is modular and that SHR projects can be viewed as controlled experiments, the scientific exploration mode provides the opportunity to continually improve SHIRA in three distinct ways. First, individual scientific concepts may have deficiencies that become apparent when rigorously tested during practical application. It is important to make a thorough inventory of sources of uncertainty and analysis of quantifiable uncertainty to either improve or replace the concept. Second, as new technologies become available, they may be evaluated for use in SHIRA. Third, scientific experiments may be needed to determine how to incorporate new ideas into the design and planning process. For example, in-channel features such as LWD and hydraulic jumps are known to be important for salmonids (Hilderbrand *et al.*, 1998), yet science-based approaches for including these in design still need development. Experimental findings should be reported in the peer-reviewed literature.

4 SHIRA phases – a practical implementation process

4.1 Phases in brief

Whereas modes are tools used at any time during SHR projects, phases represent a chronological sequence of steps (Figure 2). Aside from design, the phases in SHIRA are similar to those presented in other approaches (e.g. FISRWG, 1998) and are hence only briefly summarized here (Table 2). During the preliminary planning phase, goals, sites, and support are sought within a basin-scale context (e.g. Brookes and Shields, 1996; FISRWG, 1998; NRC, 1992). Site selection should be carefully chosen with

Table 2 Summary of key tasks performed in each phase of SHIRA. The modes used are abbreviated as follows: DCM: data collection mode; MM: modelling mode; CM: conceptualization mode; and SEM: scientific exploration mode.

Phase	Key tasks	Mode(s) used
Phase one: Preliminary planning	Baseline data collection performed	DCM
	Historical flow analysis	DCM
	Compile historical annual redd surveys and HSC	DCM
	Historical geomorphic analysis	DCM
	Historical context summarized	DCM, CM
	Basin context explicitly recognized (watershed assessment)	DCM, CM
	Problem definition and development of explicit conceptual model	CM
	State objectives, select monitoring indicators and outline monitoring timeline	CM
	Explicit recognition of how SHR project fits in basin management plan	CM
	Feedback and support from stakeholders	CM
	Project constraints identified (e.g. budget, construction access, construction timing, gravel availability)	DCM, CM
	Site selection	CM, MM?
Phase Two: Pre-project	Detailed topographic survey and habitat mapping	DCM
	Bed material characterization and collect flow validation data	DCM
	Build and run hydrodynamic, habitat suitability and sediment entrainment models	MM
	Validate and refine model until satisfactory results	MM
Phase Three: Design	See Section 4.2	CM, MM
Phase Four: Final design selection	See Section 4.2.4	CM, MM
Phase Five: Construction	Designer to communicate key goals and design elements to contractor in pre-construction meeting (including: construction access, grave handling and cleanliness, construction staging areas, identification of sensitive areas and potential hazards)	NA
	Construction staking to be provided to delineate boundaries, fill elevations, etc.	NA
	Spot grade checking to ensure finish elevations match design	DCM
	Construction observation for (clarifications, modifications and reality check)	DCM
Phase Six: Post project assessment	Detailed topographic survey and habitat mapping	DCM
	Bed material characterization and collect flow validation data	DCM
	Build and run hydrodynamic, habitat suitability and sediment entrainment models	MM
	Validate and refine model until satisfactory results	MM
	Prepare first post project appraisal	CM
Phase Seven: Long term monitoring and adaptive management	Carry out long term monitoring of pre-defined indicators and track morphological change, habitat utilization.	DCM
	Adaptive management	SEM, CM
	Publish all data as part of an information inventory	DCM, SEM

respect to the river's longitudinal profile with ample consideration of future SHR projects as well as current spawning habitat sites (Figure 4). To ensure value in later monitoring and assessment, it is crucial to establish a hypothesis-driven experimental purpose along with applied goals. Next, the pre-project phase thoroughly documents site specific baseline conditions. This begins with an intensive field campaign at least one year prior to anticipated construction and is concluded with detailed modelling analyses. In Section 4.2, the design phase is discussed more specifically. Months can be spent designing minute details of individual design scenarios. However, when construction commences, there are limits to the detail an excavator or front-end loader with a 4–6 m^3 bucket can achieve. Given these constraints, construction should focus on general design intent first and specific details second. Phase six provides the first post project appraisal (PPA) with special attention towards how well the construction matched the final design. Downs and Kondolf (2002) outline an eight-part PPA process which includes: success criteria, baseline surveys, design rationale, design drawings, post-project monitoring survey, supplementary historical data, and secondary analytical procedures. The final phase is then comprised of three parts: (1) long-term monitoring (Brookes and Shields, 1996; FISRWG, 1998), (2) adaptive management (Walters, 1986) and (3) information inventory. Numerous sources are available for developing monitoring protocols (Kondolf, 1995a; Newson, 2002).

4.2 Design

Design in SHIRA is segregated into a development phase and a final selection phase. Design development has three parts: (1) conceptual design formulation, (2) detailed design development, and (3) design testing. Design is a creative process, and its real-world utility depends on objective testing of multiple scenarios as opposed to development of a single design. In the same way Chamberlin (1890) advocates multiple working hypothesis, multiple design scenarios can include both those that designers hypothesize as appropriate solutions and "null" designs. As an example, multiple conceptual models have been proposed to explain why pool-riffle sequences tend to maintain themselves: Keller's (1971) original 'velocity reversal hypothesis', secondary flow cell convergence and divergence (Clifford and Richards, 1992) and Thompson's (1999) 'revised velocity reversal hypothesis'. Although none of these conceptual models have been proven, nor is it likely that there is a single explanation for the self-maintenance of pool-riffle sequences, they can provide a reasonable basis for design. Thompson *et al.* (2001, 1999) proposed that pool-riffle maintenance was sometimes due to width constrictions upstream of pools and width expansions upstream of riffles (which, is thought to concentrate flow through the pools and allow it to dissipate out across a riffle). Thus, a hypothesized design scenario may aim to constrain channel width in the pools and allow width to expand across riffles. The "null" design scenario would propose the opposite (constant channel width or width constriction in riffle). Hydrodynamic and SMI model results of the hypothesized and null design scenarios at flood stages can indicate whether the conceptual model indeed explains the desired process. All scenarios are designed within the specific SHR project constraints (i.e. site location, quantity of gravel available, construction access, construction equipment).

4.2.1 Conceptual design formulation

Numerous design scenarios can be formulated conceptually by drawing "form-process sketches" of designs over existing channel topography, habitat and geomorphic maps. A simple conceptual planform sketch delineating where gravel will be placed to create the desired channel forms should be drawn. More importantly, the hydrogeomorphic processes and related ecological functions hypothesized to be produced by such a design scenario are added to the map. The conceptual "form-process sketch" should document a designers' ideas for a proposed design and how they hypothesize that design will function. For example, it may be proposed to convert an incised glide with homogenized depths and velocities into a pool-riffle. Because of the past emphasis on cross-sections, little geomorphic theory exists at the sub-reach scale to constrain habitat-scale riffle morphology. Natural rivers show wide diversity (Montgomery and Bolton, 2003), thereby offering latitude in design details. Until DEM-based fluvial geomorphic theory is developed to address this critical gap in understanding, designers should draw on hydrodynamic patterns and processes known from experience or analogue conditions for designing sub-reach and hydraulic-unit scale features. Hence, the designer should not become overly attached to any single design hypothesis (Schumm, 1991).

4.2.2 Detailed design development

Detailed design development converts the conceptual design into a DEM. While many applications exist for building DEMs, computer-assisted-drafting (CAD) programs are the design industry-standard, and more efficient for drafting grading plans. DEM data can be exported to a hydrodynamic modelling interface. DEM data can be exported to a hydrodynamic modelling interface. CAD allows easy calculation of fill volumes and extraction of long profiles and cross sections from a DEM. Design gravel sizes should be specified using a combination of HSCs, literature reports of gravel sizes (e.g. Kondolf and Wolman, 1993) and physical constraints from the gravel supplier.

4.2.3 Design testing

Design testing in SHIRA uses the modelling mode to evaluate design scenarios relative to flow structure, habitat, geomorphic process, and sediment entrainment criteria. While true model validation of design scenarios is not possible, model results are directly comparable because model elements are pre-specified (Pasternack *et al.*, in press). The primary source of error in 2D modelling is DEM inaccuracy from poor field data (French and Clifford, 2000), which only plays a minor role in a design DEM. Yet, the fundamental limitations of 2D models (e.g. inability to resolve vertical components due to depth averaging) and the nature of modelling uncertainties must be understood with respect to the ability of model results to test hypotheses. However

valid a design hypothesis involving the importance of secondary flow cells with a vertical component may be, a 2D model cannot be used to assess this hypothesis (Lane *et al.*, 1999). Spatial predictions of GHSI should be used to test for design efficiency (volume of gravel added per area) and habitat patch size. A habitat patch must be larger than a single redd ($\sim$1–3 m^2) to be of spawning value. The sediment entrainment predictions can be used at spawning flows to design against potential scour and at high flows to verify or reject the validity of the designers' geomorphic process inferences made in the conceptual design formulation. In individual projects, designers will have to decide if the models discussed here are adequate to objectively test hypothesized processes resulting from design scenarios. If not, other models may be deployed or the inability to test specific aspects of design hypothesis should be explicitly reported.

4.2.4 Phase 4: final design selection

After multiple design scenarios have been developed and tested, assessment and comparisons should be made. Although the outcome of this process is normally the selection of a single design, it should be recognized that there is no single correct answer (Schumm, 1991) and that the analyses might suggest that nothing should be done. It is better to arrive at this conclusion before the expense and impact of construction are realized rather than during a post project appraisal. Findings should be presented to experts and managers to get feedback and direction before refining the final design. The final design scenario may simply be the perceived best scenario from the design phase or a combination of scenarios. Alternately, it may be the one yielding the best test of an experimental hypothesis. Ultimately, a transparent decision should be made on the basis of the early analyses. Once a final design scenario is refined, model results should be solidified and construction documents prepared. Construction document requirements will vary according to the project contractor and regulatory agencies involved. At a minimum, construction documents should include pre-project topography and a grading plan depicting configuration of placed gravel fills and highlighting critical design elements. Construction documents should convey all information necessary for a general engineering contractor to read them. If a competitive bidding process is being used to select a contractor, it may be helpful to have plans reviewed by a professional engineer before distribution.

5 Discussion – other design considerations

Restoration of regulated rivers is by definition impossible without dam removal. Dam removal has grown in popularity for the restoration of native fisheries and geomorphic processes (Doyle and Harbor, 2003). However, it is expensive and usually only proposed for small dams where there exists a clear alternative for water storage and flood control (Bednarek, 2001). On many larger salmon rivers, dam removal may not be a realistic option (Graf, 2001). However, improvement of certain geomorphic and ecologic functions on regulated rivers through rehabilitation efforts like SHR may be feasible. SHIRA can provide a framework within which SHR efforts may be effectively carried out.

5.1 Importance of habitat heterogeneity

One logical way to develop SHR design scenarios using a 2D hydrodynamic model and GHSI results, is to produce designs optimizing bed configuration to achieve the maximum area of GHSI-defined optimal habitat. This logic has guided past efforts at SHR (Kondolf *et al.*, 1996). From our experience, optimization with GHSI alone at a single discharge may produce relatively homogenous flat riffles. GHSI provides valuable insight into potential spawning habitat preferences, but many factors influencing spawning are simply not represented (Knapp and Preisler, 1999). While optimal spawning habitat is generally found in riffles, proximity of optimal spawning habitat to pools, LWD, boulder clusters, flow separations (eddies) and overhanging cover can be equally important to spawners. Such structural elements allow the female to quickly seek refuge from predation or rest while still allowing defence of her redd (McPhee and Quinn, 1998; Merz, 2001a). Another problem arises in designs based entirely on GHSI at a single flow. Spawning flows may fluctuate with downstream water demand. A flat riffle designed for optimal GHSI habitat at a single flow could potentially produce poor quality habitat over the entire homogenous riffle at a different spawning flow. Topographically diverse riffles are more likely to provide a range of GHSI-defined quality habitats over variable flows. Habitat heterogeneity should afford multiple habitat functions to different species. Finally, habitat quantity should be balanced with geomorphic sustainability, and the latter rarely suggests a long, flat riffle.

Incorporating complex features into a design can improve the quality of habitat beyond the predictive capability of current numerical models. Numerical models can reduce some uncertainties in design outcomes but need to be combined with conceptual models and practical limitations of construction to achieve spatial heterogeneity. Hydraulic structures can be used to add habitat heterogeneity and fluvial complexity in otherwise homogenized flow conditions (Hilderbrand *et al.*, 1998; Jeffries, 2002). In a true channel restoration, hydraulic structures, such as boulder clusters or LWD, may not be justified on the basis of historical evidence in reaches where SHR is now proposed. However, since SHR is intended to improve certain ecologic and geomorphic functions that are now lacking, the use of structural elements may be justified. This is probably only appropriate if the inferred processes and benefits associated from such structures can be modelled or tested in the design phase. LWD is very difficult to model in 2D (Pasternack *et al.*, in press), while boulders are manageable (Crowder and Diplas, 2000). Model results can be used to infer whether structures produce desired hydrogeomorphic processes and ecologic functions. However, model results cannot predict the rate at which boulder clusters may induce scour or rates at which LWD will break down or blow out. Thus, hydraulic structures may provide benefits in the form of habitat heterogeneity,

but considerable uncertainty in the channel response to these features must be accepted.

5.2 Integration of conceptual features into designs

A number of empirical studies and general observations of spawning activity have led to conceptual models of processes that presently cannot be numerically modelled. Is the inclusion of such conceptual models warranted in design development? For example, chinook salmon (*Oncorhynchus tshawytscha*) are thought to preferentially spawn where hyporheic flow occurs (Geist, 2000; Vronskiy, 1972). One example of bedforms thought to promote hyporheic flow is pool-exit slopes. Water is vertically constricted through a pool exit slope and then spreads over a shallow riffle, characterized by decreased depth and increased velocity. The head gradient induced in this zone can promote downwelling through permeable spawning gravels. Lisle and Lewis (1992) explain that even if eggs incubate successfully, alevins still need connected pore spaces to emerge. Hyporheic flow of water through the gravels is thought to maintain such connected pore spaces by flushing fines and increasing dissolved oxygen values critical to egg survival. Although most hydrodynamic models are not coupled to hyporheic flow models, and GHSI does not account for downwelling at pool-exit slopes, the process-inference may well justify the use of pool-exit slopes in designs.

5.3 Channel stability

Channel stasis is not an appropriate goal of SHR projects (Kondolf, 2000b). Even in severely regulated rivers that rarely experience shear stresses over a "critical threshold", Paintal (1971) shows that sediment transport will occur and can eventually yield significant change. In natural rivers spawning gravels turn over and bedforms are re-supplied from upstream. Overton (1984) noticed that some spawning sites persisted from year to year whereas others (40 to 80%) were transitory. Thus, a mix of transitory and stable bedforms may be appropriate for SHR. Montgomery *et al.* (1999) concluded that bed scour depths must constrain spawning distributions because population survival would be unsustainable if scour depths consistently exceeded egg burial depths during the incubation period. To further confuse matters, channel locations, which experience active bedload transport, may in some cases support topographically stable reaches (DeVries, 2002). Relating channel stability and sediment transport to spawning habitat is an active area of research with considerable uncertainty due to both the variability in processes and our lack of knowledge (Montgomery and Bolton, 2003). As it is difficult to draw generic design conclusions about channel stability, designers that rely on a process-based approach can grapple with the applicability of stability concepts to their sites. Shields *et al.* (2003) offer some hydraulic engineering design tools for considering channel stability in channel reconstruction that may have some utility in specific SHR contexts. We discourage the expectation that an enhanced gravel bed should necessarily remain exactly as it was placed.

5.4 Limitations

The largest limitation of SHR is that it is an active-approach to rehabilitation focused at the reach scale over inter-annual time scales. SHR may not be sustainable at longer time scales unless supporting geomorphic processes are achieved through larger spatial and temporal scale watershed-based restoration or management. Project lifetime remains the largest unknown. The assumption is that SHIRA is used as part of a larger watershed scale restoration program, but the reality may be that funding is only spent on piecemeal individual spawning bed enhancement projects without appropriate long term or large scale planning. If the latter is the case, SHIRA will likely provide cost-effective short-term benefits that may diminish with time in the absence of periodic maintenance or gravel augmentation. Conversely, gravel augmentation is unlikely to produce or sustain target habitat until larger-scale geomorphic processes have been recovered (may take decades to centuries). Pulse-flows may provide a mechanism in regulated rivers by which certain ecologic and hydrogeomorphic functions can be achieved (Andrews and Nankervis, 1995). Whiting (2002) suggests partitioning the annual hydrograph into certain functions in which the flow magnitude determines the function (e.g. pool scour, riffle-cleansing, riffle mobilization will require different magnitude flows). However, flow adjustments to improve flow-sensitive habitat characteristics are often difficult to obtain because of pre-existing water allocation. Similarly, if regular gravel augmentation is not done to alleviate coarse-grained sediment deficits, spawning bed enhancement projects will likely not last. Thus, it is apparent that a combination of gravel augmentation, spawning bed enhancement and flow augmentation will be required to achieve restoration of the full array of spatial and temporal scales of biological and geomorphic riverine processes.

Individual river systems may provide design challenges currently not explicitly outlined in SHIRA. For example, when applying SHIRA on the Mokelumne River, water quality has not been shown to be problematic for salmonids (Merz, 2001b). In rivers where water quality is a limiting factor, it may be appropriate to modify SHIRA to include water quality assessment capabilities (see Herricks, 1996 for examples). SHIRA itself can be adaptively managed and changed by practitioners as needed to include new sub-modes that address future shortcomings.

6 Conclusion

The three most common types of spawning habitat rehabilitation projects are gravel augmentation, hydraulic structure placement and spawning bed enhancement. SHIRA provides a framework and detailed design methods for undertaking spawning bed enhancement and hydraulic structure placement forms of SHR. The approach uses four separate modes as tools throughout the course of sequential project phases. The ideas embodied in the components of SHIRA are not necessarily new or conceptually difficult to understand, and this may be what makes its application useful. Still, SHIRA is a departure from many restoration approaches in that more emphasis is placed on design. While clarifying *what* to do in restoration projects plays an important role in

refocusing restoration efforts, it is also important for the scientific community to help practitioners figure out *how* to apply the findings of our research. As we have applied SHIRA on three projects to date (with three others underway), we have demonstrated SHIRA implementation is possible, but not free of problems (Wheaton, 2003). No approach should ever become a substitute for creativity and dynamic interaction with others during the design process. From a scientific perspective, implementation of habitat rehabilitation projects provides unique opportunities to test hypotheses on river system processes. The prospect of coupling future ecosystem-rehabilitation efforts with scientific studies is an exciting opportunity for practitioners and scientists to collaborate and gain improved understanding of riverine ecosystems.

Acknowledgements

Financial support for this work was provided by East Bay Municipal Utility District (Research Agreements OOK6046 & 99K3086), the University of California, the US Fish and Wildlife Service (contracting entity for CALFED Bay-Delta Ecosystem Restoration Program: Cooperative Agreement DCN# 113322G003) and a National Fish and Wildlife Federation grant through CALFED (Contract #99-NO6). We gratefully acknowledge Gonzalo Castillo, Joe Cech, Jeff Mount, James Smith, Brett Valle, Kelly Wheaton and Steve Winters for their input towards the research and manuscript. We thank Adrea Wheaton for her expertise and help with several figures. We thank Ellen Mantalica of the Center for Integrated Watershed Science and Management in the John Muir Institute for the Environment, Davis, California for management support. We wish to thank Andrew Miller and two anonymous reviewers for their critical feedback, which helped dramatically clarify earlier drafts of the manuscript.

List of Acronyms and Abbreviations

1D	one dimensional
2D	two dimensional
3D	three dimensional
CAD	computer assisted drafting
DEM	digital elevation model
dGPS	differential global positioning system
GHSI	global habitat suitability index
HSC	habitat suitability curve
IFIM	instream flow incremental methodology
LWD	large woody debris
PPA	post project appraisal
rtkGPS	real time kinematic global positioning system
SHR	spawning habitat rehabilitation
SHIRA	spawning habitat integrated rehabilitation approach
SMI	sediment mobility index
TIN	triangular irregular network

References

1. Anderson, J. L., Hilborn, R. W., Lackey, R. T., and Ludwig, D. (2003). "9. Watershed Restoration-Adaptive Decision Making in the Face of Uncertainty", in: R. C. Wissmar, P. A. Bisson, and M. Duke (eds.), Strategies for Restoring River Ecosystems: Sources of Variability and Uncertainty in Natural and Managed Systems, American Fisheries Society, Bethesda, Maryland, pp. 185–201.
2. Andrews, E. D. and Nankervis, J. M. (1995). "Effective Discharge and the Design of Channel Maintenance Flows for Gravel-Bed Rivers", *Natural and Anthropogenic Influences in Fluvial Geomorphology*, Geophysical Monograph 89, 151–164.
3. Annable, W. K. (1999). "On the Design of Natural Channels: Decisions, Direction and Design", *The Second International Conference on Natural Channel Systems*, Niagara Falls, Ontario, Canada, pp. 29.
4. Armour, C. L. and Taylor, J. G. (1991). "Evaluation of the Instream Flow Incremental Methodology by United-States Fish and Wildlife Service Field Users", *Fisheries*, 16(5), 36–43.
5. Bates, P. D., Stewart, M. D., Siggers, G. B., Smith, C. N., Hervouet, J. M., and Sellin, R. H. J. (1998). "Internal and external validation of a two-dimensional finite element code for river flood simulations", *Proceedings of the Institution of Civil Engineers-Water Maritime and Energy*, 130(3), 127–141.
6. Bednarek, A. T. (2001). "Undamming rivers: A review of the ecological impacts of dam removal", *Environmental Management*, 27(6), 803–814.
7. Bohn, B. A. and Kershner, J. L. (2002). "Establishing aquatic restoration priorities using a watershed approach", *Journal of Environmental Management*, 64(4), 355–363.
8. Booker, D. J., Sear, D. A., and Payne, A. J. (2001). "Modelling three-dimensional flow structures and patterns of boundary shear stress in a natural pool-riffle sequence", *Earth Surface Processes and Landforms*, 26(5), 553–576.
9. Boon, P. J. (1998). "River restoration in five dimensions", *Aquatic Conservation-Marine and Freshwater Ecosystems*, 8(1), 257–264.
10. Bovee, K. "Perspectives on two-dimensional river habitat models: the PHABSIM experience", *Proceedings of the 2nd International Symposium on Habitats and Hydraulics*, (1996), Quebec, Canada.
11. Brasington, J., Langham, J., and Rumsby, B. (2003). "Methodological sensitivity of morphometric estimates of coarse fluvial sediment transport", *Geomorphology*, 53(3–4), 299–316.
12. Brasington, J., Rumsby, B. T., and Mcvey, R. A. (2000). "Monitoring and modelling morphological change in a braided gravel-bed river using high resolution GPS-based survey", *Earth Surface Processes and Landforms*, 25(9), 973–990.

13. BRIERLEY, G. J. and FRYIRS, K. (2000). "River styles, a geomorphic approach to catchment characterization: Implications for river rehabilitation in Bega catchment, New South Wales, Australia", *Environmental Management*, 25(6), 661–679.
14. BROOKES, A. (1996). "9. River Restoration Experience in Northern Europe", in: A. Brookes and F. D. Shields (eds.), River Channel Restoration: Guiding Principles for Sustainable Projects, John Wiley & Sons, Chichester, UK, pp. 75–101.
15. BROOKES, A., KNIGHT, S. S., and SHIELDS, F. D. (1996). "4. Habitat Enhancement", in: A. Brookes and F. D. Shields (eds.), River Channel Restoration: Guiding Principles for Sustainable Projects, John Wiley & Sons, Chichester, UK, pp. 103–126.
16. BROOKES, A. and SEAR, D. (1996). "3. Geomorphological Principles for Restoring Channels", in: A. Brookes and F. D. Shields (eds.), River Channel Restoration: Guiding Principles for Sustainable Projects, John Wiley & Sons, Chichester, UK, pp. 75–101.
17. BROOKES, A. and SHIELDS, F. D. (1996). River Channel Restoration: Guiding Principles for Sustainable Projects, John Wiley & Sons, Chichester, UK, pp. 433.
18. BUNTE, K. and ABT, S. R. (2001). Sampling Surface and Subsurface Particle-Size Distributions in Wadable Gravel- and Cobble-Bed Streams for Analyses in Sediment Transport, Hydraulics and Stream Bed Monitoring. Gen. Tech. Rep. RMRS-GTR-74. *RMRS-GTR-74*, U.S. Department of Agriculture, Forest Service, Rocky Mountain Research Station, Fort Colins, CO, pp. 428.
19. CHAMBERLIN, T. C. (1890). "The method of multiple working hypothesis", *Science*, Reprinted 1965: 148, 754–759.
20. CHAPMAN, D. W. (1988). "Critical Review of Variables Used to Define Effects of Fines in Redds of Large Salmonids", *Transactions of the American Fisheries Society*, 117, 1–21.
21. CHURCH, M. (2002). "Geomorphic thresholds in riverine landscapes", *Freshwater Biology*, 47(4), 541–557.
22. CLARK, M. J. (2002). "Dealing with uncertainty: adaptive approaches to sustainable river management", *Aquatic Conservation-Marine and Freshwater Ecosystems*, 12, 347–363.
23. CLARK, M. J. and RICHARDS, K. J. (2002). "Supporting complex decisions for sustainable river management in England and Wales", *Aquatic Conservation-Marine and Freshwater Ecosystems*, 12, 471–483.
24. CLIFFORD, N. J. and RICHARDS, K. (1992). "2: The Reversal Hypothesis and the Maintenance of Riffle-Pool Sequences: A Review and Field Appraisal", in: P. Carling and G. Petts (eds.), Lowland Floodplain Rivers: Geomorphological Perspectives, John Wiley and Sons Ltd, Chichester, UK, pp. 43–70.
25. CROWDER, D. W. and DIPLAS, P. (2000). "Using two-dimensional hydrodynamic models at scales of ecological importance", *Journal of Hydrology*, 230, 172–191.
26. DEVRIES, P. (2002). "Bedload layer thickness and disturbance depth in gravel bed streams", *Journal of Hydraulic Engineering-Asce*, 128(11), 983–991.
27. DIETRICH, W. E. and WHITING, P. (1989). "Boundary shear stress and sediment transport in river meanders of sand and gravel", in: S. Ikeda and G. Parker (eds.), River Meandering, American Geophysical Union Water Resources Monograph 12, Washington D.C., pp. 1–50.
28. DONNELL, B. P., LETTER, J. V., and MCANALLY, W. H. (2001). User's Guide for RMA2 Version 4.5. US Army, Engineer Research and Development Center Waterways Experiment Station, Coastal and Hydraulics Laboratory, [available on web: http://chl.wes.army.mil/software/tabs/docs.htp], pp. 284.
29. DOWNS, P. W. and KONDOLF, G. M. (2002). "Post-project appraisals in adaptive management of river channel restoration", *Environmental Management*, 29(4), 477–496.
30. DOYLE, M. W. and HARBOR, J. M. (2003). "Toward Policies and Decision-Making for Dam Removal", *Environmental Management*, 31(4), 453–465.
31. EDMONDS, R. L., FRANCIS, R. C., MANTUA, N. J., and PETERSEN, D. L. (2003). "2. Sources of Climate Variability in River Ecosystems", in: R. C. Wissmar, P. A. Bisson, and M. Duke (eds.), Strategies for Restoring River Ecosystems: Sources of Variability and Uncertainty in Natural and Managed Systems, American Fisheries Society, Bethesda, Maryland, pp. 11–37.
32. FERC. (1998). "Order Approving Settlement Agreement and Amending License. East Bay Municipal Utility District Lower Mokelumne River Hydroelectric Project No. 2916." Federal Energy Regulatory Commission.
33. FISCHER, H. B., LIST, E. J., KOH, R. C., IMBERGER, J., and BROOKS, N. H. (1979). Mixing in Inland and Coastal Waters, Academic Press, Inc., New York, pp.
34. FISRWG. (1998). Stream Corridor Restoration: Principles, Processes, and Practices. *GPO Item No. 0120-A*, Federal Interagency Stream Restoration Working Group, Washington D.C., pp. 653.
35. FRENCH, J. R. (2003). "Airborne LiDAR in support of geomorphological and hydraulic modelling", *Earth Surface Processes and Landforms*, 28(3), 321–335.
36. FRENCH, J. R. and CLIFFORD, N. J. (2000). "Hydrodynamic modeling as a basis for explaining estuarine environmental dynamics: some computational and methodological issues", *Hydrological Processes*, 14, 2089–2108.
37. FRISSELL, C. A., LISS, W. J., and BAYLES, D. (1993). "An Integrated, Biophysical Strategy for Ecological Restoration of Large Watersheds", *Changing Roles in Water Resources Management and Policy: American Water Resources Association*, 29(3).
38. FROEHLICH, D. C. (1989). HW031.D – Finite Element Surface-Water Modeling System: Two-Dimensional Flow in a Horizontal Plane-Users Manual: Federal Highway Administration. *Report FHWA-RD-88-177*, Federal Highway Administration, Washington D.C., pp. 285.

39. FROTHINGHAM, K. M., RHOADS, B. L., and HERRICKS, E. E. (2002). "A multiscale conceptual framework for integrated ecogeomorphological research to support stream naturalization in the agricultural midwest", *Environmental Management*, 29(1), 16–33.
40. GALLAND, J. C., GOUTAL, N., and HERVOUET, J. M. (1991). "Telemac – a New Numerical-Model for Solving Shallow-Water Equations", *Advances in Water Resources*, 14(3), 138–148.
41. GARDE, R. J. and RAJU, K. G. R. (1985). Mechanics of sediment transportation and alluvial stream problems, Wiley Eastern Limited, New Delhi, India, pp.
42. GEIST, D. R. (2000). "Hyporheic discharge of river water into fall chinook salmon (*Oncorhynchus tshawytscha)* spawning areas in the Hanford Reach, Columbia River", *Can. J. Fish. Aquat. Sci.*, 57, 1647–1656.
43. GESSLER, D., HALL, B., SPASOJEVIC, M., HOLLY, F., POURTAHERI, H., and RAPHELT, N. (1999). "Application of a 3D mobile bed, hydrodynamic model", *Journal of Hydraulic Engineering*, 125(7), 737–749.
44. GILVEAR, D. J. (1999). "Fluvial geomorphology and river engineering: future roles utilizing a fluvial hydrosystems framework", *Geomorphology*, 31(1–4), 229–245.
45. GOMEZ, B. and CHURCH, M. (1989). "An Assessment of Bed Load Sediment Transport Formulae for Gravel Bed Rivers", *Water Resources Research*, 25(6), 1161–1186.
46. GRAF, W. L. (2001). "Damage Control: Dams and the Physical Integrity of America's Rivers", *Annals of the Association of American Geographers*, 91, 1–27.
47. HARDY, D. T. B. and ADDLEY, M. R. C. (2001). Evaluation of Interim Instream Flow Needs in the Klamath River. Institute for Natural Systems Engineering: Utah Water Research Laboratory – Utah State University, Logan, Utah, pp. 298.
48. HARDY, R. J., BATES, P. D., and ANDERSON, M. G. (1999). "The importance of spatial resolution in hydraulic models for floodplain environments", *Journal of Hydrology*, 216, 124–136.
49. HARDY, R. J., LANE, S. N., FERGUSON, R. I., and PARSONS, D. R. (2003). "Assessing the credibility of a series of computational fluid dynamic simulations of open channel flow", *Hydrological Processes*, 17(8), 1539–1560.
50. HARPER, D., EBRAHIMNEZHAD, M., and COT, F. C. I. (1998). "Artificial riffles in river rehabilitation: setting the goals and measuring the successes", *Aquatic Conservation-Marine and Freshwater Ecosystems*, 8, 5–16.
51. HASSAN, M. A., GOTTESFELD, A. S., and TUNNICLIFFE, J. F. (2002). "Sediment mobility in fish bearing streams: the influence of floods and spawning salmon", *Eos Trans. AGU Fall Meeting Supplement*, 83(47), Abstract H21C-0831.
52. HERRICKS, E. E. (1996). "7. Water Quality Issues in River Channel Restoration", in: A. Brookes and F. D. Shields (eds.), River Channel Restoration: Guiding Principles for Sustainable Projects, John Wiley & Sons, Chichester, UK, pp. 75–101.
53. HERVOUET, J. M. (2000). "TELEMAC modelling system: an overview", *Hydrological Processes*, 14(13), 2209–2210.
54. HERVOUET, J. M. and BATES, P. (2000). "The TELEMAC modelling system – Special issue", *Hydrological Processes*, 14(13), 2207–2208.
55. HEY, R. D., HERITAGE, G. L., and PATTESON, M. (1994). "Impact of Flood Alleviation Schemes on Aquatic Macrophytes", *Regulated Rivers-Research & Management*, 9(2), 103–119.
56. HILDÉN, M. (2000). "The Role of Integrating Concepts in Watershed Rehabilitation", *Ecosystem Health*, 6(1), 39–50.
57. HILDERBRAND, R. H., LEMLY, A. D., DOLLOFF, C. C., and HARPSTER, K. L. (1998). "Design Considerations for Large Woody Debris Placement in Stream Enhancement Projects", *North American Journal of Fisheries Management*, 18, 161–167.
58. JEFFRIES, R. (2002). *The effect of vegetation on the geomorphology of lowland floodplains*, Ph.D. Thesis, University of Southampton, Southampton, pp. 251.
59. KELLER, E. A. (1971). "Areal sorting of bed-load material: the hypothesis of velocity reversal", *Geological Society of America Bulletin*, 82, 753–756.
60. KNAPP, R. A. and PREISLER, H. K. (1999). "Is it possible to predict habitat use by spawning salmonids? A test using California golden trout (*Oncorhynchus mykiss aguabonita*)", *Canadian Journal of Fisheries and Aquatic Sciences*, 56(9), 1576–1584.
61. KNIGHTON, D. (1998). Fluvial forms and processes: a new perspective, Arnold, London ; New York, pp.
62. KONDOLF, G. M. (1995a). "5 Elements for Effective Evaluation of Stream Restoration", *Restoration Ecology*, 3(2), 133–136.
63. KONDOLF, G. M. (1995b). "Geomorphological Stream Channel Classification in Aquatic Habitat Restoration – Uses and Limitations", *Aquatic Conservation-Marine and Freshwater Ecosystems*, 5(2), 127–141.
64. KONDOLF, G. M. (1997). "Hungry water: Effects of dams and gravel mining on river channels", *Environmental Management*, 21(4), 533–551.
65. KONDOLF, G. M. (2000a). "Assessing salmonid spawning gravel quality", *Transactions of the American Fisheries Society*, 129(1), 262–281.
66. KONDOLF, G. M. (2000b). "Some suggested guidelines for geomorphic aspects of anadromous salmonid habitat restoration proposals", *Restoration Ecology*, 8(1), 48–56.
67. KONDOLF, G. M., VICK, J. C., and RAMIREZ, T. M. (1996). "Salmon spawning habitat rehabilitation on the Merced River, California: An evaluation of project planning and performance", *Transactions of the American Fisheries Society*, 125(6), 899–912.
68. KONDOLF, G. M. and WOLMAN, M. G. (1993). "The Sizes of Salmonid Spawning Gravels", *Water Resources Research*, 29(7), 2275–2285.

69. LACEY, R. W. J. and MILLAR, R. G. (2001). Application of two Dimensional Hydrodynamic Model for the Assessment and Design of Instream Channel Restoration Works. *Watershed Restoration Management Report No. 9*, Forest Practices Branch, B.C. Forest Service, Vancouver, B.C., pp. 72.
70. LANE, S. N., BIRON, P. M., BRADBROOK, K. F., BUTLER, J. B., CHANDLER, J. H., CROWELL, M. D., MCLELLAND, S. J., RICHARDS, K. S., and ROY, A. G. (1998). "Three-dimensional measurement of river channel flow processes using acoustic Doppler velocimetry", *Earth Surface Processes and Landforms*, 23(13), 1247–1267.
71. LANE, S. N., BRADBROOK, K. F., RICHARDS, K. S., BIRON, P. A., and ROY, A. G. (1999). "The application of computational fluid dynamics to natural river channels: three-dimensional versus two-dimensional approaches", *Geomorphology*, 29(1–2), 1–20.
72. LANE, S. N., JAMES, T. D., and CROWELL, M. D. (2000). "Application of digital photogrammetry to complex topography for geomorphological research", *Photogrammetric Record*, 16(95), 793–821.
73. LECLERC, M., BOUDREAU, P., BECHARA, J., BELZILE, L., and VILLENEUVE, D. (1994). "A Model of Habitat Dynamics Applied to Landlocked Atlantic Salmon (*Salmo-salar*) Juveniles of the Ashuapmushuan River (Quebec, Canada)", *Bulletin Francais De La Peche Et De La Pisciculture*(332), 11–32.
74. LECLERC, M., BOUDREAULT, A., BECHARA, J. A., and CORFA, G. (1995a). "2-Dimensional Hydrodynamic Modeling – a Neglected Tool in the Instream Flow Incremental Methodology", *Transactions of the American Fisheries Society*, 124(5), 645–662.
75. LECLERC, M., BOUDREAULT, A., BECHARA, J. A., and CORFA, G. (1995b). "Two-dimensional hydrodynamic modeling: a neglected tool in the instream flow incremental methodology", *Transactions of the American Fisheries Society*, 124(5), 645–662.
76. LEOPOLD, L. B. and MADDOCK, T. (1953). The Hydraulic Geometry of Stream Channels and Some Physiographic Implications. *Geological Survey Professional Paper 252*, United States Geological Survey, pp. 57.
77. LIGON, F. K., DIETRICH, W. E., and TRUSH, W. J. (1995). "Downstream Ecological Effects of Dams", *Bioscience*, 45(3), 183–192.
78. LISLE, T. E. and LEWIS, J. (1992). "Effects of Sediment Transport on Survival of Salmonid Embryos in a Natural Stream: A Simulation Approach", *Can. J. Fish. Aquat. Sci*, 49, 2377–2344.
79. MADDOCK, I. (1999). "The importance of physical habitat assessment for evaluating river health", *Freshwater Biology*, 41, 373–391.
80. MARMULLA, G. (ed.), (2001). *Dams, fish and fisheries. Opportunities, challenges and conflict resolution*. Technical Paper no. 419. FAO Fisheries Department: Rome, Itally, pp. 166.
81. MCBAIN, S. M. and TRUSH, W. J. (1997). Trinity River Maintenance Flow Study: Final Report. McBain & Trush: Prepared for Hoopa Valley Tribe Fisheries Department, Arcata, CA, pp. 482.
82. MCCULLAGH, M. J. (1981). "Creation of smooth contours over irregularly distributed data using local surface patches", *Geophysical Analysis*, 13, 51–63.
83. MCLEAN, D. G. and CHURCH, M. (1999). "Sediment transport along lower Fraser River 2. Estimates based on the long-term gravel budget", *Water Resources Research*, 35(8), 2549–2559.
84. MCPHEE, M. V. and QUINN, T. P. (1998). "Factors affecting the duration of nest defense and reproductive lifespan of female sockeye salmon, Oncorhynchus nerka", *Environmental Biology of Fishes*, 51(4), 369–375.
85. MERZ, J. E. (2001a). "Association of fall-run chinook salmon redds with woody debris in the lower Mokelumne River, California", *California Fish and Game*, 87(2), 51–60.
86. MERZ, J. E. (2001b). "Diet of juvenile fall-run chinook salmon in the lower Mokelumne River, California", *California Fish and Game*, 87(3), 102–114.
87. MERZ, J. E. and SETKA, J. D. (in press). "Evaluation of a spawning habitat enhancement site for chinook salmon in a regulated California river." *North American Journal of Fisheries Management*.
88. MILLER, D. E., SKIDMORE, P. B., and WHITE, D. J. (2001). Channel Design. Inter-Fluve, Inc. – Prepared for Washington Department of Fish and Wildlife, Boseman, MT, pp. 117.
89. MISHNALL, G. W., CUMMINS, K. W., PETERSEN, R. C., CUSHING, C. E., RUNS, D. A., SEDELL, J. R., and VANNOTE, R. L. (1985). "Developments in Stream Ecosystem Theory", *Can. J. Fish. Aquat. Sci.*, 42, 1045–1055.
90. MONTGOMERY, D. R., BEAMER, E. M., PESS, G. R., and QUINN, T. P. (1999). "Channel type and salmonid spawning distribution and abundance", *Can. J. Fish. Aquat. Sci.*, 56, 377–387.
91. MONTGOMERY, D. R. and BOLTON, S. M. (2003). "3. Hydrogemorphic Variability and River Restoration", in: R. C. Wissmar, P. A. Bisson, and M. Duke (eds.), Strategies for Restoring River Ecosystems: Sources of Variability and Uncertainty in Natural and Managed Systems, American Fisheries Society, Bethesda, Maryland, pp. 39–80.
92. MONTGOMERY, D. R., GRANT, G. E., and SULLIVAN, K. (1995). "Watershed Analysis as a Framework for Implementing Ecosystem Management", *Water Resources Bulletin*, 31(3), 369–386.
93. MOYLE, P. B. and RANDALL, P. J. (1998). "Evaluating the biotic integrity of watersheds in the Sierra Nevada, California", *Conservation Biology*, 12, 1318–1326.
94. NEHLSEN, W., WILLIAMS, J. E., and LICHATOWICH, J. A. (1991). "Pacific salmon at the crossroads: stocks at risk from California, Oregon, Idaho, and Washington." *Fisheries*, 16, 4–21.

95. NEWSON, M. D. (2002). "Geomorphological concepts and tools for sustainable river ecosystem management", *Aquatic Conservation-Marine and Freshwater Ecosystems*, 12(4), 365–379.
96. NEWSON, M. D., CLARK, M. J., SEAR, D. A., and BROOKES, A. (1998). "The geomorphological basis for classifying rivers", *Aquatic Conservation-Marine and Freshwater Ecosystems*, 8(4), 415–430.
97. NRC. (1992). Restoration of aquatic ecosystems: science, technology, and public policy, National Academy Press, Washington DC, pp. 552.
98. OLSEN, N. R. B. (2003). A Three Dimensional Numerical Model for Simulation of Sediment Movements in Water Intakes with Multiblock Option: Version 1.1 and 2.0 User's Manual. Department of Hydraulic and Environmental Engineering, The Norwegian University of Science and Technology, Oslo, Norway, pp. 138.
99. OVERTON, C. K. (1984). "Evaluation of Stream Channel Enhancement Needs", *Pacific Northwest Stream Habitat Management Workshop: American Fisheries Society*, Humboldt State University, CA, pp. 156–164.
100. PAINTAL, A. S. (1971). "Concept of critical shear stress in loose boundary open channels", *Journal of Hydraulic Research*, 9(1), 91–113.
101. PARSONS, D. R. (2002). *Flow Separation in Meander Bends*, Ph.D. Thesis, University of Sheffield, Sheffield, U.K., pp. 300.
102. PASTERNACK, G. B., WANG, C. L., and MERZ, J. E. (in press). "Application of a 2D Hydrodynamic Model to Design of Reach-Scale Spawning Gravel Replenishment on the Mokelumne River, California", *River Research and Applications*.
103. PEDROLI, B., BLUST, G. d., LOOY, K. V., and ROOIJ, S. V. (2002). "Setting targets in strategies for river restoration", *Landscape Ecology*, 17(Suppl. 1), 5–18.
104. PESS, G. R., BEECHIE, T. J., WILLIAMS, J. E., WHITAL, D. R., LANGE, J. I., and KLOCHAK, J. R. (2003). "8. Watershed Assessment Techniques and the Success of Aquatic Restoration Activities", in: R. C. Wissmar, P. A. Bisson, and M. Duke (eds.), Strategies for Restoring River Ecosystems: Sources of Variability and Uncertainty in Natural and Managed Systems, American Fisheries Society, Bethesda, Maryland, pp. 185–201.
105. POUDEVIGNE, I., ALARD, D., LEUVEN, R. S. E. W., and NIENHUIS, P. H. (2002). "A Systems Approach to River Restoration: A case study in the Lower Seine Valley, France", *River Research and Applications*, 18, 239–247.
106. REID, L. M. and DUNNE, T. (1996). Rapid evaluation of sediment budgets, GeoEcology Paperbacks, Resikrchen, Germany, pp.
107. RICHTER, B. D., BAUMGARTNER, J. V., POWELL, J., and BRAUN, D. P. (1996). "A method for assessing hydrologic alteration within ecosystems", *Conservation Biology*, 10, 1163–1174.
108. RONI, P., BEECHIE, T. J., BILBLY, R. E., LEONETTI, F. E., POLLOCK, M. M., and PESS, G. R. (2002). "A review of stream restoration and a hierarchal strategy for prioritizing restoration in Pacific Northwest watersheds", *North American Journal of Fisheries Management*, 22, 1–20.
109. SCHUMM, S. A. (1991). To Interpret the Earth: Ten ways to be wrong, Cambridge University Press, Cambridge, UK, pp. 132.
110. SEAR, D. (1996a). "6. The Sediment System and Channel Stability", in: A. Brookes and F. D. Shields (eds.), River Channel Restoration: Guiding Principles for Sustainable Projects, John Wiley & Sons, Chichester, UK, pp. 149–177.
111. SEAR, D. A. (1994). "River Restoration and Geomorphology", *Aquatic Conservation-Marine and Freshwater Ecosystems*, 4(2), 169–177.
112. SEAR, D. A. (1996b). "Sediment transport processes in pool-riffle sequences", *Earth Surface Processes and Landforms*, 21(3), 241–262.
113. SEAR, D. A., NEWSON, M. D., and BROOKES, A. (1995). "Sediment related river maintenance: the role of fluvial geomorphology", *Earth Surface Processes and Landforms*, 20, 629–647.
114. SHIELDS, F. D., COPELAND, R. R., KLINGEMAN, P. C., DOYLE, M. W., and SIMON, A. (2003). "Design for stream restoration", *Journal of Hydraulic Engineering-Asce*, 129(8), 575–584.
115. SLANEY, P. A. and ZALDOKAS, D. (Eds). (1997). *Fish Habitat Rehabilitation Procedures, Watershed Restoration Technical Circular No. 9*. 9. Ministry of Environment, Lands and Parks: Vancouver, B.C., pp. 337.
116. SOAR, P. J. and THORNE, C. R. (2001). Channel Restoration Design for Meandering Rivers. *ERDC/CHL CR-01-1*, U.S. Army Corps of Engineers, Engineer Research and Development Center, Vicksburg, MS, pp. 437.
117. STANFORD, J. A., WARD, J. V., LISS, W. J., FRISSELL, C. A., WILLIAMS, R. N., LICHATOWICH, J. A., and COUTANT, C. C. (1996). "A General Protocol for Restoration of Regulated Rivers", *Regulated Rivers-Research & Management*, 12, 391–413.
118. STEFFLER, P. and BLACKBURN, J. (2002). River2D: Two-Dimensional Depth Averaged Model of River Hydrodynamics and Fish Habitat, Introduction to Depth Averaged Modeling and User's Manual. University of Alberta, Edmonton, Alberta, Canada, pp. 120.
119. SWINDALE, N. (1999). *Numerical Modelling of River Rehabilitation Schemes*, Ph.D. Thesis, University of Nottingham, Nottingham, UK, pp. 302.
120. THOMPSON, D. M. and HOFFMAN, K. S. (2001). "Equilibrium pool dimensions and sediment-sorting patterns in coarse-grained, New England channels", *Geomorphology*, 38(3–4), 301–316.
121. THOMPSON, D. M., WOHL, E. E., and JARRETT, R. D. (1999). "Velocity Reversal and sediment sorting in pools and riffles controlled by channel constrictions", *Geomorphology*, 27, 229–241.

122. THOMSON, J. R., TAYLOR, M. P., FRYIRS, K. A., and BRIERLEY, G. J. (2001). "A geomorphological framework for river characterization and habitat assessment", *Aquatic Conservation-Marine and Freshwater Ecosystems*, 11(5), 373–389.
123. THORNE, C. R. (1998). Stream reconnaissance handbook: geomorphological investigation and analysis of river channels, John Wiley, New York, pp.
124. VAN-ZYLL-DE-JONG, M. C., COWX, I. G., and SCRUTON, D. A. (1997). "An Evaluation of Instream Habitat Restoration Techniques of Salmonid Populations in a Newfoundland Stream", *Regulated Rivers-Research & Management*, 13, 603–614.
125. VRONSKIY, B. B. (1972). "Reproductive biology of the Kamchatka River chinook salmon", *Journal of Ichthyology*, 12, 259–273.
126. WAAL, L. C. D., LARGE, A. R. G., and WADE, P. M. (eds.) (1998). *Rehabilitation of Rivers: Principles and Implementation*. John Wiley & Sons: Chichester, UK, pp.
127. WALKER, J., DIAMOND, M., and NAURA, M. (2002). "The development of Physical Quality Objectives for rivers in England and Wales", *Aquatic Conservation-Marine and Freshwater Ecosystems*, 12(4), 381–390.
128. WALTERS, C. J. (1986). Issues of adaptive management of renewable resources, Macmillan, New York, pp. 374.
129. WALTERS, C. J. (1997). "Challenges in adaptive management of riparian and coastal ecosystems", *Conservation Ecology [online]*, 1(2), 1. Available from the Internet. URL: http://www.consecol.org/vol1/iss2/art1.
130. WARD, J. V., TOCKNER, K., UEHLINGER, U., and MALARD, F. (2001). "Understanding Natural Patterns and Processes in River Corridors as the Basis for Effective River Restoration", *Regulated Rivers-Research & Management*, 17, 311–323.
131. WHEATON, J. M. (2003). *Spawning Habitat Rehabilitation*, M.S. Thesis, University of California at Davis, Davis, CA, pp. 223.
132. WHEATON, J. M., PASTERNACK, G. B., and MERZ, J. E. (2004). "Spawning Habitat Rehabilitation – II. Using Hypothesis Testing and Development in Design, Mokelumne River, California, U.S.A." *International Journal of River Basin Management*, 2(1), 21–37.
133. WHITING, P. J. (2002). "Streamflow necessary for environmental maintenance", *Annual Review of Earth and Planetary Sciences*, 30, 181–206.
134. WILCOCK, P. (1997). "Friction Between River Science and Practice: The Case of River Restoration", *EOS, Transactions of the American Geophysical Union*, 78(40).
135. WILCOCK, P. R. (1996). "Estimating Local Bed Shear Stress From Velocity Observations", *Water Resources Research*, 32(11), 3361–3366.
136. WILCOCK, P. R. (2001). "Toward a Practical Method for Estimating Sediment-Transport Rates in Gravel-Bed Rivers", *Earth Surface Processes and Landforms*, 26, 1395–1408.
137. WILCOCK, P. R., BARTA, A. F., SHEA, C. C., KONDOLF, G. M., MATTHEWS, W. V. G., and PITLICK, J. (1996). "Observations of flow and sediment entrainment on a large gravel-bed river", *Water Resources Research*, 32(9), 2897–2909.
138. WILLSON, M. F. and HALUPKA, K. C. (1995). "Anadromous Fish as Keystone Species in Vertebrate Communities", *Conservation Biology*, 9(3), 489–497.
139. WISSMAR, R. C. and BESCHTA, R. L. (1998). "Restoration and management of riparian ecosystems: a catchment perspective", *Freshwater Biology*, 40, 571–585.
140. WISSMAR, R. C., BRAATNE, J. H., BESCHTA, R. L., and ROOD, S. B. (2003). "5. Variability of Riparian Ecosystems: Implications for Restoration", in: R. C. Wissmar, P. A. Bisson, and M. Duke (eds.), Strategies for Restoring River Ecosystems: Sources of Variability and Uncertainty in Natural and Managed Systems, American Fisheries Society, Bethesda, Maryland, pp. 107–127.
141. WOLMAN, M. G. and LEOPOLD, L. B. (1957). River flood plains: some observations on their formation: Geological Survey Professional Paper 282-C. United States Geological Survey, Washington D.C., pp. 87–107.
142. WOLMAN, M. G. and MILLER, J. P. (1960). "Magnitude and frequency of forces in geomorphic processes", *Journal of Geology*, 68, 54–74.
143. YOSHIYAMA, R. M., FISHER, F. W., and MOYLE, P. B. (1998). "Historical abundance and decline of chinook salmon in the Central Valley region of California", *North American Journal of Fisheries Management*, 18, 487–521.

Intl. J. River Basin Management Vol. 2, No. 1 (2004), pp. 21–37

Spawning habitat rehabilitation – II. Using hypothesis development and testing in design, Mokelumne River, California, U.S.A.

JOSEPH M. WHEATON, *Department of Land, Air, and Water Resources, University of California at Davis, One Shields Avenue, Davis, CA 95616*
Corresponding Author: School of Geography, University of Southampton, Highfield, Southampton SO17 1BJ
E-mail: Joe.Wheaton@soton.ac.uk

GREGORY B. PASTERNACK, *Department of Land, Air, and Water Resources, University of California at Davis, One Shields Avenue, Davis, CA 95616*

JOSEPH E. MERZ, *East Bay Municipal Utility District, 1 Winemasters Way, Lodi, CA 95240; Department of Wildlife, Fish and Conservation Biology, University of California at Davis, One Shields Avenue, Davis, CA 95616*

ABSTRACT
Rehabilitation of salmonid spawning habitat in regulated rivers through spawning bed enhancement is commonly used to mitigate altered sediment and flow regimes and associated declines in salmonid communities. Partial design-phase predictive results are reported from the application of SHIRA (Spawning Habitat Integrated Rehabilitation Approach) on the lower Mokelumne River, California. The primary management goal of the project was to improve habitat for spawning and incubation life stages of fall-run chinook salmon (*Oncorhynchus tshawytscha*). In the summer of 2001, we conducted a pre-project appraisal followed by development and testing of 12 design scenarios. A subsample of eight design hypotheses, used in three of the design scenarios, is presented. Hydrodynamic, habitat suitability and sediment entrainment model results were used to test five of the eight design hypotheses. Two of the three hypotheses not tested were due to inadequate data on flow boundary conditions at high discharges. In September 2001, the project was constructed in a 152 m reach of the LMR from a final design based on all eight of the design hypotheses presented. Transparent hypothesis development and testing in design is emphasized as opposed to declaring success or failure from an ongoing long-term monitoring campaign of the case study presented.

Keywords: river restoration design; gravel augmentation; spawning gravels; habitat enhancement; Mokelumne River; fall-run chinook salmon (*Oncorhynchus tshawytscha*).

1 Introduction

In the Central Valley of California, U.S.A., rivers that once sustained robust runs of chinook salmon (*Oncorhynchus tshawytscha*) are now regulated or otherwise impacted by dams, diversions, chanelisation and instream gravel mining (Yoshiyama *et al.*, 1998). The decline of salmonids in regulated rivers has been linked to many perturbations including over-harvest and the deterioration, inaccessibility and reduction of spawning habitat for these fish (Maddock, 1999; Moyle and Randall, 1998; Nehlsen *et al.*, 1991). In an inventory of gravel injection projects within California's Central Valley from 1976 to 1999, Lutrick and Kondolf (p. comm.) identified 73 spawning habitat rehabilitation (SHR) projects, on 19 different rivers, totalling over 45 US$ million, and involving the addition of over 1.2 million m^3 (1.8 million metric tons) of gravel. Wheaton *et al.* (2004) segregate SHR projects into three categories: (1) gravel augmentation, (2) hydraulic structure placement and (3) spawning bed enhancement. The two most dominant forms of SHR in California are gravel augmentation and spawning bed enhancement and most have not included a detailed design process but instead relied on prescriptive treatments (Kondolf, 2000b). SHR as a type of river restoration is an indicator-species-centred endeavour that focuses on a specific ecological function connected to and indicative of other functions in an effort to promote broader ecosystem recovery. Benefits to a diverse range of other ecological functions, dependent on hydrogeomorphic processes across a range of spatiotemporal scales, are presumed to follow (Maddock, 1999).

Despite the popularity of SHR in practice, it has received little attention in the peer-reviewed literature (Wheaton *et al.*, 2004). Kondolf *et al.* (1996) reviewed a case study of a riffle construction (spawning bed enhancement) on the Merced River, California; and found geomorphic considerations to be lacking. Kondolf (2000b) offered suggestions for SHR, emphasizing the importance of geomorphic assessment across multiple spatiotemporal scales. Merz and Setka (in press) outlined several techniques they used to evaluate and monitor a spawning bed enhancement project constructed in 2000 on the Mokelumne River, California and

Received and accepted

implemented without a design approach. In a separate spawning bed enhancement project constructed in 1999 on the Mokelumne River, California, Pasternack *et al.* (in press) established that more efficient use of gravel and spawning habitat could have been achieved had 2D hydrodynamic and habitat suitability models been used to develop design alternatives. Measurement of habitat enhancement success has been variable with little work assessing design, implementation or longevity of projects. Despite numerous sources of uncertainty in the restoration process, which make developing specific or appropriate performance measures difficult, methods to cope with uncertainty in restoration are almost non-existent in the literature.

In a companion paper (Wheaton *et al.*, 2004) we reviewed the application of a variety of existing science-based tools and concepts to design and analyze SHR projects in regulated rivers and suggested the SHIRA (Spawning Habitat Integrated Rehabilitation Approach) framework to be employed with those tools. Ideally, the utility of this approach might be tested by monitoring fish populations at experimental rehabilitation sites. In practice, such trends are strongly influenced by many external factors and internal intermediate mechanisms related to flow and sediment dynamics, run-size and timing, changes in harvest regulations, and ocean harvesting and predation (Yoshiyama *et al.*, 1998). Thus, comprehensive post project appraisal evaluating specific mechanistic links among hydrodynamics, geomorphology, and ecology is an important aspect of river restoration (Downs and Kondolf, 2002). This topic has been investigated repeatedly in the peer reviewed literature, though the degree of practicality implementing post project appraisal remains uncertain.

Rather than providing the story of a rehabilitation project through post project appraisal, the aim of this paper is to illustrate the utility of hypothesis development and testing during design. The river restoration literature is rich with case-by-case criticism but lacks detailed SHR design advice for practitioners (Wilcock, 1997). Traditional scientific hypothesis testing takes many forms (after Schumm, 1991):

- Falsification – trying to disprove a hypotheses (Popper, 1968)
- Statistical Inference – deduce statistical hypotheses (H_0 & H_A) and iteratively refine a scientific hypothesis based on inference and rejection of null hypothesis (Anderson, 1998)
- Ruling hypothesis – induction of a single hypothesis (Beveridge, 1980)
- Multiple working hypothesis (Chamberlin, 1890) – formulation of as many sequential, parallel or composite hypotheses as possible (Schumm, 1991)

Design hypothesis testing, as presented here, differs from traditional scientific hypothesis testing. The latter aims to universally corroborate or disprove a tentative explanation based on observed evidence. In contrast, a design hypothesis is a mechanistic inference, formulated on the basis of scientific literature review, and thus is assumed true as a general scientific principle. Hence, design hypothesis testing examines for presence of generally accepted functional or process attributes inherent in a design hypothesis in the specific, relevant setting. Design hypothesis testing does not test the overall validity of the scientific principle. Design hypothesis falsification of a specific site design could be a highly useful and cost-effective tool. Under some circumstances, such falsification may also provide insight and testing of underlying scientific principles that would be of great value to the larger scientific community as well (Cao and Carling, 2002). Selected results from the design phase of a spawning bed enhancement project implemented with SHIRA on the lower Mokelumne River, California are used as to demonstrate the utility of design hypothesis testing (see Wheaton, 2003 for details).

2 Study reach

The Mokelumne River of central California drains a 1700 km^2 catchment westward to the Sacramento-San Joaquin Delta (see also Merz, 2001a). Sixteen major dams or diversions, including the 0.24 km^3 Pardee and the 0.51 km^3 Camanche reservoirs, have dramatically altered the Lower Mokelumne River's (LMR) flow regime (Pasternack *et al.*, in press). A flood frequency analysis using a Log Pearson III distribution reveals a dramatic reduction in discharge after the construction of Pardee and Camanche Reservoirs. The two, five, ten and one hundred year recurrence interval flows were reduced from pre Camanche dam levels by 67%, 59%, 73% and 75% respectively. The fragmentation of the Mokelumne River basin via damming has completely altered the hydrology, and disconnected the flux of sediment from the upper basin to the LMR. Hence, spawning gravels have not been replenished from the upper basin since the construction of Pardee Reservoir in 1929. Excluding enhancement, all sediment now supplied in the LMR is derived from erosion of existing relic deposits, its own bed and fine-grained sediment primarily from agricultural runoff. In basins like the Mokelumne where dam removal is not under consideration, SHR is a compromise to provide some ecological function in a new downscaled system positioned downstream of a major dam (Trush *et al.*, 2000).

The LMR spans 72 km from the Delta to Camanche Dam, which has a chinook salmon and steelhead (*O. mykiss*) fish hatchery but no fish ladder (Figure 1A). The majority of salmonid spawning now takes place in a 14-km reach between Camanche Dam and Elliot Road (Merz and Setka, in press). In addition to native anadromous steelhead and fall-run chinook salmon, at least 34 other fish species occur in the LMR (Merz, 2001a). Slopes throughout the current spawning reaches are low (ranging from 0.0005 to 0.002). The study reach begins 580 m downstream of Camanche Dam and 76 m downstream of the confluence of Murphy Creek (a 13.4 km^2 subbasin). From June to July of 2001, the pre project phase was carried out within the 272 m long study reach (Figure 1B). From early July to mid August the design phases detailed in this paper were conducted on 152 m reach contained within the study reach.

3 Methods

3.1 Specific application of SHIRA to lower Mokelumne River

As detailed in the companion paper (Wheaton *et al.*, 2004), SHIRA is organized into a set of science-based tools, termed

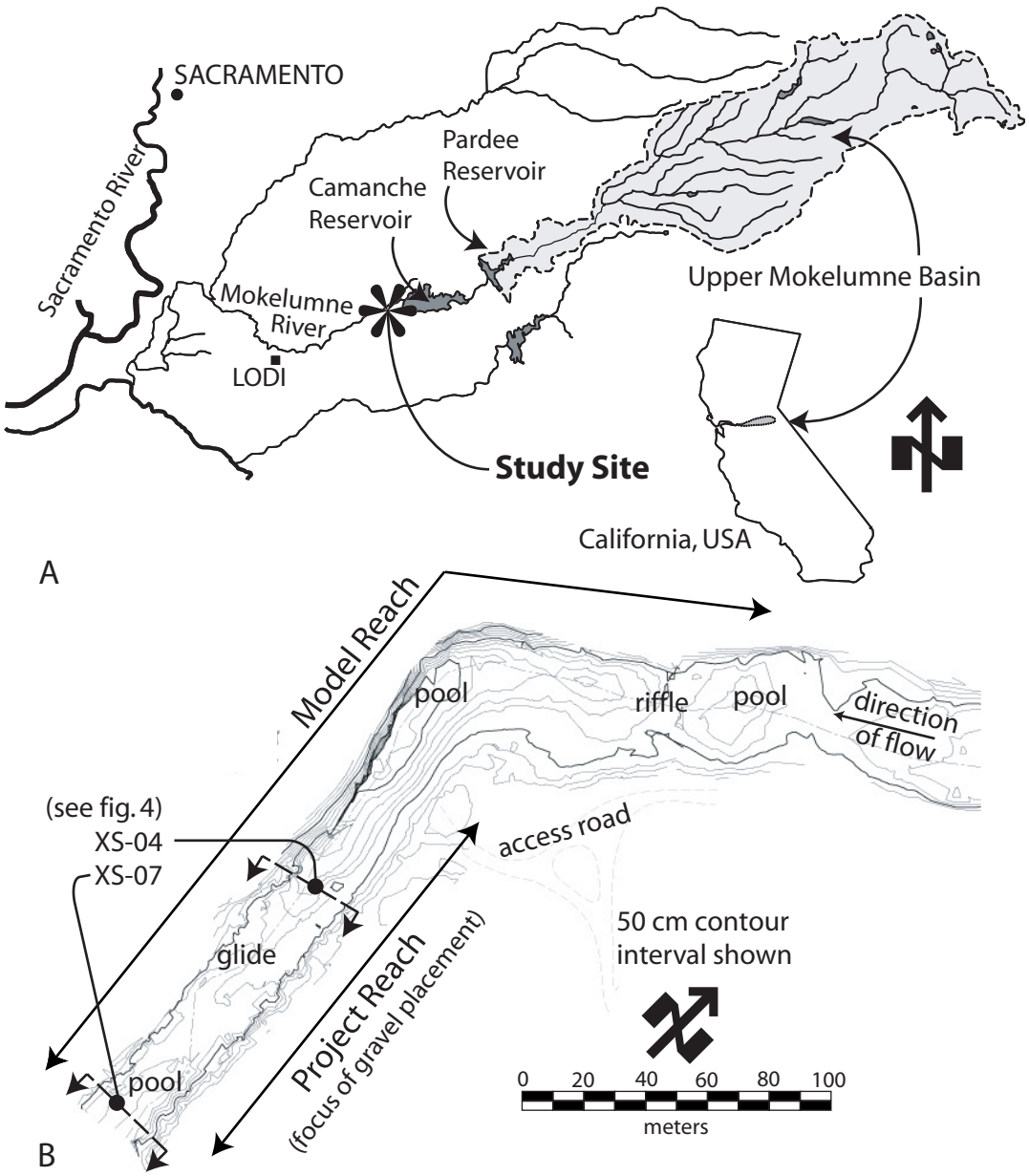

Figure 1 Study site maps. (A) Mokelumne River catchment location map. (B) Topographic survey of study reach showing extent of model domain versus project domain.

modes, used throughout a sequence of project phases. In the methods here, we explain only how specific SHIRA modes were used during the design phase for a specific LMR study. SHIRA is not a prescriptive, cookbook approach and the details of its application will vary from river to river.

On the LMR, a handful of assumptions guided the choices made during data collection, modelling and conceptualization modes. Fall-run chinook salmon are the focus of management efforts on the LMR (FERC, 1998). Reduced quantity and quality of spawning habitat on the LMR was identified by FERC (1993) as the second most important factor restricting population goals. The 2001 experiment site was located just downstream of a major dam incapable of passing coarse-grained sediment. Due to flow reductions, the LMR is largely disconnected from its floodplain and once-active alluvial deposits are now armoured with vegetation (Edwards, 2001). As such, it was assumed that the sediment supply from upstream was negligible and recruitment of gravels in floodplain storage unlikely. Grain size distributions for placed gravels (supplied from a LMR floodplain quarry) were determined from a mix of fork length data for LMR adult female fall-run chinook salmon (Miyamoto, 2001) and related envelope curves reported in the literature (Kondolf and Wolman, 1993). Spawning habitat suitability models were built using only depth and velocity habitat suitability curves (HSC). Grain-size HSCs were not used because source gravels from a local quarry have shown little variability in projects dating back to 1991. Thus, during design inclusion of grain-size HSC acts as a constant and only further emphasizes the poor quality habitat of pre-project conditions. All designs were based on an assumed 1150 m^3 of gravel available for construction (768 m^3 from a quarry and 382 m^3 from retired hatchery spawning beds). This volume was dictated by available funds for the project as opposed to being derived from sediment budget calculations, which suggest a bedload deficit of $\sim$40,000 to 47, 000 m^3 accruing since the construction of Pardee

reservoir in 1929. The flow regime of the LMR is heavily regulated with a maximum Camanche release of 141 cumecs, a minimum mandated fish flow of 4.25 cumecs and spawning flows typically between 5.7 (exceeded 80% of time) and 14.2 cumecs (exceeded 45% of time) depending on water deliveries to downstream users (for detailed hydrologic analysis: Pasternack *et al.*, in press). Due to the absence of project site rating curves, lack of availability of vegetated floodplain topographic data, and lack of high flows during the 2001 water year, hydrodynamic modelling was primarily conducted at an 11.46 cumecs spawning flow, for which validation data was collected. The 11.46 cumecs flow is exceeded 54% of the time under the current flow regime (1963–2003). The above assumptions and limitations helped determine the specific methods and metrics used in the data collection mode (Table 1). Although not included explicitly in this study, monitoring of previous enhancement sites since 1991 has involved macroinvertebrate, fish community, alevin egg tube survival and water quality studies (Merz, 2001a,b; Merz, 2002; Merz and Setka, in press). This biological foundation strongly influenced the assumptions described above.

3.2 Incorporating established concepts into designs

Drawing on SHIRA's Conceptualization Mode, key concepts from the literature were documented, including related processes, the geomorphic forms thought to promote and interact with those processes and the presumed ecological benefits. In the development of designs, we took several design objectives and established design hypotheses for them (Table 2). These concepts were then incorporated into 12 competing design scenarios. We report how some of the concepts led to conceptual designs for three of twelve scenarios: Design Five – Flat Riffle, Design Six – Constricted Pools, and Design Twelve – Central Bar Complex. For each design, form-process sketches and finished grading plans

Table 1 Data collection mode. Description of purpose, methods and metrics for various data collection mode components for project.

Data collection component	Purpose	Method	Metric: pre	Metric: Design
Topographic Reach Survey	Build Digital Elevation Models	Total station w/true datum and coordinate system; feature-based irregular surveying (high density around topographically complex areas; low density on floodplains)	1886 points; Avg. density: 0.17 pt./m^2; 1.09 ha; Surface complexity: 1.05	NA (grading plans used to create DEMs)
Flow/ Hydrodynamics	Rating curves; Hydrodynamic Model Validation; Model boundary condition specifications; eddy viscosity estimation from theory and velocity measurements	Depth-averaged estimates (0.6 depth if <0.75 m; average of 0.2 and 0.8 depth if >0.75 m): Wadable cross sections: Marsh McBirney Electromagnetic current meter and top setting rod. Non-wadable cross sections: Flat bottom boat and Price AA current meter	Seven cross sections (4 wadable; 3 non-wadable); 219 points	No validation possible (Pre-project boundary conditions used)
Geomorphic Analysis	Characterize active and inactive geomorphic processes and limitations	Hydraulic geometry analysis, channel classification, geomorphic process inventory, rough bedload sediment budget using ACRONYM	Seven cross sections, field reconnaissance and 59 years of flow record	NA
Flow Regime Analysis	Identify timing, duration and intensity of peak flows, spawning flows and various recurrence interval flows	Pre dam USGS daily records (1904–1963); Post dam EBMUD daily records (1964–2001); Log Pearson III flood frequency analysis	59 years of pre dam records; 37 years of post dam records	NA (same used)
Spawning Habitat Characterization	Quantify hydrodynamic characteristics of spawning habitat; habitat typing; redd utilization	Velocity and depth habitat suitability curves from (CDFG, 1991); River styles characterization; weekly redd surveys (1994–2001) (Merz and Setka, in prep.)	Velocity and depth HSC; *Redd surveys* (*1994–2000*): Total LMR: 6483 redds ($\approx$926/year) Project reach: 55 redds ($\approx$7/year)	Same velocity and depth HSC used;
Substrate Characterization	Quantify surface grain size distributions; Estimate model roughness parameters	Wolman Pebble Counts; Roughness estimation (Manning's n)	3 transects (100 samples each); $n = 0.043$	Quarry specified distribution; $n = 0.043$

Table 2 Some examples of design concepts used. The table illustrates how to start with basic design objectives, develop specific design hypotheses, incorporate the hypotheses into channel design and test them.

Design objective	Possible design hypothesis	How to include hypothesis in design	How to test design hypothesis
1. Provide higher quantity of higher quality spawning habitat.	1A. Spawning habitat should be provided that is as close to GHSI defined high quality habitat as possible.	Design features that will promote shallower water depths, swifter velocities and locally steepened water surface slopes (e.g. riffles; transverse bars, ribs; point bars; longitudinal bars).	Use GHSI models of designs at spawning flows to predict habitat quality of modeled design scenarios.
2. Spawning habitat should be geomorphically sustainable.	2A. Pool riffle sequences should be self-maintaining when provided with an upstream gravel supply if at high flows an entrainment reversal promotes net deposition over riffles and net scour within pools.	Place riffles where flow width expansions are permissible and place pools where flow width constrictions may be used at pool heads.	Model velocity, shear stress, and sediment entrainment over range of flows and look for entrainment reversal at high flows.*
	2B. Deposition of coarse bedload at high flows should be encouraged over spawning habitat (e.g. riffles and bars) and scour should be promoted in pools.	Design bed morphology and channel width variations over a range of flows to encourage convergent flow paths in pools and divergent flow paths over spawning habitat.	Use 2D hydrodynamic model flow vector solution to test for presence of convergent and divergent flow paths at high flows.*
	2C. Although active scour and deposition is presumed to take place at higher flows, there should not be significant erosion of spawning habitat during spawning flows.	Design spawning habitat to be stable at spawning flows by not using channel narrowing or excessively steep water surface and/or bed slopes in spawning habitat zones.	Model sediment entrainment at spawning flows and check that entrainment of spawning habitat not occurring.
3. Provide intergravel conditions to support higher alevin survival rates.	3A. Higher rates of hyporheic exchange (e.g. upwelling or downwelling through gravels) should be promoted to maintain connectivity of intergravel pore space, maintain high levels of dissolved oxygen and promote flushing of fines and metabolic wastes.	Include broad bowl-shaped pool-exit slopes at pool-riffle transitions (tend to increase hydraulic head gradient rapidly and induce downwelling).	Use a hyporheic flow model to test for downwelling; OR calculate hydraulic head gradients (based on some major assumptions) and test for downwelling.**
4. Provide refugia in close proximity to spawning habitat.	4A. Structural refugia in close proximity to spawning habitat should provide resting zones for adult spawners, protection from predation and holding areas for juveniles.	Place spawning habitat in close (>5 m) proximity to pools; overhanging cover, boulder complexes, and LWD.	Measure distance from medium and high GHSI quality habitats to structural refugia and check to see that most spawning habitat is within reasonable proximity.
	4B. Shear zone refugia (characterized by two distinct blocks of flow moving in opposite directions; e.g. eddies) in close proximity to spawning habitat should provide resting zones for adult spawners and drift feeding opportunities for juveniles and macroinvertebrates.	Through design of bed features, irregular shaped banks, channel width variations, LWD or boulder complexes, promote shear zones in close (>5 m) proximity to spawning habitat.	Look for presence of shear zones in hydrodynamic model results at spawning flows and measure distances from high and medium GHSI quality habitats to check for reasonable proximity.
5. Providing morphological diversity should support biological diversity.	5A. Designs should promote habitat heterogeneity to provide a mix of habitat patches that serve multiple species and lifestages.	Avoid GHSI optimization of excessively large contiguous areas of habitat; design for functional mosaic of geomorphic forms and habitat.	Large (>2 to 4 channel widths) patches of homogenized flow conditions in hydrodynamic model and homogenized habitat quality in GHSI model results should not be present at spawning flows.

*Due to inadequate data on high flows, these hypotheses were only partially tested at spawning flows and it was presumed that desired patterns would be preserved at high flows.
**Not tested in this study.

depict the utility of SHIRA's conceptualization mode at creatively incorporating scientific concepts into designs (Wheaton, 2003).

Finished grading plans were drawn in AutoCAD and TIN-based digital elevation models (DEMs) were created in AutoDesk's Land Desktop R3. A finished grading plan specifies finished grade elevations in reference to a pre-project DEM. A pre-project DEM was made from detailed topographic surveys. Design DEMs combined the pre-project DEM with grading plans for hypothetical designs (Table 1). DEMs were each iteratively developed using (1) visualization, (2) editing, (3) data augmentation and (4) interpolation stages. Point data augmentation was used to improve pre-project DEM representation of areas with lower point resolution or inadequate data (typically deep pools). Three types of point augmentation were used: (1) additional field surveys, (2) interpolation between known points and (3) user-specified spacing along contours. When iterative DEM development finally yielded realistic terrain representation, refined point and breakline data were extrapolated from Land Desktop for later use in hydrodynamic model mesh characterization.

3.3 Numerical models for process predictions

SHIRA's Modelling Mode was used to create hydrodynamic, sediment entrainment and spawning habitat models that in turn were used to test specific design hypotheses (Table 2). Model results are presented for the pre-project (for validation and comparison) and three design scenarios. Emphasis is placed on the ability or inability of these models to test the design hypotheses made. The models used are reviewed briefly below (see also Pasternack *et al.*, in press).

The 2D Finite Element Surface Water Modelling System (FESWMS) and Surfacewater Modelling System graphical interface were used to analyze steady state hydrodynamics. The boundary conditions required to run FESWMS are: (1) a discharge at the upstream boundary, (2) a corresponding water surface elevation at the downstream boundary and (3) channel topography. Due to inadequate flow variation during the 2001 water year, lack of forested floodplain topographic data, and lack of historical rating curves for the reach, discharge and water surface boundary conditions were identified only for spawning flows (11.46 cumecs). Refined DEM data were used to discretize channel topography to a finite element model mesh at an approximately uniform node spacing (~45 cm apart). This resulted in model meshes with between 49,000 and 53,000 computational nodes comprising between 15,000 and 16,500 quadrilateral and triangular elements. The most noteworthy model parameters include Manning's roughness and Boussinesq's eddy viscosity coefficient for turbulence closure. Manning's roughness (n) was estimated as 0.043 for entire study site using a McCuen summation method (McCuen, 1989). This was used instead of a spatially explicit application of Strickler's equation for roughness based on substrate size variations, because in this instance there was a narrow and homogenized range of gravel substrate sizes. Eddy viscosity is a fourth-order tensor (33 terms), which describes the property of the flow and arises from the closure problem when averaging the velocity terms in the Navier-Stokes equations. We used Boussinesq's analogy to parameterize eddy viscosity, which crudely approximates eddy viscosity as an isotropic scalar. Doing so allows a theoretical estimate of eddy viscosity as 60 percent of the product of shear-velocity (u*) and depth (Froehlich, 1989). Pasternack *et al.* (in press) were unable to achieve model stability for a reach with a shallow riffle and a relatively deep, in-channel mining pit using a single constant eddy viscosity value estimated from field measured depth and velocity data with a mesh built on unrefined DEM data at a study site located 220 m upstream. In fact, model stability was only achieved when the constant eddy viscosity was kept above $0.065\,m^2/sec$. During a flow of 11.46 cumecs at the study site reported here, an average eddy viscosity of $0.017\,m^2/sec$ was calculated from 219 velocity and depth measurements. Due to significantly less topographic variation as well as higher mesh and DEM quality in this study, model stability and convergence was achieved even using the actual calculated eddy viscosity value of $0.017\,m^2/sec$. No model calibration was performed as all model parameters were specified with actual measured or theoretically calculated values. Pre project model results (velocity and depth) were compared against measured values at five cross sections for validation.

Habitat suitability curves for fall-run chinook on the LMR were used to develop a global habitat suitability index (GHSI) for spawning (Wheaton *et al.*, 2004). In principle, this is similar to PHABSIM habitat simulations with the major exception that a 2D instead of 1D hydrodynamic model is used (Leclerc *et al.*, 1995). The index yields spatial predictions of spawning habitat suitability based on 2D hydrodynamic model results (Pasternack *et al.*, in press). Whereas the hydrodynamic model results can be used to test specific hydrodynamic process predictions and make ecological function inferences, the habitat suitability model tests the claim that specific forms will produce preferable spawning habitat conditions.

A sediment entrainment sub-model based on hydrodynamic model results and representative grain sizes (d_{16}, d_{50} and d_{84}) was used to test for potential scour at spawning flows. A common approach to modelling sediment entrainment using Shields' incipient motion criterion (Garde and Raju, 1985), and Einstein's log velocity profile equation was employed (Wheaton *et al.*, 2004). The theoretical HSC and entrainment functions were analyzed by plotting them as a third dimension on velocity versus depth plots. Actual measured hydraulic conditions (velocity and depth) could then be overlaid on the same plot to assess both habitat suitability and sediment entrainment thresholds. Sediment entrainment model results were used to test for erosion at low spawning flows, but could not be used to test hypothesized erosion processes at higher flows due to lack of adequate rating curve data coupled with an un-surveyed, wide, and complex vegetated floodplain.

4 Results

4.1 Incorporating established concepts into designs

The pre-project topographic survey and geomorphic habitat classification revealed a pre-project reach-averaged slope of

Table 3 Summary grading statistics.

Design	Volume of gravel used (m^3)	Gravel placement footprint (m^2)	Maximum fill depth (m)	Bed elevation at riffle crest (m)	Local slope
Pre	NA	NA	NA	26.90	0.0011
Five	961	2225	1.5	27.66	0.0080
Six	956	2457	1.4	27.51	0.0049
Twelve	1146	2402	1.5	27.44*	0.0020

*Upper riffle reported (central bar raised from 27.02 to 27.75 and lower riffle raised from 26.66 m to 27.44 m).

0.0011 and a pool-glide morphology dominating the project area (Figure 1B). Excessive depths on the LMR are attributed to a history of instream gravel mining and channel re-alignment. All designs were intended to improve spawning habitat within the glide portion of the uniform and homogenized reach (Figure 1B). Design alternatives included: tight alternate bars, constricted riffle, broad flat riffle, constricted pools, braided and complex channel geometries. Only three of the twelve design scenarios, which illustrate a range of different concepts, are reported below. Summary earthwork statistics are provided in Table 3.

The conceptual design formulation for Scenario Five was based primarily on optimizing the area of GHSI-defined high quality spawning habitat with a pool-riffle unit (hypothesis 1A of Table 3). A broad flat riffle with a slope of 0.008 was specified across the entire width of the channel and extended longitudinally roughly 60 m (Figure 2A). The upstream portion of the project was to transition out of an existing confined pool onto a broad pool-exit slope. Pool-exit slopes are bedforms at the pool-riffle transition that we hypothesized (hypothesis 3A) would promote hyporheic exchange or downwelling of water due to an increased hydraulic head gradient and vertically contracting streamlines (Kondolf, 2000a). The inferred ecological benefits of hyporheic exchange for salmonids are realized during egg-incubation through potential flushing of metabolic wastes, maintenance of interstitial voids and elevated dissolved oxygen levels, all of which could promote higher alevin survival rates (Chapman, 1988). Furthermore, chinook salmon have been found to preferentially spawn where downwelling occurs (Geist, 2000; Vronskiy, 1972). The broad flat riffle was to provide a large area of contiguous high quality spawning habitat. It was hypothesized that the riffle would decrease water depths, increase water surface slope and increase velocities to those optimal for spawning (hypothesis 1A). Modelling of earlier design scenarios (e.g. constricted riffle) suggested scour even at spawning flows and this design was modified to discourage scour during spawning and incubation flows (hypothesis 2C in Table 2). Finally, the large flat riffle was a simple design commonly used in spawning bed enhancement projects and a good benchmark for comparison.

The conceptual design formulation for Scenario Six also specified a broad riffle (hypothesis 1A in Table 2), but used some of the design volume of gravel to further constrict flow width through pools both upstream and downstream of the riffle (hypothesis 2A) using two submerged bars (Figure 2B). The bars were designed roughly four channel widths apart (consistent with empirical observations (e.g. Brookes and Sear, 1996). Pool constriction was sought (hypothesis 2B) to promote convergent flow and focus scour in pools at higher flows based on mass conservation (Carling, 1991) and convective acceleration force mechanisms for pool maintenance (Dietrich and Whiting, 1989). Divergent flow over the riffle was intended to promote gravel deposition on the riffle at higher flow as suggested by Booker *et al.* (2001) and Thompson *et al.* (1999). It was hypothesized that the bar pattern would encourage the flow thalweg to switch from river right to river left as it diverges across the riffle and further concentrate flow in the downstream pool (hypothesis 2B). This was intended to compliment the transitional classification of the channel between a straight and meandering river and work in harmony with the existing upstream meander bend hydraulics. Whereas in design scenario five the majority of gravel was used to create contiguous spawning habitat, here a significant portion of the gravel was used to achieve geomorphic goals thought to promote sustaining fluvial processes.

In Design Scenario Twelve, two flat riffle areas with finish grades at an elevation slightly lower than the single riffle in previous designs (limiting backwater impact on an upstream riffle with riffle crest elevation of 27.55 m) were bridged by a central longitudinal bar (Figure 2C). The central bar has multiple hypothesized functions. First, it yields flow divergence across both flat riffle areas (promoting gravel deposition there) and flow convergence over adjacent pools (reducing gravel deposition there; hypothesis 2B). Booker *et al.* (2001) found that grains seeded in riffles in a channel with a small width to depth ratio were routed and deposited around the perimeters of pools. Second, it provides needed construction access for the downstream riffle area. Third, Pasternack *et al.* (in press) previously found central bars to be highly gravel-efficient and yield large contiguous areas of high quality habitat (hypothesis 1A). Existing deeper areas along both sides of the central bar were maintained as small pools, and like the central bar, they too serve several hypothesized purposes. First, recirculating eddies induced by the constriction of flow through the pools could lead to aggradation of gravels on pool exit slopes or along the central bar (hypothesis 2A). Second, designs with only one riffle introduce only one pool-exit slope. Thus, by incorporating two small pools into the design, a total of three pool-exit slopes were present (hypothesis 3A). Third, the sloping bed around the small pools provides habitat heterogeneity (hypothesis 5A). Fourth, the small pools provide adult holding areas proximal to spawning habitat (hypothesis 4A). Finally, the existing banks on both sides of the bar were highly irregular due to tree roots and overhanging cover. Maintaing pools on both sides of the bars was hoped to preserve existing shear zones along these irregular banks; thus providing shear zone refugia (hypothesis 4B).

4.2 Numerical models for process predictions

4.2.1 Comparison with pre project

Pre-project hydrodynamic model results at a representative spawning flow of 11.46 cumecs highlight several interesting flow

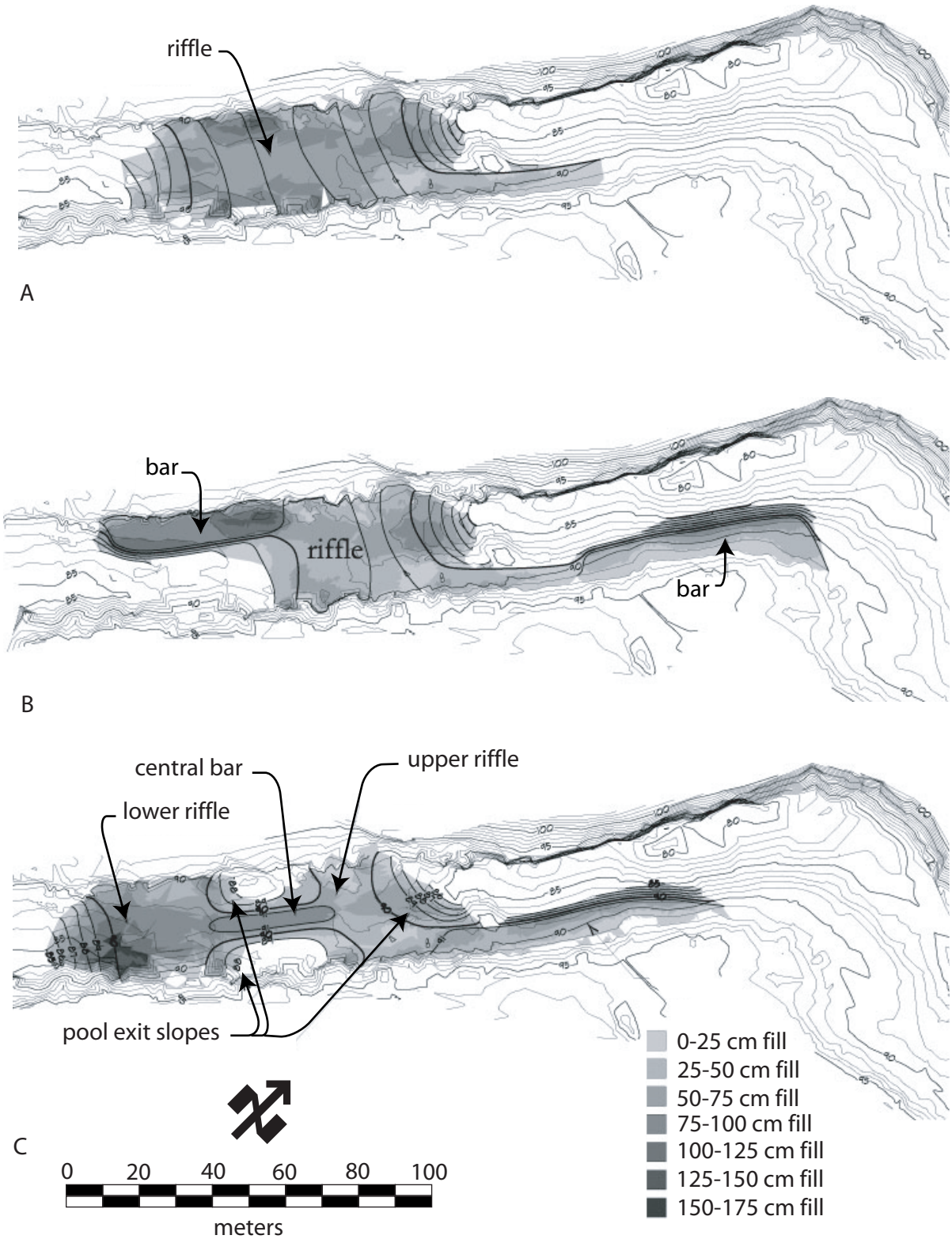

Figure 2 Conceptual designs and grading plans for selected design scenarios. (A) Design scenario 5 (flat riffle). (B) Design scenario 6 (constricted pools). (C) Design scenario 12 (final design – complex channel geometry). Shaded areas represent depth of design specified gravel placement; whereas faded contours represent pre project topography.

features (Figure 3A). Pronounced eddies on the inside bend of the river and downstream of irregularities that protrude into the channel along the banks are correctly captured in model results and qualitatively verifiable in the field. The pre-project model results highlight the swifter velocities over an existing riffle upstream of the bend, the concentration of flow through the deep pool on the outside bend, and the rather homogenous flow patterns and sluggish velocities through the glide where gravel addition is proposed.

Pre-project flow data collection and model validation at five cross sections (Figure 4), during an 11.46 cumecs discharge, show a generally good agreement between field data and model

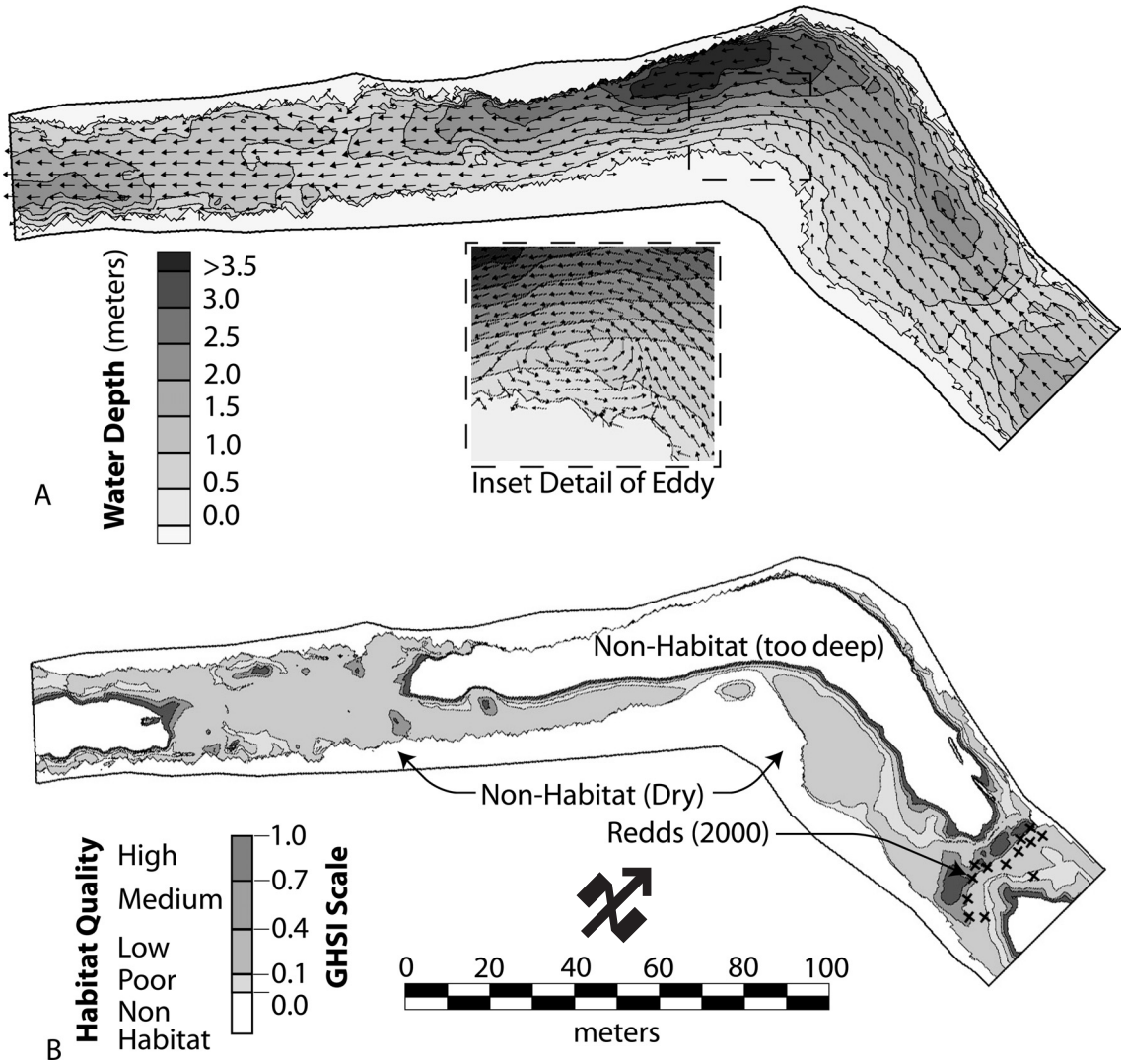

Figure 3 Pre-project Model Results at 11.46 cumecs for comparison. (A) Hydrodynamic Model Results. Shading corresponds to depth solutions and arrows correspond to velocity vectors (scaled to magnitude). (B) Spawning habitat suitability model (GHSI) results w/2000 redd survey results overlaid (redds delineated by black x's).

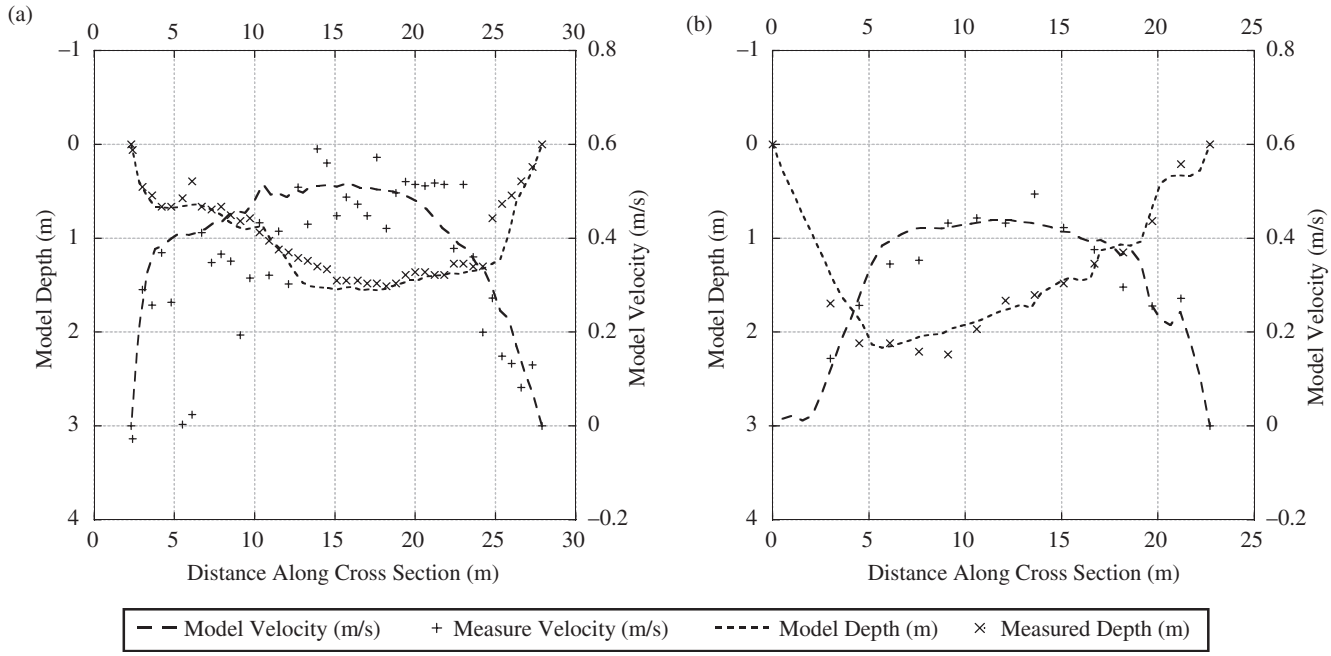

Figure 4 Examples of Pre-project Model validation at two cross sections. (A) Cross section four. (B) Cross section seven. (See Figure 1 for cross section locations.) Generally, poor velocity validation is attributed to areas of poor topographic quality (indicated by errors in measured and predicted depth) and to a lesser extent local-scale measured velocity fluctuations are muted by the model.

predictions (see Wheaton 2003 for full results). The largest errors in velocity predictions are where model bathymetry inaccurately describes the bed. The use of an intermediate AutoCAD-driven DEM process in this study represented a significant advance in model prediction compared to an earlier study (Pasternack *et al.*, in press) in which raw survey data were directly interpolated to yield the model mesh.

For comparison, pre-project GHSI modelling results confirm the lack of substantial areas of high or medium quality spawning habitat within the proposed enhancement area (Figure 3B).

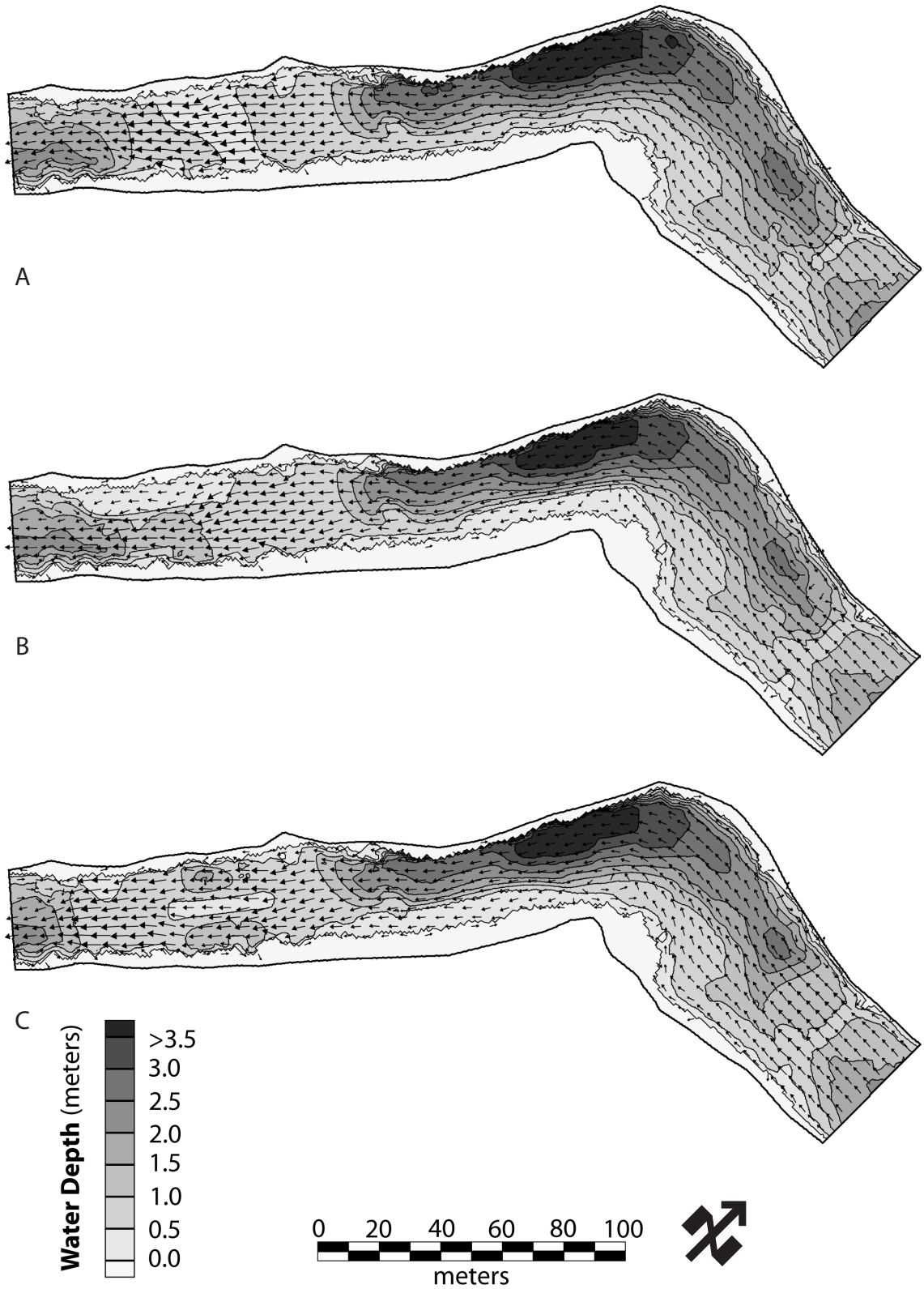

Figure 5 Design Phase Hydrodynamic Model Results at 11.46 cumecs. Shading corresponds to depth solutions and arrows correspond to velocity vectors (scaled to magnitude). (A) Design scenario 5 (flat riffle). (B) Design scenario 6 (constricted pools). (C) Design scenario 12 (final design – complex channel geometry).

Conversely, the best suited spawning habitat is highlighted in an existing riffle upstream of the project area (at the top of the model reach) and the locations of redds from the year 2000 survey (x's in Figure 3B) illustrate these preferences. Note that no redds were located in the project area in 2000. However, the thirteen redds located on the riffle upstream of the bend show good agreement with GHSI predictions and reveal clustering at a pool exit slope (hypothesis 3A). Roughly 56% of the model reach was found to be non-spawning habitat. Of the 44% considered potential spawning habitat, only 2.8% was found to be of high quality, 7.5% was of medium quality, 23.1% was of low quality and 67.6% was of poor quality.

4.2.2 Comparison of three designs

The hydrodynamic model results at an 11.46 cumec discharge are depicted in Figure 5 for all three designs and can be directly compared with the pre project results in Figure 3A. Table 4 shows the results of hypothesis testing inferred from hydrodynamic, habitat suitability (GHSI) and sediment entrainment modelling results. Figure 6 shows a direct comparison of GHSI habitat suitability predictions for the three designs and can be compared directly with pre project results in Figure 3B. Figure 7A shows a summary evaluation of the respective percentages of GHSI spawning habitat and non-habitat throughout the entire modelled reach for the three designs and pre project. Much of modelled area received no gravel by design, since it is necessary to model a larger reach than just the project site. Figure 7B recasts the GHSI results in terms of three different metrics of gravel efficiency (based on volume of gravel used in Table 3).

Figure 8 synthesizes the hydrodynamic, habitat suitability and sediment entrainment model results into a single graph. The plots of Figure 8 depict both the depth and velocity distributions as small black points for the pre project (8A) and all three designs (8B–8D). Each point represents a velocity and depth prediction at one of over 50,000 nodes. Overlaid behind these distributions are the GHSI habitat suitability predictions (same shading scheme as

Table 4 Hypothesis testing results summarized.

Design hypothesis used (refer to Table 2)	Hypothesis tested?	Results of hypothesis testing or reason for not testing
Design Five		
1A – Optimize HSC habitat	Yes	Ranks 4th in terms of new habitat created (Figure 7A), 1st in terms of high quality habitat production efficiency (Figure 7B), and provides a large contiguous area of high quality spawning habitat.
2C – No scour during spawning	Yes	Sediment entrainment model showed no prediction of scour at spawning flows (Figure 8B).
3A – Pool exit slopes	No	No hyporheic exchange model. One pool exit slope provided based on empirical evidence of habitat utilization (e.g. Figure 3B).
Design Six		
1A – Optimize HSC habitat	Yes	Ranks 3rd in terms of new habitat created (Figure 7A), 2nd in terms of high quality habitat production efficiency (Figure 7B), and provides a large contiguous area of high quality spawning habitat.
2A – Pool-riffle maintenance	No	No data for specifying hydrodynamic and sediment entrainment model boundary conditions at high flows.
2B – Flow paths for maintenance	No	(see 2A above)
2C – No scour during spawning	Yes	Sediment entrainment model showed no prediction of scour at spawning flows (Figure 8C).
3A – Pool exit slopes	No	No hyporheic exchange model. One pool exit slope provided based on empirical evidence of habitat utilization (e.g. Figure 3B).
Design Twelve		
1A – Optimize HSC habitat	Yes	Ranks 1st in terms of new habitat created (Figure 7A), 4th in terms of high quality habitat production efficiency (Figure 7B), yet provides less contiguous or homogenized areas of high quality spawning habitat.
2A – Pool-riffle maintenance	No	(see 2A above)
2B – Flow paths for maintenance	No	(see 2A above)
2C – No scour during spawning	Yes	Sediment entrainment model showed no prediction of scour at spawning flows (Figure 8D).
3A – Pool exit slopes	No	No hyporheic exchange model. Three pool exit slopes provided based on empirical evidence of habitat utilization (e.g. Figure 3B).
4A – Structural refugia	Yes	All GHSI high and medium quality habitat found in close proximity to pools.
4B – Shear zone refugia	Yes	All GHSI high and medium quality habitat found in close proximity to shear zones at bank edges.
5A – Habitat Heterogeneity	Yes	More fluvial complexity apparent in hydrodynamic model predictions and GHSI habitat is more heterogeneous than previous designs.

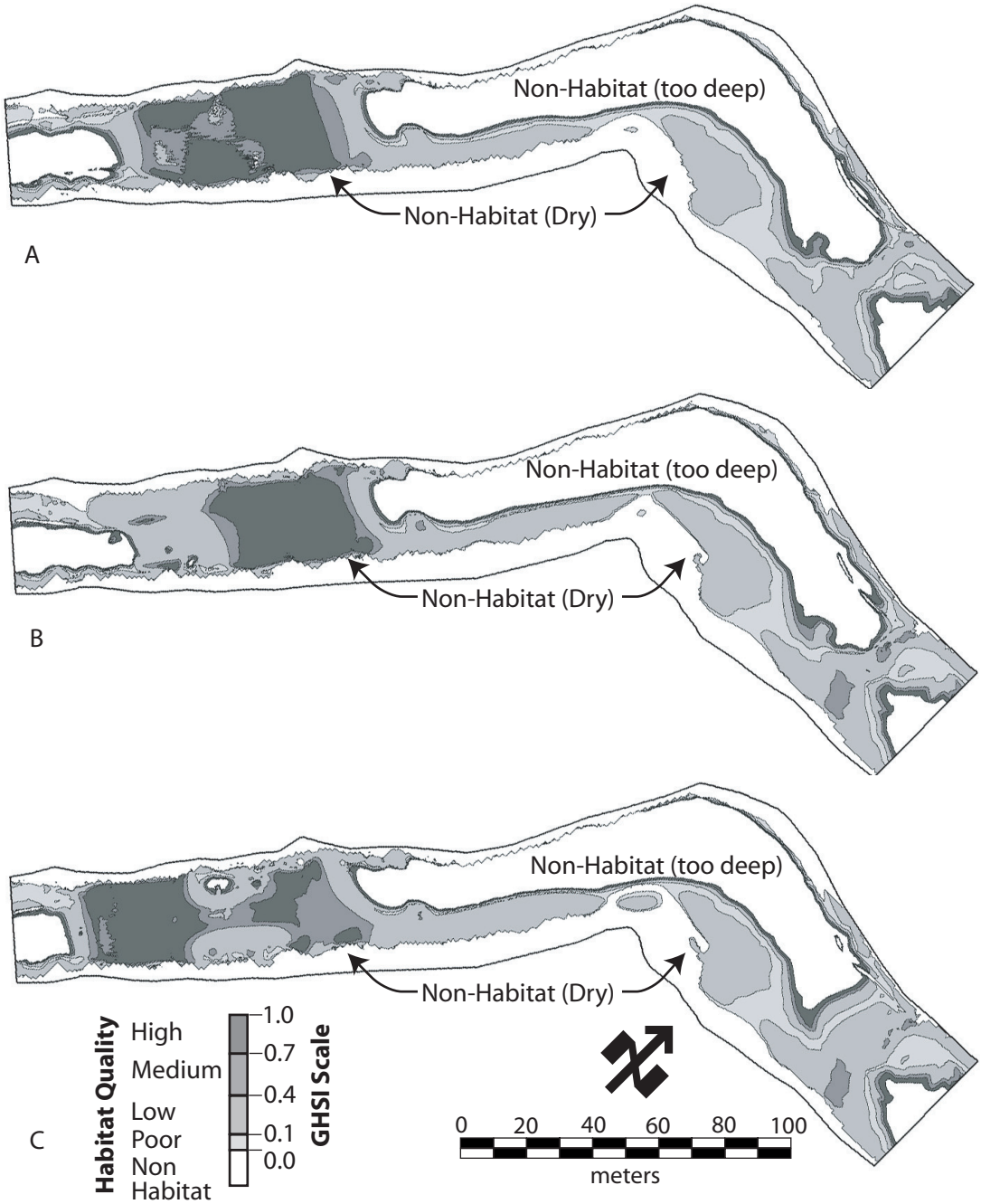

Figure 6 Design Phase Spawning Habitat Suitability Model (GHSI) results at 11.46 cumecs. (A) Design scenario 5 (flat riffle). (B) Design scenario 6 (constricted pools). (C) Design scenario 12 (final design – complex channel geometry).

Figure 6) and sediment entrainment thresholds for four different grain sizes. In general, the pre project distribution (8A) occupies the lower velocity region of the graph which corresponds to generally poorer spawning habitat. All of the plots show more variability in depth (spread horizontally) than velocity (compacted vertically). However, the three designs shift portions of these distributions to lower depth (i.e. gravel placement) higher velocity regions that correspond with higher quality spawning habitat. The darkened vertical streaks of the distributions found in the three designs represent areas graded to a consistent depth but that yield significant variations in velocity. Notice that the homogenized flat riffle of Design Five (8B) has only one vertical streak, whereas the more heterogeneous Design Twelve (8D) has four vertical streaks. Finally, as the distributions are all for an 11.46 cumecs spawning discharge, none of the distributions exceed any of the thresholds for sediment entrainment.

This paper focused on the utility of hypothesis testing in design development of SHIRA, and as such does not report the results of construction, post project appraisal or long-term monitoring. Incidentally, design scenario twelve was chosen as the final design because it showed the best mix of model-defined spawning habitat and conceptually identified important features (Table 4). Construction was carried out in September of 2001 based on this design and the first spawning activity was recorded later that year (see Wheaton, 2003 for full results). From 1991 to 2001 East Bay Municipal Utility District placed over 8500 m^3

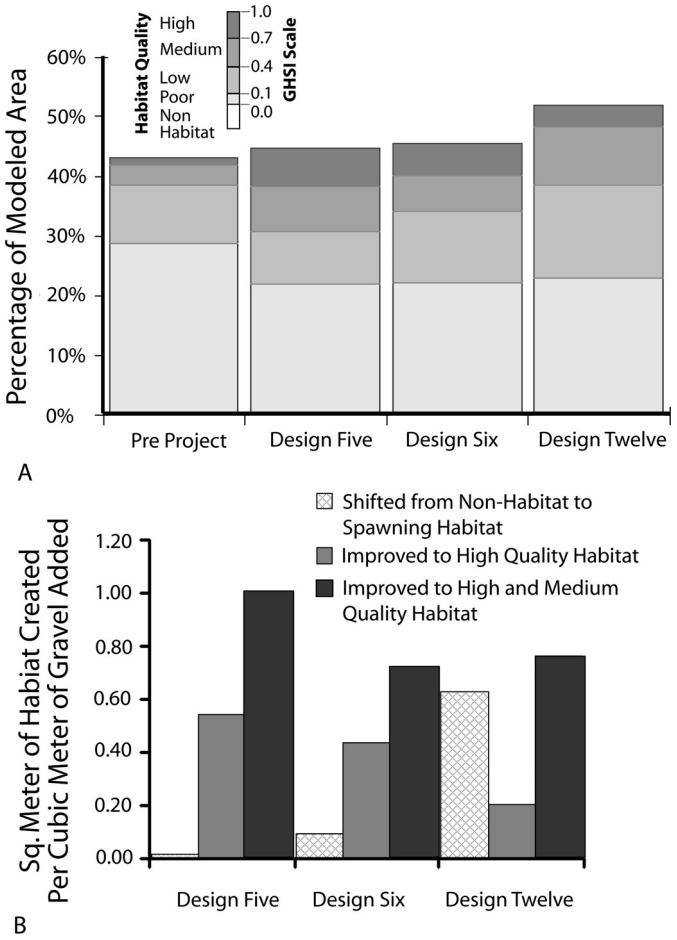

Figure 7 Design Phase Spawning Habitat Suitability Model comparisons. (A) In terms of percentage of total model domain. Notice that a large percentage (48 to 57%) of the model domain is not spawning habitat (i.e. pools comprise a large portion of the model reach) and that a significant portion (22 to 28%) remains as poor quality spawning habitat. Such areas provide important adult holding and refugia as well as juvenile rearing habitat. (B) In terms of three different gravel efficiency measures.

of gravel at 12 spawning habitat enhancement sites along the LMR and has a geomorphic and biological monitoring program encompassing all of these projects extending at least to 2009.

5 Discussion

5.1 Active versus passive … form-based or process-based?

In river restoration practice, designs are most often developed on the basis of form mimicry. In other words, designs are produced by imitating the attributes of either a present day or a historical 'natural' analogue. As form and process are intimately linked (Ritter *et al.*, 1995), form-based restoration sometimes works (Annable 1999). In many cases, 'form-based' templates digress towards a prescriptive specification of structures and treatments thought to improve a site (e.g. placement of groins, LWD, riffles without careful consideration). Although concepts drawn from scientific research may well enlighten a form-based design process, what often lacks is a systematic consideration of the interaction between geomorphic processes and ecologic functions (Annable, 1999). Wilcock (1997) suggests basing design goals on general physical principles instead of empirical relations between channel geometry and flow frequency. For example, what hydrologic and geomorphic processes are necessary to provide a specific ecological function? What form will produce those processes under various flow and sediment regimes? Given the water and sediment supply, how will those forms adjust? Such questions point towards a 'process-based' approach mindful of processes ranging from the grain scale to the catchment scale.

Most investigators of river restoration are comfortable claiming 'process-based' rehabilitation is better than 'form-based' rehabilitation (Wheaton *et al.*, 2004). In the case of 'passive approaches' to restoration (e.g. pulse flows, changes in basin landuse), using a 'process-based' approach makes intuitive sense. For example, providing flow releases from a reservoir to mimic a natural hydrograph and encourage mobilization and reorganization of sediments, may restore the processes that 'allow the river to do the work' (Stanford *et al.*, 1996; Trush *et al.*, 2000). Yet 'active approaches' are chosen in place of 'passive approaches' when river managers decide that a 'passive approach' will take an unacceptably long amount of time (Montgomery and Bolton, 2003). The FERC dam re-licensing agreement for Camanche Reservoir (FERC, 1998), which requires that EBMUD provide SHR on the LMR, is an example of an 'active approach' chosen because a 'passive approach' was deemed too slow.

'Active approaches', by definition, involve direct manipulation of channel structure or form (Montgomery and Bolton, 2003). But does this mean they are 'form-based' rehabilitation? In 'active' SHR channel design, you can not consider process without considering form, but it is quite easy and tempting to base "active" channel design on form without considering process. We argue that explicit development of design hypotheses, which articulate processes and functions expected from placed forms, allows one to undertake a 'process-based' active approach. Using accepted scientific hypotheses found in the peer reviewed literature to drive conceptual design development is not necessarily new or novel. With three design scenario examples, we demonstrated the incorporation of ecological function and geomorphic process concepts to produce conceptual designs and detailed finished grading plans.

5.2 Numerical models to test design hypothesis

Neither modelling nor conceptualization alone can constrain the potential uncertainties arising from design decision making. At a minimum, conceptual consideration of uncertainties in restoration design can yield more realistic expectations of restoration outcomes. Modelling can not definitively prove design hypotheses correct or incorrect because of inherent model uncertainties (Cardwell and Ellis, 1996). For example, design decisions based solely on GHSI defined velocity and depth criteria will neglect potentially important characteristics such as proximity to refugia (Quinn and Kwak, 2000). Conversely, employing a conceptual design (e.g. "build a riffle") without testing for desired hydraulic and flow conditions could easily lead to construction

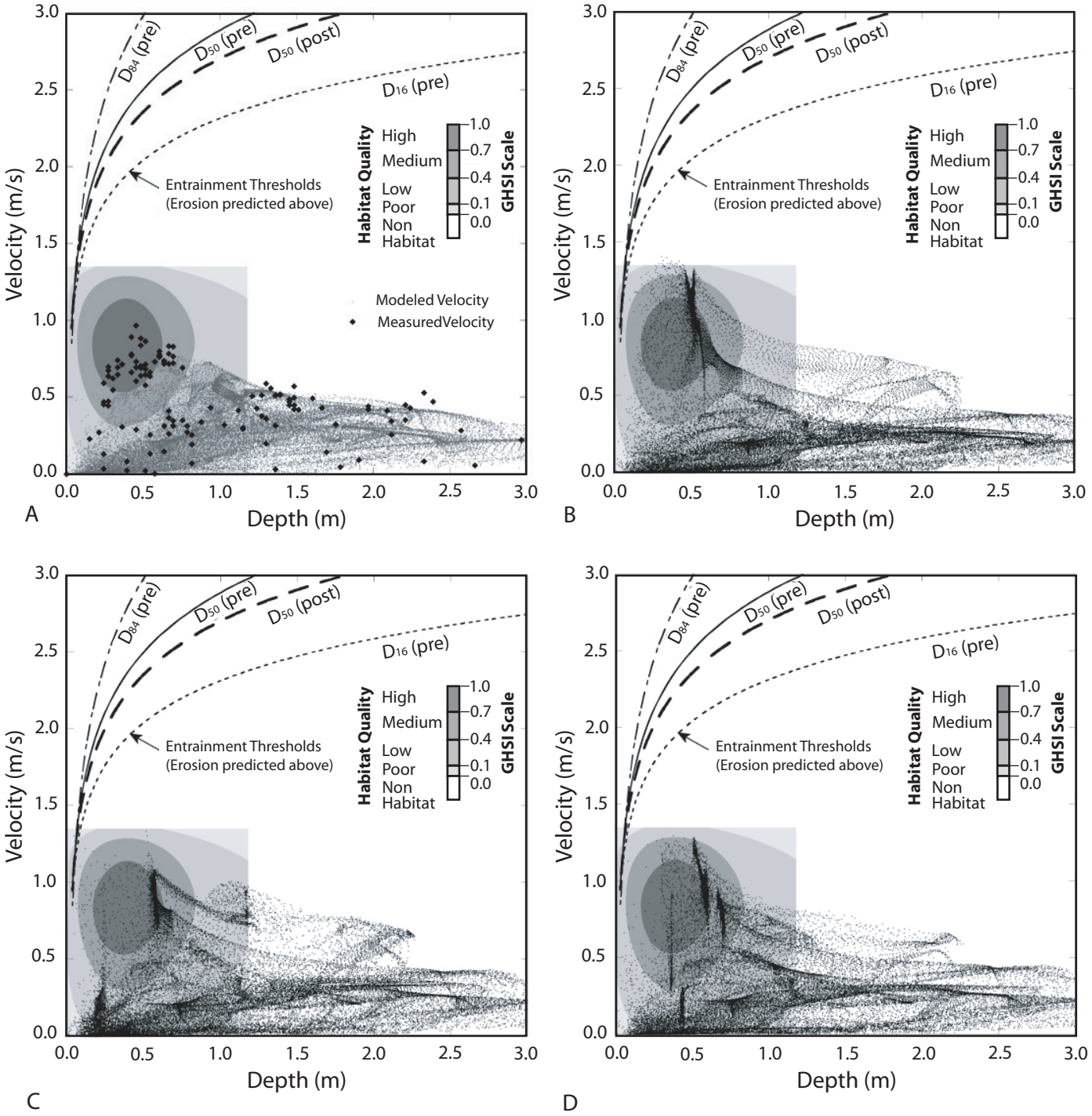

Figure 8 Design phase velocity vs. depth plots at 11.46 cumecs. (A) Pre project. (B) Design scenario 5 (flat riffle). (C) Design scenario 6 (constricted pools). (D) Design scenario 12 (complex channel geometry).

of a feature which does not provide the crucial characteristics. However, conceptual design development in conjunction with modelling can be viewed as a reasonable decision support system to make the restoration design process more transparent (Clark and Richards, 2002).

In this project, design hypotheses were tested systematically with off-the-shelf numerical models before project construction (Tables 2 and 3). We were forced to accept a higher degree of uncertainty in implementing a design scenario (design 12) based partially on untested design hypotheses. Proceeding on the best available information is a central tenant of adaptive management (Clark, 2002) and the precautionary principle (deFur and Kaszuba, 2002). Ideally, design scenarios would have been modelled over a range of flows to test stage dependence of conceptual design hypotheses. For example, habitat suitability should be analyzed over a range of spawning flows, whereas sediment entrainment should be analyzed at spawning flows and geomorphically relevant high flows. Of the three design hypotheses we were unable to test, two were due to inadequate model boundary conditions for high flows (hypotheses 2A and 2B). The

lack of stage data from higher flows was due to a flat-lined low flow regime over a relatively dry study period, absence of a DEM for the floodplain, and inadequacy of artificially constructed rating curves (Wheaton, 2003). Partial data has subsequently been collected during a prescribed pulse flow and was used in design of a project built in 2003. A vegetated floodplain DEM is under production now.

Although ecological function inferences and hypotheses reported were largely limited to spawning and incubation life stages of a single species, it is easy to include conceptual ideas that benefit other life stages (e.g. rearing, out-migration), other organisms (e.g. steelhead and macroinvertebrates), food webs or energy budgets. Additional models beyond those used in this study, including those that model water quality, 1D sediment transport, fine sediment deposition, alevin survival, hyporheic exchange, habitat suitability for other fish species, lifestages and/or macroinvertebrates are available and could be incorporated into other applications of the SHIRA framework. Final designs can be chosen with the help of these analyses, but in balance with conceptual ideas that are not necessarily easy to analyze quantitatively.

5.3 Does hypothesis testing insure success?

As in any hypothesis testing, supportive results do not prove a project (even if constructed exactly as designed) will respond as hypothesized. In the earth sciences especially, Schumm (1991) suggests that convergence (when different processes produce similar effects) and divergence (when similar processes produce different effects) complicate drawing simple conclusions from hypothesis testing. For example, we relied on two hypotheses from the recent literature (hypotheses 2A and 2B) for the maintenance of pool riffle sequences. Neither has been proven and both are based on limited empirical evidence from a handful of sites (Booker *et al.*, 2001; Thompson *et al.*, 1999). However, a major advantage of using and testing transparent design hypotheses emerges during the post project appraisal and long term monitoring phases. Consider a design hypothesis that was accepted based on design testing and a project then constructed based on that evidence. Perhaps long term monitoring data then suggests that the scientific hypothesis was incomplete or false for a particular application. Such a scenario provides the perfect setting to use SHIRA's 'Scientific Exploration Mode' and the results then feed back through adaptive management (Walters, 1997). The conceptual models that drive the development of the design hypothesis and/or the numerical models used to test it may then be revised based on a more complete understanding of their limitations.

Alternatively, unforeseen problems not considered during design may arise. An example currently under consideration on the LMR has emerged from monitoring habitat utilization through redd surveys and substrate composition through time (Merz *et al.*, in press). In brief, habitat utilization and substrate quality are quite high in the first few years following rehabilitation. Yet under a homogenized low-flow regime, substrate quality drops due to establishment of aquatic vegetation and colmation of fines normally mobilized by higher flows (Brunke, 1999). Preliminarily, the corresponding ecologic response appears to be at least a temporary drop in habitat utilization. For this example, the conceptual model of spawning habitat (Figure 3 in Wheaton *et al.*, 2004) can be used to explain the observed declines in substrate quality and habitat utilization. One working hypothesis emerging from these observations could be that regular substrate mobilization is necessary to maintain habitat quality so long as it does not coincide with the incubation period (Montgomery *et al.*, 1999; Montgomery *et al.*, 1996). Although, sediment mobility models could be used to test what flows entrainment is likely to occur, better testing is likely to come out of experimental pulse flows and continued long term monitoring of substrate conditions and habitat utilization.

6 Conclusion

This paper presents partial results of hypothesis development and testing as used in the design phases of a spawning habitat bed enhancement project on the Lower Mokelumne River implemented using SHIRA. We developed multiple conceptual designs based on specific design hypotheses and used modelling analyses to test hypotheses where possible. Even though hypothesis testing does not insure project success, it provides mechanistic understanding and predictive capability to restoration practitioners; as well as experimental opportunities to test how underlying scientific concepts fare at a local site. This arguably constrains uncertainties in project outcomes and fosters more realistic expectations.

Acknowledgements

Financial support for this work was provided by East Bay Municipal Utility District (Research Agreements OOK6046 & 99K3086), the University of California, the US Fish and Wildlife Service (contracting entity for CALFED Bay-Delta Ecosystem Restoration Program: Cooperative Agreement DCN# 113322G003) and a National Fish and Wildlife Federation grant through CALFED (Contract #99-NO6). We gratefully acknowledge Joe Cech, Gonzalo Castillo, Jeff Mount, Carlos Puente, James Smith, Brett Valle, Chien Wang, Kelly Wheaton, Steve Winter for input towards the research and manuscript. We thank Adrea Wheaton for her expertise and help with several figures. The authors thank Ellen Mantalica and Diana Cummings of the Center for Integrated Watershed Science and Management in the John Muir Institute for the Environment, Davis, California for providing grant management support. Waren Jung, Russ Taylor, Richard Walker and other East Bay Municipal Utility District staff were instrumental in assisting with field work and data collection as well as several University of California at Davis undergraduates: Evan Buckland, Eric Buer, Adam Fishback, Andrew Gilbert and Pascal Nepesca. We wish to thank Andrew Miller and three anonymous reviewers for their critical feedback, which helped dramatically clarify earlier drafts of the manuscript.

References

1. ANDERSON, J.L. (1998). "Chapter 6: Errors of Inference", in: V. Sit and B. Taylor (eds.), Statistical Methods for Adaptive Management Studies, B.C. Ministry of Forests, Victoria, B.C., pp. 69–87.
2. ANNABLE, W.K. (1999). "On the Design of Natural Channels: Decisions, Direction and Design", *The Second International Conference on Natural Channel Systems*, Niagara Falls, Ontario, Canada, pp. 29.
3. BEVERIDGE, W.I.B. (1980). *The Seeds of Discovery*, Norton, New York.
4. BOOKER, D.J., SEAR, D.A. and PAYNE, A.J. (2001). "Modeling three-dimensional flow structures and patterns of boundary shear stress in a natural pool-riffle sequence", *Earth Surface Processes and Landforms*, 26(5), 553–576.
5. BROOKES, A. and SEAR, D. (1996). "3. Geomorphological Principles for Restoring Channels", in: A. Brookes and F.D. Shields (eds.), River Channel Restoration: Guiding Principles for Sustainable Projects, John Wiley & Sons, Chichester, UK, pp. 75–101.
6. BRUNKE, M. (1999). "Colmation and Depth Filtration within Streambeds: Retention of Particles in Hyporheic Interstices", *International Rev. Hydrobiology*, 84(2), 9–117.
7. CAO, Z. and CARLING, P.A. (2002). "Mathematical modelling of alluvial rivers: reality and myth. Part I: General review", *Proceedings of the Institution of Civil Engineers-Water and Maritime Engineering*, 154(3), 207–219.
8. CARDWELL, H. and ELLIS, H. (1996). "Model uncertainty and model aggregation in environmental management", *Applied Mathematical Modelling*, 20(2), 121–134.
9. CARLING, P.A. (1991). "An Appraisal of the Velocity-Reversal Hypothesis for Stable Pool Riffle Sequences in the River Severn, England", *Earth Surface Processes and Landforms*, 16(1), 19–31.
10. CDFG (1991). Lower Mokelumne River Fisheries Management Plan. California Department of Fish and Game: The Resources Agency, Sacramento, CA, pp.
11. CHAMBERLIN, T.C. (1890). "The method of multiple working hypothesis", *Science*, Reprinted 1965: 148, 754–759.
12. CHAPMAN, D.W. (1988). "Critical Review of Variables Used to Define Effects of Fines in Redds of Large Salmonids", *Transactions of the American Fisheries Society*, 117, 1–21.
13. CLARK, M.J. (2002). "Dealing with uncertainty: adaptive approaches to sustainable river management", *Aquatic Conservation-Marine and Freshwater Ecosystems*, 12, 347–363.
14. CLARK, M.J. and RICHARDS, K.J. (2002). "Supporting complex decisions for sustainable river management in England and Wales", *Aquatic Conservation-Marine and Freshwater Ecosystems*, 12, 471–483.
15. DEFUR, P.L. and KASZUBA, M. (2002). "Implementing the precautionary principle", *The Science of The Total Environment*, 288(1–2), 155–165.
16. DIETRICH, W.E. and WHITING, P. (1989). "Boundary shear stress and sediment transport in river meanders of sand and gravel", in: G. Parker (ed.), River Meandering, American Geophysical Union Water Resources Monograph 12, Washington D.C., pp. 1–50.
17. DOWNS, P.W. and KONDOLF, G.M. (2002). "Post-project appraisals in adaptive management of river channel restoration", *Environmental Management*, 29(4), 477–496.
18. EDWARDS, B.R. (2001). Vegetation of the Lower Mokelumne River: 1927, Advanced Spatial Analysis Facility, Humboldt State University, Arcata, CA.
19. FERC (1993). Final Environmental Impact Statement, proposed modifications to the Lower Mokelumne River Project, California, FERC Project No. 2916-004. Federal Energy Regulatory Commission, Washington D.C.
20. FERC (1998). "Order Approving Settlement Agreement and Amending License. East Bay Municipal Utility District Lower Mokelumne River Hydroelectric Project No. 2916." Federal Energy Regulatory Commission.
21. FROEHLICH, D.C. (1989). HW031.D – Finite Element Surface-Water Modeling System: Two-Dimensional Flow in a Horizontal Plane-Users Manual: Federal Highway Administration. *Report FHWA-RD-88-177*, Federal Highway Administration, Washington D.C., pp. 285.
22. GARDE, R.J. and RAJU, K.G.R. (1985). Mechanics of sediment transportation and alluvial stream problems, Wiley Eastern Limited, New Delhi, India, pp.
23. GEIST, D.R. (2000). "Hyporheic discharge of river water into fall chinook salmon (*Oncorhynchus tshawytscha)* spawning areas in the Hanford Reach, Columbia River", *Can. J. Fish. Aquat. Sci*., 57, 1647–1656.
24. KONDOLF, G.M. (2000a). "Assessing salmonid spawning gravel quality", *Transactions of the American Fisheries Society*, 129(1), 262–281.
25. KONDOLF, G.M. (2000b). "Some suggested guidelines for geomorphic aspects of anadromous salmonid habitat restoration proposals", *Restoration Ecology*, 8(1), 48–56.
26. KONDOLF, G.M., VICK, J.C. and RAMIREZ, T.M. (1996). "Salmon spawning habitat rehabilitation on the Merced River, California: An evaluation of project planning and performance", *Transactions of the American Fisheries Society*, 125(6), 899–912.
27. KONDOLF, G.M. and WOLMAN, M.G. (1993). "The Sizes of Salmonid Spawning Gravels", *Water Resources Research*, 29(7), 2275–2285.
28. LECLERC, M., BOUDREAULT, A., BECHARA, J.A. and CORFA, G. (1995). "Two-dimensional hydrodynamic modeling: a neglected tool in the instream flow incremental methodology", *Transactions of the American Fisheries Society*, 124(5), 645–662.
29. MADDOCK, I. (1999). "The importance of physical habitat assessment for evaluating river health", *Freshwater Biology*, 41, 373–391.
30. MERZ, J.E. (2001a). "Association of fall-run chinook salmon redds with woody debris in the lower Mokelumne River, California", *California Fish and Game*, 87(2), 51–60.

31. MERZ, J.E. (2001b). "Diet of juvenile fall-run chinook salmon in the lower Mokelumne River, California", *California Fish and Game*, 87(3), 102–114.
32. MERZ, J.E. (2002). "Comparison of diets of prickly sculpin and juvenile fall-run chinook salmon in the lower Mokelumne River, California", *Southwestern Naturalist*, 47(2), 195–204.
33. MERZ, J.E. and SETKA, J.D. (in prep). "Evaluation of a chinook salmon spawning habitat enhancement project in a California Central Valley Stream".
34. MERZ, J.E. and SETKA, J.D. (in press). "Evaluation of a spawning habitat enhancement site for chinook salmon in a regulated California river." *North American Journal of Fisheries Management*.
35. MERZ, J.E., SETKA, J.D., PASTERNACK, G.B. and WHEATON, J.M. (in press). "Predicting fry production benefits from salmonid spawning habitat rehabilitation in a regulated California river".
36. MIYAMOTO, J.J. (2001). Mokelumne River Spawning Habitat Improvement Project. East Bay Municipal Utility District, Orinda, CA, pp. 11.
37. MONTGOMERY, D.R., BEAMER, E.M., PESS, G.R. and QUINN, T.P. (1999). "Channel type and salmonid spawning distribution and abundance", *Can. J. Fish. Aquat. Sci.*, 56, 377–387.
38. MONTGOMERY, D.R. and BOLTON, S.M. (2003). "3. Hydrogemorphic Variability and River Restoration", in: R.C. Wissmar, P.A. Bisson, and M. Duke (eds.), Strategies for Restoring River Ecosystems: Sources of Variability and Uncertainty in Natural and Managed Systems, American Fisheries Society, Bethesda, Maryland, pp. 39–80.
39. MONTGOMERY, D.R., BUFFINGTON, J.M., PETERSON, N.P., SCHUETT-HAMES, D. and QUINN, T.P. (1996). "Stream-bed scour, egg burial depths, and the influence of salmonid spawning on bed surface mobility and embryo survival", *Canadian Journal of Fisheries and Aquatic Sciences*, 53(5), 1061–1070.
40. MOYLE, P.B. and RANDALL, P.J. (1998). "Evaluating the biotic integrity of watersheds in the Sierra Nevada, California", *Conservation Biology*, 12, 1318–1326.
41. NEHLSEN, W., WILLIAMS, J.E. and LICHATOWICH, J.A. (1991). "Pacific salmon at the crossroads: stocks at risk from California, Oregon, Idaho, and Washington." *Fisheries*, 16, 4–21.
42. PASTERNACK, G.B., WANG, C.L. and MERZ, J.E. (in press). "Application of a 2D Hydrodynamic Model to Design of Reach-Scale Spawning Gravel Replenishment on the Mokelumne River, California", *River Research and Applications*.
43. POPPER, K.R. (1968). The Logic of Scientific Discovery, Harper and Row, New York, pp. 480.
44. QUINN, J.W. and KWAK, T.J. (2000). "Use of Rehabilitated Habitat by Brown Trout and Rainbow Trout in an Ozark Tailwater River", *North American Journal of Fisheries Management*, 20, 737–751.
45. RITTER, D.F., KOCHEL, R.C. and MILLER, J.R. (1995). Process geomorphology, Wm. C. Brown, Dubuque, IA, pp.
46. SCHUMM, S.A. (1991). To Interpret the Earth: Ten ways to be wrong, Cambridge University Press, Cambridge, UK, pp. 132.
47. STANFORD, J.A., WARD, J.V., LISS, W.J., FRISSELL, C.A., WILLIAMS, R.N., LICHATOWICH, J.A. and COUTANT, C.C. (1996). "A General Protocol for Restoration of Regulated Rivers", *Regulated Rivers-Research & Management*, 12, 391–413.
48. THOMPSON, D.M., WOHL, E.E. and JARRETT, R.D. (1999). "Velocity Reversal and sediment sorting in pools and riffles controlled by channel constrictions", *Geomorphology*, 27, 229–241.
49. TRUSH, W.J., MCBAIN, S.M. and LEOPOLD, L.B. (2000). "Attributes of an alluvial river and their relation to water policy and management", *Proceedings of the National Academy of Sciences of the United States of America*, 97(22), 11858–11863.
50. VRONSKIY, B.B. (1972). "Reproductive biology of the Kamchatka River chinook salmon", *Journal of Ichthyology*, 12, 259–273.
51. WALTERS, C.J. (1997). "Challenges in adaptive management of riparian and coastal ecosystems", *Conservation Ecology [online]*, 1(2), 1. Available from the Internet. URL: http://www.consecol.org/vol1/iss2/art1.
52. WHEATON, J.M. (2003). *Spawning Habitat Rehabilitation*, M.S. Thesis, University of California at Davis, Davis, CA, pp. 223.
53. WHEATON, J.M., PASTERNACK, G.B. and MERZ, J.E. (2004). "Spawning Habitat Rehabilitation – I. Conceptual Approach and Methods", *International Journal of River Basin Management*, 2(1), ?-?
54. WILCOCK, P. (1997). "Friction Between River Science and Practice: The Case of River Restoration", *EOS, Transactions of the American Geophysical Union*, 78(40).
55. YOSHIYAMA, R.M., FISHER, F.W. and MOYLE, P.B. (1998). "Historical abundance and decline of chinook salmon in the Central Valley region of California", *North American Journal of Fisheries Management*, 18, 487–521.

Section 2
Is 2D Modeling Accurate?

Introduction

The most important tool used in SHIRA is 2D hydrodynamic modeling. This tool is thought to be capable of quantitatively testing many important hydrogeomorphic and ecological predictions of a river rehabilitation design. Thus a central goal of this demonstration project was to thoroughly evaluate the accuracy of 2D models for use in river restoration.

A common question about SHIRA is whether 2D modeling is required for SHIRA. We believe that the biggest problem with many river projects today is that their designs are inadequately evaluated prior to construction. The fact that so many experts have concluded that so many river rehabilitation projects are "failures" (i.e. projects didn't meet their stated goals) leads to the conclusion that subjective evaluations of project design solely reliant on the professional judgment of the designer are extremely uncertain and prone to catastrophic error. Empirical and analytical tools for evaluating designs have some use in evaluating some geomorphic design hypotheses, but they often have orders of magnitude uncertainty due to differences in local conditions from the conditions used to create the empirical functions. Also, they are incapable of evaluating spatially complex projects with design features that cannot be represented by cross-sections. 1D hydrodynamic models such as HEC-RAS and MIKE11 provide the capability of considering unsteady conditions and to some extent non-uniform conditions, but they cannot account for transitional dynamics where no cross-sections are measured nor secondary flow processes. 3D models such as UNTRIM and SSIIM go the farthest by including vertical fluid fluxes, and thus require extensive data collection for validation. Few ecological and geomorphic processes have been quantitatively linked to 3D flow dynamics yet, limiting the interpretation of 3D model output. Thus, 2D models are uniquely positioned to provide the right balance between sufficient resolution and available linkages to valued river functions (e.g. habitat conditions, sediment transport regimes, an geomorphic functioning).

Like any model, 2D models are not perfect representations of nature. Thus, the question is whether they are accurate enough to predict the key conditions and processes associated with evaluating the design hypothesis included in a design alternative? To be accurate enough, the models must be able to accurately predict water depth and velocity, as a first step. Then they must be coupled with empirical or analytical tools to extend their fundamental results to the realm of a particular function, such as physical habitat quality. 2D models need to be evaluated for the accuracy at each step of the way, before they will be accepted more broadly.

In the subsections that follow, 2D models are evaluated for their accuracy and utility with regard to different functions. In the first subsection, the question is answered as to whether the use of 2D models would in fact yield improved physical habitat conditions for salmon spawning relative to an ad hoc project built with no forethought design at all. There is also some evaluation of the accuracy of 2D models in predicting water depth and velocity. In the second subsection, the question is asked as to how accurately 2D models predict bed shear stress relative to field methods for estimating it. Sources of error in bed shear stress prediction are thoroughly

evaluated. In the third subsection, the results of 1D, 2D, and 3D models of a riffle-pool sequence are compared to evaluate whether 2D models can accurately capture the central hydrogeomorphic mechanism responsible for riffle-pool self-sustainability. Here the cross-comparison of all the different types of models provides the clearest picture of the pros and cons of each predictive strategy. Although this inter-model comparison was not performed on the Mokelumne River, it is part of this project, because the project involved using SHIRA, and one component of SHIRA is the "Scientific Exploration Mode" that involves tracking down sources of uncertainty in SHIRA tools. Dry Creek near Winters, CA turned out to be the place where extensive data was available to do the model inter-comparison. Because the models involve the laws of physics and both Dry Creek and Mokelumne River follow the same laws of physics, the results regarding hydrodynamic processes and geomorphic functioning obtained from the Dry Creek study are directly applicable to the Mokelumne River SHIRA demonstration project.

An assessment of the ability of 2D models to accurately predict the spatial pattern of fish utilization is a critical need that is answered in this report, but not in this section. Instead, that question is analyzed in section 3 where it is also possible to evaluate the ecological outcome of the implemented demonstration projects on the lower Mokelumne River.

Once the benefits and uncertainties associated with 2D modeling are understood, then river managers and restoration practitioners will seek education and training on their usage. The 2D model used in this project was FESWMS 3, which is a public domain program developed by the Federal Highway Administration. To simplify and enhance the usage of FESWMS, a commercial package called Surfacewater Modeling System (SMS) was developed and sold by Environmental Modeling Systems, Incorporated (http://www.ems-i.com). The current version is SMS 9.2. This program not only contains the latest version of FESWMS, but it also contains several other 2D modeling codes, including RMA2 and HIVEL2D. We evaluated all models early on, but ultimately selected FESWMS because it can handle supercritical flow, which is a common phenomenon observed at gravel-placement project sites. There is no reason why other 2D models within SMS or those beyond SMS couldn't be used in place of FESWMS as long as the user understands how the model works and how to address their model's sensitive uncertainties.

RIVER RESEARCH AND APPLICATIONS

River Res. Applic. **20**: 205–225 (2004)

Published online 12 February 2004 in Wiley InterScience
(www.interscience.wiley.com). DOI: 10.1002/rra.748

APPLICATION OF A 2D HYDRODYNAMIC MODEL TO DESIGN OF REACH-SCALE SPAWNING GRAVEL REPLENISHMENT ON THE MOKELUMNE RIVER, CALIFORNIA

GREGORY B. PASTERNACK,[a]* C. LAU WANG[a] and JOSEPH E. MERZ[b]

[a] *Department of Land, Air, and Water Resources, University of California, 1 Shields Avenue, Davis, CA 95616-8626, USA*
[b] *East Bay Municipal Utility District, 1 Winemasters Way, Lodi, CA 95240, USA*

ABSTRACT

In-stream chinook salmon (*Oncorhynchus tschawytscha*) spawning habitat in California's Central Valley has been degraded by minimal gravel recruitment due to river impoundment and historic gravel extraction. In a recent project marking a new direction for spawning habitat rehabilitation, 2450 m^3 of gravel and several boulders were used to craft bars and chutes. To improve the design of future projects, a test was carried out in which a commercial modelling package was used to design and evaluate alternative gravel configurations in relation to the actual pre- and post-project configurations. Tested scenarios included alternate bars, central braid, a combination of alternate bars and a braid, and a flat riffle with uniformly spaced boulders. All runs were compared for their spawning habitat value and for susceptibility to erosion. The flat riffle scenario produced the most total, high, and medium quality habitat, but would yield little habitat under flows deviating from the design discharge. Bar and braid scenarios were highly gravel efficient, with nearly 1 m^2 of habitat per 1 m^3 of gravel added, and yielded large contiguous high quality habitat patches that were superior to the actual design. At near bankfull flow, negligible sediment entrainment was predicted for any scenario. Copyright © 2004 John Wiley & Sons, Ltd.

KEY WORDS: river restoration; 2D modelling; salmon; gravel; numerical modelling; salmon spawning; physical habitat

INTRODUCTION

In California salmonid spawning habitat has been degraded or depleted by a plethora of instream human activities and upland land uses (Nehlsen *et al.*, 1991; Moyle and Randall, 1998; Yoshiyama *et al.*, 1998). Dam construction and operation (Kondolf, 1997; Brandt, 2000), gravel extraction (Gilvear *et al*., 1995; Kondolf *et al.*, 1996), historic gold mining (Harvey and Lisle, 1998), channelization (Nagasaka and Nakamura, 1999), water diversion (Petts, 1996; Douglas and Taylor, 1998), deforestation (Platts and Megahan, 1975; Marks and Rutt, 1997), and intensive agriculture (Soulsby *et al.*, 2000) are specific activities that disrupt healthy stream ecology (Allan and Flecker, 1993; Poff *et al.*, 1997). While California's commercial landings of chinook salmon (*Oncorhynchus tschawytscha*) show wide annual variability, a consistent downward trend in decadal harvest during 1950–2000 from 33 621 to 18 980 tonnes indicates a serious threat to species survival (National Marine Fisheries Service, 2001).

For Sierra Nevada streams, dams prevent salmon from reaching historic spawning sites (Moyle and Randall, 1998). Spawning areas below the lowest impassable dams are now critical to survival of seasonal runs. As a result, maintenance flows are provided during different spawning seasons (Castleberry *et al.*, 1996; Moyle *et al.*, 1998). However, even with a minimal flow regime in place, spawning areas below dams suffer gravel losses in winter floods, have little gravel recruitment, and experience channel changes. Thus, dams have altered flow regimes and created out-of-balance sediment budgets that hurt chinook salmon populations.

* Correspondence to: Gregory B. Pasternack, Department of Land, Air, and Water Resources, University of California, 1 Shields Avenue, Davis, CA 95616-8626, USA. E-mail: gpast@ucdavis.edu

Received 11 April 2002
Revised 26 November 2002
Accepted 9 December 2002

Instream mining has exacerbated the problem by severely depleting available gravel. Mining alters channel geometry and elevation, and involves extensive clearing, flow diversion, sediment stockpiling, and deep pit excavation (Sandecki, 1989). Tens to hundreds of millions of tons of gravel are being removed from California's rivers creating a serious gravel deficit.

Gravel replenishment projects had been undertaken to mitigate severely degraded spawning areas below Sierra Nevada dams in more than 13 rivers in California as of 1992 (Kondolf and Matthews, 1993). The largest of these efforts is on the Upper Sacramento River where gravel replenishment has been conducted from 1979 to 2002. Gravel replenishment has been used to raise beds to pre-regulation elevations, prevent channel incision, and in rare cases to create features such as islands and pool–riffle sequences.

Even though these projects may provide some short-term habitat, the amount of gravel added is a small fraction of the bedload deficit. Gravels placed in the main channel have washed downstream during high flows, requiring continued addition of more imported gravel (California Department of Water Resources, 1995). Also, few objective criteria exist for designing and placing in-channel features. Project failure often results from a lack of understanding of geomorphic processes. In many cases designs have been based on 'folklore' or aesthetic criteria rather than application of hydrology and hydrodynamics (National Research Council, 1992).

Post-construction monitoring of gravel replenishment in California has been limited. One exception was a study of the Merced, Tuolumne, and Stanislaus rivers (Kondolf *et al.*, 1996). Ten sites were excavated and back-filled with smaller gravel to create spawning habitat for chinook salmon from 1990 to 1994, but placed gravel sizes were mobile at high flows recurring at 1.5–4 year intervals. Channel surveys showed that augmented gravels washed out.

Based on limited assessment and uncertain success of gravel projects to date, it is apparent that current strategies are not yielding optimal usable habitat while minimizing gravel losses by flow-induced sediment entrainment. The goal of this study was to test the applicability of a commercial modelling package with a two-dimensional (2D) hydrodynamic model for use in designing fine-scale gravel placement to rehabilitate and augment salmon spawning habitat as well as to reintroduce fluvial complexity. 2D hydrodynamic models quantify depth, velocity, and shear stress at ecologically relevant scales, such as a pool–riffle reach or in the vicinity of a single boulder. When model output is coupled with quantitative estimates of preferred physical habitat conditions, the result is a powerful tool for characterizing instream habitat (Leclerc *et al.*, 1995). If this tool could be used prescriptively, then many potential alternative scenarios could be assessed for habitat quality and geomorphic sustainability prior to project construction.

The test site for this study was a gravel project by the East Bay Municipal Utility District (EBMUD) on the Mokelumne River downstream of Camanche Dam in the Central Valley, California (Figure 1). Commercial software was used to build and compare alternative scenarios with actual pre- and post-project conditions. Habitat suitability indices assessed low-flow chinook salmon spawning habitat, while a sediment mobility index predicted entrainment at near-bankfull discharge. Specific objectives were to: (1) build and analyse 2D models of an alluvial reach before and after gravel replenishment; (2) create four alternative design scenarios—alternate bars, channel braid, alternate bars + braid, and flat with boulders; and (3) compare the pre- and post-project hydrodynamic, habitat, and geomorphic conditions with those of the alternative scenarios. This study provides lessons for future gravel-bar design worldwide.

ECOLOGICAL APPLICATION OF HYDRODYNAMIC MODELS

2D models using depth-averaged Saint-Venant equations are increasingly used for aquatic biology and geomorphology. Their primary advantage over 1D models (e.g. HEC-2 and MIKE-11) for these applications is that they yield fine-scale distributions of velocity vectors (including lateral components) as opposed to ecologically and geomorphically insignificant cross-sectional average downstream speeds. Nodal velocity vectors can be used to estimate local habitat and shear stress conditions. It is very well known that the trade-off for this improvement is the expense of pre-project fine-scale field mapping because the quality of model results is strongly dependent upon the accuracy and spatial resolution of the underlying topographic and parameter measurements as well as the resultant digital elevation model (Leclerc *et al.*, 1995; Ghanem *et al.*, 1996). Most 2D models assume a hydrostatic pressure distribution and are thus incapable of handling substantial vertical accelerations or bed gradients >0.10 (Miller and Cluer, 1998). Lane *et al.* (1999) evaluated the extent 3D models improved predictive ability over 2D

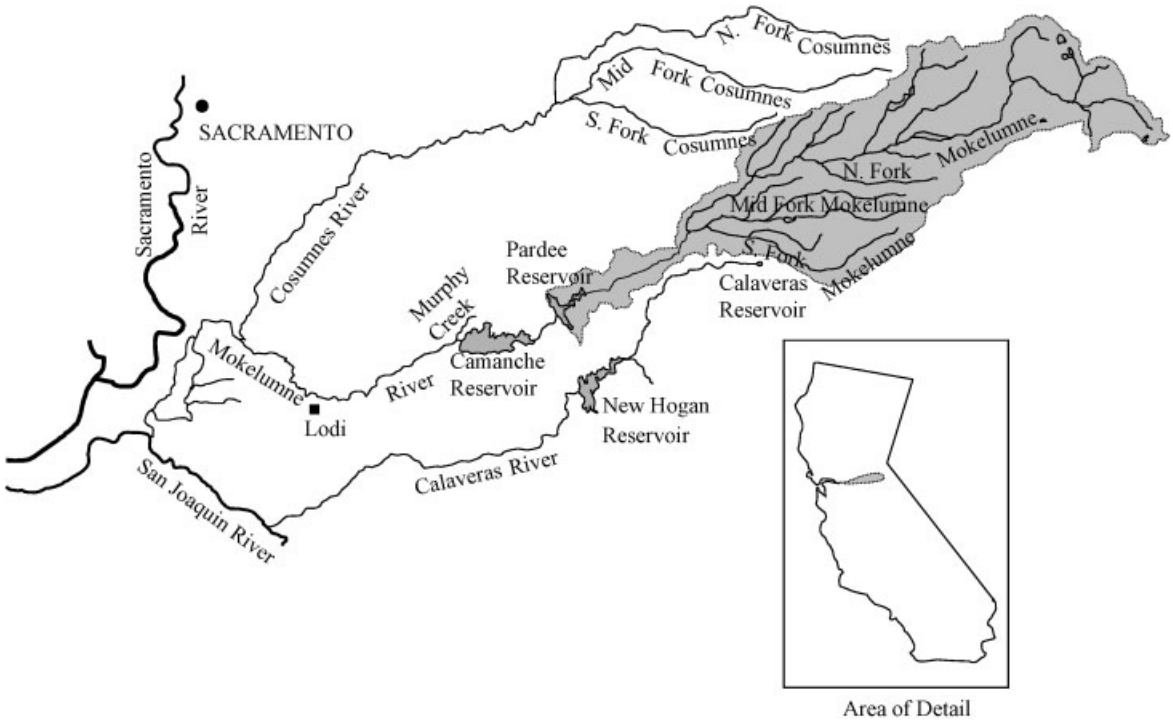

Figure 1. Map of the Mokelumne River basin showing locations of Camanche Reservoir and Murphy Creek

ones. They reported an extreme non-linear sensitivity in 3D models to minor variations in bed geometry and channel network, thus yielding dramatically different flow predictions and bed shear stresses. Given the limits of technology to get field data to calibrate and validate 3D models at the necessary sub-reach scale, 2D models are now the most promising tools for gravel replenishment.

Crowder and Diplas (2000) showed that 2D models can simulate sub-reach-scale stream features with ecological relevance. Small obstructions create velocity gradients, velocity shelters, transverse flows, etc. that were not evident when the obstructions were omitted from their model. Geomorphic applications of 2D models include Miller (1994, 1995), and Cluer (1997).

2D models of habitat require parameters associated with preferred conditions (Vadas, 2000). The Instream Flow Incremental Method is the most widely used approach for combining biology and life habit data of aquatic species with models to predict how water management impacts habitat (Bovee, 1982). Habitat suitability functions defining stream utility have been developed for different life stages of many species. While this approach simplifies complex spatio-temporal interactions, studies have found a significant correlation between predictions and actual community diversity (Gore and Nestler, 1998; Gallagher and Gard, 1999).

STUDY SITE

Mokelumne River basin

The Mokelumne River is a tributary of the San Joaquin River in central California, draining part of Sierra Nevada's western slope (Figure 1). The river drains *c.* 1700 km^2 and heads at 3050 m. The basin grades from forested mountains in the east to grassy foothills and agricultural floodplains in the west. Precipitation ranges from *c.* 1200 mm in the headwaters to *c.* 510 mm in the lowlands and falls during October to April. Channel widths in the lower river range from 19 to 43 m with a mean of 30 m. The river is connected to its floodplain in the spawning reaches, but is constrained by levees downstream. Adjacent lands are heavily used for recreation and grazing. A

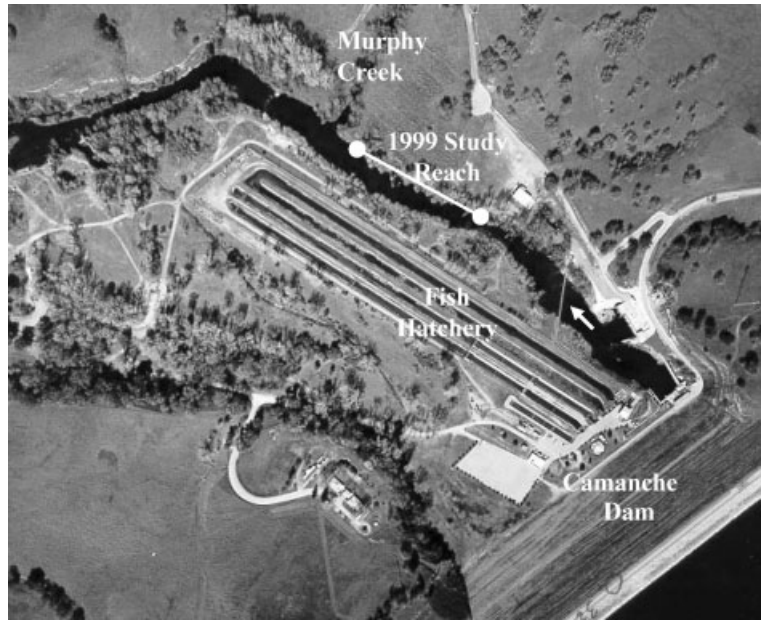

Figure 2. Aerial photo of Mokelumne River below Camanche Dam showing the location of the project reach, the adjacent fish hatchery, and the inlet of Murphy Creek

small tributary, Murphy Creek, enters the river *c.* 1 km downstream of the dam (Figure 1). Detailed hydrology, geology, and ecology for the basin were presented in Wang and Pasternack (2000).

Flow regime

The Mokelumne River has 16 major water projects with four large reservoirs. The two most downstream reservoirs non-passable to anadromous fish are Pardee (completed in 1929) and Camanche (completed in 1964). Camanche aids flood control and river regulation. A fish hatchery built below Camanche to mitigate fishery losses, forced a realignment and excavation of the river (Figure 2). The subsequent altered flow regime stabilized active sediment and enabled in-channel vegetation survival. Changes are documented in historical sources, notably aerial photos. The active channel is now half its former width and overdeepened. The lower Mokelumne begins at Camanche and drains to the Sacramento–San Joaquin Delta.

Hydrologic analysis of pre-dam (1904–1963) and post-dam (1964–1999) annual peak flows below Camanche Dam (USGS ID 11323500) shows the dam's impact. Prior to it, annual peaks exceeded 200 cm for 21 of 57 years. Since 1964, annual peaks have never exceeded 200 cm (Figure 3). Pre-dam mean monthly flow had a typical snowmelt hydrograph (Figure 4a), with highest flow during May and June, after the peak in precipitation (Figure 4b). The post-dam hydrograph shows a significant reduction in the late spring snowmelt runoff below the dam. A flood frequency analysis using annual extreme pre- and post-dam data shows a dramatic reduction in flow for all recurrence intervals after the dam was built (Figure 5). Estimated using Log Pearson III distributions, Q_2, Q_5, Q_{10}, and Q_{100} decreased by 67, 59, 73, and 75%, respectively (Wang and Pasternack, 2000). The statistical bankfull discharge ($Q_{1.5}$) prior to Camanche was 120 cm, which is now released only about every five years. Flow out of Camanche has a step hydrograph, with lows near the minimum (4.25 cm) prescribed in the Joint Settlement Agreement for relicensing (Federal Energy Regulatory Commission (FERC), 1998).

Gravel rehabilitation projects

Significant fishery declines during the 1976–1977 and 1987–1992 droughts led to a focus on improving fish habitat. EBMUD and collaborators have replenished gravels below Camanche since 1990 (Table I). FERC (1993) encouraged it as a non-flow alternative for improving habitat, citing lack of gravel recruitment and clogging

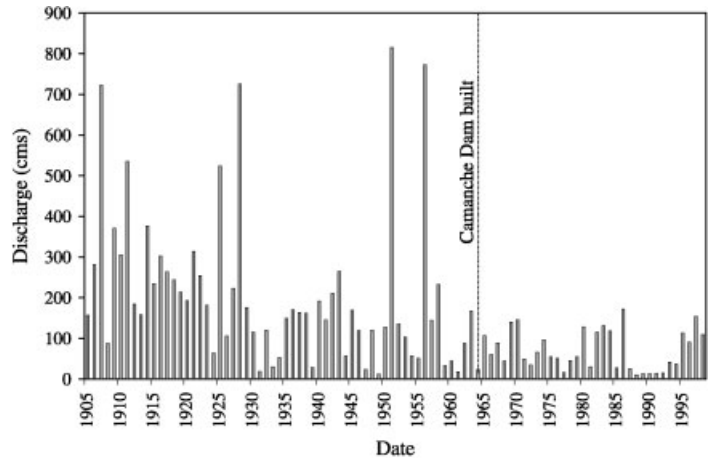

Figure 3. Annual peak flows 1904–1999 from the gauge below Camanche Dam showing significant decrease in peaks with the dam's management regime

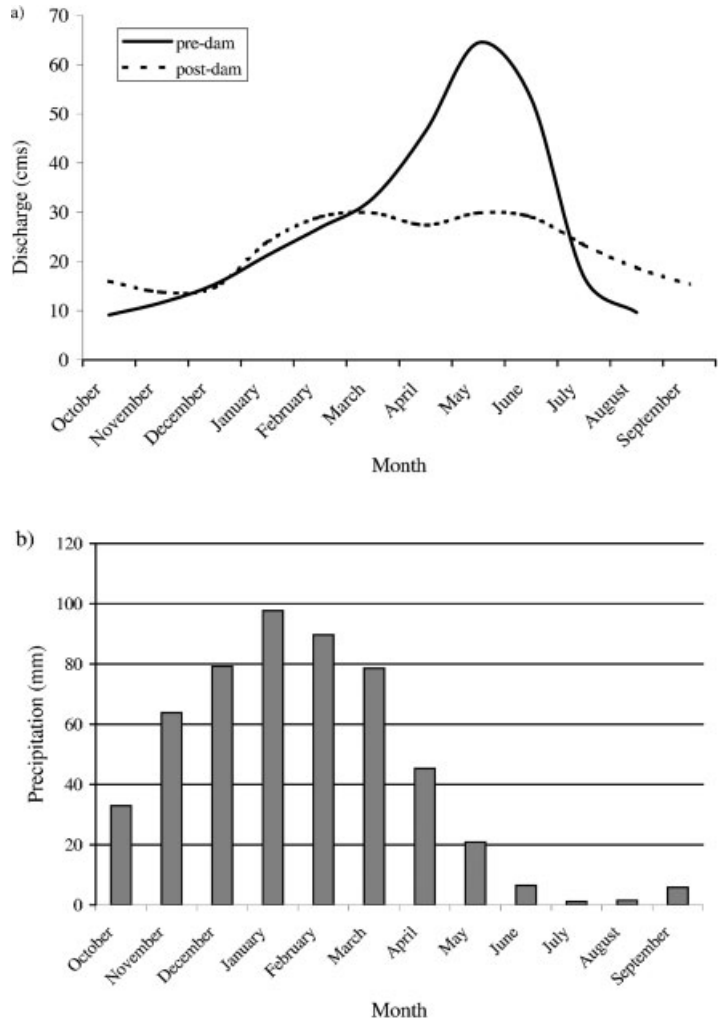

Figure 4. Mean monthly (a) discharge below Camanche Dam for both pre- and post-dam periods and (b) precipitation at Pardee Dam

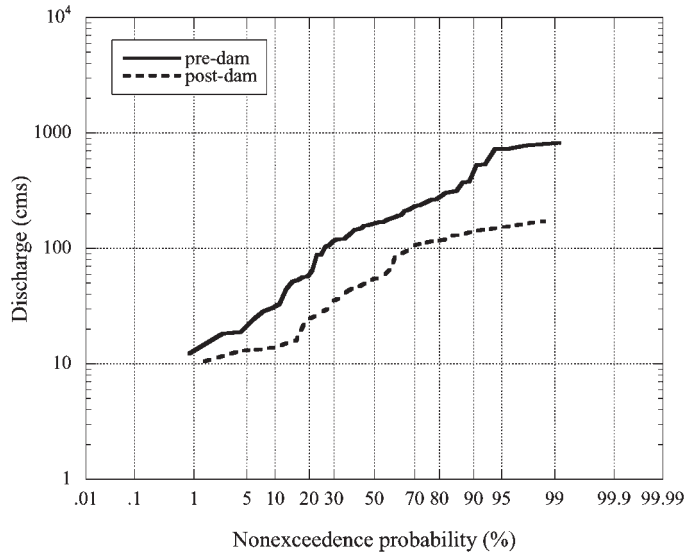

Figure 5. Pre- and post-dam flood frequency curves using annual peak flow series

Table I. History of gravel augmentation/enhancement projects below Camanche Dam

Year	Gravel volume (m^3)[a]	Distance downstream from Camanche Dam (km)[a]
1990	199	0.21
1992	230	0.58
1994	382; 76	0.61; 1.27
1996	268; 268	1.27; 6.88
1997	230; 230	7.84; 9.60
1998	459; 459	0.97; 8.64
1999	2450	0.40
2000	920	1.16

[a] Multiple sites in a year separated by semi-colon.

of bed pores. Since 1998, project sites have been monitored for inter-gravel permeability, dissolved oxygen content, water temperature, macro-invertebrate diversity, and redd counts. Some sites will be monitored until 2009.

The site reported here was replenished in fall 1999 (Figure 2). The channel was fairly uniform with a low slope amenable to the model. The right bank was steep with a narrow riparian zone. The low-lying left bank had an accessible floodplain that has heavy recreational use. Initial modelling was done on a 300 m reach past Murphy Creek, but to raise resolution the reach was cut to 150 m ending just upstream of the junction with Murphy Creek.

FIELD METHODS

In fall 1999, EBMUD placed 2450 m^3 of washed floodplain gravel in the river below Camanche, creating exposed boulders, chutes, pools, and riffles. Channel topography, water depth and velocity, and substrate sizes were measured for 2D model use. Because this work was initiated after EBMUD's project was underway, there was no chance to measure pre-project velocities. Once the 2D model reasonably replicated post-project flow conditions, four alternative gravel scenarios were designed and compared.

Channel topography

Detailed topography was mapped with 1155 points. Surveying was performed by licensed professionals and was done before and after gravel placement while flow was low. Surveying resolution was high (*c.* 1 point per 3.6 m^2). Rather than using a uniform distribution (time-consuming in the field) or many transects (do not capture true topography), care was taken to accurately map bed features with a high density of points measured in the vicinity of natural slope breaks and fewer points over flat surfaces. In addition to coordinates, wet/dry channel boundaries, water surface elevation, and bed exposure were carefully documented.

Observation data

Depth and velocity were measured after the gravel was placed at a typical spawning-season low flow (9.3 cm) and a higher flow (31 cm). The high flow was close to the post-dam $Q_{1.5}$, which is the Q_{bf} suitable for evaluating gravel scour (California Department of Fish and Game (CDFG), 1991). Though the peak for 1999 was 68 cm, this could not be modelled because it spread over the unmapped floodplain.

Post-project depth and velocity were measured at four cross-sections. Endpoints were marked with steel pins to define location and alignment. Endpins were surveyed with a Trimble Pathfinder Pro XRS differential GPS whose resolution was *c.* 0.3 m. GPS coordinates were overlaid in the model to locate the nearest node to each endpin thereby defining comparable cross-sections. Cross-sections 4 (just upstream of placed gravel) and 7 (over gravel bars) were waded at 9.3 cm and sampled every 0.3 m with careful position control. Depths were measured with a stadia rod. At cross-section 4, velocity was averaged over 1 min with a Unidata Starflow depth-averaging ultrasonic Doppler velocity meter (± 1 mm s^{-1}). At cross-section 7, a Marsh-McBirney Flo-mate (± 33 mm s^{-1}) and a depth-setting wading rod were used to estimate average velocity as the point velocity at 0.6 of depth. Cross-sections 1 (upstream boundary for coarse mesh runs) and 10 (below placed gravel) were observed at 31 cm with a cable-mounted USGS Price AA current meter from a flat-bottomed boat locked onto a high-tension steel cable every 1.5 m with careful position control. Standard USGS procedure for calculating depth-averaged velocity from point measurements was used. Positional accuracy and observation resolution were much finer than the scale of bed features (*c.* 5–10 m) and similar to model node spacing.

Substrate size

Wolman pebble counts were conducted before and after replenishment (Kondolf and Li, 1992). Counts were made along three randomly located 30 m longitudinal transects yielding 300 particles. The first particle encountered by the tip of the index finger with closed eyes was sampled. This was done for 100 particles per transect. Each particle was placed into 0.5 phi size class over the range of 3–8 phi including lumped <3 and >8 size fractions (Vyverberg *et al.*, 1996). Cumulative percentages of each class were calculated.

MOKELUMNE MODEL

Model description

The Finite Element Surface Water Modelling System Two-Dimensional Flow in a Horizontal Plane model (FESWMS-2DH v. 2) simulates steady or unsteady 2D surface-water flows, including sub- and super-critical conditions (Froehlich, 1989). FESWMS solves the vertically integrated equations of motion and continuity with a finite element scheme. It uses a robust wetting and drying routine that determines channel boundary location. An element is 'dry' when depth is below a user-defined threshold (0.12 m here) at all of its nodes.

FESWMS was implemented in the Boss International Surface Water Modelling System v. 7.0 (SMS). SMS was used for finite element mesh creation and interpolation of topography to mesh nodes with a TIN-based linear topographic interpolation scheme. Initially a coarse mesh including Murphy Creek was used, but then model area was reduced to 5091 m^2 with the project and adjacent pool downstream. Elements were *c.* 1 m^2 with a nodal distance of *c.* 0.5 m (i.e. node centred in each element). Pre- and post-project meshes were trimmed close to the known wetted perimeter for each flow to allow for a favourable balance between resolution of relevant bed features and computation time as well as to reduce wetting and drying computations.

Model parameterization

Model parameters were determined using theory and measurement. Camanche outflow was the discharge at the upstream boundary. Water surface elevation was field-surveyed at the downstream boundary (28.1 m for 9.3 cm, 28.6 m for 31 cm). A global constant roughness coefficient (Manning's n) of 0.043 was estimated based on roughness tables for a straight, coarse gravel channel with no vegetation (McCuen, 1989). A spatially explicit algorithm for roughness based on substrate size variations was unwarranted in this study for two reasons. First, the reach had a narrow range of gravel substrate sizes, especially after gravel placement. Second, the form drag of gravel bars caused much more significant roughness. Tests of spatially explicit roughness yielded no significant effect, matching Miller and Cluer (1998).

FEWSMS uses the Boussinesq eddy viscosity to resolve turbulence closure. Eddy viscosity coefficient values that are too high suppress flow separation, whereas values too low cause model instability (Miller, 1994). Eddy viscosity was calculated as $v = C\,u* R_h$, where $C = 0.6$, $u* =$ shear velocity, and $R_h =$ hydraulic radius (Froehlich, 1989). Shear velocity was calculated from velocity observations using Einstein's log-velocity equation for turbulent flow over rough beds. Even though calculated eddy viscosities were mostly $<0.05\,m^2\,s^{-1}$, values $<0.065\,m^2\,s^{-1}$ led to model instability, so $0.065\,m^2\,s^{-1}$ was used for all pre- and post-project model runs.

Scenario construction

Four alternative scenarios were designed using the SMS Scatter Point Module to compare against the actual ad hoc placement. Even though SMS was not intended for topographic design, it was possible to create topography using its scatter point module. Bed features were first created with artificial points and then pasted over existing topography. Transitions between the pre-existing bed and artificial features were smoothed with additional topographic points.

Given the numerous artificial degrees of freedom in designing alternative reach topography (*c.* $30^{25\,000}$), an objective search for the optimal solution to habitat goals and sediment entrainment constraints was not feasible. Instead, different channel configuration types were tested. The scenarios developed were alternate bars, channel braid, alternate bars + braid, and flat riffle with boulders (Figure 6). All designs except the last used large, coherent bed features that were thought to offer high quality contiguous habitat while also limiting isolated protrusions susceptible to erosion. The downstream half of the model area encompassed a channel-wide pool (*c.* 2.52 m deep). The pool was kept because it was too deep to fill economically and it may provide habitat for other life stages of salmonids. Further, the pool also provided an opportunity to observe any possible important flow dynamics such as recirculating eddies. These eddies are zones of rapid change in flow velocity and direction, which may provide rest sites for spawners between nest-site preparation efforts. Bowl-shaped pool to riffle transitions were also considered beneficial, as they promote stream water downwelling, aid oxygenation of gravels, and are preferentially used by salmonids (Kondolf, 2000).

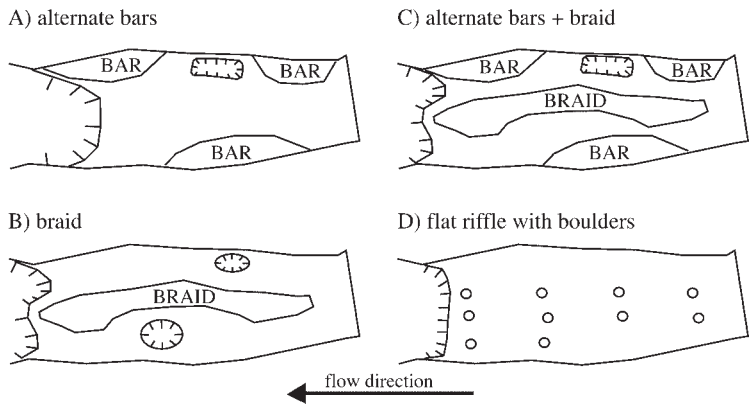

Figure 6. Schematic illustrations of the four alternative gravel placement scenarios. Hatched areas are pools while circles in (D) are boulders. Gravel was used not only to make features, but also to raise bed elevation globally. Detailed topographic maps available in Wang and Pasternack (2000) or upon request

Because the gravel needed for different scenarios varied by up to 30%, comparisons were made based on efficiency—habitat area per cubic metre of gravel added. Gravel volumes were calculated by digital elevation model (DEM) differencing in ArcInfo. Instream features were exposed at low flow by design. Gravel was used not only to make features, but also to decrease water depths globally, as depth was universally greater than the optimal habitat suitability value. Depth and velocity distribution statistics were taken from nodal data sets.

Model parameters were nearly the same as those used in pre- and post-project runs. The roughness coefficient was 0.043 for all cases. Eddy viscosity was $0.065\,m^2\,s^{-1}$ for all runs, except for the low flow alternate bars + braid run, for which it was $0.09\,m^2\,s^{-1}$ due to model instability. Meshes had equal numbers of nodes and nearly equal numbers of elements.

Scenario comparison

Scenarios were compared using habitat and sediment entrainment criteria. A global habitat suitability index (GHSI) was calculated from velocity (VHSI) and depth (DHSI) suitability curves derived from 98 observed redds at seven sites on the lower Mokelumne (CDFG, 1991). These curves were compared against independent data from the Yuba and Sacramento rivers and found to be similar (CDFG, 1991). The GHSI is specifically for chinook salmon spawning in the lower Mokelumne River under the assumption of perfect substrate quality, which holds when new gravel is placed. DHSI and VHSI range from 0 to 1.13 m and 0 to $1.55\,m\,s^{-1}$ with optimal conditions at 0.40 m and $0.82\,m\,s^{-1}$, respectively. These criteria were combined using $GHSI = DHSI^{(0.5)} \times VHSI^{(0.5)}$. GHSI was classed as poor (0–0.1), low (0.1–0.4), medium (0.4–0.7) and high (0.7–1.0) quality habitat (*sensu* Leclerc *et al.*, 1995). GHSI is calculated at each node and thus cannot assess spatially related habitats. Areas of each GHSI category in each alternative design were calculated and compared.

To assess if placed gravels would wash away at the modelled flows, the ratio of actual to critical velocity was used as a sediment mobility index (SMI). The depth-average critical velocity for movement of the median grain size at a node was calculated using Einstein's log-velocity equation for turbulent flows over rough beds combined with Shield's incipient motion criteria (Garde and Ranga Raju, 1985) assuming a dimensionless shear stress of 0.045:

$$\bar{u}_{\text{critical}} = \left[5.75 \log\left[12.2\frac{H}{k_s}\right]\right]\left[\frac{0.045(\gamma_s - \gamma_f)d_{50}}{\rho f}\right]^{0.5} \quad (1)$$

where H = water depth, d_{50} = median bed material grain size, k_s = boundary roughness, γ_s = sediment specific weight, γ_f = fluid specific weight, and ρ_f = fluid density. For the Mokelumne's highly homogeneous bed, d_{50} was taken as k_s (Smart, 1999). This parameter should not be confused with the Z_0 boundary roughness of a more general form of Equation 1, though the two are linearly related (Smart, 1999). Because sediment is unlikely to move under the low flow at which fish spawn (unless flow becomes supercritical), reported SMIs were calculated under near-bankfull flow conditions. SMI >1 predicts entrainment. For SMI <1, entrainment potential was divided into low (0–0.33), medium (0.33–0.67), and high (0.67–1.0) categories. Other causes of entrainment that are not quantifiable in this model include fishermen walking on the gravel, gravel consolidation over time, local scour around large woody debris (LWD), and salmon activity.

RESULTS

Gravel placement resulted in significant changes to the channel. Prior to the project, the channel was deep and fairly uniform (Figure 7A) and had a bed composed of poorly sorted, compacted gravels of poor quality for salmon spawning. Grain size frequency analysis showed a pre-project bed d_{50} of 41 ± 43 mm (1 standard deviation) (Figure 8). A fraction (13%) of bed particles were <8 mm in diameter, potentially clogging large pores. After the project the channel was shallow and diverse, with several longitudinal bars separated by fast-running chutes (Figure 7B). The far right side of the channel had gravel scattered in small mounds to create exposed bars and riffles under low flow. Exposed boulders were also used to create habitat features. Post-project d_{50} was 48 ± 21 mm yielding a homogeneous bed with large interstices (Figure 8). For both pre- and post-project

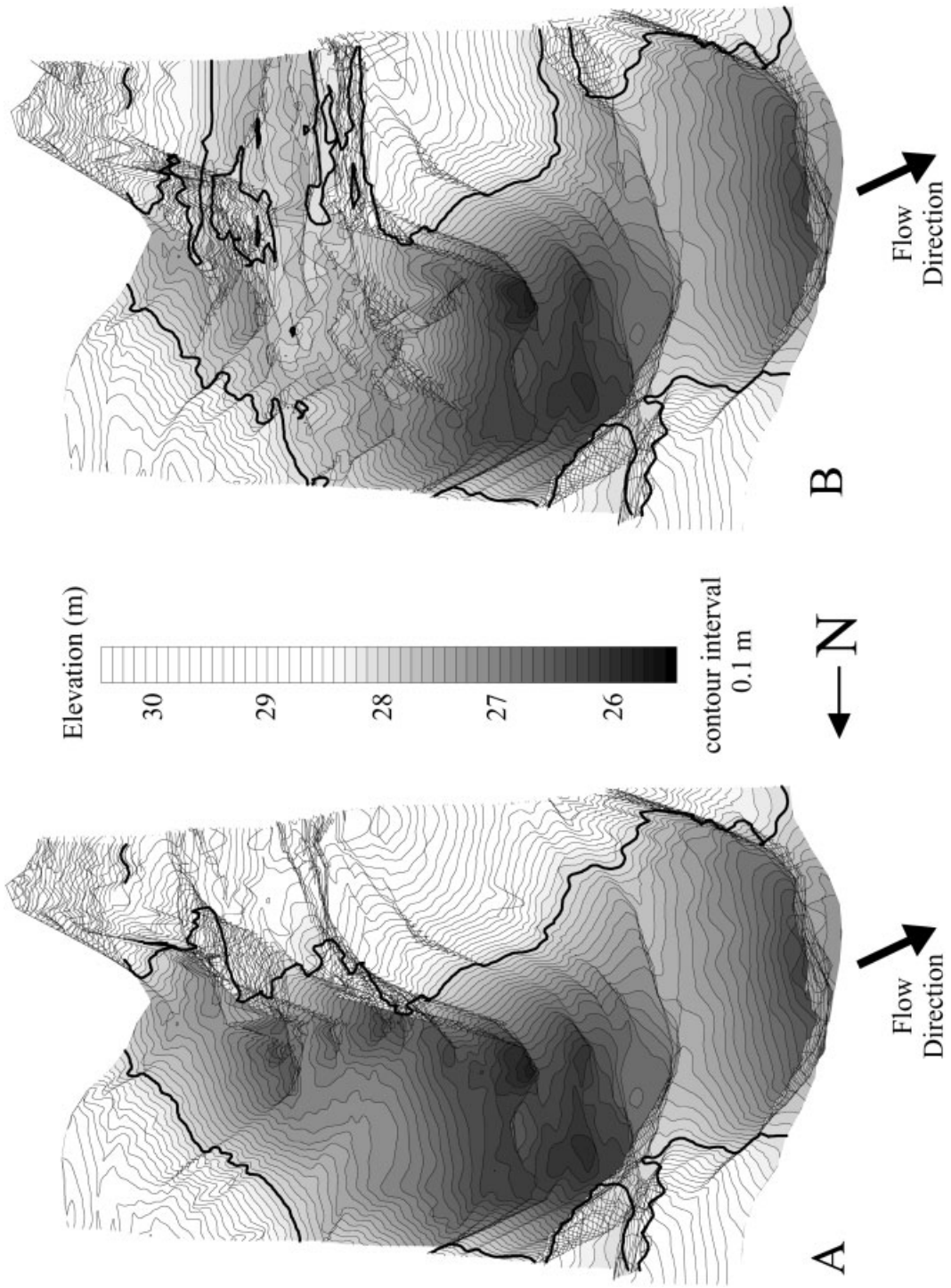

Figure 7. Oblique visualizations looking upstream at (a) pre- and (b) post-project channel geometry. Heavy contour is the 28 m level. Contour interval is 0.1 m

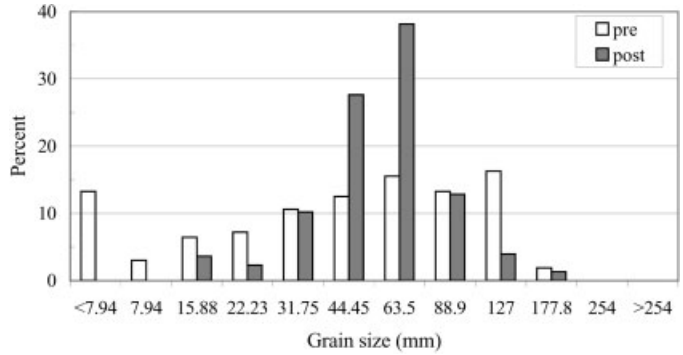

Figure 8. Comparison of bed material grain size distributions before and after gravel replenishment

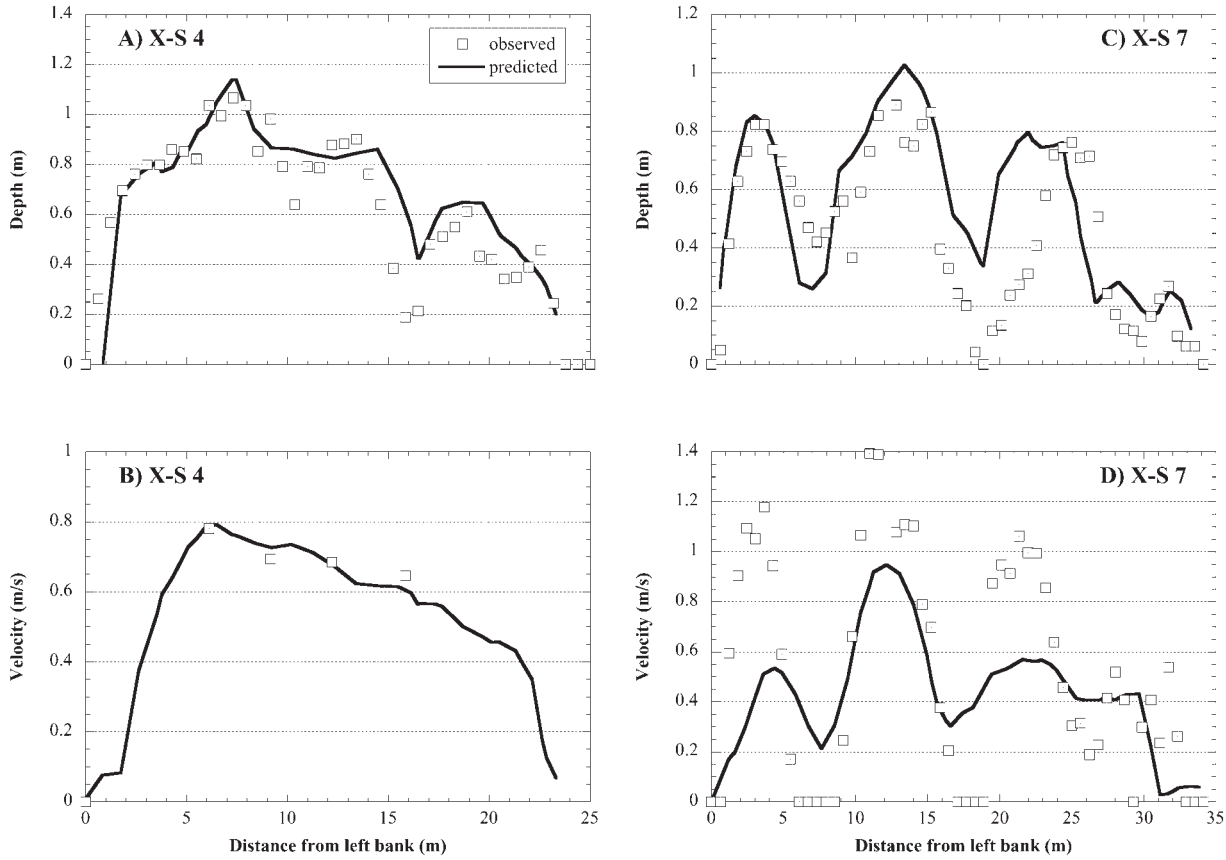

Figure 9. Comparisons of observed versus predicted depths and velocities during a low discharge representative of salmon spawning conditions at cross-sections 4 (A,B) and 7 (C,D)

substrates, the lack of clay, silt, and sand simplified habitat and entrainment conditions so that GHSI and SMI assumptions were reasonable.

Model validation

For the post-project low flow run the model showed very high sensitivity to topographic interpolation error inherent to the simple linear SMS approach. For cross-sections 4 and 7 observed depths ranged from 0 to 1.07 m (Figure 9A,C). The interpolated bathymetry was deeper than observed despite a high density of survey

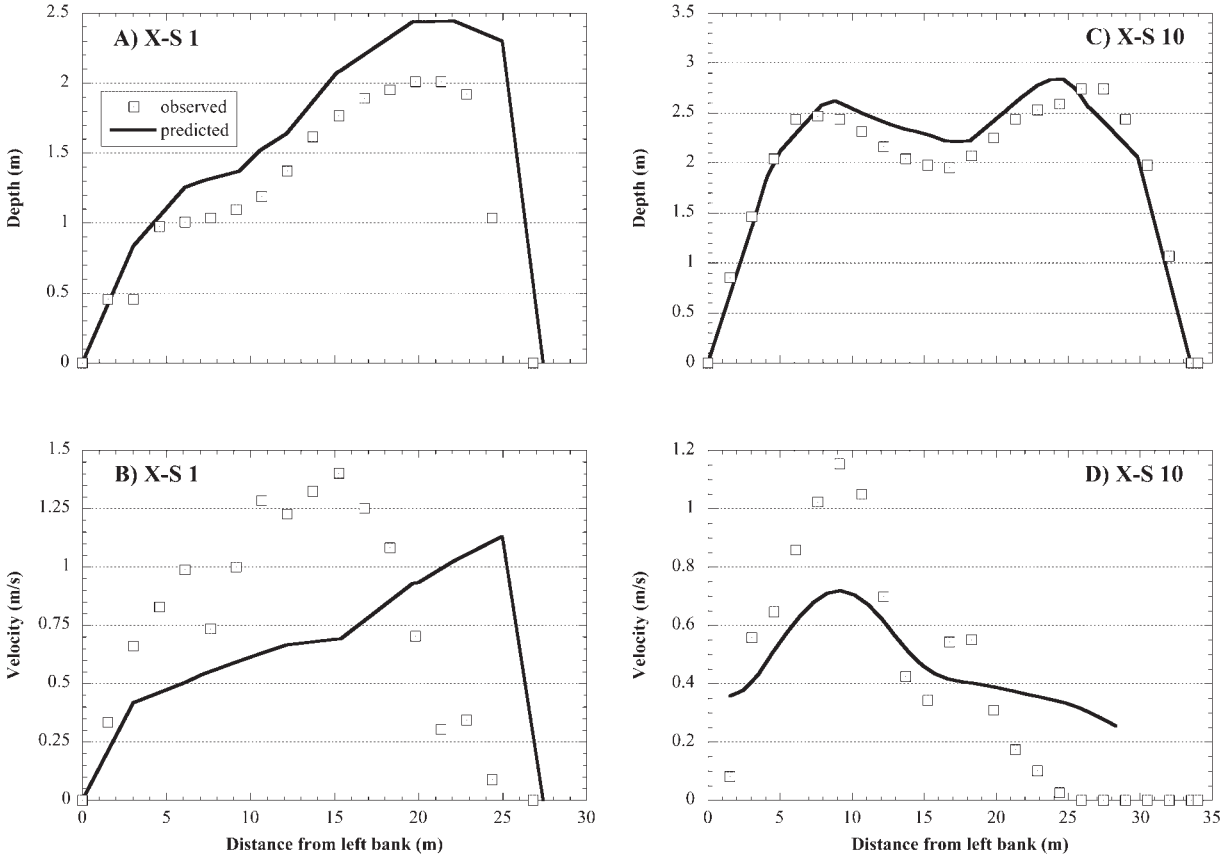

Figure 10. Comparisons of observed versus predicted depths and velocities during a high discharge representative of sediment entrainment conditions at cross-sections 1 (A,B) and 10 (C,D)

points. Cross-section 7 had three bars, three chutes, and a small side channel on the right bank yielding a significant challenge for SMS.

Differences in observed versus predicted velocity primarily stemmed from the topographic interpolation error. Cross-section 4 had an observed peak velocity of 0.78 m s^{-1}. Predicted velocities nearly equalled the five observed values (Figure 9B). Data were lost for the right side of the channel due to battery failure. At cross-section 7, observed velocities were underpredicted in chutes and overpredicted over gravel bars (Figure 9D).

For high flow, model performance at cross-sections 1 and 10 was seriously degraded by LWD and affected by interpolation error. At cross-section 1, validated using a coarse mesh covering that location, depth peaked near the right bank where there was highly branched LWD under water (Figure 10A). Modelled depths were greater than observed, with the worst outcome at the debris. Low flow topographic mapping for model creation avoided the debris whereas high flow observations by boat could not. Observed depths at cross-section 10, where debris was present upstream of the right half of the channel, showed the channel divided into two deep chutes (Figure 10C). Model depths showed some smoothing in relation to observations. Because of the LWD at both cross-sections, velocity transects underpredicted peak velocity and did not capture lateral flow distribution (Figure 10B, D). The effects of LWD will be discussed in detail later.

In summary, validation of the model revealed serious problems with using a simple TIN-based linear interpolation approach on raw topographic data. Where bathymetry was modelled properly and woody debris was absent, the model performed well. These apparent constraints were fully considered in the design phase of the study.

Scenario results

Even though model validation showed that SMS provided poor topographic interpolation in complex terrain so that depth and velocity were underestimated, this deficiency has no impact on comparison of different scenarios with prescribed topography. To compare between real channel configurations and prescribed alternatives required the assumption of accurately interpolated topography. For the pre-project case, the channel was uniform enough that the model reasonably represented topography. For the post-project case, the model was accurate away from bars and chutes but not over such features. Thus, post-project results presented below underestimate details of flow and habitat conditions.

Overall, bed, flow, habitat, and sediment entrainment conditions for the six different bed topographies varied significantly. Model output is illustrated in a series of four maps per scenario: depth, velocity, GHSI at low flow, and SMI at high flow. For the sake of brevity, depth and SMI plots are excluded, though relevant aspects of these plots are summarized below. All plots and raw data sets from this study are available in Wang and Pasternack (2000) or by request.

The pre-project baseline consisted of a uniform channel with low velocities, minimal spawning habitat, and no sediment entrainment (Figure 11A,C). Depths spanned 0–1.82 m, while velocities ranged from 0 to 0.60 m s^{-1}. Velocity vectors were generally parallel and showed little deviation from the longitudinal axis (Figure 11A). Depth controlled GHSI values given low and nearly constant velocities (Figure 11C). The channel was too deep to yield habitat for 74% of the area, leaving a usable fringe along the banks. No high quality habitat was predicted. Monitoring from 1990 to 1998 showed no salmon spawning activity (Setka, 2000), confirming the model prediction. High depths and low velocities uniformly yielded very low SMI values.

EBMUD's gravel replenishment yielded significantly different and highly complex fluvio-geomorphic conditions (Figure 11B, D). Depth decreased to 0.15–1 m, with the bed exposed over boulders and bar tops. Shallow depths produced faster flows that funnelled between exposed features (Figure 11B). Chute velocities ranged from 1.64 to 2.04 m s^{-1}. A large eddy behind a boulder in both observed and modelled conditions indicated accurate representation of flow pattern, if not flow magnitude. GHSI values were dramatically enhanced due to decreased depth, though the best habitat was highly patchy (Figure 11D). Except for exposed bar tops, the entire project area became usable habitat. Velocities in the fastest chute were too high and produced low quality habitat. Other chutes and some riffle areas produced high quality habitat. Shallower depths and faster velocities increased SMI values, but no entrainment was predicted. Critical velocities were nearly exceeded in cells adjacent to exposed bars. Because the model underpredicted chute velocities, the site was field inspected and these small areas were found to indeed be eroding while other areas were stable as predicted.

In the alternate bars scenario, two small bars were placed on the right bank and one big bar on the left bank (Figure 6A). Opposing bars were connected by riffles; a pool separated the two riffles. Because the reach was short, bars were not intended to mimic natural riffle–pool spacing, but rather to provide simple, coherent bed structures with low risk of erosion during spawning season. The alternate bars decreased channel width, causing flow meandering as well as recirculating eddies downstream of all bars. Bar tops were dry at low flow. Velocities ranged from 0 to 1.28 m s^{-1} (Figure 12A). Despite lacking habitat on exposed bars, the same amount of high quality habitat was predicted as for the actual post-project case (Figure 13A). Habitat was concentrated in three large patches on shallow riffles. SMIs showed no erosion. The highest SMI occurred at the head of the first alternate bar.

In the braided scenario, an exposed 76×5 m sinuous braid was placed mid-channel to divide flow into two spawning chutes. A riffle–pool–riffle sequence was made in each chute yielding three pool–riffle transitions promoting water downwelling and substrate oxygenation (Figure 6B). Velocities ranged from 0 to 1.13 m s^{-1} (Figure 12B). Recirculating eddies formed in the shear zone along the braid's upper half. A large two-cell eddy formed over the braid's lower section and a single-cell eddy formed downstream along the right bank. High quality habitat occurred along riffle sections (Figure 13B). Depth and velocity conditions conflicted with each other limiting potential habitat. SMIs were higher over riffles but still too low for entrainment.

The alternate bars + braid scenario had two meandering chutes with riffle–pool–riffle sequences (Figure 6C). The left sequence was highly constricted between the braid and the bar because the left bar was much bigger than the two bars forming the right bank. The size of the bar limited the size and depth of the pool in the left chute. This formed a narrow chute over a riffle that led to a shallow pool and then to another riffle. Once again there were three

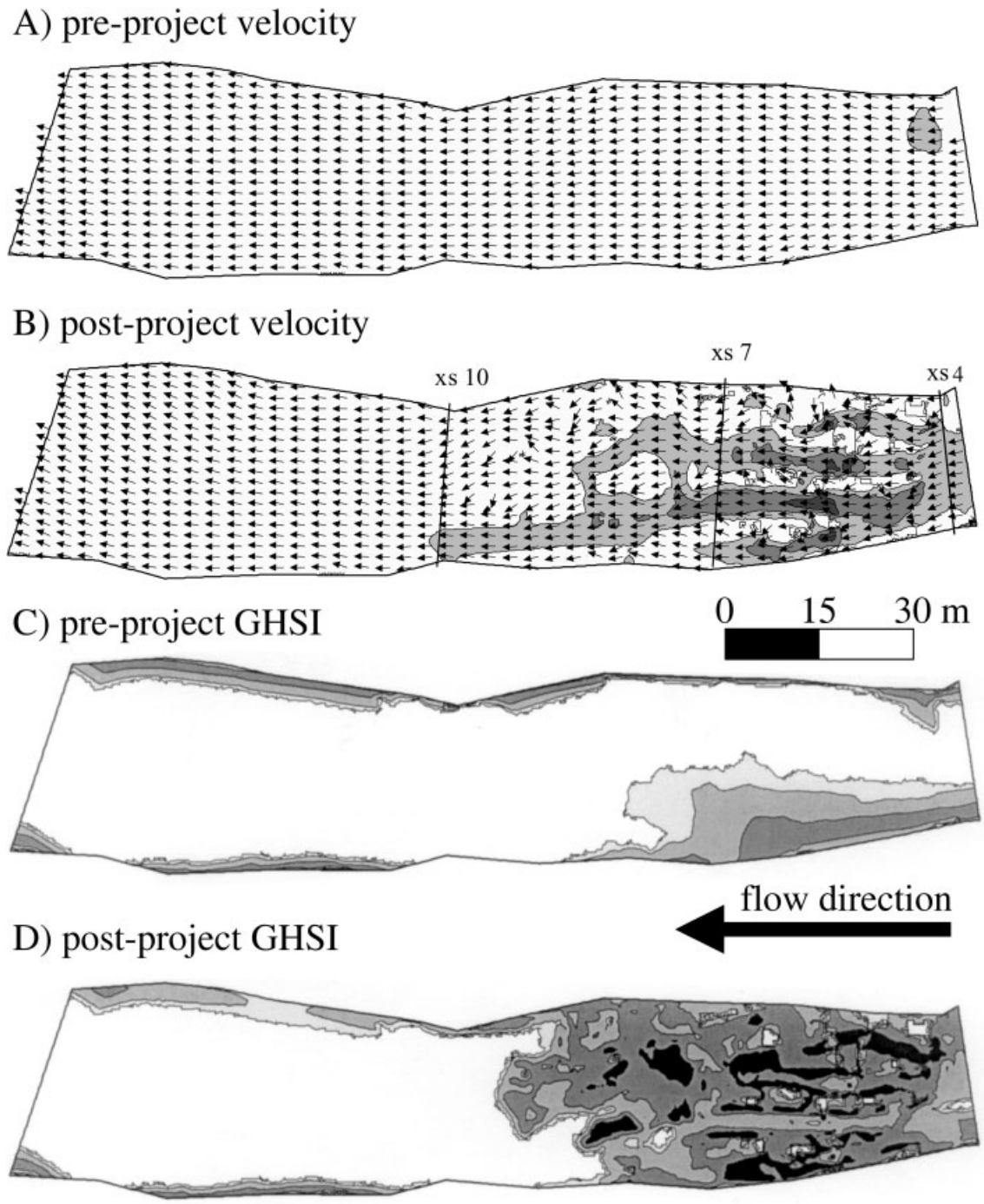

Figure 11. Simulation results for (A) pre- and (B) post-project velocity vectors as well as (C) pre- and (D) post-project GHSI. Validation cross-sections (xs) are shown, except xs 1 upstream of the project reach that was used with a coarser-scale model run. Velocity magnitude is represented with shading such that white = 0–0.5 m s^{-1}, light grey = 0.5–1 m s^{-1}, medium grey = 1–1.5 m s^{-1}, and dark grey = 1.5–2 m s^{-1}. GHSI is represented with shading such that white = 0 (dry areas and deep pools), light grey $\leqslant$0.1 (very poor quality), medium grey = 0.1–0.4 (low quality), dark grey = 0.4–0.7 (medium quality), and black = 0.7–1 (high quality)

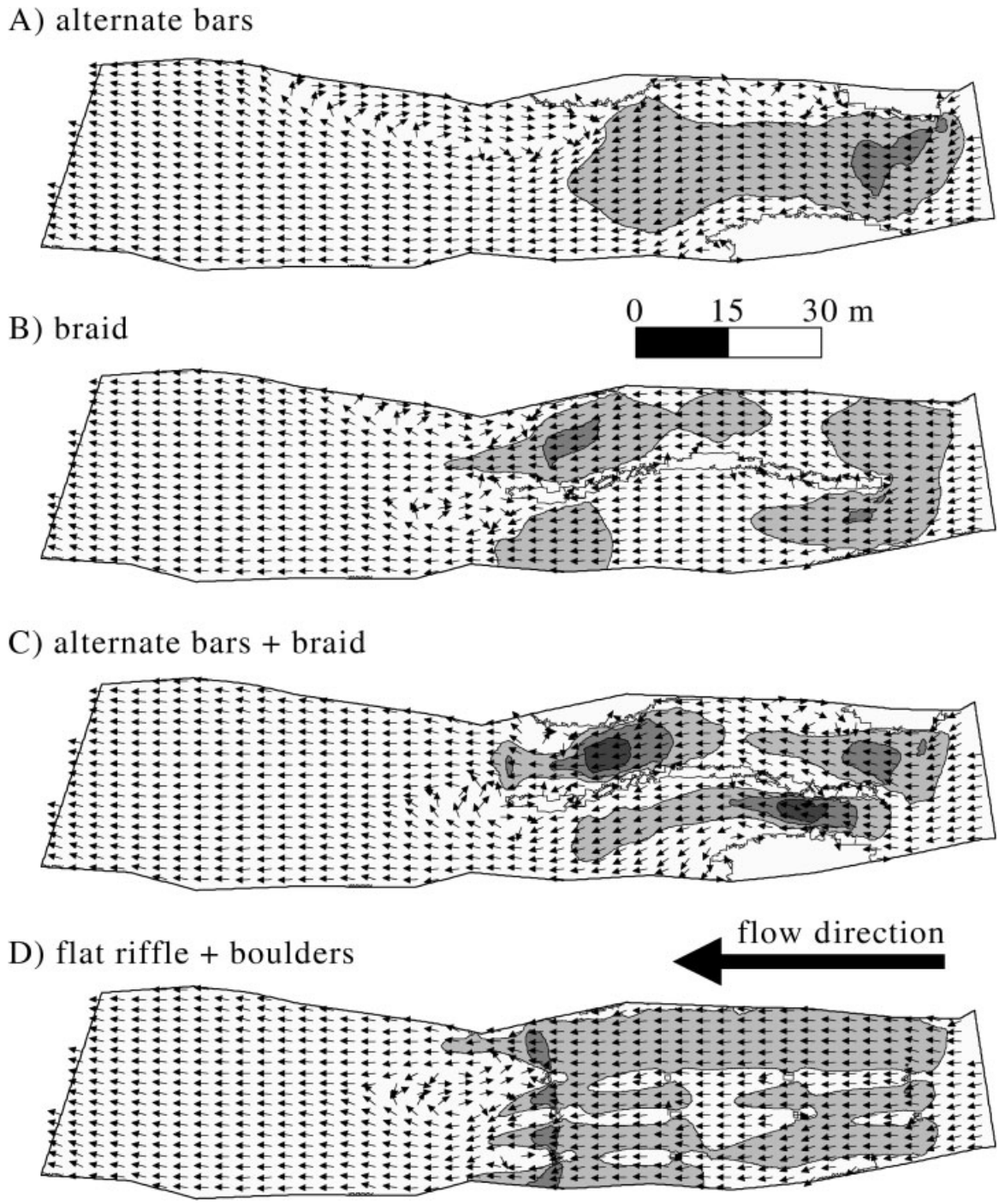

Figure 12. Comparison of velocity magnitude (shading) and direction (arrows) among the four alternative gravel placement scenarios. Dry areas have no arrows. Velocity magnitude is represented with shading such that white = 0–0.5 m s^{-1}, light grey = 0.5–1 m s^{-1}, medium grey = 1–1.5 m s^{-1}, and dark grey = 1.5–2 m s^{-1}

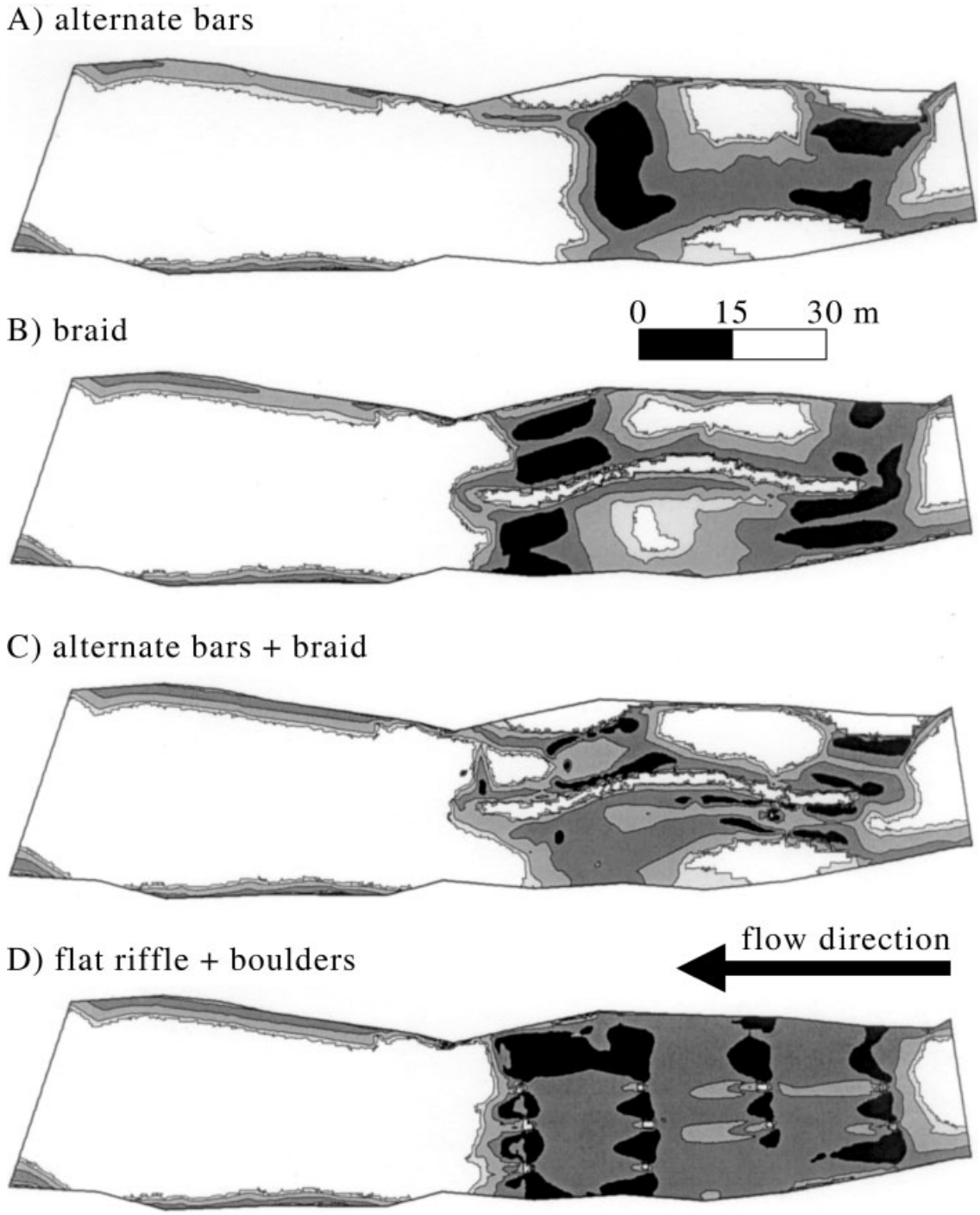

Figure 13. Comparison of GHSI values among the four alternative gravel placement scenarios. White = 0 (dry areas and deep pools), light grey ⩽0.1 (very poor quality), medium grey = 0.1–0.4 (low quality), dark grey = 0.4–0.7 (medium quality), and black = 0.7–1 (high quality)

pool-exit slopes promoting substrate oxygenation. Velocity was fastest over the riffle sections, with a peak of $2.0\,\mathrm{m\,s^{-1}}$ (Figure 12C). Eddies formed behind each exposed bar. In comparison to the braided scenario, chute asymmetry changed the mid-channel eddy to a single cell. The large number of exposed features built into this design resulted in too much unusable area (Figure 13C). Deep pools also provided no habitat. Few high quality

habitat areas existed, as optimal depth coincided with excessive velocity, while optimal velocity occurred in excessive depth. Relatively high SMI values were concentrated at the head of the first alternate bar.

For the flat riffle + boulders scenario, gravel was set uniformly over the site. Ten boulders were spaced evenly over the left 67% of the channel to constrict flow, create high velocities, and obtain small recirculating eddies providing resting locations for juveniles and adults (Figure 6D). Boulders were *c.* 3 m in diameter and exposed at low flow. The upstream end of the riffle had a broad pool-exit slope for water downwelling. The fastest velocities occurred in the constrictions between boulders, typically 0.5–1.22 m s^{-1} (Figure 12D). Velocities were lowest behind boulders (*c.* 0.01–0.5 m s^{-1}). Due to the uniformity of gravel and lack of exposed areas, this scenario yielded the most habitat area, though the most gravel was used too (Figure 13D). Boulder symmetry produced regularly distributed high quality habitat patches in the optimal velocity chutes between boulders. Highest SMIs occurred in grid cells just upstream of each boulder.

DISCUSSION

Several studies explain the effect of sparse topographic data on 2D modelling (Anderson and Bates, 1994; French and Clifford, 2000; Marks and Bates, 2000), but few have addressed the significance of DEM-generation limitations within 2D modelling packages. This project had dense data surveyed by professionals yielding a high quality baseline at the scale of habitat-relevant features. This assisted the design of alternatives and enabled a test of SMS and FESWMS in comparing designs on the basis of habitat and sediment entrainment patterns. Unfortunately, SMS v. 7.0 proved unable to generate a digital elevation model that accurately reflected complex natural topography, even with a node spacing of 0.5 m. Lacking that, FESWMS could not match observed conditions. SMS does not have enough tools for accurate terrain modelling. While its topographic interpolation scheme is identical to other DEM software, what is needed is better management of large and layered topographic datasets as well as options to apply accepted civil engineering methods that manually adjust the terrain model to yield an accurate representation as can be done with many CAD programs, such as AutoDesk's AutoCAD. DEMs made using engineering software may be imported into SMS and used with a 2D model to yield more computationally stable and accurate simulations. Thus, in addition to collecting dense topographic datasets, one must work hard at DEM generation to obtain an accurate representation of the bed for 2D modelling.

Even with an accurate terrain model, a serious problem was encountered in representing flow conditions near LWD. While woody material was not widespread, two large pieces altered the flow pattern of the model validation cross-sections. Resulting errors affected habitat quality estimates and location as well as potential for sediment entrainment. As large woody debris can provide significant instream habitat (Abbe and Montgomery, 1996; Merz, 2001) and is part of channel rehabilitation, this poses a limitation on the use of a 2D model where wood is present. Changing local flow parameters to better mimic woody debris can help a model match observed conditions, but this is not possible in a design mode predicting future velocities under alternatives. Further, habitat provided by woody debris is not accounted for in habitat suitability indices, so the use of model results to predict habitat conditions would be tenuous.

Gravel replenishment yielded a dramatic change in flow conditions and thus in quantity and quality of habitat. Mean depth decreased from 1.38 m to 1.09 m, while predicted mean velocity increased from 0.21 to 0.34 m s^{-1} (Table II). More importantly, the range of predicted velocities increased from 0–0.6 to 0–2.07 m s^{-1}. Because the model underestimated actual velocity (Figures 9 and 10), and higher velocity would have yielded higher GHSI values, habitat quality was underestimated. Even so, the site went from having no high quality habitat to having at least 362 m^2 of it. Total usable habitat changed from 945 to over 2350 m^2, with the largest increase occurring for medium quality habitat. The efficiency of the gravel project was 0.96 m^2 m^{-3}. Whereas no spawning occurred in the reach in prior years, after gravel placement redds were observed on-site within two months. The follow year there were 29 redds on-site (out of 987 for the whole lower river). These changes show gravel replenishment significantly improves quantity and quality of habitat, even without an objective design process.

Comparing the predicted quantity of habitat under different scenarios showed that many produced similar outcomes (Table III). Even though designed bed features had large exposed areas that provided no habitat, their structures yielded more efficient habitat generation in between so overall gravel efficiency was 0.91–0.99 m^2 m^{-3}, which was comparable to the ad hoc project. The only scenario that resulted in a very poor utilization of gravel

Table II. Depth and velocity distributions for each scenario

Scenario	Mean[a] depth (m)[b]	Velocity ($m\,s^{-1}$)		Gravel (m^3)
		Mean[a]	Range	
Pre-1999	1.38 ± 0.52	0.21 ± 0.08	0–0.60	n/a
Post-1999	1.09 ± 0.66	0.34 ± 0.32	0–2.07	2450
Alternate bars	1.15 ± 0.68	0.29 ± 0.27	0–1.31	1911
Braided	1.10 ± 0.64	0.31 ± 0.24	0–1.14	2370
Bars + braided	1.09 ± 0.70	0.30 ± 0.31	0–2.03	2675
Flat riffle + boulders	1.08 ± 0.62	0.37 ± 0.24	0–1.37	2675

[a] Mean ± 1 SD of spatial data from whole area of scenario mesh.
[b] Depths for all scenarios depths ranged from 0 to 2.52 m.

Table III. Estimated area and gravel efficiency of each quality of spawning habitat

Scenario	Low			Medium			High			Total		
	%	m^2	$m^2\,m^{-3}$	%	m^2	$m^2\,m^{-3}$	%	m^2	$m^2\,m^{-3}$	%	m^2	$m^2\,m^{-3}$
Pre-1999	11	581	n/a	7	364	n/a	0	0	n/a	17	945	n/a
Post-1999	16	840	0.34	23	1146	0.47	7	362	0.15	46	2348	0.96
Alternate bars	13	671	0.35	14	720	0.38	7	356	0.19	34	1747	0.91
Braided	17	879	0.37	17	843	0.36	9	459	0.19	43	2181	0.92
Bars + braided	16	792	0.30	17	856	0.32	3	177	0.07	36	1825	0.68
Flat riffle + boulders	9	465	0.17	32	1617	0.60	11	560	0.21	52	2642	0.99

was the alternate bars + braid scenario, which generated $0.68\,m^2\,m^{-3}$. In that case, the exposed areas of the alternate bar and braid features were too large. The flat riffle + boulders scenario used the most gravel, but was also the most efficient at generating habitat.

Focusing on the quantity and distribution of high quality habitat areas, the alternatives yielded much more favourable results than the actual design (Table III). According to EBMUD's subsequent spawning survey, 10% of redds were superimposed (Setka, 2000), so habitat connectivity and patch size were used to compare scenarios. The flat riffle scenario yielded the most high quality habitat area ($560\,m^2$) and had many sizable patches. Despite the small amount of gravel used in the alternate bars scenario, it had nearly the same quantity of high quality habitat as the actual design, yielding improved gravel efficiency. In this case, high quality habitat was focused into three patches that were the largest sizes of all patches in all scenarios, which is a desirable outcome. Similarly, the braided scenario resulted in five large patches and the secondmost area of high quality habitat. The alternate bars + braided scenario yielded very little high quality habitat despite the large amount of gravel used.

Design scenarios may also be differentiated on the basis of other qualitative considerations. Geist and Dauble (1998) proposed that salmon redd distribution in large alluvial rivers was a function of the interaction of surface water and groundwater via the hyporheic zone. In contrast to the actual design, the alternative designs explicitly include zones of surface water downwelling into the gravel. Both the braided and alternate bars + braided scenarios had the most downwelling zones built into them. Similarly, 2% of observed redds in the follow-up survey were along boulders (Setka, 2000), which provide refugia for salmonids and add fluvial complexity, though they tend to promote gravel entrainment (House and Boehne, 1985; Fuller, 1990). Crowder and Diplas (2000) showed that SMS can model flow conditions around boulders, and that has been corroborated here. Boulders were essential to the flat riffle scenario for controlling flow and generating habitat patches. Boulders can be placed in any scenario and will be explored further in future studies. Even without boulders, alternative scenarios had exposed bars that created eddies and refugia.

Because the flat riffle scenario was designed to have optimal flow conditions for a single design discharge, it yielded the best outcome. However, Camanche outflow during the spawning season can vary from 14 to *c.* 46 cm

between years. Under such a range, matching a single design flow in any given year is unlikely unless dam operations specify it. Deviation from the design discharge would yield little to no usable habitat. In contrast, the other design approaches would provide a suitable area of habitat under a range of flows because of their topographic complexity.

No sediment entrainment for the median grain size was predicted for any scenarios at near-bankfull flow (31 cm). The scenarios with sites that were approaching an entrainment condition were the actual design and the flat riffle with boulders. In both cases potential entrainment was located at the heads of boulders and bars. Ideally, the model would be used to simulate higher flows, but above-bankfull conditions induce flooding of the adjacent forested floodplain, which could not be modelled at a reasonable cost. In 1986 the California Department of Fish and Game performed a simple sediment study for the Mokelumne River using HEC-6 (CDFG, 1991). At a cross-section just upstream of the site, they predicted that at *c.* 30 cm, grain sizes of $\leqslant 4.6$ mm would be entrained. Even at a flow of *c.* 142 cm, HEC-6 predicted that only sizes smaller than 12.5 mm would be transported. As the added gravel had a median size of 48 mm, constructed features should be well protected against flow-induced gravel loses. Based on observation, a greater concern may be erosion by supercritical flow at extremely low flow depths.

In this study it was found that an off-the-shelf 2D modelling package could be used to design and compare alternative scenarios for gravel rehabilitation of salmon spawning sites on the basis of multiple quantitative and qualitative habitat and sediment mobility criteria. When an accurate DEM is generated using a high-density topographic survey and professional design engineering software, then a hydrodynamic model can accurately simulate spatial patterns in velocity, depth, sediment entrainment, and spawning habitat in streams. By comparing these variables for six different channel configurations it was possible to distinguish design features that generated and enhanced physical habitat from those that were counterproductive. The strongest conclusion reached is that ad hoc gravel replenishment yields highly patchy habitat conditions that are less gravel-efficient and more likely to erode. Even with large areas of exposed gravel, alternative designs matched or exceeded the actual design. The use of exposed gravel at the design flow is warranted when higher than normal discharges are planned for. In this case, flow may be lower than the design discharge, so it would have been better to keep bars submerged. With that additional area, alternatives would probably greatly exceed the actual design in habitat area and gravel efficiency. Among alternatives, the braided scenario would have been selected for construction because of its large amount of total and high quality habitat, its gravel efficiency, its generation of multiple oxygenation zones and one- or two-cell recirculating eddies, and its lack of sediment entrainment. This choice is probably unique to this site, and many other possible alternatives were not considered in the design phase.

ACKNOWLEDGEMENTS

We gratefully acknowledge James Smith, Dr Jeff Mount, Dr David Galut, Dr Michel Leclerc, Joe Wheaton, Brett Valle, Jose Constantine, and anonymous reviewers for input to the research and manuscript. Russ Taylor and other EBMUD staff helped with data collection while Ellen Mantalica at UC Davis provided logistical support.

REFERENCES

Abbe TB, Montgomery DR. 1996. Large woody debris jams, channel hydrodynamics and habitat formation in large rivers. *Regulated Rivers: Research & Management* **12**: 201–221.

Allan JD, Flecker AS. 1993. Biodiversity conservation in running waters. *BioScience* **43**: 32–43.

Anderson MG, Bates PD. 1994. Evaluating data constraints on two-dimensional finite element models of floodplain flow. *Catena* **22**: 1–15.

Bovee K. 1982. *A guide to stream habitat analysis using the Instream Flow Incremental Methodology.* Instream Flow Information Paper No. 12. USDA Fish and Wildlife Service, Office of Biological Services. FWS/OBS-82/26.

Brandt SA. 2000. Classification of geomorphological effects downstream of dams. *Catena* **40**: 375–401.

California Department of Fish and Game. 1991. *Lower Mokelumne River Fisheries Management Plan*. The Resources Agency: Sacramento, CA.

California Department of Water Resources. 1995. *Sacramento River Gravel Restoration Phase II Study: A Plan for Continued Spawning Gravel Replenishment Between Keswick Dam and Clear Creek*. Technical Information Record TIR ND-95-1, Northern District: Red Bluff, CA.

Castleberry DT, Czech JJ, Erman DC, Hankin D, Healey M, Kondolf GM, Mangel M, Mohr M, Moyle PB, Nielsen J, Speed TP, Williams JG. 1996. Uncertainty and instream flow standards. *Fisheries* **21**: 20–21.

Cluer BL. 1997. *Eddy bar responses to the sediment dynamics of pool-riffle environments*. PhD Dissertation, Colorado State University, Fort Collins.

Crowder DW, Diplas P. 2000. Using two-dimensional hydrodynamic models at scales of ecological importance. *Journal of Hydrology* **230**: 172–191.

Douglas AJ, Taylor JG. 1998. Riverine based eco-tourism: Trinity River non-market benefits analysis. *International Journal of Sustainable Development and World Ecology* **5**: 136–148.

Federal Energy Regulatory Commission. 1993. *Final Environmental Impact Statement, Proposed Modifications to the Lower Mokelumne River Project, California, FERC Project No. 2916–004*. Federal Energy Regulatory Commission: Washington, DC.

French JR, Clifford NJ. 2000. Hydrodynamic modeling as a basis for explaining estuarine environmental dynamics: some computational and methodological issues. *Hydrological Processes* **14**: 2089–2108.

Froehlich DC. 1989. *Finite Element Surface-Water Modeling System: Two-dimensional Flow in a Orizontal Plane User's Manual*. US Department of Transportation, Publication #FHWA-RD-88-177.

Fuller DD. 1990. *Seasonal utilization of instream boulder structures by anadromous salmonids in Hurdygurdy Creek, California*. Fish Habitat Relationships Bulletin, FHR Currents No. 3. USDA Forest Service, Region 5. 8pp.

Gallagher SP, Gard MF. 1999. Relationship between Chinook salmon (Oncorhynchus tshawytscha) redd densities and PHABSIM-predicted habitat in the Merced and Lower American rivers, California. *Canadian Journal of Fisheries and Aquatic Sciences* **56**: 570–577.

Garde RJ, Ranga Raju KG. 1985. *Mechanics of Sediment Transportation and Alluvial Stream Problems*. Wiley Eastern Limited: New Dehli.

Geist DR, Dauble DD. 1998. Redd site selection and spawning habitat use by fall Chinook salmon: the importance of geomorphic features in large rivers. *Environmental Management* **22**: 655–669.

Ghanem A, Steffler P, Hicks F. 1996. Two-dimensional hydraulic simulation of physical habitat conditions in flowing streams. *Regulated Rivers: Research & Management* **12**: 185–200.

Gilvear DJ, Waters TM, Milner AM. 1995. Image analysis of aerial photography to quantify changes in channel morphology and instream habitat following placer mining in interior Alaska. *Freshwater Biology* **34**: 389–398.

Gore JA, Nestler JM. 1998. Instream flow studies in perspective. *Regulated Rivers: Research & Management* **2**: 93–101.

Harvey BC, Lisle TE. 1998. Effects of suction dredging on streams: a review and an evaluation strategy. *Fisheries* **23**: 8–17.

House R, Boehne P. 1985. Evaluation of instream enhancement structures for salmonid spawning and rearing in a coastal Oregon stream. *North American Journal of Fisheries Management* **5**: 283–295.

Kondolf GM. 1997. Hungry water: effects of dams and gravel mining on river channels. *Environmental Management* **21**: 533–551.

Kondolf GM. 2000. Assessing salmonid spawning gravel quality. *Transaction of the American Fisheries Society* **129**: 262–281.

Kondolf GM, Li S. 1992. The pebble count technique for quantifying surface bed material size in instream flow studies. *Rivers* **3**: 80–87.

Kondolf GM, Matthews WVG. 1993. *Management of Coarse Sediment in Regulated Rivers of California*, Report No. 80. University of California Water Resources Center: Riverside.

Kondolf GM, Vick JC, Ramirez TM. 1996. *Salmon Spawning Habitat Rehabilitation in the Merced, Tuolumne, and Stanislaus Rivers, California: An Evaluation of Project Planning and Performance*, Report No. 90. University of California Water Resources Center: Berkeley, CA.

Lane SN, Bradbrook KF, Richards KS, Biron PA, Roy GA. 1999. The application of computational fluid dynamics to natural river channels: three-dimensional versus two-dimensional approaches. *Geomorphology* **29**: 1–20.

Leclerc M, Boudreault A, Bechara JA, Corfa G. 1995. Two-dimensional hydrodynamic modeling: a neglected tool in the instream flow incremental methodology. *Transactions of the American Fisheries Society* **124**: 645–662.

Marks K, Bates P. 2000. Integration of high-resolution topographic data with floodplain flow models. *Hydrological Processes* **14**: 2109–2122.

Marks SD, Rutt GP. 1997. Fluvial sediment inputs to upland gravel bed rivers draining forested catchments: potential ecological impacts. *Hydrology and Earth System Sciences* **1**: 499–508.

McCuen RH. 1989. *Hydrologic Analysis and Design*. Prentice Hall: Englewood Cliffs.

Merz JE. 2001. Association of fall-run chinook salmon redds with woody debris in the lower Mokelumne River, California. *Caliornia Fish and Game* **87**: 51–60.

Miller AJ. 1994. Debris-fan constrictions and flood hydraulics in river canyons: some implications from two-dimensional flow modelling. *Earth Surface Processes and Landforms* **19**: 681–697.

Miller AJ. 1995. Valley morphology and boundary conditions influencing spatial patterns of flood flow. In *Natural and Anthropogenic Influences in Fluvial Geomorphology*, Costa JE, Miller AJ, Potter KW, Wilcock PR (eds). American Geophysical Union: Washington, DC; 57–81.

Miller AJ, Cluer BL. 1998. Modeling considerations for simulation of flow in bedrock channels. In *Rivers Over Rock: Fluvial Processes in Bedrock Channels*, Wohl EE, Tinkler KJ (eds). American Geophysical Union: Washington, DC; 61–104.

Moyle PB, Randall PJ. 1998. Evaluating the biotic integrity of watersheds in the Sierra Nevada, California. *Conservation Biology* **12**: 1318–1326.

Moyle PB, Marchetti MP, Baldrige J, Taylor TL. 1998. Fish health and diversity: justifying flows for a California stream. *Fisheries* **23**: 6–15.

Nagasaka A, Nakamura F. 1999. The influences of land-use changes on hydrology and riparian environment in a northern Japanese landscape. *Landscape Ecology* **14**: 543–556.

National Marine Fisheries Service. 2001. *Annual Commercial Landing Statistics*. NMFS Fisheries Statistics and Economic Division: Washington, DC.

National Research Council. 1992. *Restoration of Aquatic Ecosystems: Science, Technology, and Public Policy*. NRC Committee on Restoration of Aquatic Ecosystems: Washington, DC.

Nehlsen W, Williams JE, Lichatowich JA. 1991. Pacific salmon at the crossroads: stocks at risk from California, Oregon, Idaho, and Washington. *Fisheries* **16**: 4–21.

Petts GE. 1996. Water allocation to predict river ecosystems. *Regulated Rivers: Research and Management* **12**: 353–365.

Platts WS, Megahan W. 1975. *Time Trends in Channel Sediment Size Composition in Salmon and Steelhead Spawning Areas: South Fork Salmon River, Idaho*. USDA Forest Service General Technical Report. Internountal Forest and Range Experiment Station: Ogden, Utah.

Poff NL, Allan JD, Bain MB, Karr JR, Prestegaard KL, Richter BD, Sparks RE, Stromberg JC. 1997. The natural flow regime. *BioScience* **47**: 769–784.

Sandecki M. 1989. Aggregate mining in river systems. *California Geology* **42**: 88–94.

Setka JD. 2000. *Fall-run Chinook Salmon and Steelhead Trout Spawning Survey, September 1999 Through January 2000 Mokelumne River, California*. East Bay Municipal Utility District: Lodi, CA.

Smart GM. 1999. Turbulent velocity profiles and boundary shear in gravel bed rivers. *Journal of Hydraulic Engineering* **125**: 106–116.

Soulsby C, Youngson AF, Moir HJ, Malcolm IA. 2000. Fine sediment influence on salmonid spawning habitat in a lowland agricultural stream: a preliminary assessment. *The Science of the Total Environment* **265**: 295–307.

Vadas RL. 2000. Instream-flow needs for anadromous salmonids and lamprey on the Pacific Coast, with special reference to the Pacific Southwest. *Environmental Monitoring and Assessment* **64**: 331–358.

Vyverberg K, Snider B, Titus RG. 1996. *Lower American River Chinook Salmon Spawning Habitat Evaluation*. California Department of Fish and Game: Sacramento.

Yoshiyama RM, Fisher FW, Moyle PB. 1998. Historical abundance and decline of chinook salmon in the Central Valley region of California. *North American Journal of Fisheries Management* **18**: 487–521.

Wang CL, Pasternack GB. 2000. *Application of a 2-D Hydraulic Model to Reach-scale Spawning Gravel Replenishment*. University of California.

Journal of Hydrology (2006) 328, 227–241

available at www.sciencedirect.com

SCIENCE DIRECT®

journal homepage: www.elsevier.com/locate/jhydrol

Error propagation for velocity and shear stress prediction using 2D models for environmental management

Gregory B. Pasternack [a,*], Andrew T. Gilbert [a], Joseph M. Wheaton [a,b], Evan M. Buckland [a]

[a] *Department of Land, Air, and Water Resources, University of California at Davis, 211 Veihmeyer Hall, One Shields Avenue, Davis, CA 95616-8626, USA*
[b] *Institute of Geography and Earth Sciences, University of Wales, Aberystwyth, Llandinam Building, Penglais Campus, Aberystwyth, Ceredigion SY23 3DB, Wales, UK*

Received 2 May 2005; received in revised form 9 November 2005; accepted 17 December 2005

KEYWORDS
Shear stress;
2D models;
River restoration;
Hydraulics

Summary Resource managers, scientists, government regulators, and stakeholders are considering sophisticated numerical models for managing complex environmental problems. In this study, observations from a river-rehabilitation experiment involving gravel augmentation and spawning habitat enhancement were used to assess sources and magnitudes of error in depth, velocity, and shear velocity predictions made at the 1-m scale with a commercial two-dimensional (depth-averaged) model. Error in 2D model depth prediction averaged 21%. This error was attributable to topographic survey resolution, which at 1 pt per 1.14 m^2, was inadequate to resolve small humps and depressions influencing point measurements. Error in 2D model velocity prediction averaged 29%. More than half of this error was attributable to depth prediction error. Despite depth and velocity error, 56% of tested 2D model predictions of shear velocity were within the 95% confidence limit of the best field-based estimation method. Ninety percent of the error in shear velocity prediction was explained by velocity prediction error. Multiple field-based estimates of shear velocity differed by up to 160%, so the lower error for the 2D model's predictions suggests such models are at least as accurate as field measurement. 2D models enable detailed, spatially distributed estimates compared to the small number measurable in a field campaign of comparable cost. They also can be used for design evaluation. Although such numerical models are limited to channel types adhering to model assumptions and yield predictions only accurate to ~20–30%, they can provide a useful tool for river-rehabilitation design and assessment, including spatially diverse habitat heterogeneity as well as for pre- and post-project appraisal.

* Corresponding author. Tel.: +1 530 754 9243; fax: +1 530 752 5262.
E-mail address: gpast@ucdavis.edu (G.B. Pasternack).

0022-1694/$ - see front matter
doi:10.1016/j.jhydrol.2005.12.003

Introduction

Two-dimensional hydrodynamic numerical (2D) models are now widely available at low cost and are being used in environmental science and management. Many previous studies have tested the spread in model predictions to variability in initial and boundary conditions (contingency analysis), parameter values (sensitivity analysis), wetting and drying schemes, and mesh discretization (e.g., Bates and Anderson, 1996; Tchamen and Kahawita, 1998; Hardy et al., 1999; Byrd and Furbish, 2000; French and Clifford, 2000). Some studies have used 2D models as a surrogate for large-scale manipulative experimentation that is impractical or disallowed in nature (Miller, 1995; Cao et al., 2003). Others have used 2D models for investigating geomorphic processes (e.g., Miller and Cluer, 1998; Nicholas and Walling, 1998; Rathburn and Wohl, 2003), flood inundation (Bates et al., 1992; Stewart et al., 1999), water quality and soil contamination (Moulin and Ben Slama, 1998; Stewart et al., 1998), and aquatic microhabitat quality (Leclerc et al., 1995; Ghanem et al., 1996; Tiffan et al., 2002). Beyond characterizing existing conditions, 2D models are now even being used to aid design and evaluation of river-rehabilitation projects in regulated gravel-bed rivers (Pasternack et al., 2004; Wheaton et al., 2004a,b). In these cases, model limitations are recognized and valued.

While all management tools have residual uncertainty that can never be eliminated, there are sources of quantifiable error whose constraint would boost confidence in the practical application of 2D models among a sometimes skeptical audience of academic scientists, resource managers, government regulators, and private consultants who are being confronted with such models with increasing frequency. One large source of uncertainty is model validation. Similar to the advancement from lumped to distributed hydrological models, changing from 1D to 2D hydrodynamic models should increase the breadth of model validation needed.

Previous environmental applications have used either cross-section or point-based measurements of downstream-directed flow components to determine depth and velocity prediction deviation from observations, often with little to no analysis of causes of error (e.g., Rathburn, 2001; Gard, 2003; Pasternack et al., 2004; Gard, 2005). Although flood inundation area can be validated using aerial photos or Synthetic Aperture Radar satellite imagery as a large-scale surrogate for the 2D depth pattern (Bates and De Roo, 2000), analogous approaches for validating large-scale 2D velocity pattern are lacking. Qualitative surface velocity-vector patterns may be observed using floating ropes or buoys that trace 2D particle paths as well as hand-sketches or movies of flow pattern. However, such approaches cannot identify subaqueous 2-layer velocity patterns.

To assess point-scale velocity vectors through depth in wadable gravel-bedded reaches, 2D or 3D sensors may be used (e.g., Rhoades and Kenworthy, 1995; Biron et al., 1998; Lane and Richards, 1998; Nicholas and Sambrook Smith, 1999). This approach is highly time-consuming and expensive. It is challenging to accurately record multiple flow components through depth over a $\sim 10^4$ m^2 area, while accurately referencing measurement direction to the 2D model's coordinate system, and impossible to do so simultaneously (Booker et al., 2001). Furthermore, it is unclear how to scale-up 0.5 mm point measurements to compare against averages over $\sim 0.5-3$ m^2 model cells. Also, moving 3D sensor data into a 2D model can introduce error through averaging methods. Attempts are being made to use boat-based 3D velocity profilers coupled to RTK GPS units for water depths >2 m (e.g., Shields et al., 2003), but this approach also averages over variable spatial scales that do not match the 2D-model computational scale and does not resolve the log-linear vertical velocity profile.

For regulated, gravel-bed river management, there is a need to predict sediment entrainment, which adds more error through the propagation of potentially inaccurate depth and velocity predictions through additional equations as well as the error inherent in shear velocity equations (Lane et al., 1999). Because gravel-bed rivers have a lower ratio of water depth to grain size than sand-bed rivers, they have more complex fluid mechanics and sediment transport boundary regimes. By definition, 2D models cannot produce vertical velocity gradients in lateral or downstream directions or produce up- and down-welling, all of which are important contributors to drag and lift forces responsible for grain entrainment (Nelson et al., 2001). Also, they do not represent hyporheic flow mechanics responsible for grain vibrations and possible ejections from the bed.

These deterministic limitations raise a serious challenge to the suitability of 2D models for use in sediment entrainment prediction. Are the ''lumped'' physics in 2D models sufficient to produce predictions at least as accurate as standard field-measurement methods and better than widely used 1D models? Through a detailed evaluation of the performance of 2D models in matching observed point velocity measurements, Lane et al. (1999) found that optimization of the bed roughness parameter within realistic limits yielded highly accurate estimates of downstream velocity, a primary variable governing sediment entrainment.

Despite this, Lane et al. (1999) proposed that 2D models be abandoned in favor of 3D models for predicting fluid dynamics and associated processes in gravel-bed rivers. 3D models ought to be superior given their more detailed representation of physics, and they do provide more accurate predictions of the lateral velocity component. However, depending on the particular environmental management application, 2D models may be more appropriate than 3D models. First, it is presently infeasible to collect 3D velocity data and transform it to calibrate and validate 3D models over $>10^4$ m^2 area. Second, many important geomorphic and ecological functions critical to environmental management have been related to depth-average hydraulics and are yet to be related to 3D fluid dynamics. Third, even where a geomorphic process has been related to 3D fluid dynamics, such as in the case of outer bank erosion in a meander bend, it is unclear which model node's shear stress component should be used to drive the process. Fourth, the number and configuration of secondary circulation cells in 3D models exhibit a sensitive dependence on boundary and initial conditions in some channel configurations, necessitating further basic research. Finally, although 3D models

include more physics than 2D models, they too are flawed representations of even more complex sediment entrainment phenomena, and thus involve ''lumped'' evaluation. The selection of 1D, 2D, or 3D predictive capability should hinge on predictive success relative to field observation for the particular environmental problem at hand, rather than theoretical grounds alone.

Improving the evaluation of depth, velocity, and shear velocity prediction in 2D models is an important basic science need prior to community acceptance or rejection of expanded utilization of 2D models in gravel-bed river management. In this study, 1906 metric tons of gravel were placed in a regulated river as a manipulative river-rehabilitation experiment according to a design that had been iteratively vetted with the aid of a 2D model. The overall question addressed here is whether the 2D model predictions of depth, velocity, and shear velocity used in the rehabilitation design and post-project evaluation process were sufficiently accurate for that purpose. Specific study objectives were to: (1) measure and characterize vertical velocity profiles over the artificially contoured gravel bed; (2) compare observed and 2D-model-predicted flow kinematics, including depth, velocity, and total shear velocity; (3) assess practical methods for estimating bed shear velocity from model-predicted total shear velocity. The conclusions suggest practical means of reducing prediction error for use of 2D models. As a next step beyond previous important contributions in this area (e.g., Lane et al., 1999), this study tests the utility of 2D models for use in regulated-river-rehabilitation projects.

Study site

River rehabilitation in Central Valley, California

River rehabilitation by gravel augmentation is being implemented in the Central Valley of California, USA in accordance with the CALFED Bay-Delta Program's Ecosystem Restoration Program Draft Stage 1 Implementation Plan to enhance aquatic habitat and rehabilitate fluvial geomorphic processes. Many rehabilitation projects are founded on research demonstrating that salmon-spawning habitat is a primary limiting constraint on fish populations in the Sacramento–San Joaquin river system (Moyle, 1994; Fisher, 1994; Brown, 2000). Access to historic spawning habitat has been blocked by dams (Moyle and Randall, 1998), with remaining downstream habitat suffering from flow regulation and water quality degradation due to adjacent land use (e.g., agriculture, gravel mining, and residential development).

In this study the Spawning Habitat Integrated Rehabilitation Approach (SHIRA) was used to aid experimental design. SHIRA integrates concepts from hydrology, ecology, biology, geomorphology, and engineering to design and evaluate alternative channel configurations for a degraded river (Pasternack et al., 2004; Wheaton et al., 2004a,b). Central to this approach is testing of predictions made by transparent design hypotheses regarding environmental processes over 10^{-1}–10^{4} m scales. In this SHIRA application, a 2D model aided evaluation of the relative performance of design alternatives and the final as-built experimental configuration down to the 0.1–1 m scale that fish are attune to (methodology detailed in Wheaton et al. (2004b)). Monitoring is used to evaluate SHIRA predictions (Merz and Setka, 2004; Merz and Ochikubo Chan, 2005; Merz et al., 2004; Wheaton et al., 2004c; Merz et al., in press) and drive adaptive management. Between 2001 and 2005 SHIRA was used on the Mokelumne River to manage placement and monitoring of 1633–5214 metric tons of gravel per year.

2002 Rehabilitation site

The present study was performed at the 2002 site located on the Lower Mokelumne River ~4 km downstream of Camanche Reservoir (Fig. 1(a)). The 2002 project included topographic feature creation at three spatial scales (Fig. 1(b)). At the reach scale (10^{2} channel widths), gravel was used to meet the river's coarse sediment budget demand, elevate the bed, and increase riffle slopes. At the geomorphic-unit scale (10^{1}–10^{2} channel widths), flow was routed through a sequence of 3 broad riffles and narrow pools to promote deposition on riffles and scour in pools. At the hydraulic unit scale (10^{-1}–10^{0} channel widths), 3 boulder complexes were used to encourage localized scour and create shear-zones, channel constrictions, hydraulic jumps, and standing waves. Also, pool exit slopes at pool-riffle transitions were shaped to promote intragravel flow and encourage flow to diverge across riffles.

Methods

To assess accuracy in 2D model predictions of depth, velocity, and shear velocity under typical post-rehabilitation conditions, field measurements and model predictions were made for the 2002 rehabilitation site for two different kinds of spatially explicit data. To assess spatially coherent lateral variability in depth and velocity associated with 10-m scale pool-riffle structure and 1-m scale bed-feature variability, depth and velocity were characterized along two cross-sections (Fig. 1(b)) with the same recently placed bed material. The cross-sections happened to be numbered 4 and 7 based on the pre-project model validation experimental design, but only 2 cross-sections were assessed post-project in favor of the second method of validation reported next. To assess variability in depth, velocity, and shear velocity in response to differing point-scale bed-material grain size, bed-features, and 2D flow patterns, measurements were made over twenty-three sediment tracer-cores (Fig. 1(b)) placed in regions of different flow patterns (e.g., convergent, divergent, uniform) as predicted by the 2D model within different geomorphic units (e.g., riffle, bar, glide). Each tracer-core contained individually sized grains taken from alluvial deposits along the Mokelumne River (~13,000 total), cleaned, measured, painted and sorted into four size classes: size class 1 = 8–32 mm, size class 2 = 32–64 mm, size class 3 = 64–128 mm, and size class unsorted with d_{50} = 27 mm and d_{84} = 43 mm (Table 1). Existing substrates were excavated down 37 cm with a modified McNeal sampler and replaced with tracer rocks (Fig. 2). One core with each grain-size class was placed in ~1 m intervals across a hydraulic region, yielding 6 different core-set locations (Fig. 1(b)). One of the 24 cores had flow

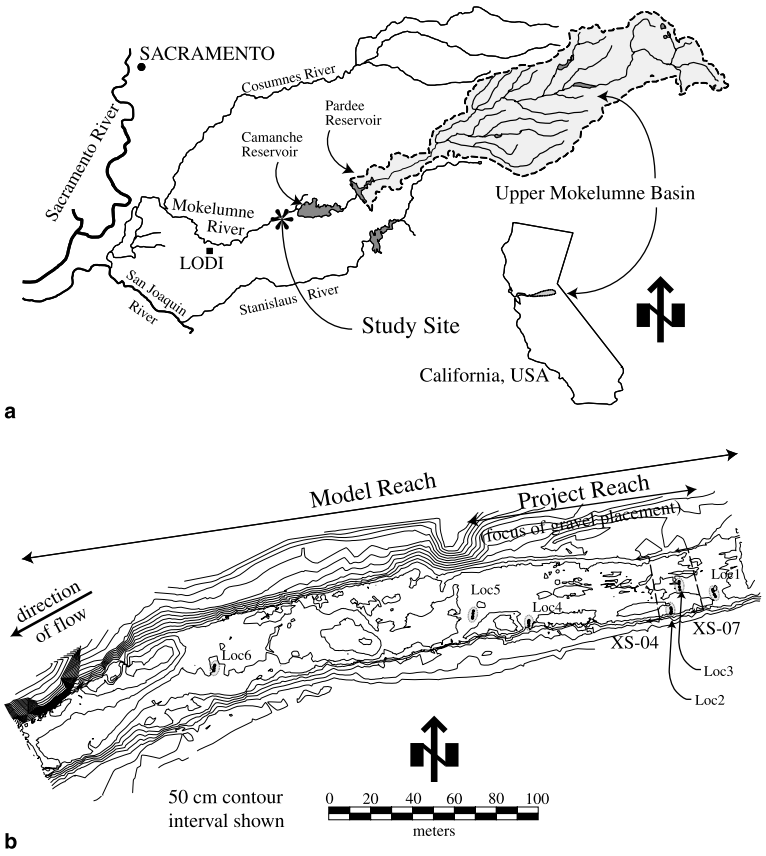

Figure 1 Study site maps: (a) Mokelumne River basin map; (b) topographic map of model domain showing gravel placement area as well as 2 cross-sections and 6×4 tracer-core locations.

over it that was too shallow to obtain data from for this study. Core points are denoted by location number and size class number (e.g., L1-sc1 for location 1 size class 1).

Observation data

Field observations of depth and velocity were made at 0.6-m intervals across the two cross-sections on 11/21/02 three months after project construction when the discharge was 7.73 $m^3 s^{-1}$, while depth and vertical velocity profiles at the 23 tracer-core points were collected through January 2003 when discharge was at a low spawning/incubation flow rate of 7.51 $m^3 s^{-1}$. For reference, the statistical bankfull discharge ($Q_{1.5}$) prior to Camanche Dam construction was 120 $m^3 s^{-1}$. In all cases, depth was measured using a stadia rod to a resolution of ±1 cm and point velocity was measured using an electromagnetic Marsh-McBirney Flo-Mate (±33 mm s^{-1} root mean square) sampling at 30 Hz and averaged over 10 s. For cross-section velocity data, a depth-setting wading rod was used to position the sensor at 0.6 of the depth to obtain a measure of the depth-averaged velocity. For vertical velocity profiles over tracer cores, the diameter of the sensor head (3 cm) limited the resolution of the profile and constrained the number of points obtainable depending on water depth at each point. Thus, measurements were made at elevations of 2 and 5 cm above the bed, and then at 5-cm intervals through depth yielding 3–10 measurements per profile. The depth-averaged velocity at a tracer-core point (U) was calculated as the mean of vertical profile measurements.

2D hydrodynamic modelling

The two-dimensional (depth-averaged) Finite Element Surface Water Modelling System model code (Froehlich, 1989) and Surface-water Modelling System (SMS) graphical interface (Environmental Modeling Systems, Incorporated) were used to predict site hydrodynamics at the 0.1–1 m scale relevant to microhabitat utilization and sediment entrainment. This 2D model uses a wetting and drying routine to determine channel boundary location. An element is ''dry'' when depth is below a user-defined threshold (set at 1 $D_{90} \sim 0.12$ m here) at all of its nodes. Model output included point-predictions of water depth, water velocity, and bed shear velocity. The equations built into the model for estimating bed shear velocity at each node were

$$u^* = U\sqrt{C_d} \text{ and } C_d = 9.81\frac{n^2}{d^{1/3}} \quad (1,2)$$

where u^* is shear velocity, U is depth-averaged velocity, C_d is the drag coefficient, n is Manning's n, and d is water depth (Froehlich, 1989). Shear velocity and Shields stress may be calculated from the available data, but this was not necessary for the assessment of uncertainty sought in this study, for which values of u^* were appropriate.

Table 1 Field-measured and model-predicted bed and flow characteristics at tracer-core locations

Site	Grain-size parameters			Measured		Model-predicted	
	D_{50} (m)	D_{84} (m)	D_{90} (m)	d (m)	U (ms^{-1})	d (m)	U (ms^{-1})
Yellow tracers at top flat riffle							
L1-scU	0.027	0.043	0.055	0.33	0.85	0.41	0.80
L1-sc1	0.021	0.028	0.029	0.32	1.20	0.36	0.96
L1-sc2	0.046	0.058	0.060	0.33	0.92	0.33	0.93
L1-sc3	0.088	0.138	0.153	0.24	0.70	0.41	0.89
Green tracers at front end of pool along left bank							
L2-scU	0.027	0.043	0.055	0.50	0.98	0.62	0.82
L2-sc1	0.021	0.028	0.029	0.50	1.01	0.27	0.16
L2-sc2	0.046	0.058	0.060	0.40	1.01	0.55	0.33
L2-sc3	0.088	0.138	0.153	0.40	1.12	0.55	0.58
Orange tracers on shallow bar in center of channel							
L3-scU	0.027	0.043	0.055	0.26	0.55	0.25	0.63
L3-sc1	0.021	0.028	0.029	0.18	0.36	0.24	0.51
L3-sc2	0.046	0.058	0.060	0.18	0.44	0.21	0.49
L3-sc3	0.088	0.138	0.153	0.28	0.53	0.31	0.57
Blue tracers between pools							
L4-scU	0.027	0.043	0.055	0.40	1.18	0.46	1.06
L4-sc2	0.046	0.058	0.060	0.36	1.04	0.40	1.09
L4-sc3	0.088	0.138	0.153	0.36	1.16	0.45	1.17
Pink tracers along pool to riffle transition							
L5-scU	0.027	0.043	0.055	0.26	0.53	0.19	0.88
L5-sc1	0.021	0.028	0.029	0.32	0.96	0.26	0.88
L5-sc2	0.046	0.058	0.060	0.24	1.04	0.24	0.84
L5-sc3	0.088	0.138	0.153	0.34	0.72	0.26	0.89
Dark green and white tracers on un-changed riffle downstream of project							
L6-scU	0.027	0.043	0.055	0.18	0.59	0.18	1.05
L6-sc1	0.021	0.028	0.029	0.20	0.92	0.19	0.93
L6-sc2	0.046	0.058	0.060	0.22	0.74	0.16	1.11
L6-sc3	0.088	0.138	0.153	0.20	0.80	0.16	1.19

Pasternack et al. (2004) and Wheaton et al. (2004b) detail validation and utilization of the model on the Mokelumne River. A site DEM was made in AutoCAD Land Desktop 2002i based on 3185 points surveyed with a Topcon GTS802A total station on a staggered-grid with supplemental features (average density of 0.88 pts m^{-2}). Point data augmentation (e.g., interpolation and user-specified spacing along contours) improved the DEM in areas with inadequate data. Refined topographic point and breakline data were exported to SMS. The 2D mesh was generated using a built-in adaptive tessellation algorithm without reference to the independently located depth and velocity measurement points. This independence provided a fair test of the accuracy of a 2D model without special attention to the mesh in the vicinity of validation locations. Node elevations were interpolated from imported DEM data using a TIN-based scheme. The mesh covered 16,930 m^2 of channel and banks with 23,957 computational nodes comprising 7830 elements, with the highest density near boulder clusters. The mesh's node density varied, but averaged 1.42 pts m^{-2}, which was significantly higher than that for the DEM.

Other than topography, the model's boundary conditions were steady state discharge (7.25 $m^3 s^{-1}$), corresponding water surface elevation at the downstream boundary (25.11 m in the NAVD88 vertical datum system), Manning's n bed roughness for well-mixed, placed gravels (0.043), and eddy viscosity (0.028 $m^2 s^{-1}$). Discharge was obtained from Camanche Dam (USGS station #11323500) for the flow used to compare pre-project, alternate design, and post-project conditions, so it was 5% lower than the average discharge of the field observations, which is a small unaccounted source of error. Water surface elevations associated with the studied flows were surveyed using the aforementioned total station with a vertical accuracy of ±2 cm. Manning's roughness (n) was estimated as 0.043 using a standard linear summation method (McCuen, 1989; Pasternack et al., 2004) over the spatially explicit Strickler's equation for roughness because the bed was artificially created using a homogenized source of gravel. A constant eddy viscosity value for the model was estimated from pre-project, cross-section based, field observations of depth and velocity; as $\nu = Cu^*R_h$ (Froehlich, 1989), where $C = 0.6$, R_h = hydraulic radius, and u^* was estimated using independent depth-averaged velocity data and the global z_0 velocity profile method explained below (using velocity at 0.6 of depth as depth-averaged velocity). Field-estimated

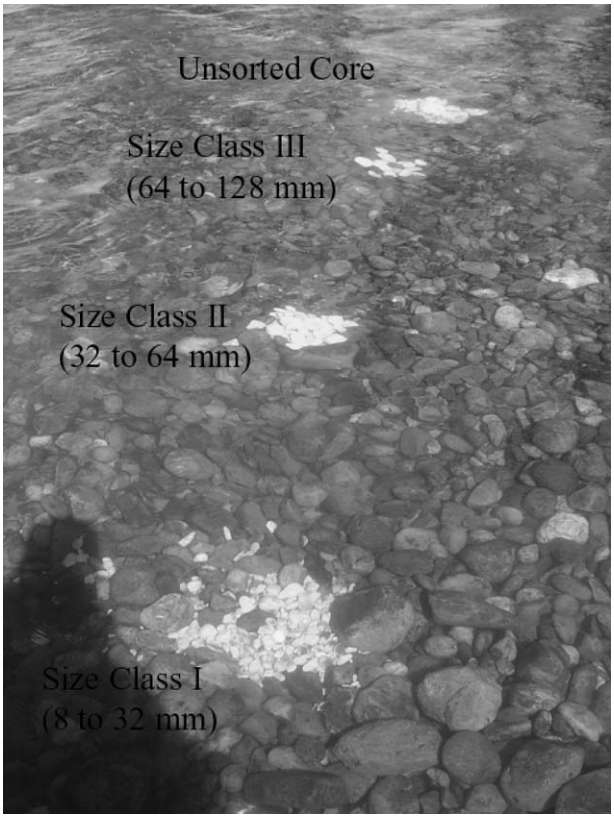

Figure 2 Photo of installed tracer-cores at location 1 illustrating size classes of cores and the size distribution of surrounding artificially placed coarse sediment.

v-values ranged from 9.3×10^{-4} to 0.033 $m^2 s^{-1}$, with a mean of 0.015 $m^2 s^{-1}$. The minimum stable value attainable with the model and subsequently used to obtain all results was 0.0279 $m^2 s^{-1}$. Field estimates and the final model value were in the same range to those reported by Pasternack et al. (2004) and Wheaton et al. (2004b).

Horizontal coordinates of cross-section endpins and tracer-cores were located within 5 cm using a GTS802A total station and imported into the 2D modelling domain. For the cross-sectional evaluation, model predictions at computational nodes along the line between endpins were extracted and plotted on the same graph with the cross-sectional field data, with no explicit matching of measurement locations. For tracer core comparisons, model depths and velocities at the exact locations of field measurement were obtained using TIN-based interpolation. Specifically, the centroid of an element is calculated, triangles are constructed in the element through the centroid, and then linear interpolation along the triangles is used to obtain data values. Since these data are from matching locations, predicted versus observed scatter plots and regression analysis were used to evaluate predictive accuracy.

Velocity profiles

The vertical velocity profile for steady, uniform, subcritical flow in a wide, straight channel with total roughness dominated by skin friction may be logarithmic over the whole flow depth (Wilcock, 1996). To assess this for tracer-core locations within the rehabilitation site with a known bed-material size, whole vertical velocity profiles were inspected for their shape and fitted with the logarithmic function

$$\frac{u}{u^*} = 5.75 \log_{10}\left(\frac{30.2z}{k_s}\right) \quad (3)$$

where u is velocity in the direction of flow, z is elevation above the bed and $k_s = 33z_o$ is the boundary roughness (Smart, 1999). The bed material placed at the site was the same across the whole area, so that reduced the error that would otherwise result from having a variable k_s. For each tracer-core, the bed material was nearly uniform in grain size, further reducing potential error in estimating k_s. When the stated assumptions are violated, Eq. (3) only applies to the bottom ~20% of the water column, above a near-bed ''roughness'' region and below an outer ''turbulent'' region (Wiberg and Smith, 1991; Wilcock, 1996). To test this assumption, depth-normalized velocity profiles may be assessed for slope breaks differentiating log-linear inner and outer profiles (Lawless and Robert, 2001), yielding skin friction and form drag, respectively. Unfortunately, in this study the size of the sensor head and low water depth limited the number of points available for profiles and proximity to the bed introducing uncertainty (Biron et al., 1998). However, previous studies have used a similar approach and successfully resolved profiles (e.g., Robert, 1997). Tiny sensors (<5 mm) may be more precise, but their measurements are strongly influenced by strong velocity variability induced by complex scales of bed roughness (Lawless and Robert, 2001), which is beyond the scope of Eq. (3) to address anyway.

Shear velocity estimation

Shear velocity in the form of u^* was estimated from field measurements using five methods and from model output using three methods, because there is no general consensus as to which approach is best for shallow gravel-bed river conditions. Eqs. (1,2) were applied to tracer-core and model-output datasets using depth-averaged velocity and were additionally applied to the field data substituting the near-bed (z = 2 cm) velocity for the depth-averaged velocity. Whole velocity profiles were fitted with Eq. (3) and values of u^* and k_s were obtained as a third method of estimating u^* from the field data. Wilcock (1996) compared the utility of depth-averaged velocities, point velocities in the lowest 20% of the flow, and slopes of whole velocity profiles for estimating local bed shear velocity. He noted that errors in u^* estimates from the slope of a velocity profile are ~8–9 times larger than those in u^* estimates based on depth-averaged velocities. Thus, u^* was calculated two different ways using the depth-integrated form of (3) assuming that $d \gg z_0$ (Wilcock, 1996; Smart, 1999).

$$u^* = \frac{U}{5.75 \log\left(12.2 \frac{d}{33 z_o}\right)} \quad (4)$$

where z_0 was calculated once as a global constant for all locations equal to $D_{84}/10$ (Wilcock, 1996) using the overall pebble-count grain size distribution for the site to get D_{84} and once individually derived for each location from the log-velocity profile according to Eq. (3). The two measures

of u^* from Eq. (4) were used for both tracer-core and model-output datasets.

To account for the error in u^* estimates due to limitations in field measurement, Wilcock (1996) linear error propagation formula was utilized for the depth-averaged u^* estimates. Expressed in proportional form, the standard error, $\alpha(u^*)$, for u^* was estimated as

$$\frac{\alpha(u^*)}{u^*} = \sqrt{\left(\frac{\alpha_U}{U}\right)^2 + \left(\frac{\alpha_d}{d\xi_d}\right)^2 + \left(\frac{\alpha_{D_p}}{D_p\xi_d}\right)^2} \quad (5)$$

where α_U and α_d are errors in U and d, respectively, α_{D_p} is taken to be $D_{90}/16$, D_p is taken as D_{84}, and $\alpha_d = \ln[11d/(3D_{84})]$ (Wilcock, 1996). The error in depth measurement was 1 cm. Because the method for u^* estimation assumes a logarithmic velocity profile, the error metric used as an estimate of α_U was taken as the deviation of actual profiles from the logarithmic ideal, which also accounts for sensor error. This was calculated as the mean plus two standard deviations in the data set ($n = 23$) of absolute values of the difference between the calculated mean velocity for a profile and the velocity value at 0.6* depth taken from the fitted logarithmic curve.

Results

Velocity profiles

All twenty-three vertical velocity profiles had statistically significant, highly correlative fits with a logarithmic profile over the whole flow depth (Fig. 3). Locations L2_sc2 and LS-scU had S-shaped profiles, while L2_sc1 had a nearly uniform profile for the upper 80% of depth overlying a linear profile for the lower 20% of depth. Individual log-profiles were significantly different in velocity magnitudes and velocity gradient as a function of depth. The deepest areas-L2 and L4- had more points in their velocity profiles allowing better resolution of the flow regions. Underlying tracer-core grain-size distributions did not explain differences between sites. The average ratio of velocity at 0.6* depth to depth-average velocity was 1.06 (±0.14 SD). The ratio of velocity at 2 cm above the bed to depth-averaged velocity showed more variability, averaging 0.41 (±0.23 SD). Locations L1_sc3 and L2_sc1 had upstream-directed near-bed velocities due to flow separation downstream of grain protrusions.

2D Model results

The model region contained three riffles and two pools, with the largest riffle being artificially constructed and including significant heterogeneity. According to the design and post-project model predictions (Fig. 4), initially planar flow over the upstream riffle crest was split into a main streamtube and a secondary streamtube by a boulder complex, where a streamtube is a 2D flow region of approximately parallel flow trajectories. Downstream the main streamtube was split again by a second boulder complex, with the majority of it constricted into a peripheral pool. Flow from secondary streamtube moved slower and diverged strongly around the second boulder complex and over the shallower riffle zone to cover the majority of channel width. The main flow tube was highly constricted along the left bank, but continued through a sequence of mid-depth diverging glides and constricting pools with high velocity variability. Meanwhile, the secondary streamtube was divided by a central longitudinal bar yielding more local divergence and convergence zones providing significant velocity variability. The shallow glide along the right bank was slow moving. At the end of the central bar, the main stream tube diverged out of a peripheral pool across a riffle crest and converged with the secondary streamtubes to yield high velocities over a stream-wide glide. An exposed sand and mud bar constricts the channel at this point accelerating the flow into the first of two deep pools in the study area. After that, flow strongly diverges over a wide, flat riffle and then becomes planar until it converges strongly yielding very high velocities over the second major pool. Finally, flow diverges over the last riffle entrance and flows planar over the riffle crest.

Depth prediction

Model depth predictions were compared against cross-sectional data for spatial patterns and tracer-point data for quantitative analysis. For the cross-sections, the DEM and 2D model captured the cross-channel variability of bed-features with a relief >20 cm but over-predicted depth (Fig. 5(a) and (c)). At tracer-core locations model predictions deviated from observed depths by an average of 21% (±17% SD), with a tendency to over-predict (Table 1; Fig. 6). No trend in predictability was found as a function of depth or local bed-material grain size, on the chance that local bed roughness could be a systematic source of error. The L2 points located on a pool entrance slope along the left bank (Fig. 1(b)) had the worst predictability. Of those, the one closest to the bank had the most under-predicted depth (45%) of all measured locations. In the 2D model this point was located between wet and dry nodes that were only 1 m apart. Model predictions in this zone should be treated with scepticism, because no effort was made address sub-grid scale variations in bank topography. If the bed elevation of the measurement point is manually subtracted from the water surface elevation of the adjacent wet node, then the resulting depth is predicted to be 0.41 m, which is within 18% of the measured value. The point with the worst over-prediction (71%) was L1_sc3 located on the first riffle crest. Since this location had the coarsest bed material ($D_{90} = 153$ mm), it is possible that the wading rod was randomly placed on top of a protruding cobble. Such an effect is at the sub-grid scale of the model.

Velocity prediction

Similar to the depth results, cross-sectional variations revealed the spatial pattern of velocity prediction accuracy while tracer-core comparisons provided quantitative metrics of accuracy. Due to short sampling times and the location of some sites in the vortex shedding zone downstream of placed boulders, measured velocities showed high fluctuations over short lateral distances. To counter this effect, a curve was fit to the data using the locally weighted Least Squared error method. Both cross-sections had structured lateral variations in velocity magnitude of 0.1—1 m s^{-1} at the 1—10 m

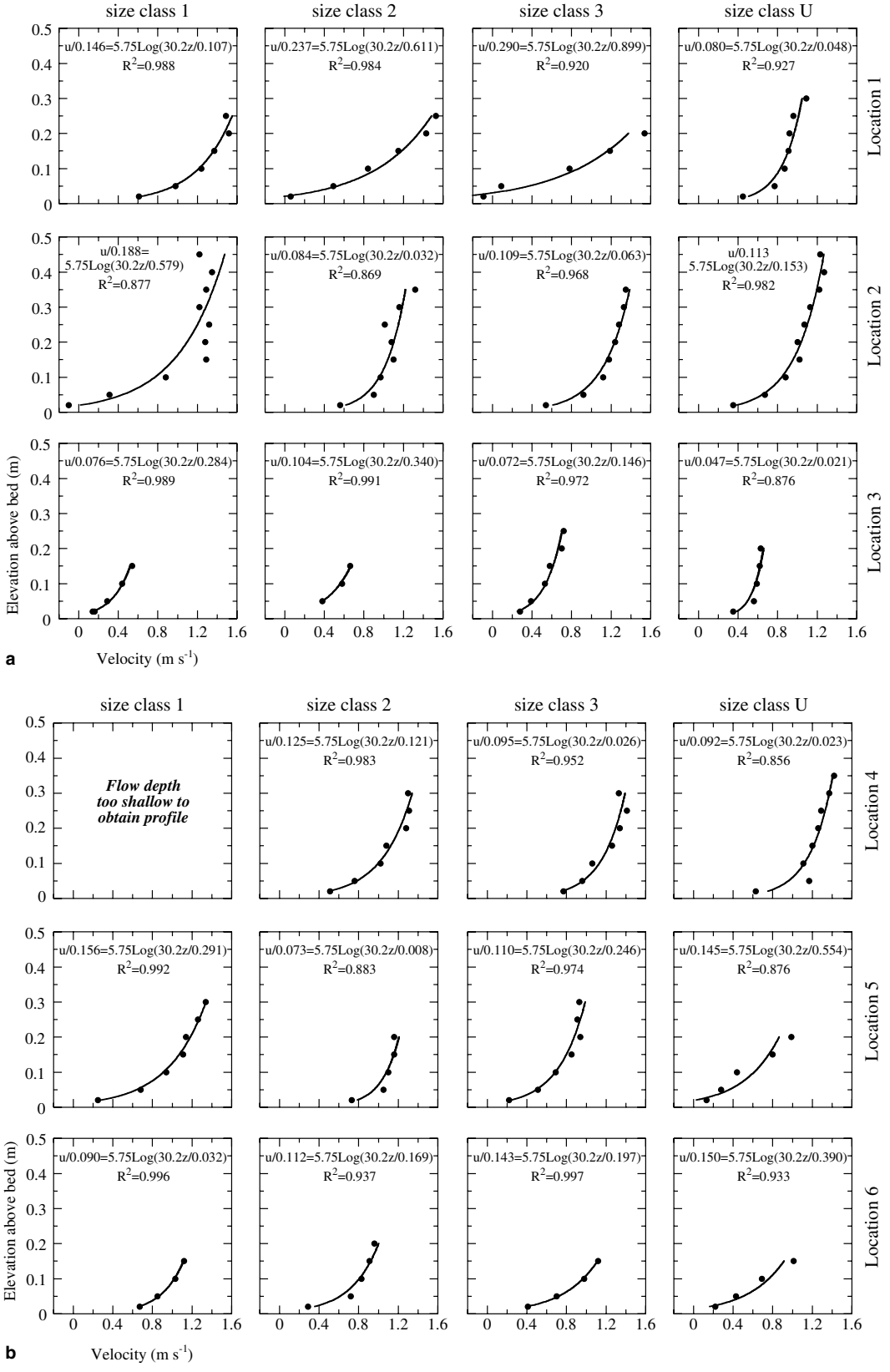

Figure 3 Vertical velocity profiles over 23 tracer-cores organized by location and size class.

spatial scale due to converging/diverging and accelerating/decelerating streamtubes around and over constructed bar features. Observed lateral variations in velocity were captured by the 2D model (Fig. 4(b) and (d)). Cross-section 4 showed a general over-prediction, with a 30—50% over-prediction over the central bar top. Given that both depth

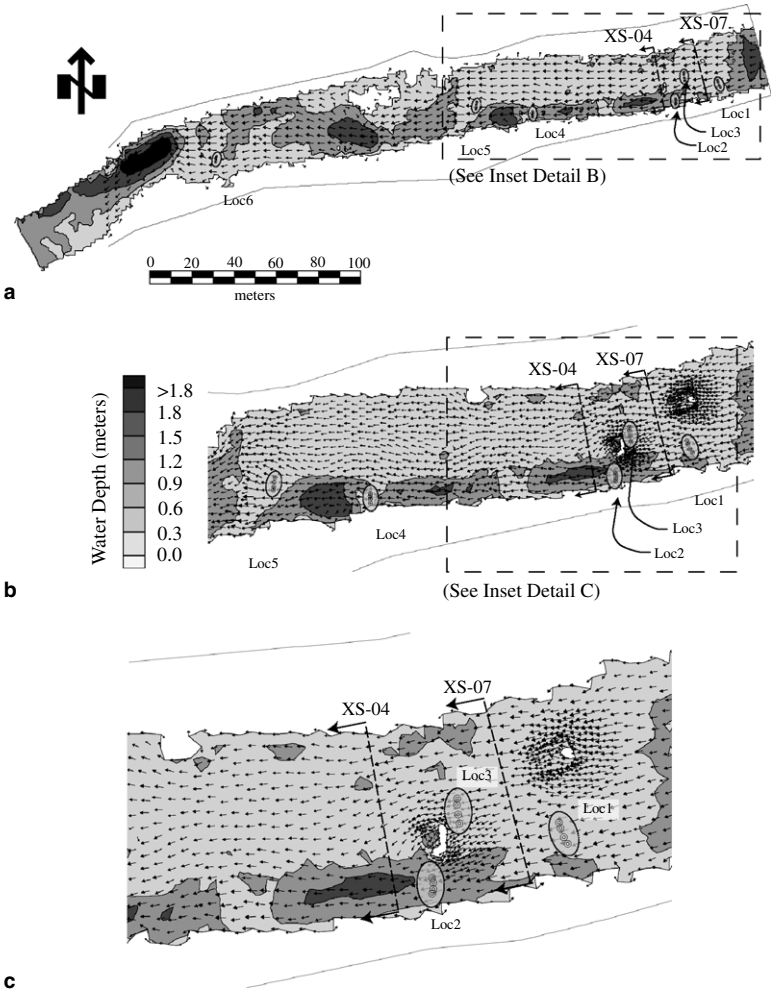

Figure 4 Post-project 2D model hydrodynamic predictions for the 2002 rehabilitation site at 7.25 cumecs. Shading corresponds to depth solutions and arrows correspond to velocity vectors (scaled to magnitude). Vector density reflects computation mesh resolution. Ovals with circles inside are tracer-core locations.

and velocity were over-predicted, optimization of the bed roughness parameter could not improve predictions of one without making the other worse. Cross-section 7 showed a close match between observed and predicted velocities. At tracer-core locations, velocities predicted by the 2D model deviated from velocity-profile mean velocities by an average of 29% (±26% SD) (Table 1; Fig. 7(a)).

Errors in velocity prediction were not a function of depth, local bed-material grain size, or velocity. Instead, the absolute value of error in depth prediction accounted for 56% of the variability in the absolute value of velocity error, with $p < 0.0001$ (Fig. 7(b)). According to the trend (excluding 2 outliers), each additional 1% increase in depth prediction error yielded a 1.5% error in velocity prediction overall. The data shows that where depth prediction error was 0—20%, velocity prediction error randomly varied between 0% and 20%. Also, whereas sites with depth prediction error >25% had velocity prediction errors varying randomly between 40% and 85%. The locations with the best predictability occurred on riffle tops (L1, L3, and L5). Those with the worst predictability occurred at the pool entrance close to the river-left bank (L2) and at the most downstream riffle (L6). Depths at L2 points were over-predicted, causing an under-prediction in velocity, and this effect was compounded by the retarding effect of the nearby bank in the model. For the highly over-predicted velocities of the L6 tracer points, the model had under-predicted the depth over sorted cores yielding the shallowest predicted depths of all test points. This depth-error produced skimming flow close to the Fr supercritical threshold, which may have increased the error. For L6-scU, there was no error in depth prediction, but the velocity was over-predicted by 78%. The velocity profile for this spot showed very low velocities (Fig. 3) that may have been so low because of the local roughness due to the unsorted bed material, which was not represented in the 2D model.

Total shear velocity prediction

Differences among field-observational methods for estimating u^* were larger than those between corresponding field-estimation and model-prediction u^* methods (Table 2). Minimum and maximum estimates of total shear velocity based

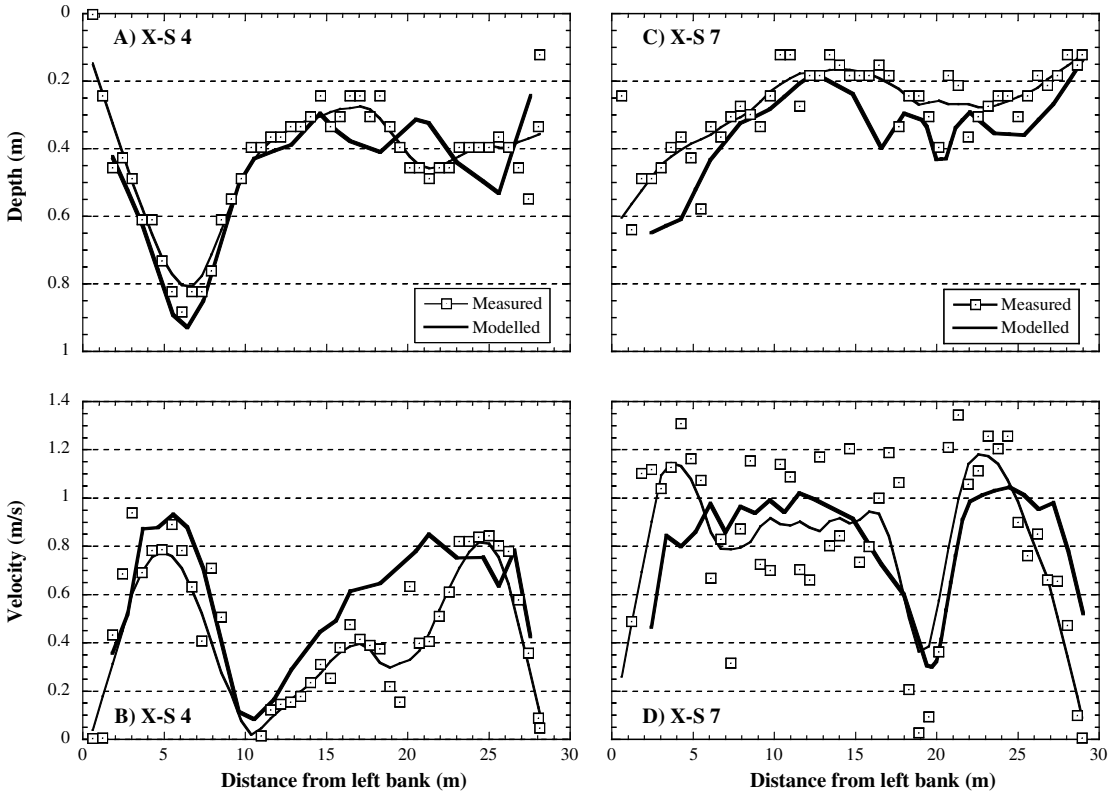

Figure 5 Comparisons of observed versus predicted depths and velocities at cross-sections 4 (a,b) and 7 (c,d). Field observations were fit with a curve using the locally weighted Least Squared error method to reduce measurement noise.

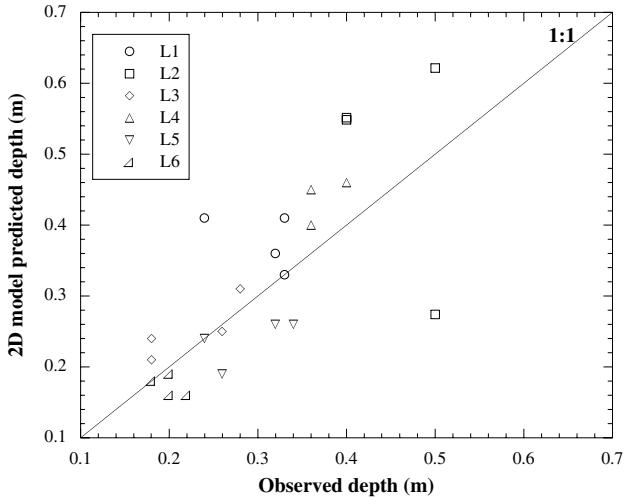

Figure 6 Observed versus predicted depths at 23 tracer-core locations showing the largest errors near the wet-dry boundary and where the DEM was faulty.

on four observational methods over each tracer-core differed by an average of 64% with a range of 5.6—160%. A comparison of field-estimation methods for u^* using U in Eqs. (1,2) versus using it in Eq. (4) shows that there is only a small difference between the two (Fig. 8). Meanwhile, shear velocities predicted by the 2D model deviated from field-estimated values by lower averages (and ranges) of 36% (0.6—99%), 31% (0.6—92% range), 31% (0.4—103%) using comparable Eqs. (1,2) and (4) with a global z_o, and Eq. (4) with a local z_o, respectively. For this case, this result contradicts the qualitative remarks of Lane et al. (1999) who state that their 2D model over-predictions of bed shear stress were ''ridiculous''. For the method of Eqs. (1,2), field-estimated and model-predicted values of C_d were similarly low (~0.02—0.03), with the only source of difference stemming from differences in depth, according to Eq. (2). For the method of Eq. (4) with a global z_o, more than half of predicted values fell within the 95% confidence limits of field-estimation uncertainty predicted using Eq. (5) (Fig. 9). Sixty-three percent of predictions using that method had less than 25% error. Of the 7 points with >50% error, 3 were at L6 where depth was <0.2 m (Fig. 3(b)) and 3 were at L2, whose challenging local conditions have already been described. The most poorly predicted point with an error of 91% was L5-scU. Error in the absolute value of velocity prediction accounted for 90% of the error in the absolute value of shear velocity model prediction (Fig. 10). When the 7 most poorly predicted points were corrected for velocity error, they had an average remaining error of 11% (±7.3% SD).

Bed shear velocity prediction

Because of the lack of distinguishable inner and outer regions with distinct log-linear vertical velocity profiles (Fig. 3), the only available method for estimating bed shears stress using the field data was to use Eqs. (1,2) with u

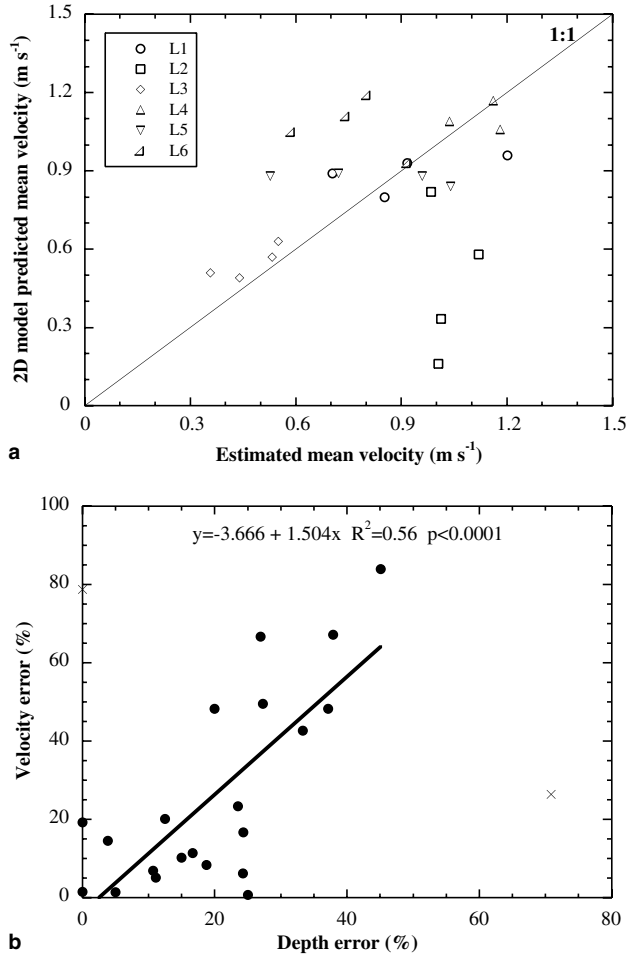

Figure 7 Assessment of velocity predictions at 23 tracer-core locations: (a) observed versus predicted depths and (b) analysis showing that depth error was the primary cause of error in velocity prediction (outliers have X-symbols).

measured at the position closest to the bed over each tracer-core. Compared to that estimated using Eqs. (1,2) with U, u^* estimated using the near-bed velocity averaged 57% lower, ranging from 27% to 93% lower. The variability in the difference between total versus near-bed u^* is primarily explained by the differing profile shapes (Fig. 3), with steeper velocity gradients as a function of depth corresponding to higher deviations between total and bed shear velocity (Fig. 11). Unfortunately, none of depth, depth-averaged velocity, or bed-material grain size explain the variability in whole-profile vertical velocity gradient. Instead, that variability is due to a complex array of variability in bed topography and resulting 3D flow structure processes. In general steeper vertical velocity gradients occurred over flat riffles with planar 2D flow patterns (L1 and L6) whereas gentle gradients occurred over pools with convergent flow (L2), riffle exits with divergent flow (L3), and mid-depth glides (L4). An exception to this was tracer-core L2-sc1, which had a sharp near-bed gradient underlying nearly uniform flow.

For practical application of 2D models for sediment entrainment prediction in shallow gravel-bedded rivers, an accurate estimate of near-bed u^*, not total u^* is needed. Despite the unaccountable sources of error inherent in the observed data due to the complex bed topography, a significant improvement in the prediction of near-bed u^* can be obtain by adjusting model output u^* with a constant multiplier. Using the Solver add-on to Microsoft Excel, the constant reduction multiplier in total u^* that yielded the lowest average absolute difference (29.5%) in total versus near-bed u^* was evaluated and found to be 0.51, though the standard deviation went up from 0.19 to 0.29. This shift brings the 2D model prediction of u^* well within the range of uncertainty for field-estimation of near-bed u^*. More studies are needed to determine the generality of a ~50% reduction in 2D model estimates to match observations, but the finding of this study substantiates that 2D models can be used to accurately estimate shear velocity in environmental management applications as long as significant effort is placed on accurately discretizing the topographic boundary condition and the difference between total and near-bed shear stress estimates is accounted for.

Discussion

In this study it was found that the error in 2D model predictions of depth, velocity, and shear velocity over well-mixed, double washed gravel averaged 21%, 29%, and 31%, respectively. These accuracies reflect the very challenging field conditions on a carefully constructed geomorphic-unit with highly complex 3D features by design. Depth error prediction was directly attributable to error in the DEM and thus was not primarily an error of the 2D model itself. More than half the error in velocity was in turn caused by depth error, and then 90% of the shear velocity error was caused by velocity error. Thus, the single most important factor in determining 2D model prediction accuracy is DEM accuracy.

Pasternack et al. (2004) addressed the topic of DEM accuracy in terms of the topographic survey (resolution and accuracy) and DEM generation methodology. In this study, the bed was surveyed with a resolution of 1 point every 1.14 m^2, which is quite high relative to previously published efforts and above that specified to capture typical gravel-bed morphology (Brasington et al., 2000). Even this resolution is still inadequate for comparison against typical 0.01-m scale positional measurements. Unlike sand-beds, gravel beds can have significant interlocking grain friction that is capable of sustaining complex pebble cluster morphologies, depressions, and bars at length scales of 0.001—1 m. These features may be created by flow processes and fish pedoturbation. It is now apparent that reducing the error of 2D model predictions at individual nodes from the 20% to 30% range to the <10% range must require higher survey-point densities than 1 point every 1.2 m^2. Robotic total station or RTK GPS surveys of wadable gravel beds with complex geometries are cost-effective for densities as high as ~2 pts per m^2. LIDAR remains problematic due to the biohazard of electromagnetic frequencies and amplitudes capable of penetrating water to sufficient depths clouded by sediment and bubbles. Boat-based echo sounder surveys yield extremely high resolution along boat transects, but also result in large gaps between transects. Tighter transects and future application of multi-beam sonar for shallow streams

Table 2 Field-estimated and model-predicted parameters and shear velocities at tracer-core locations

Site	Field estimated		Field-estimated u^* (ms^{-1})[a]					Model-predicted	Model-predicted u^* (ms^{-1})[a]		
	ks	Cd	a	b	c	d	e	Cd	a	d	e
Yellow tracers at top flat riffle											
L1-scU	0.048	0.026	0.138	0.073	0.080	0.130	0.077	0.024	0.125	0.113	0.069
L1-sc1	0.107	0.027	0.196	0.099	0.146	0.186	0.134	0.025	0.153	0.142	0.103
L1-sc2	0.611	0.026	0.149	0.010	0.237	0.141	0.195	0.026	0.151	0.142	0.198
L1-sc3	0.899	0.029	0.120	0.015	0.290	0.122	0.239	0.024	0.139	0.126	0.208
Green tracers at front end of pool along left bank											
L2-scU	0.153	0.023	0.149	0.053	0.113	0.129	0.107	0.021	0.120	0.101	0.084
L2-sc1	0.579	0.023	0.152	0.015	0.188	0.133	0.171	0.028	0.027	0.027	0.037
L2-sc2	0.032	0.025	0.159	0.088	0.084	0.144	0.081	0.022	0.049	0.042	0.025
L2-sc3	0.063	0.025	0.176	0.085	0.109	0.160	0.103	0.022	0.086	0.074	0.050
Orange tracers on shallow bar in center of channel											
L3-scU	0.021	0.028	0.093	0.059	0.047	0.093	0.044	0.029	0.107	0.108	0.051
L3-sc1	0.284	0.032	0.064	0.029	0.076	0.072	0.070	0.029	0.087	0.089	0.088
L3-sc2	0.34	0.032	0.079	0.025	0.104	0.088	0.094	0.031	0.086	0.091	0.097
L3-sc3	0.146	0.028	0.089	0.047	0.072	0.086	0.068	0.027	0.093	0.089	0.070
Blue tracers between pools											
L4-scU	0.023	0.025	0.185	0.099	0.092	0.168	0.088	0.023	0.162	0.144	0.077
L4-sc2	0.121	0.025	0.166	0.081	0.125	0.148	0.116	0.025	0.171	0.155	0.118
L4-sc3	0.026	0.025	0.185	0.123	0.095	0.165	0.091	0.024	0.180	0.160	0.088
Pink tracers along pool to riffle transition											
L5-scU	0.554	0.028	0.089	0.022	0.145	0.089	0.121	0.032	0.156	0.171	0.246
L5-sc1	0.291	0.027	0.156	0.041	0.156	0.149	0.148	0.028	0.148	0.148	0.148
L5-sc2	0.008	0.029	0.178	0.125	0.073	0.181	0.071	0.029	0.144	0.146	0.057
L5-sc3	0.246	0.026	0.116	0.035	0.110	0.109	0.102	0.028	0.150	0.150	0.139
Dark green and white tracers on un-changed pre-existing riffle downstream of project											
L6-scU	0.39	0.032	0.105	0.039	0.150	0.117	0.136	0.032	0.188	0.209	0.243
L6-sc1	0.032	0.031	0.162	0.118	0.090	0.174	0.085	0.032	0.165	0.180	0.087
L6-sc2	0.169	0.030	0.129	0.050	0.112	0.134	0.107	0.033	0.203	0.235	0.182
L6-sc3	0.197	0.031	0.141	0.072	0.143	0.151	0.128	0.033	0.218	0.252	0.208

[a] Methods are a = Eqs. (1,2) using U; b = Eqs. (1,2) using u_bed; c = Eq. (3); d = Eq. (4) using global z_o; e = Eq. (4) using local z_o.

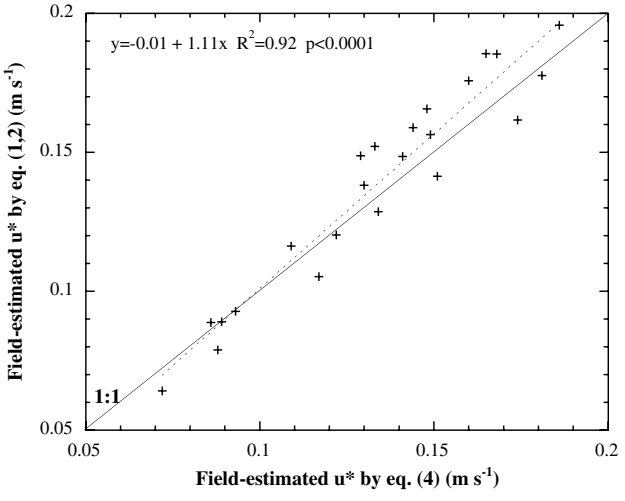

Figure 8 Comparison of u^* estimation methods using field-measured depth-averaged velocity and either Eq. (4) with a global z_o (open symbols) or Eqs. (1,2) (closed symbols).

may eventually provide progress towards solving the problem, and thus have the most promise for solving this fundamental problem with 2D model application.

Even though there is error in 2D model predictions, there is also substantial error in field measurements. Velocity measurement involves a sensor-size trade-off. Sensors that function at the 1—10 cm scale may not resolve all theoretical factors impacting vertical-velocity pattern, but appear to accurately measure depth-averaged velocity. With substantial effort they can map cross-channel velocity patterns. Conversely, those that function at the 0.1—10 mm scale may distinguish skin friction from form drag, but do so at the cost of high sensitivity to even more complex micro-scale flow patterns that cannot be addressed theoretically. This level of detail would not be cost-effective as a tool for spatial flow mapping for 2D model validation in river management applications. Meanwhile, shear velocity may be estimated using many different equations involving various field measurements. Resulting values typically differ by ~50—70%. The error in 2D model predictions of shear veloc-

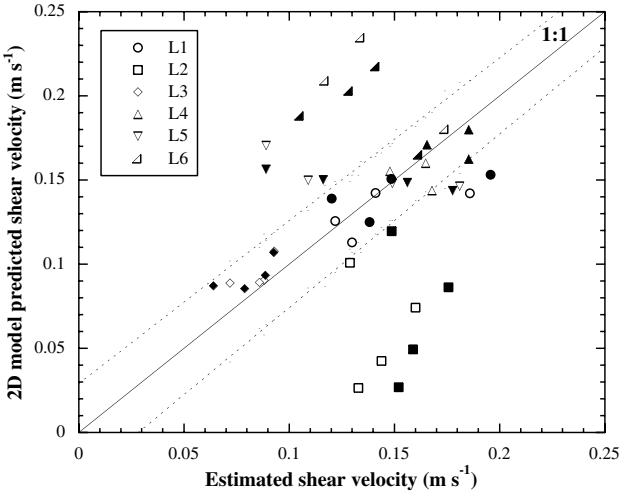

Figure 9 Estimated versus 2D-model-predicted u^* based on Eqs. (1,2) with depth-averaged velocity (filled symbols) and based on Eq. (4) using a global z_o (open symbols). Solid line is 1:1 while dashed lines are 95% confidence limits on open symbol estimates.

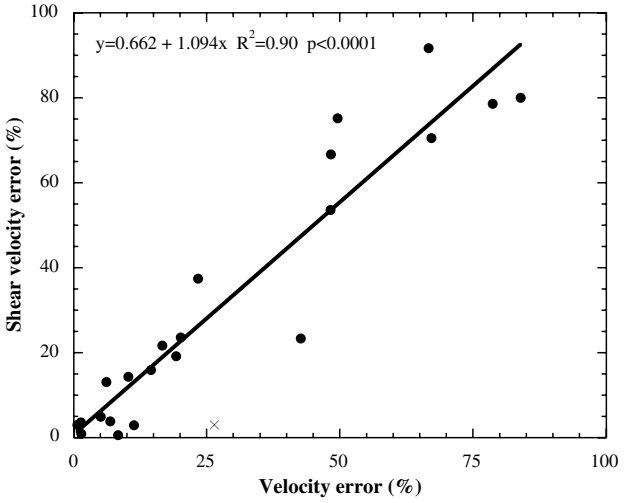

Figure 10 Analysis showing that velocity error was the predominant cause of error in u^* prediction (outlier has an X-symbol).

ity were within the 95% confidence limits of estimates based on field measurement ~60% of the time.

Given the errors reported above, it remains to be determined whether the 2D model application in this case is ''validated'' in light of the resultant numbers. Even though computational models solving the 2D St. Venant equations have been published, evaluated, and available for over 30 years, their increasing usage in scientific evaluation and societal management of complex river phenomena spanning hydrology, geomorphology, and ecology has re-raised the issue of model validation among a broader community. It is necessary to re-evaluate model assumptions for usage within the new settings they are being used as well as to validate model predictions for new functions that are extrapolated

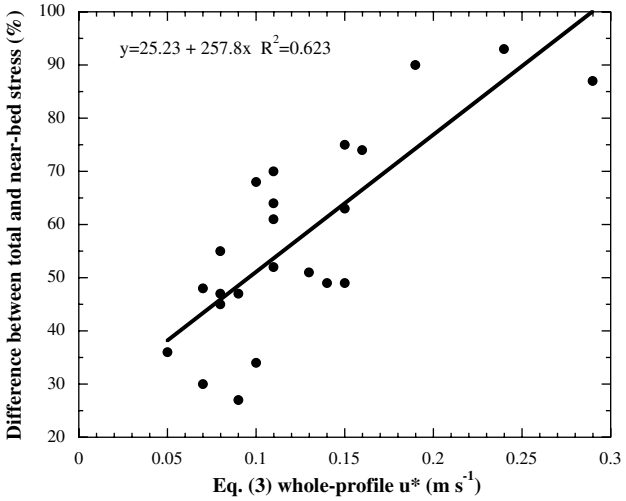

Figure 11 Analysis showing that the velocity gradient of the whole vertical velocity profile was the primary cause of the difference between total and near-bed u^*.

from model results through analytical, semi-analytical, or empirical relations. However, exactly what amount of error constitutes ''validation'' is unsettled in hydrology. Some rainfall-runoff studies as well as hydraulic studies use spatial or temporal pattern mimicry as sufficient validation, rarely presenting direct predicted versus observed plots and error estimates. This situation translates into confusion and conflict in the management arena.

At a minimum, when model predictions are within the range of error obtained in direct measurement or estimation based on measurement, then a model is at least as valid as measurement. This is the case with the 2D model shear velocity predictions made in this study. Despite the propagation of DEM errors through the model, the final predictions were accurate, except in very shallow locations close to the model threshold for drying. Thus, the 2D model is validated with respect to shear velocity. The magnitude of bed shear velocity predicted by the 2D model overestimates that obtained using near-bed velocity measurements by a factor of 2. Usage of this correction coefficient provides a simple and functional solution to the problem.

Validation of depth and velocity predictions depends on choosing a threshold level of error that is acceptable, and no universal threshold is identifiable. The threshold will depend on the purpose of the predictions and the associated level of accuracy needed. A finding from this study is that as much as 25% error in depth and 35% error in velocity prediction does not adversely affect shear velocity prediction enough to distinguish it from field-based estimation. Such thresholds will need to be determined for each new variable of interest as 2D model usage is expanded to address complex hydraulic—ecologic—geomorphic problems facing society.

Finally, it does appear that 2D depth, velocity, and shear velocity predictions were sufficiently accurate to conclude that 2D models can be an effective tool aiding river-rehabilitation design and pre- or post-project appraisal. Aquatic ecologists sought to include significant habitat heterogeneity in the rehabilitation project to reflect their occurrence

in undisturbed reference reaches. Neither steady, uniform flow equations (empirical or analytical) nor 1D computation models could resolve such 3D features. The 2D model could and did so successfully at the scale of 3–100 m. Where the 2D model did not perform well, was in resolving 0.1–1 m features that were inadequately mapped. At the scales where topographic features were resolved, post-project conditions were close to those predicted in the SHIRA design process, with most deviation due to the challenge of building the design using a rubber-tire front loader with limited depth capability. When viewed as one tool with its own limits and uncertainties among many such tools within a framework for site evaluation, a 2D model can shed significant insight into post-project conditions and help avoid costly mistakes.

Acknowledgements

Financial support for this work was provided by the US Fish and Wildlife Service (contracting entity for CALFED Bay-Delta Ecosystem Restoration Program: Cooperative Agreement DCN# 113322G003). The authors gratefully acknowledge EBMUD, Joe Merz, Jim Smith, Ellen Mantalica, Diana Cummings Brett Vallé, and Steven Winter for fieldwork assistance, helpful advice, administrative support, and equipment provision.

References

Bates, P.D., Anderson, M.G., 1996. A preliminary investigation into the impact of initial conditions on flood inundationpredictions using a time/space distributed sensitivity analysis. Catena 26, 115–134.

Bates, P.D., De Roo, A.P.J., 2000. A simple raster-based model for floodplain inundation. Journal of Hydrology 236, 54–77.

Bates, P.D., Anderson, M.G., Baird, L., Walling, D.E., Simm, D., 1992. Modelling floodplain flows using a two-dimensional finite element model. Earth Surface Processes and Landforms 17, 575–588.

Biron, P.M., Lane, S.N., Roy, A.G., Bradbrook, K.F., Richards, K.S., 1998. Sensitivity of bed shear velocity estimated from vertical velocity profiles: the problem of sampling resolution. Earth Surface Processes and Landforms 23, 133–139.

Booker, D.J., Sear, D.A., Payne, A.J., 2001. Modelling three-dimensional flow structures and patterns of boundary shear velocity in a natural pool–riffle sequence. Earth Surface Processes and Landforms 26, 553–576.

Brasington, J., Rumsby, B.T., Mcvey, R.A., 2000. Monitoring and modelling morphological change in a braided gravel-bed river using high resolution GPS-based survey. Earth Surface Processes and Landforms 25 (9), 973–990.

Brown, L.R., 2000. Fish communities and their associations with environmental variables, lower San Joaquin River drainage, California. Environmental Biology of Fishes 57, 251–269.

Byrd, T.C., Furbish, D.J., 2000. Magnitude of deviatoric terms in vertically averaged flow equations. Earth Surface Process and Landforms 25, 319–328.

Cao, Z., Carling, P., Oakley, R., 2003. Flow reversal over a natural pool-riffle sequence: a computational study. Earth Surface Processes and Landforms 28, 689–705.

Fisher, F., 1994. Past and present status of Central Valley chinook salmon. Conservation Biology 8 (3), 870–873.

French, J.R., Clifford, N.J., 2000. Hydrodynamic modeling as a basis for explaining estuarine environmental dynamics: some computational and methodological issues. Hydrological Processes 14, 2089–2108.

Froehlich, D.C., 1989. Finite Element Surface-water Modeling System: Two-dimensional Flow in a Orizontal Plane User's Manual. US Department of Transportation, Publication #FHWA-RD-88-177, p. 285.

Gard, M., 2003. Flow-habitat Relationships for Spring-run Chinook Salmon Spawning in Butte Creek. United States Fish and Wildlife Service, Energy Planning and Instream Flow Branch, Sacramento, CA, p. 86.

Gard, M., 2005. Monitoring of Restoration Projects in the Merced River Using 2-dimensional Modelling Methodology. United States Fish and Wildlife Service, Energy Planning and Instream Flow Branch, Sacramento, CA, p. 86.

Ghanem, A., Steffler, P., Hicks, F., 1996. Two-dimensional hydraulic simulation of physical habitat conditions in flowing streams. Regulated Rivers: Research and Management 12, 185–200.

Hardy, R.J., Bates, P.D., Anderson, M.G., 1999. The importance of spatial resolution in hydraulic models for floodplain environments. Journal of Hydrology 216, 124–136.

Lane, S.N., Richards, K.S., 1998. High resolution, two-dimensional spatial modelling of flow processes in a multi-thread channel. Hydrological Processes 12, 1279–1298.

Lane, S.N., Bradbrook, K.F., Richards, K.S., Biron, P.M., Roy, A.G., 1999. The application of computational fluid dynamics to natural river channels: three-dimensional versus two-dimensional approaches. Geomorphology 29, 1–20.

Lawless, M., Robert, A., 2001. Scales of boundary resistance in coarse-grained channels: turbulent velocity profiles and implications. Geomorphology 39, 221–238.

Leclerc, M., Boudreault, A., Bechara, J.A., Corfa, G., 1995. Two-dimensional hydrodynamic modeling: a neglected tool in the instream flow incremental methodology. Transactions of the American Fisheries Society 124, 645–662.

McCuen, RH., 1989. Hydrologic Analysis and Design. Prentice Hall, Englewood Cliffs.

Merz, J.E., Ochikubo Chan, L.K., 2005. Effects of gravel augmentation on macroinvertebrate assemblages in a regulated California river. River Research and Applications 21, 61–74.

Merz, J.E., Setka, J.D., 2004. Evaluation of a spawning habitat enhancement site for chinook salmon in a regulated California river. North American Journal of Fisheries Management 24, 397–407.

Merz, J.E., Setka, J., Pasternack, G.B., Wheaton, J.M., 2004. Predicting benefits of spawning habitat rehabilitation to salmonid fry production in a regulated California river. Canadian Journal of Fisheries and Aquatic Science 61, 1433–1446.

Merz, J.E., Pasternack, G.B., Wheaton, J.M., in press. Sediment Budget for Salmonid Spawning Habitat Rehabilitation in the Mokelumne River. Geomorphology, doi:10.1016/j.geomorph.2005.11.004.

Miller, A.J., 1995. Valley morphology and boundary conditions influencing spatial patterns of flood flow. In: Costa, J.E., Miller, A.J., Potter, K.W., Wilcock, P.R. (Eds.), Natural and Anthropogenic Influences in Fluvial Geomorphology. American Geophysical Union, Washington, DC, pp. 57–81.

Miller, A.J., Cluer, B.L., 1998. Modeling considerations for simulation of flow in bedrock channels. In: Wohl, E.E., Tinkler, K.J. (Eds.), Rivers Over Rock: Fluvial Processes in Bedrock Channels. American Geophysical Union, Washington, DC, pp. 61–104.

Moulin, C., Ben Slama, E., 1998. The two-dimensional transport module SUBIEF. Applications to sediment transport and water quality processes. Hydrological Processes 12, 1183–1195.

Moyle, P.B., 1994. The decline of anadromous fishes in California. Conservation Biology 8 (3), 869–870.

Moyle, P.B., Randall, P.J., 1998. Evaluating the biotic integrity of watersheds in the Sierra Nevada, California. Conservation Biology 12, 1318–1326.

Nelson, J.M., Schmeeckle, M.W., Shreve, R.L., 2001. Turbulence and particle entrainment. In: Mosley, M.P. (Ed.), Gravel-Bed Rivers V. New Zealand Hydrological Society, pp. 221–248.

Nicholas, A.P., Sambrook Smith, G.H., 1999. Numerical simulation of three-dimensional flow hydraulics in a braided channel. Hydrological Processes 13, 913–929.

Nicholas, A.P., Walling, D.E., 1998. Numerical modelling of floodplain hydraulics and suspended sediment transport and deposition. Hydrological Processes 12, 1339–1355.

Pasternack, G.B., Wang, C.L., Merz, J.E., 2004. Application of a 2D hydrodynamic model to reach-scale spawning gravel replenishment on the lower Mokelumne River, California. River Research and Applications 20 (2), 205–225.

Rathburn, S.L., 2001. Modeling Pool Sediment Dynamics in a Mountain River. Colorado State University, Ph.D Thesis. p. 204.

Rathburn, S.L., Wohl, E.E., 2003. Predicting fine sediment dynamics along a pool-riffle mountain channel. Geomorphology 55 (1–4), 111–124.

Rhoades, B.L., Kenworthy, S.T., 1995. Flow structure at an asymmetrical stream confluence. Geomorphology 11 (4), 273–293.

Robert, A., 1997. Characteristics of velocity profiles along riffle-pool sequences and estimates of bed shear velocity. Geomorphology 19, 89–98.

Shields, F.D., Knight, S.S., Testa, S., Cooper, C.M., 2003. Use of acoustic doppler current profilers to describe velocity distributions at the reach scale. Journal of the American Water Resources Association 39 (6), 1397–1408.

Smart, G.M., 1999. Turbulent velocity profiles and boundary shear in gravel bed rivers. Journal of Hydraulic Engineering 125, 106–116.

Stewart, M.D., Bates, P.D., Price, D.A., Burt, T.P., 1998. Modelling the spatial variability in floodplain soil contamination during flood events to improve chemical mass balance estimates. Hydrological Processes 12, 1233–1255.

Stewart, M.D., Bates, P.D., Anderson, M.G., Price, D.A., Burt, T.P., 1999. Modelling floods in hydrologically complex lowland river reaches. Journal of Hydrology 223, 85–106.

Tchamen, G.W., Kahawita, R.A., 1998. Modelling wetting and drying effects over complex topography. Hydrological Processes 12, 1151–1182.

Tiffan, K.F., Garland, R.D., Rondorf, D.W., 2002. Quantifying flow-dependent changes in subyearling fall chinook salmon rearing habitat using two-dimensional spatially explicit modeling. North American Journal of Fisheries Management 22, 713–726.

Wheaton, J.M., Pasternack, G.B., Merz, J.E., 2004a. Spawning habitat rehabilitation-1. Conceptual approach and methods. Journal of River Basin Management 2, 3–20.

Wheaton, J.M., Pasternack, G.B., Merz, J.E., 2004b. Spawning habitat rehabilitation-2. Using hypothesis development and testing in design, Mokelumne River, California, USA. Journal of River Basin Management 2, 21–37.

Wheaton, J.M., Pasternack, G.B., Merz, J.E., 2004c. Use of habitat heterogeneity in salmonid spawning habitat rehabilitation design. In: Fifth International Symposium on Ecohydraulics: Aquatic Habitats: Analysis and Restoration, IAHR-AIRH, Madrid, Spain. pp. 791–796.

Wiberg, P.L., Smith, J.D., 1991. Velocity distribution and bed roughness in high-gradient streams. Water Resources Research 27, 825–838.

Wilcock, P.R., 1996. Estimating bed shear velocity from velocity observations. Water Resources Research 32, 3361–3366.

WATER RESOURCES RESEARCH, VOL. 42, W10427, doi:10.1029/2005WR004391, 2006

Flow convergence routing hypothesis for pool-riffle maintenance in alluvial rivers

Michael L. MacWilliams Jr.,[1] Joseph M. Wheaton,[2,3] Gregory B. Pasternack,[3] Robert L. Street,[1] and Peter K. Kitanidis[1]

Received 29 June 2005; revised 28 April 2006; accepted 19 June 2006; published 31 October 2006.

[1] The velocity reversal hypothesis is commonly cited as a mechanism for the maintenance of pool-riffle morphology. Although this hypothesis is based on the magnitude of mean flow parameters, recent studies have suggested that mean parameters are not sufficient to explain the dominant processes in many pool-riffle sequences. In this study, two- and three-dimensional models are applied to simulate flow in the pool-riffle sequence on Dry Creek, California, where the velocity reversal hypothesis was first proposed. These simulations provide an opportunity to evaluate the hydrodynamics underlying the observed reversals in near-bed and section-averaged velocity and are used to investigate the influence of secondary currents, the advection of momentum, and cross-stream flow variability. The simulation results support the occurrence of a reversal in mean velocity and mean shear stress with increasing discharge. However, the results indicate that the effects of flow convergence due to an upstream constriction and the routing of flow through the system are more significant in influencing pool-riffle morphology than the occurrence of a mean velocity reversal. The hypothesis of flow convergence routing is introduced as a more meaningful explanation of the mechanisms acting to maintain pool-riffle morphology.

Citation: MacWilliams, M. L., Jr., J. M. Wheaton, G. B. Pasternack, R. L. Street, and P. K. Kitanidis (2006), Flow convergence routing hypothesis for pool-riffle maintenance in alluvial rivers, *Water Resour. Res.*, *42*, W10427, doi:10.1029/2005WR004391.

1. Introduction

[2] The velocity reversal hypothesis was introduced by *Keller* [1971] as a mechanism for understanding the maintenance of pool-riffle sequences in alluvial streams. This hypothesis was based on observations from Dry Creek, California, that "at low flow the bottom velocity is less in the pool than in the adjacent riffles" and that "with increasing discharge the bottom velocity in pools increases faster than in riffles" [*Keller*, 1971, p. 754]. The velocity reversal hypothesis proposes the removal of fine sediment from riffles into pools during low flows since velocity (or shear stress) is at a maximum over riffles [*Sear*, 1996]. As discharge rises, the velocity in pools increases and becomes greater than over riffles, resulting in a "velocity reversal." *Gilbert* [1914] first described this phenomenon noting that "at high stage ... the greater and smaller velocities have exchanged places," though it was *Keller* [1969, 1971] who first used the term 'velocity reversal' to describe this process. Since then, the velocity reversal hypothesis has initiated significant discussion in the literature and underlies a variety of conceptual models which attempt to describe the maintenance of pool-riffle morphology.

[3] Although Keller's proposal of the hypothesis focused on mean bottom velocities, subsequent studies have expanded the hypothesis to apply to mean boundary shear stress [*Lisle*, 1979], section-averaged velocity [*Keller and Florsheim*, 1993], and section-averaged shear velocity [*Carling*, 1991]. Other studies have focused on point measures of velocity and shear stress [*Petit*, 1987, 1990]. A brief synopsis of the primary studies which have addressed the velocity reversal hypothesis, including the type of study, the parameter evaluated, and our evaluation of the authors' support for the velocity reversal is given in the first three columns of Table 1. A more thorough discussion is presented by *MacWilliams* [2004].

[4] As seen in Table 1, the literature does not provide a clear consensus or single governing hypothesis for the mechanisms controlling pool-riffle morphology. Although there has been significant debate about whether a reversal of one or more flow parameters takes place, there is more general agreement that many cross-sectional average flow parameters in pools and riffles tend to converge as discharge increases [*Carling and Wood*, 1994]. While the literature suggests that a velocity reversal does occur in some cases, it is not clear whether a reversal of some type is a requisite for pool maintenance or whether the reversal hypothesis is applicable for all pool-riffle sequences. For example, *Clifford and Richards* [1992] found that a reversal or its absence could be demonstrated simultaneously for a given pool riffle sequence depending on the parameter evaluated, and the location of the measurement or cross section.

[1]Environmental Fluid Mechanics Laboratory, Department of Civil and Environmental Engineering, Stanford University, Stanford, California, USA.
[2]River Basin Dynamics and Hydrology Research Group, University of Wales, Aberystwyth, UK.
[3]Department of Land, Air, and Water Resources, University of California, Davis, California, USA.

0043-1397/06/2005WR004391$09.00

Table 1. Primary References Pertaining to the Velocity Reversal Hypothesis, With Our Best Assessment of the Type of Study, the Parameters Evaluated for a Reversal, and the Authors' Support for the Velocity Reversal and Flow Convergence Routing Hypotheses[a]

Reference	Type of Study	Reversal Parameter(s)	Support for Velocity Reversal	Support for Flow Convergence Routing
Keller [1969]	field	near-bed velocity	stated support	implied support
Keller [1970, 1971]	field	near-bed velocity	stated support	implied support
Keller [1972]	theoretical	N/A	not discussed	assumed support
Richards [1978]	1-d model	section average velocity and shear	inconclusive	not discussed
Lisle [1979]	field	mean shear stress	stated support	not discussed
Bhowmik and Demissie [1982]	field	N/A	negative	not discussed
Jackson and Beschta [1982]	field	near-bed velocity	stated support	assumed support
Lisle [1986]	field	N/A	not discussed	assumed support
Petit [1987, 1990]	field	point shear stress and velocity	inconclusive	assumed support
Carling [1991]	field	velocity, shear velocity	negative	implied support
Clifford and Richards [1992]	field	point and section-averaged velocity and shear stress	negative	implied support
Keller and Florsheim [1993]	1-D model	section average velocity	stated support	not discussed
Clifford [1993a, 1993b]	field	N/A	negative	assumed support
Carling and Wood [1994]	1-D model	section average velocity and shear velocity	conditional support	not discussed
Miller [1994]	2-D model	N/A	not discussed	assumed support
Sear [1996]	field, review	N/A	negative	not discussed
Thompson et al. [1996, 1998, 1999]	field, laboratory, 2-D model	Velocity	conditional support	assumed support
Booker et al. [2001]	3-D model	section average velocity, near-bed velocity, bed shear stress	conditional support	assumed support
Cao et al. [2003]	2-D model	bed shear stress, depth average velocity	conditional support	assumed support

[a]For the velocity reversal hypothesis, stated support indicates that the study supports the velocity reversal hypothesis for the case(s) analyzed; conditional support indicates that the study supported the velocity reversal under some conditions; inconclusive indicates that no firm statement of support or lack of support was made in the study; negative means the study rejected the hypothesis. For the flow convergence routing hypothesis, assumed support is applied to studies that explicitly discuss the significance of either a flow convergence or restriction for the study site(s), and it is assumed that these sites would support the flow convergence routing hypothesis; implied support applies to studies where these features were noted at the study site but not characterized as an important mechanism.

Support for a reversal hypothesis based on reversals in different types of flow parameters (as seen in Table 1) should be considered as a suite of multiple working hypotheses for explaining pool-riffle morphology rather than a single ruling hypothesis because different maintenance mechanisms may operate in different pool-riffle sequence. However, a review of all the published field data for sediment transport in pool-riffle sequences [*Sear*, 1996] has shown that a velocity or shear stress reversal does not explain all of the published evidence of sediment transport. Thus a more fundamental motivating question is that within systems that exhibit reversals of some kind, is the reversal an adequate explanation for pool maintenance? If not, and some alternative maintenance mechanism is hypothesized, can that alternative hypothesis explain pool maintenance in pool-riffle sequences that do not exhibit reversals?

[5] The extension of Keller's velocity reversal hypothesis from mean bottom velocity (as it was originally proposed) to section-averaged variables has been driven in part by the use of one-dimensional models to analyze pool-riffle sequences. *Keller and Florsheim* [1993] used a one-dimensional hydraulic model (HEC-RAS) to evaluate the velocity reversal hypothesis using Keller's original field data. They found that during high flows the mean pool velocity exceeded that of adjacent riffles, and that during low flows, the condition was reversed. Applying a similar model (HEC-2), *Carling and Wood* [1994] demonstrate the effect of varying channel width, riffle spacing, and channel roughness on the shear velocity, section mean velocity, and energy slope. However, in their results a reversal in the mean velocity took place only when the riffle was considerably wider than the pool. Similarly a "shear velocity reversal" took place only when the pool was rougher than the riffle. Both of these conclusions severely limit the conditions when a section-averaged velocity or shear velocity reversal could potentially occur and suggest that other mechanisms may be necessary to explain sediment transport in pool-riffle sequences. *Carling* [1991] found a convergence in mean velocity in pools and riffles in his study site, but concluded that riffles were not sufficiently wide at high flows to accommodate the known discharge with a velocity lower than in pools, and thus no velocity reversal was identified. Similarly, *Richards* [1978] found a narrowing of the difference in mean depth and velocity with discharge, but neither of these variables, nor surface slope or bed shear showed any tendency to equalize at the highest flow simulated. On the basis of their results, *Keller and Florsheim* [1993] concluded that more sophisticated models of the hydraulics associated with pool-riffle sequences will be able to explain in more detail the interaction between channel form and process in pool-riffle sequences in alluvial streams.

[6] There is a growing recognition that section-averaged data are not sufficient to explain the dynamics of pool-riffle sequences. Several studies have implemented two-dimensional models to simulate flow in pool-riffle sequences [e.g., *Miller*, 1994; *Thompson et al.*, 1998; *Cao et al.*, 2003]. Although *Miller* [1994] focused primarily on flow around a debris fan, his results identified the influence of flow convergence at the upstream end of the fan leading to the development of scour holes; thus his results demonstrate the importance of flow convergence in the formation of a riffle-pool sequence. Note that in this context "convergence" is used to define the physical process of funneling of flow rather than in the context of a narrowing difference between mean parameter values as it was used previously. Similarly, *Thompson et al.* [1998] identified the importance of a constriction at the head of the pool in creating a jet of locally high velocities in the pool center, and the formation of a recirculating eddy. *Cao et al.* [2003] found that at low discharge there exists a primary peak zone of bed shear stress and velocity at the riffle tail in line with the maximum energy slope, and a secondary peak at the pool head. With increasing discharge, the secondary shear stress peak at the head of the pool increases and approaches or exceeds the primary shear stress peak over the riffle. They also attributed the existence of a flow reversal in their simulation to the constriction at the pool head. *Booker et al.* [2001] applied a three-dimensional CFD model to a natural pool-riffle sequence. In their study, only three out of eight possible pool-riffle couplets experienced a mean velocity reversal. They found a tendency for near-bed velocity direction to route flow away from the deepest part of pools and suggest that this flow routing may have an important influence on sediment routing and the subsequent maintenance of pool-riffle morphology.

[7] Extensive field and laboratory observations have been made on the effects of flow constrictions on flow convergence and divergence, recirculating flow, and sediment routing. Constrictions resulting from debris fans [e.g., *Miller*, 1994; *Kieffer*, 1985, 1989; *Schmidt*, 1990] have been characterized by a flow regime consisting of a convergent flow upstream of the constriction, a beginning divergence out of the constrictions, and ultimately a downstream state of uniform flow not influenced by the constriction [*Kieffer*, 1985,1989]. *Schmidt* [1990] identifies the presence of a scour hole immediately downstream from most channel constrictions, and notes that recirculating currents can develop between the jet of flow exiting the constriction and the bank. *Thompson* [2004] has used laboratory experiments to investigate the influence of pool length on recirculating eddies and jet strength. Both *Thompson* [2004] and *Schmidt et al.* [1993] observed significant variation in instantaneous velocity field resulting in the recirculation zone, which indicates that average flow parameters are not sufficient to explain sediment transport. *Lisle and Hilton* [1992] observed nonuniform sediment deposition in pools which showed little correlation to water depth. They found that deposits were thickest under eddies and backwaters, but were commonly absent under the thalweg. Further, *Lisle and Hilton* [1992, p. 380] observed that "although some fine sediment is deposited in pools, boundary shear stress along the major sediment pathways in pools remained sufficient to maintain continued transport downstream." Similarly, *Jackson and Beschta* [1982] observed a nonuniform distribution of bedload transport across the channel resulting from a relatively large increase in velocity with discharge along the channel thalweg, with relatively little change in the lower velocities along the channel edges. This increase in velocity did not result in significant scour, but instead enabled bed material from the upstream riffle to be efficiently routed through the pool. These observations indicate that flow constrictions and a

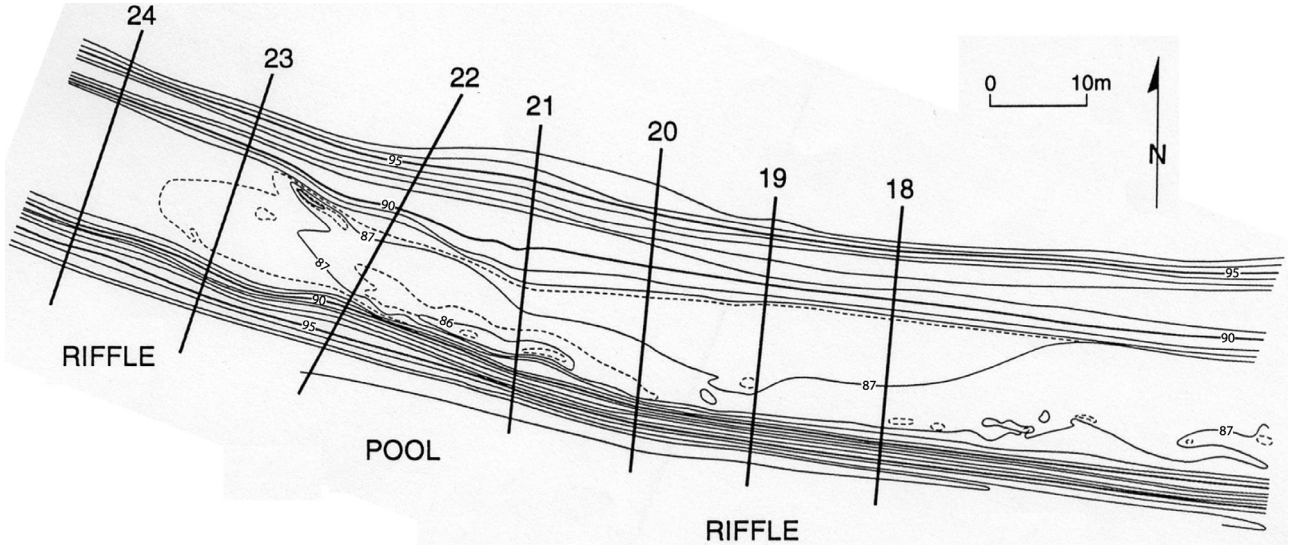

Figure 1. Topographic map of a riffle-pool-riffle sequence in Dry Creek near Winters, California. Contour interval is 1 foot (1 foot = 0.3048 m). Modified from *Keller and Florsheim* [1993]. Copyright 1993 John Wiley & Sons Limited. Reproduced with permission.

resulting nonuniform distribution of flow can have a significant impact on routing of sediment through pools.

[8] Drawing on this extensive literature, *Thompson et al.* [1996, 1998] have revised the traditional velocity reversal model to incorporate the effects of a channel constriction at the head of a pool. Their study demonstrated how the upstream constriction resulted in higher local velocities in the pool in comparison to adjacent riffles, despite a similar cross-sectional area. As noted by *Booker et al.* [2001], this concept links the concept of velocity reversal with work by *Keller* [1972] which suggested that the regular pattern of scour and deposition required for pools and riffles may be provided by an alternation of convergent and divergent flow patterns along the channel. This connection is significant because the pool-riffle sequence on Dry Creek has a point bar (on the north bank between sections 22 and 20 on Figure 1) which acts as constriction at the head of the pool. *Cao et al.* [2003] conclude that a channel constriction can, but may not necessarily, lead to [sediment transport] competence reversal, depending on channel geometry, flow discharge, and sediment properties. *Booker et al.* [2001] conclude that an analysis of near-bed velocity patterns suggested that the near-bed flow direction can cause routing of sediments away from the deepest part of the pools. Their results indicate maintenance of pool-riffle morphology by a lack of sediment being routed into pools rather than an increased ability to erode based on convergence of flow into the pool.

[9] The velocity reversal hypothesis was proposed by *Keller* [1971] based on bed velocity measurements in a pool-riffle sequence on Dry Creek, CA. The bed-velocity data [*Keller*, 1969, 1970] support a convergence of near-bed velocity, and a reversal in near-bed velocity is predicted for higher discharges. *Keller and Florsheim*'s [1993] one-dimensional modeling study support a reversal in mean velocity for the pool-rifle sequence on Dry Creek. The overall goal of this paper is to return to Keller's original data set to evaluate the flow processes in a pool-riffle sequence using two-dimensional and three-dimensional numerical simulations that may be able to explain the hydrodynamic mechanics underlying the observed conditions, which was not possible by previous one-dimensional simulation. Using both types of models not only provides a more complete assessment of the physical processes, but it also completes the systematic evaluation of the utility of different levels of process resolution. Specific objectives include (1) identifying pool-riffle "reversals" in near-bed velocity, depth-averaged velocity, section-averaged velocity, and bed shear stress, (2) evaluating the roles of secondary circulation and width constriction at the site, and (3) assessing whether the velocity reversal hypothesis is an adequate explanation for the maintenance of the pool-riffle morphology for this pool-riffle sequence. Although the study only investigates one site in detail, the hydrodynamic processes simulated in these models are transferable to other sites, and our analysis draws on both the extensive literature on pool-riffle morphology and experience on other rivers. On the basis of our analysis, a new "flow convergence routing" hypothesis for pool-riffle maintenance in alluvial rivers is proposed, which is consistent with Dry Creek conditions and those observed other sites reported in the literature. The new hypothesis is significant for its ability to explain why past studies on other field sites have differed in their assessment of the originally proposed velocity reversal mechanism.

2. Methods

[10] In this study, the Dry Creek reach mapped in Keller's original field study was modeled using both a two-dimensional and a three-dimensional hydrodynamic model. The models were validated using field data collected by *Keller* [1969] and compared against one-dimensional results from *Keller and Florsheim* [1993]. This approach allows for a detailed assessment of the capacity of one-, two- and three-dimensional models to capture the hydrodynamics and a strong basis for inference of important morphological processes that operate on this pool-riffle sequence. Specif-

ically, the one-dimensional results from *Keller and Florsheim* [1993] and the results from the two- and three-dimensional models applied in this study were used to assess whether a reversal in mean velocity occurred on Dry Creek. Further, the three-dimensional model was used to compare predicted bed velocity to the measurements from *Keller* [1971] and to evaluate whether a near-bed velocity reversal occurs, as Keller originally predicted. Lastly, the predicted bed shear stresses from the two- and three-dimensional simulations were used to evaluate whether a reversal in bed shear stress occurred and whether the spatial or temporal distribution of bed shear stresses indicate any other important mechanisms that could account for a reversal in sediment transport competence.

2.1. Two- and Three-Dimensional Modeling

[11] Two different numerical models were applied in this study. Although the two- and three-dimensional models were applied independently, to the extent possible, the model parameters used in the two- and three-dimensional simulations were equivalent to the model parameters used in the one-dimensional model presented by *Keller and Florsheim* [1993], to allow for a balanced comparison between the three models. The specific formulation of roughness, eddy viscosity, and boundary conditions were different in each model as described below, but the parameter values were calibrated to produce equivalent water surface elevations and cross-sectional area.

[12] Three-dimensional simulations were made using the three-dimensional nonhydrostatic hydrodynamic model for free surface flows on unstructured grids, UnTRIM, described by *Casulli and Zanolli* [2002]. The UnTRIM model solves the full three-dimensional momentum equations for an incompressible fluid under a free surface given by

$$\frac{\partial u}{\partial t}+u\frac{\partial u}{\partial x}+v\frac{\partial u}{\partial y}+w\frac{\partial u}{\partial z}-fv=-\frac{\partial p}{\partial x}+\nu^h\left(\frac{\partial^2 u}{\partial x^2}+\frac{\partial^2 u}{\partial y^2}\right)+\frac{\partial}{\partial z}\left(\nu^v\frac{\partial u}{\partial z}\right)$$

$$\frac{\partial v}{\partial t}+u\frac{\partial v}{\partial x}+v\frac{\partial v}{\partial y}+w\frac{\partial v}{\partial z}+fu=-\frac{\partial p}{\partial y}+\nu^h\left(\frac{\partial^2 v}{\partial x^2}+\frac{\partial^2 v}{\partial y^2}\right)+\frac{\partial}{\partial z}\left(\nu^v\frac{\partial v}{\partial z}\right)$$

$$\frac{\partial w}{\partial t}+u\frac{\partial w}{\partial x}+v\frac{\partial w}{\partial y}+w\frac{\partial w}{\partial z}=-\frac{\partial p}{\partial z}+\nu^h\left(\frac{\partial^2 w}{\partial x^2}+\frac{\partial^2 w}{\partial y^2}\right)+\frac{\partial}{\partial z}\left(\nu^v\frac{\partial w}{\partial z}\right)-g$$

where $u(x, y, z, t)$ and $v(x, y, z, t)$ are the velocity components in the horizontal x and y directions, respectively; $w(x, y, z, t)$ is the velocity component in the vertical z direction; t is the time; $p(x, y, z, t)$ is the normalized pressure defined as the pressure divided by a constant reference density; f is the Coriolis parameter; g is the gravitational acceleration; and ν^h and ν^v are the coefficients of horizontal and vertical eddy viscosity, respectively [*Casulli and Zanolli*, 2002]. Conservation of mass is expressed by the continuity equation for incompressible fluids

$$\frac{\partial u}{\partial x}+\frac{\partial v}{\partial y}+\frac{\partial w}{\partial z}=0.$$

The free surface equation is obtained by integrating the continuity equation over depth and using a kinematic condition at the free surface; this yields [*Casulli and Zanolli*, 2002]

$$\frac{\partial \zeta}{\partial t}+\frac{\partial}{\partial x}\left[\int_{-H^0}^{\zeta} u dz\right]+\frac{\partial}{\partial y}\left[\int_{-H^0}^{\zeta} v dz\right]=0,$$

where $h(x, y)$ is the prescribed bathymetry measured downward from the reference elevation and $\eta(x, y, t)$ is the free surface elevation measured upward from the reference elevation. Thus the total water depth is given by $H(x, y, t) = h(x, y) + \eta(x, y, t)$. The discretization of the above equations and model boundary conditions is presented in detail by *Casulli and Zanolli* [2002] and is not reproduced here. The UnTRIM model was modified to include an inflow boundary condition for volume and momentum, a radiation outflow boundary condition, and a modified formulation of bed drag and vertical eddy viscosity as described by *MacWilliams* [2004].

[13] The two-dimensional finite element surface water modeling system (FESWMS) was used to analyze depth-averaged hydrodynamics following the approach of *Pasternack et al.* [2004]. FESWMS solves the vertically integrated conservation of momentum and mass equations using a finite element method to acquire depth averaged 2D velocity vectors and water depths at each node in a finite element mesh. The model is capable of simulating both steady and unsteady two-dimensional flow as well as subcritical and supercritical flows. The basic governing equations for vertically integrated momentum in the x and y directions under the hydrostatic assumption are given by

$$\frac{\partial}{\partial t}(HU)+\frac{\partial}{\partial x}(\beta_{uu}HUU)+\frac{\partial}{\partial y}(\beta_{uv}HUV)+gH\frac{\partial z_b}{\partial x}+\frac{1}{2}g\frac{\partial H^2}{\partial x}+\frac{1}{\rho}\left[\tau_x^b-\frac{\partial}{\partial x}(H\tau_{xx})-\frac{\partial}{\partial y}(H\tau_{xy})\right]=0$$

and

$$\frac{\partial}{\partial t}(HV)+\frac{\partial}{\partial x}(\beta_{vu}HVU)+\frac{\partial}{\partial y}(\beta_{vv}HVV)+gH\frac{\partial z_b}{\partial y}+\frac{1}{2}g\frac{\partial H^2}{\partial y}+\frac{1}{\rho}\left[\tau_y^b-\frac{\partial}{\partial x}(H\tau_{yx})-\frac{\partial}{\partial y}(H\tau_{yy})\right]=0,$$

respectively, where H is the water depth, U and V are the depth-averaged velocity components in the horizontal x and y directions, z_b is the bed elevation, β_{uu}, β_{uv}, β_{vu}, and β_{vv} are the momentum correction coefficients that account for the variation of velocity in the vertical direction, τ_x^b and τ_y^b are the bottom shear stresses acting in the x and y directions, respectively, and τ_{xx}, τ_{xy}, τ_{yx} are the τ_{yy} shear stresses caused by turbulence. Conservation of mass in two dimensions is given by

$$\frac{\partial H}{\partial t}+\frac{\partial}{\partial x}(HU)+\frac{\partial}{\partial y}(HV)=0.$$

Discretization of the above equations for the FESWMS model is presented by *Froehlich* [1989], and is not reproduced here.

[14] The bathymetry for the Dry Creek field site [*Keller*, 1969] was digitized from a plane table survey contour map to generate a Digital Elevation Model (DEM) of the study reach in Autodesk's LandDesktop R3 Terrain Manager (Figure 1). The refined DEM data was then exported and interpolated onto each of the model grids. The total reach modeled is approximately 135 m long and ranges in width between 20 and 25 m. The FESWMS model used a finite element mesh with an approximately uniform node spacing of 0.45 m. This resulted in a model mesh with roughly 12,600 computational nodes comprising approximately 3500 mixed quadrilateral and triangular elements. For the UnTRIM model, an unstructured horizontal grid consisting of 23,655 cells triangular in planform was developed using TRIANGLE [*Shewchuk*, 1996]. The average grid cell size was 0.12 m^2. The seven cross sections in the study reach (Figure 1) were preserved in the model grids by aligning the edges of the model grid cells along the section lines. This facilitated direct comparison of model results with Keller's field data at specific cross sections. A uniform vertical grid spacing of 0.05 m was used for the UnTRIM simulations.

[15] *Keller* [1971] found that at low flow the Manning's *n* roughness coefficient in the pool-riffle sequence was 0.040 for the pool and 0.042 for the riffle. *Keller and Florsheim* [1993] used a roughness of 0.041 over pools and 0.043 over riffles in their simulations. *Keller and Florsheim* [1993] did a sensitivity analysis of bottom roughness by comparing their results using these values to a case where the roughness values were reversed and a case where a roughness of 0.041 was used in both the riffles and pools, and found no change in the relative velocities in the pools and riffles. They found that relative velocities are more dependent on channel geometry than on variation in roughness. Specification of bed roughness in a two- and three-dimensional model requires a spatially distributed roughness specified at each grid point, rather than coefficient at each cross section. In addition, this parameter represents only the effect of bed roughness, rather than encompassing all forms of energy loss in the channel as it does in a one-dimensional model. In the FESWMS model and the UnTRIM model, the bed roughness value is the principal calibration parameter used to calibrate the water surface slope. As a result, the bed roughness values were selected such that the predicted water surface matched the observed water surface. Because a detailed mapping of roughness for the Dry Creek site was not available, a constant roughness parameter was applied in both the FESWMS and the UnTRIM simulations. In the FESWMS simulations the Manning's *n* roughness was estimated as 0.041 for entire study site. For the UnTRIM simulations a constant z_o roughness of 1.5×10^{-3} m was applied. On the basis of the method described by *MacWilliams* [2004], this roughness height corresponds to a Manning's *n* value of approximately 0.041 for the range of flow depths simulated. The results from the UnTRIM and FESWMS simulations suggest that the roughness values selected primarily influence the water surface slope, and that the primary flow features are controlled by the channel geometry. Although local variations in roughness are likely to influence local shear stress values and bed velocity values, the large-scale flow features observed in this study are primarily controlled by the geometry of the pool-riffle sequence. This corroborates *Keller and Florsheim*'s [1993] conclusion that relative velocities are more dependent on channel geometry than on variation in roughness.

[16] For the FESWMS simulations, Boussinesq's analogy was applied to parameterize eddy viscosity, which crudely approximates eddy viscosity as an isotropic scalar. Doing so allows a theoretical estimate of eddy viscosity as 60 percent of the product of shear velocity and depth [*Froehlich*, 1989]. A constant eddy viscosity value of 0.027 m^2/sec was used for all FESWMS model runs. It is well known that the eddy viscosity has a nearly parabolic distribution with depth in an open channel flow and that the use of a constant eddy viscosity for three-dimensional simulations is likely to yield unrealistic vertical velocity profiles [*Rodi*, 1993]. As a result, in uniform open channels, the velocity profile is often assumed to be logarithmic, resulting in a parabolic eddy viscosity distribution [*Celik and Rodi*, 1988]. For the UnTRIM simulations, a parabolic vertical eddy viscosity model was applied following the approach of *Celik and Rodi* [1988].

[17] Keller's original field measurements [*Keller*, 1969, 1971] were made at discharges of 0.42, 0.97, and 4.5 m^3/s. The HEC-RAS model simulations by *Keller and Florsheim* [1993] were conducted for five steady flow rates, including the three discharges measured by *Keller* [1969] and two larger discharges of 8.5 and 17 m^3/s. These five flow rates were modeled as five separate steady flow simulations in FESWMS; in UnTRIM a transient simulation of each flow rate was run until the flow field reached a "steady state." In both UnTRIM and FESWMS, the inflow discharge was specified at the upstream end of the channel using a uniform velocity distribution; at the downstream end of the channel, the water surface elevation was specified based on the elevations predicted at the downstream cross section from the modeled results of *Keller and Florsheim* [1993]. To allow direct comparison with previous studies, we evaluated the model results at the pool cross section (section 19, Figure 1) and riffle cross section (section 21, Figure 1) used in the analysis of *Keller* [1971] and *Keller and Florsheim* [1993].

2.2. Model Validation

[18] The UnTRIM and FESWMS models have previously been validated in a number of applications [cf. *Casulli and Zanolli*, 2002; *MacWilliams*, 2004; *Froehlich*, 1989; *Pasternack et al.*, 2004]. For this application, the models were validated using field data collected by *Keller* [1969] to the extent possible recognizing the technological limitations and differing purpose of the original work. Validation of detailed numerical models against historical field data poses a significant challenge, because only sparse data are available for validation purposes. At the Dry Creek field site, the primary objective of the data collection effort was for the bed load movement experiments reported by *Keller* [1969, 1970], and only limited point velocity and water surface elevation data are available. Bed velocity measurements were made at the pool cross section (section 21) and riffle cross section (section 19) for 0.42, 0.97, and 4.5 m^3/s discharges. Velocity was also measured at 0.6 times the depth for the 0.42 and 0.97 m^3/s discharges. Observed cross-sectional areas for the pool and riffle cross sections were reported by *Keller and Florsheim* [1993], while observed depths at these cross sections are available only for the 0.97 m^3/s discharges (E. A. Keller, unpublished field

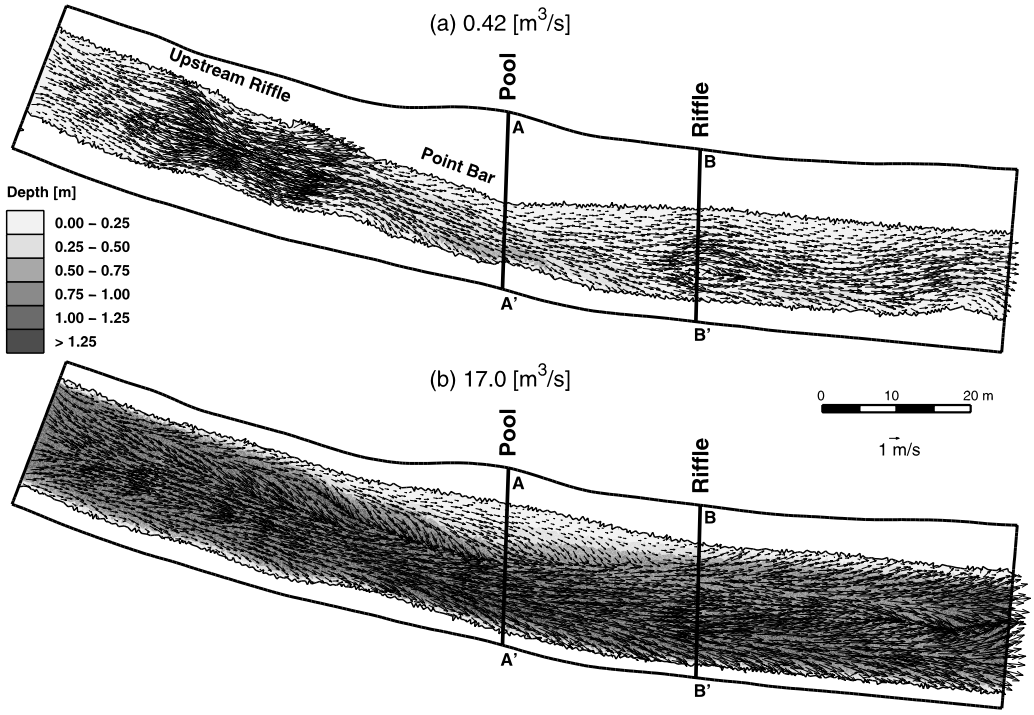

Figure 2. Predicted surface velocity vectors and depth on Dry Creek for (a) 0.42 and (b) 17.0 m^3/s flow rates. Surface velocities are shown for a subset of the UnTRIM computational cells.

notebook, 1969). The stations where these point data were collected are measured along each cross section but the exact starting position for each transect is not precisely reported; the alignment used was estimated using water surface edges and depths where available. While more detailed data collection using modern instruments would allow for more thorough model validation, we recognize that the available data was collected for a different purpose, and with relatively little quality control. Where the model results deviate from the available data, multiple data types have been used to help understand these differences. These comparisons highlight some potential shortcomings in the available data, and suggest that, while a reasonable level of validation can be achieved, some remaining differences may result from uncertainty in available observation data rather than model uncertainty.

2.3. Bed and Depth-Averaged Velocity

[19] On the basis of bed velocity measurements on Dry Creek, *Keller* [1971] predicted the occurrence of a bed velocity reversal. *Keller* [1969] believed that the "bottom velocity is much more significant in analyzing bed load movement than the mean velocity of the entire stream." Keller collected velocity measurements near the bed at three foot intervals along each of four cross sections during measured discharges of 0.42, 0.97, and 4.5 m^3/s. Velocities near the bed were measured with at rod-mounted, pigmy Price current meter [*Keller*, 1970]. For comparison with the bottom velocity measured by Keller, the velocity predicted using UnTRIM in the bottom two cells in each water column was interpolated to estimate the average velocity at a depth of 5 cm. On the basis of the geometry of the instrument used, this seems to be a reasonable estimate of the lowest height at which the velocity could feasibly be sampled. Because the pigmy Price current meter method does not measure flow direction and assumes all flow is in one direction, the overall velocity magnitude predicted by UnTRIM is used rather than only the downstream flow component. This distinction is significant for areas in which significant secondary circulation exists near the channel bed. Comparisons of bed velocity were not made using the FESWMS results, since FESWMS is a depth-averaged model. Depth-averaged velocities from FESWMS were compared to velocities measured at 0.6 times the depth for the 0.42 and 0.97 m^3/s discharges.

2.4. Section-Averaged Velocity

[20] *Keller and Florsheim* [1993] extended *Keller*'s [1969] original proposal of a reversal in bed velocity to a reversal in mean cross-section velocity. In their analysis, the field measurements from *Keller* [1969] were averaged over the pool and riffle cross sections and HEC-RAS was used to model section-averaged velocity. In this study, the predicted flow fields from FESWMS and UnTRIM at the pool and riffle cross sections were also averaged at the pool and riffle cross sections to obtain the cross-sectional average velocities for each of the five flow rates. These average velocities were compared to the results presented by *Keller and Florsheim* [1993].

2.5. Bed Shear Stress

[21] The predicted bed shear stress was calculated over the model domain for both the UnTRIM and FESWMS simulations. For the FESWMS simulations, the depth-averaged shear stress was calculated from depth, velocity, and bed roughness using a drag force relation [*Froehlich*, 1989]. Bed shear stress for the FESWMS simulation was calculated as 0.51 times the depth-averaged shear stress based on a detailed validation study (*Pasternack et al.*, submitted for

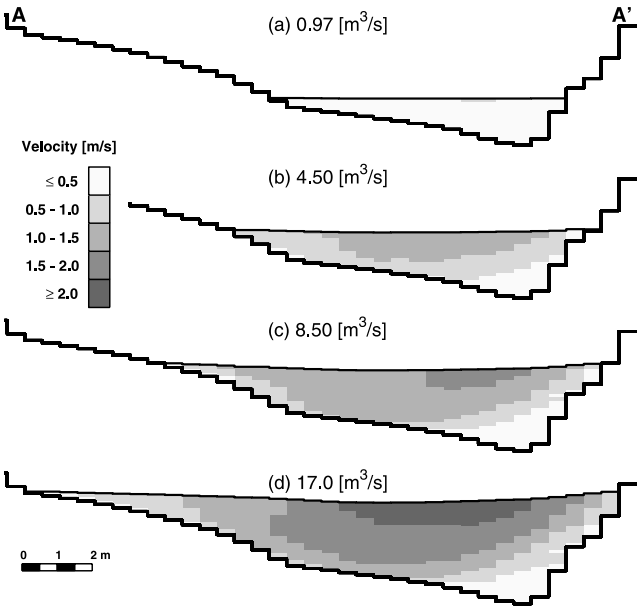

Figure 3. Downstream velocities at pool cross section predicted using UnTRIM for five flow rates. Cross sections are shown with 2 times vertical exaggeration.

publication, 2005). In the UnTRIM simulations, the bed shear stress was calculated from the near-bed velocity by assuming a log law near the bed [*MacWilliams*, 2004].

3. Results

[22] The predicted surface velocity and flow depth from the UnTRIM simulation for the 0.42 and 17.0 m^3/s discharges are shown in Figure 2. At a discharge of 0.42 m^3/s the highest surface velocities are predicted over the riffle upstream of the pool cross section and over the riffle cross section. The pool cross section is significantly narrower than the upstream riffle or the downstream riffle due to the point bar, and there is little variation of surface velocity across the pool cross section. The flow width increases downstream of the point bar, and flow is diverted around a local topographic high near the riffle cross section. Downstream of the riffle cross section the flow is more uniform. At a discharge of 17.0 m^3/s, the flow is fairly uniform across the upstream riffle but there is a noticeable deflection of surface velocities away from the shallow portions of the point bar as the flow approaches the pool cross section. The point bar is flooded, but low surface velocities are predicted in the shallower areas on the point bar; the highest predicted surface velocities at the pool cross section occur within a narrow zone midway across the section. As seen in Figure 2, the pool cross section widens more with discharge than the riffle cross section, such that at the 17.0 m^3/s discharge the flow width is relatively uniform over the entire reach; the shallow channel margins on the riffle cross section are much smaller than on the pool cross section. The predicted downstream velocities from the UnTRIM simulation at the pool cross section (section 21) are shown in Figure 3. The highest velocities occur near the surface, and the flow tends to be concentrated in the center section of the pool, with the highest velocities near the bed occurring over the point bar side of the pool rather than in the deepest section of the pool. This effect becomes more pronounced at higher discharges. Downstream of the pool, the flow diverges as the width of the point bar decreases; flow is more uniform across the channel the at the riffle cross section and further downstream.

3.1. Water Surface Elevation

[23] The water surfaces predicted at the pool and riffle cross sections for the UnTRIM and FESWMS simulations are compared with the observed water surfaces in Figure 4. Because observed water surface elevations were not available, the observed water surface was calculated at each discharge from the observed cross-sectional areas at the pool and riffle cross sections reported by *Keller and Florsheim* [1993] using the cross section geometries shown in Figure 4. At the pool cross section, the FESWMS and UNTRIM simulations predict a water surface approximately 0.07 to 0.08 m higher than the observed water surface for the 0.42 m^3/s discharge and 0.06 to 0.08 m lower than the observed water surface for the 0.97 m^3/s discharge. For the 4.5 m^3/s discharge, the UnTRIM simulation predicts a water surface within 0.01 m for most of the flow width, while the FESWMS simulation predicts a slightly higher water surface. At the riffle cross section, the water surface elevations predicted using both FESWMS and UnTRIM differ from the observed values by less than 0.02 m for all three flow rates for which observed data are available. For the 0.97 m^3/s discharge, depth measurements are available at the stations where velocity was measured (E. A. Keller, unpublished field notebook, 1969). The depth measurements are reported to an accuracy of 0.03 m (0.1 ft). These measurements of depth are plotted upward from the pool topography on Figure 4. These measurements show a large scatter (0.27 m between the maximum and minimum "observed" depth), which suggests variation between the local bathymetry where the measurement was taken and the bathymetry from the plane table survey topography used in this study. A similar level of scatter is also seen when the observed depths are plotted at the riffle cross section. The observed depths at the pool cross section show better agreement with the water surface predicted by UnTRIM and FESWMS than the observed water surface calculated from the observed cross-sectional area. The average elevation of the observed depths plotted for the 0.97 m^3/s discharge differs by less than 0.02 m from the average elevation predicted by both FESWMS and UnTRIM. This suggests that the water surfaces predicted for this discharge are reasonable, and that there may be some reliability uncertainties with the observed cross-sectional area at the pool cross section. Namely, the model cross sections were derived from topographic data from a plane table survey whereas the observed cross sections are approximately located on this survey and collected with a separate hand-level survey. Additionally, the original calculation of flow area was from a limited number of depth collection stations, variations between the surveyed topography and the stations where data was collected exist, and errors are introduced by back calculating the water depth from the reported observed cross-sectional area. Despite these potential sources of error, very good agreement between observed and predicted water surfaces are achieved at the riffle cross section for all three

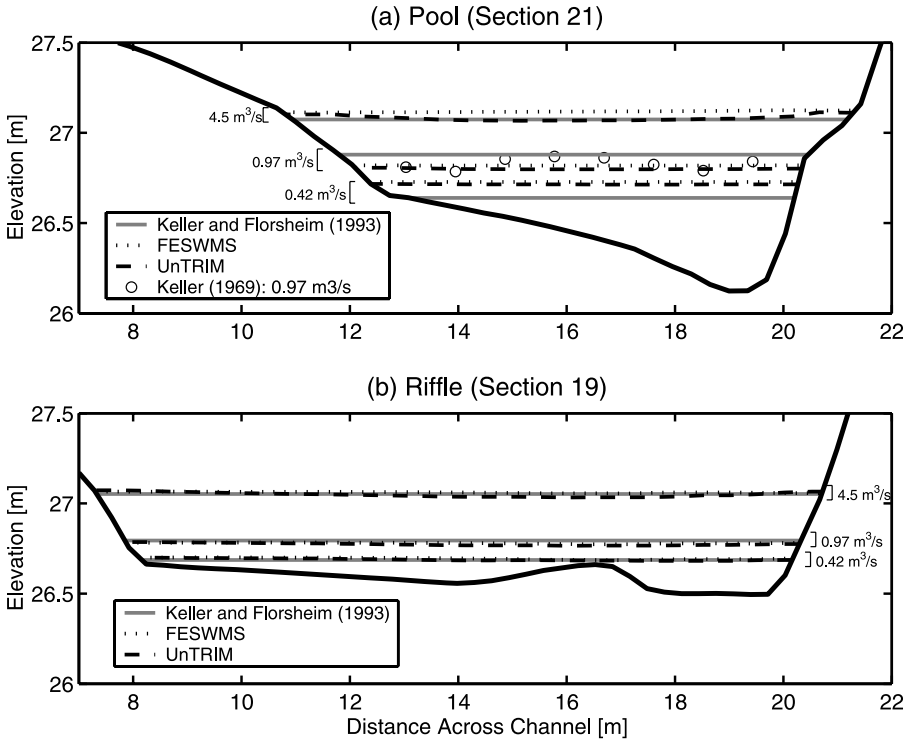

Figure 4. Predicted and observed water surface elevations at the (a) pool and (b) riffle cross sections for 0.42, 0.97, and 4.5 m^3/s discharges.

discharges, and reasonable agreement is achieved at the pool cross section.

3.2. Bed and Depth-Averaged Velocity

[24] The bed velocity measurements at the pool and riffle cross sections are compared with the predicted near-bed velocity from UnTRIM on Figures 5 and 6, respectively. There is generally good agreement between the measured bed velocity and the bed velocity predicted by UnTRIM at the pool cross section for each of the three discharges at which data was collected (Figure 5). No data were collected in the deepest part of the pool for the 4.5 m^3/s flow rate because the water was too deep and swift to collect measurements (E. A. Keller, unpublished field notebook, 1969). At all three discharges, the maximum measured and maximum predicted bed velocity at the pool cross section does not occur in the deepest part of the pool.

[25] For the riffle cross section, shown in Figure 6, there is also very good agreement between the measured and modeled bed velocity for each of the three discharges at which data was collected. The biggest observed difference between the field observations and the model predictions occurs on the right margin of the riffle cross section for a discharge of 4.5 m^3/s. As will be discussed below, this area of the riffle cross section exhibits significant secondary circulation at a discharge of 4.5 m^3/s and higher; for these discharges the predicted cross-stream velocity component near the bed is of a comparable magnitude to the downstream velocity component in this portion of the riffle. This flow complexity, and any unsteadiness associated with these flow patterns, appears to be the primary mechanism responsible for the difference between the predicted and observed bed velocity on the right edge of the riffle cross section. However, overall the simulation results show good agreement with the field observations at the riffle cross section. The agreement between the predicted and measured bed velocity at both the pool and riffle sections for the three discharges at which data is available indicates that the UnTRIM model is accurately simulating flow in Dry Creek at these discharges.

[26] The velocity measurements collected at 0.6 times the depth at the pool and riffle cross sections are compared with the predicted depth-averaged velocity from FESWMS on Figures 7. At the pool cross section the predicted depth-averaged velocity agrees well with the observed velocity at 0.6 times the depth for the 0.42 m^3/s discharge except at a distance of 14 m along the section where velocities were observed to be zero. For the 0.97 m^3/s discharge FESWMS slightly overpredicts velocities between 12 and 14 m along the section, and slightly under predicts velocity between 18 and 20 m. At the riffle cross section, the velocities predicted for the 0.42 m^3/s discharge show good agreement with observed velocities, while FESWMS consistently predicts lower velocities than the observed velocities at the 0.97 m^3/s. Differences between the observed velocity and the depth-averaged velocity predicted by FESWMS may result from the assumption that the velocity at 0.6 times the depth is equivalent to the depth-averaged values. For example, since the observed and predicted water surface and cross-sectional area at the riffle cross section (Figure 4) is nearly identical and the flow rates are identical, consistently higher observed depth-averaged velocities at the 0.97 m^3/s discharge is not consistent with continuity. Given this limitation in assuming that the velocity at 0.6 times the depth is equivalent to the depth-averaged values, the depth-

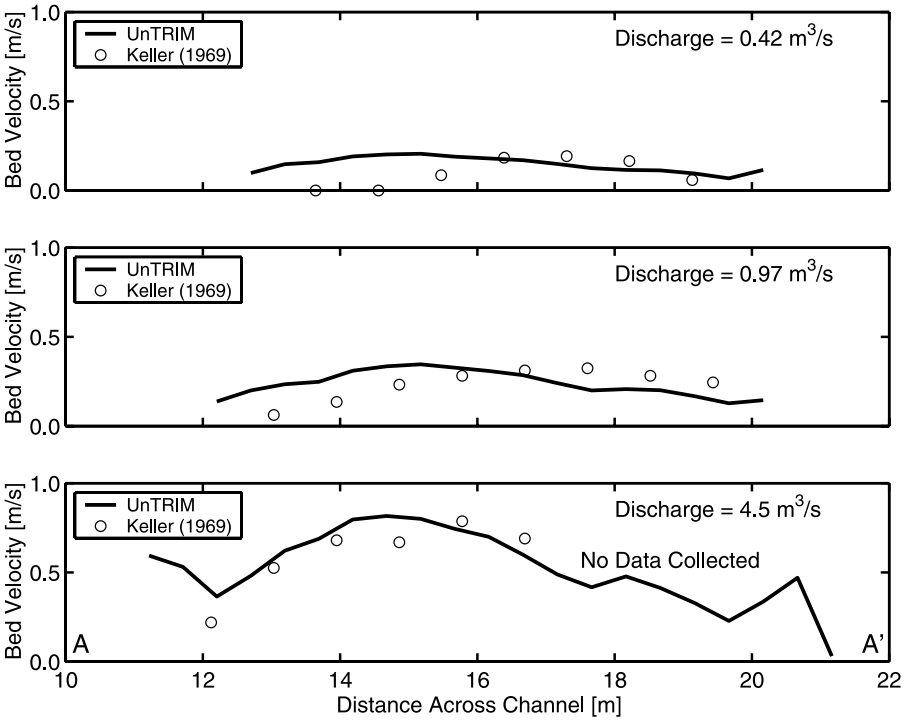

Figure 5. Predicted and observed near-bottom velocity at pool cross section for 0.42, 0.97, and 4.5 m^3/s discharges.

averaged velocities predicted by FESWMS show a reasonable agreement with the observed values.

3.3. Section-Averaged Velocity

[27] The predicted cross-sectional average velocities at the pool and riffle cross sections are shown as a function of discharge in Figure 8. For all flows, the HEC-RAS model [*Keller and Florsheim*, 1993] predicted a somewhat lower mean velocity (larger cross-sectional area) at the riffle cross section than the 2-D and 3-D models, with the largest differences occurring for the lower discharges. The 2-D and 3-D models show better agreement with the field data

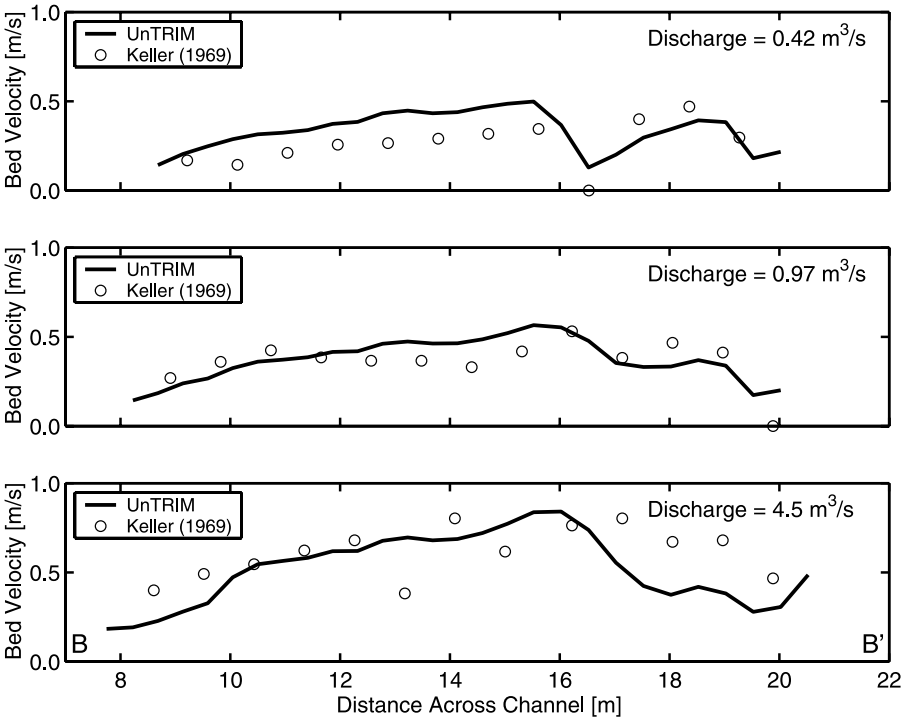

Figure 6. Predicted and observed near-bottom velocity at riffle cross section for 0.42, 0.97, and 4.5 m^3/s discharges.

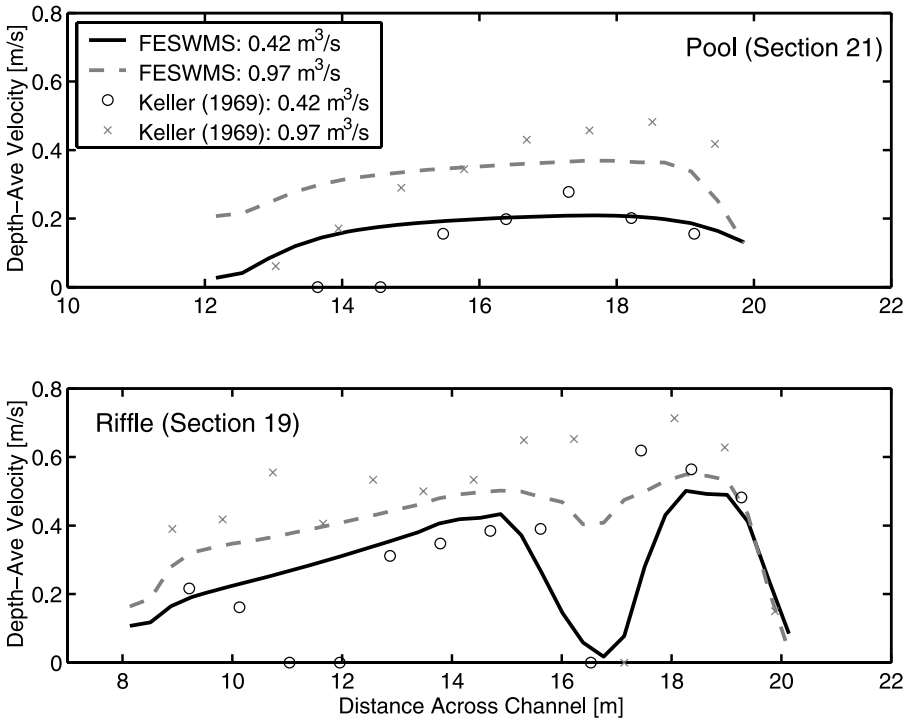

Figure 7. Observed velocity at 0.6 times the depth and predicted depth average velocity from FESWMS and for 0.42 and 0.97 m^3/s discharges at the (a) pool and (b) riffle cross sections.

for the riffle cross section. At the pool cross sections, all three models consistently underpredict the cross-sectional average velocity relative to the observed value at the 0.42 m^3/s discharge, and overpredict the cross-sectional average velocity at the 0.97 m^3/s discharge. All three models show good agreement with the observed cross-sectional average velocity at the pool cross section for the 4.5 m^3/s discharge. This is consistent with the differences in predicted and observed cross-sectional area at the pool cross section shown in Figure 4. Using HEC-RAS, *Keller and Florsheim* [1993] predicted a reversal in mean velocity at approximately 3.3 m^3/s. The FESWMS (2-D) simulation

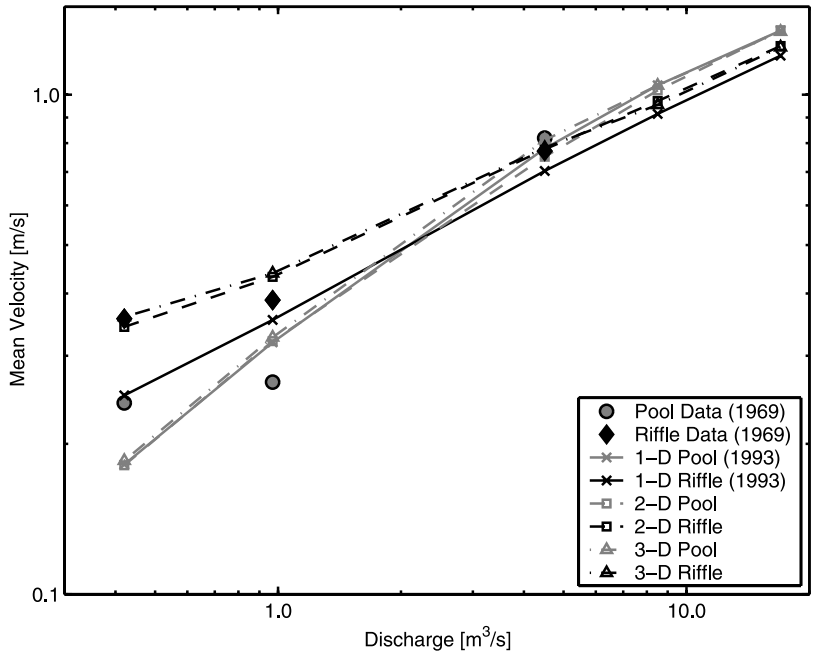

Figure 8. Mean cross-section velocity as a function of discharge at pool and riffle cross sections from field measurements [*Keller*, 1969] and predicted using a 1-D model [*Keller and Florsheim*, 1993], 2-D model (FESWMS), and 3-D model (UnTRIM).

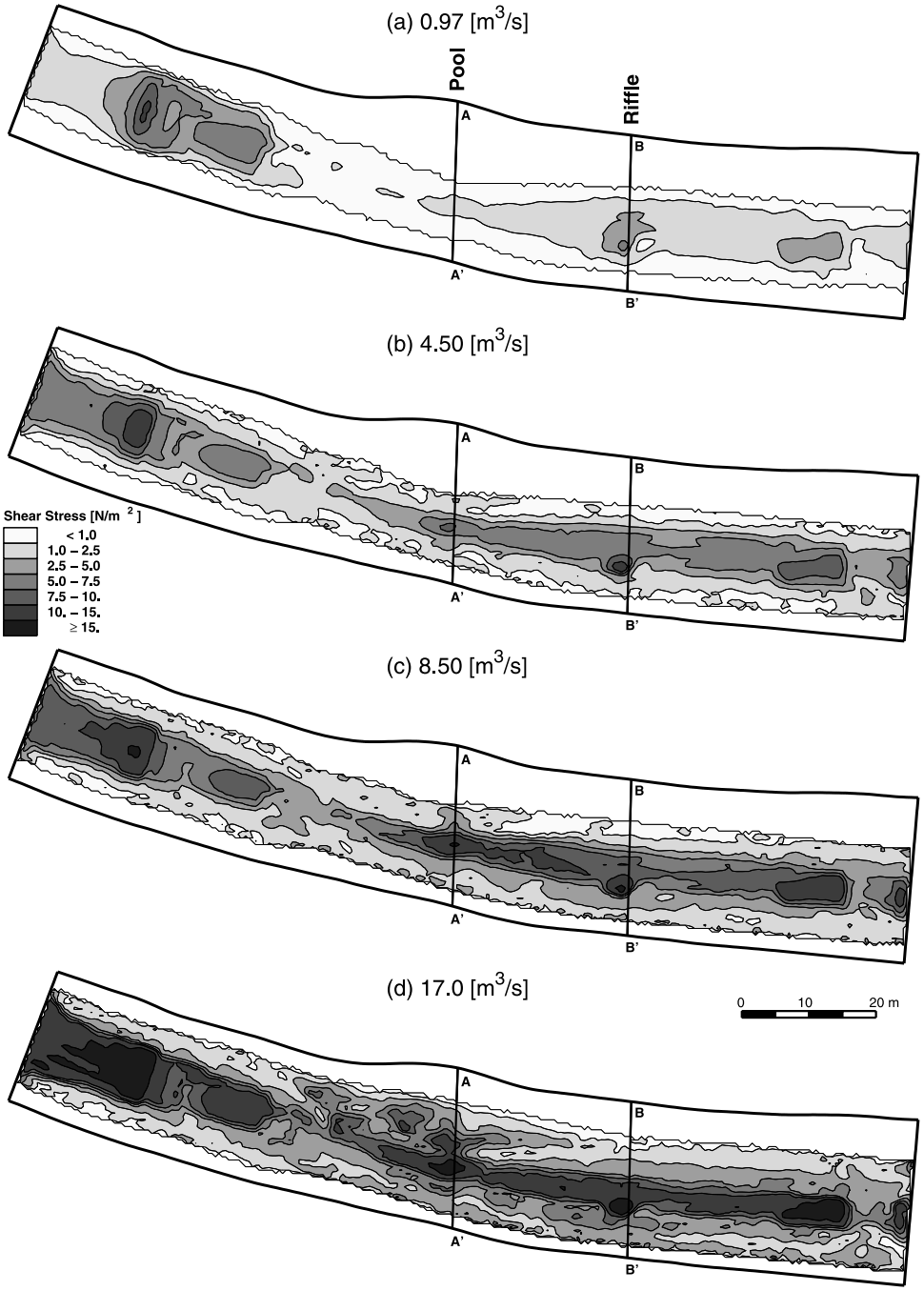

Figure 9. Bed shear stress distribution for four flow rates on pool-riffle sequence on Dry Creek from UnTRIM simulations.

predicts a reversal in cross-sectional average velocity at approximately 5.9 m^3/s, and the UnTRIM (3-D) simulation results predict a reversal in mean cross-sectional velocity at a discharge of approximately 3.8 m^3/s. This analysis shows that all three models predict a reversal in cross-sectional average velocity for this pool-riffle sequence on Dry Creek.

3.4. Bed Shear Stress

[28] Planform maps of bed shear stress for four of the five discharges simulated from the UnTRIM and FESWMS simulations are shown in Figures 9 and 10, respectively. For the 0.97 m^3/s flow (Figures 9a and 10a) the UnTRIM and FESWMS simulations predict a similar distribution of shear stress, with the highest shear stresses occurring over the upstream riffle and a narrower zone of high shear stresses through the pool cross section which widens downstream over the riffle cross section. This zone of higher shear stress along the center of the channel becomes more pronounced with increasing discharge. The UnTRIM simulations predict a more distinct band of higher shear stresses along the center of the channel with lower shear stresses along the channel margins (and in the deepest part of the pool). The shear stress distribution predicted by the FESWMS simulations shows a more uniform distribution of

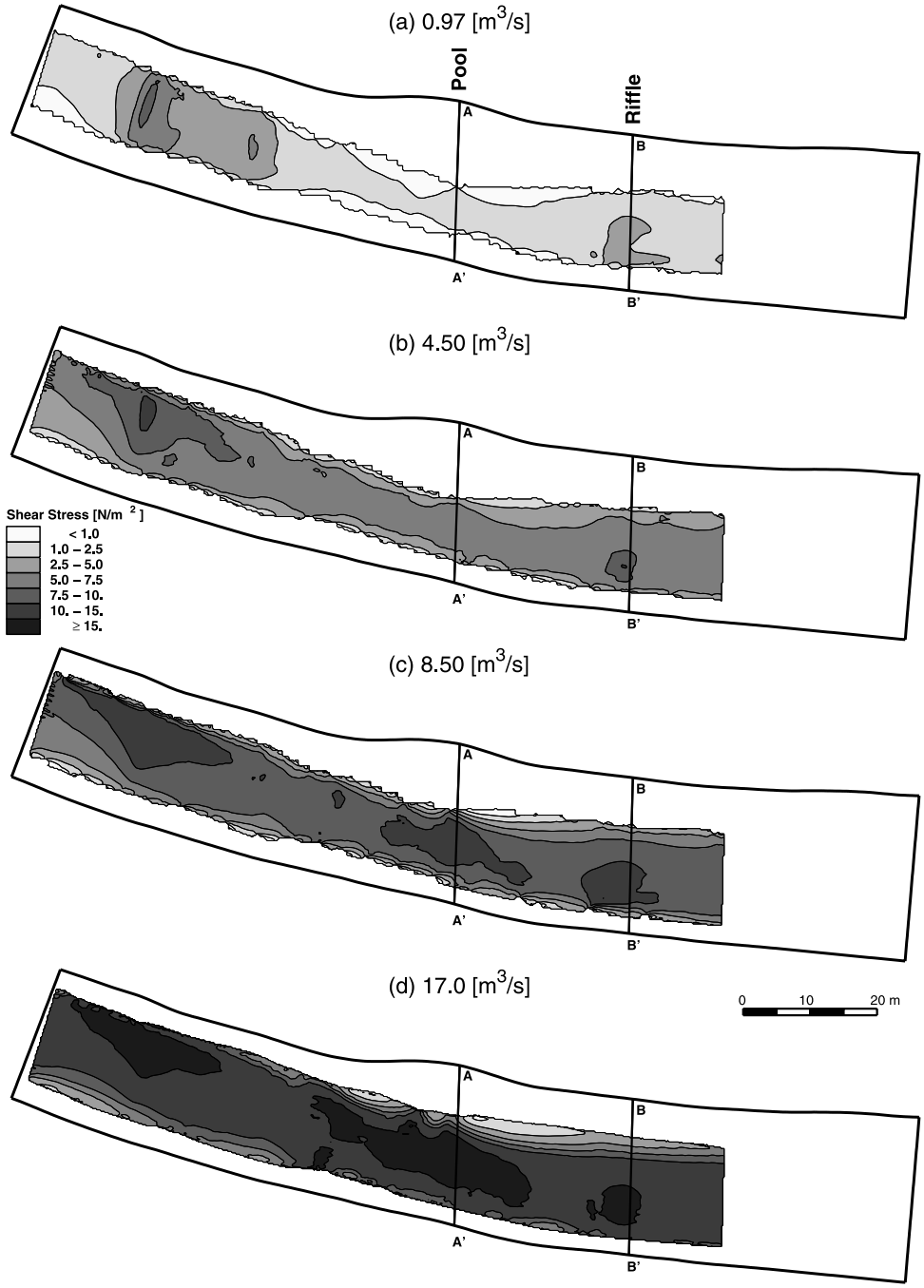

Figure 10. Bed shear stress distribution for four flow rates on pool-riffle sequence on Dry Creek from FESWMS simulations (the modeled reach for the FESWMS simulations was shorter than for the UnTRIM simulations but is shown on the same scale to facilitate comparison).

shear stresses across the channel, but still show the highest shear stresses concentrated in the center of the channel. As with the near-bed velocity (Figure 5), the maximum bed shear stresses predicted at the pool cross section occur on the slope of the point bar, rather than in the deepest part of the pool for both models and at all discharges. At the riffle cross section, the bed shear stress at the lower two flow rates is fairly uniform across the channel, with the highest values occurring near the middle of the cross section and at a local topographic high point (e.g., Figure 4). In general, the bed shear stresses predicted from the FESWMS simulations (Figure 10) tend to be slightly higher than the bed shear stresses predicted from the 3-D UnTRIM simulations (Figure 9). This discrepancy results from calculating the bed shear stress from the depth-averaged velocity rather than the near-bed velocity. However, these comparative results confirm the practical utility of scaling the depth-averaged shear stress predictions by a factor of 0.51 to yield a reasonable estimate of bed shear stress.

[29] The bed shear stresses shown in Figure 9 were averaged over the pool and rifle cross sections. Figure 11 shows the cross-sectional average and cross section maxi-

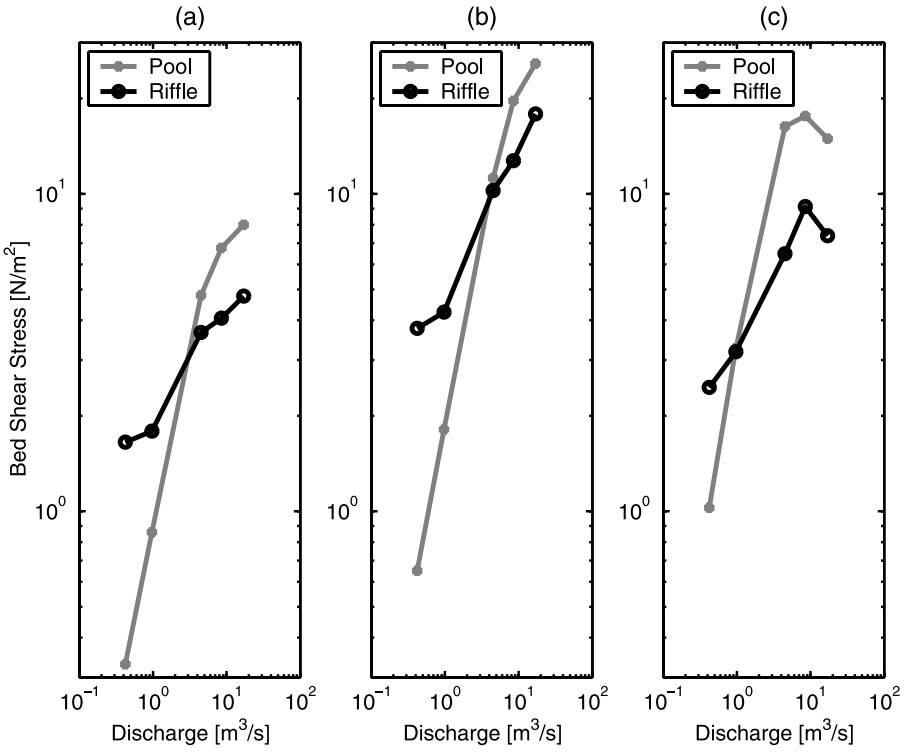

Figure 11. Bed shear stress as a function of discharge at the pool and riffle cross sections: (a) Section average bed shear stress predicted using UnTRIM. (b) Section maximum bed shear stress predicted using UnTRIM. (c) Bed shear stress calculated using the depth-slope product for pool and riffle cross sections using depth and water surfaces from UnTRIM simulations.

mum shear stresses at the pool and riffle cross sections predicted using UnTRIM. The shear stress predicted by applying the depth-slope product at the pool and riffle cross sections is also shown for comparison. A reversal in cross-sectional averaged bed shear stress occurs at a discharge of 3.0 m^3/s and a reversal in maximum cross-section bed shear stress occurs at a discharge of 3.9 m^3/s. The shear stresses predicted using the depth-slope product show a reversal at a discharge of 0.94 m^3/s.

3.5. Secondary Circulation

[30] Although the analysis of cross-sectional average parameters provides a relatively simple metric for analyzing flow processes, cross-sectional average parameters do not reliably account for flow complexity in systems where significant secondary circulation exists. Figure 12 shows the magnitude and direction of the cross-stream flow component along the pool cross section (section 21) for four of the five discharges studied. As seen in Figure 12, significant secondary circulation cells develop at the pool cross section for the discharges of 4.5 m^3/s and greater. The degree of secondary circulation predicted at the pool cross section increases significantly with discharge. At the 0.42 (not shown) and 0.97 m^3/s flow rates, a single small secondary circulation cell is visible in the deepest part of the pool. As the discharge increases, the magnitude of the transverse velocities increases significantly and a separate weaker circulation cell develops over the shallow section of the point bar. These results are consistent with field observations made by Keller at the Dry Creek site. His field observations suggest there is considerably more turbulence at high flows in pools than in adjacent point bars and that some pools in Dry Creek appear to be formed by "vertical vortexes" scouring the pool bottom [*Keller*, 1969]. By "vertical vortices" it is assumed that Keller is referring to the large vertical circulation cells visible in Figure 12 at higher discharges. These circulation cells are also likely to play a significant role in mobilizing sediments in the deepest portion of the pool as discharge increases. It should also be noted that in general the secondary flow at the pool cross section shows a dominant flow direction from left to right. This tendency becomes more pronounced as discharge increases, especially near the surface over the point bar where the downstream velocities are largest. This effect indicates that the cross-section line is not exactly perpendicular to the primary flow direction (cross-section location on Figure 1; flow direction on Figure 2). However, since this cross-section alignment was used by *Keller* [1969, 1971] and *Keller and Florsheim* [1993], this alignment is maintained in this study. Figure 13 shows the magnitude and direction of the cross-stream flow component along the riffle cross section for four of the five discharges studied. At the 0.97 m^3/s discharge, a small circulation cell is visible on the right side of the cross section. The magnitude of this circulation cell increases significantly with increasing discharge. A second weaker eddy is visible on the left side of the cross section for discharges of 4.5 m^3/s and greater.

4. Discussion

4.1. Bed Velocity

[31] Keller's original bed velocity measurements showed a convergence rather than a reversal in mean bed velocity;

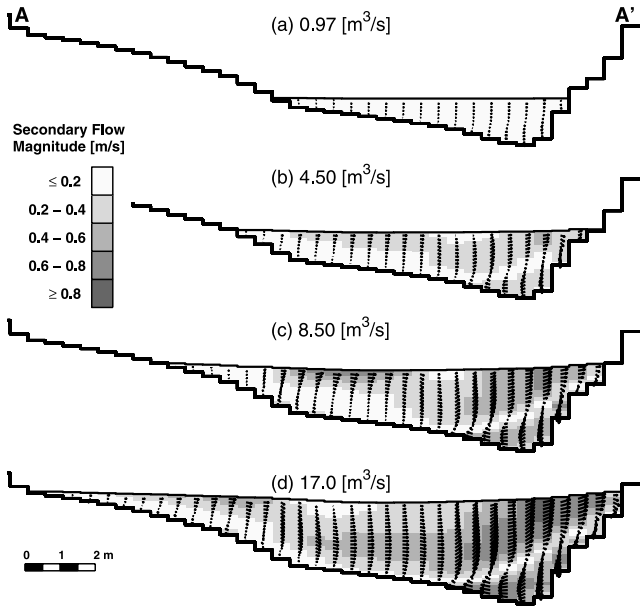

Figure 12. Secondary flow magnitude and direction at pool cross section A-A′ predicted using UnTRIM for five flow rate. Cross sections are shown with 2 times vertical exaggeration.

however, *Keller* [1969, 1971] postulated that a reversal in mean bed velocity would occur at a discharge above 4.5 m^3/s. By averaging the near-bed velocity at the pool and riffle cross sections for each of the five flow rates, it is possible to determine whether a reversal in mean near-bed velocity occurs in Dry Creek. The UnTRIM simulations predict a reversal in mean cross-section bed velocity at approximately 4.0 m^3/s and a reversal in maximum cross-section bed velocity at approximately 5.1 m^3/s. The consideration of the maximum bed velocity is significant because it is the locally maximum bed velocity in the cross section rather than the cross-sectional average value which gives a better indication of the local sediment transport competence. A reversal in mean bed velocity occurred prior to a reversal in maximum bed velocity, while the predicted reversal in mean bed velocity occurred at a slightly lower discharge than was predicted by *Keller* [1971]. However, these results support *Keller*'s [1971] original prediction that a reversal in near-bed velocity would occur on his pool-riffle study site on Dry Creek.

4.2. Section-Averaged Velocity

[32] A velocity reversal refers to the discharge at which the cross-sectional average velocity at the pool cross section exceeds the cross-sectional average velocity at the riffle cross section. Because the instantaneous discharge in both cross sections is identical, a reversal in mean cross-section velocity corresponds identically with a reversal in mean cross-sectional area. This reversal in cross-section area is largely a function of the site geometry. Through a systematic modeling study using a 1-D model, *Carling and Wood* [1994] found that a reversal in mean cross-section velocity only took place when the riffle was considerably wider than the pool. In their study, the ratio of pool to riffle width did not vary as a function of discharge. In contrast, at the Dry Creek field site, the riffle is approximately 50% wider than the pool at a flow rate of 0.42 m^3/s, but then only 25% wider than the pool at a flow rate of 4.5 m^3/s, and slightly narrower than the pool at a discharge of 17.0 m^3/s (e.g., Figure 9). The widening of the pool at a higher rate with increasing discharge in this case served as the geometric mechanism that led to a reversal in cross-sectional area and thus a reversal in section-averaged velocity. Depending on the absolute values of width and depth at low flow in an adjacent pool and riffle, the trajectory in changes in those variables that leads to a reversal in cross-sectional area can be quite different. Thus the particular trajectory observed in Dry Creek should not be viewed as a unique solution leading to a velocity reversal.

4.3. Bed Shear Stress

[33] *Carling and Wood* [1994] found that a "shear velocity reversal" took place whenever the pool had a significantly higher roughness coefficient than the riffle, but under no other conditions. In their study, the shear velocity, U_*, was calculated as

$$U_*^2 = gdS,$$

where g is gravity, d is the average water depth, and S is the energy slope. On the basis of this equation, commonly referred to as the depth-slope product, a higher value of the shear velocity is highly dependent on the energy slope. The average predicted cross-sectional depth and water surface slope (as a proxy for energy slope) at the pool and riffle cross sections from the UnTRIM simulations were used to calculate the shear velocity using this equation. The simulation results showed a significant variation in water surface elevation and downstream water surface slope along the cross section, making the calculation of a meaningful cross-sectional average energy slope difficult. As a result, the average water surface slope was calculated over a 10 m reach centered on the pool and riffle cross sections. The average depth of the riffle was less than the average depth of

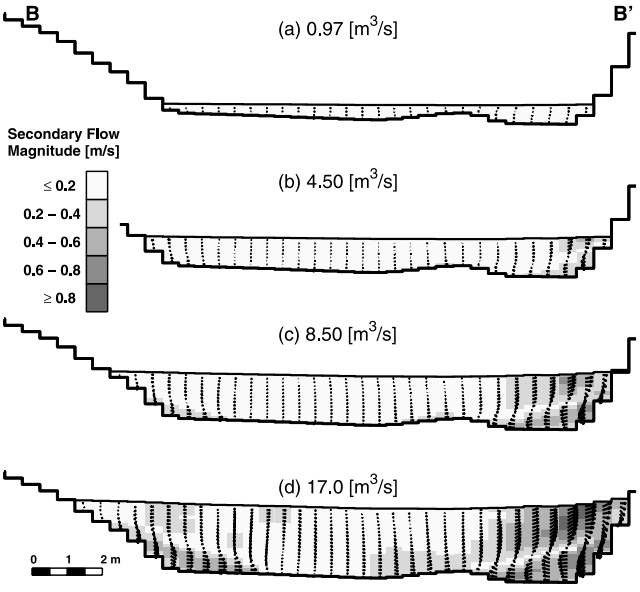

Figure 13. Secondary flow magnitude and direction at riffle cross section B-B′ predicted using UnTRIM for five flow rates. Cross sections are shown with 2 times vertical exaggeration.

the pool for the discharges less than 17.0 m^3/s, but greater than the average depth of the pool for a discharge of 17.0 m^3/s. This reversal in average depth occurs due to the widening of the pool onto the shallow areas of the point bar with increasing discharge (seen in Figure 2), whereas the riffle width does not increase as significantly with discharge. At the riffle cross section, the increase in flow depth with discharge is more pronounced than the increase in width. The water surface slope at the riffle cross section decreases with discharge; the water surface at the pool cross section steepens with discharge for the first three discharges and then decreases in slope for higher discharges. The difficulty associated with calculating a representative average water surface slope increases with discharge because the water surface elevation along and across the cross section becomes more complex at higher discharges. Thus there is a significant degree of uncertainty in the estimates of water surface slope at higher discharges. Applying the average depth and water surface slope parameters to the above equation predicts a reversal in bed shear stress at a discharge of 0.94 m^3/s. This result is not consistent with the predicted mean and maximum bed shear stresses shown in Figure 11. Similarly, the shear stress maps shown on Figure 9 and 10 do not support the drop in shear stress at the pool and riffle cross sections for the highest discharge, as is predicted by the application of the depth-slope product.

[34] This analysis of shear velocity using a one-dimensional approach illustrates the inappropriateness of applying one-dimensional equations to flows where significant cross-stream flow patterns are evident. In flows where significant two- and three-dimensional flow patterns are significant, one-dimensional step backwater models (such as HEC-RAS) do not provide a reliable estimate of friction slope and the slope-depth product does not yield a reliable estimate of shear velocity. *Thompson et al.* [1996] have argued that water surface slope is of little use in the calculation of shear stresses in systems where complex wave patterns and localized flow conditions influence longitudinal water surface slopes. In addition, variations in water surface elevation along a given cross section also lead to a range of possible water surface slopes between two given cross sections [*Miller*, 1994]. These factors all suggest that a one-dimensional approach is not appropriate for estimating bed shear stress in this pool-riffle sequence.

[35] A comparison of the predicted shear stresses from the FESWMS and UnTRIM simulations (Figures 9 and 10) provides insight into the relative importance of three-dimensional flow processes in predicting bed shear stress on Dry Creek. As mentioned above, one of the important mechanisms identified by the UnTRIM simulation is the convergence of the highest shear stresses into a narrow zone of flow routing through the channel. A qualitative comparison of Figures 9 and 10 shows that the width of higher shear stresses relative to the overall width of the channel is much narrower in the UnTRIM simulation than the FESWMS simulations. Part of this difference results because the secondary circulation cells on both margins of the channel (Figures 12 and 13) act to enhance the concentration of the flow in the center of the channel. Additionally the use of a horizontal eddy diffusivity in the FESWMS model acts to smooth out the horizontal velocity gradients, thereby reducing cross-stream flow variability. These conclusions are supported by additional 2-D simulations made using UnTRIM which show less flow convergence than the 3-D UnTRIM simulations, but more flow convergence than the FESWMS simulations. This effect could be reduced in the FESWMS simulations by using a spatially distributed eddy viscosity.

4.4. Secondary Circulation

[36] *Clifford and Richards* [1992, p. 67] have argued that "the interaction of channel form and channel flow at any point within a riffle-pool unit depends in part on flow and sediment behavior in upstream and downstream units," and that "if anything, explanations relying on cross-sectional averages complicate, rather than clarify, the characteristics of flow and form interaction." *Clifford and Richards* [1992] base this argument in part on the difficulty in accurately calculating the energy slope in the presence of complex secondary flow, and conclude that in the presence of a complex secondary flow the application of a 1-D equation of the form of equation discussed above is unacceptable. The results presented in the previous section, which demonstrate the significant secondary circulation patterns at both the pool and riffle cross sections, and the apparent inconsistencies found when applying the depth-slope equation to the range of flows simulated on Dry Creek, support this conclusion.

4.5. Flow Constriction

[37] *Keller* [1969] found that the at-a-point maximum bottom velocities at the pool cross section (Figure 5) showed a tendency for the highest velocities to be located on the point bar side of the pool rather than in the center of the pool. His bottom velocity measurements suggest that the area of high bottom velocity is "never in the center of the pool" and that "with increasing velocity there is a tendency for the area of high bottom velocity to migrate toward the point bar side of the pool" [*Keller*, 1969]. This feature is also observed in the shear stress distribution predicted by the UnTRIM simulations shown in Figure 9. The highest near-bed velocities, and thus the highest bed shear stresses, occur on the point bar and not in the deepest part of the pool. The alignment of this area of high flow velocity and shear stress with the flow constriction upstream of the pool on Dry Creek suggest that the upstream flow constriction is playing an important role in flow routing through the pool cross section.

[38] To test the influence of the upstream constriction on the velocity and shear stress distribution in the pool cross section on Dry Creek, an additional UnTRIM simulation was made with a modified numerical method that neglects the advective acceleration terms in the three-dimensional model. In effect, this approach removes any potential effects resulting from the flow convergence associated with the constriction at the head of the pool. The velocity distribution at the pool cross section for the simulation which neglects advective acceleration, shown in Figure 14, shows a dramatically different velocity distribution than was observed in the simulation results shown in Figure 3. For the simulation without advective acceleration, the maximum velocities and shear stresses occur over the deepest part of the pool instead of over the point bar as was observed by *Keller* [1969] and seen in the simulation results presented in the previous section. This result shows that the constriction

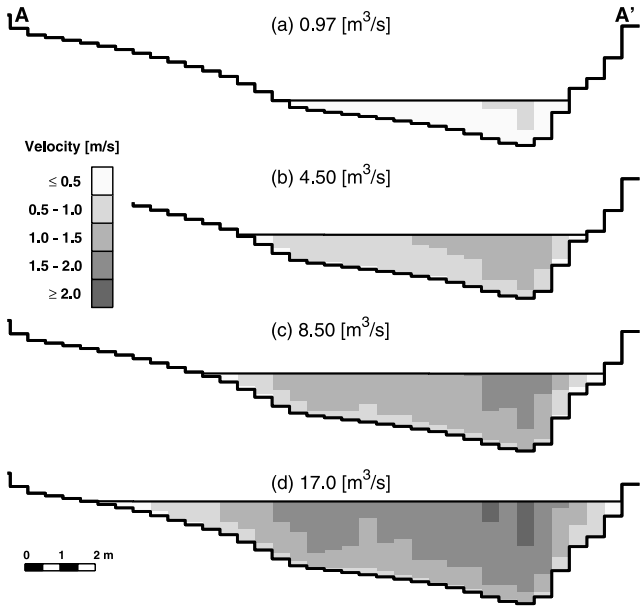

Figure 14. Downstream velocities at pool cross section for five flow rates predicted by UnTRIM simulation without advective acceleration. Cross sections are shown with 2 times vertical exaggeration.

at the head of the pool on Dry Creek is having a significant impact on the hydrodynamics of the pool-riffle sequence on Dry Creek. It also demonstrates that models that do not incorporate the full complexity of three-dimensional hydrodynamics and advective acceleration cannot accurately predict the important flow processes that occur in the pool-riffle sequence on Dry Creek. This result supports the results of *Whiting and Deitrich* [1991] which show that convective acceleration terms are important where topographic forcing leads to significant cross-stream and downstream flow accelerations. Another interesting outcome of this simulation without advective acceleration is that the results still predict a reversal in mean velocity at a discharge of 4.5 m^3/s. This result supports the conclusion that the occurrence of a mean velocity reversal is controlled more by the relative width of the pool and riffle than by the dominant flow processes in the pool-riffle sequence.

4.6. Flow Convergence Routing

[39] *Clifford and Richards* [1992] concluded that there is a need to formulate explanations of the maintenance of pool-riffle sequences that are sensitive to local variation and the existence of spatially distributed form process feedbacks. The results of the three-dimensional simulations of the pool-riffle sequence on Dry Creek support this conclusion. While the simulation results support a reversal in mean velocity, mean bed velocity, mean bed shear stress, and a variety of other cross-sectional average parameters, a reversal in mean parameters is not sufficient to explain the geomorphic processes that are necessary to maintain the pool-riffle sequence on Dry Creek. Fundamentally, this is because a reversal in mean velocity is not, in and of itself, sufficient to explain the important mechanisms occurring in the pool-riffle sequence on Dry Creek. A reversal in mean velocity does not explain the occurrence of the high velocities observed on the point bar rather than in the deepest part of the pool and it does not explain the important effects that advective acceleration have on the distribution of predicted velocities in the pool cross section. While a velocity reversal, or a convergence of cross-sectional average flow parameter values is observed in many pool-riffle sequences, there is a significant body of evidence in the literature that suggests that more complicated flow processes are significant in the maintenance of pool-riffle morphology. The flow complexity evident in almost all field studies and every two- and three-dimensional modeling study of pool-riffle sequences to date indicate that one-dimensional parameters and one-dimensional models are not adequate to capture the flow complexity in pool-riffle sequences. As a result, it is a reasonable conclusion that a hypothesis for pool-riffle morphology based on cross-sectional average parameters is not appropriate for explaining all of the processes important for maintaining pool-riffle morphology.

[40] A working hypothesis for defining the important processes for maintaining pool-riffle morphology can be introduced based on the processes observed on Dry Creek. It is called here the hypothesis of 'flow convergence routing' and is thought to be a more meaningful mechanism for explaining the key processes maintaining the pool-riffle morphology in Dry Creek than the occurrence of a velocity reversal. The hypothesis draws on elements of the work of *Booker et al.* [2001] and *Thompson et al.* [1996, 1998], but considers the maintenance mechanisms more explicitly. Under this hypothesis, the formation and maintenance of a pool depends on the occurrence of an upstream flow constriction which results in a convergence and acceleration of flow at the head a pool; this effectively generates a jet of flow through and downstream of the constriction. The effect of this convergence increases with discharge, and results in the development of a zone of high velocity and shear stress along a well-defined zone within the channel. Near bed flow is routed through this zone of high velocity resulting in high shear stress; this zone of high velocity and shear stress is the primary pathway for sediment movement through the pool. This zone of flow routing corresponds to the highest near-bed velocities, shear stresses, and maximum particle size. This zone is the primary pathway for sediment routing through the pool and can serve to route the coarsest sediment away from the deepest part of the pool. The lateral variation of flow along the edge of the convergence zone creates a lateral shear between the faster moving water over the point bar and the slower moving water over the deeper portion of the pool. This lateral shear zone has a significant impact on the secondary circulation pattern observed at the pool cross section, and this circulation plays a role in mobilizing sediment in the deepest part of the pool. Depending on the geometry of the site, a separation zone and recirculating eddy may also develop. At the tail of the pool, the flow diverges at the head of the riffle leading to deposition on the riffle and the maintenance of a topographic high at the tail of the pool. This hypothesis of flow convergence routing can explain how hydrodynamic processes evident in Dry Creek result in maintenance of the pool-riffle sequence, is supported by the data and observations of *Keller* [1969], and is supported by the results of other studies of pool-riffle sequences.

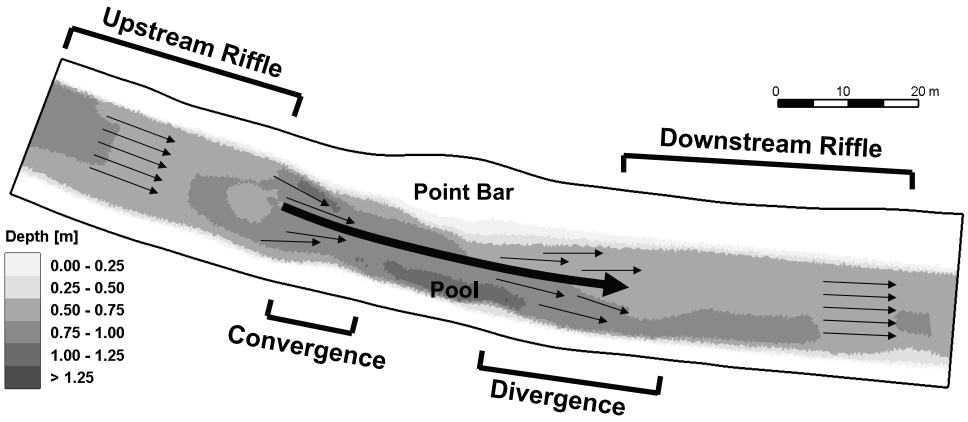

Figure 15. Conceptual model of flow convergence routing for pool-riffle sequence on Dry Creek. Depths shown for 4.5 m^3/s discharge.

[41] A conceptual model of the flow convergence routing mechanism during high flows on Dry Creek is shown in Figure 15. At the upstream riffle, the flow is fairly uniform across the channel. The point bar at the pool cross section acts as a constriction, and the flow is concentrated over a smaller width of channel. This funneling of flow results in a zone of higher velocity and sediment transport competence (depicted by wide dark arrow) that acts to route flow and sediment through the pool reach. Downstream of the point bar, the flow diverges and spreads out over the downstream riffle. At a sufficient distance downstream of the constriction, the flow on the downstream riffle is again fairly uniformly distributed across the riffle.

[42] The introduction of the flow convergence routing hypothesis is not a rejection of the results of *Keller* [1969, 1971]. Rather, the introduction of a more detailed hypothesis is a recognition that cross-sectional average parameters are not sufficient to explain the important processes in maintaining pool-riffle morphology. However, *Keller* [1969] also identified the significance of flow convergence routing on Dry Creek. He observed that "the point bar, which is slightly upstream, also tends to converge water into the pool. This is not significant at low flow, but may be important in producing fast bottom velocities at high flow. Water coming out of the pool diverges on the riffle, and this is probably responsible for the slower bottom velocity in the riffle at high flow." Further, Keller concluded that "it is assumed that at high flow the convergence of the pool produces fast bottom velocity which has a jetting action on the bed material; when the material reaches the divergent and slower bottom velocity of the riffle, the coarser material may be dropped from the moving traction load."

[43] The occurrence of flow routing in Dry Creek is also supported by Keller's observations that the highest velocities in the pool tended to be located on the point bar side of the pool rather than in the center of the pool. The bedload movement experiments on Dry Creek reported by *Keller* [1969, 1970] found that 35 percent of the variability of the distance a bed load particle will move at the field site can be explained by the variability of the bottom velocity in the vicinity of the particle, and 68 percent can be explained by the combination of velocity and particle parameters. Keller found that on riffles movement was most influenced by differences in bottom velocity. However, particle parameters, i.e., volume, weight in water, specific gravity, and shape, are considerably more important than velocity for the movement of particles through pools. Because, velocity tends to be more uniform over the riffle, the bed velocity shows a high correlation with movement over the riffles. However at the pool cross section, two important sediment transport mechanisms occur. In the convergence zone where the near-bed velocities are highest, the significance of locally high bed velocity and shear stress is likely to be important. However, in the deeper part of the pool where bed velocities are much lower sediment mobilization is likely to rely on mobilization due to secondary circulation driven processes. In these areas, particle parameters are likely to be more significant than downstream bed shear stress as an indicator for particle movement.

[44] *Keller* [1969] reports that on Dry Creek bed material is significantly larger on bars and riffles than in the deeper parts of pools. In addition, Keller found that the large material on the point bar gradually decreases in size across the stream to the bottom of the pool. Figure 16 shows the lateral sorting of largest bed material for the pool and riffle cross sections. There is a significant peak in largest bed material at a distance of approximately 15 m. This peak in the size of the largest bed material on both the pool and riffle cross sections corresponds to the zone of maximum shear stress which is visible on Figure 9 at the higher discharges. This peak in coarsest bed material corresponds to the zone of flow convergence and supports the hypothesis that the largest bed materials are being routed around the deepest part of the pool rather than through it. This routing of sediment around the deepest part of the pools rather than through them resolves the paradox of why coarse sediment is not left in the pool on the receding discharge. *Lisle and Hilton* [1992] observed a similar mechanism with dropping stage, noting that although some fine sediment was deposited in pools, boundary shear stress along the major sediment pathways was sufficient to maintain continued transport downstream.

[45] *Lisle* [1986] has observed that both large obstructions and bends cause intense, quasi-steady secondary circulation in scour holes and goes on to suggest that "obstructions and bends are similar enough in their effects on channel form and the pattern of flow and sediment transport ... to suggest that they lie on a continuum of

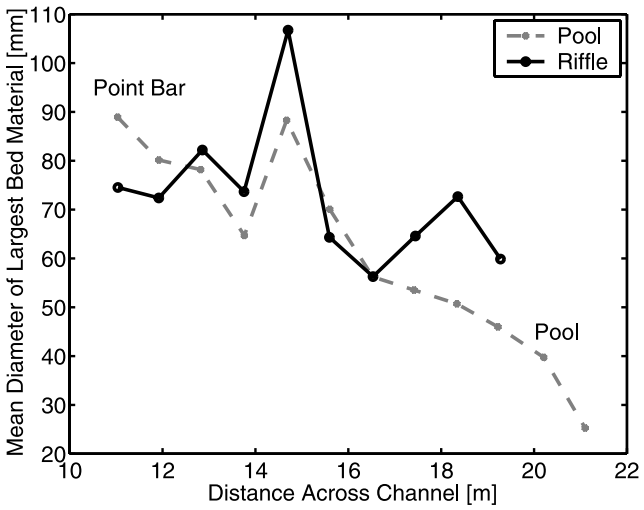

Figure 16. Lateral sorting of largest bed material size through a pool and adjacent riffle (data from *Keller* [1969]). The exact starting points for sediment sampling across the cross sections are not available, so channel distances are approximate.

bank forms affecting channel morphology." In this context, the hypothesis of flow convergence routing provides an important link with the work of *Dietrich et al.* [1979] on flow and sediment transport in meandering systems. *Dietrich et al.* [1979] found that the zone of maximum boundary shear stress is near the inside bank in the upstream bend (rather than in the deeper outside portion of the pool) and then crosses the outside bank as it enters the central segment of the bend. Similarly, the downstream velocity distribution at the upstream bend presented by *Dietrich et al.* [1979] shows a similar distribution to that predicted for the pool cross section on Dry Creek, with the highest velocities occurring over the point bar rather than the deeper part of the pool on the outside bend. *Dietrich et al.* [1979] also identified a zone of maximum sediment transport corresponding to the zone of maximum boundary shear stress and the zone of maximum particle size. This zone of coarse sediment shows a similar effect of flow convergence and sediment routing over a distinct band as is observed in the sediment distribution shown in Figure 16. As seen in Figure 9, the UnTRIM simulations predict a narrow band of high shear stress which develops downstream of the constriction at the head of the pool. The predicted shear stress distributions at discharges of 4.5 and 8.5 m^3/s show a well developed zone of high shear stress along the zone of flow convergence. At the highest discharge simulated, 17.0 m^3/s, this zone of convergence is somewhat less pronounced. As seen in Figure 9, the overall flow width at the highest discharge is more uniform and the constriction is less pronounced. This suggests the constriction may be sufficiently submerged at this discharge, whereby its influence on flow through the pool-riffle unit is reduced relative to that at lower discharges.

[46] Although the hypothesis of flow convergence routing is introduced based on the processes observed and simulated in Dry Creek, this hypothesis is consistent with observations of the significance of flow constrictions observed in other studies of pool-riffle sequences on alluvial streams [e.g., *Thompson et al.*,1998; *Booker et al.*, 2001; *Cao et al.*, 2003]. As seen in Table 1, many of the primary references pertaining to the velocity reversal hypothesis offer either stated or implied support for the hypothesis of flow convergence routing, since flow constrictions and flow convergence have been discussed in many of these references. The majority of the studies which do not directly support the flow convergence routing hypothesis are one-dimensional modeling studies, which cannot evaluate this mechanism.

[47] The model simulations presented in this study cannot directly identify the mechanisms of pool formation from a plane bed regime; however the significance of the constriction in maintaining pool-riffle morphology suggests that the presence of a constriction may also play an important role in pool formation. A study by *Lisle* [1986] found that 85% of pools were next to large obstructions or bends and that, conversely, 92% of large obstructions or bends had pools. Similarly, *Clifford* [1993b] suggested that pool-riffle units are initiated with the generation of eddies at a major flow obstacle. Further, *Clifford* [1993b] describes an autogenic process whereby the deposition downstream of a pool formed by an obstruction generates the next downstream flow irregularity. This process is consistent with the converging and diverging flow patterns fundamental to the flow convergence routing hypothesis. However, neither this study nor any of the previous studies of which we are aware rigorously track the persistence of pool-riffle sequences through time. A field reconnaissance of the Dry Creek field site in 2003 revealed that, though Keller's original pool-riffle site was still identifiable, significant incision on much of Dry Creek prohibited drawing conclusions about long-term maintenance at the site.

[48] The mechanism of flow constriction and routing observed in Dry Creek is somewhat different from the mechanism proposed by *Thompson et al.* [1996, 1998]. At their field site, *Thompson et al.* [1996, 1998] identify a constriction that blocks a portion of the channel rather than the more subtle narrowing constriction on Dry Creek. Because the channel width immediately opens up downstream of their constriction, *Thompson et al.* [1996, 1998] identify a separation zone and a recirculating eddy that form downstream of the constriction, while the primary flow is funneled into the deepest part of the pool. Although the geometry is somewhat different, the field site of *Thompson et al.* [1996] also can be explained by the hypothesis of flow convergence routing. However, in their case the flow is diverted through, rather than around, the deepest part of the pool. For this geometry, the flow convergence routing mechanism is consistent with their observations that the coarsest materials found in the pool unit are in the deepest part of the pool. *Booker et al.* [2001] identify flow routing around the deepest section of the pool for all of the pool units studied, which is identical to the flow routing observed on Dry Creek. Further, *Booker et al.* [2001] note that a recirculating eddy forms in only one of their pool units, and they suggest that the presence of recirculating zones at the pool head is a phenomenon that may act to maintain pool morphology but is of secondary importance in comparison to sediment routing. This suggests that a flow constriction is likely to be a more prominent feature in a composite hypothesis for pool-riffle morphology than the presence of

a recirculating eddy. Further consideration of the hypothesis of flow convergence routing on additional field sites is likely to yield insight into the relative importance of each of these processes on the maintenance of pool-riffle morphology in alluvial rivers.

5. Conclusions

[49] Two- and three-dimensional simulations of flow in the pool-riffle sequence on Dry Creek, CA are presented. The predicted flow velocities agree well with measured bed velocities by *Keller* [1969] and with average velocities predicted by *Keller and Florsheim* [1993] using a one-dimensional model. The model results show a reversal in mean velocity, mean near-bed velocity, maximum near-bed velocity, mean bed shear stress, and maximum bed shear stress in the pool-riffle sequence at discharges between 3.0 and 6.8 m^3/s. These results agree well with previous predictions of a reversal of bed velocity by *Keller* [1971] and a reversal in mean velocity by *Keller and Florsheim* [1993]. The application of the UnTRIM and FESWMS models to the Dry Creek pool-riffle sequence is significant because this field site served as the basis for the introduction of the velocity reversal hypothesis for pool-riffle sequences.

[50] The results of both the two-dimensional and three-dimensional simulations demonstrate that the presence of a flow constriction at the head of the pool results in a flow convergence that causes the maximum velocities to occur on the point bar of the pool rather than in the deepest part of the pool. The three-dimensional model shows a greater degree of flow and shear stress convergence and further reveals that this flow convergence drives a significant secondary circulation cell in the deepest part of the pool. It is believed that flow convergence serves to route sediment across the point bar rather than through the deepest part of the pool, while secondary circulation in the pool cross section has the potential to cause mobilization of the fine sediments in the deepest part of the pool.

[51] Though the pool-riffle sequence on Dry Creek does experience a reversal in cross-sectional average and near-bed parameters, the results presented in this study suggest that the velocity reversal hypothesis does not explain the primary mechanisms for maintaining pool-riffle morphology on Dry Creek. In light of these results that show that nonuniform flow effects are important in driving flow and sediment routing processes in the pool-riffle sequence, the velocity reversal hypothesis, which is based on cross-sectional average values, does not seem to be an adequate hypothesis to explain the important processes in maintaining pool-riffle morphology at this site. Although many studies of pool-riffle sequences have shown a convergence in mean parameters at pools and riffles, there is no evidence to suggest that a reversal in velocity must occur, and in fact many studies have shown that reversals do not occur at all pool-riffle sequences. For a hypothesis to be meaningful it must be able to explain the dominant processes; the velocity reversal hypothesis does not meet this criteria.

[52] On the basis of the processes observed on Dry Creek, the hypothesis of flow convergence routing is introduced as a new working hypothesis for defining the important processes for maintaining pool-riffle morphology in alluvial rivers. Under this hypothesis, the formation and maintenance of a pool depends on the occurrence of an upstream flow constriction which results in a convergence and acceleration of flow at the head of a pool. Flow through the pool is routed through a narrow zone within the cross section. This zone of flow routing corresponds to the highest near-bed velocities, shear stresses, maximum particle size. This zone is the primary pathway for sediment routing through or around the pool and can serve to route the coarsest sediment away from the deepest part of the pool. At the tail of the pool, the flow diverges at the head of the riffle leading to deposition on the riffle and the maintenance of a topographic high at the tail of the pool. This hypothesis is consistent with the field measurements and observations of *Keller* [1969], with the simulation results presented in this study, and with other recent studies which have identified flow constrictions as playing a major role in defining pool-riffle morphology.

[53] **Acknowledgments.** The authors would like to acknowledge Edward Keller for providing access to his unpublished data and field notebooks. The UnTRIM code was provided by V. Casulli of the University of Trento, Italy. This material is based upon work supported by National Science Foundation (grant EAR-0087842, Program Manager: L. Douglas James). Additional funding was provided to M.L.M. by a Stanford Graduate Fellowship and a NSF Graduate Research Fellowship. Financial support for this work was also provided by the U.S. Fish and Wildlife Service (contracting entity for CALFED Bay-Delta Ecosystem Restoration Program: Cooperative Agreement DCN 113322G003). We thank Edward A. Keller, Douglas M. Thompson, and an anonymous reviewer for their careful review of the manuscript and suggestions for improvements.

References

Bhowmik, N. G., and M. Demissie (1982), Bed material sorting in pools and riffles, *J. Hydraul.*, *108*, 1227–1231.

Booker, D. J., D. A. Sear, and A. J. Payne (2001), Modeling three-dimensional flow structures and patterns of boundary shear stress in a natural pool-riffle sequence, *Earth Surf. Processes Landforms*, *26*, 553–576.

Cao, Z., P. Carling, and R. Oakley (2003), Flow reversal over a natural pool-riffle sequence: A computational study, *Earth Surf. Processes Landforms*, *28*, 689–705.

Carling, P. A. (1991), An Appraisal of the velocity-reversal hypothesis for stable pool-riffle sequences in the River Severn, England, *Earth Surf. Processes Landforms*, *16*, 19–31.

Carling, P. A., and N. Wood (1994), Simulation of flow over pool-riffle topography: A consideration of the velocity reversal hypothesis, *Earth Surf. Processes Landforms*, *19*, 319–332.

Casulli, V., and P. Zanolli (2002), Semi-implicit numerical modeling of non-hydrostatic free-surface flows for environmental problems, *Math. Comput. Model.*, *36*, 1131–1149.

Celik, I., and W. Rodi (1988), Modeling suspended sediment transport in nonequilibrium situations, *J. Hydraul. Eng.*, *114*(10), 1157–1191.

Clifford, N. J. (1993a), Differential bed sedimentology and the maintenance of a riffle-pool sequence, *Catena*, *20*, 447–468.

Clifford, N. J. (1993b), Formation of riffle-pool sequences: Field evidence for an autogenetic process, *Sediment. Geol.*, *85*, 39–51.

Clifford, N. J., and K. S. Richards (1992), The reversal hypothesis and the maintenance of riffle-pool sequences: A review and field appraisal, in *Lowland Floodplain Rivers: Geomorphological Perspectives*, edited by P. A. Carling and G. E. Petts, pp. 43–70, John Wiley, Hoboken, N. J.

Dietrich, W. E., J. D. Smith, and T. Dunne (1979), Flow and sediment transport in a sand bedded meander, *J. Geol.*, *87*, 305–315.

Froehlich, D. C. (1989), Finite element surface-water modeling system: Two-dimensional flow in a horizontal plane-users manual, *Rep. FHWA-RD-88–177*, 285 pp., Fed. Highway Admin., Washington, D. C.

Gilbert, G. K. (1914), The transportation of debris by running water, *U.S. Geol. Surv. Prof. Pap.*, *86*.

Jackson, W. L., and R. L. Beschta (1982), A model of two-phase bedload transport in an Oregon coast range stream, *Earth Surf. Processes Landforms*, *7*, 517–527.

Keller, E. A. (1969), Form and fluvial processes of Dry Creek, near Winters, California, M.S. thesis, Univ. of Calif., Davis.

Keller, E. A. (1970), Bed-load movement experiments: Dry Creek, California, *J. Sediment. Petrol.*, *40*, 1339–1344.

Keller, E. A. (1971), Areal sorting of bed-load material: The hypothesis of velocity reversal, *Geol. Soc. Am. Bull.*, *82*, 753–756.

Keller, E. A. (1972), Development of alluvial stream channels: A five stage model, *Geol. Soc. Am. Bull.*, *83*, 1531–1536.

Keller, E. A., and J. L. Florsheim (1993), Velocity-reversal hypothesis: A model approach, *Earth Surf. Processes Landforms*, *18*, 733–740.

Kieffer, S. W. (1985), The 1983 hydraulic jump in Crystal Rapid: Implications for river-running and geomorphic evolution in the Grand Canyon, *J. Geol.*, *93*, 385–406.

Kieffer, S. W. (1989), Geologic nozzles, *Rev. Geophys.*, *27*, 3–38.

Lisle, T. (1979), A sorting mechanism for a riffle-pool sequence, *Geol. Soc. Am. Bull., Part II*, *90*, 1142–1157.

Lisle, T. E. (1986), Stabilization of a gravel channel by large streamside obstructions and bedrock bends, Jacoby Creek, northwest California, *Geol. Soc. Am. Bull.*, *97*, 999–1011.

Lisle, T. E., and S. Hilton (1992), The volume of fine sediment in pools: An index of sediment supply in gravel-bed streams, *Water Resour. Bull.*, *28*, 371–383.

MacWilliams, M. L. (2004), Three-dimensional hydrodynamic simulation of river channels and floodplains, Ph.D. dissertation, 222 pp., Stanford Univ., Stanford, Calif.

Miller, A. J. (1994), Debris-fan constrictions and flood hydraulics in river canyons: Some implications from two-dimensional flow modelling, *Earth Surf. Processes Landforms*, *19*, 681–697.

Pasternack, G. B., C. L. Wang, and J. E. Merz (2004), Application of a 2D hydrodynamic model to design of reach-scale spawning gravel replenishment on the Mokelumne River, California, *River Res. Appl.*, *20*, 202–225.

Petit, F. (1987), The relationship between shear stress and the shaping of the bed of a pebble-loaded river La Rulles–Ardenne, *Catena*, *14*, 453–468.

Petit, F. (1990), Evaluation of grain shear stresses required to initiate movement of particles in natural rivers, *Earth Surf. Processes Landforms*, *15*, 135–148.

Richards, K. S. (1978), Simulation of flow geometry in a riffle-pool stream, *Earth Surf. Processes*, *3*, 345–354.

Rodi, W. (1993), *Turbulence Models and Their Application in Hydraulics: A State-of-the-Art Review*, 3rd ed., A. A. Balkema, Brookfield, Vt.

Schmidt, J. C. (1990), Recirculating flow and sedimentation in the Colorado River in Grand Canyon, Arizona, *J. Geol.*, *98*, 709–724.

Schmidt, J. C., D. M. Rubin, and H. Ikeda (1993), Flume simulation of recirculating flow and sedimentation, *Water Resour. Res.*, *29*, 2925–2939.

Sear, D. A. (1996), Sediment transport processes in pool-riffle sequences, *Earth Surf. Processes Landforms*, *21*(3), 241–262.

Shewchuk, J. R. (1996), Triangle: Engineering a 2D quality mesh generator and Delaunay triangulator, in *Applied Computational Geometry: Towards Geometric Engineering*, vol. 1148, edited by M. C. Lin and D. Manocha, pp. 203–222, Springer, New York.

Thompson, D. M. (2004), The influence of pool length on local turbulence production and energy slope: A flume experiment, *Earth Surf. Processes Landforms*, *29*, 1341–1358.

Thompson, D. M., E. E. Wohl, and R. D. Jarrett (1996), A revised velocity-reversal and sediment sorting model for a high-gradient, pool-riffle stream, *Phys. Geogr.*, *17*(2), 142–156.

Thompson, D. M., J. M. Nelson, and E. E. Wohl (1998), Interactions between pool geometry and hydraulics, *Water Resour. Res.*, *34*(12), 3673–3681.

Thompson, D. M., E. E. Wohl, and R. D. Jarrett (1999), Velocity reversals and sediment sorting in pools and riffles controlled by channel constrictions, *Geomorphology*, *27*, 229–241.

Whiting, P. J., and W. E. Deitrich (1991), Convective accelerations and boundary shear stress over a channel bar, *Water Resour. Res.*, *27*(5), 783–796.

P. K. Kitanidis, R. L. Street, and M. L. MacWilliams Jr., Environmental Fluid Mechanics Laboratory, Department of Civil and Environmental Engineering, Stanford University, Stanford, CA 94305-4020, USA. (mmacwill@stanford.edu)

G. B. Pasternack and J. M. Wheaton, Department of Land, Air, and Water Resources, University of California, Davis, 1 Shields Avenue, Davis, CA 95616-8626, USA.

Section 3
Does SHIRA Actually Yield Ecological Benefits?

Introduction

SHIRA was created to yield immediate ecological benefits to help sustain riverine populations over years, while also promoting longer term interdecadal to centennial ecological restoration by decreasing the gravel deficit downstream of a dam. The purpose of this section is to evaluate the actual ecological benefits observed after SHIRA was implemented on the lower Mokelumne River. This evaluation depended on the close collaboration with fisheries biologists at EBMUD who collected all the biological data evaluated.

The words "spawning habitat" in SHIRA are often misconstrued to mean that SHIRA only addresses the short-sighted need for increased fish spawning habitat. That is not true. Instead, SHIRA is a systemic framework for river rehabilitation. The challenge in doing systemic rehabilitation is determining whether every aspect of an ecosystem has in fact been rehabilitated. In the discipline of ecology, one approach for addressing this challenge is to identify *indicator* species whose habitat and population status provide a measure of the overall integrity of the ecosystem. SHIRA employs this concept. By increasing the amount of high-quality salmon spawning habitat and carefully designing the spatial distribution of that spawning habitat, SHIRA aims to not only improve spawning conditions, but also improve the ecosystem as a whole.

This central tenant in SHIRA has been tested to the extent possible with the available resources for this demonstration project. In the first subsection, a thorough evaluation is made of whether the 2D model central to SHIRA can accurately predict the spatial pattern of Chinook spawner utilization in a river. It also provides an assessment of whether the demonstration projects on the lower Mokelumne River actually increased spawner utilization of high-quality habitat. It also provides insight as to whether rehabilitation of less than 3% of the total channel length can have a population-scale impact on the river's fall-run Chinook salmon.

In the second subsection an evaluation is made of the ecological success or failure of qualitatively designed habitat heterogeneity elements used in one of the demonstration projects ostensibly to enhance spawning activity. Past efforts at spawning riffle installation below dams during the 1980s were reported to only provide barren flat surfaces that fish ended up not utilizing. Our results show that riffle enhancements should include diverse features, because fish are strongly attracted to them for spawning.

In the third subsection an evaluation is made of the benefits of gravel placement on the lower Mokelumne River to the survival of salmon embryos to the fry life stage. This evaluation was done on a site that was not designed using SHIRA (because of the timing of the test), but was constructed *ad hoc* in similar fashion as SHIRA using augmented gravels. The outcome showed that placing gravel for riffle enhancement not only increasing numbers of redds, but also increases the production of fry.

Though not in this report, EBMUD has done extensive monitoring of the response of fish species in many lifestages as well as macroinvertebrates and aquatic plants to gravel placement on the lower Mokelumne River. Published scientific journal articles and technical reports explain the diverse benefits that have been observed since significant gravel placement has been adopted beginning in 1999. These are available on the SHIRA website and from EBMUD. Although it was not possible to test every species and lifestage across all those of interest, the indications from evaluations of benthic macroinvertebrates and fish is that river rehabilitation using SHIRA does provide broad ecological benefits.

Title: The Use of Slope Creation for Rehabilitating Incised, Regulated, Gravel-Bed Rivers

Running Title: Slope Creation in Regulated Rivers

Authors: Eve M. Elkins[1], Gregory B. Pasternack[1*], Joseph E. Merz[2]

*Corresponding Author

Addresses:

[1]Department of Land, Air, and Water Resources, University of California, One Shields Avenue, Davis, CA 95616; [2]East Bay Municipal Utility District, 1 Winemasters Way, Lodi, CA 95240.

ABSTRACT

Gravel bedded channels often become incised and degraded below dams. Gravel can be added to the channel to rehabilitate hydrogeomorphic conditions, including those promoting salmon spawning. When implemented without increasing bed slope, gravel addition at downstream riffles backfloods upstream riffles. A 2-year gravel-augmentation project was done to test the efficacy of a new method for "slope creation". Riffle-to-riffle slope was raised from 0.002 to 0.008 by adding gravel to the most upstream riffle. When gravel was added to the next downstream riffle a year later, riffle-to-riffle slope decreased to the sought after 0.004. After the study, the area of high-quality Chinook salmon spawning habitat increased 471%. The number of redds observed went from 62 to 161 during the study despite a 50% decline of in-river spawners. This eliminates variations in migrant population size and hatchery take as alternative explanations. Slope creation can be a useful aid for rehabilitating regulated rivers.

KEYWORDS: Eco-hydrology (1813), restoration (0481); gravel augmentation; habitat enhancement; dams (1808), Erosion (1815); Geomorphology: fluvial (1825)

INTRODUCTION

Dams alter a stream's hydrologic and geomorphic regimes leading to channel narrowing, incision, armoring, increased stability, and decreased slope [*Ligon et al.*, 1995; *Lisle and Church*, 2002; *Williams and Wolman*, 1984]. Physical habitat quality is the degree of suitability of local depth, velocity and river-bed substrate size in a stream to support a particular ecological function. Together with other stressors, dam-related degradation of physical habitat quality for salmonid spawning is responsible for interdecadal declines in anadromous populations [*Moyle*, 1994; *Moyle and Randall*, 1998; *Nehlsen et al.*, 1991; *Yoshiyama et al.*, 2000].

To mitigate the ecological impacts of river regulation, "gravel augmentation", defined as adding washed gravel and cobble to a stream, is widely performed in California. This is done to reduce bed armoring, improve river-bed substrate quality, increase flow velocity, reduce water depth, increase habitat heterogeneity, and increase hyporheic exchange [*DWR*, 2000; 2001; *Kondolf et al.*, 1996; 2001; 2004; *McBain et al.*, 2000; *Wheaton et al., 2004a*]. Such projects often emphasize rehabilitation of spawning habitat for key salmon species whose status strongly indicates that of the aquatic ecosystem [*Merz et al.*, 2004; *Merz and Ochikubo Chan*, 2005].

Because regulated streams are often incised, the benefits of in-channel gravel augmentation may be limited by the maximum riffle crest elevation achievable. As gravel is added at one degraded riffle the next-upstream riffle may be flooded out and lose its functionality. This backwater effect may diminish the gains of a project or make conditions worse overall [*Sear and Newson*, 2004; *Wheaton et al.*, 2004a]. To address this problem, gravel can be added at the base of a dam to increase the local bed elevation, and then a steeper slope can be built down the reach (Fig. 1). We term this artificial increase in riffle-to-riffle bed slope

"slope creation". This is conjectured to improve hydrogeomorphic conditions, including those comprising the physical habitat quality preferred for native Chinook salmon (*Oncorhynchus tschawytscha*) spawning.

Although river rehabilitation that enhances in-river fish production will aid spawning fish of both wild and hatchery origins, the consensus of the scientific [*Botsford and Brittnacher*, 1998; *Marchetti and Moyle*, 2001] and policy [*Flosi et al.*, 1995; *USFWS*, 2001; *DWR*, 1994; *CMARP*, 1999] communities in California is that in-channel habitat restoration is a necessary component of species recovery. According to Marchetti et al. [2004], "the restoration of natural processes in aquatic systems can be expected to minimize the establishment of alien fishes while helping to maintain native fish populations". This wide consensus is reflected in the millions of dollars being spent at this time to rehabilitate most Central Valley streams. The more spawning that can be achieved in-stream, the more hatchery production may be reduced.

This study investigated the short-term hydrodynamic, physical-habitat, and sediment-transport-regime responses of a degraded river reach to slope creation. Channel manipulation, defined as re-contouring a river's topography with the aid of washed coarse sediment brought in from a nearby quarry, was done to increase the riffle-to-riffle slope from 0.002 to 0.004 immediately below a dam. Although a single carefully monitored and modeled channel manipulation cannot fully corroborate the slope creation procedure, specific predictions (formally defined later) were evaluated to better understand the role of slope in regulated streams: 1) slope creation improves salmon spawning habitat quality, 2) spawning salmon prefer areas predicted in advance to be high-quality habitat, and 3) slope creation can provide a sediment transport regime that keeps high-quality habitat stable during spawning and incubation life stages. These predictions were tested by analyzing patterns of flow, scour potential, and

spawning habitat quality at a site on the Mokelumne River in northern California prior to (pre-project), after the first (mid-project) and after the second (post-project) channel manipulation. Observed counts of up-migrating fish, hatchery take, and redds for each spawning season were also used to test predictions and assess the slope-creation approach. The significance of this study is that specific predictions regarding hydrogeomorphic and fish response to slope creation were tested to reveal mechanisms underlying complex linkages among flow, morphology, and habitat regimes.

Slope Creation

When examining geomorphic units at a sub-reach scale, slope and discharge control in-channel hydraulics and morphodynamic change [*Knighton*, 1998]. In regulated reaches where channel slope has declined slowly over decades, depth is increased, velocity is decreased, and substrates become clogged, yielding poor habitat quality (Fig. 1a). Bed relief typically yielding riffles and pools decreases to produce a single long glide. Moreover, in most cases re-instatement of the historic (or a "naturalized") flow regime is politically infeasible. Thus, raising slope back to its pre-dam state can quickly undo decades of degradation. Not only might this improve physical habitat quality, but it is hypothesized to restore many key geomorphic processes that maintain high-quality habitat.

To address this complex water resources issue a slope creation approach was developed, implemented, and assessed. Slope creation involves adding coarse sediment to the channel below a dam in a staged manner (Figs. 1b, 1c) heavily relying on iterative design development, design evaluation, and adaptive monitoring over many years (Fig. 2). It was conceived of in response to observations of detrimental backwater effects at 4 previous isolated gravel

augmentation projects [*Wheaton et al.*, 2004a]. It was also added onto the previously reported SHIRA gravel-augmentation framework [*Wheaton et al.*, 2004a; *Wheaton et al., 2004b*]. Because it is often unaffordable or infeasible to undo decades of degradation in a single, one-year project, the slope creation approach was designed to be implemented in small stages over many years.

The ultimate length of reach whose longitudinal profile may be restored using this approach depends on the magnitude of slope change needed, the history of incision, and the total elevation gain permitted at the base of a dam in light of dam operations. *Williams and Wolman* [1984] reported examples of meters of channel incision as far as 60 km downstream of dams. Any depth of bed incised in the past may be recreated using slope creation. Restoring each increment of 0.1% slope to the uppermost 1-km reach below a dam requires 1 m of elevation gain. Because the critical region of habitat-limited fish spawning at the base of a dam may be <1 km in length, much steeper slopes may be achieved over shorter distances in this critical zone for the same amount of elevation gain. If a longer regulated reach was historically used for spawning, then restoring the bed elevation at the base of the dam to its pre-dam elevation and distributing the pre-dam slope downstream should yield the desired hydrogeomorphic conditions over the total length of the historical spawning reach.

Several limitation of slope creation must be considered. The most important is that as long as a dam remains, constructed channel features and the rehabilitated slope must be maintained with periodic gravel injections below the dam to sustain short-term gains. Longer-term issues associated with this maintenance regime are not addressed in this study, but are covered in an investigation of longer-lived rehabilitation sites [*Merz et al.*, 2006]. In addition, slope creation only deals with structural enhancement; the minimum requirements for water

quality parameters such as temperature and dissolved oxygen are assumed to be within an acceptable range [*Merz and Setka*, 2004] and are not addressed in this approach. Finally, the maximum slope that should be built is constrained by the unnatural and undesirable onset of bed material transport of the added gravels during spawning or early incubation, times when flow is normally low and abnormally high transport would destroy fish embryos.

Study Area

The snow-fed Mokelumne River drains 1624 km^2 of the central Sierra Nevada (Fig. 3). It has 16 major water impoundments, including Salt Springs (175 million m^3), Pardee (259 million m^3) and Camanche (531 million m^3) reservoirs. Prior to Camanche Dam, annual peak flows 1904-1963 exceeded 200 m^3/s for 21 of 57 years. Since 1964, releases are capped at 142 m^3/s. Pre-dam, the annual hydrograph was snowmelt-dominated, with highest flow in May-June, well after peak precipitation. Post-dam, snowmelt runoff is greatly reduced. Flood frequency analysis revealed a dramatic reduction in flow magnitude for all recurrence intervals [*Pasternack et al.*, 2004]. From May 2000 to the completion of this study, flow was near the 4.25 m^3/s minimum prescribed in re-licensing [*FERC*, 1998].

The lower Mokelumne River has been impacted by direct anthropogenic intervention and slow, long-term morphologic degradation. Hydraulic mining, gravel extraction, dam construction, water diversion, altered flow regimes, deforestation, artificial bank protection, channelization and levee construction have resulted in depleted, degraded and otherwise, inaccessible gravel beds within the river. The first 750 m of channel below Camanche Dam was re-engineered to accommodate sluicing, power generation, and hatchery operations. Also, reduced flood peaks and durations stabilized formerly active gravel deposits and permitted

encroachment of vegetation into the channel [*FERC*, 1998]. Presently, the lower Mokelumne River between Camanche Dam and Highway I-5 has a low slope (0.0002-0.002 instead of 0.001-0.006), narrow width (19-43 m instead of 40-90 m), and poor salmonid spawning bed substrates (compacted coarse sediment partially overgrown with aquatic vegetation and organic-rich mud instead of clean, loose gravel and cobble).

For the 19-year period before Camanche Reservoir was impounded, runs averaged 3,300 spawners, though spawning areas were estimated to accommodate ~15,000 adult Chinook salmon [*CDFG*, 1959]. Presently, average annual lower Mokelumne River Chinook escapement averages 5500 [*Workman*, 2003]. Between 1994 and 2002, the percent of length of the upper 1-km of channel observed to have redds varied between 19-34%, with high densities focused at a few riffles. The Mokelumne River Fish Hatchery uses the majority of up-migrating fish to produce 3-9 million juvenile Chinook salmon. *USFWS* [1997] called for a fall-run Chinook salmon population target of 9,300.

METHODS

Channel Manipulation

To evaluate slope creation, a channel manipulation was performed 2003-2004 on the lower Mokelumne River in the top 300-m reach downstream of Camanche Dam (Fig. 3) located at the coordinates 38°13’3” N, 121°1’43” W. This is the farthest upstream migratory point accessible to spawners . The SHIRA framework [*Wheaton et al.*, 2004a] was used to study the baseline condition of the river, design and implement a 2–year slope creation project, evaluate the viability of iterative slope creation, and perform as-built, post-spawning, and interannual

assessments. A detailed map (~1 pt/m^2) of channel topography was surveyed. Surveying accuracy was assessed using control network checks and was found to average ±0.35 cm horizontal and ±0.39 cm vertical. Topographic data were imported into Autodesk Land Desktop 3 to create a digital elevation model for each year (Fig. 4a).

Several slope-creation designs were developed, iteratively refined, and reduced to a final selection in spring 2003. Local expert experience and diverse concepts regarding Chinook salmon habitat requirements [*Healey*, 1991; *Geist and Dauble*, 1998], habitat heterogeneity [*Gibbins and Acornley*, 2000; *Brooks et al.*, 2004; *Wheaton et al.*, 2004c], pool-riffle maintenance [e.g. *Carling*, 1991; *MacWilliams et al.*, 2006], and effects of dams [*Grant et al.*, 2003] guided design development. Also, design elements related to other life stages were utilized, such as submerged wood and boulder clusters [*Abbe and Montgomery*, 1996; *Inoue and Nakano*, 1998; *Urabe and Nakano*, 1998; *Merz*, 2001] as well as hyporheic flow [*Geist and Dauble*, 1998; *Baxter and Hauer*, 2000; *Gayraud et al.*, 2002]. These have been shown to correlate with higher redd and fish densities [*Zalewski et al.*, 1998; *Horan et al.*, 2000; *Gibson*, 2002; *Brooks et al.*, 2004]. Shaded, deep, cool pools were enhanced to provide adult holding habitat [*Nielsen and Lisle*, 1994], while slow and backwater areas were incorporated to provide rearing and juvenile habitat [*Bozek and Rahel*, 1991]. Spawning habitat quality and scour patterns predicted by 2D model simulations aided design evaluation and improvement.

The use of these design elements would appear to diminish the ability to attribute study outcomes solely to slope creation. However, one of the riffles manipulated in this study (riffle 2) was previously enhanced in 1999 with all of the above features *ad hoc* without considering slope creation, SHIRA, or 2D modeling [*Pasternack et al., 2004*]. No spawners utilized the site in the first season after enhancement in 1999. The hatchery took 60% of the run that year. Between

2000-2003 its habitat quality degraded sharply, as detailed later [*Merz et al.*, 2006]. Thus, use of slope creation, SHIRA, and 2D modeling at this site provides a direct test of riffle rehabilitation with versus without slope creation at the same spawning discharge of ~8.5 m^3/s.

The final design for 2003 incorporated a 0.5-m fill depth at the riffle crest, a large riffle, a peripheral chute, and a small secondary riffle crest (Fig. 4b). Fill depth was limited by the maximum sustainable increase in slope and riffle entrance/exit slopes of 0.005-0.01. The length of the project was constrained by the target slope and the 3217 metric tons of coarse sediment available. The design was constructed in summer 2003.

Based on mid-project observations and modeling, the design goal for the second phase of slope creation was to raise the elevation of riffle 2, thereby creating new high-quality habitat there and imposing a backwater effect on riffle 1 (Fig. 1c). In this case a backwater effect would be beneficial, because the first phase of slope creation maximized the local elevation gain to sustain several years of downstream slope re-distribution. This came at the cost of excessively high local velocities and shallow depths (Fig. 1b), partially mitigated against in the first year using the peripheral chute. The second-phase, final design raised riffle 2 by 0.5 m resulting in a broad, relatively flat riffle. It also called for the crest of riffle 1 to be lowered by 0.2 m and the peripheral chute to be partially filled in (Fig. 4c). In summer 2004, 3,012 metric tons of coarse sediment were used to construct the design.

2D Mokelumne Model

Finite Element Surface Water Modeling System 3.0 (FESWMS) was used to simulate and compare depth-averaged 2D flow hydrodynamics, spawning habitat quality, and sediment transport regime. FESWMS solves the vertically integrated conservation of momentum and

mass equations using a finite element method to acquire local water depth and depth-averaged 2D velocity vectors at each node in a computational mesh [*Froehlich*, 1989]. Application of FESWMS to gravel-bed rivers has been extensively validated on the Lower Mokelumne River using observed velocity and depth at 35 cross-sections, indicating good predictions for the gravel bed and poor predictions around large woody debris or complex banks [*Pasternack et al.*, 2004; *Wheaton et al.*, 2004b; *Pasternack et al.*, 2006]. *Pasternack et al.* [2006] reported details regarding FESWMS model uncertainty. They found that FESWMS could predict local shear stress over gravel-bed riffles as accurately as 5 common field estimation methods. *MacWilliams et al.* [2006] compared FESWMS with 1D and 3D models of gravel-bed river hydrodynamic and found that the 2D model was capable of simulating key stage-dependent processes responsible for riffle-pool maintenance. FESWMS is a long-established model best viewed as a conceptual guide of likely outcomes, rather than literal truth. In this study, validation is taken further by directly testing habitat-quality model predictions against salmon-spawning observations.

FESWMS was implemented using Surface Water Modeling System v. 8.1 graphical user interface (EMS-I, South Jordan, UT). Discharge and downstream boundary water surface elevation were obtained from flow records and by surveying the water surface at the desired flow conditions, respectively. A constant Manning's n of 0.043 was estimated for placed gravel features [*Pasternack et al.*, 2004]. A constant eddy viscosity of 0.028 m^2/s was used. Digital elevation model data were interpolated to the mesh with a typical internodal spacing of 1.2 m.

Local habitat-suitability curves for depth and velocity based on observations in the lower Mokelumne River [*CDFG*, 1991; *Pasternack et al.*, 2004] were used to make habitat-quality predictions (Fig. 5). Since placed gravel was specified to meet spawning requirements, grain-size suitability curves were not needed. During extended years of below average flow, aquatic

vegetation is observed in low-gradient geomorphic units on the lower Mokelumne River [*Smith et. al.,* 2004]. Minimal vegetation existed on steeper riffles that were rehabilitated in 2000 and 2002. Lacking direct literature on the habitat suitability of vegetated gravels, this uncertainty was addressed by recognizing that salmonids generally do not spawn in reaches covered in aquatic vegetation, because it slows velocities, stabilizes substrates, and accumulates sand, mud, and organic muck [*Sand-Jensen*, 1998; *Madsen et al.*, 2001]. On the lower Mokelumne, there is no significant source of sand or mud in the study area, but organic fines grow and accumulate *in situ* as long as flow remains very low and steady. Thus, where aquatic vegetation was present, it was considered a complete deterrent to spawning and spawning habitat quality was assigned a value of 0. Where aquatic vegetation was not present, a global habitat suitability index (GHSI) for spawning was calculated at each mesh node as the geometric mean of the depth and velocity suitability. GHSI values of 0, 0-0.1, 0.1-0.4,0.4-0.7, and 0.7-1.0 were interpreted as predicting non-habitat, very poor habitat, low-quality habitat, medium-quality habitat, and high-quality habitat, respectively [*Leclerc et al.*, 1995]. This classification was independently validated using observed fish utilization data. GHSI does not directly account for the value of aggregate habitat-heterogeneity features or hyporheic water quality [*Geist*, 2000].

To evaluate coarse sediment entrainment risk at the flow during which spawning and embryo incubation occur, Shields stress was calculated at each node in the model as described in *Pasternack et al.* [2006]. Wolman pebble counts [Kondolf and Li, 1992] were completed pre-, mid- and post-project for Shields stress calculations. Shields-stress values were categorized based on transport regimes defined by Lisle et al. [2000] where values of $\tau^*<0.01$ correspond to no transport, $0.01<\tau^*<0.03$ correspond to intermittent entrainment, $0.03<\tau^*<0.06$ corresponds to "partial transport", and $\tau^*>0.06$ corresponds to full transport.

Model Validation

To validate 2D depth and velocity predictions, cross-sectional hydraulic data were collected along multiple transects using the methods of *Pasternack et al.* [2004, 2006] before and after each channel manipulation. Field observations along each cross-section were fit with a curve using the locally weighted Least Squared error method to reduce measurement noise. A 2D model simulation was performed for the corresponding flows that were observed. Modelled and measured curves were compared for cross-channel patterns.

To assess fish utilization of manipulated riffles and validate spawning habitat-quality predictions, redd surveys were conducted by wading and canoeing. Redd locations were recorded using a Trimble Pro XR Global Positioning System and a laser range finder (Atlanta Advantage) [*Merz and Setka*, 2004] resulting in a horizontal accuracy of ±1 m. A 2D model simulation was performed for the corresponding average autumn spawning flows that occurred pre-, mid-, and post-project (6.0, 9.5 and 6.0 m^3/s). The predicted GHSI for each redd location was extracted from the 2D model. Due to the hatchery take, 73-91% of up-migrating Chinook salmon during this study, density-dependency in spawning-location selection was significantly reduced. Minimal redd superposition was observed, so redd location is a good indicator of physical habitat preference.

PREDICTION TESTING

A prediction is a statement that is testable by observation. Predictions about specific outcomes of the channel manipulation in the study area were developed to test key issues, such as whether spawning improved and whether slope creation was responsible for it. Prediction

testing involved comparing field observations against model predictions for each project stage and cross-comparing 2D model simulations among the different stages. For 2D model cross-comparison, it was necessary to simulate a common flow, which was chosen as 11.33 m^3/s- a typical spawning discharge for the lower Mokelumne River.

Prediction 1 – Habitat quality will improve

To determine whether the quantity of high-quality and medium-quality habitat increased the spatial distribution of predicted habitat quality was compared for the pre-, mid- and post-project scenarios at 11.33 m^3/s. Arc GIS 9 was used to determine and compare the predicted area of each type of habitat quality. An increase in habitat quality would corroborate the prediction and support the use of slope creation to improve spawning habitat quality. Comparison of spawning at riffle 2 in 1999 and 2004 provided a direct test of the efficacy of slope creation relative to other rehabilitation measures.

Prediction 2- Spawners will preferentially utilize high-quality habitat

To determine whether predicted high-quality habitat was preferentially used by spawning fall-run Chinook salmon, pre-, mid-, and post-project, GHSI predictions were validated against redd observations. Percent habitat availability ($\%A_i$) and percent utilization ($\%U_i$) for each habitat quality class (*i)* defined earlier were solved for pre-, mid-, and post-manipulation scenarios using

$$\%A_i = 100 \times \frac{bed\,area_i}{total \cdot area} \qquad \text{and} \qquad \%U_i = 100 \times \frac{\#\cdot redds_i}{total \cdot \#\cdot redds}. \qquad (3,4)$$

To determine whether salmon preferred certain predicted habitat types as opposed to randomly selecting available habitat, habitat quality preference was calculated using Strauss' linear index

(*L*) as described in the work of *Lechowicz* [1982]. *L* is calculated by subtracting $\%U_i$ from $\%A_i$. This index yields values that range from –1 (avoidance) to 1 (preference). A value of 0 indicates a random selection. As an additional test, an analysis of variance (ANOVA) was used to compare the spawning preference index to the habitat quality index. These analyses test whether spawners prefer model-predicted high-quality habitat. If the tests corroborate the prediction, then that also validates the conclusions from the first prediction, showing not only that slope creation improved 2D model predicted habitat quality, but also that it improved it in reality.

An analysis was performed to account for fluctuations in the number of fish returning from the ocean to the lower Mokelumne River as well as fluctuations in hatchery take on variations in observed numbers of redds. The number of spawners was counted using a video recorder that images up-migrating fish at Woodbridge Dam (located downstream of any spawning habitat). A few fish may sneak past the video system or be missed in the count due to human error [*Workman*, 2006]. The number of fish taken into the hatchery was obtained from a manual hatchery count. These data were used to calculate the actual number of spawners in the river relative to the number of redds observed in the study area. If the number of in-river spawners decreased during each stage of slope creation, but the number of observed redds increased in the study area, then that would eliminate variation in migrant population size and hatchery take as possible explanations for increases in redds.

To assess the utilization of the rehabilitated sites relative to the utilization of the much larger area of non-rehabilitated sites, the redds observed at the study site each year was divided by the total number of redds observed throughout the river. An increase in fraction of redds at the study site relative to the rest of the river over the course of the study would demonstrate that the fish were preferentially selecting the rehabilitated sites.

Prediction 3 –Riffles will not scour during spawning flows

To determine whether detrimental scour at spawning flows is inevitable when implementing slope creation, model-predicted Shields stresses were compared pre-, mid- and post-project at 11.33 m^3/s. Evidence of full transport in the mid- and post-project would refute the prediction and indicate the inevitability of scour when implementing a staged slope-creation project, regardless of the lack of a flood regime. Modeling higher flows would be useful for examining sustainability of observed improvements and maintenance mechanisms but necessary floodplain topography and roughness data as well as a stage-discharge rating curve for > 22.65 m^3/s does not exist. Bed scour at high flows is both expected and ideal for gravel maintenance.

RESULTS

To aid the presentation and evaluation of study results, the 2D model predictions for pre-, mid- and post-project are first described. Hydrodynamic validation at the 9 new cross-sections measured in 2003 and 2004 showed similar results to previous validations reported for the lower Mokelumne River [*Pasternack et al.* 2004; *Wheaton et al.* 2004b; *Pasternack et al.* 2006]. Depth was predicted with high accuracy (Fig. 6a,b), except near submerged wood (Fig. 6c). Lateral velocity patterns were mimicked by the model, but showed smoothing (Fig. 6d-f).

Prior to construction, the study reach consisted of three deep pools alternating with two riffles degraded into glides (Figs. 4a, 7a). The reach was relatively homogeneous and lacking hydraulic variability (Fig. 8a). Riffle 1 consisted of low-relief transverse ridges formed by the tailspills of redds constructed in previous spawning seasons. Velocity was locally accelerated

over the ridges. The remaining areas consisted of several deep, low velocity pools and a long uniform glide at "riffle" 2. Mean depth and velocity for each riffle and the study area are given in Table 1.

After the first manipulation, riffle-to-riffle slope was increased from 0.0022 in 2002 to 0.0084 in 2003 (Fig. 4b, 7b). Riffle entrance and exit slopes ranged from 0.002 to 0.060 with the steepest slopes over the study-area terminus. According to the mid-project longitudinal profile, after the first stage of gravel augmentation, water backed up into pool 1 with the water surface rising approximately 0.5 m, equivalent to the increase in riffle 1 crest elevation. Flow accelerated through the chute, completely bypassing the crest of riffle 1, making flow very shallow on the crest of riffle 1 (Fig. 8b). Flow was sent obliquely across the riffle over the secondary crest of riffle 1 with accelerating velocities at the project's terminus. Mean depth on riffle 1 was reduced and mean velocity was increased and more variable (Table 1). No changes were made to riffle 2.

During the second manipulation the increase in riffle 2 elevation created a backwater effect, raising depths upstream on riffle 1 and resulting in a final slope of 0.0039 (Fig. 4c, 7c). The crest elevation of riffle 1 was slightly lowered and a backwater condition was imposed by the increase in elevation on riffle 2. This eliminated overly fast and excessively shallow areas for spawning on riffle 1 that resulted from the first phase (Fig. 8c). The post-project condition on riffle 1 maintained the same mean depth, increased the mean velocity and reduced the range of both. On riffle 2 depths were reduced and velocities increased (Table 1).

Prediction 1 – Habitat quality will improve

Prior to construction the high-quality habitat was arranged in transverse bars along the

ridges in riffle 1. There was a large area unsuitable for spawning in pools 1 and 2 (Fig. 9a). High- and medium-quality habitat made up 20% of the study reach. Very little spawning habitat was predicted on riffle 2 as it was covered with aquatic vegetation.

Following the first manipulation, high-quality habitat was rearranged into longitudinal patches that bordered the chute and the riffle crest (Fig. 9b). The total area of non-habitat for spawning was increased by 1,517 m^2 (Table 2). The increase in the crest of riffle 1 induced a backwater effect in pool 1 converting very poor- and low-quality habitat into non-habitat for spawning. The high velocities and shallow depths on riffle 1 caused a 149 m^2 loss in medium quality habitat providing less than ideal spawning habitat. Regardless, there was a 109 m^2 increase in high-quality habitat mostly bordering the crest of riffle 1 and the chute. Much of the altered channel was on the verge of being too steep and shallow for spawning. The changes in the upstream conditions had no significant effect on habitat quality for un-modified riffle 2.

After the second manipulation, habitat quality was significantly improved across riffle 1, in the chute, and across riffle 2 (Fig. 9c). The non-habitat area was reduced by 3,870 m^2 as large portions of the deeper areas were filled in with gravel (Table 2). There was a dramatic increase (876 m^2) in medium-quality and high-quality habitat (2,540 m^2) relative to the initial condition. The combined two stages of slope creation resulted in a 471% increase in high-quality habitat. This predicted increase in habitat quality corroborates prediction 1, if the model's predictions are accurate, as assessed next.

Prediction 2- Spawners will preferentially utilize high-quality habitat

The numbers of fish migrating upstream past Woodbridge Dam pre-, mid-, and post-project were 10752, 10266, and 11416, respectively. Hatchery take during those three seasons

was 7929 (74%), 8117 (79%), and 10355 (91%), respectively. Thus, the number of spawners actually in the river declined from 2833 pre-project to 2149 mid-project, and then plummeted down to 1061 post-project.

The number of redds observed pre-, mid-, and post-project were 62, 79, and 161, respectively. Thus, the number of redds in the manipulated study area increased steadily, even while in-river spawners declined. From 2003-2004, the number of spawners dropped by 51%, but the number of redds in the study area increased by 104%. These numbers eliminate variation in migrant population size and hatchery take as possible explanations for observed increases in numbers of redds in the study area.

The redds observed in the study area during the three seasons equaled 7%, 11%, and 20% of all redds recorded river-wide, chronologically. These relative increases occurred despite the fact that the study area made up only ~2% of lower Mokelumne River's total spawning reach, fish could freely move in and out of the study area, the number of total spawners in the river decreased sharply in 2004, and the area should already have been highly preferred prior to rehabilitation, because it is located at the upstream limit of fish migration. Thus, not only were there more fish spawning in the study area with each successive manipulation, but the percent of the total spawners river-wide choosing this reach increased as well.

Analysis of the observed spatial distribution of redds validated the habitat-quality predictive capability of the 2D model. Using ANOVA, there was a highly significant positive relationship between GHSI and the actual spawning preference index ($p=0.0004$). This statically validated model predictions. When utilization was adjusted by availability (eqs. 3, 4), high-quality habitat was strongly preferred all years, while non- and low-quality habitats were avoided (Fig. 10), providing an independent validation of model predictions. Thus, both predictions 1 and

2 were corroborated in the study.

Even though predicted high-quality habitat was highly preferred and non habitat avoided in all years, fish preferences shifted noticeably throughout the study as the sites were manipulated (Fig. 10). Over the study, the percents of redds constructed in model-predicted medium- and high-quality habitat at spawning flows trended upward from 48% pre-project to 58% mid-project to 88% post project. Very poor quality habitat and non-habitat were avoided during all stages, even though the number of spawners increased appreciably after the final stage, again indicating a lack of density dependence.

Prediction 3 –Riffles will not scour during spawning flows

Prior to manipulation intermittent entrainment of the median bed surface particle size, D_{50} (40.8 mm), was predicted along the crest of the transverse bars on riffle 1 at the spawning flow (Fig. 11a). Following the first manipulation intermittent entrainment and partial transport was predicted for the D_{50} (50.4 m) in the chute, across the crest of riffle 1 and at the tail spill at the end of riffle 1 (Fig. 11b). This indicates that the elevation gain is close to the maximum possible without initiating significant scour during spawning and incubation periods. There was no change in grain size with the second manipulation, as the same size and range of gravel was added to the site (Table 3). After the second manipulation areas of partial transport at the spawning flow were almost completely eliminated, with a few small areas of intermittent entrainment predicted over the crest of riffle 1 and along the end of riffle 2 (Fig. 11c). This indicates that raising riffle 2 stabilized riffle 1, enabling future rounds of slope creation once this initial effort is extended as far downstream as possible.

DISCUSSION

Ecological Assessment

Widespread changes in channel hydrodynamics and spawner utilization occurred during a 2-year controlled manipulation of a regulated, gravel-bed river channel. Hydrodynamic and spawning-habitat preference predictions made with a 2D model were accurate enough to be statistically validated using observed redd counts. Controlled channel manipulations resulted in a 471 % increase in high-quality Chinook salmon spawning habitat area and more than a doubling in spawner utilization of the study reach, even after the number of in-river spawners dropped by half.

An important outcome of the study was that changing two riffle-pool units had an impact on the population-scale abundance of redds. Even as the river-spawning population declined steady over the study, the number of redds in the study area increased steadily. The study area makes up only ~2% of lower Mokelumne River's spawning reach, but prior to the project, 7% of the population used the site, with this overrepresentation likely due to the site's location at the head of the reach and its proximity to the hatchery. After enhancement, the proportion of the total run spawning at this site tripled, with 20% of the total population using the study area in 2004.

With this population-scale shift toward using rehabilitated sites preferentially, *Merz and Setka* [2004] and *Merz et al*. [2004] showed that spawners on those sites are accessing clean porous gravel, large areas of ideal depth and velocity, complex flow patterns and boulder clusters combining to create some of the most desirable habitat on the lower Mokelumne River. Sites that have been enhanced have shown as high as a 35% increase in survival of incubating

embryos to the fry stage as compared to un-enhanced sites [*Merz et al.*, 2004]. If 20% of the fish are spawning in areas where there is a 35% increase in fry production, then this manipulation will have a highly beneficial impact on river production of Mokelumne Chinook salmon.

Throughout the study, spawning Chinook salmon preferentially used areas predicted by the 2D model to be medium and high quality spawning habitat while avoiding areas predicted to be very poor quality and non spawning habitat. Despite the general validation of prediction 2, the assumptions made about substrate quality may mask the effect of various factors. Qualitative evidence suggests vegetation plays a key role in the choice of spawning location and thus should be incorporated into habitat quality predictions, as done in this study. A more detailed substrate suitability curve incorporating dominant and sub-dominant sediment size as well as organic mud and live aquatic vegetation ought to provide more accurate substrate suitability predictions. The lack of vegetation growing on riffles 1 and 2 during 2003-2006 as well as the on-going lack of vegetation over several more years on the 2000 and 2002 sites rehabilitated with steeper slopes shows that increasing riffle slope and providing periodic spring flow releases of >55 m^3/s effectively eliminates the previous problem observed in *ad hoc* gravel augmentation at the 1999 and 2001 sites on the lower Mokelumne River. The 1999 site was built *ad hoc* and 30% less gravel arrived for construction of the 2001 site relative to the design specification [*Wheaton et al.*, 2004b]. Both of these projects were limited by the upstream backwater effect they created. These factors explain the differences in outcome observed at different riffles after ~5 years.

Spawner utilization of habitat changed as channel conditions improved (Fig. 10). Based on the sequence of utilization over the course of the study, spawners have more relaxed hydraulic criteria for choosing redd locations when a river is degraded. It is likely that under such degraded conditions, surface hydraulics are not adequately indicative of hyporheic water quality, and that

fish are choosing sites based on their assessment of hyporheic conditions. Nevertheless, after rehabilitation improved hydraulic conditions, increased hyporheic exchange, and added new heterogeneous habitat features, spawners became more discerning, with more utilizing high-quality physical habitat in the final state relative to the initial and mid-study states (Fig. 10).

It seems reasonable to conclude that lack of available high-quality habitat forced fish to spawn in lower quality habitat areas initially, but the habitat quality maps show there is available, unused, good habitat in 2002. The fish packed more tightly into the high-quality habitat in 2003 and 2004, indicating something must be turning fish away from the relatively better habitat in 2002. This could be due to the model's inability to capture the effect of intraspecies and interspecies interactions and/or the effect of complex flow structures and hyporheic flow on the choice of redd location. An example of the former is when early spawners choose a site, and then subsequent spawners use the same locations. This may be because the gravel is loosened, and cleaned improving substrate quality, hydraulic conditions and making redd construction easier [*Essington et al*., 1998]. It may be a mechanism to out-compete the early spawners [*Ferguson and Rice,* 1980] or it may simply be one fish following the lead of another. Regardless this phenomenon would be more evident in the pre-project stage when the gravel has yet to be worked over. Early redd construction will improve substrate quality dramatically in a degraded channel, but after clean gravel is added during channel manipulation, all the placed substrates would be loose, clean and easy to move. In this state, the work of early spawners would have less beneficial impact on hyporheic flow and substrate quality. Additionally, most redds are clustered near specific channel features; channel margins, boulder clusters, and along the upstream edge of riffle crests (Fig. 9). Clear patterns of clustering around boulder clusters, riffle crests, and large wood have been observed throughout past Mokelumne

augmentation projects [*Merz*, 2001; *Wheaton et al.*, 2004c] and elsewhere [*Piegay et al.*, 2000; *Rosenfeld et al.*, 2000; *Roni and Quinn*, 2001]. Boulder clusters and large woody debris have been shown to improve spawning habitat by increasing eddies and shear zones [*Abbe and Montgomery*, 1996; *Bouckaert and Davis*, 1998] and providing resting habitat and cover from predators. Redd clustering evident throughout this study (Fig. 9) illustrates the necessity for developing designs not only based on habitat suitability curves and 2D models but on a wider range of qualitative information and established concepts regarding ideal salmon spawning habitat.

Isolating Impact of Slope Creation

By introducing slope directly below the dam the driving force required to raise the flow velocity and lower flow depth was restored, allowing for the introduction of complex flow patterns, improving spawning habitat quality and corroborating prediction 1. Even though fish migration size and hatchery take were eliminated as factors explaining observed increases in redd numbers, a complication arises in attributing the improvements to slope creation as opposed to ancillary improvements associated with gravel placement, including substrate quality improvement, addition of habitat heterogeneity, improved hyporheic flow, flushing of fines and nutrients, etc. For example, major improvements in spawning conditions were observed at riffle 2, but the cause cannot be isolated by this manipulation alone due to the presence of aquatic vegetation and other degraded conditions during the pre-project phase. However, the cause for the improvement can be isolated by comparing the outcome of this manipulation with a previous *ad hoc* non-SHIRA project done at riffle 2 in 1999 [*Pasternack et al.*, 2004; *Merz et al.*, 2006]. That effort used a comparable amount of gravel at the same location, but was built with no

design process or consideration of slope. The upstream riffle remained un-altered while the project on riffle 2 improved substrate quality, used habitat heterogeneity, decreased the cross-sectional area, increased velocity, decreased depth, and flushed fines and nutrients. Despite those changes, no spawners used the site in the first season immediately following construction when substrate quality was highest. In contrast, the same metric after SHIRA-based slope creation in 2004 showed 65 redds. Discharge was ~8.5 m^3/s in both years. Thus, the immediate utilization differences between 1999 and 2004 can be directly attributed to the use of SHIRA and slope creation.

Subsequent utilization of riffle 2 has differed markedly after slope creation in comparison to previous enhancement without it. During 2000-2003 when no manipulations were made to riffle 2, there were 30, 5, 2, and 6 redds present, respectively [*Merz et al.*, 2006]. Inadequate slope and low winter flow releases during this sequence of dry years explain why this site had poor substrate quality and vegetation growth. In contrast, in the second spawning season after the 2004 slope creation, 187 redds were observed on riffle 2 alone. As of October 2006, the study area was clear of vegetation and substrate quality was high. It remains to be seen what future utilization of the site will be, but this comparison of rehabilitation with versus without slope creation at the same location and using the same material strongly suggests that slope creation was primarily responsible for the dramatic gains in redd abundance.

Slope creation effectively provided the opportunity to improve the spawning habitat in the entire reach without drowning upstream riffles. Because slope creation was implemented below a dam and staged over a two-year period, detrimental backwater effects were avoided. This was only possible because the 2D model proved to be accurate enough for this purpose.

Hydrogeomorphic Assessment

Bed scour during low flows associated with spawning and incubation periods can have a significant influence on salmonid embryo survival [*Lisle and Lewis*, 1992]. Artificially cleaned material may exacerbate the potential for scour mortality [*Nawa and Frissell*, 1993]. Consequently, it was important to assess the potential for localized scour in the study area. Little to no intermittent or partial sediment transport was predicted throughout this study at spawning flows, indicating slope creation can be implemented in a staged manner without unwanted scour and sediment transport during the sensitive periods of spawning and embryo incubation. This corroborates prediction 3. No scour was observed between stages. The peak winter flows (42.7 m^3/s) caused no measurable difference in digital elevation model elevations, even in the chute, predicted to exhibit sub-critical intermittent sediment transport. This indicates the need for higher flushing flows to be released from the dam in order to maintain the short-term benefits of slope creation over the longer term. Regardless of the features created, coarse sediments at past Mokelumne rehabilitation projects have accumulated organic fines that may degrade hyporheic water quality. Organic fines build up over years and promote vegetation growth. However, with average to above average water years in 2005 and 2006, transport of placed gravels did take place during late winter and spring after the incubation period. This well-timed runoff was observed to dislodge organic fines, remove vegetation from spots that had it, and redistribute gravel among channel features. Annual injection of 500 tons of gravel upstream of riffle 1 has been implemented to sustain the observed sediment budget in light of the active transport regime that is developing [*Merz et al.*, 2006].

During this study it became apparent that an understanding of the interplay between riffles is critical to managing regulated riffle-pool streams. A single riffle cannot be rehabilitated

without considering the impact on upstream riffles. When gravel augmentation is implemented below a dam there is no upstream riffle affected in the first stage but in the second stage the relationship between riffle 1 and 2 became evident and essential to manage. The increase in elevation at riffle 2 did create a backwater effect in the second stage but turned out to be critical to improving conditions on riffle 1. As more riffles crests are rehabilitated downstream, the interplay becomes more complex, and interdependent. This is metaphorically termed a "reverse domino" effect, with upstream crests dependent on the functioning of downstream crests, just as an individual domino placed in a series depends upon the stability of those around it.

Although not quantified in this study, subsequent gravel augmentations in 2005 and 2006 have been able to distribute this initial elevation gain downstream by an additional 230 m. In part, this has been possible because the next 2 riffle-pool units had such a large cross-sectional area due to historic in-channel gravel mining that filling them in yielded substantial increases in velocity associated with depth constriction without having to raise the slope much. Filling in the channel has also reduced the flow necessary for bankfull discharge, providing a longer duration of floodplain inundation. Changing the channel's width:depth ratio has promoted bank scour, increasing the width of the active channel. As long as active management continues, this positive trajectory should continue.

CONCLUSIONS

A channel manipulation was performed to test aspects of a newly proposed slope-creation methodology. Results indicated 1) habitat quality was maintained in the first stage while providing the opportunity to significantly improve habitat quality in the second stage, 2) spawning Chinook salmon preferentially used 2D model predicted high-quality habitat, and 3)

detrimental sediment entrainment at spawning and embryo-incubation flows was avoided. Alternate explanations for observed increases in numbers of redds in the study area, including fish migration size, hatchery take, and substrate quality improvement were disproved through careful analysis. The results of this study demonstrated the utility of slope creation as a methodology for salmon spawning habitat restoration implemented below dams.

ACKNOWLEDGEMENTS

This project relied heavily on previous research completed on the Mokelumne River in collaboration with Chein Wang, Joe Wheaton, Jose Setka, and Jim Smith. Financial support for this work was provided by East Bay Municipal Utility District (Research Agreement OOK6046), the University of California, and U.S. Fish and Wildlife Service (contracting entity for CALFED Bay-Delta Ecosystem Restoration Program: Cooperative Agreement DCN# 113322G003). We acknowledge Marisa Escobar, Rocko Brown, Hamish Moir, Peng Gao and Professor Jeff Mount for their critical input and support. Ellen Mantalica and Diana Cummings at the UC Davis Center for Watershed Sciences provided valuable administrative support. We thank Warren Jung, Russ Taylor and other East Bay Municipal Utility District staff who were instrumental in assisting with field work and data collection. We thank the undergraduate students Andy Tranmer, April Sawyer, Carlos Alvarado, Dave Van Herrick, Evan Buckland, Kashaul Parikh, Mike Bezemek and Mike Bounrisavong for help with field work, modeling, and data analysis.

REFERENCES

Abbe, T. B., and D.R. Montgomery (1996), Large woody debris jams, channel hydraulics and habitat formation in large rivers, *Reg. River Res. Manage. 12*(2-3), 201-221.

Baxter, C. V., and F.R. Hauer (2000), Geomorphology, hyporheic exchange, and selection of spawning habitat by bull trout (Salvelinus confluentus), *Can. J. Fish. Aquat. Sci., 57*(7), 1470-1481.

Botsford, L. W., and J. G. Brittnacher (1998), Viability of Sacramento River winter-run Chinook salmon, *Cons. Biol.*, *12*(1), 65-79.

Bouckaert, F. W., and J. Davis (1998), Microflow regimes and the distribution of macroinvertebrates around stream boulders, *Freshwater Biol., 40*(1), 77-86.

Bozek, M. A., and F.J. Rahel (1991), Assessing Habitat Requirements of Young Colorado River Cutthroat Trout by Use of Macrohabitat and Microhabitat Analyses, *Trans. Am. Fish. Soc., 120*(5), 571-581.

Brooks, A. P., P.C. Gehrke, J.D. Jansen, and T.B. Abbe (2004), Experimental reintroduction of woody debris on the Williams River, NSW: Geomorphic and ecological responses, *River Res. Appl., 20*(5), 513-536.

Carling, P. A. (1991), An appraisal of the velocity-reversal hypothesis for stable pool riffle sequences in the River Severn, England, *Earth Surf. Processes Landforms, 16*(1), 19-31.

CDFG. (1959), The influences of proposed water projects on the fisheries of the lower Mokelumne River: Amador, Calaveras, and San Joaquin counties, California Department of Fish and Game, Sacramento, California.

CDFG. (1991), Lower Mokelumne River fisheries management plan, California Department of

Fish and Game: The Resources Agency, Sacramento, CA.

CMARP. (1999). CALFED's comprehensive monitoring, assessment, and research program for chinook salmon and steelhead in the central valley rivers, CALFED, Sacramento, CA.

Downs, P. W., and G.M. Kondolf (2002), Post-project appraisals in adaptive management of river channel restoration, *Environ. Manage., 29*(4), 477-496.

DWR. (1994). Comprehensive needs assessment for Chinook salmon habitat improvement projects in the San Joaquin River Basin.

DWR. (2000), Merced River Robinson/Gallo Project - Ratzlaff Reach Engineering Report, California Department of Water Resources, San Joaquin District River Management Section, CA.

DWR. (2001), The Merced River salmon habitat enhancement project Robinson Reach (Phase III) Engineering Report, DWR, CDFG, CALFED, USFWS, San Joaquin District.

Essington, T. E., P.W. Sorensen, and D.G. Paron (1998), High rate of redd superimposition by brook trout (Salvelinus fontinalis) and brown trout (Salmo trutta) in a Minnesota stream cannot be explained by habitat availability alone, *Can. J. Fish. Aquat. Sci., 55*(10), 2310-2316.

FERC. (1998), Order approving settlement agreement and amending license. East Bay Municipal Utility District Lower Mokelumne River Hydroelectric Project No. 2916, Federal Energy Regulatory Commission.

Ferguson, H. W., and D.A. Rice (1980), Post-spawning mortalities in brown trout Salmo-Trutta-L, *J. Fish Diseases, 3*(2), 153-160.

Flosi, G. Downie, S., Hopelain, J., Bird, M., Coey, R., and Collins, B. (1995), California salmonid stream habitat restoration manual, 3rd Edition. California Department of Fish and

Game, Sacramento.

Froehlich, D. C. (1989), HW031.D - Finite Element Surface-Water Modeling System: two-dimensional flow in a horizontal plane--users manual: Federal Highway Administration, *Report FHWA-RD-88-177*, Fed. Highway Admin.

Gayraud, S., E. Herouin, and M. Philippe (2002), The clogging of stream beds: A review of mechanisms and consequences on habitats and macroinvertebrate communities, *Bulletin Francais Peche Pisciculture 365/366*, 339-355.

Geist, D. R. (2000), Hyporheic discharge of river water into fall Chinook salmon (*Oncorhynchus tshawytscha*) spawning areas in the Hanford Reach, Columbia River, *Can. J. Fish. Aquat. Sci, 57*, 1647-1656.

Geist, D. R., and D.D. Dauble (1998), Redd site selection and spawning habitat use by fall Chinook salmon: The importance of geomorphic features in large rivers, *Environ. Manage., 22*(5), 655-669.

Gibbins, C. N., and R.M. Acornley (2000), Salmonid habitat modelling studies and their contribution to the development of an ecologically acceptable release policy for Kielder Reservoir, North-East England, *Reg. River Res. Manage., 16*(3), 203-224.

Gibson, R. J. (2002), The effects of fluvial processes and habitat heterogeneity on distribution, growth and densities of juvenile Atlantic salmon (Salmo salar L.), with consequences on abundance of the adult fish, *Ecol. Freshwater Fish, 11*(4), 207-222.

Grant, G. E., J.C. Schmidt, and S.L. Lewis (2003), A geological framework for interpreting downstream effects of dams on rivers, in *A Peculiar River, Water Science and Application 7*, edited by J. E. O'Connor and Grant, G. E., p. 209-223 American Geophysical Union.

Healey, M. C. (Ed.) (1991), Life history of chinook salmon, in *Pacific Salmon Life Histories*,

edited by C. Groot and L. Margolis, pp. 313-393, UBC Press, Vancouver.

Horan, D. L., J.L. Kershner, C.P. Hawkins, and T.A. Crowl (2000), Effects of habitat area and complexity on Colorado River cutthroat trout density in Uinta Mountain streams, *Trans. Am. Fish. Soc., 129*(6), 1250-1263.

Inoue, M., and S. Nakano (1998), Effects of woody debris on the habitat of juvenile masu salmon (Oncorhynchus masou) in northern Japanese streams, *Freshwater Biol., 40*(1), 1-16.

Knighton, D. (1998), *Fluvial Forms and Processes: A New Perspective*., 398pp., HodderArnold, New York.

Kondolf, G. M., and S.G. Li (1992), The pebble count technique for quantifying surface bed material size in instream flow studies, *Rivers, 3*, 80-87.

Kondolf, G. M. and J. T. Minear (2004), Coarse sediment augmentation on the Trinity River below Lewiston Dam: geomorphic perspectives and review of past projects. Final Report to the Trinity River Restoration Program, University of California, Berkeley, CA.

Kondolf, G. M., J.C. Vick, and T.M. Ramirez (1996), Salmon spawning habitat rehabilitation on the Merced River, California: An evaluation of project planning and performance, *Trans. Am. Fish. Soc., 125*(6), 899-912.

Kondolf, G. M., M. W. Smeltzer, and S. F. Railsback (2001). "Design and performance of a channel reconstruction project in a coastal California gravel-bed stream." *Environ. Manage., 28*(6), 761-776.

Lechowicz, M. J. (1982), The sampling characteristics of electivity indicies, *Oecologia, 52*, 22-30.

Leclerc, M., A. Boudreault, J.A. Bechara, and G. Corfa (1995), 2-Dimensional hydrodynamic modeling - a neglected tool in the instream flow incremental methodology, *Trans. Am. Fish.*

Soc., 124(5), 645-662.

Ligon, F. K., W.E. Dietrich, and W.J. Trush (1995), Downstream ecological effects of dams, *Bioscience, 45*(3), 183-192.

Lisle, T. E., and M. Church (2002), Sediment transport-storage relations for degrading, gravel bed channels, *Water Resour. Res., 38*(11).

Lisle, T. E., and J. Lewis (1992), Effects of sediment transport on survival of salmonid embryos in a natural stream: a simulation approach. *Can. J. Fish. Aquat. Sci.*, *49*, 2337-2344.

Lisle, T. E., J.M. Nelson, J. Pitlick, M.A. Madej, and B.L. Barkett (2000), Variability of bed mobility in natural, gravel-bed channels and adjustments to sediment load at local and reach scales, *Water Resour. Res., 36*(12), 3743-3755.

MacWilliams, M.L., Wheaton, J.M., Pasternack, G.B., Kitanidis, P.K., Street, R.L., 2006. the flow convergence-routing hypothesis for pool-riffle maintenance in alluvial rivers. Water Resources Research *42*, doi:10.1029/2005WR004391.

Madsen, J.D., P.A. Chambers, W.F. James, E.W. Koch, and D.F. Westlake (2001) The interaction between water movement, sediment dynamics and submersed macrophytes, *Hydrobiologia 44*(1-3), 71-84.

Marchetti, M. P., and P. B. Moyle (2001), Effects of flow regime on fish assemblages in a regulated California stream, *Ecol. Appl.*, *11*(2), 530-539.

Marchetti, M. P., T. Light, P. B. Moyle, J. H. Viers (2004), Fish invasions in California watersheds: testing hypotheses using landscape patterns, *Ecol. Appl.*, 14(5), 1507-1525

McBain, S., M. Trush, and G. Matthews (2000), Lower Clear Creek floodway rehabilitation project. channel reconstruction, riparian vegetation and wetland creation and design document, McBain and Trush, Arcata, CA.

Merz, J. E. (2001), Association of fall-run Chinook salmon redds with woody debris in the lower Mokelumne River, California, *Ca. Fish Game, 87*(2), 51-60.

Merz, J. E., and J.D. Setka (2004), Evaluation of a spawning habitat enhancement site for Chinook salmon in a regulated California River, *N. Am. J. Fish. Manage., 24*(2), 397-407.

Merz, J.E., L.K. Ochikubo Chan (2005), Effects of gravel augmentation on macroinvertebrate assemblages in a regulated California river, *River Resear. Appl.*, *21*, 61-74.

Merz, J. E., G.B. Pasternack, and J.M. Wheaton (2006), Sediment budget for salmonid spawning habitat rehabilitation in a regulated river. *Geomorphology, 76*(1-2), 207-228.

Merz, J. E., J.D. Setka, G.B. Pasternack, and J.M. Wheaton (2004), Predicting benefits of spawning-habitat rehabilitation to salmonid (Oncorhynchus spp.) fry production in a regulated California river, *Can. J. Fish. Aquat. Sci., 61*(8), 1433-1446.

Moyle, P. B. 1994. The decline of anadromous fishes in California. Conservation Biology 8:3:869-870.

Moyle, P. B., and P.J. Randall (1998), Evaluating the biotic integrity of watersheds in the Sierra Nevada, California, *Conserv. Biol., 12*, 1318-1326.

Nawa, R. K., and C. A. Frissell (1993), Measuring scour and fill of gravel streambeds with scour chains and sliding bead monitors. *N. Amer. J. Fish. Manage.*, 5, 480-488.

Nehlsen, W., J.E. Williams, and J.A. Lichatowich (1991), Pacific salmon at the crossroads: stocks at risk from California, Oregon, Idaho, and Washington, *Fisheries, 16*, 4-21.

Nielsen, J. L., and T. E. Lisle (1994), thermally stratified pools and their use by steelhead in northern California streams, *Trans. Am. Fish. Soc., 123*, 613-626.

Pasternack, G.B., A.T. Gilbert, J.M. Wheaton, and E.M. Buckland (2006), 2D model fluid mechanics error propagation for velocity and shear stress prediction, *J. Hydrol. 328*, 227-241

Pasternack, G.B., C.L. Wang, and J.E. Merz (2004), Application of a 2D hydrodynamic model to design of reach-scale spawning gravel replenishment on the Mokelumne River, California, *River Res. Appl., 20*(2), 205-225.

Piegay, H., A. Thevenet, G.M. Kondolf, and N. Landon (2000), Physical and human factors influencing potential fish habitat distribution along a Mountain River, France, *Geografiska Annaler Series a-Physical Geography, 82A*(1), 121-136.

Roni, P., and T.P. Quinn (2001), Density and size of juvenile salmonids in response to placement of large woody debris in western Oregon and Washington streams, *Can. J. Fish. Aquat. Sci, 58*, 282-292.

Rosenfeld, J., M. Porter, and E. Parkinson (2000), Habitat factors affecting the abundance and distribution of juvenile cutthroat trout (Oncorhynchus clarki) and coho salmon (Oncorhynchus kisutch), *Can. J. Fish. Aquat. Sci., 57*(4), 766-774.

Sand-Jensen, K. (1998) Influence of submerged macrophytes on sediment composition and near-bed flow in lowland streams. *Freshwater Biology*, *39*(4) 663-679.

Sear, D.A., and M.D. Newson (2004), The hydraulic impact and performance of a lowland rehabilitation scheme based on pool-riffle installation: The River Waveney, Scole, Suffolk, UK, *River Res. Appl., 20*(7), 847-863.

Smith, J. R., J.E. Merz, and M.L. Workman (2004), Effect of a controlled flow release on rooted aquatic vegetation in Chinook salmon spawning habitat in the lower Mokelumne River, California, East Bay Municipal Utility District, Lodi, CA.

Urabe, H., and S. Nakano (1998), Contribution of woody debris to trout habitat modification in small streams in secondary deciduous forest, northern Japan, *Ecol. Res., 13*(3), 335-345.

USFWS. (1997), Revised draft restoration plan for the Anadromous Fish Restoration Program,

Department of the Interior, Washington, D.C.

USFWS. (2001), Final restoration plan for the Anadromous Fish Restoration Program. Anadromous Fish Restoration Program. Department of Interior. Washington, D.C.

Wheaton, J. M., G.B. Pasternack, and J.E. Merz (2004a), Spawning habitat rehabilitation - I. Conceptual approach and methods, *Int. J. River Basin Manage., 2*(1), 3-20.

Wheaton, J. M., G.B. Pasternack, and J.E. Merz (2004b), Spawning habitat rehabilitation - II. Using hypothesis development and testing in design, Mokelumne River, California, U.S.A., *Int. J. River Basin Manage., 2*(1), 21-37.

Wheaton, J. M., G.B. Pasternack, and J.E. Merz (2004c), Use of habitat heterogeneity in salmonid spawning habitat rehabilitation design, presented paper at Fifth International Symposium on Ecohydraulics: Aquatic Habitats: Analysis and Restoration, IAHR-AIRH, Madrid, Spain.

Williams, G. P., and M.G. Wolman (1984), Downstream effects of dams on alluvial rivers, *Professional Paper, 1286*, U.S. Geol. Surv., Washington, D.C.

Workman, M. L. (2003), Lower Mokelumne River upstream fish migration monitoring conducted at Woodbridge irrigation District Dam (08/02-07/03), East Bay Municipal Utility District, Lodi, CA.

Workman, M. L. (2006), Lower Mokelumne River fall run Chinook salmon escapement report, October through December 2005, East Bay Municipal Utility District, Lodi, CA.

Yoshiyama, R. M., E.R. Gerstung, F.W. Fisher, and P.B. Moyle (2000), Chinook salmon in the California Central Valley: an assessment, *Fisheries, 25*(2), 6-20.

Zalewski, M., B. Bis, M. Lapinska, P. Frankiewicz, and W. Puchalski (1998), The importance of the riparian ecotone and river hydraulics for sustainable basin-scale restoration scenarios,

Aquat. Conserv. Marine Freshwater Ecosys., 8(2), 287-307.

FIGURE CAPTIONS

Figure 1. Longitudinal profile of a stream illustrating a 2-stage addition of gravel for "slope creation", such as performed in this study. After the first stage, riffle-to-riffle slope is steeper than desired, but that is resolved in the second stage.

Figure 2. Conceptual model describing slope creation methodology used in this study for Chinook salmon spawning habitat rehabilitation. Before using this, preliminary planning including goal setting should be performed, such as described in *Wheaton et al*. [2004a].

Figure 3. Map of the Mokelumne River basin showing locations of Camanche and Pardee Reservoirs. The study site was located immediately downstream of the tailpool at the base of Camanche Dam.

Figure 4. Digital elevation models of the study site during A) pre-, B) mid- and C) post-manipulation stages. Darker shading equals lower elevation.

Figure 5. Habitat Suitability Curves developed for the Mokelumne River by *CDFG* [1991]. Curves predict habitat quality based on flow depth, velocity and substrate type.

Figure 6. Comparisons of observed versus predicted depths and velocities at a representative cross-section for the pre- (A, D), mid- (B, E) and post- (C, F) project stages. Field observations were fit with a curve using the locally weighted Least Squared error method to reduce

measurement noise.

Figure 7. Longitudinal profiles showing change in thalweg elevation (solid line) and water surface elevation (dashed line) for the A) pre-, B) mid- and C) post- manipulation stages of the study.

Figure 8. 2D model velocity predictions at 11.33 m^3/s for the A) pre-, B) mid- and C) post-manipulation stages. Arrows indicate velocity direction, while darker shading equals higher velocity.

Figure 9. 2D model habitat-quality predictions at 11.33 m^3/s showing the global habitat suitability index (GHSI) at the A) pre-, B) mid- and C) post- manipulation stages. Validation is provided by comparison against actual redd locations for each stage, shown as targeted disks.

Figure 10. Utilization and availability of spawning habitat as predicted for the A) pre-, B) mid- and C) post- manipulation stages using the three analysis methods. Utilization values larger than availability indicates a preference while availability larger than utilization indicates avoidance.

Figure 11. 2D model predictions of Shield stress at 11.33 m^3/s for the A) pre-, B) mid- and C) post- manipulation stages of the study.

Table 1. Mean and ± 1 standard deviation of depth and velocity modeled at 11.33 m^3/s in the project reach, on riffle 1 and riffle 2.

Location	Pre-Project	Mid-Project	Post-Project
		Depth (m)	
Study Area	0.76 ±0.45	0.68 ±0.51	0.68 ±0.50
Riffle 1	0.63 ±0.29	0.45 ±0.34	0.45 ±0.23
Riffle 2	0.59 ±0.29	0.60 ±0.30	0.44 ±0.15
		Velocity (m s^{-1})	
Study Area	0.45 ±0.24	0.47 ±0.38	0.52 ±0.35
Riffle 1	0.51 ±0.21	0.63 ±0.46	0.68 ±0.29
Riffle 2	0.62 ±0.19	0.65 ±0.26	0.85 ±0.26

Table 2. Channel area in each spawning habitat quality category modeled at 11.33 m^3/s.

			Habitat Quality				
Project Stage	Metric	Non	Very Poor	Low	Medium	High	Total Habitat Area (m^2)*
Pre-Project	Area (m^2)	4173	444	4204	1433	539	6619
	Area (%)	-	7	64	22	8	100
Mid-Project	Area (m^2)	5690	901	2595	1284	648	5427
	Area (%)	-	17	48	24	12	100
Pre to Mid Change	Area (m^2)	1517	457	-1609	-149	109	-1192
Post-Project	Area (m^2)	1819	782	3128	2308	3079	9297
	Area (%)	-	8	34	25	33	100
Mid to Post Change	Area (m^2)	-3870	-119	533	1025	2431	3870

*Excludes non-habitat

1

2

3

Table 3. Measured low, median, and high surface grain sizes (mm) for each stage of the study.

Size Parameter*	Pre-Project	Mid-Project	Post-Project
D_{16}	22.8	32.5	32.5
D_{50}	40.8	50.4	50.4
D_{90}	69.6	85.1	85.1

*subscript denotes percent of particles smaller than

4

5

6

7

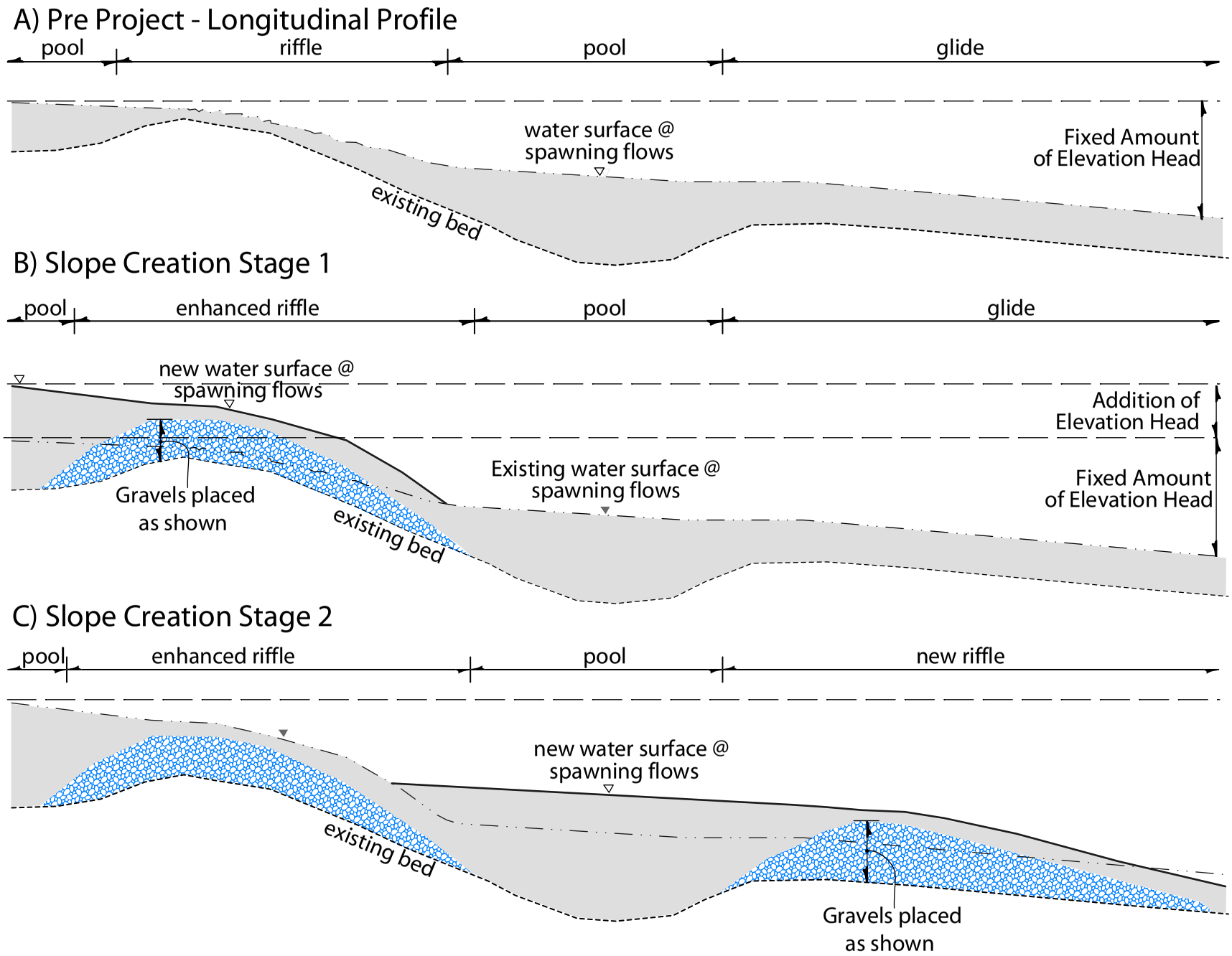
A) Pre Project - Longitudinal Profile
pool
riffle
pool
glide
water surface @
spawning flows
existing bed
Fixed Amount
of Elevation Head
B) Slope Creation Stage 1
pool
enhanced riffle
pool
glide
new water surface @
spawning flows
Addition of
Elevation Head
Existing water surface @
spawning flows
Fixed Amount
of Elevation Head
Gravels placed
as shown
existing bed
C) Slope Creation Stage 2
pool
enhanced riffle
pool
new riffle
new water surface @
spawning flows
existing bed
Gravels placed
as shown

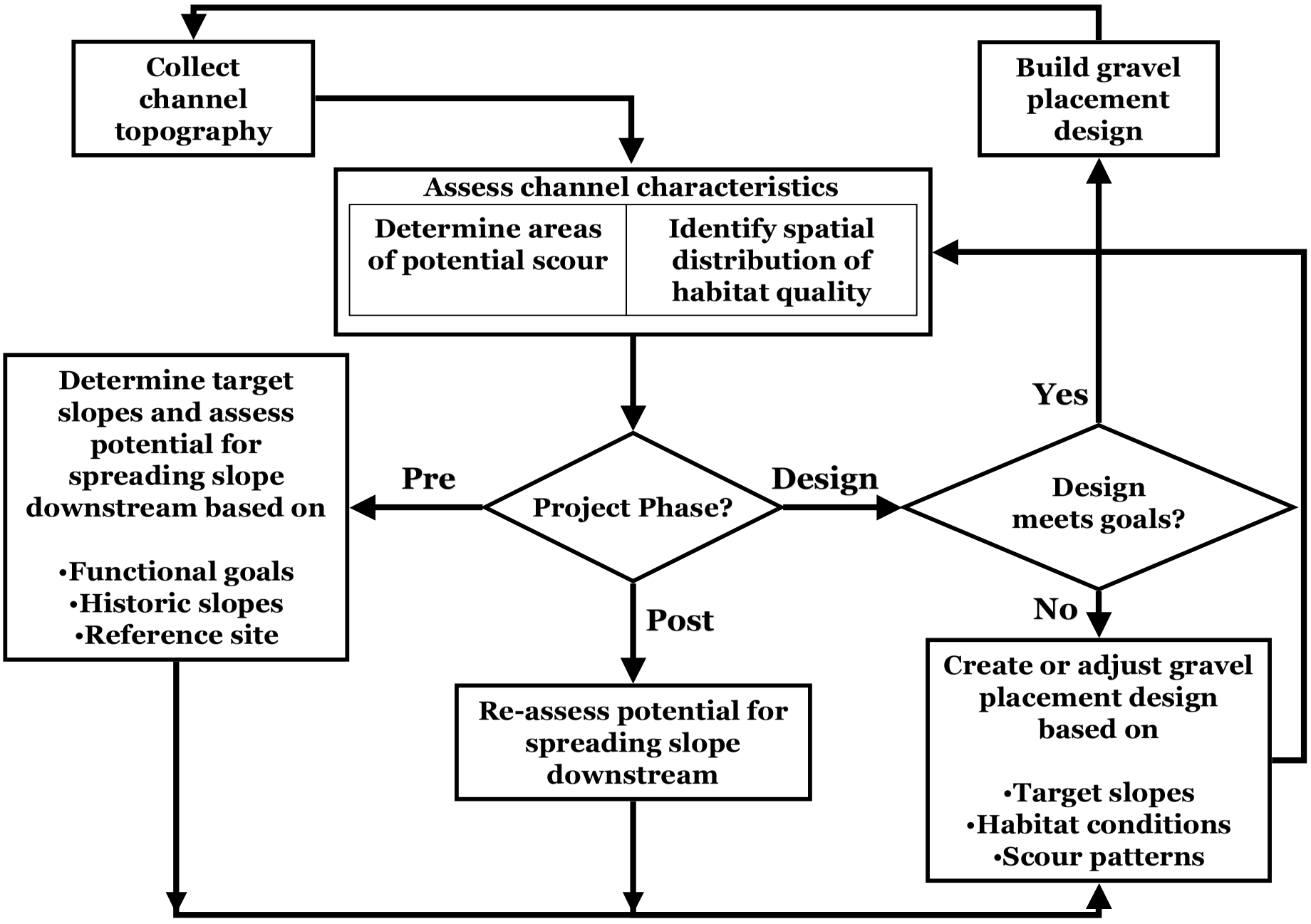
Collect channel topography
Assess channel characteristics
Determine areas of potential scour
Identify spatial distribution of habitat quality
Build gravel placement design
Determine target slopes and assess potential for spreading slope downstream based on
•Functional goals
•Historic slopes
•Reference site
Pre
Project Phase?
Design
Post
Yes
Design meets goals?
No
Re-assess potential for spreading slope downstream
Create or adjust gravel placement design based on
•Target slopes
•Habitat conditions
•Scour patterns

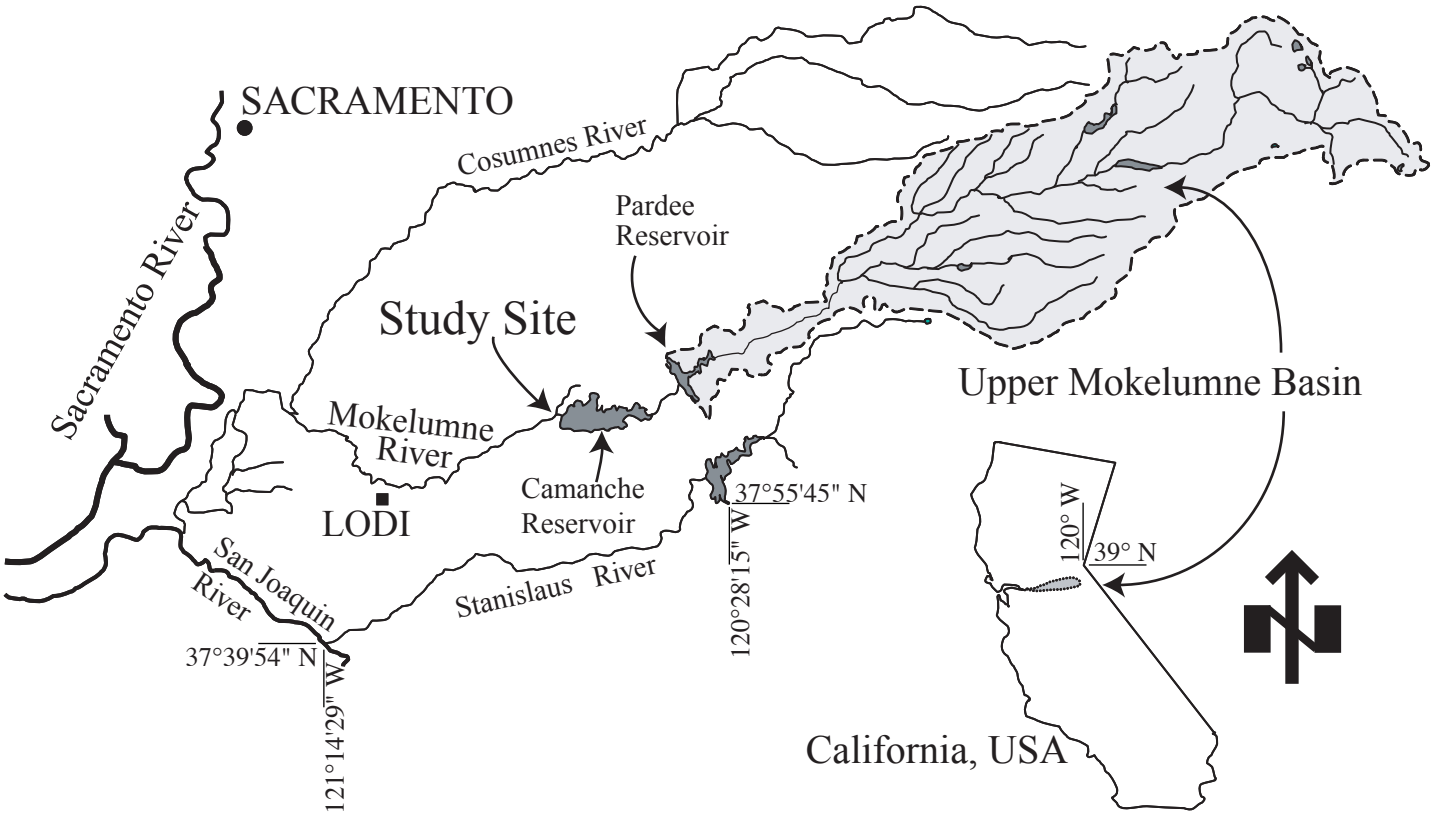
SACRAMENTO
Cosumnes River
Sacramento River
Pardee
Reservoir
Study Site
Upper Mokelumne Basin
Mokelumne
River
Camanche
Reservoir
37°55'45" N
LODI
120° W
39° N
San Joaquin
River
Stanislaus River
37°39'54" N
120°28'15" W
121°14'29" W
California, USA

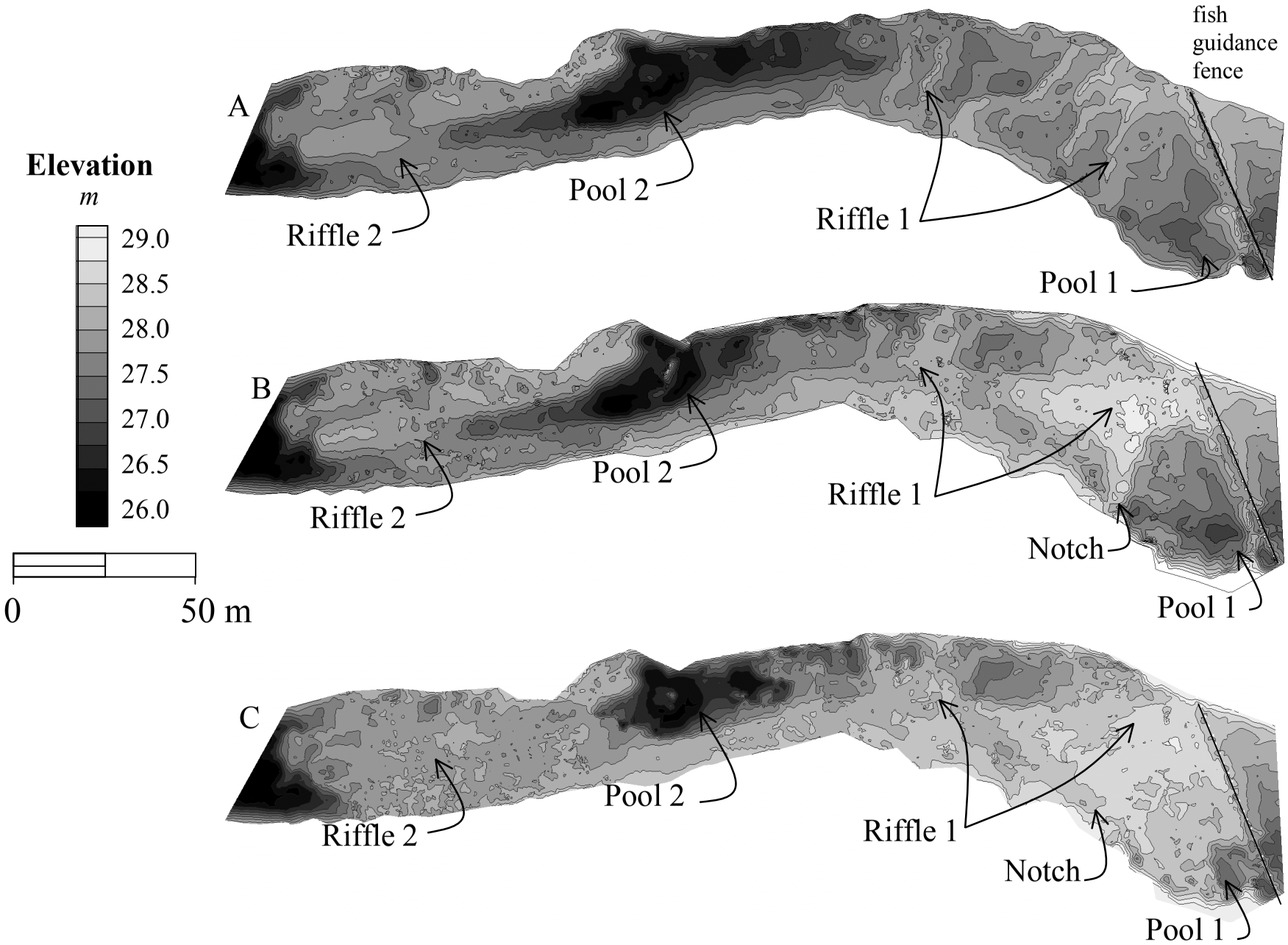
Elevation
m
29.0
28.5
28.0
27.5
27.0
26.5
26.0
0
50 m
A
Riffle 2
Pool 2
Riffle 1
Pool 1
fish
guidance
fence
B
Riffle 2
Pool 2
Riffle 1
Notch
Pool 1
C
Riffle 2
Pool 2
Riffle 1
Notch
Pool 1

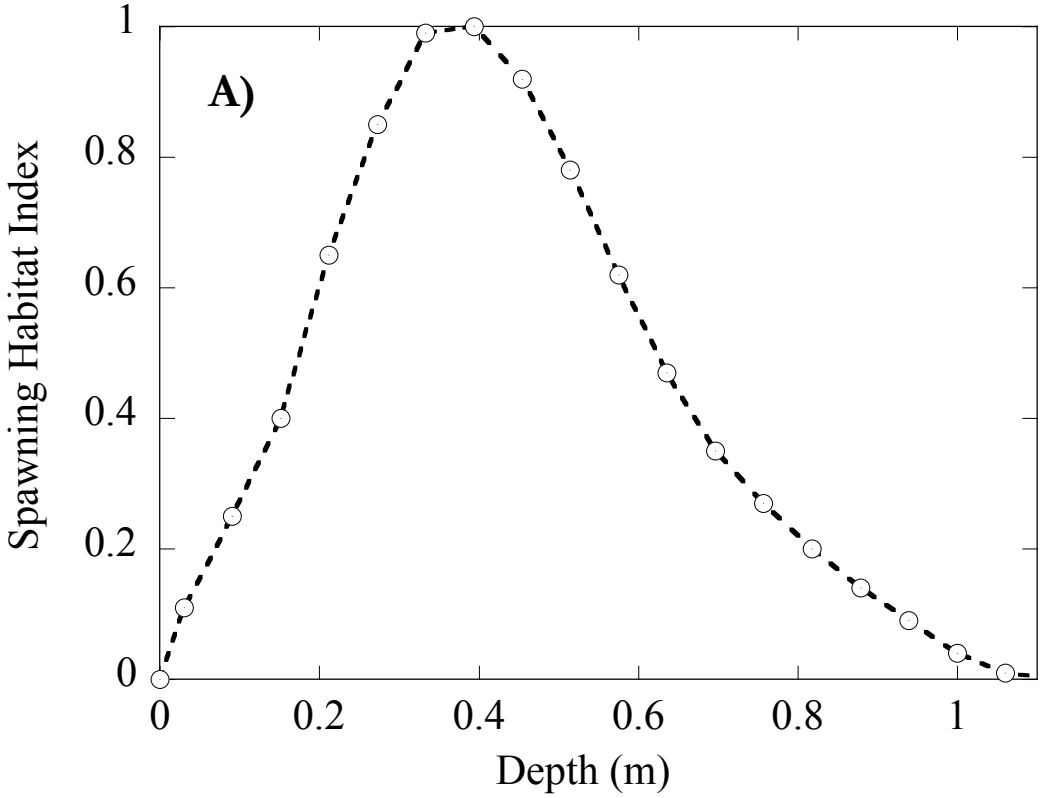
A)
Spawning Habitat Index
Depth (m)
0
0.2
0.4
0.6
0.8
1

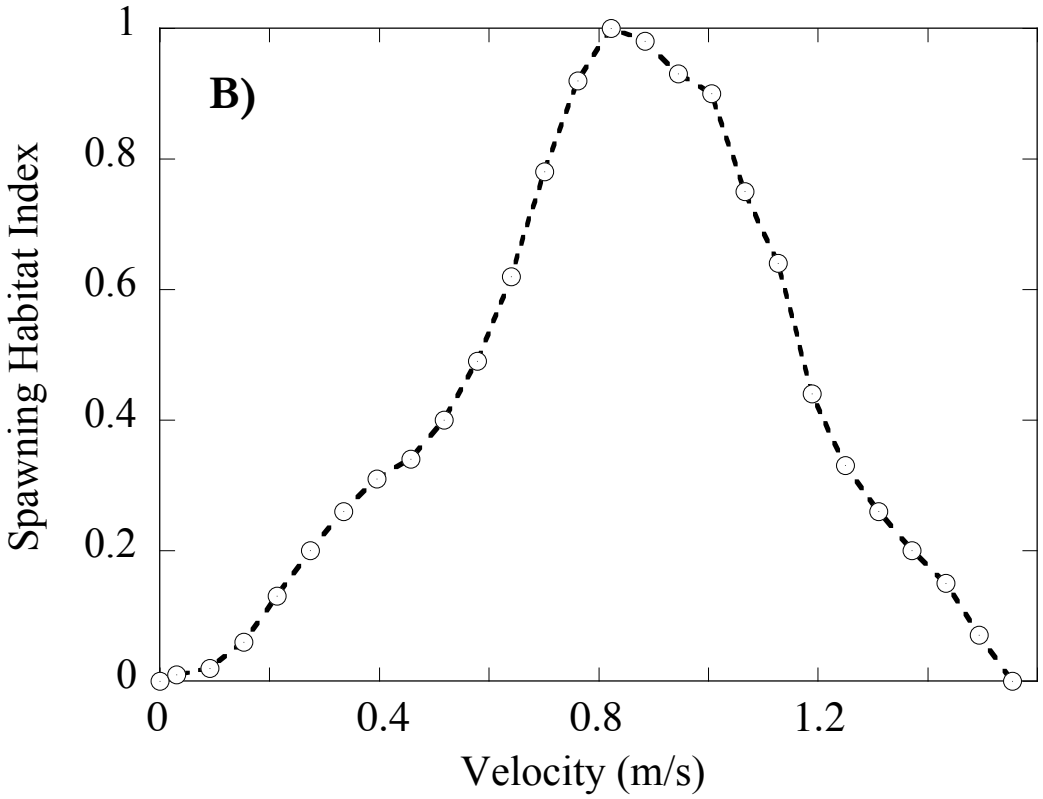
B)
Spawning Habitat Index
Velocity (m/s)
0
0.4
0.8
1.2
0.2
0.6
1

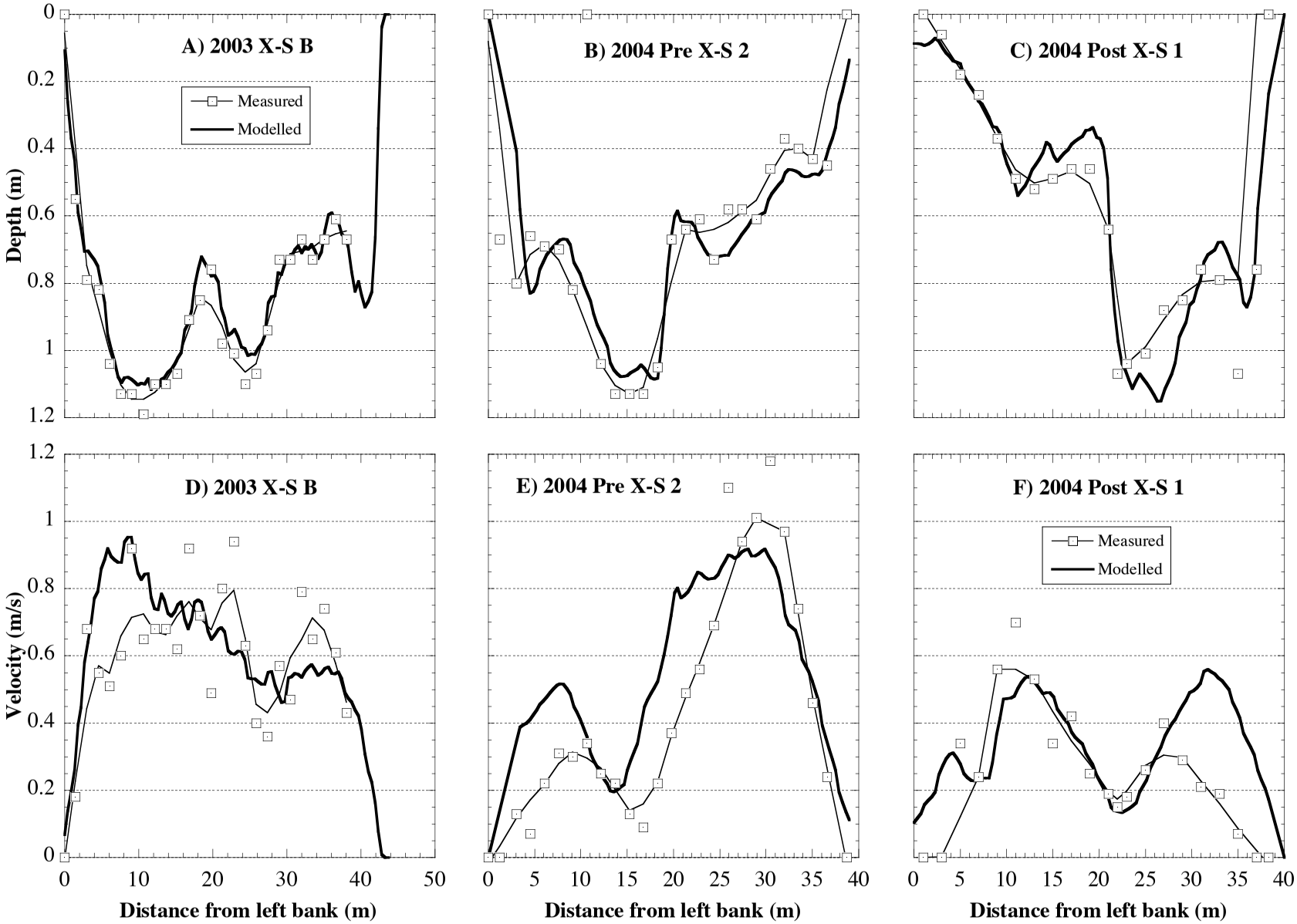
A) 2003 X-S B
B) 2004 Pre X-S 2
C) 2004 Post X-S 1
D) 2003 X-S B
E) 2004 Pre X-S 2
F) 2004 Post X-S 1
Measured
Modelled
Depth (m)
Velocity (m/s)
Distance from left bank (m)
Distance from left bank (m)
Distance from left bank (m)

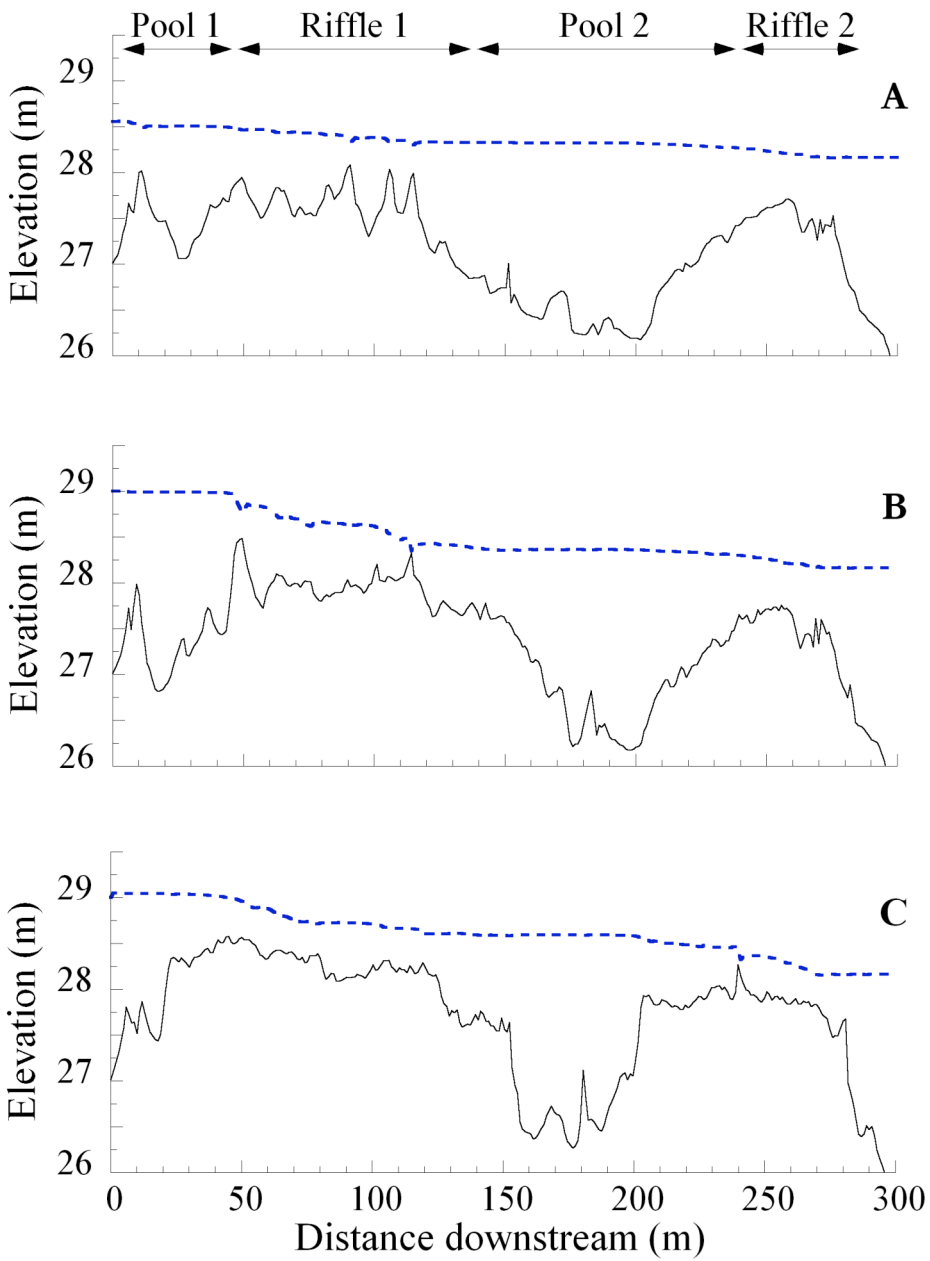
Pool 1
Riffle 1
Pool 2
Riffle 2
A
B
C
Elevation (m)
29
28
27
26
0
50
100
150
200
250
300
Distance downstream (m)

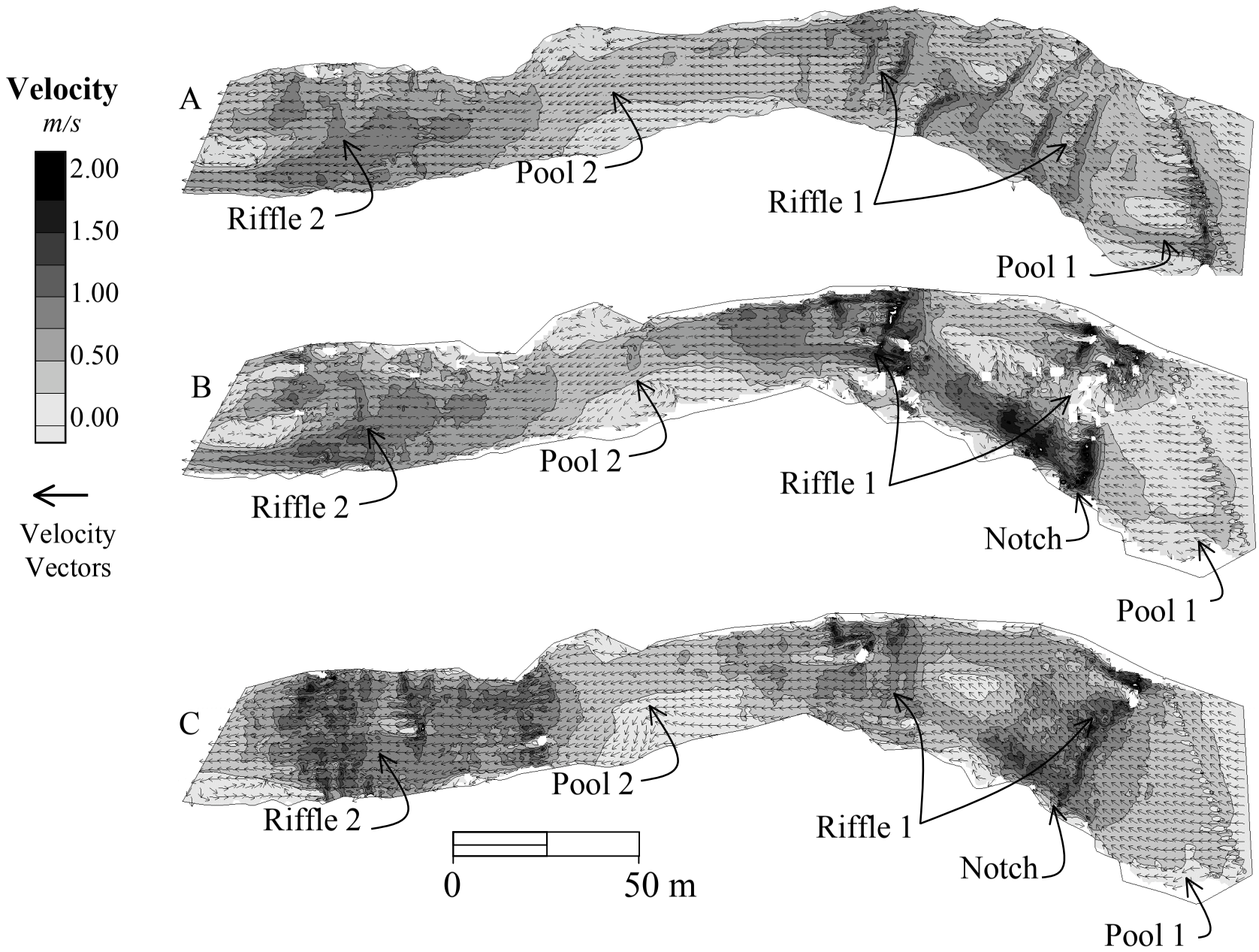
Velocity
m/s
2.00
1.50
1.00
0.50
0.00
Velocity Vectors
A
Riffle 2
Pool 2
Riffle 1
Pool 1
B
Riffle 2
Pool 2
Riffle 1
Notch
Pool 1
C
Riffle 2
Pool 2
Riffle 1
Notch
Pool 1
0
50 m

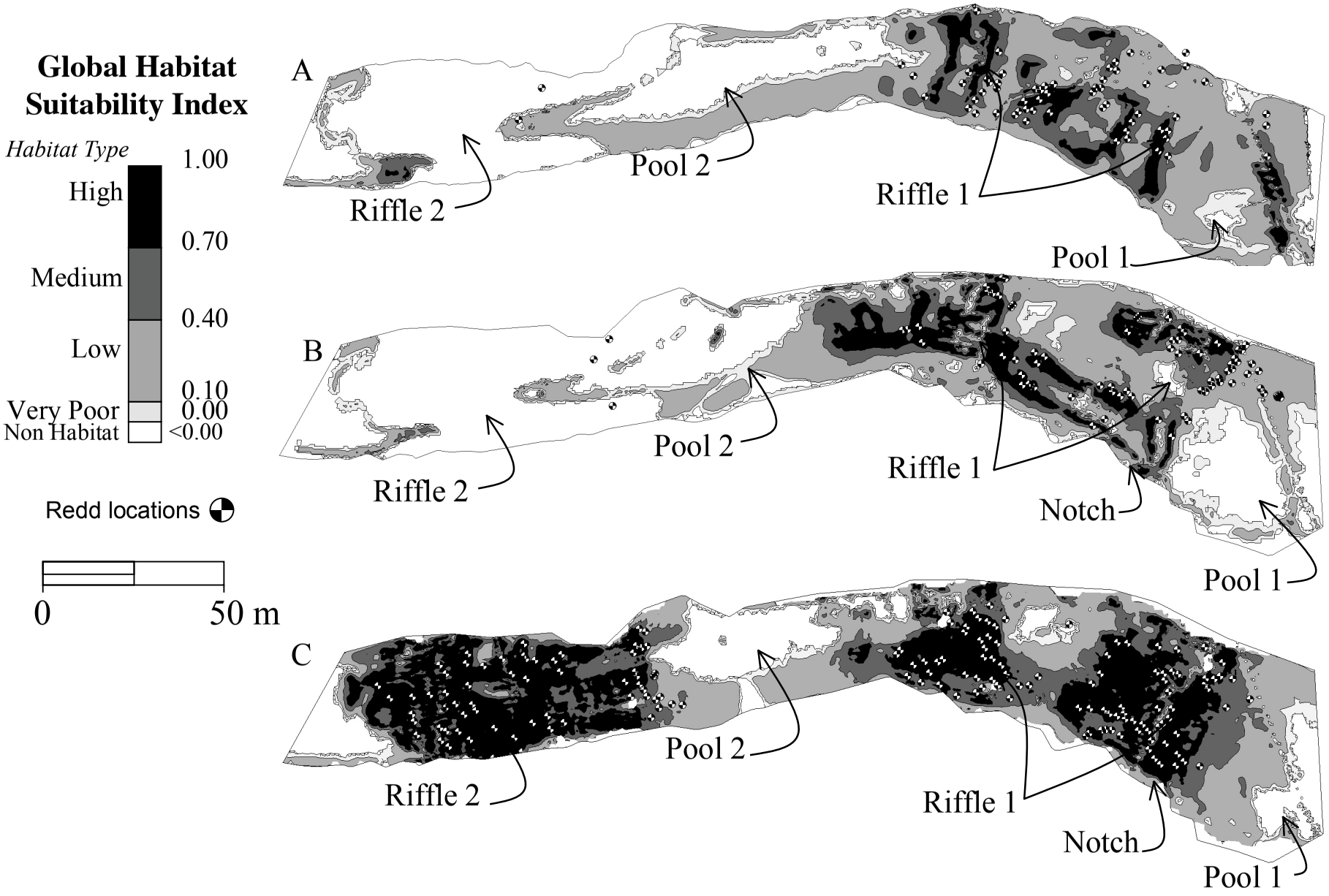
Global Habitat Suitability Index
Habitat Type
1.00
High
0.70
Medium
0.40
Low
0.10
Very Poor
0.00
Non Habitat
<0.00
Redd locations
0
50 m
A
Riffle 2
Pool 2
Riffle 1
Pool 1
B
Riffle 2
Pool 2
Riffle 1
Notch
Pool 1
C
Riffle 2
Pool 2
Riffle 1
Notch
Pool 1

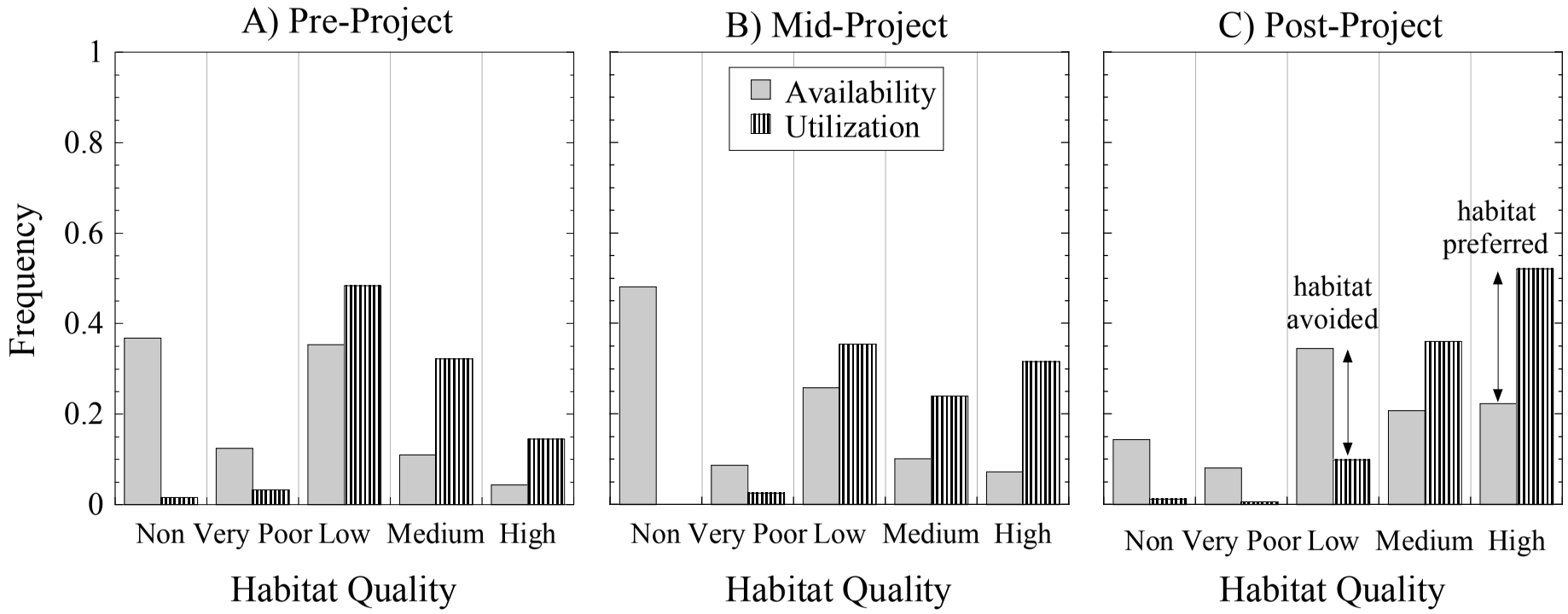
A) Pre-Project
B) Mid-Project
C) Post-Project
Frequency
1
0.8
0.6
0.4
0.2
0
Availability
Utilization
habitat
avoided
habitat
preferred
Non Very Poor Low Medium High
Habitat Quality

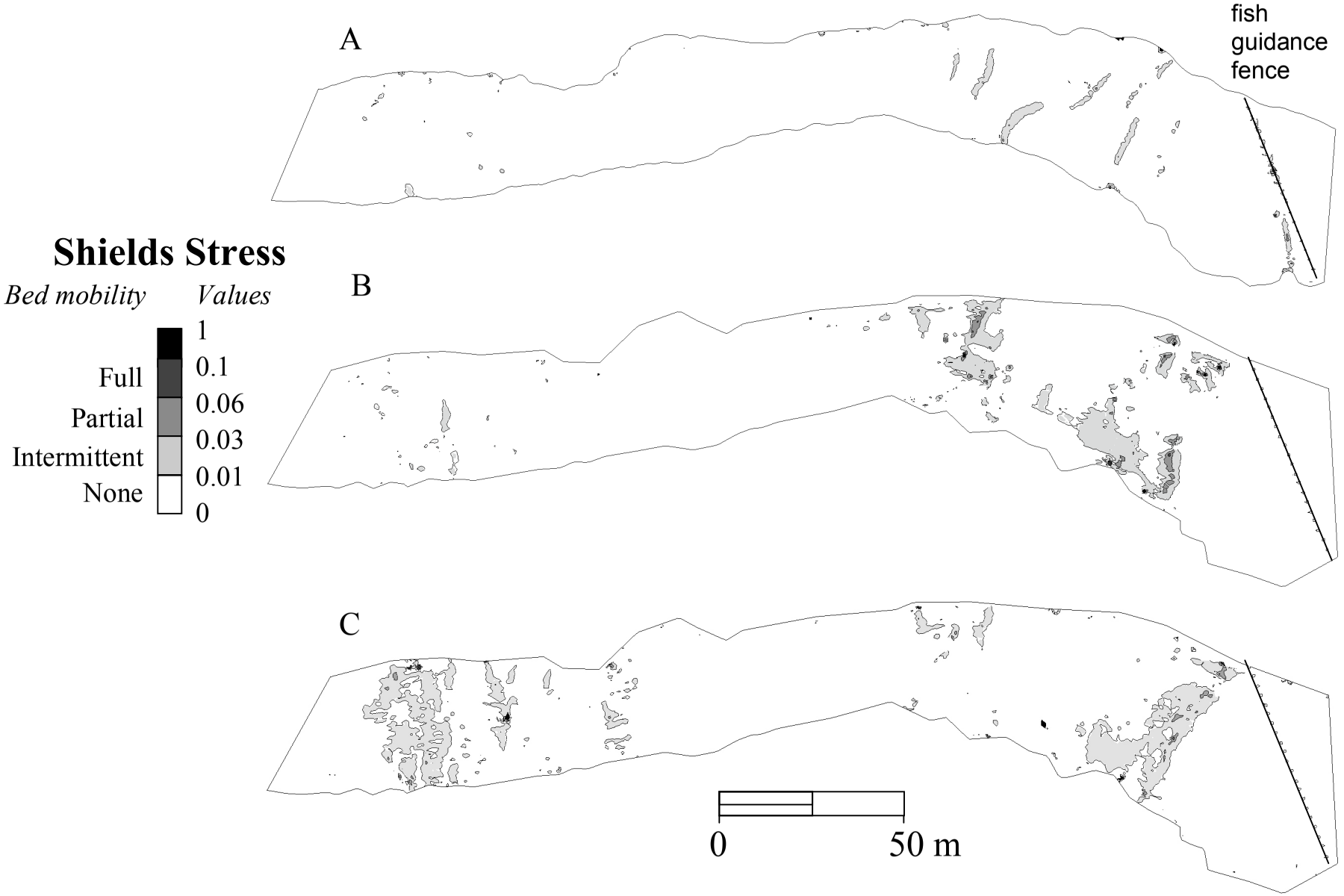
A
fish
guidance
fence
B
C
Shields Stress
Bed mobility
Values
Full
Partial
Intermittent
None
1
0.1
0.06
0.03
0.01
0
0
50 m

Use of habitat heterogeneity in salmonid spawning habitat rehabilitation design

J.M. Wheaton*, G.B. Pasternack
Department of Land, Air and Water Resources, University of California at Davis, Davis, California, U.S.A.
**currently: School of Geography, University of Southampton, Southampton, U.K: Joe.Wheaton@soton.ac.uk.*

J.E. Merz
Department of Wildlife, Fish and Conservation Biology, University of California at Davis, Davis, California, U.S.A.

ABSTRACT: A shortage of salmonid spawning habitat on dammed and regulated rivers has led to the popularity of spawning habitat rehabilitation projects. Habitat heterogeneity is thought to be an important feature of aquatic ecosystems, but specific metrics for design and assessment are lacking. In August 2002, ~ 2,786 metric tons of spawning gravels and 7 large boulders were placed in a 155 meter reach on the lower Mokelumne River, California, USA. Habitat heterogeneity was incorporated into the design as part of a spawning habitat integrated rehabilitation approach (SHIRA) developed by the authors. A mix of conceptual and numerical models (2D hydrodynamic with habitat suitability and sediment entrainment submodels) were used to test the effectiveness of design scenarios. Although optimal spawning habitat as defined by habitat suitability models is generally found in riffles, proximity of habitat to structural cover (pools, large woody debris, boulder clusters and overhanging vegetation) and hydrodynamic shear zones provide equally important refuge from predation and resting zones for energy conservation. The increased heterogeneity appeared highly effective in terms of redd utilization with 70 redds located in close proximity to 93% of the available structural cover, and 42 redds located in close proximity to 90% of the available shear zone refugia. Partial results emphasizing habitat heterogeneity availability and utilization metrics are presented to illustrate their potential in rehabilitation design and assessment.

1 INTRODUCTION

In both the ecology and geomorphology literature, the importance of habitat heterogeneity is usually presumed to positively influence biodiversity (NRC 1992; Palmer et al. 1997); but habitat heterogeneity can manifest benefits in terms of specific ecologic functions as well (Wheaton et al. 2004b). In a review of 85 papers on habitat heterogeneity in terrestrial ecosystems from 1960-2003, Tews et al. (2004) found 85% reported a positive correlation between species diversity and habitat heterogeneity; but caution that metrics for measuring species and structural diversity are inconsistently defined and highly scale-dependent. This highlights a vague distinction between the presumed benefits of habitat heterogeneity and the impacts of habitat fragmentation. The notion of the importance of habitat heterogeneity is also well engrained in the habitat restoration community (Pretty et al. 2003), but how this is achieved in practice remains ambiguous. In many rivers of North America and Europe, declines in salmonid populations have been partially attributed to elimination, degradation and homogenization of physical habitat (Cowx & Welcomme 1998; Hendry et al. 2003; Nehlsen et al. 1991). This has prompted the allocation of millions of euros, dollars and pounds towards spawning habitat rehabilitation (SHR) efforts (Kondolf 2000; Nijland & Cals 2000). Wheaton et al. (2004b) segregate SHR into a passive approach: gravel augmentation; and two active approaches: hydraulic structure placement (e.g. large woody debris, boulders, deflectors) and spawning bed enhancement (e.g. riffle construction). Hydraulic structures are frequently intended in habitat rehabilitation to increase heterogeneity, with intended benefits to juvenile lifestages and macroinvertebrates (Muotka et al. 2002); but are usually only used in SHR to promote deposition of spawning gravels (Wheaton et al. 2004b). Here, we focus on specific ecological benefits of habitat heterogeneity to spawning salmonids (e.g. Merz 2001). Presumed ecosystem benefits of increased species diversity from habitat heterogeneity are not addressed.

This paper illustrates how habitat heterogeneity can be incorporated to SHR through use of habitat availability metrics in design and their effectiveness assessed through habitat utilization in pre and post project appraisal. A SHR project constructed in August 2002 on the lower Mokelumne River (LMR), California, USA is used as a case study. The SHIRA (spawning habitat integrated rehabilitation approach)

framework was used to plan, design, construct and monitor the project; but details of the approach, provided in Wheaton et al. (2004a; 2004b), are not discussed here. The structural features used to provide habitat heterogeneity are themselves microhabitat scale (10^{-1} to 10^{0} m) features but produce heterogeneity over the macrohabitat or morphological-unit scale (10^{0} to 10^{1} m).

2 STUDY SITE

The Mokelumne River of central California drains a 1700 km^2 basin out of the Sierra Nevada westward to the Sacramento-San Joaquin Bay Delta (see Merz 2001). Sixteen major dams or diversions have dramatically altered the LMR's flow regime reducing the two year recurrence interval flow from 164 to 54 cumecs (Pasternack et al. 2004). The dams have blocked the replenishment of spawning gravels to the LMR since 1963. SHR for fall-run chinook salmon (*Oncorhynchus tschawytscha*) is now required as part of dam relicensing on the LMR (FERC 1998). The upper 9.6 km of the LMR is a gravel bed river (surface D_{50} ~ 45 mm at study reach). The 220 m long study reach is located roughly 4 km downstream of the lowest non-passable reservoir to anadromous fish. The study reach is the site of a 155 m long SHR site designed by the authors, in which ~2786 metric tons of spawning gravels and 7 large boulders were placed in August 2002. The project increased local reach slopes from 0.0015 to 0.0032 by elevating the upper riffle crest roughly 0.5 m, but maintained the same planform geometry and ~30 m channel widths.

3 METHODS

To include habitat heterogeneity in design, we focused on providing high quality spawning habitat in close proximity to a variety of structural features thought to provide specific benefits to salmonids. Wheaton et al. (2004a) demonstrated development and testing of habitat heterogeneity and other design hypothesis for SHR at a separate project roughly 3 km upstream. In the interest of space, the reader is referred to Wheaton et al. (2004b) for a complete description of the SHIRA methodology used in both projects and Wheaton et al. (2004a) for specific details about the FESWMS 2D hydrodynamic model, model validation, Global Habitat Suitability Index (GHSI) submodel, and Sediment Mobility Index (SMI) entrainment submodel used to test design hypotheses and assess pre and post project conditions. Results from representative steady-state simulations using FESWMS and the GHSI spawning habitat suitability submodel at representative spawning flows were used to quantify habitat quality and availability for pre (2001: ~9.34 cumecs) and post (2002: ~7.24 cumecs) project conditions. Metrics of habitat availability for the three different design scenarios developed are not reported here (incidentally the post project metrics are very similar to the final design). Thus, spawning habitat quality was assessed on the basis of depth and velocity habitat suitability curves for fall-run chinook salmon from the LMR and m^2 of availability calculated from GHSI predictions. Utilization of spawning habitat was assessed by counting the number of redds in the different GHSI-defined areas.

Habitat heterogeneity was provided by locating structural features, intended to increase fluvial complexity, in close proximity to spawning habitat. 'Close proximity' was loosely defined based on empirical analysis of proximity to seven types of structural elements with 136 individual redds from the LMR. Structural features were to serve specific ecologic functions without fragmenting habitat. We focused on two types of structural features: those that provide cover and those that produce hydrodynamic shear zones, which in turn generate 'dead zones' or eddies large enough for fish utilization. The importance of structural cover to aquatic fauna is well established (Pretty et al. 2003). Benefits to salmonids include protection from predation, resting, primary production and water temperature regulation (Merz 2001; Hendry et al. 2003). We calculated the availability of structural cover in terms of area (in m^2) and a count of distinct units of bank vegetation, LWD complexes, boulder clusters and deep pools (Bisson et al. 1981). The availability of shear zones was also calculated in terms of area and a count of distinct units depicted within 2D hydrodynamic model simulations. The presence of hydrodynamic shear zones were attributed to one of four surveyed features: bank irregularities, LWD complexes, boulder clusters and bedforms. Utilization was then assumed to be indicated by the number of redds (acquired from weekly redd surveys with a dGPS) in close proximity to distinct structural units. 'Close' proximity varied between 1 and 10 m and individual redds often utilized more than one structural unit. Anecdotal evidence from over 10 years of monitoring on the LMR and weekly site visits during spawning support these assumptions. A GIS was developed to assess the above metrics from a combination of field reconnaissance, detailed topographic surveys, 2D hydrodynamic model results (for shear zones), spawning habitat suitability model results (for habitat quality predictions) and weekly redd surveys (Merz & Setka In Press).

4 RESULTS & DISCUSSION

The availability of pre project (2001) spawning habitat was dominated by low quality habitat (52%) with

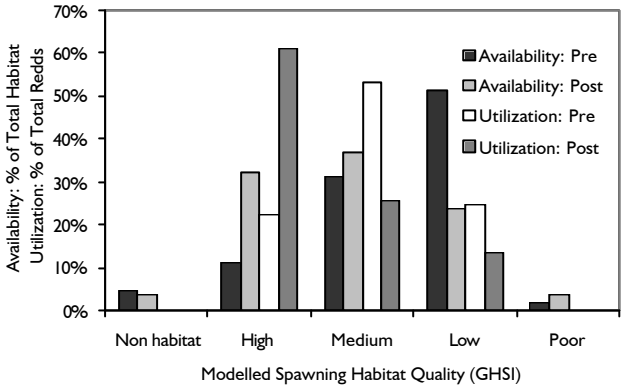

Figure 1. Comparison of pre and post project modeled spawning habitat quality availability and utilization

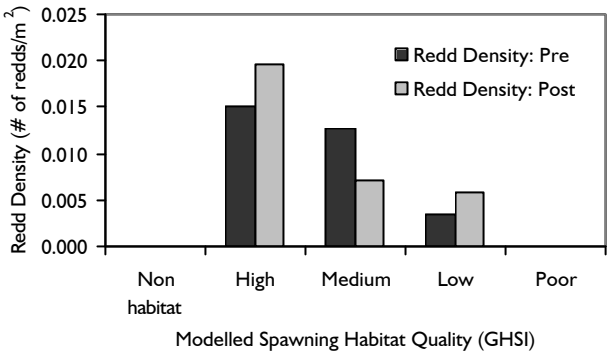

Figure 2. Redd Densities as validation of GHSI model predictions of habitat quality.

a low availability (11%) of high quality spawning habitat (Fig. 1). The best quality spawning habitat was segregated in two distinct zones 100 m apart: an upper 'crossing riffle' and a lower 'island riffle', which together comprised only 26% of the total available habitat. Post project (2002) availability shifted the distribution towards higher quality habitat raising high and medium quality habitats from 11% and 31% respectively to 32% and 37% (Fig. 1). This was accomplished primarily by extending the 'crossing riffle' further downstream and building a central bar extending down to the 'island riffle', which divided the flow and created three distinct small pools. Spawning habitat utilization then shifted from two to five distinct areas comprising 35% of the total study reach.

Although there are strong annual fluctuations in ocean harvest, adult escapement, river spawners and hatchery intake, the total number of redds in the LMR in 2001 and 2002 showed only minor variation with 843 and 826 redds respectively. Similarly, it is difficult and questionable to attribute the modest increase in redds observed at the site from 2001 to 2002 (49 to 59 redds) to the SHR project. However, the patterns of habitat utilization and availability provide a mechanistic explanation of habitat preference that is directly attributable to changes brought about by the SHR project. The predictive capability of the GHSI model is well validated by redd densities, which although higher in 2002 show consistent agreement with the high, medium and low quality habitat predictions (Fig. 2). Further, the GHSI effectively segregates poor and non-habitat (deep pools or dry areas) with no redd utilization experienced in these areas. In 2001, only 22% of the redds were located in high quality habitat and 53% settled for medium quality habitat; a strong reflection of the limited availability of high quality spawning habitat. In 2002 by contrast, 61% were located in high quality habitat and 25% in medium quality habitat; again, a reflection of the increased availability of high quality spawning habitat. On the basis of this analysis alone, the merit of increasing spawning habitat quality is questionable if lesser quality habitat is still used. However, Merz et al. (In Press) have shown increased survival of salmonid embryos from 12 separate SHR projects on the LMR. Hence considerations other than simply providing high quality spawning habitat and utilization are essential.

The SHR project also increased habitat heterogeneity through introduction of more structural cover (from 12 to 21 distinct aerial units) and hydrodynamic shear zones (from 5 to 18 distinct slack water areas). The majority of the existing structural cover was bank vegetation, with a few deep pools (Fig. 3). The increases were provided through placement of three distinct boulder complexes, and placing gravel in the channel to accentuate bank irregularities and promote zones of flow convergence and divergence. In addition two LWD complexes floated in and deposited within the site shortly after construction. In 2001, only 10% of the total study site area provided structural cover utilized by spawners and none of the shear zone refugia was utilized (Fig. 3 and 4). This is most likely because the limited amount of such structural heterogeneity was not in close proximity to the two riffles providing reasonable quality spawning habitat. In 2002, over 23% of the total study area provided structural cover (Fig. 3) and 14% provided shear zone refugia. This increased heterogeneity appeared highly effective in terms of redd utilization (i.e. redd proximity) with 70 redds using 93% of the available structural cover in one or

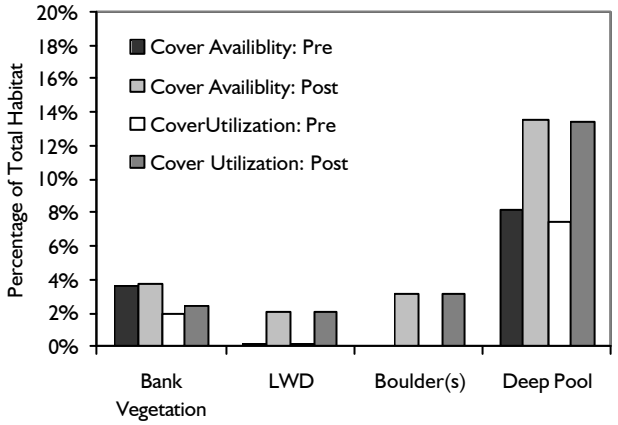

Figure 3. Habitat heterogeneity expressed in terms of structural cover. Comparison of pre and post project availability and utilization.

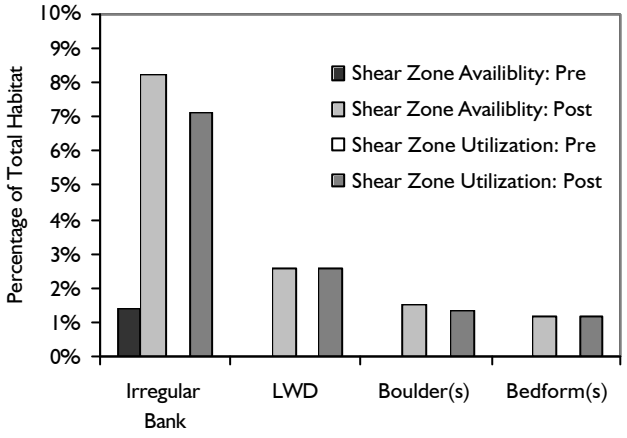

Figure 4. Habitat heterogeneity expressed in terms of shear zone refugia. Comparison of pre and post project availability and utilization.

more ways, and 42 redds using 90% of the available shear zone refugia. Deep pools and irregular banks were the most available and utilized structural cover and shear zones respectively. LWD on the LMR has been reduced from historic levels and the banks are artificially armored with vegetation that has established following the highly regulated flow regime (Merz 2001).

5 CONCLUSION

Although these results highlight the importance of habitat heterogeneity and some potential metrics for expressing it, the dependence of any empirical observations of habitat utilization is intimately tied to habitat availability. None-the-less, these results quantitatively capture ecohydraulic mechanisms (shear zones) and structural features that produce habitat heterogeneity and apparent benefits to salmonids. Thus, the methods and metrics for assessing habitat heterogeneity should be easily transferable to a variety of habitat restoration projects. However, the longevity of techniques used to produce desired processes (in this case shear zones) and structural features (in this case cover) will depend on an adequate consideration (e.g. SHIRA) of sustaining hydro-geomorphic processes and anticipated disturbances.

6 ACKNOWLEDGEMENTS

Financial support for this work was provided by East Bay Municipal Utility District (Research Agreements OOK6046 & 99K3086), the University of California, the US Fish and Wildlife Service (contracting entity for CALFED Bay-Delta Ecosystem Restoration Program: Cooperative Agreement DCN# 113322G003) and a National Fish and Wildlife Federation grant through CALFED (Contract #99-NO6).

REFERENCES

Bisson, P.A., Nielsen, J., Palmason, R.A., & Grove, L.E. 1981. A system of naming habitat types in small streams, with examples of habitat utilization by salmonids during low streamflow, In Armantrout, N.B. (ed.), Acquisition and utilization of aquatic habitat inventory information: American Fisheries Society Western Division.

Cowx, I.G., & Welcomme, R.L. (Eds) 1998. Rehabilitation of Rivers for Fish. Oxford, UK: Fishing News Books.

FERC 1998. Order Approving Settlement Agreement and Amending License. East Bay Municipal Utility District Lower Mokelumne River Hydroelectric Project No. 2916.: Federal Energy Regulatory Commission.

Hendry, K., Cragg-Hine, D., Grady, M.O., Sambrook, H., & Stephen, A. 2003. Management of habitat for rehabilitation and enhancement of salmonid stocks, Fisheries Research, 62: 171-192.

Kondolf, G.M. 2000. Some suggested guidelines for geomorphic aspects of anadromous salmonid habitat restoration proposals, Restoration Ecology, 8(1): 48-56.

Merz, J.E. 2001. Association of fall-run chinook salmon redds with woody debris in the lower Mokelumne River, California, California Fish and Game, 87(2): 51-60.

Merz, J.E., & Setka, J.D. In Press. Evaluation of a spawning habitat enhancement site for chinook salmon in a regulated California river., N. Amer. J. of Fisheries Management.

Merz, J.E., Setka, J.D., Pasternack, G.B., & Wheaton, J.M. In Press. Predicting fry production benefits from salmonid spawning habitat rehabilitation in a regulated California river, Canadian Journal of Fisheries and Aquatic Sciences.

Muotka, T., Paavola, R., Haapala, A., Novimkee, M., & Laasonen, P. 2002. Long-term recovery of stream habitat structure an benthic invertebrate communities from in-stream restoration, Biological Conservation, 105: 243-253.

Nehlsen, W., Williams, J.E., & Lichatowich, J.A. 1991. Pacific salmon at the crossroads: stocks at risk from California, Oregon, Idaho, and Washington., Fisheries, 16: 4-21.

Nijland, H.J., & Cals, M.J.R. (Eds) 2000. River Restoration in Europe: Practical Applications. Conference on River Restoration: Proceedings. Wageningen, The Netherlands.

NRC 1992. Restoration of aquatic ecosystems: science, technology, and public policy, Washington DC: National Academy Press.

Palmer, M.A., Ambrose, R.F., & Poff, N.L. 1997. Ecological theory and community restoration ecology, Restoration Ecology, 5(4): 291-300.

Pasternack, G.B., Wang, C.L., & Merz, J.E. 2004. Application of a 2D hydrodynamic model to design of reach-scale spawning gravel replenishment on the Mokelumne River, California, River Research & Applications, 20(2): 202-225.

Pretty, J.L., Harrison, S.S.C., Shepherd, D.J., Smith, C., Hildrew, A.G., & Hey, R.D. 2003. River rehabilitation and fish populations: assessing the benefit of instream structures, J Appl Ecology, 40(2): 251-265.

Tews, J., Brose, U., Grimm, V., Tielbörger, K., Wichmann, M. C., Schwager, M., & Jeltsch, F. 2004. Animal species diversity driven by habitat heterogenity/diversity: the importance of keystone structures, J of Biogeography, 31: 79-92.

Wheaton, J. M., Pasternack, G. B., & Merz, J. E. 2004a. Spawning Habitat Rehabilitation - II. Using Hypothesis Testing and Development in Design, Mokelumne River, California, U.S.A., International Journal of River Basin Management, 2(1).

Wheaton, J. M., Pasternack, G. B., & Merz, J. E. 2004b. Spawning Habitat Rehabilitation - I. Conceptual Approach and Methods, International Journal of River Basin Management, 2(1).

Predicting benefits of spawning-habitat rehabilitation to salmonid (*Oncorhynchus* spp.) fry production in a regulated California river

Joseph E. Merz, Jose D. Setka, Gregory B. Pasternack, and Joseph M. Wheaton

Abstract: We tested the hypothesis that spawning-bed enhancement increases survival and growth of chinook salmon (*Oncorhynchus tshawytscha*) embryos in a regulated California stream with a gravel deficit. We also examined how 12 physical parameters correlated within spawning sites and how well they predicted survival and growth of chinook salmon and steelhead (*Oncorhynchus mykiss*) embryos. Salmon embryos planted in enhanced gravels had higher rates of survival to the swim-up stage than embryos planted in unenhanced spawning gravels. No significant increase in growth was observed. Intergravel temperature and substrate size were strongly correlated with distance downstream from the lowest nonpassable dam. Intergravel turbidity and total suspended and volatile solids were also strongly correlated. Multiple-regression models were built with a combination of physical measurements to predict survival and length of salmon and steelhead embryos. Survival models accounted for 87% of the variation around the mean for salmon and 82% for steelhead. Growth models accounted for 95% of the variation around the mean for salmon and 89% for steelhead. These findings suggest that spawning-bed enhancement can improve embryo survival in degraded habitat. Additionally, measurements of a suite of physical parameters before and after spawning-bed manipulation can accurately predict benefits to target species.

Résumé : Nous avons éprouvé l'hypothèse selon laquelle l'aménagement des sites de reproduction augmente la survie et la croissance des embryons du saumon quinnat (*Oncorhynchus tshawytscha*) dans un cours d'eau de Californie soumis à la régulation et ayant une pénurie de gravières. Nous avons aussi déterminé la corrélation entre 12 variables physiques dans les sites de fraye et examiné comment elles peuvent prédire la survie et la croissance des embryons de saumons quinnat et de truites arc-en-ciel anadromes (*Oncorhynchus mykiss*). Les oeufs de saumons insérés dans des gravières améliorées ont une meilleure survie jusqu'au stade du début de la nage que ceux qui sont mis dans des gravières de fraye non améliorées. Il n'y a pas d'accélération significative de la croissance. La température dans le gravier et la taille du substrat sont en forte corrélation avec la distance en aval du barrage infranchissable le plus en aval. La turbidité dans le gravier, les solides totaux en suspension et les solides volatils affichent aussi la même forte corrélation. L'élaboration de modèles de régression multiple basés sur une combinaison de mesures physiques permettent de prédire la survie et la longueur des embryons de saumons quinnat et de truites arc-en-ciel anadromes. Les modèles de survie expliquent 87 % de la variation autour de la moyenne chez le saumon et 82 % chez la truite. Les modèles de croissance expliquent 95 % de la variation autour de la moyenne chez le saumon et 89 % chez la truite. Ces résultats montrent que l'amélioration des sites de fraye dans les habitats dégradés peut accroître la survie des embryons. De plus, la mesure des variables physiques avant et après la manipulation des sites de fraye peut permettre de prédire les avantages escomptés pour les espèces visées par l'aménagement.

[Traduit par la Rédaction]

Introduction

Salmonids have specific substrate and water-quality requirements for successful spawning, incubation, and embryo development. Riverine salmonids typically spawn in cool, clear, well-oxygenated streams with distinct depth, current velocity, and gravel size for each species (Bjornn and Reiser 1991; Groot and Margolis 1991). Salmonid eggs and embryos remain in the gravel for a relatively long time, ranging between roughly 2 and 8 months. The length of time between egg deposition and alevin emergence depends on species, redd location, and numerous physical parameters

Received 8 August 2003. Accepted 25 February 2004. Published on the NRC Research Press Web site at http://cjfas.nrc.ca on XX October 2004.
J17698

J.E. Merz.[1] Wildlife, Fish and Conservation Biology Department, University of California, One Shields Avenue, Davis, CA 95616–8751, USA.
J.D. Setka. East Bay Municipal Utility District Fisheries and Wildlife Division, 500 San Pablo Dam Road, Orinda, CA 94563, USA.
G.B. Pasternack and J.M. Wheaton. Department of Land, Air, and Water Resources, University of California, One Shields Avenue, Davis, CA 95616–8626, USA.

[1]Corresponding author (e-mail: sac26419@saclink.csus.edu).

 doi: 10.1139/F04-077

(DeVries 1997). Timing of spawning, egg burial depth, and embryo development are tied to the dynamic hydrologic regime of a river, including disturbances such as streambed scour (Montgomery et al. 1999).

Interannual mobilization of channel-bed sediment provides renewal of substrate conditions, and infrequent large floods reset spatially complex channel morphology (Trush et al. 2000). Alteration of flow, sediment transport, and continuity of river systems by dams, water diversions, levees, armoured banks, and mining may have deleterious affects on these processes, impacting upon one or more salmonid life stages (Nelson et al. 1987; Heaney et al. 2001; Soulsby et al. 2001). Elimination of a natural flow and sediment transport regime causes channel stabilization and narrowing, reduced formation of point gravel bars and secondary channels, accumulation of finer sediment in gravels, and reduced water quality (Poff et al. 1997). These physical degradations contribute to decreased substrate permeability and dissolved oxygen content (DO). Impaired water quality is presumed to cause a decrease in the health and survival of developing salmonid embryos within the substrate (Olsson and Persson 1988; Reiser and White 1988; Beacham and Murray 1990).

Since the early 1970s, numerous projects have been undertaken to ameliorate anthropogenic impacts on indigenous salmonid populations (House 1996; Scruton et al. 1997). In the Central Valley of California, 73 spawning habitat rehabilitation projects on 19 different rivers were carried out between 1976 and 1999, but their success has been poorly evaluated (Kondolf et al. 1996; Wheaton 2003). Nevertheless, concerns over the fate of California Central Valley steelhead (*Oncorhynchus mykiss*) and several runs of chinook salmon (*Oncorhynchus tshawytscha*) resulted in the United States National Marine Fisheries Service (NOAA) listing these populations as threatened or endangered under the Endangered Species Act (NOAA 1994, 1998). Salmonid spawning-habitat rehabilitation within California has received increasing attention as a tool to enhance these dwindling populations (Buer et al. 1981; Kondolf and Mathews 1993; California Department of Water Resources 2002). Wheaton (2003) developed a systematic approach to designing salmon spawning habitat rehabilitation projects using spawning-bed enhancement. While gravel augmentation typically entails dumping of appropriate materials in or near the channel to allow distribution via stream flow, spawning-bed enhancement involves placement of gravel as specific bed features (typically riffles or bars), potentially providing immediate spawning habitat. Merz and Setka (2004) showed that spawning-bed enhancement not only attracted spawning salmon to previously unused areas, but improved intergravel physical parameters associated with spawning and embryo development. Spawning-bed enhancement has been shown to benefit nontarget aquatic fauna as well (Merz and Chan 2004). Yet there is much uncertainty as to how well projects mitigate degradation of spawning habitat or improve survival of developing embryos (Roni et al. 2002). Additional research is needed to evaluate how substrate and associated hyporheic environment directly influence embryo survival (Kondolf et al. 1996; Merz and Setka 2004). In this paper, results from two embryo-survival experiments are reported. In the first experiment, we test the hypothesis that spawning-bed enhancement increases survival and growth of riverine chinook salmon embryos to the swim-up stage. In the second experiment, we propose embryo survival and growth models based on measurable physical parameters. We then test the validity of four multiple-regression models to predict the benefits of spawning-habitat enhancement on developing chinook salmon and steelhead embryos in a regulated California river.

Material and methods

Study site

The Mokelumne River, California, drains approximately 1624 km^2 of the central Sierra Nevada. Sixteen major dams or diversions, including the 0.24-km^3 Pardee and the 0.51-km^3 Camanche reservoirs, have dramatically altered the flow regime of the lower Mokelumne River (LMR) (Pasternack et al. 2004). Prior to completion of the Camanche Dam in 1964, annual peaks exceeded 200 $m^3 \cdot s^{-1}$ for 21 of 57 years. Since 1964, annual peaks have never exceeded 200 $m^3 \cdot s^{-1}$, with the discharges associated with the 2-, 5-, 10-, and 100-year recurrence intervals decreased by 67%, 59%, 73%, and 75%, respectively.

The LMR is approximately 54 km of regulated river between Camanche Dam, a nonpassable barrier to anadromous fish, and its confluence with the Sacramento – San Joaquin Delta. The river between Camanche Dam and Lake Lodi (Fig. 1), is characterized by alternating bar-complex and flatwater habitats, and is above tidal influence, with a gradient of approximately 0.00017. The drainage consists of 87 km^2 of mostly agricultural and urbanized land. Several small streams and storm drains enter the lower river. At least 35 fish species occur in the LMR, including two native anadromous salmonids, fall-run chinook salmon, and winter steelhead (Merz 2001). Both populations are supplemented by Mokelumne River Fish Hatchery (MRFH) production and fish imported from the Feather River and Nimbus (American River) hatcheries. Most chinook salmon and steelhead spawning on the LMR now takes place in the 14-km reach immediately below Camanche Dam.

Compared with other major barriers on Sierra rivers, Camanche Dam is positioned in an area of relatively low elevation and relief. Accordingly, slopes throughout the current spawning reaches remain low (ranging from 0.0005 to 0.0020). Tailings from abandoned gravel-mining operations are frequent along the upper 11 km of the LMR. While many of the tailings are isolated from the river by berms and levees, several large pits are now incorporated into the main river channel. It has been estimated that approximately 80% of historical spawning habitat is now inaccessible, owing to construction of Camanche Dam, and remaining habitat quality is a limiting factor to Mokelumne River salmonid production, second only to ocean harvest (Menchen 1961; Federal Energy Regulatory Commission 1993). East Bay Municipal Utility District, owner and operator of Camanche Dam, has placed over 11 000 m^3 of gravel at 12 spawning-bed enhancement sites along the LMR since 1991 and has a monitoring program encompassing all of these projects that will extend to at least 2009 (Pasternack et al. 2004). The projects typically consist of placing approximately 350–1200 m^3 of washed river rock in berms, staggered bar, riffle, or complex channel geometry configurations to improve

Fig. 1. Locations of 10 egg-tube study sites (○) within the lower Mokelumne River, California. C, Mokelumne River Hatchery (control); E, enhanced site; U, unenhanced site; F, Feather River; A, American River; M, Lower Mokelumne River.

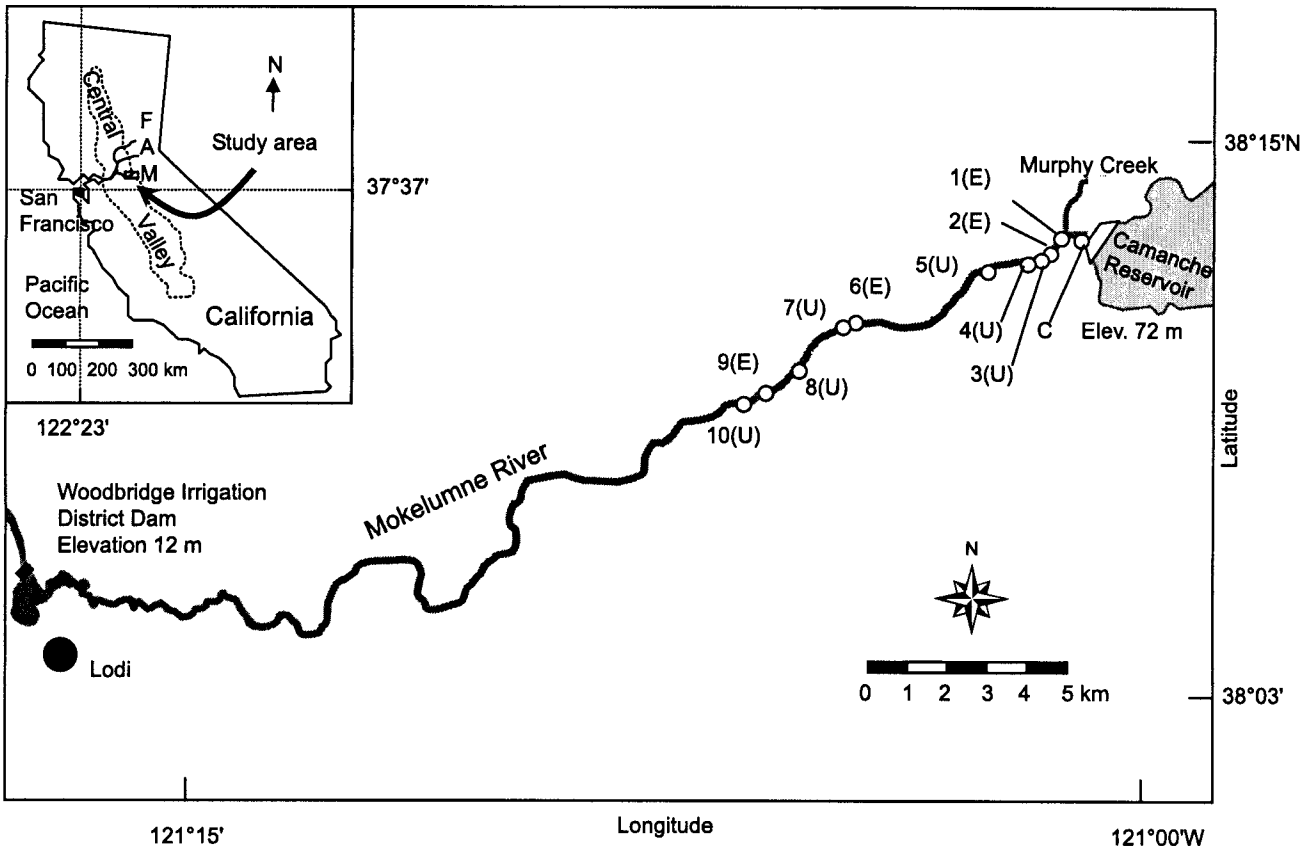

spawning habitat. Chinook salmon and steelhead typically begin spawning in the new gravels within 3–24 months of gravel placement. For this study, 10 sites were evaluated based on access and how many could be assessed within a single day. The sites are spread out within the upper 11.3 km of the LMR, four of them being spawning bed enhancement sites (Fig. 1).

Egg-incubation tubes

The focus of the first experiment was to compare survival and growth (as indicated by length) of chinook salmon embryos in enhanced and unenhanced spawning gravel sites. The second experiment was conducted to develop a predictive model of chinook salmon and steelhead survival and growth using associated physical parameters within spawning beds. In both experiments, egg-incubation tubes were buried in gravels to test survival and growth of fertilized eggs and embryos.

Egg tubes were constructed of standard dimension ratio 35-polyvinyl chloride (PVC) pipe with two PVC caps to close the tube ends (Fig. 2). Eighteen, evenly spaced, 19-mm-diameter holes were drilled into each tube. The tube's inner surface was covered with 0.35 mm mesh plastic screen typically used for egg incubation in steelhead and chinook salmon hatcheries (Leitritz and Lewis 1980). An artificial "redd" was constructed at each site for egg-tube placement. A series of depressions were made by hand in the gravel streambed for each set of egg tubes (Fig. 2). Pockets were constructed in an upstream progression, following the description of DeVries (1997). At each study site, egg-incubation tubes were buried horizontally and perpendicular to stream flow at a depth of 22 cm, the approximate depth of egg pockets in chinook salmon and steelhead redds according to Healey (1991) and Montgomery et al. (1999). Bed material from subsequent pockets was used to cover each egg tube.

Experiment 1: survival and growth in enhanced versus unenhanced sites

To compare survival of chinook salmon embryos in enhanced and unenhanced gravel sites, egg tubes were buried at four enhanced-substrate locations (constructed between 1994 and 2001) and six unenhanced-substrate locations within the LMR (Fig. 1). Unenhanced sites were selected on the basis of consistent spawning use by chinook salmon and accessibility. Ten tubes with approximately 200 chinook salmon eggs each from the MRFH were buried at each site. A control group of 2000 eggs was placed in incubation tubes (200 eggs each) at the MRFH to monitor embryo development. Eggs were taken from approximately 22 female chinook salmon at the MRFH on 21 November 2001. Fertilized eggs were "eyed" and 18 days old (average hatchery water

Fig. 2. Diagram of constructed "redd" with egg tubes, stand pipe, and temperature logger (top view). The figure is not drawn to scale.

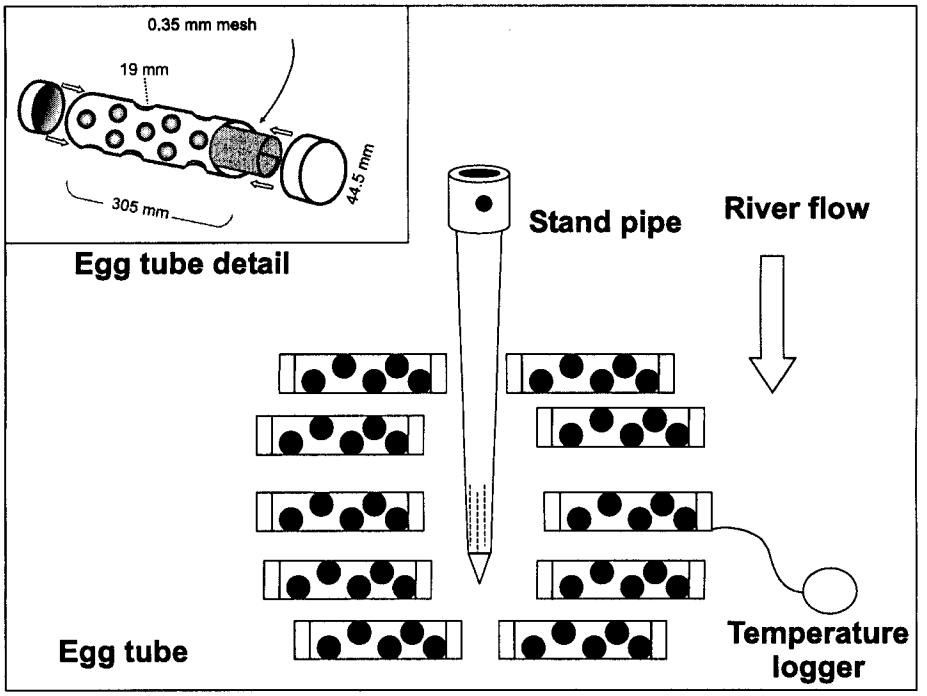

temperature was 12.3 °C) when placed in the egg tubes and buried in the gravel. MRFH water is sand-filtered and piped from Camanche Reservoir.

Experiment two: predictive models of survival and growth

To test predictive models of chinook salmon and steelhead embryo survival and growth from associated physical measurements, approximately 20 000 chinook salmon and steelhead embryos were buried in egg tubes at various spawning habitats located throughout the LMR (see Habitat selection and evaluation below). Five tubes with approximately 200 eyed chinook salmon embryos and five tubes with approximately 200 eyed steelhead embryos were buried at each site. A control group of five chinook salmon egg tubes and five steelhead egg tubes (200 embryos each) were placed in rearing troughs at the MRFH to monitor embryo development and survival. Chinook salmon eggs were taken from 15 female salmon spawned on 23 December 2001 at the MRFH. Fertilized eggs were eyed and 18 days old (average hatchery water temperature was 10.12 °C) when placed in egg tubes and buried in the gravel on 9 January 2002. An insufficient number of steelhead spawned at the MRFH to provide embryos for this study, therefore eggs were taken from 12 female steelhead spawned on 18 December 2001 at the Feather River Hatchery, California. Fertilized steelhead eggs were approximately 22 days old when placed in the egg tubes and buried in the gravel on 9 January 2002 (average hatchery water temperature was 10.3 °C).

Habitat selection and evaluation

For experiment 2, 10 sites were selected within the upper 11.3 km of the LMR, based on historical spawning use and enhancement activities (Fig. 1). Although, the sites were located in the vicinity of experiment 1 sites, the sites did not overlap and were not selected on the basis of enhanced versus unenhanced gravels. The 10 sites each consisted of similar riffle morphologies with comparable substrate compositions ($D_{50} \approx$ 150–450 mm gravels), channel slopes (0.002–0.006) and hydraulic conditions (shallow (<0.36 m), and swift current (>0.6 $m \cdot s^{-1}$). Hydraulics at each site were crudely characterized from one point measurement of depth and velocity positioned between the egg tube placement locations (at the standpipe location; Fig. 2). This measurement was performed on 9 December 2001 during a discharge of 6.5 $m^3 \cdot s^{-1}$, which was representative of hydraulics experienced throughout the incubation period. Depth was recorded from a top-setting velocity rod and depth-averaged velocity was approximated by assuming a logarithmic velocity profile and taking a measurement at 60% of the depth with an electromagnetic Marsh McBirney Flo-Mate velocimeter.

Substrate evaluation

Both surface and subsurface grain-size distributions were used to characterize the substrate during the post-study period (after egg-tube removal) at each site. Grain-size distributions were assumed not to have changed from pre- to post-analysis based on previous studies (Merz and Setka 2004). Subsurface samples were collected at the location of the standpipe at each site using a McNiel core sampler (St-Hilaire et al. 1997). Samples were placed in sealed containers and transported to the laboratory for analysis. Substrate was sieved through screens of the following sizes: 0.5, 1.0, 2.4, 4.7, 9.5, 12.7, 15.9, 22.2, 31.8, 44.5, 63.5, 88.9, 127.0, 177.8, and 254.0 mm. Each size class was weighed and recorded. Residual water and associated suspended sediment was poured through 15-cm No. 595 filter paper. The paper and sediment residual was dried at 70 °C for 24 h, weighed,

Table 1. Observed survival rates and total lengths (TL) of chinook salmon embryos incubated in egg tubes from 12 December 2001 through 7 January 2002 and from 9 January through 31 January 2002 at the Mokelumne River Fish Hatchery and at four enhanced and five unenhanced spawning sites.

Experiment/group	Species	Mean survival rate (%)	SE*	Lower 95%	Upper 95%	Mean TL (mm)	SE*	Lower 95%	Upper 95%
Experiment 1									
Hatchery	Chinook salmon	60	0.05	0.50	0.70	26.9	0.38	26.19	27.68
River									
Enhanced sites	Chinook salmon	29	0.03	0.24	0.35	25.2	0.12	24.77	25.55
Unenhanced sites	Chinook salmon	22	0.02	0.18	0.26	25.1	0.02	24.81	25.43
Experiment 2									
Hatchery	Chinook salmon	88	0.04	0.76	1.00	22.6	0.44	21.32	23.78
	Steelhead	84	0.08	0.62	1.00	22.2	0.19	21.69	22.73
River gravel	Chinook salmon	58	0.04	0.50	0.65	18.5	0.84	16.81	20.21
	Steelhead	61	0.03	0.54	0.68	19.0	0.89	17.20	20.79

*A pooled estimate of error variance was used.

and recorded. Surface samples were collected by pebble count at three randomly selected transects (~100 samples per transect) at each site using methods similar to those of Bauer and Burton (1993). Three 30-m longitudinal transects were randomly placed at each site. Surveyors collected substrate samples by hand every 0.3 m along the transect and used a round-holed template to measure size. Substrate from pebble counts was categorized into 12 sizes: <8.0, 8.0, 16.0, 22.2, 31.8, 44.5, 63.5, 89.0, 127.0, 177.8, 254.0, and > 254.0 mm. Categorization was based on the largest slot (round hole with specified diameter) through which an individual pebble could not be passed.

Intergravel permeability, DO, temperature, and turbidity

Intergravel water-quality measurements were taken at each site prior to egg-tube placement and immediately after egg-tube removal. A modified Terhune Mark VI standpipe was driven into the gravel to measure gravel permeability, DO, and water temperature following Barnard and McBain (1994). We collected water samples from the standpipe with a vacuum hand pump apparatus (Saiki and Martin 1996). Samples were taken at depths of 15, 30, and 45 cm to evaluate stratification of compaction and sedimentation within the known depth ranges of chinook salmon and steelhead spawning (Vronskiy 1972; Chapman 1988; Bjornn and Reiser 1991). Approximately 200 mL of water was collected from each sample and transported to the laboratory to measure turbidity in nephelometric turbidity units (NTU), total suspended solids (TSS), and volatile suspended solids (VSS). Turbidity was measured with a Hach 2100P turbidimeter. TSS samples were filtered through a 50-μm sieve, then passed through a precombusted gas fiber filter, dried to 60 °C, and weighed (American Public Health Association et al. 1995). Ambient DO and stream temperature (15 cm below the water surface) as well as intergravel DO and water temperature were recorded with a YSI 55 dissolved-oxygen meter. An Onset StowAway TidbiT temperature logger (–4 °C to +37 °C) was buried with the eighth tube (starting with top left tube No. 1) at each monitoring location (Fig. 2). Loggers recorded water temperature within the gravel every 60 min for the duration of the monitoring period (approximately 26 days). Hourly temperature data were totaled to calculate temperature-hours for each site.

Survival, development, and general condition

Based on observation of the hatchery control group, egg tubes were removed from the gravel when embryos reached the alevin stage and at least 10% showed capability of self-orientation in water current, typical of the swim-up stage. Live alevins were counted, measured for total length (TL), and assessed for anomalies (such as disease or deformities). Alevin mortalities and unhatched embryos were enumerated and recorded.

Data analyses

We used a one-way *t* test to compare mean survival rates and lengths of chinook salmon alevins buried in enhanced and unenhanced gravels (Zar 1999). To build a survival and growth model for chinook salmon and steelhead embryos, principal components analysis (PCA) was used to reduce the number of physical condition variables in the data set. This analysis was performed with SPSS® version 10 (SPSS Inc. 1997). We used the B4 selection method, as described in Joliffe (1972) and prescribed by Talmage et al. (2002), to select representative environmental variables indicated by the first four axes. We used multiple linear regression to build preliminary models with these independent variables to predict mean survival and mean TL of chinook salmon and steelhead alevins using the JMP linear regression model function, which performs an analysis of variance (ANOVA) (Sall et al. 2001). Alternate variables were then exchanged to strengthen the models. We also used ANOVA to compare the independent variables with alevin survival and TL. A significance level of 0.05 was used in statistical tests.

Results

Experiment 1: chinook salmon embryo survival and growth in enhanced and unenhanced spawning gravels

Chinook salmon embryos used to compare enhanced and unenhanced gravels were recovered on 8 January 2002, 28 days after egg-tube placement. Survival of chinook salmon

Table 2. Physical parameters associated with 10 egg tube monitoring sites and the Mokelumne River Fish Hatchery (control site)

					Peizometer measurements taken at time of egg-tube planting								
					Temperature (°C)			DO (ppm)			Permeability (mL·s^{-1})		
Site No.	DFCD[a] (km)	Water depth (m)	Stream velocity (m·s^{-1})	AT[b] (°C)	15 cm	30 cm	45 cm	15 cm	30 cm	45 cm	15 cm	30 cm	45 cm
Control	0.1			10.15	9.8			10.7			63		
1	0.8	0.3	0.65	10.10	9.8	10.0	10.2	10.2	7.7	6.1	38	41	28
2	1.4	0.2	0.78	9.97	9.6	10.0	10.0	9.9	9.5	9.1	42	17.5	9.25
3	1.7	0.2	0.67	9.79	10.3	9.8	9.8	9.2	6.9	5.9	40.5	14	25
4	1.8	0.2	0.75	9.88	10.6	10.1	9.9	8.0	8.2	8.5	41.5	19	16.5
5	2.3	0.2	0.75	10.11	10.1	10.0	9.7	10.3	10.1	10.1	35.5	9.25	5.5
6	6.3	0.2	0.89	9.73	9.8	9.9	9.8	9.3	8.5	6.9	44.9	43.6	32.5
7	7.1	0.2	0.65	9.79	9.9	9.5	9.5	9.6	7.3	6.4	44.8	42.5	35.5
8	8.5	0.4	0.96	9.87	9.5	9.5	9.6	9.2	6.4	6.1	44.1	23.85	8.5
9	9.5	0.3	1.02	9.61	9.4	9.1	9.2	9.2	7.3	7.1	47.6	12.5	1.2
10	10.5	0.3	0.65	9.72	8.7	8.7	8.9	9.0	8.1	7.2	18.2	21.5	11.5

Note: DFCD, distance from Camanche Dam; AT, average temperature in egg tubes at 15 cm; DO, dissolved oxygen; NTU, nephelometric turbidity

Fig. 3. Mean daily discharge rate and temperature of water released from Camanche Dam into the lower Mokelumne River from 1 November 2001 to 31 January 2002. The broken line indicates the temperature of the Camanche Dam release; the solid line indicates the rate of the Camanche Dam release.

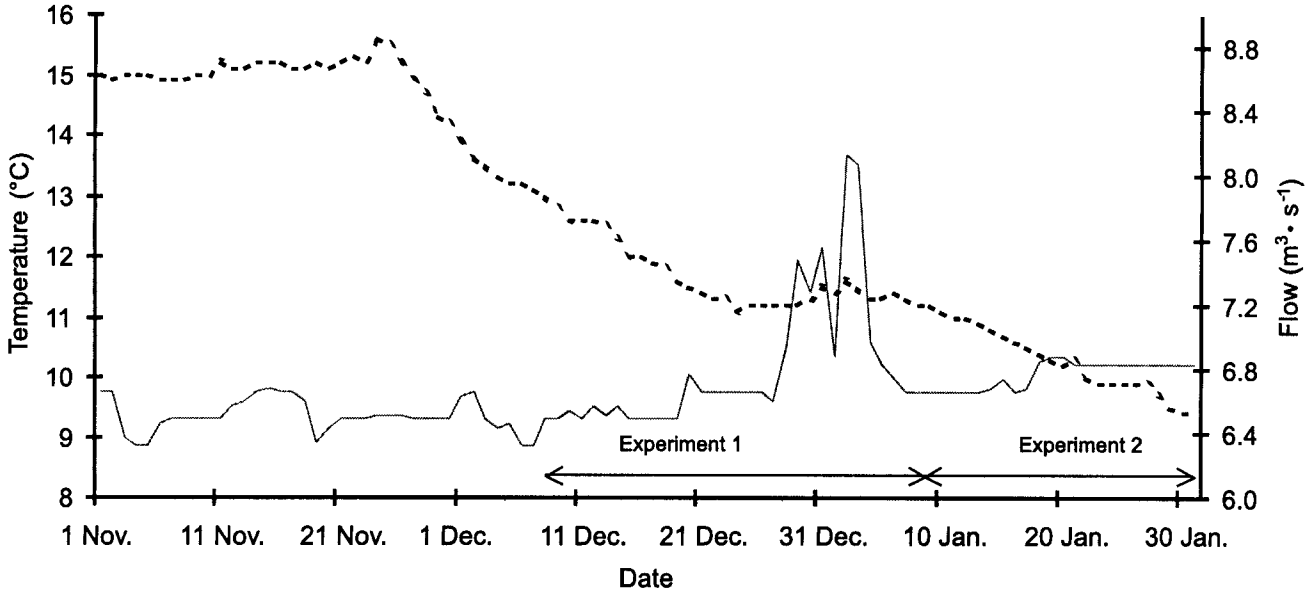

embryos was highly variable. The chinook salmon embryo survival rate ranged from 0% in several unenhanced-gravel tubes to over 63% in tubes used as controls within the MRFH (Table 1).

Growth of chinook salmon was also variable. Chinook salmon embryos ranged from 11 to 31 mm TL in tubes incubated at the MRFH, while embryos incubated in river-gravel tubes ranged from 13 mm TL (site 3) to 30 mm TL (sites 4 and 5). Survival of chinook salmon alevins was significantly higher in enhanced gravel than in unenhanced gravel (Table 1; $t = 2.022$, df = 8, $P < 0.039$). No significant difference was observed for growth in enhanced and unenhanced gravel ($t = 0.038$, df = 8, $P = 0.485$).

Experiment 2: physical parameters associated with 10 spawning sites and their predictive power for salmonid survival and growth

Camanche Dam releases to the LMR ranged from 6.6 m^3·s^{-1} on 1 December 2001 to 6.8 m^3·s^{-1} on 31 January 2002, with a peak of 8.1 m^3·s^{-1} on 2 January 2002 (Fig. 3). Physical parameters associated with the spawning sites are provided (Table 2). Average daily temperature varied within the constructed redds. Although temperatures were somewhat consistent during experiment 1, during experiment 2, mean gravel temperature was inversely correlated with distance downstream of Camanche Dam (Fig. 4). Moreover, daily temperature variation was also greater downstream.

within the lower Mokelumne River, California, from 9 to 31 January 2002.

Turbidity (NTU)			TSS (mg·L^{-1})			VSS (mg·L^{-1})			d_{50} (mm)	
15 cm	30 cm	45 cm	15 cm	30 cm	45 cm	15 cm	30 cm	45 cm	Pebble count	Core
3.8			4.0			2.8				
24	1312	1024	14.6	362.4	809.7	6.3	61.8	122.4	385.6	370.5
970	1404	1328	297.2	547.8	573.3	30.1	59.2	73.9	423.3	455.5
24	1080	818	31.3	439.0	232.3	12.4	48.8	27.6	356.6	351.6
369	6137	4145	113.6	1150.7	1030.6	22.5	135.9	126.7	414.0	394.2
117	194	517	54.4	81.3	226.9	10.3	13.9	36.6	299.2	370.5
20	481	3050	32.3	365.6	1410.0	5.4	41.1	166.0	375.2	474.3
354	4450	3300	101.0	1504.7	465.7	18.8	175.3	57.3	203.7	159.2
18	369	374	55.1	226.1	577.0	6.3	25.8	67.9	251.5	314.6
343	378	1971	182.2	419.6	1194.0	28.6	48.9	95.0	203.4	74.1
696	1013	1180	177.0	377.6	471.1	25.0	46.8	59.5	152.2	156.7

units; TSS, total suspendeds olids; VSS, volatile suspended solids; d_{50}, median particle size.

Fig. 4. Temperatures recorded 15 cm below the gravel surface at 10 spawning sites and 15 cm below the water surface within the Mokelumne River Fish Hatchery (Hatchery). Average, minimum, and maximum hourly temperatures are shown for the monitoring period from 12 December 2001 through 8 January 2002 (experiment 1) (■) and for the monitoring period from 9 through 31 January 2002

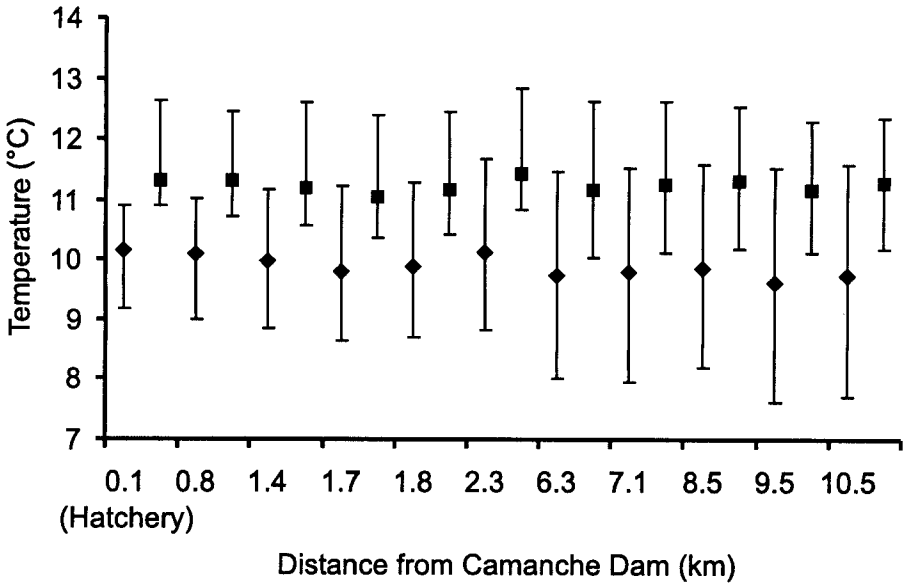

Intergravel DO ranged from 6.1 mg·L^{-1} at 45 cm below the gravel surface to 10.11 mg·L^{-1} at 15 cm below the gravel surface. Intergravel permeability ranged from 1.2 mL·s^{-1} at 30 cm beneath the site 9 gravel surface to 48 mL·s^{-1} at 15 cm beneath the surface at the same site. We were able to draft 63 mL·s^{-1} through the standpipe in filtered hatchery water.

Spatial (i.e., distance from Camanche Dam) trends were observed in the variables collected (Table 3). As distance from Camanche Dam increased, average temperature within the gravels decreased and diurnal temperature fluctuations increased (Fig. 4). Surface substrate sizes, as indicated by pebble-count d_{50} (Pd_{50}) and general bed material size, as indicated by core-sample d_{50} (Cd_{50}), decreased as samples were taken farther from the dam. Correlations between turbidity, TSS, and VSS were strong, as were Cd_{50} and Pd_{50} measurements.

Chinook salmon and steelhead eggs used for the survival and growth models were recovered on 31 January 2002, 22 days after tube placement. Chinook salmon survival ranged from 0% to 100% in river gravel and from 74% to 98% within the MRFH. Similarly, steelhead survival ranged from 15% to 100% within river gravel and from 56% to 97% within the MRFH. Chinook salmon lengths ranged from 14 mm TL at site 5 to 25 mm TL within the tubes incubated at the MRFH. Steelhead lengths ranged from 13 mm TL at site 3 to 24 mm TL at all but two of the river sites. Chinook salmon and steelhead embryos tended to grow more slowly

farther downstream from Camanche Dam, as indicated by average embryo size (Table 3).

While Cd_{50} and water depth appeared to have the strongest correlation with average rates of survival of chinook and steelhead embryos, respectively, no single physical parameter influenced both species strongly. The first four PCA axes explained over 87% of the total variance in physical conditions associated with the spawning locations (Table 4). The variables with the greatest loadings on each axis were distance from Camanche Dam, average VSS, and stream velocity.

Survival models

We used Cd_{50}, average VSS, and total temperature-hours as predictors of chinook salmon survival (Table 5A). The F ratio in the ANOVA for the overall model was significant at $F_{prob} < 0.01$ and the model accounted for 87% of the variation around the mean. We used average DO, temperature-hours, and average turbidity as predictors of steelhead survival (Table 5B). The F ratio in the ANOVA for the overall model was significant at $F_{prob} < 0.05$ and the model accounted for over 82% of the variation around the mean.

Growth models

We used temperature-hours, average permeability, average DO, and Cd_{50} as the independent variables to predict chinook salmon length at the time of egg-tube removal (Table 6A). The growth model accounted for 95% of the variation around the mean, with a significant F ratio for the ANOVA. We used Cd_{50}, average permeability, redd depth, and stream velocity as independent variables to predict steelhead length at the time of egg-tube removal (Table 6B). The growth model accounted for 89% of the variation around the mean, with a significant F ratio for the ANOVA.

Discussion

Growth and survival

Benefits documented for spawning salmonids and their developing embryos as a result of enhancement projects have been anecdotal, and typically inferred from measurements of physical habitat characteristics and observations of spawning activity (Zeh and Donni 1994; Van-Zyll-De-Jong et al. 1997). Our results indicate that LMR spawning gravel enhancements significantly increased chinook salmon embryo survival to swim-up stage up to 5 years after placement. Survival of salmonid embryos has been tied to DO (Coble 1961), temperature (Heming 1982), percent fines (Sear 1993), and permeability (Kondou et al. 2001) within spawning gravels. Merz and Setka (2004) showed that strategically placed gravel within the LMR significantly increased velocities and permeability, and decreased depths and fines, equilibrating the hyporheic and water-column environments, which supports our findings in this study. However, the short-term benefits of spawning-gravel enhancements may diminish through time if inter-annual bed mobilization from flushing flows is not provided (Wheaton 2003).

Although we observed no significant increase in embryonic growth in enhancement gravels during experiment 1, our preliminary egg-tube test showed a 24% average increase in survival and a 11% increase in growth of chinook salmon embryos placed in two enhanced sites when compared with two unenhanced sites in December 2000 (unpublished data). Embryo quality may have been a significant factor in the reduced benefits to growth observed in this study, considering that we observed 65%–100% survival in enhancement gravels in tubes buried for 4 weeks during our preliminary test and only 1%–67% within enhancement gravels during this study. Similar survival rates were also observed by hatchery staff monitoring the same egg lots incubated in the MRFH.

Physical correlations

The principal component correlations explain a few trends with respect to median grain sizes that are consistent with conventional geomorphic theory. First, surface bed material was consistently coarser than subsurface material. In gravel-bed streams, this is known as paving or armouring (Parker et al. 1982) and is thought to arise from differential erosion of coarse and fine grains in heterogeneous bed mixtures. Briefly, finer grains require less energy to erode than coarser grains, primarily because of their differences in mass. For example, a prolonged intermediate-flow event may produce hydraulic forces competent to erode fine- and medium-grained particles from the surface of a heterogeneous gravel bed, but not strong enough to erode the coarser grain particles. This, in turn, can lead to an armoured layer comprised of a higher percentage of coarse grains compared with a subsurface layer, which is not subjected to hydraulic forces adequate to winnow finer material away. Kondolf (1997) explains that, in regulated rivers like the LMR, surface armouring is often accentuated owing to flow-regulation conditions because larger particles that lag behind are less easily mobilized by hungry water below dams. Furthermore, dams block the passage of gravels, and once finer material (including spawning gravels) has winnowed away it is not replenished. Although the subsurface layers may provide a finite source of appropriately sized spawning gravels, they can become inaccessible or erodable under the protection of a coarse-armour veneer.

The second trend apparent in the principal component correlations is a reduction in grain size with distance downstream from Camanche Dam (fining). This fining of bed material is evident in both the surface median grain size and to a lesser extent the subsurface, consistent with the literature (e.g., Schumm and Stevens 1973; Ashworth and Ferguson 1989). Constantine et al. (2003) documented downstream fining in the gravel-bed reaches of the neighbouring Cosumnes River, but also noted the presence of a confined gravel-bed reach where downstream fining was not evident. They attributed the lack of decrease in grain size in that discrete reach to equal mobility of all bed material and incised channel morphologies that limit the freedom of the channel to migrate laterally. Given the incised nature of the LMR channel and the artificial reset of grain sizes at enhanced sites located throughout the LMR, one might suspect that the downstream fining trend would not persist in similarity to the Cosumnes River. However, the rather small percentage of the entire spawning reach actually covered by enhanced gravels (<2%) may prevent a noticeable influence on the general fining trend (Merz and Setka 2004). Furthermore, the equal mobility of all grain sizes observed in the Cosumnes River is in response to a nonregulated natural

Table 3. Principal component correlations among dependent and independent variables for chinook salmon and steelhead embryos developing in spawning gravel of the lower Mokelumne River from 9 to 31 January 2002.

	Physical variable											
Variable	DFCD	WD	SV	TH	TA	PA	DOA	TURA	TSSA	VSSA	PD_{50}	Cd_{50}
Chinook salmon												
CSSurvival	–0.273	–0.302	0.353	0.063	0.339	–0.257	0.113	–0.373	–0.386	–0.449	0.487	0.635
CSAS	**–0.721**	–0.412	–0.090	0.681	0.554	–0.466	0.495	–0.170	–0.418	–0.320	0.685	0.690
CSSM	–0.661	–0.244	–0.405	**0.794**	0.408	–0.136	0.491	–0.464	–0.665	–0.493	0.546	**0.708**
CSSMX	–0.600	–0.173	–0.110	**0.788**	0.500	–0.249	0.411	–0.158	–0.385	–0.226	0.614	**0.731**
Steelhead												
STHSurvival	0.108	–0.625	–0.171	–0.142	–0.133	–0.302	0.386	0.505	0.298	0.215	–0.116	–0.099
STHAS	**–0.710**	–0.629	0.006	0.511	0.634	–0.182	0.549	–0.122	–0.262	–0.247	**0.781**	**0.831**
STHSM	0.381	0.325	0.246	–0.087	–0.343	0.101	0.237	0.216	0.451	0.441	–0.124	–0.037
STHMX	–0.535	–0.188	0.327	0.563	0.565	–0.309	0.544	–0.395	–0.428	–0.424	0.498	0.528
Physical variable												
WD	0.651											
SV	0.423	0.429										
TH	**–0.753**	–0.208	–0.385									
TA	**–0.883**	–0.209	–0.391	0.608								
PA	–0.103	–0.016	–0.149	–0.052	0.356							
DOA	–0.410	–0.408	–0.104	0.572	0.247	–0.372						
TURA	–0.122	–0.494	–0.258	–0.162	0.273	0.344	–0.078					
TSSA	0.132	–0.169	0.143	–0.433	0.091	0.487	–0.215	**0.836**				
VSSA	–0.360	–0.214	–0.078	–0.221	0.224	0.586	–0.183	**0.880**	0.954			
Pd_{50}	**–0.863**	–0.592	–0.104	0.524	**0.866**	0.240	0.289	0.178	0.107	0.220		
Cd_{50}	**–0.724**	–0.509	–0.089	0.579	**0.757**	0.214	0.380	–0.022	–0.127	–0.003	**0.891**	

Note: Boldface type denotes correlations greater than 0.7. CSSurvival, average chinook salmon survival rate; CSAS, chinook salmon average size; CSSM, chinook salmon minimum size; CSSMX, chinook salmon maximum size; STHSurvival, average steelhead survival rate; STHAS, steelhead average size; STHSM, steelhead minimum size; STHMX, steelhead maximum size; WD, water depth; SV, stream velocity; DFCD, distance from Camanche Dam; TH, temperature-hours; TA, average temperature within gravel; PA, average gravel permeability; DOA, average dissolved oxygen content within gravel; TURA, average water turbidity within gravel; TSSA, average total suspended solids within gravel; VSSA, average volatile suspended solids within gravel; Pd_{50}, pebble-count d_{50}; Cd_{50}, core-sample d_{50}.

Table 4. Principal component loadings for the first four axes for physical conditions associated with 10 spawning sites within the lower Mokelumne River.

Characteristic	Axis 1	Axis 2	Axis 3	Axis 4
Distance from Camanche Dam	**–0.9280**	–0.1830	–0.0372	0.0344
Average ambient temperature	0.8790	–0.2220	0.0037	–0.2330
Temperature-hours	0.8780	–0.2210	0.0093	–0.2340
Core-sample d_{50}	0.8110	0.1470	0.4170	0.1830
Pebble-count d_{50}	0.7950	0.3620	0.3660	0.2090
Average dissolved oxygen concn.	0.6190	–0.1980	–0.3420	0.4270
Water depth	–0.5930	–0.4490	0.3800	–0.2980
Average volatile suspended solids	–0.1180	**0.9490**	–0.0025	–0.0313
Average total suspended solids	–0.3020	0.9060	0.0128	0.1710
Average turbidity	–0.0134	0.9030	–0.3450	0.0386
Average permeability	–0.0040	0.6330	0.4700	–0.4860
Stream velocity	–0.4250	–0.1610	**0.5580**	**0.6270**
Percent total variance explained	39.30	29.05	10.19	9.33

Note: Values in boldface type indicate the component with the highest loading on each axis.

Table 5. Statistics and associated multiple regression results for two models used to predict (A) chinook salmon and (B) steelhead embryo survival in Mokelumne River spawning gravel.

(A) Chinook salmon.					
Summary of fit	R^2	R^2 adj.	Root mean square error	Mean of response	Sum of weights
	0.8650	0.7975	0.0807	0.5723	10
Source	df	Sum of squares	Mean square	F ratio	Prob > F
Model	3	0.2503	0.0834	12.8116	0.0051
Error	6	0.0391	0.0065		
Corrected total	9	0.2893			
Effect tests	N_{param}	df	Sum of squares	F ratio	Prob > F
Core-sample d_{50}	1	1	0.1917	29.4346	0.0016
Average VSS	1	1	0.0934	14.3472	0.0091
Temperature-hours	1	1	0.0760	11.6651	0.0142
(B) Steelhead.					
Summary of fit	R^2	R^2 adj.	Root mean square error	Mean of response	Sum of weights
	0.8232	0.6818	0.0717	0.6139	10
Source	df	Sum of squares	Mean square	F Ratio	Prob > F
Model	4	0.1196	0.0299	5.8201	0.0402
Error	5	0.0257	0.0051		
Corrected total	9	0.1453			
Effect tests	N_{param}	df	Sum of squares	F ratio	Prob > F
Average DO	1	1	0.0373	7.2675	0.0430
Temperature-hours	1	1	0.0356	6.9339	0.0464
Average turbidity	1	1	0.0361	7.0257	0.0454
Average permeability	1	1	0.0072	1.4078	0.2887

Note: N_{param}, number of parameters; adj., adjusted.

flow regime with no major dams blocking the replenishment of sediment. Thus, the armoured surface substrates of the LMR may exhibit downstream fining through the coarse relic deposits left behind from the pre-regulation flow and sediment regime.

We also observed a strong correlation between water temperature and distance downstream from Camanche Dam, evident in both average temperature and temperature-hours. Preece and Jones (2002) observed a 3-week lag in and a 5.0 °C reduction of annual maximum daily temperature on Australia's Namoi River after construction of a dam. Similarly, Camanche Reservoir acts as an insulator, cooling water within the spawning reaches of the LMR during summer and fall. However, this pattern is reversed during the winter period, with water actually cooling farther downstream from the dam.

Correlations between physical and biological parameters

Substrate-size Cd_{50} was significantly correlated with chinook salmon survival and, along with temperature-hours and

Table 6. Statistics and associated multiple regression results for two models used to predict chinook salmon (A) and steelhead (B) growth in Mokelumne River spawning gravel.

(A) Chinook salmon.					
Summary of fit	R^2	R^2 adj.	Root mean square error	Mean of response	Sum of weights
	0.9472	0.9050	0.3162	20.6088	10
Source	df	Sum of squares	Mean square	F ratio	Prob > F
Model	4	8.9686	2.2422	22.4320	0.0022
Error	5	0.4998	0.1000		
Corrected total	9	9.4684			
Effect tests	N_{param}	df	Sum of squares	F ratio	Prob > F
Temperature hours	1	1	0.6773	6.7766	0.0481
Average permeability	1	1	3.2321	32.3358	0.0023
Average dissolved oxygen	1	1	0.3008	3.0094	0.1433
Core d_{50}	1	1	2.7874	27.8869	0.0032
(B) Steelhead.					
Summary of fit	R^2	R^2 adj.	Root mean square error	Mean of response	Sum of weights
	0.8857	0.7943	0.1825	21.1139	10
Source	df	Sum of squares	Mean square	F ratio	Prob > F
Model	4	1.2910	0.3228	9.6898	0.0142
Error	5	0.1665	0.0333		
Corrected total	9	1.4576			
Effect tests	N_{param}	df	Sum of squares	F ratio	Prob > F
Core d_{50}	1	1	0.5481	16.4557	0.0098
Average permeability	1	1	0.1379	4.1391	0.0976
Depth	1	1	0.0859	2.5776	0.1693
Velocity	1	1	0.0294	0.8815	0.3909

Note: N_{param}, number of parameters; adj., adjusted.

VSS, explained 86% of the variability in predicted survival. Likewise, growth regression equations for both chinook and steelhead included Cd_{50}. The mechanistic pathway of the Cd_{50} effect likely involved a relationship with permeability (Sowden and Power 1985). Interestingly, while we observed strong correlations between Cd_{50} chinook alevin survival and growth, Cd_{50} only appeared to be strongly correlated with steelhead growth, not survival. According to Chapman (1988), mean particle size is not as good an indicator of steelhead survival as for other salmonid species. Usefulness of mean particle size may be limited because gravel mixtures with the same geometric mean can have different size compositions. While our study design focused on survival of salmonid embryos within the hyporheic environment, the placement of eggs in a tube provided protection from physical impacts from all but the smallest substrates (<2.9 mm diameter). It is expected that Cd_{50} would have a direct egg-size-dependent effect on survival of eggs deposited directly in substrate. Likely, direct impacts related to substrate size include physical abrasion and crushing in the case of smaller gravel and interstitial space or, in the case of larger interstitial space, increased trauma due to currents and decreased cushioning. In a similar vein, egg size varies between salmonid species and even within species. Fecundity and egg size are inversely related in Pacific salmon and vary over latitudinal clines, with northernmost populations producing more but smaller eggs (Flemming and Gross 1990). Quinn et al. (1995) showed that there was a correlation between egg and substrate size for sockeye salmon (*Oncorhynchus nerka*), implying a selective effect of gravel size on egg size. Natural-selection effects on salmonid egg size can occur over decades and may be influenced by hatchery production (Kinnison et al. 1998). Independent of body size, there is little variation in egg size within populations of salmonids and we assumed that the egg sizes in our study were similar for each species for each experiment (Flemming and Gross 1990).

Development rates in sockeye and chinook salmon embryos are optimized for thermal regimes present within a given population's home spawning area, suggesting a genetic component that may vary between populations (Hendry et al. 1998; Kinnison et al. 1998). Although we used Feather River steelhead eggs, we assume that there is little difference between the present populations considering the high egg-importation rate by hatcheries over the past four decades (Bryant 2000). Even so, genetic influence on development rates should be considered when compiling information on restoration techniques and resulting salmonid physiological performance (growth, behaviour, mortality).

Intra-watershed variation must also be considered. For instance, the thermal shift in the LMR below Camanche Dam appears to affect embryo survival and growth. We observed both slower growth with cooling downstream of the dam late in the season and increased growth with warming earlier in

the season (unpublished data). The reservoir insulating effect (i.e., warming water in winter and cooling water in summer and fall) will affect oxygen-saturation levels as well.

Numerous studies have documented correlations between individual physical parameters and embryo survival (Coble 1961; Heming 1982; Sear 1993). However, a specific action, such as increasing substrate permeability, may also influence temperature, DO, or even predator access to developing embryos. Shepherd et al. (1986) showed that the thermal mass of the substrate in Pacific Northwest coastal streams caused parallel but lagged and buffered heating and cooling trends in infiltration-source intergravel water compared with surface water. Similarly, this study and other work performed on LMR spawning gravel enhancement demonstrated that during the early portion of the fall-run chinook salmon spawning season (October through early November), intergravel water may be as much as 2.3 °C warmer than surface water, potentially influencing growth and development within the different embryo life stages. Salmonid egg to fry development is generally partitioned into three phases: prehatch, posthatch, and terminal phase. During the posthatch phase, yolk utilization increases markedly concurrently with increased somatic growth and organogenesis. The terminal phase is when the fish begins the transfer to exogenous feeding. It is during the terminal phase that suboptimal environmental conditions effects are manifested in either reduced physiological performance or increased mortality. Prior to the terminal phase suboptimal conditions generally affect growth rates and yolk-utilization efficiencies, whereas sublethal or critical conditions lead to developmental arrest and death. Progression of embryonic development is highly susceptible to regulation by extraneous factors such as temperature and DO, both of which are correlated with hyporheic flow (Chapman 1988). During the study period intergravel temperatures ranged from 7.6 to 12.8 °C, well within the optimal incubation range for chinook salmon and steelhead (Bjornn and Reiser 1991). Results from experiment 2 indicate that, as expected, temperature affected the growth and presumably the yolk-utilization efficiency of the embryos, but had no significant impact on survival. However, this study was performed during the middle of the LMR redd incubation period (October through April) and results could be different at either end of this period.

The use of several physical-parameter measurements to construct a predictive model of chinook salmon and steelhead survival and growth worked well. In addition to the parameters discussed above, VSS, DO, permeability, depth, and water velocities were all used in regression equations to predict growth and survival. While literature and previous work on the LMR support the fact that each of the parameters listed can influence salmonid physiology, their inclusion in our predictive model is not necessarily indicative of a significant effect individually (Garric et al. 1990). In our analysis we found that there were significant differences in the predictive power of regression equations based on what combination of parameters was used. While individually some parameters, such as average temperature, had a higher correlation with average steelhead size, when included in a suite of parameters they were not as useful as stream velocity in maximizing the predictive power of the regression equation. While the bulk of variation in growth and survival is explained by two or three parameters, the inclusion of minimally correlated measures may act to fine-tune equations to particular sites or systems. Leftwich et al. (1997) compared the predictive power of local and regional habitat models for the tangerine darter (*Percina aurantiaca*). Their results indicate significant differences in the relative importance of limiting factors between habitats, which limited the transferability of local-habitat models. It is likely that the influence of nonlimiting parameters in predictive models would also vary geographically, emphasizing the importance of collecting a full suite of data when evaluating restoration projects and the significant relatedness between some parameters (Koslow et al. 2002).

Management implications

It is important to note that the steelhead and chinook salmon embryos were not exposed to the test environment during their earliest development period. Even so, our results suggest that survival and development effects from manipulation of the spawning and incubation environment can be accurately measured. By increasing substrate porosity, hyporheic and surface water quality can be equilibrated. However, these synergistic effects greatly complicate evaluation of enhancement benefits, especially when parameters are assessed individually. These effects may explain documented low correlations between alevin survival and substrate-permeability measurements.

The simple test comparing embryo survival in enhanced and unenhanced gravels performed here provides some of the first evidence of short-term biological benefits of spawning-habitat rehabilitation. From a subset of the 12 parameters we were able to develop predictive multiple regression models for chinook salmon and steelhead embryo survival and growth, which suggests that benefits from gravel augmentation can be predicted and measured. However, this is not to suggest that all forms of spawning-habitat rehabilitation will or should yield similar improvements in embryo survival. Instead, there are logical explanations for differences between substrate conditions in enhanced and unenhanced gravels that may then explain the observed differences in survivability. The four spawning bed enhancement sites consisted of riffles constructed between 1994 and 2001. Unlike gravel augmentation or hydraulic structure placement forms of rehabilitation, these projects involve the direct placement of clean, optimally sized spawning gravels to form immediate spawning habitat (Wheaton 2003). On the LMR, typical fill depths of these projects are greater than egg-burial depths (>25 cm). Merz and Setka (2004) showed significant reductions in channel depth, sediment fines, and intergravel temperature and significant increases in stream velocities, intergravel permeability, and DO. Therefore, strategic gravel placement equilibrated the hyporheic and water-column environments and related positively to embryo survival rates. As Pasternack et al. (2004) point out, ad hoc implementation (as done on the LMR from 1991 to 2000) of spawning bed enhancement projects without a systematic design process (e.g., Wheaton 2003) can lead to less efficient gravel placement. To better gauge the benefits of such projects to the effort applied, we suggest appropriate cost-benefit analysis of material and effort in terms of actual embryo or fry production. Furthermore, while site-specific

augmentation appears promising, it is important to note that the LMR is a relatively low gradient stream with a highly regulated flow. Using the methods presented here in other river systems should increase our understanding of how gravel-enhancement projects work in different situations. This understanding, in turn, can be linked to the establishment of healthy ecosystem, hydrologic, and geomorphic processes.

Acknowledgements

We thank James Smith, Michelle Workman, Leigh Chan, Dr. Peter Moyle, and Dr. Joseph Cech for their contributions to this project. We are also grateful to Dillon Collins, Dr. Randy Dahlgren, Leslie Ferguson, Liz Gordon, James Jones, Nina Kogut, Gina Ladd, Donna Maniscalco, Bert Mulchaey, Audrey Peller, Kent Reeves, Matt Saldate, Jason Shillam, John Strelka, and Dr. Erwin Van Nieuwenhuyse, who assisted at various times with field and laboratory work. Finally, we thank the Mokelumne River and Feather River hatchery staff of the California Department of Fish and Game for providing chinook salmon and steelhead eggs for this project. Support from the United States Fish and Wildlife Service through the Central Valley Project Improvement Act Restoration Funds, California State Park Funding, and East Bay Municipal Utility District is gratefully acknowledged.

References

American Public Health Association, American Water Works Association, and Water Pollution Control Federation. 1995. Standard methods for the examination of water and wastewater. 19th ed. American Public Health Association, Washington, D.C.

Ashworth, P., and Ferguson, R.I. 1989. Size-selective entrainment of bed load in gravel bed streams. Water Resour. Res. **25**: 627–634.

Barnard, K., and McBain, S. 1994. Standpipe to determine permeability, dissolved oxygen, and vertical particle size distribution in salmonid spawning gravels. Fish Habitat Relationships Tech. Bull. No. 15, U.S. Forest Service, Region 5, Eureka, Calif.

Bauer, S.B., and Burton, T.A. 1993. Monitoring protocols to evaluate water quality effects of grazing management on western rangeland streams. United States Environmental Protection Agency, Water Division, Surface Water Branch, Region 10, Seattle, Washington. pp. 145–148.

Beacham, T.D., and Murray, C.B. 1990. Temperature, egg size, and development of embryos and alevin of five species of Pacific salmon: a comparative analysis. Trans. Am. Fish. Soc. **119**: 927–945.

Bjornn, T.C., and Reiser, D.W. 1991. Habitat requirements of salmonids in streams. Am. Fish. Soc. Spec. Publ. No. 16. pp. 41–82.

Bryant, R.J. 2000. Mokelumne River Fish Hatchery 1999–2000. Region 2, Inland Fisheries Administrative Report. California Department of Fish and Game, Sacramento.

Buer, K., Scott, R., Parfitt, D., Serr, G., Haney, J., and Thompson, L. 1981. Salmon spawning gravel enhancements on northern California rivers. *In* Proceedings: propagation, enhancement, and rehabilitation of anadromous salmonid populations and habitat symposium, 15–17 October, Humboldt State University, Arcata, California. *Edited by* T.J. Hassler. American Fisheries Society, Bethesda, Md. pp. 149–154.

Coble, D.W. 1961. Influence of water exchange and dissolved oxygen in redds on the survival of steelhead trout embryos. Trans. Am. Fish. Soc. **90**: 469–474.

California Department of Water Resources. 2002. Merced River salmon habitat enhancement project Phase II – Ratzlaff Reach Spring 2001 Geomorphic Monitoring Report. California Department of Water Resources San Joaquin District River Management Section, Sacramento.

Chapman, D.W. 1988. Critical review of variables used to define effects of fines in redds of large salmonids. Trans. Am. Fish. Soc. **117**: 1–21.

Constantine, C.R., Mount, J.F., and Florsheim, J.L. 2003. The effects of longitudinal differences in gravel mobility on the downstream fining pattern in the Cosumnes River, California. J. Geol. **111**: 233–241.

DeVries, P. 1997. Riverine salmonid egg burial depths: review of published data and implications for scour studies. Can. J. Fish. Aquat. Sci. **54**: 1685–1698.

Federal Energy Regulatory Commission. 1993. Proposed modifications to the Lower Mokelumne River Project, California. Final Environmental Impact Statement. Division of Project Compliance and Administration, Federal Energy Regulatory Commission, Washington, D.C.

Flemming, I.A., and Gross, M.R. 1990. Latitudinal clines: a trade-off between egg number and size in Pacific salmon. Ecology, **71**: 1–11.

Garric, J., Migeon, B., and Vindimian, E. 1990. Lethal effects of draining on brown trout: a predictive model based on field and laboratory studies. Water Res. **24**: 59–65.

Groot, C., and Margolis, L. (*Editors*). 1991. Pacific salmon life histories. University of British Columbia Press, Vancouver, B.C.

Healey, M.C. 1991. Life history of chinook salmon (*Oncorhynchus tshawytscha*). *In* Pacific salmon life histories. *Edited by* C. Groot and L. Margolis. University of British Columbia Press, Vancouver, B.C.

Heaney, S.I., Foy, R.H., Kennedy, G.J.A., Crozier, W.W., and O'Connor, W.C.K. 2001. Impacts of agriculture on aquatic systems: lessons learnt and new unknowns in Northern Ireland. Mar. Freshw. Res. **52**: 151–163.

Heming, T. A. 1982. Effects of temperature on utilization of yolk by chinook salmon (*Oncorhynchus tshawytscha*) eggs and alevins. Can. J. Fish. Aquat. Sci. **39**: 184–190.

Hendry, A.P., Hensleigh, J.E., and Reisenbichler, R.R. 1998. Incubation temperature, development biology, and the divergence of sockeye salmon (*Oncorhynchus nerka*) within Lake Washington. Can. J. Fish. Aquat. Sci. **55**: 1387–1394.

House, R. 1996. An evaluation of stream restoration structures in a coastal Oregon stream, 1981–1993. N. Am. J. Fish. Manage. **16**: 272–281.

Joliffe, I.T. 1972. Discarding variables in a principal component analysis. I: Artificial data. J. R. Statist. Soc. **21**: 160–173.

Kinnison, M.T., Unwin, M.J., Hershberger, W.K., and Quinn, T.P. 1998. Egg size, fecundity, and development rate of two introduced New Zealand chinook salmon (*Oncorhynchus tshawytscha*) populations. Can. J. Fish. Aquat. Sci. **55**: 1946–1953.

Kondolf, G.M. 1997. Hungry water: effects of dams and gravel mining on river channels. Environ. Manag. **21**: 533–551.

Kondolf, G.M., and Mathews, W.V.G. 1993. Management of coarse sediment in regulated rivers of California, Report No. 80. University of California Water Resources Center, Riverside.

Kondolf, G.M., Vick, J.C., and Ramirez, T.M. 1996. Salmon spawning habitat rehabilitation on the Merced River, California: an evaluation of project planning and performance. Trans. Am. Fish. Soc. **12**: 899–912.

Kondou, T., Takeshita, N., Nakazono, A., and Kimura, S. 2001. Egg survival in a fluvial population of Masu salmon in relation to intragravel conditions in spawning redds. Trans. Am. Fish. Soc. **130**: 969–974.

Koslow, J.A., Hobday, A.J., and Boehlert, G.W. 2002. Climate variability and marine survival of coho salmon (*Oncorhynchus kisutch*) in the Oregon production area. Fish. Oceanogr. **11**: 65–77.

Leftwich, K.N., Angermeier, P.L., and Dolloff, C.A. 1997. Factors influencing behavior and transferability of habitat models for a benthic stream fish. Trans. Am. Fish. Soc. **126**: 725–734.

Leitritz, E., and Lewis, R.C. 1980. Trout and salmon culture. California Fish Bull. No. 164, Agricultural Sciences Publications, University of California, Berkeley.

Menchen, R.S. 1961. The Mokelumne River artificial spawning channel experiment 1960–61 spawning season. Marine Resources Branch Administrative Rep. No. 61, California Department of Fish and Game, Sacramento, Calif.

Merz, J.E. 2001. Diet of juvenile chinook salmon in the lower Mokelumne River, California. Calif. Fish Game, **87**: 102–114.

Merz, J.E., and Chan, L.K. 2004. Effects of gravel augmentation on macroinvertebrate assemblages in a regulated California River. River Res. Appl. **21**: 1–14.

Merz, J.E., and Setka, J.D. 2004. Evaluation of a spawning habitat enhancement site for chinook salmon in a regulated California river. N. Am. J. Fish. Manag. **25**: 48–56.

Montgomery, D.R., Pess, G., Beamer, E.M., and Quinn, T.P. 1999. Channel type and salmonid spawning distributions and abundance. Can. J. Fish. Aquat. Sci. **56**: 377–387.

Nelson, R.W., Dwyer, J.R., and Greenberg, W.E. 1987. Regulated flushing in a gravel-bed river for channel habitat maintenance: a Trinity River [California, USA] fisheries case study. Environ. Manag. **11**: 479–494.

National Oceanic and Atmospheric Administration (NOAA). 1994. Endangered and threatened species; status of Sacramento River winter-run chinook salmon. Fed. Regist. **59**: 440–450.

NOAA. 1998. Endangered and threatened species: threatened status for two ESUs of steelhead in Washington, Oregon, and California. Fed. Regist. **53**: 13347–13371.

Olsson, T.I., and Persson, B.G. 1988. Effects of deposited sand on ova survival and alevin emergence in brown trout (*Salmo trutta* L.). Arch. Hydrobiol. **113**: 621–627.

Parker, G., Dhamotharan, S., and Stefan, H. 1982. Model experiments on mobile, paved gravel bed streams. Water Resour. Res. **18**: 1395–1408.

Pasternack, G.B., Wang, C.L., and Merz, J.E. 2004. Application of a 2D hydrodynamic model to design of reach-scale spawning gravel replenishment on the Mokelumne River, California. River Res. Appl. **20**: 205–225.

Poff, N.L., Allan, J.D., Bain, M.B., Karr, J.R., Prestegaard, K.L., Richter, B.D., Sparks, R.E., and Stromberg, J.C. 1997. The natural flow regime. Bioscience, **47**: 769–784.

Preece, R.M., Jones, H.A. 2002. The effect of Keepit Dam on the temperature regime of the Namoi River, Australia. River Res. Appl. **18**: 397–414.

Quinn, T.P., Hendry, A.P., and Wetzel, L.A. 1995. The influence of life history trade-offs and the size of incubation gravels on egg size variation in sockeye salmon (*Oncorhynchus nerka*). Oikos, **74**: 425–438.

Reiser, D.W., and White, R.G. 1988. Effects of two sediment size-classes on survival of steelhead and chinook salmon eggs. N. Am. J. Fish. Manag. **8**: 432–437.

Roni, P., Beechie, T.J., Bilby, R.E., Leonetti, F.E., Pollock, M.M., and Pess, G.R. 2002. A review of stream restoration techniques and a hierarchical strategy for prioritizing restoration in Pacific Northwest watersheds. N. Am. J. Fish. Manag. **22**: 1–20.

Saiki, M.K., and Martin, B.A. 1996. Vacuum hand pump apparatus for collecting water samples from a horizontal intragravel pipe. N. Am. J. Fish. Manag. **16**: 231–232.

Sall, J., Lehman, A., and Creighton, L. 2001. JMP start statistics: a guide to statistics and data analysis using JMP and JMP IN software. 2nd ed. Duxbury, Pacific Grove, Calif.

Schumm, S.A., and Stevens, M.A. 1973. Abrasion in place: a mechanism for rounding and size reduction of coarse sediments in rivers. J. Geol. **1**: 37–40.

Scruton, D.A., Clarke, K.D., Anderson, T.C., Hoddinott, A.S., van Zyll De Jong, M.C., and Houston, K.A. 1997. Evaluation of habitat improvement and restoration initiatives for salmonids in Newfoundland, Canada. Can. Manuscr. Rep. Fish. Aquat. Sci. **2413**: 1–35.

Sear, D.A. 1993. Fine sediment infiltration into gravel spawning beds within a regulated river experiencing floods: ecological implications for salmonids. Regul. Rivers Res. Manag. **8**: 373–390.

Shepherd, B.G., Hartman, G.F., and Wilson, W.J. 1986. Relationships between stream and intergravel temperatures in coastal drainages, and some implications for fisheries workers. Can. J. Fish. Aquat. Sci. **43**: 1818–1822.

Soulsby, C., Youngson, A.F., Moir, H.J., and Malcolm, I.A. 2001. Fine sediment influence on salmonid spawning habitat in a lowland agricultural stream: a preliminary assessment. Sci. Total Environ. **265**: 295–307.

Sowden, T.K., and Power. G. 1985. Prediction of rainbow trout embryo survival in relation to groundwater seepage and particle size of spawning substrates. Trans. Am. Fish. Soc. **114**: 804–812.

SPSS Inc. 1997. SPSS®. Version 10 [computer program]. SPSS Inc., Chicago.

St-Hilaire, A., Caissie, D., Cunjak, R.A., and Bourgeois, G. 1997. Spatial and temporal characterization of suspended sediments and substrate composition in Catamaran Brook, New Brunswick. Can. Tech. Rep. Fish. Aquat. Sci. No. 2165.

Talmage, P.J., Perry, J.A., and Goldstein, R.M. 2002. Relation of instream habitat and physical conditions to fish communities of agricultural streams in the Northern Midwest. N. Am. J. Fish. Manag. **22**: 825–833.

Trush, W.J., McBain, S.M., and Leopold, L.B. 2000. Attributes of an alluvial river and their relation to water policy and management. Proc. Natl. Acad. Sci. U.S.A. **97**: 11858–11863.

Van-Zyll-De-Jong, M.C., Cowx, I.G., and Scruton, D.A. 1997. An evaluation of instream habitat restoration techniques of salmonid populations in a Newfoundland stream. Regul. Rivers Res. Manag. **13**: 603–614.

Vronskiy, B.B. 1972. Reproductive biology of the Kamchatka River chinook salmon (*Oncorhynchus tshawytscha* (Walbaum)). J. Ichthyol. (Engl. Transl. Vopr. Ikhtiol.), **12**: 259–273.

Wheaton, J.M. 2003. Spawning habitat rehabilitation. M.S. thesis, Department of Land, Air and Water Resources – Hydrologic Sciences, University of California, Davis.

Zar, J.H. 1999. Biostatistical analysis. 4th ed. Prentice–Hall, Inc. Englewood Cliffs, N.J.

Zeh, M., and Donni, W. 1994. Restoration of spawning grounds for trout and grayling in the river High-Rhine. Aquat. Sci. **56**: 59–69.

Section 4
What are the Geomorphic Consequences Resulting from the Use of SHIRA?

Introduction

A guiding principle underlying SHIRA is that the best ecological outcome associated with rehabilitating a regulated gravel-bed river will be obtained by re-configuring a channel and/or adjusting the flow regime to produce the necessary geomorphic processes that promote self-sustainable river functionality. In order to achieve this outcome, one must identify what those key geomorphic processes are and then be able to re-configure the channel and/or adjust the flow regime to produce them. However, even if one develops the perfect design for river rehabilitation, it is only worthwhile if the design can actually be built according to the specifications. The first subsection of this section tests whether the common approach used to re-configure accessible regulated streams can meet the demands of SHIRA's sophisticated science-based designs that include a lot of heterogeneity at multiple spatial scales. A key finding was that uncertainty in the final dry bulk density of gravel placed into the as-built configuration is a major problem that needs to be addressed by future research. Also, construction using front loaders results in several challenges that limit the ability to accurately reproduce bed features with elevational variations of <0.5 m.

Because geomorphic change occurs slowly over time, especially in a heavily regulated river such as the Mokelumne, the testing of the geomorphic principles used in SHIRA can only occur years after a project is built. This CALFED-sponsored project was not intended to or of sufficient duration to monitor beyond 2005 the 2003-2005 sites whose designs were produced in this project. However, it was possible to monitor the 1999-2000 baseline sites and the 2001 preliminary SHIRA site to see what happened to them by 2005. In the second subsection, a sediment budget approach for tracking individual geomorphic processes responsible for changing spawning habitat rehabilitation sites is reported and applied to the 1999-2001 sites. The resulting sediment budgets yielded the important finding that on a low-slope, low-flow river such as the Mokleumne, gravel settlement over the first few years represents a dominant cause of site change relative to flow-induced scour and other mechanisms.

Finally, although SHIRA was initially used to only rehabilitate individual riffles in 2001 and 2002 prior to this demonstration project, baseline evaluation of the LMR revealed that the whole sequences of riffles and pools below the dam require rehabilitation. To facilitate this, a "slope creation" tool was added to SHIRA as described in section 3b. From a geomorphic perspective, once slope creation was going to be used to rehabiulitate the river's longitudinal profile, it became apparent that knowledge of how individual riffle-pool units ordered into a sequence influenced each other would be necessary. In other words, each riffle-pool unit does not function in a vacuum, but is influenced particularly by those downstream of it. In the third subsection of this section, two theoretical pool-riffle-pool morphologies were tested for their spawning habitat quantity/quality and susceptibility to scour as a result of downstream riffle crest elevation to illustrate and evaluate inter-riffle interactions. A key ecological finding of this evaluation was that backwater conditions are required in order to obtain high-quality habitat. Since PHABSIM is not capable of simulating backwater conditions, that commonly used tool is

thus inadequate for use in SHIRA and for spawning habitat rehabilitation in general. A key geomorphic finding of this investigation was that sequences of riffles are most susceptible to degradation and destruction in a "reverse domino" sequence, with damage to downstream riffles facilitating damage of upstream riffles.

Long-term geomorphic evaluation of SHIRA was not possible with 3 years of funding, but the results reported in this project demonstrate that the LMR is much more hydraulically and geomorphically diverse now than it was before 2001. Flow can now access the floodplain more frequently, the bed slope is generally steeper, and the lateral complexity of riffles and pools is much greater. Monitoring of how the river responds to these changes will have to occur over many more years before any conclusions may be drawn about the rehabilitation utility of the geomorphic principles incorporated into SHIRA.

Construction constraints on geomorphic-unit rehabilitation on regulated gravel-bed rivers

Authors:

April M. Sawyer[1], Gregory B. Pasternack[1*], Joseph E. Merz[2], Marisa Escobar[1], Anne E. Senter[1]

Addresses:

[1]Department of Land, Air, and Water Resources, University of California, One Shields Avenue, Davis, CA 95616-8626, USA;

[2] East Bay Municipal Utility District, 1 Winemasters Way, Lodi, CA 95240.

*Corresponding author

ABSTRACT

Construction of a river rehabilitation project may have limitations hindering the integrity of the final outcome in relation to the design. For example, designs for salmonid spawning habitat enhancement by gravel augmentation based on analysis of geomorphic processes can be very detailed to meet habitat requirements, with some features at a scale of 0.5 m relief. Given equipment and contouring methods typical of such projects, it is necessary to determine whether design features are practicable before widespread adoption of such detailed designs. In this study, we compared design and as-built topography for 5 spawning habitat rehabilitation projects at riffle-pool geomorphic units on the lower Mokelumne River, California that were built in-stream using front loaders. Digital Elevation Models (DEMs) of each site were produced for pre-project, design, and as-built conditions. DEM differencing of the as-built surface against pre-project and design surfaces for each site was used to identify deviations from the design, including gravel supply deficits and bulk density differences, providing insight into construction accuracy. The causes of each identified deviation were assessed based on subjective observations during construction. Across the projects, 70% of as-built topography showed insignificant deviation from design within -0.15 to 0.15 m. Of the 30% deviating from the design, 41% was overfilled and 59% underfilled as a result of gravel deficits, bulk density differences and observed construction difficulties. The difficulties encountered as a result of construction in an aqueous environment caused as-built topography to differ from design. They included front loader fording depth, poor operator elevation estimation, operator spatial disorientation, and obstructions by wood. In addition, funding and project management uncertainties were responsible for gravel supply deficits and gravel bulk density estimation errors. It is concluded that construction of the broad (> 0.5-m relief) features of process-based salmonid spawning habitat rehabilitation projects built using augmented gravel is practicable, but shaping detailed (<0.5-m relief) features and gently sloping riffle entrance and exit slopes is not practicable with a front loader.

Keywords: river restoration, fluvial geomorphology, river engineering, spawning habitat

1. INTRODUCTION

Analytical, empirical, and numerical methods for evaluating fluvial processes and landforms exist from microscopic to global spatial scales and corresponding temporal scales. While further improvements in basic river science continue, periodic evaluation of the practical utility of existing knowledge is necessary to promote advancement of environmental management. A common critique of one type of environmental management, applied river restoration, is that it often does not make use of the best available science (e.g. Brooks and Shields, 1996; Kondolf, 2000; Downs and Kondolf, 2002; Wohl et al., 2005). However, it has also been noted that the best available science is often not practicable (Wilcock 1997; Wheaton et al., 2004a). Thus, there appears to be a critical scientific gap in evaluating the sensible utility of using best-available scientific theories in applied river restoration.

Grading plans are documents that direct how a landscape is re-contoured during construction. In this study we evaluated the practicability of implementing highly detailed river-bed grading plans that were generated based on thorough scientific analysis. Grading plans were implemented using rubber-tire front loaders (i.e. the standard method in accessible California streams) at a reasonable cost. Evaluated grading plans included elements to re-configure the channel, build hydraulic structures using boulders, and supply coarse sediment below a dam for the river's sediment budget. This study focuses on construction constraints and does not debate the merits of the rehabilitation principles (i.e. Wheaton et al., 2004a,b; Elkins et al., in press) used in the specific projects evaluated. The significance of this research is that it offers the geomorphology community insight into practical constraints on implementing designs using advanced process-based principles.

Within a river channel, construction of carefully designed topographic features using a rubber-tire front loader has limitations and sources of error as revealed through this investigation. A streambed-enhancement project design is based on an expected volume of gravel pre-determined to meet project goals within set cost constraints. At no fault of the construction process, the as-built volume may deviate from the design volume if the delivered weight of gravel does not match the expected weight (i.e. "gravel deficit"). This can occur if funding is uncertain, gravel purchase and/or delivery costs change between the dates of funding allocated and construction, the supplier cannot produce the contracted amount of the specified gravel, alternate supplies turn out to be inadequate, or other such unexpected reasons.

To understand why as-built topography might deviate from design, it is helpful to conceive of possible sources of error. One major limiting factor may be that both front loaders and operators are being employed in a unique working environment with significant constraints. For instance, each front loader has a maximum depth to which it can ford before engine flooding occurs; making construction into deep pools a hazard for the machinery. Additionally, operators have different levels of skill, experience, and anxiety operating in a river. Each operator must decide how far to push gravel into deep areas such as pool/riffle transitions, while risking potential engine, transmission and gear box damage in excess of $200,000 to repair, thus making construction highly subjective in these areas and more susceptible to error.

Even in areas where a front loader may be safely operated, it could be difficult for the operator to achieve the desired grade. Placing the gravel in the correct location depends on the ability of the operator to orient themselves and their work in the real world relative to the grading plans on maps of the stream. However, depending on what markers are used on site, how they are organized, and who places them, the operator may be at a disadvantage because they are

trying to follow instructions and were not directly involved in design or construction preparation. Instream placement and manipulation of gravel with the front loader to match the designed grade may be hindered by decreased visibility due to suspended sediments, waves created by front loader movement, reflection from the sun, and refraction through water. These factors may impede the operator's judgment of depth, even with tire submergence as a reference estimate. Also, the correct design depth may be achieved in this manner, but at the wrong bed elevation depending on what variables are controlling channel hydraulics. Finally, overhanging vegetation and submerged wood may limit tractor accessibility close to the banks.

Other challenging sources of error include loose gravel packing and compressibility of placed, subaqueous gravel. Merz et al. (2006) studied bulk density effects at a single streambed-enhancement site within the same river reach as investigated in this study. They reported that the bulk density of dry gravel measured during tests made at a nearby quarry by weighing a 19-L (5-gal) bucket filled with coarse sediment 6 times was 1.645 metric tons per m^3. However, when a large amount of gravel is poured onto the river bed it might be loosely packed, yielding a significantly lower bulk density. Furthermore, the size distribution of material delivered from the quarry might be different from that anticipated, yielding a different packing density. Continual front loader movement over the riverbed during construction might cause significant gravel compaction, but perhaps less than normally achieved using vibratory or rolling compactors on unsubmerged road aggregate. During construction a front loader enters the river at designated points to limit the amount of riparian damage and thus drives over built gravel paths many times going to and from placement points. As a result of repeated traffic by the front loader, areas closest to the placement points may have a greater bulk density and contribute to deviation from the design. All of the above potential sources of error were evaluated in this

investigation.

2.STUDY AREA

The snow-fed Mokelumne River in California drains ~1600 km^2 of the central Sierra Nevada (Fig. 1). It presently has 16 major water impoundments, including Salt Springs (175,032,089 m^3), Pardee (258,909,341 m^3) and Camanche reservoirs (531,387,061 m^3) that have dramatically altered the late spring snowmelt flow regime (Pasternack et al., 2004). Below Camanche Dam, the Lower Mokelumne River (LMR) bed slope ranges from 0.10 % near Camanche Dam to 0.02 % near the Cosumnes River confluence, with the active channel now half its former width (present average 30 m; range 19-43 m). Post-dam channel incision has disconnected the remaining floodplain from the channel during all but the highest infrequent flow releases. As far as ~15 km downstream of Camanche Dam, the degraded channel bed has limited amounts of compacted gravels and cobbles associated with higher bed slope and shallow riffle-run hydraulics, yet is the only reach on the LMR available for salmonid spawning. Camanche Dam not only blocks gravel delivery from upstream, it also blocks spawners from traveling any further upstream. During the 1980s and 1990s, limited amounts of gravel were placed in the river to enhance spawning riffles. Murphy Creek, a minor tributary close to the dam, contributes a small amount of fine gravel since a dam on it was removed in 2002. Historic mining operations depleted instream gravel storage and yielded deep pits that are sediment-transport barriers. Channel-mining tailings exist along the upper third of the LMR, but are isolated behind berms and levees. Flow releases cannot access and mobilize them. Channel and banks are highly stable and banks are moderately vegetated, limiting gravel recruitment from

bank scour.

Presently, the LMR supports over 35 native and non-native fish species including native Chinook salmon (*Oncorhynchus tschawytscha*) and steelhead (*O. mykiss*) (Merz et al., 2004). For the 19-year period before Camanche Reservoir was impounded, runs averaged 3,300 spawners, though spawning areas were estimated to accommodate ~15,000 adult Chinook salmon at 11.3 m^3/s (CDFG, 1955). Post-Camanche Dam, Chinook salmon runs have averaged ~3,800 spawners producing ~800-1000 redds. USFWS (1997) called for a LMR fall-run Chinook salmon population target of 9,300. Average annual LMR salmon escapement has been monitored by video at Woodbridge Dam 1990-2004, with Chinook escapement averaging 5,825 and ranging from 410-10,759 (Workman, 2003). Most spawning occurs in the 15 km between Camanche and Elliott Road. The Federal Energy Regulatory Commission (FERC) ranked factors limiting salmonid production in the LMR and determined that salmon-spawning habitat quality and quantity were highly most important factors (FERC 1993).

Research on abiotic-biotic linkages on the LMR has found that the amount and quality of Chinook salmon-spawning habitat serves as an effective ecological indicator of the health of this regulated river's aquatic ecosystem. High-quality spawning habitat was found to have high intergravel permeability and dissolved oxygen content (Merz and Setka, 2004), high diversity and abundance of macroinvertebrates (Merz and Ochikubo Chan, 2005), and high survival of embryos to the fry life stage (Merz et al., 2004). Creating high-quality spawning riffles has been observed to enhance pools that serve as adult holding habitat, increase the area of shallow water habitat for fry rearing, and raise the streambed to enhance floodplain connectivity. Based on these observed ecosystem linkages, river rehabilitation below Camanche Dam 1999-2005 has focused on spawning habitat rehabilitation including gravel augmentation, hydraulic structure

placement, and spawning bed enhancement (Wheaton et al., 2004a,b; Elkins et al., in press).

Rehabilitation planning, design, implementation, and long-term monitoring on the LMR has been guided by the Spawning Habitat Integrated Rehabilitation Approach (SHIRA). SHIRA integrates concepts from hydrology, ecology, biology, geomorphology, and engineering to design and evaluate alternative channel configurations for a degraded regulated river prior to construction (Pasternack et al., 2004; Wheaton et al, 2004a,b). Central to this approach is the testing of mechanistic predictions made by transparent design hypotheses regarding environmental processes over 10^{-1}-10^{4} m scales using 2D hydrodynamic modelling (Pasternack et al., 2006). 2D models aid evaluation of the relative performance of design alternatives and the final as-built project configuration down to the 0.1-1 m scale that fish are attuned to (evaluation methodology detailed in Wheaton et al. (2004b)). Monitoring is used to evaluate SHIRA predictions and drive adaptive management (Merz et al., 2006; Elkins et al., in press). While 2D models and other tools used in SHIRA have uncertainty (Pasternack et al., 2006; MacWilliams et al., 2006), they help stakeholders gain a deeper understanding of what a particular rehabilitation project can and cannot do, thus yielding realistic project goals and providing significant cost-savings.

3. METHODS

The methodology for this study was to employ SHIRA to develop final grading plans for river rehabilitation sites (Fig. 2), apply cost-effective practices to construct the projects according to the grading plans as closely as possible, conduct a detailed topographic survey to characterize each site's as-built condition, and then compare and contrast design plans against actual construction outcomes. The scientific and management foundations of each specific design are

presented elsewhere (e.g. Wheaton and Pasternack, 2002; Wheaton et al., 2004b; Pasternack et al., 2006; Elkins et al., in press) and are not directly relevant to answering the scientific question posed in this study. It is important to keep the focus of this research on construction constraints; therefore this paper is not the place to debate the merits of rehabilitation principles. Each evaluated project's design is briefly summarized next.

3.1 Grading Plans

To create the grading plan for each project, a baseline digital elevation model (DEM) was first developed for the pre-project state of each site. Next, alternative design scenarios were developed, evaluated, and reduced to the final design based on various selection criteria (Wheaton et al., 2004a,b; Elkins et al., in press). Finally, the design DEM was used to generate a set of grading-plan documents for use in construction.

Topographic data was obtained using a Topcon GTS-802A or LEICA TPS1100 (or TPS1200) robotic total station following these 5 steps: 1) setting up the total station within the established control network, 2) wading into the channel in a dry suit with a prism pole to measure bed positions on a staggered grid with a sampling density of ~1-1.5 pt/m^2, 3) capturing key breaklines (bank toes, boulders, slope breaks), 4) performing supplemental surveying of boulders, redds and other features with a higher point density of ~10 pts/m^2, and 5) surveying un-wadable pools by lowering the prism pole from a small rubber raft held in position by ropes. Surveying accuracy was assessed using control network checks and was found to average ±0.0035 m horizontal and ±0.0039 m vertical.

Topographic data were imported into Autodesk Land Desktop 3 to create each baseline DEM. The four iterative stages of DEM development as described by French and Clifford

(2000) were implemented: interpolation, visualization, editing, and augmentation. First, survey data were interpolated and a surface defined respecting breaklines. Next, the surface was visualized as a map and edited to remove obvious interpolation errors. The revised surface was visually verified in the field to check for poorly represented areas in the DEM. Further iteration was done as needed.

Final design scenario DEMs were developed using the pre-project DEM as a baseline. Points and contours were modified and augmented in Autodesk to describe the final design surface. The gravel volume of each design was determined by DEM differencing between the design and pre-project DEMs. This volume was converted to a weight based on the previously mentioned average dry bulk density from bucket tests at a nearby quarry (1.645 metric tons per m^3). Designs were iterated to yield estimated design weights close to the expected contractual purchase weights of 907, 1906, 2087, 3554, and 3301 metric tons for each year chronologically 2001-2005.

Grading plans consisted of a set of laminated maps and placed markers to help the front loader operator with coarse sediment placement and to provide workers checking channel grade using a total station or autolevel with reference points. The set of maps included a pre-project topographic map, a final design topographic map, a gravel-fill depth map, and a map of the spatial pattern of water depth predicted by a 2D hydrodynamic model for the discharge present at the time of construction. In addition, zoomed views of components of the final design were provided on multiple pages. In 2001-2004, bright marker paint was used on trees on the banks to denote key reference points associated with the major bed features to help the front-loader operator contour the sediment properly while operating in the river. Visual inspection of the 2D hydraulic pattern was made by wading around the site as another way of inspecting whether the

construction process was yielding the desired outcome.

In 2005, the feature-based reference points and grade checking measures were replaced with a grid-based approach. A 6.1x6.1 m bed-elevation grid was extracted from the final design DEM and imported into a Leica TPS1200 total station. Labeled and brightly-painted wood stakes were posted in 6.1-m (20') intervals down the channel for the front loader operator to use as a visual aid. These stakes were used to thoroughly check elevations in the grid during and after construction. Wading with a stadia rod provided a visual depth reference for the operator to follow the surveyor's instructions.

3.2 Construction Approach

Each year 2001-2005, a single geomorphic unit on the LMR was augmented with coarse sediment and re-contoured using a front loader according to the given grading plan for that year (Fig. 2). The amount of coarse sediment used for each project varied depending upon available funding and project costs. The augmented sediment consisted of washed 25-150 mm diameter river gravel (CDFG, 1991; Kondolf and Wolman, 1993) from an open floodplain quarry located 0.5 km from the active channel. The material was transported to each site in 15.3-m^3 (20-yd^3) dump trucks and poured directly into the channel to avoid losses on the floodplain (Merz et al., 2006). Concurrent with sediment delivery, the front loader was used to re-contour the bed by scooping up a bucket full of material, transporting it to the desired location, and dropping it into place. After the gravel and cobble bed was contoured, the front loader placed ~10-20 boulders (0.6-1.2 m diameter) and ~5-10 pieces of wood (trunks up to 0.6 m diameter) throughout each site to increase downwelling, channel complexity, and cover for spawning salmonids (Geist and Dauble, 1998; House, 1996; Merz, 2001). No boulders or wood were artificially cabled together

or into place, so they were free to adjust or transport naturally. Depending on the amount of material placed and the number of dump trucks available to bring in the sediment, construction took 3-8 days.

Each project utilized a ~20 metric-ton, front-wheel front loader with rubber tires and a 3.82-m^3 (5-yd^3) bucket capacity to construct the design features in the wetted channel. Construction equipment manufacturer's websites and subsequent phone correspondence with dealers were used to compile information about front loader capabilities. Since front loaders were used during flows of 7-13 m^3/s, a primary concern was the maximum depth of fording below which the engine would not flood. Manufacturers recommend not exceeding the height of the center of the wheel hub that generally coincides with the bottom of the oil pan on which the engine sits. Fording to this depth is also problematic because if the breather tube in the engine is submerged, water can be sucked into the transfer cases and transmission where expensive damage may result, as experienced in 2003.

Because gravel bulk density is an important variable in determining gravel erodibility and hyporheic water quality, the effect of a front loader on bulk density is necessary to consider. The footprint of compaction for each tractor was calculated from construction photos of loader wheels not submerged in water. On average loaders sank into the gravel half the radius of the wheel hub due to compaction. From this approximation, the surface area in contact with gravel was calculated using tire dimensions. Finally, each tractor's weight was divided by the total in-contact surface area of the four tires to obtain the stress imposed by the front loader on the gravel bed (Table 1). Knowledge of the stress due to compaction is important to qualify the effect of the front loader's repetitive traffic over the bed as a source of deviation from expected bulk-density.

3.3 As-built DEM

Once construction was completed the site was allowed to rest for 1-3 days to account for rapid settling before a detailed topographic survey of the as-built condition was performed and a DEM generated. Both the topographic survey and DEM generation were done using the approaches previously described for the baseline topographic characterization. The as-built DEM represents the condition that spawners find the site in during the months right after construction. For a comparison of design versus as-built topography for each project year, see Figures 3-7.

3.4 DEM Analysis

Using the DEM-differencing algorithm in Surfer 8 (Golden Software, Golden, CO), as-built DEMs were compared against design DEMs to determine the magnitude and spatial pattern of volume difference. Sets of DEMs for each site were imported into Surfer and used to generate identical high-resolution DEM grids. The grid-blanking feature was used to limit subsequent analyses to only the in-channel area. Using the matching design and as-built gridded DEMs (Figs. 3-7), Surfer calculated gross cut (in underfilled areas), gross fill (in overfilled areas), and net volume difference. Also, Surfer's Grid Math function subtracted design elevations from the as-built elevations to yield a DEM-difference map with areas of positive (excess) and negative (deficit) as-built elevation relative to the design surface. As-built DEMs were also differenced against pre-project DEMs to obtain the actual as-built volume, enabling calculation of the as-built dry bulk density of the placed material knowing its dry weight from gravel delivery documents.

A key constraint on the study was to determine the amount of local underfilling or overfilling indicative of a significant variation worthy of investigation. To address this, DEM difference error was evaluated on an elevation and volumetric basis. Topographic surveying error included vertical set-up accuracy of ~ ±0.004 m and prism-pole placement errors of ~ ±0.01 m. Given that bed particle size was in the 0.1-0.15 m range, vertical resolution was thus not limited by surveying accuracy, but by natural surface heterogeneity. As a conservative limit, as-built surfaces within ±0.15 m of the design surface were considered accurate. Thus, significant variation was defined as more than a 0.15-m absolute difference from the design elevation. The direction of the deviation was either a fill (> +0.15 m) or a cut (< -0.15 m) relative to the design.

A volumetric error analysis to constrain deviations resulting from varying point densities and point locations between two DEMs made for the same area on the LMR was performed by Merz et al. (2006). They reported an average error of ±2 m^3 per 100 m^2 of channel surface area. Since project areas were ~2000-4000 m^2, volumetric errors are ±40-80 m^3. Thus, a DEM difference between design and as-built surface must have more deviation than this range for the difference to be attributable to real surface variation.

For black and white visualization, DEM difference maps use shades of grey (darkest shade corresponds to lowest elevation) to depict areas of gravel deficit and shades of grey with dots (lightest shaded dots corresponds to highest elevation) for areas of gravel surplus. For each project year, these difference data were exported from Surfer and analyzed in Microsoft Excel with histograms that showed the frequency of areas categorized into 0.15-m contour intervals as well as the percentage of occurrence of cut, fill and insignificant areas.

3.5 Construction Observations

The identification of elevational errors in construction was made using quantitative DEM analyses as previously explained. Causes of error for each sizable area deviating from the design were organized into the broad categories of gravel supply uncertainty, construction operations, and gravel bulk-density differences. Determination of gravel-supply uncertainties and bulk-density differences as causes of elevation error was based on comparing and contrasting calculated design, purchased, and as-built gravel volumes for each project. Also, if the available gravel supply ran out prior to completion of the design, then the cause of error associated with unfilled areas was objectively attributable to gravel supply uncertainty.

Determination of the cause of each significant error associated with construction operations depended on the subjective interpretation of each design crew member. Discussion among observers, participants, and operators was used to generate an expert consensus for the problems encountered for each project. It was often agreed that individual areas of elevation error could be attributed to multiple causes. Using this subjective expert consensus approach, causes of errors were tabulated for each year and compared across years to reveal common patterns that transcend the uncertainty associated with unavoidable subjectivity.

4. RESULTS

The DEM difference plots show a consistent pattern of construction difficulties in achieving specified elevations to within ±0.15 m. Overall as-built gravel volumes deviated from design volumes by 29 % (Table 2). Actual starting locations for gravel placement to begin a riffle tended to be too far upstream and with a steep riffle entrance slope using too much gravel. That often led to inadequate gravel supplies to build the desired riffle exit slopes, so those were

underfilled. Complex bed features tended to be built with excessive relief, yielding higher bar tops and lower chute troughs. Detailed results for each project are presented to demonstrate these and other significant deviations. For each project, specific locations of significant deviation are numbered to simplify presentation. For simplification in this section, areas of significant deviation are reported as the absolute value of volume difference: either >0.15 m underfilled or >0.15 m overfilled.

4.1 The 2001 Project

The 2001 project design was specified to have an as-built volume of 1147 m^3, corresponding to an estimated supply of 1887 metric tons of gravel, with 980 metric tons of that needing to be salvaged from the beds of adjacent hatchery channels at no cost (Table 3). As it turned out, the salvage operation only yielded 400 metric tons of usable gravel, making on-site design changes necessary to account for an overly ambitious design relative to gravel supply. Nevertheless, 81% of the 2001 as-built project area was within ±0.15 m of the design surface. Of the 19% of areas with significant deviation, 83 % was >0.15 m underfilled and 17% was >0.15 m overfilled.

The comparison of design versus as-built DEMs yielded six specific areas of significant difference (Fig. 8). Lacking the anticipated amount of gravel, it was decided to not fill area 1. A small area peripheral to the upstream pool was also overfilled by 0.3 m (area 2). Area 3 was the primary area that was significantly overfilled at the riffle entrance and riffle crest, which were built too far upstream and were as much as 1.50 m higher than specified. The majority of the site, including area 4 at the pool-constricting point bar and area 5 at the central bar, was underfilled by 0.15-0.45 m, mainly due to the gravel deficit. Gravel supplies ran out before area

6 was reached, so that area was 1.5 m below design grade.

For the 2001 project, the sources of error were gravel deficits (half of all errors), operator spatial disorientation, and operator mis-estimation of elevation/depth (Tables 4, 5). The *ad hoc* adjustments to account for the reduced gravel supply included eliminating gravel placement in areas 1 and 6 as well as reduced placement in areas 4 and 5 (Fig. 8). Operator's spatial disorientation was responsible for significantly overfilling areas 2 and 3. Operator's poor elevation and depth estimation partly accounted for underfilling areas 4 and 5. Whereas the project volume for 1307 metric tons of placed gravel was estimated to be 794 m^3, the actual as-built volume relative to the pre-project DEM was 649 m^3 (Table 3). The observed difference in as-built volume stems from net gravel compaction. As-built bulk density exceeded the quarry value by ~22%, yielding a higher density of 2.013 metric tons per m^3 as opposed to the bucket-test estimate of 1.645 metric tons per m^3.

4.2 The 2002 Project

The 2002 project design included small placements of varying priority to account for uncertainty in gravel supply and as-built bulk density. The design specified an as-built volume of 1448 m^3 assuming all staged components could be completed (Table 3). A supply of 2786 metric tons of gravel estimated to yield 1694 m^3 was purchased, indicating that an excess of gravel should have been available to achieve all design features. Overall, 79% of the 2002 complete design versus as-built project area was within ±0.15 m of the design surface. Of the 21% of areas that deviated from the design, 43% of the as-built survey area elevations were >0.15 m overfilled, and 57% were >0.15 m underfilled.

The comparison of design versus as-built survey results found eleven areas of significant

difference (Fig. 9). Starting at the upstream limit of the site where the riffle entrance was located, the entrance slope at area 1 was underfilled by 0.15-0.45 m. Just downstream at area 2, the riffle crest was overfilled by 0.15-0.45 m, and the backside of the riffle crest, area 3, was 0.15-0.45 m lower than specified. Downstream of the crest, the flow was designed to be split into a thalweg on river left and a side channel on river right, with a longitudinal bar in between. On river left, an alternating sequence of deeper and shallower microhabitats was built with excessive relief such that a small pool, area 4, was underfilled by 0.60 m and a small riffle crest, area 5, was overfilled by 1.2 m. On river right at area 6, the whole length of the side channel was overfilled by 0.30 m. At area 7, the central bar dividing the two threads was 0.30 m lower than specified. Visual observations and 2D model simulations showed that the flow was divided, but not to the extent originally intended. At area 8, beyond the central bar, the next riffle area and riffle exit slope were underfilled by 0.45 m. Area 9 shows a cluster of points on river left where a boulder cluster was intended to be placed on a point bar to constrict the flow in a pool, but the exact number and positioning of the boulders turned out different than designed. Areas 10 and 11 are on the next riffle after the pool and were specified for construction if enough gravel was available, but those areas ended up not being filled.

For the 2002 project several factors played a role in causing the deviations, with operator mis-estimation of elevation/depth (31%) and fording depth limitations (25%) being the largest problems (Tables 4, 5). As shown in Fig. 9, design deviations in areas 1 and 5 resulted from the tractor not going far enough upstream and from mistakenly filling a designed pool, respectively. These deviations were related to operator spatial disorientation problems. Operator mis-estimation of elevation resulted in overfill in areas 2 and 6 as well as underfilling in areas 3, 4, and 7. These elevation errors yielded less relief between the central bar and side channel.

Another error arose when adding boulders because the operator did not place them at the exact locations as designed, which results in surveying errors around boulder clusters, this is seen at area 9. Area 8 was underfilled due to overfilling upstream. Due to overfilling upstream, low-priority areas 10 and 11 were left unfilled. The DEM difference between as-built and pre-project conditions yielded an as-built volume and bulk density of 1410 m^3 and 1.976 metric tons per m^3, respectively (Table 3). Once again, as-built bulk density exceeded the quarry value by ~20%.

4.3 The 2003 Project

The 2003 project was the first phase of a 2-year scheme to rehabilitate the stream's longitudinal profile and enhance its floodplain connectivity starting at the base of Camanche Dam. In this project the adaptive design was not only sectional as in 2002, but also temporal in that any deviations would be revisited and addressed in 2004. The final design for the 2003 portion of the project was specified to have an as-built volume of 2020 m^3 (Table 3). The purchased gravel supply was 3217 metric tons, estimated to yield 1955 m^3, indicating a small 3.2% gravel deficit. Overall, 64% of the 2003 project area had insignificant deviation from the design of within ± 0.15 m elevation difference. Of the 36% of areas that had significant deviation from the design, 31% of the as-built survey area elevations were >0.15 m overfilled, and 69% were >0.15 m underfilled.

A comparison of the design versus as-built project results (Fig.10) revealed eight differences from the design starting from the upstream end of the project site. At area 1, the riffle crest was overfilled 0.15-0.75 m. Just downstream on river right at area 2, the long back slope of the riffle was 0.15-0.75 m underfilled, with the deepest deviation closest to the bank at the transition into the pool where a lot of existing wood obstructed placement. The elevation of

the entrance to the river-left chute adjacent to the riffle crest at area 3 was overbuilt by 0.45 m whereas the chute's length, area 4, was 0.15-0.75 m underfilled. This resulted in a much longer but shallower chute along the left bank. Downstream, half of a left-bank point bar at area 6 was 0.45 m too low and the thalweg to the right of it, area 5, was 0.60 m too high. A small area at the entrance of the next riffle crest, area 7, was 0.30 m overfilled. The majority of that riffle, area 8, was 0.5-1.35 m underfilled due to existing wood obstructions that made it difficult to maneuver the front loader. The few openings in between wood obstructions tended to be overfilled.

Design deviations in 2003 resulted from nearly equal amounts of all factors. Operator errors accounted for 55% of deviations, while channel conditions accounted for 28% (Tables 4, 5). Area 1 shows the riffle crest built too far upstream and too high, contributing to the deficit in area 2 where there were also wood obstructions hindering placement and creating fording limitations (Fig.10). Operator spatial disorientation was worse in 2003 because the channel was much wider at this year's rehabilitation site, making it more difficult for the operator to orient relative to markers on the distant banks. Area 3 was built too high because that location was the site of gravel dumping by delivery trucks. Areas 4 and 6 were underfilled due to over sizing the thalweg as a result of operator mis-estimation of depth. Area 8 was underfilled due to fording limitations and existing wood hindrances. Where wood and excessive depth complicated gravel placement, operator skill, experience, and willingness becomes a factor in determining the degree to which an effort is made to succeed with the design or not, as constructing features in such situations is very difficult. Although there was a slight gravel deficit to start with (3323 metric tons by design versus 3217 metric tons purchased), the highest observed as-built bulk density over all project years of 2.120 metric tons per m^3 meant that the material was packed more tightly in the river, yielding a significantly larger net volumetric deficit of 503 m^3 (Table

3). This gravel deficit affected areas 2, 6, and 8.

4.4 The 2004 Project

The 2004 project completed the two-phase design plan directly below Camanche Dam that sought to facilitate rehabilitation of downstream riffles while at the same time maintaining the high quality habitat the 2003 and 2004 projects were designed to provide. The design volume of 1667 m^3 required an estimated 2743 metric tons, when converted using the quarry value of bulk density (Table 3). This time 3012 metric tons of gravel was supplied, indicating a sufficient supply to achieve the design, even if some compaction occurred. Overall, 68% of the 2004 project area had insignificant deviation from the design of within ± 0.15 m elevation difference. Of the 32% of areas that had significant deviation from the design, 58% of the as-built survey area elevations were >0.15 m overfilled, and 42% were >0.15 m underfilled.

A comparison of the design versus as-built survey results found 11 significant differences deviating from the design (Fig.11). First, at area 1 near the left bank, the most upstream pool was underfilled by 0.3-0.60 m. In the channel center at the uppermost riffle head, area 2 was overfilled by 0.15-0.60 m. At area 3, along river left spanning in the downstream direction, the riffle was overfilled by 0.15-0.90 m, while adjacent at area 4 the riffle at channel center was underfilled between 0.15-0.30 m. At area 5, small areas around a set of placed boulders near the left bank were underfilled by 0.75-0.90 m. Closer to river right at area 6, the transition into the channel chute downstream of the riffle toward channel center was underfilled by 0.6-1.0 m. Just downstream at area 7, the deep area of the pool in mid-channel and near the right bank was underfilled by up to 1.2 m. At area 8 along the left bank, a large portion of the lateral bar was overfilled by up to 1.2 m, with the highest point adjacent to the deepest area of the pool, yielding

a very steep slope/transition. A small localized spot at area 9 near a boulder placed at the downstream end of lateral bar was too low by 0.75 m. At area 10 near the right bank, three small areas of the main downstream riffle were underfilled by 0.15 to 0.75 m. At the bottom of the project reach, area 11, the pool near the left bank was underfilled by 0.5-1.65 m.

During the 2004 project, operator error was responsible for half of the problems encountered during construction (Tables 4, 5). Areas 2, 3, and 8 illustrate the repeated tendency toward overfilling the upstream section of a project area, leaving downstream areas such as 6, 7, and 11 significantly underfilled (Fig.11). This was exacerbated by the preference of this project's operator to only operate in very shallow water. For example, area 3 was used as the pathway to transport gravel to the top section of the project, but after construction that section was not re-graded back down to the design elevation. Areas 5 and 9 illustrate localized DEM deviations due to minor boulder misalignment relative to the design. Submerged wood and riparian shade trees played a role in limiting placement in areas 5, 6, 7, and 10.

In terms of bulk density errors, the as-built density of 1.502 metric tons per m^3 was the closest observed as-built value to the estimated value based on quarry measurements (Table 3). Notably, it was the first time as-built bulk density was observed to be lower than the quarry value. The consequence was that an extra 338 m^3 of fill was achieved, and this was primarily consumed by overfilled areas due to spatial disorientation in area 8.

4.5 The 2005 Project

The 2005 project served to extend the rehabilitated longitudinal profile constructed in the 2003 and 2004 projects further downstream. The design volume was 1950 m^3 (3208 metric tons), and a slight excess of 3384 metric tons of gravel was supplied for construction (Table 3).

Overall, 62% of the 2005 project area had insignificant deviation from the design of within ± 0.15 m elevation difference. Of the 38% of areas that had significant deviation from the design, 58% of the as-built survey area elevations were >0.15 m overfilled, and 42% were >0.15 m underfilled.

The comparison of design versus as-built topography for 2005 yielded 10 areas of significant difference (Fig. 12). For the upper half of the project area there was a consistent pattern of paired underfilled upstream holes followed by downstream overfilled bars. Areas 1 and 2 were localized holes with deficits of 0.75 m and 1.35 m, respectively. In the channel center just downstream of underfilled area 1, the bed was 0.15-0.45 m overfilled at area 3. Area 4 was a long section of the left half of the riffle crest that was underfilled by 0.15-0.30 Area 5 downstream of underfilled area 2 received extra gravel and a few pieces of wood placed *ad hoc* into the bed yielding 0.3- 0.9 m overfill. Downstream of that was section 6, overfilled by 0.15-0.3 m. In the lower half of the project area the channel was generally overfilled except for area 7, a narrow, deep hole along the river-right bank that was left at the original elevation. Area 8 was designed to be the main thalweg. It was overfilled by 0.15-0.60 m, pushing the thalweg further toward the left bank than designed. The area of fill was extended too far downstream past the designed project area, yielding area 9 with the largest volume of overfill for this project year. To the right of this over-extended area was a hole with a deficit of 1.05 m.

The 2005 site's main causes of error were related to gravel placement methods. The operator had substantial aid by a surveyor who periodically checked elevations referencing a grid with corresponding stakes placed at 6.1 m (20') intervals along the bank (Tables 4,5). The same person operated the front loader in 2005 as in 2004, and in both cases there was an excess of gravel available relative to the design specification. Design deviations in areas 2, 3, 4, 5 and 6

were generally small and are attributable to poor elevation estimation by the operator. The ability of the surveyor to guide the operator for improved grading of areas with ~0.3 m of deviation down to within 0.15 m were found to be limited, since the weight of the front loader yielded tire tracks 0.15-0.3 m deep that couldn't be avoided. Design deviations in right-bank areas 1, 5, and 7 were caused by multiple wood obstructions that hindered access, placement, and surveying. The outcome of not being able to place gravel along the right bank was a subtle shifting of the design to river left by the operator, which resulted in overfilling of the thalweg at area 8. Also, the combination of excess gravel for the project, an inability to place it along the right bank, and proximity to the front loader access point along the left bank, led the operator to place an excessive amount of gravel in area 9. Given the depth of water in the pool downstream of the site, it was not possible to shift the gravel placed in area 9 over into area 10. The as-built bulk density of the project was 1.434 metric tons per m^3, which was lower than the estimated quarry value enabling an extra 409 m^3 of fill to be built into the site than expected (Table 3).

5. DISCUSSION

5.1 Supply Uncertainties

The actual supply of gravel delivered for 2001 was deficient by 31%, but thereafter was within a few percent of the specified amount or in significant excess (Table 3). In 2001, the deficit was due to an incorrect assumption as to how much gravel could be salvaged from an old hatchery channel. The solution to such uncertainty as encountered in 2001 was to over-design subsequent projects and then designate low priority sections that could be left unfilled if the largest potential amount of gravel was not delivered. Also, even as design was underway, more

funding for additional gravel than the guaranteed minimum amount was sought after from other funding sources. Flexible designs and aggressive pursuit of more gravel solved the supply deficit problem for the subsequent years. Although not experienced on the Mokelumne, another important supply uncertainty may arise when the time between funding allocation and actual construction is delayed over several years during which time gravel and diesel fuel prices may fluctuate widely, eroding the purchasing-power of the allocated funding.

5.2 Construction operations

Over all project years, the most common construction error was the operator's poor elevation/depth estimation, which accounted for 28% of all errors (Table 5). Operator spatial disorientation, wood hindrances, gravel deficits, and fording limitations had nearly equal occurrences accounting for 13-18 % of errors each (Table 5). Surveying errors, boulder placement deviations, and operator willingness contributed a small amount of error to each project.

A consistent problem encountered was the tendency of the operator to consume a disproportionate amount of gravel in constructing riffle entrances, leaving a deficit for building riffle exits. Part of this problem was due to inadequate staking on the banks adjacent to pools and glides to clearly identify where the first amount of gravel should be dumped. However, this problem persisted even when those locations were clearly marked, because of the fording limitations of the front loader that prevent it from creating the designed riffle entrance and exit slopes. By their nature, front loaders can only build steeply-sloped features because of grading capabilities and fording depth limitations. Gravel will tend to landslide down those slopes over time as a result of the steep slope, eventually yielding an improved gradient. If sufficient

resources are available, the preferred solution to this problem is to use an excavator located on the bank to grade riffle entrance and exit slopes to match designs and eliminate fording limitations. To be practicable when only a front loader will be used, the design must to be simplified and lack gentle slopes. Such a simplified design was used in 2005 and proved highly practicable. The construction outcome would have closely matched the design had not living, overhanging vegetation and dead wood obstructions been present along the right bank. Thus, a key finding is that front loaders cannot safely place gravel around wood pieces associated with pools or beneath low overhanging riparian trees. If the project does not include removal of wood and trees outright, then the project design should work around them and not incorporate those areas into the rehabilitation plans.

Speaking with the 2004-2005 operator on-site during the 2005 project, insight into the operator's methodology for placing gravel in the unfamiliar setting was obtained. The operator stated that it is easier on the front loader and operator to first underfill an area and then add the necessary gravel on top later to achieve grade. In concurrence, his experience indicated that initial overfilling of an area is much more difficult to change, because it involves back-scraping the surface to remove the excess. These statements are supported by the net overfilling in 2004 and 2005 that were not corrected due to operator's unwillingness and front loader's inability to back-scrape to the desired depth.

In evaluating feature-based versus grid-based stake-outs to aid the operator, grid-based stake-outs were found to be more effective. The feature based method provides a smaller number of markers and require the operator to use more judgment in estimating designed gravel placement locations. In this situation operators tend to misalign and accentuate features. Grid-based markers spaced in 20' intervals along the banks substantially aided the operator in locating

placements relative to grading plan maps. It was not possible to place grade markers in the channel itself because they would obstruct the front loader's path, but that would have been even more helpful. Surveyor elevation checks and flow path evaluations helped the operator improve grading, but once the bed was within 0.3 m it was difficult to obtain further improvements due to the weight and footprint of compaction of the front loader. Tire tracks ~0.1-0.2 m deep streaked the length of each project in 2001 and 2002. In 2003-2005 the front loader was run cross-channel at the end of construction to yield transverse tracks instead of longitudinal tracks to see if Chinook would use them as proto redd dunes, but subsequent spawning showed no pattern in relation to the tracks.

5.3 As-built Bulk Density

An important finding of this study is that the as-built bulk density of a large amount of placed gravel in a river can vary significantly, and this needs to be accounted for in the design and construction process or else the as-built volume may not yield the designed channel morphology. Averaging across all projects, the bulk density of the as-built riffles was 1.809 metric tons per m^3, which is within 10.0% of the bucket-test value of 1.645 metric tons per m^3. However, the range of values was 1.434-2.120 metric tons per m^3, corresponding with deviations of 9-29 % from the estimated quarry value. No consistent, definitive trend is evident in the data to explain the source of the deviations quantitatively. The best explanation is that the 2001-2003 sites were constructed using a single access point at the upstream end of each site, whereas the 2004 and 2005 sites were constructed using 2 access points each. Having multiple access points reduces the number of times that the loader drives over the placed material, thereby significantly reducing the amount of compaction. Using multiple access points or placing material with an

excavator instead of a front loader should result in a more predictable as-built bulk density. However, since designs are made on the basis of volume and gravel is purchased on the basis of weight, this represents a major uncertainty in project implementation that requires further investigation.

Ideally, placed gravel would be compacted during construction as is the standard for road construction, but that is not typically done for a subaqueous gravel bed. Merz et al. (2006) monitored through 2003 the fate of gravel placement projects built on the Mokelumne in 1999, 2000, and 2001. At the end of the first year of existence, each site was observed to have a 14-20 % volumetric loss. Subsequent annual losses were a much lower 3-10%. Although some of the losses were attributable to surficial scour, detailed analysis of a variety of mechanisms revealed that the majority of loss was attributable to deflation and compaction (Merz et al., 2006). One approach to addressing this problem is to build projects over multiple years in vertical layers to give the gravel time to self-adjust and to enable adaptive design in response to observed changes. This is the approach being used on the LMR for the 2003 to 2005 projects.

6. CONCLUSION

In this investigation, the construction of detailed river rehabilitation designs was monitored and the sources of design deviations assessed. Overall, the 5 projects assessed showed a 70% spatial adherence to design surfaces. Construction with a front loader reasonably mimicked the design features of more than 0.5 m relief. As evaluated in other studies (Wheaton et al., 2004b; Merz et al., 2006; Pasternack et al., 2006; Elkins et al., in press), the resulting mimicry yielded the desired hydrologic and geomorphic processes in support of enhanced ecological productivity. Of the 30 % of total project area that did not match the design surface,

there were regions of underfilling and overfilling in all years. In the 2001, 2002, and 2003 projects, the areas of significant difference were on average underfilled. In 2004 and 2005, the areas of significant difference were overfilled.

Three major categories of deviations were found - gravel supply deficits, construction errors, and as-built bulk density differences. Gravel supply deficits and as-built bulk density differences were found to be difficult to eliminate because of project management uncertainties. The recommended approach for addressing these problems is to develop spatially sectional designs with an established prioritization and stage gravel placement over multiple years to enable adaptive design and construction. Gravel supply deficits were consistently exacerbated by the operator's tendency to place too much gravel building riffle entrances. This is partly a result of operator spatial disorientation and partly a result of fording depth limitations of front loaders, both of which prevent the operator from accurately constructing the desired riffle entrance slope at the correct location. The recommended solutions for this problem include grid-based staking, frequent elevation checks, use of an excavator for grading riffle entrance and exit slopes, and amending designs to not have depths >0.7 m at the flow released from the dam when the front loader will be in the channel where the front-loader is intended to operate. Finally, it is recommended that thorough evaluation be made of the potential for existing wood and overhanging riparian trees to hinder gravel placement according to the proposed design.

Using a large machine like a front loader to build specific design features based on geomorphic principles in an unfamiliar fluvial setting was found to be reasonably effective when attempting to rehabilitate a gravel-bed river. Despite irreducible uncertainties, limitations, and errors that exist, following the recommendations reported in this study would further improve the as-built adherence to design specifications for future projects. What is left to be considered is

the longevity of the effectiveness of such projects over many years to decades.

7. ACKNOWLEDGEMENTS

Financial support for this work was provided by the US Fish and Wildlife Service (contracting entity for CALFED Bay-Delta Ecosystem Restoration Program: Cooperative Agreement DCN# 113322G003). Construction projects were funded by EBMUD and CVPIA. Dr. Joseph Wheaton (2001-2002) and Eve Elkins (2003-2004) worked in collaboration with co-authors Pasternack and Merz on the SHIRA process to gather topographic data and produce the DEMs used in this investigation. The authors gratefully acknowledge EBMUD and UC Davis staff and students who assisted with topographic surveys. Administrative support was provided by Ellen Mantalica and Diana Cummings at the Center for Watershed Sciences at UC Davis.

REFERENCES

Brookes, A., Shields, F.D., 1996. River Channel Restoration: Guiding Principles for Sustainable Projects. John Wiley & Sons, Chichester, UK.

California Department of Fish and Game, 1955. Memo on available spawning habitat on the Mokelumne River, 11/2/55. Mokelumne file, Rancho Cordova, California.

Downs, P.W., Kondolf, G.M., 2002. As-built appraisals in adaptive management of river channel restoration. Environmental Management, 29 (4): 477–496.

Elkins, E.E., Pasternack, G.B., Merz, J.E., in press. The Use of Slope Creation for Rehabilitating Incised, Regulated, Gravel-Bed River. Water Resources Research.

Federal Energy Regulatory Commission, 1993. Final Environmental Impact Statement, proposed modifications to the Lower Mokelumne River Project, California, FERC Project No. 2916-

004. Federal Energy Regulatory Commission. Washington, DC.

French, J.R., Clifford, N.J., 2000. Hydrodynamic modelling as a basis for explaining estuarine environmental dynamics: some computational and methodological issues. Hydrological Processes 14, 2089-108.

Kondolf, G.M., 2000. Some suggested guidelines for geomorphic aspects of anadromous salmonid habitat restoration proposals. Restoration Ecology 8 (1), 48–56.

MacWilliams, M.L., Wheaton, J.M., Pasternack, G.B., Kitanidis, P.K., Street, R.L., 2006. The Flow Convergence-Routing Hypothesis for Pool-Riffle Maintenance in Alluvial Rivers. Water Resources Research 42, doi:10.1029/2005WR004391.

Merz, J.E., Setka, J.D., 2004. Evaluation of a spawning habitat enhancement site for chinook salmon in a regulated California river. North American Journal of Fisheries Management 24, 397-407.

Merz, J.E., Ochikubo Chan, L.K., 2005. Effects of gravel augmentation on macroinvertebrate assemblages in a regulated California river. River Research and Applications 21, 61-74.

Merz, J.E., Pasternack, G.B., Wheaton, J.M., 2006. Sediment Budget for Salmonid Spawning Habitat Rehabilitation in the Mokelumne River. Geomorphology 76 (1-2), 207-228.

Merz, J.E., Setka, J., Pasternack, G.B., Wheaton, J.M., 2004. Predicting benefits of spawning habitat rehabilitation to salmonid fry production in a regulated California river. Canadian Journal of Fisheries and Aquatic Science 61, 1433-1446.

Merz, J. E., Workman, M. L., Saldate, M. S. 2004. Lower Mokelumne river fish community survey (1/1/97-8/3/04). East Bay Municipal Utility District, Lodi, CA.

Pasternack, G.B., Wang, C.L., Merz, J., 2004. Application of a 2D hydrodynamic model to reach-scale spawning gravel replenishment on the lower Mokelumne River, California. River

Research and Applications 20, 2:205-225.

Pasternack, G.B., Gilbert, A.T., Wheaton, J.M., Buckland, E.M. 2006. Error Propagation for Velocity and Shear Stress Prediction Using 2D Models For Environmental Management. Journal of Hydrology 328, 227-241.

Wheaton, J.M., Pasternack, G.B., Merz, J.E., 2004a. Spawning Habitat Rehabilitation- 1. Conceptual Approach & Methods. International Journal of River Basin Management 2(1), 3-20.

Wheaton, J.M., Pasternack, G.B., Merz, J.E., 2004b. Spawning Habitat Rehabilitation- 2. Using hypothesis development and testing in design, Mokelumne River, California, U.S.A. International Journal of River Basin Management 2 (1), 21-37.

Wheaton, J.M., Pasternack, G.B. Merz, J.E., 2004c. Use of habitat heterogeneity in salmonid spawning habitat rehabilitation design. In: IAHR-AIRH, Proceedings of the Fifth International Symposium on Ecohydraulics, Volume 1. Aquatic habitats: analysis and Restoration, Madrid, Spain, p. 791-796.

Wohl, E., Angermeier, P.L., Bledsoe, B. Kondolf, G.M., MacDonnell, L., Merritt, D.M., Palmer, M.A., Poff, N.L., Tarboton, D., 2005. River restoration. Water Resources Research 41, W10301, doi:10.1029/2005WR003985.

Workman, M.L. 2003. Lower Mokelumne River upstream fish migration monitoring conducted at Woodbridge irrigation District Dam (08/02-07/03). East Bay Municipal Utility District, Lodi, CA.

Table 1. Tractor Specifications for LMR Project Sites by Year

Year	Tractor Model	Weight (kg)	Height to Center of Hub (m)	Tires	Footprint**
2001	Volvo 120E	20043	0.69	23.5R25	61.7 (8.95)
2002	Caterpillar 966G*	23752	0.86	26.5R25	61.2 (8.87)
2003	Caterpillar 966F*	23752	0.86	26.5R25	61.2 (8.87)
2004	Caterpillar 966F*	23752	0.86	26.5R25	61.2 (8.87)
2005	Caterpillar 950F*	18380	0.74	23.5-25-20PR	55.5 (8.05)
Reference	Komatsu WA400-5	18682	0.71	23.5-25-16PR	58.4 (8.47)

*Actual models used; specifications taken from newer 966H and 950H models.
**units of kPa (psi).

Table 2. Average Areas of Overfill, Underfill and Insignificant Variation

Year	Percent of total area within ±0.15 m difference	Percent of total area of >±0.15 m difference	Percent of Area Overfilled*	Percent of Area Underfilled*
2001	81	19	17	83
2002	79	21	43	57
2003	64	36	31	69
2004	68	32	58	42
2005	62	38	58	42
Average	71	29	41	59

*Relative to area of >±0.15 m difference.

Table 3. Design, purchased, and as-built gravel metrics for each project year

Metric	2001	2002	2003	2004	2005
Design Volume (m3)	1147	1448	2020	1667	1950
Required Supply (tons)	1887	2382	3323	2743	3208
Purchased Supply (tons)	1307	2786	3217	3012	3384
Supply deviation (%)	-31	17	-3	10	5
Estimated Density (tons/m3)	1.645	1.645	1.645	1.645	1.645
Purchased Volume (m3)	794	1694	1955	1831	2057
As-built Volume (m3)	649	1410	1517	2005	2359
As-built Density (tons/m3)	2.013	1.976	2.120	1.502	1.434
Density deviation (%)	22	20	29	-9	-13

Table 4. Potential sources for deviation in construction of a project design.

	Area ID for each location of deviation from design				
Causes of Error	2001	2002	2003	2004	2005
Gravel deficit	1,4,5,6	8,10,11	2,6,8		
Fording depth limitations		1,4,8,9	2,8	6,7	10
Operator's skill/experience/willingness			2,8		
Operator's spatial disorientation	2,3	1,5	1,2,6,5	1,8,11	8,9
Operator's poor elevation estimation	4,5	2,3,4,6,7	1,3,4,5	2,3,4,8	2,3,4,5,6
Intruding vegetation hindering access		8	2,7,8	5,6,7,10	1,7
Gravel bulk density error					
Surveying errors/boulder placement		9		5,9	1,5,7

Table 5. Distribution of causes of design deviations by percentage for each year.

Causes of Error	2001	2002	2003	2004	2005	All Years
Gravel deficit	50	19	17	0	0	14
Fording depth limitations	0	25	11	13	7	13
Operator's skill/experience/willingness	0	0	11	0	0	3
Operator's spatial disorientation	25	13	22	20	14	18
Operator's poor elevation estimation	25	31	22	27	36	28
Intruding vegetation hindering access	0	6	17	27	21	15
Gravel bulk density error	0	0	0	0	0	0
Surveying errors/boulder placement	0	6	0	13	21	8

FIG. CAPTIONS

Figure 1. Map of the Mokelumne River basin showing locations of Camanche and Pardee Reservoirs. The project sites were located in the gravel-bed reach downstream of Camanche Dam.

Figure 2. Regional map showing the locations of each project site by year.

Figure 3. Contour maps with 0.5 m intervals of the 2001 design (top) and as-built (bottom) topographies for comparison of desired designed elevations to constructed elevations.

Figure 4. Contour maps with 0.5 m intervals of the 2002 design (top) and as-built (bottom) topographies for comparison of desired designed elevations to constructed elevations.

Figure 5. Contour maps with 0.5 m intervals of the 2003 design (top) and as-built (bottom) topographies for comparison of desired designed elevations to constructed elevations.

Figure 6. Contour maps with 0.5 m intervals of the 2004 design (top) and as-built (bottom) topographies for comparison of desired designed elevations to constructed elevations.

Figure 7. Contour maps with 0.5 m intervals of the 2005 design (top) and as-built (bottom) topographies for comparison of desired designed elevations to constructed elevations.

Figure 8. Contour map with 0.15 m intervals of magnitude of elevation change between post and design for the 2001 project.

Figure 9. Contour map with 0.15 m intervals of magnitude of elevation change between post and design for the 2002 project.

Figure 10. Contour map with 0.15 m intervals of magnitude of elevation change between post and design for the 2003 project.

Figure 11. Contour map with 0.15 m intervals of magnitude of elevation change between post and design for the 2004 project.

Figure 12. Contour map with 0.15 m intervals of magnitude of elevation change between post and design for the 2005 project.

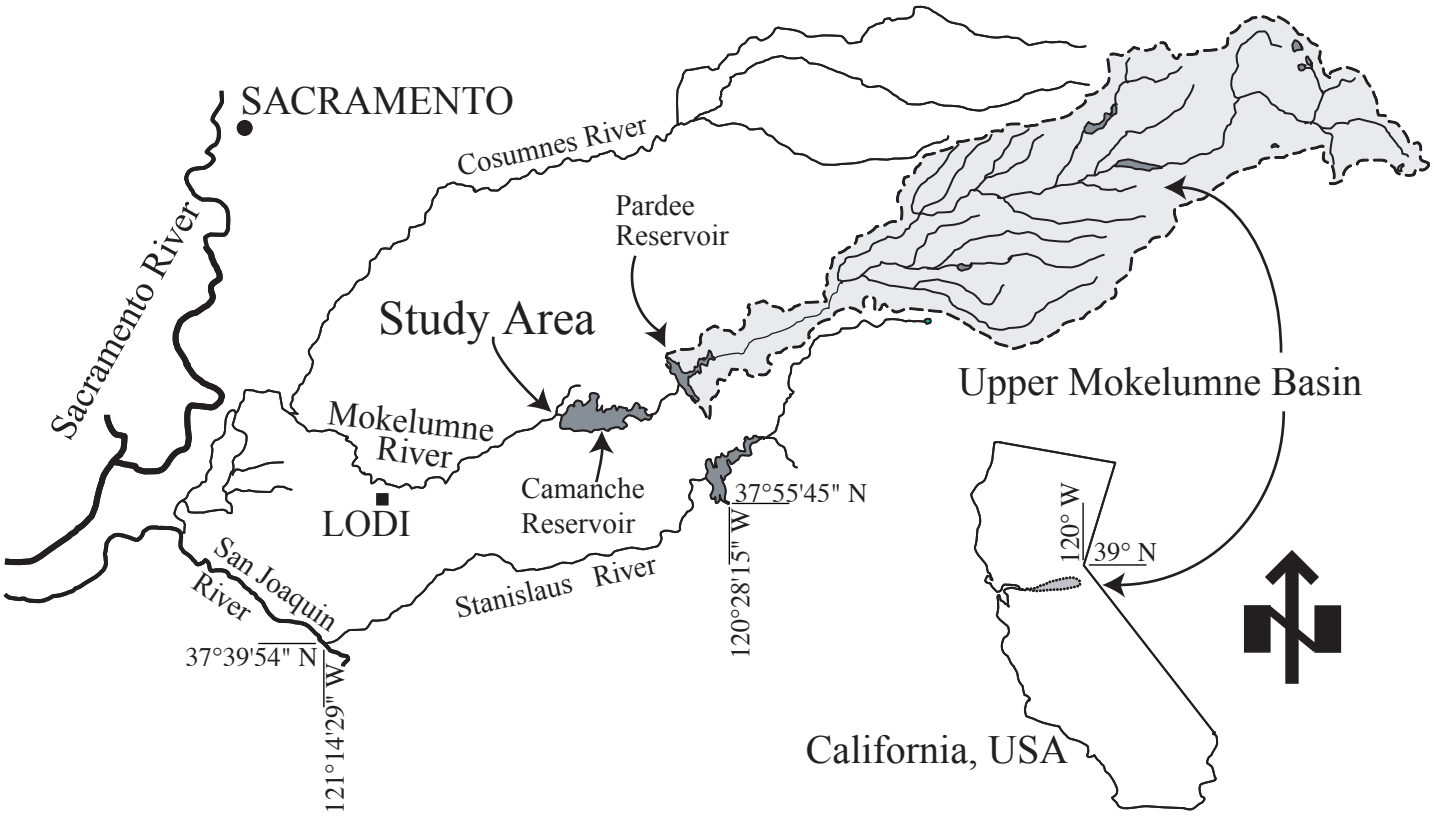
SACRAMENTO
Cosumnes River
Sacramento River
Pardee
Reservoir
Study Area
Upper Mokelumne Basin
Mokelumne
River
Camanche
Reservoir
37°55'45" N
LODI
San Joaquin
River
Stanislaus River
37°39'54" N
121°14'29" W
120°28'15" W
120° W
39° N
California, USA

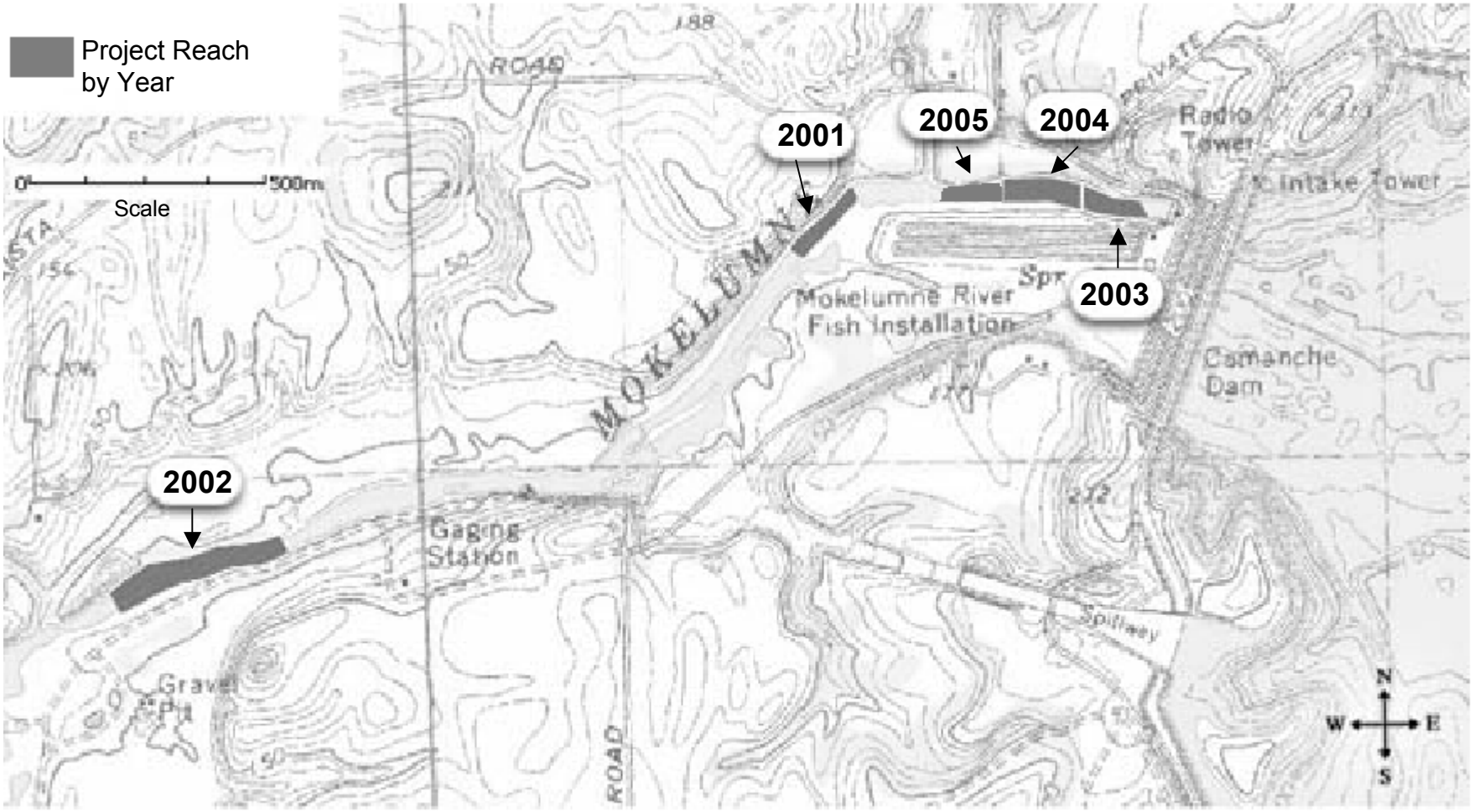
Project Reach by Year
2001
2002
2003
2004
2005
0
500m
Scale
ROAD
Mokelumne River Fish Installation
Gaging Station
Gravel Pit
Radio Tower
Intake Tower
Camanche Dam
Spillway
PRIVATE
ROAD
N
W
E
S

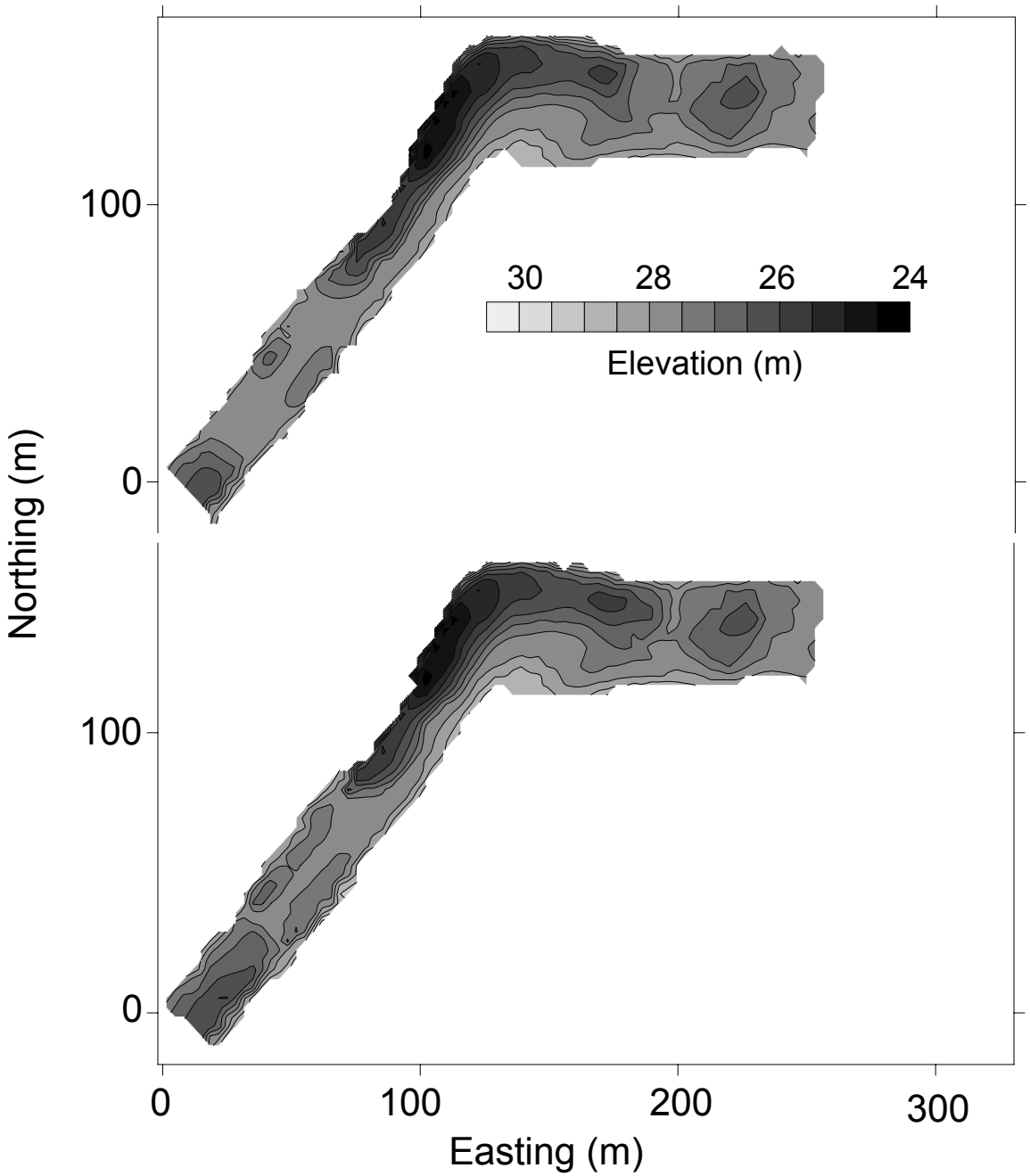
30
28
26
24
Elevation (m)
100
0
100
0
Northing (m)
0
100
200
300
Easting (m)

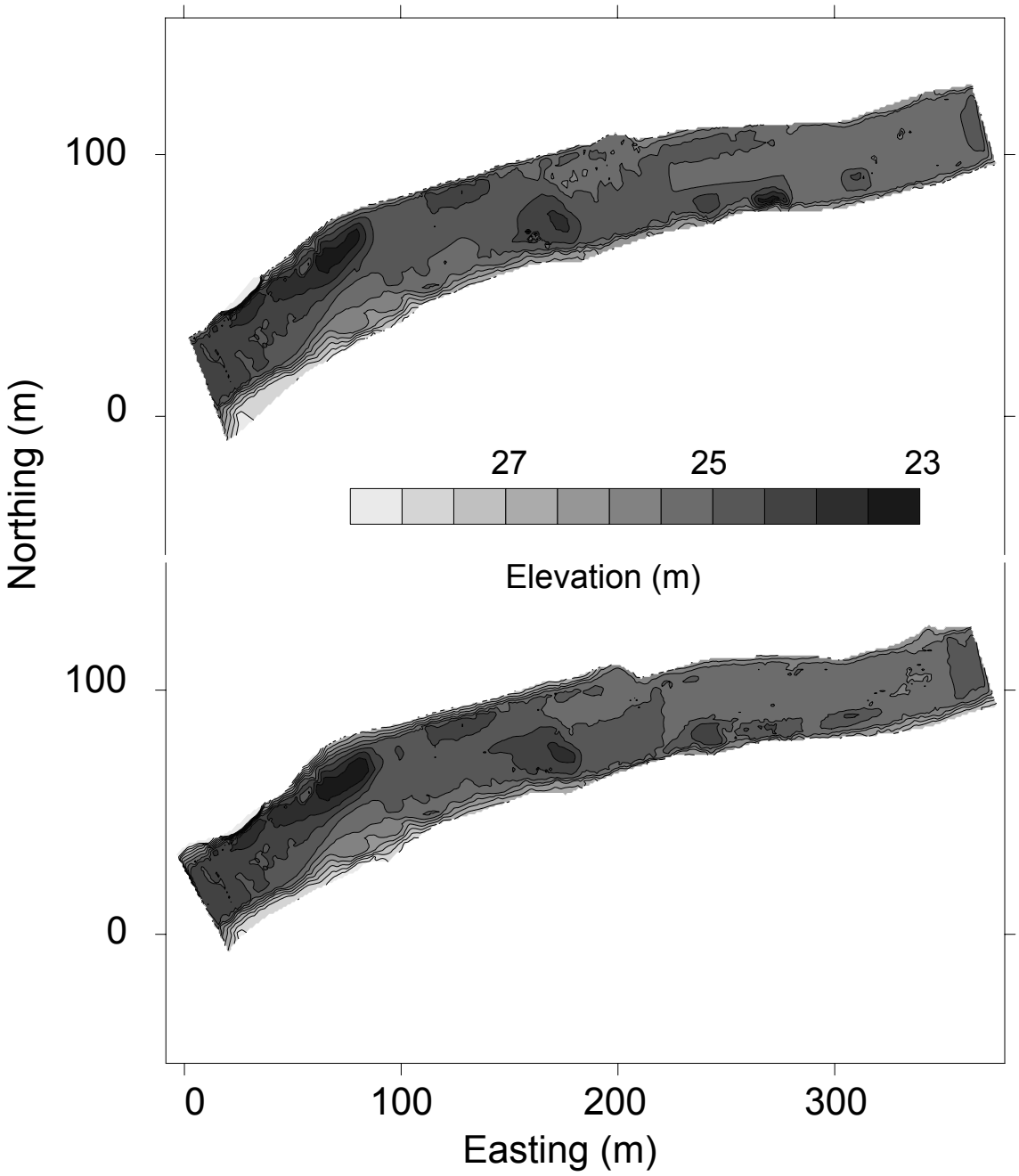
100
0
Northing (m)
27
25
23
Elevation (m)
100
0
0
100
200
300
Easting (m)

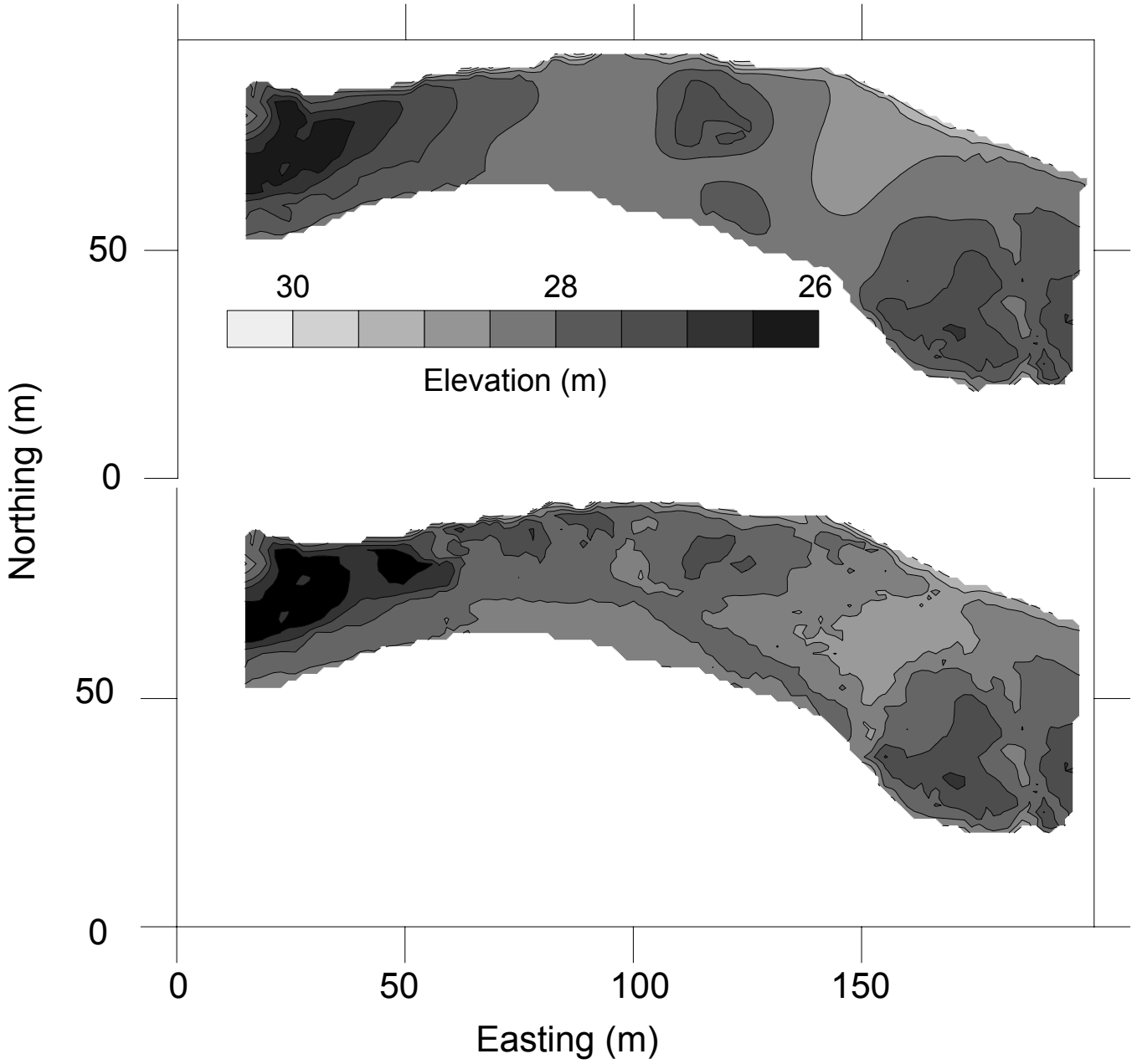
30
28
26
Elevation (m)
50
0
50
0
Northing (m)
0
50
100
150
Easting (m)

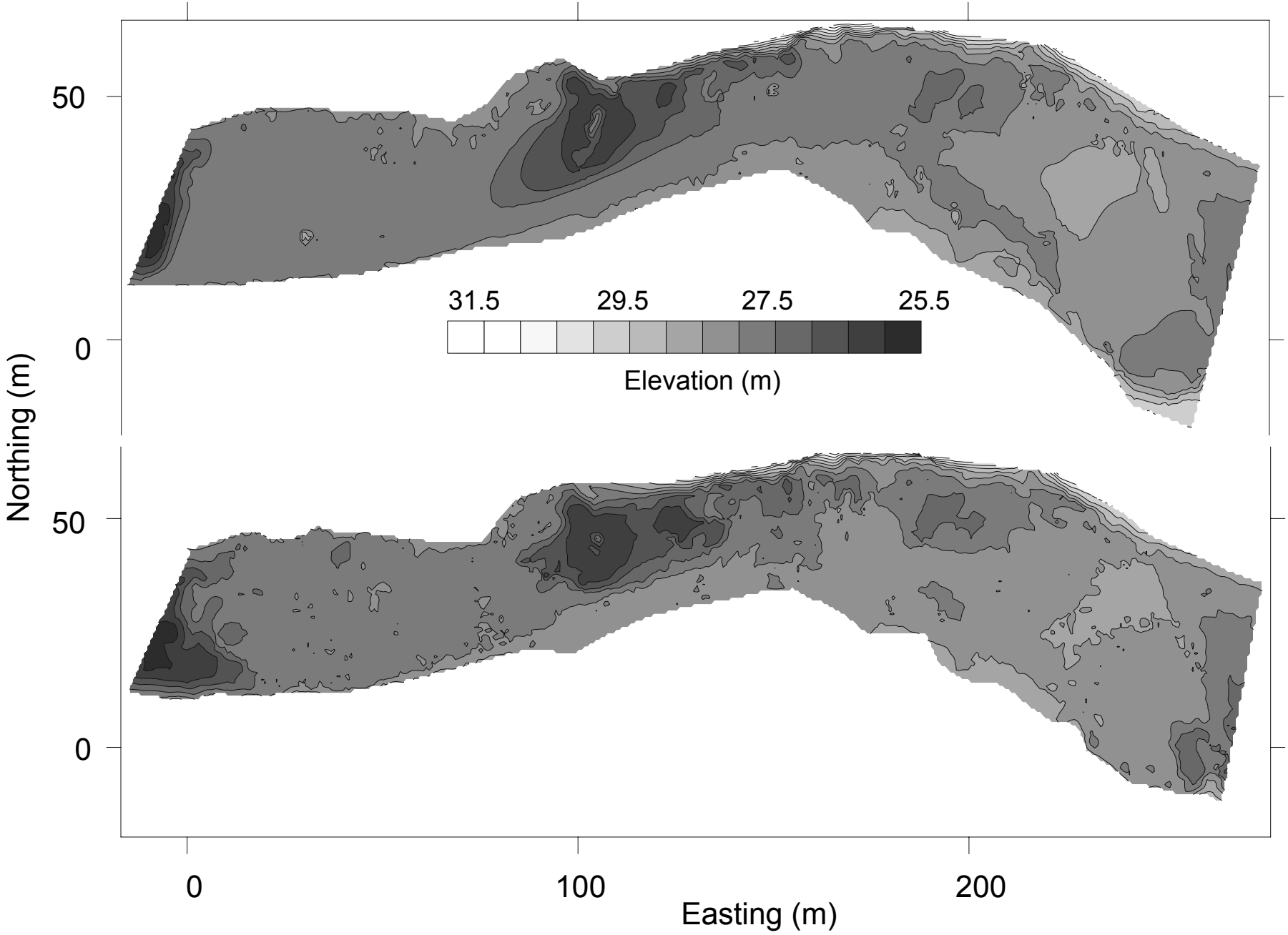
31.5
29.5
27.5
25.5
Elevation (m)
50
0
50
0
Northing (m)
0
100
200
Easting (m)

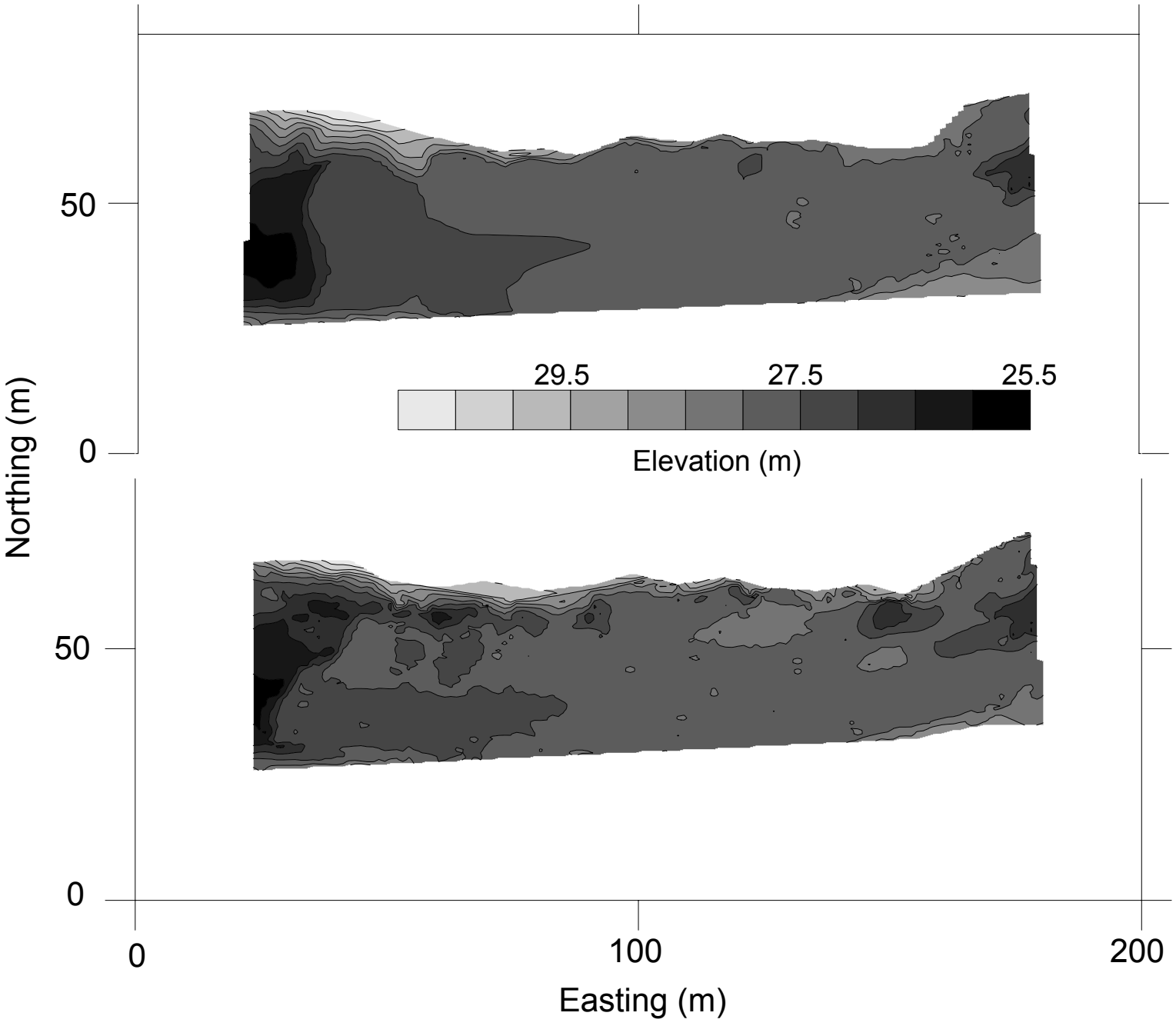
29.5
27.5
25.5
Elevation (m)
50
0
50
0
Northing (m)
0
100
200
Easting (m)

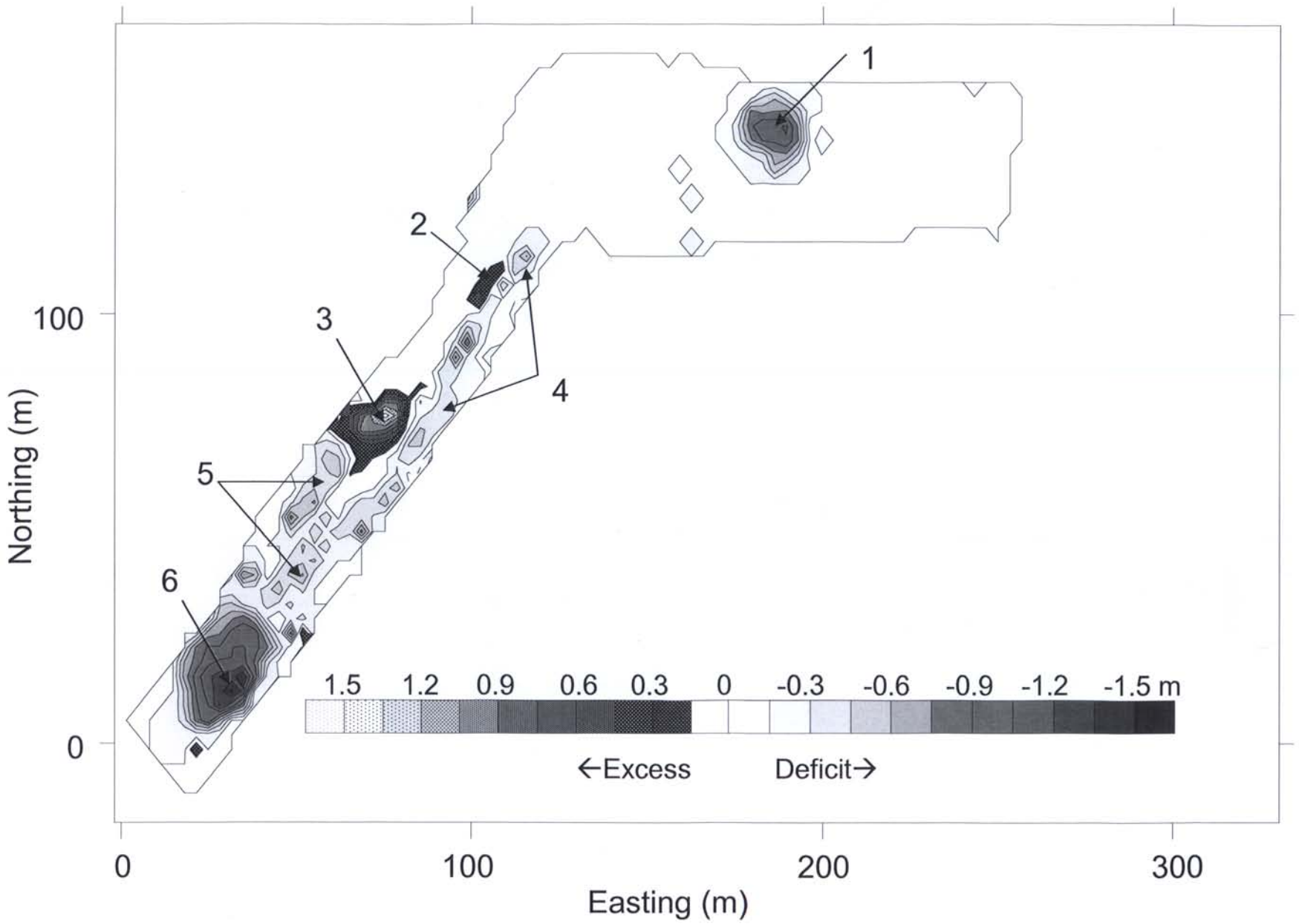
1
2
3
4
5
6
100
0
Northing (m)
1.5 1.2 0.9 0.6 0.3 0 -0.3 -0.6 -0.9 -1.2 -1.5 m
←Excess
Deficit→
0
100
200
300
Easting (m)

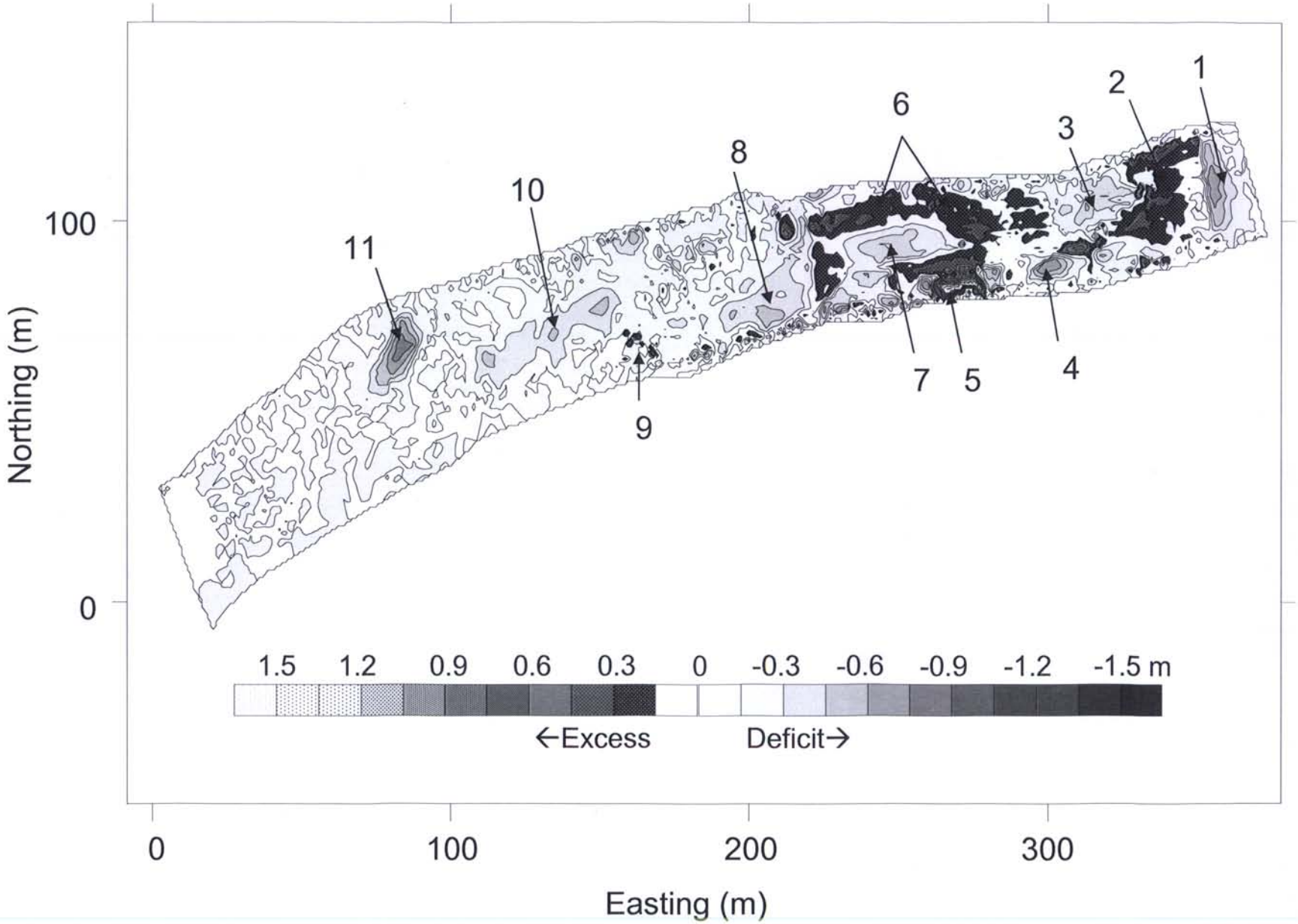
1
2
3
6
8
10
11
9
7
5
4
100
0
Northing (m)
1.5
1.2
0.9
0.6
0.3
0
-0.3
-0.6
-0.9
-1.2
-1.5 m
←Excess
Deficit→
0
100
200
300
Easting (m)

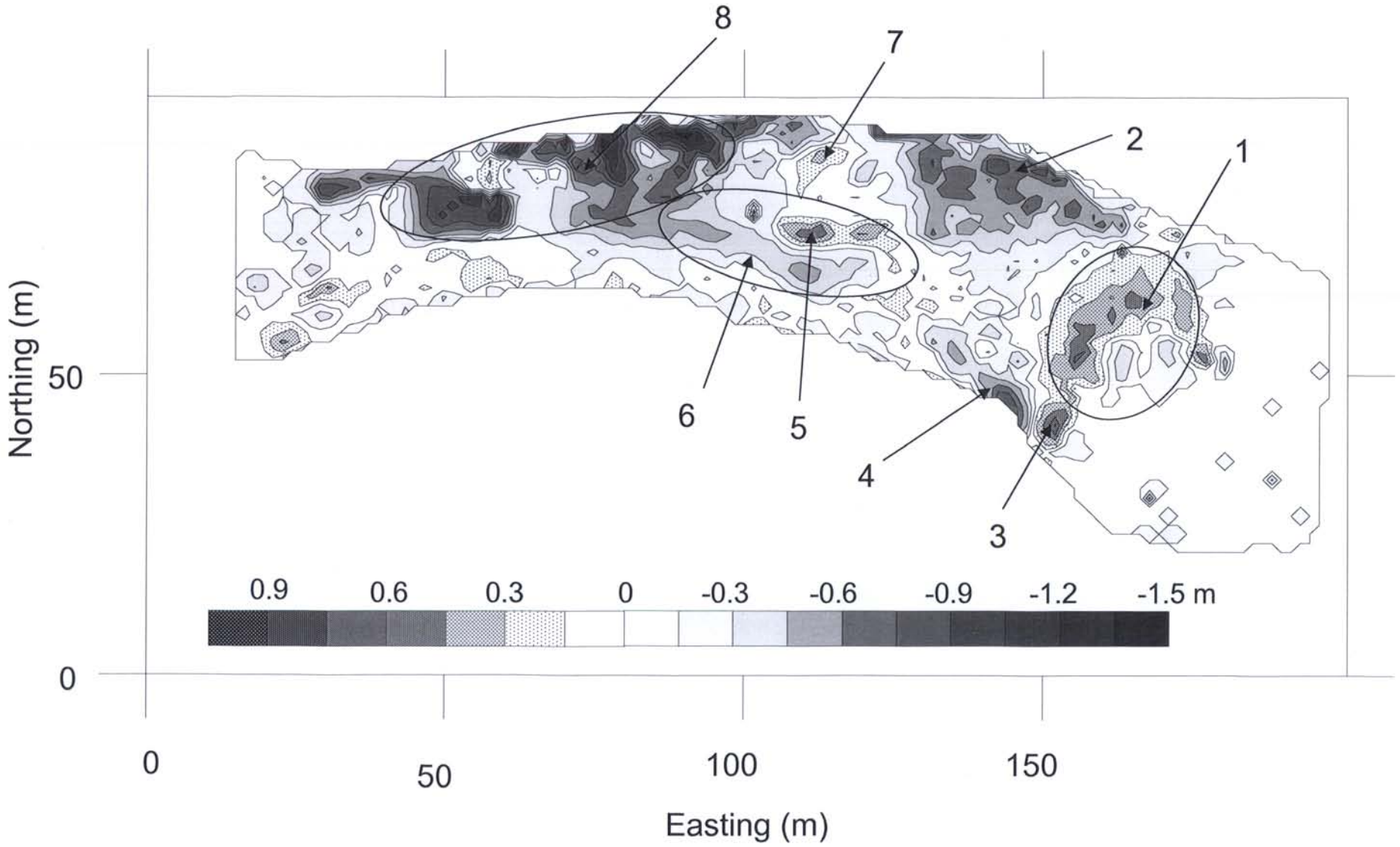
8
7
2
1
6
5
4
3
0.9
0.6
0.3
0
-0.3
-0.6
-0.9
-1.2
-1.5 m
Northing (m)
0
50
0
50
100
150
Easting (m)

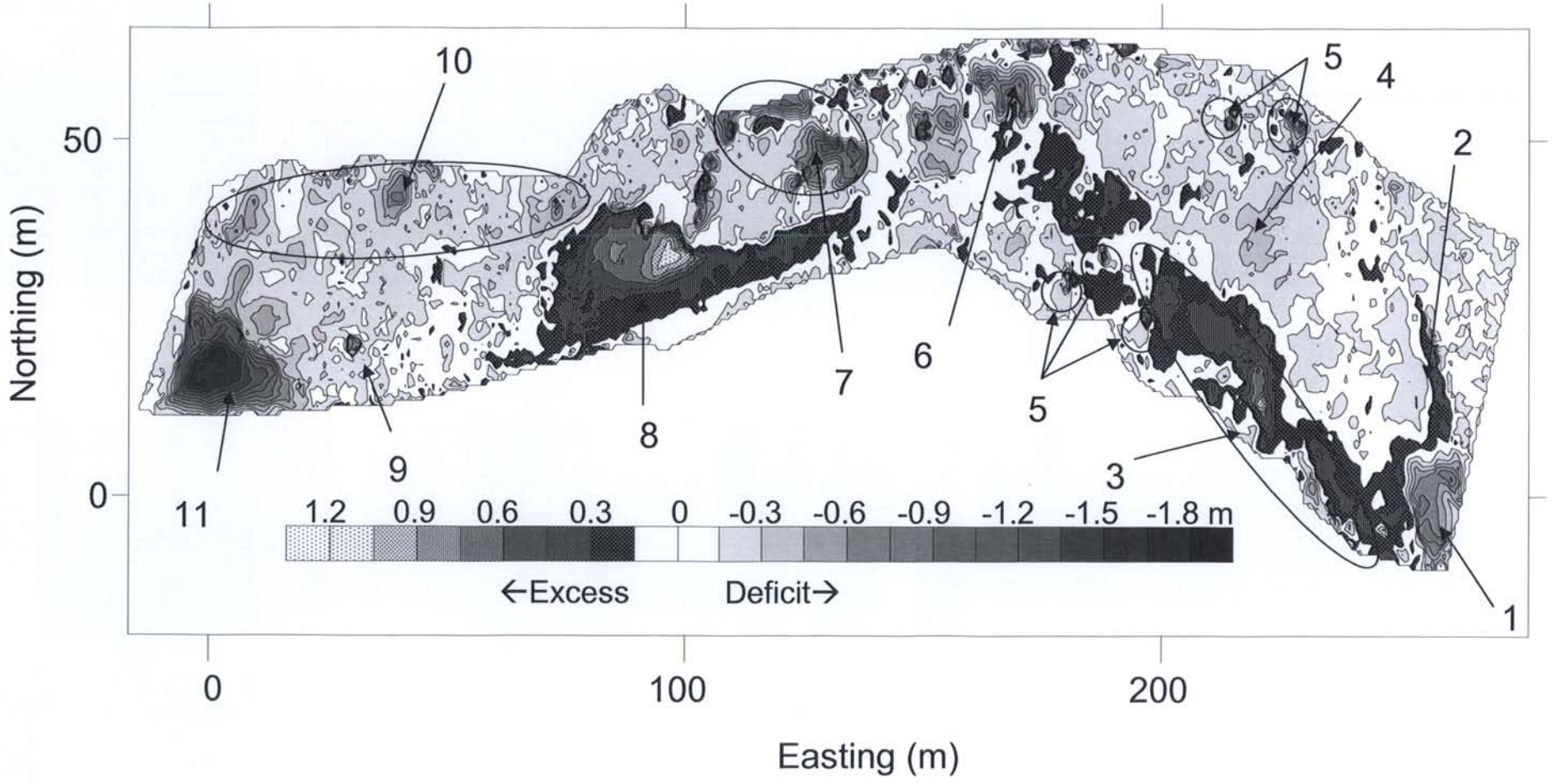
Northing (m)
50
0
0
100
200
Easting (m)
10
5
4
2
6
7
5
8
9
3
11
1
1.2 0.9 0.6 0.3 0 -0.3 -0.6 -0.9 -1.2 -1.5 -1.8 m
←Excess
Deficit→

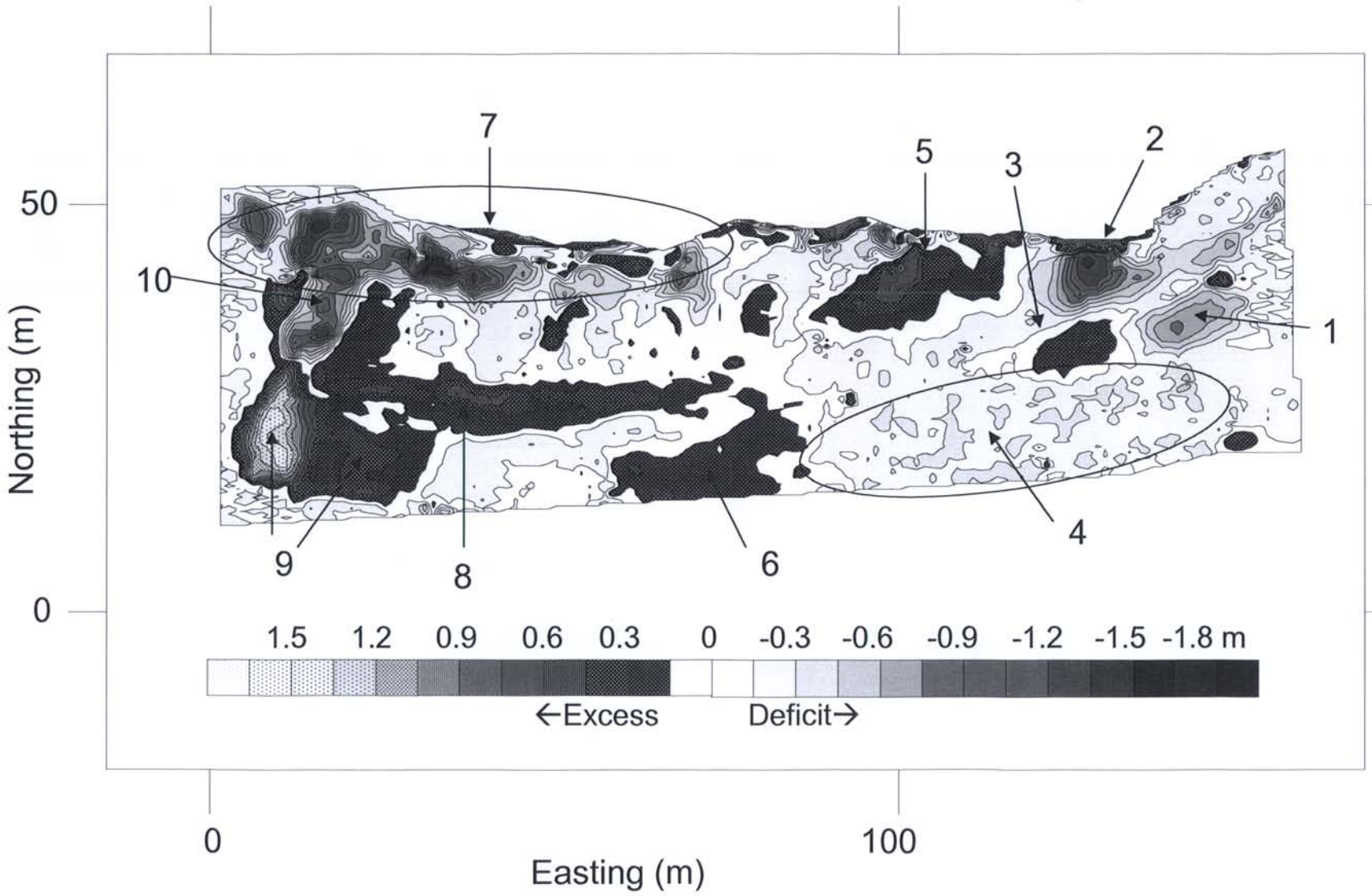
7
5
3
2
50
10
1
Northing (m)
9
8
6
4
0
1.5 1.2 0.9 0.6 0.3 0 -0.3 -0.6 -0.9 -1.2 -1.5 -1.8 m
←Excess
Deficit→
0
100
Easting (m)

Available online at www.sciencedirect.com
SCIENCE DIRECT
Geomorphology 76 (2006) 207–228
GEOMORPHOLOGY
www.elsevier.com/locate/geomorph

Sediment budget for salmonid spawning habitat rehabilitation in a regulated river

Joseph E. Merz [a,b,*], Gregory B. Pasternack [c], Joseph M. Wheaton [c,1]

[a] Department of Wildlife, Fish and Conservation Biology, University of California at Davis, One Shields Avenue, Davis, CA 95616, USA
[b] East Bay Municipal Utility District, Fisheries and Wildlife, 1 Winemasters Way Suite K2, Lodi, CA 95240, USA
[c] Department of Land, Air, and Water Resources, University of California at Davis, One Shields Avenue, Davis, CA 95616, USA

Received 15 July 2005; received in revised form 10 November 2005; accepted 14 November 2005
Available online 18 January 2006

Abstract

Bed elevation, feature adjustments, and spawning use were monitored at three Chinook salmon (*Oncorhynchus tschawytscha*) spawning habitat rehabilitation sites to measure project longevity in a regulated river. Sites enhanced with 649–1323 m^3 of gravel lost from 3–20% of remaining gravel volume annually during controlled flows of 8–70 m^3/s and 2.6–4.6% of placed material during a short-duration (19 days) release of 57 m^3/s. The oldest site lost ~50% of enhancement volume over 4 years. Of the mechanisms monitored, gravel deflation was the greatest contributor to volumetric reductions, followed by hydraulic scour. Spawning, local scour around placed features, and oversteepened slopes contributed to volumetric changes. As sites matured, volumetric reductions decreased. Sites captured as much large woody debris as was lost. While complexity is an extremely important aspect of ecological function, artificial production of highly diverse and complex habitat features may lead to limited longevity without natural rejuvenation.

Keywords: Salmonid; Spawning habitat; Rehabilitation; Restoration; Morphometric budgets; Digital elevation model differencing

1. Introduction

A sediment budget quantifies sediment fluxes and storage in a designated area over a specific time period. Budgets can be performed for whole basins (Dietrich et al., 1982; Reid and Dunne, 1996) or individual channel reaches (Fuller et al., 2003). The morphometric sediment budget approach quantifies erosion and deposition volumetrically by differencing observed topographic changes (Brasington et al., 2003; Lane and Chandler, 2003). Morphometric sediment budgets largely reflect changes from bedload transport (Fuller et al., 2003). In regulated rivers, bedload is rarely transported past large dams, hence virtually eliminating the (volumetric) input term of the sediment budget from upstream (Vaithiyanathan et al., 1992). In these areas, sediment-starved flow may erode the channel bed and banks, producing channel incision, bed material coarsening, and gravel loss (Waldichuk, 1993; Gilvear and Bradley, 1997; Kondolf, 1997; Shields et al., 2000). Such changes typically result in habitat modifications for numerous aquatic organisms, including anadromous salmonids (Osmundson et al., 2002).

* Corresponding author. East Bay Municipal Utility District, Fisheries and Wildlife, 1 Winemasters Way Suite K2, Lodi, CA 95240, USA.
E-mail address: jmerz@ebmud.com (J.E. Merz).
[1] Current address: Institute of Geography and Earth Sciences, The University of Wales, Aberystwyth, Llandinam Building, Penglais Campus, Ceredigion SY23 3DB, Wales, UK.

0169-555X/$ - see front matter © 2005 Elsevier B.V. All rights reserved.
doi:10.1016/j.geomorph.2005.11.004

Sediment budgets provide a record of relative channel stability and thus a means of assessing physical habitat change. For instance, because of declining salmonid populations (Yoshiyama et al., 1998), coarse sediment and physical structures [such as large woody debris (LWD), boulder complexes, and groins] are being added to streams to augment deficiencies, create meandering channels, and enhance spawning riffles (Scheeler, 1990; Chapman, 1995). Reviews of such spawning habitat rehabilitation (SHR) projects are detailed elsewhere (e.g., Kondolf, 2000; Wheaton et al., 2004c). While SHR projects appear to attract spawning fish and may increase embryo survival and fry production (Merz and Setka, 2004; Merz et al., 2004), numerous failures have also been documented (Frissell and Nawa, 1992; Avery, 1996). Expectations of stability are one of the greatest inadequacies associated with SHR (Wheaton et al., 2004c). Even with low flows, without further sediment input, natural and placed gravels eventually scour (Paintal, 1971). While the placement of structures (such as boulders and woody debris) is designed to improve habitat for fish, it can also accelerate scour locally (Kuhnle et al., 2002). For placed gravel, scour has been viewed as a failure (Kondolf et al., 1996); whereas the failure may not be scour itself, but rather the expectation that it should stay there. A site-scale sediment budget to estimate residence times of placed gravels and requirements for habitat maintenance might produce more reasonable expectations.

In this study, sediment budgets were used to track the fate of gravel, boulders, and LWD placed according to complex SHR designs and to identify mechanisms controlling project longevity. Site-scale (i.e. $\sim 10^1$ channel widths) sediment budgets were calculated for three spawning bed enhancement projects in a low-slope regulated river impacted by in-stream mining. Sediment input (from construction), change in storage, and gravel loss were measured volumetrically at each site and compared with process-based analyses of compaction, slope failure, and entrainment potential to assess specific mechanisms of morphological change after gravel placement. This study is significant for its insight into the relative roles of mechanisms for gravel-bed change under low flow, low-slope conditions, with lessons for future gravel placement design and monitoring strategies.

1.1. Site-scale sediment budget

A volumetric sediment budget for an SHR project on a regulated river at the typical site-scale of $\sim 10^1$ to 10^2 channel widths should account for all gravel sources and losses associated with project implementation and subsequent changes (Fig. 1). Because SHR projects involve gravel placement in a generally gravel-deficient setting, we emphasize the volumetric loss components.

1.1.1. Sources for gravel placement

Gravel for SHR is typically purchased from floodplain quarries or in-channel mining sources (Kondolf, 2000). In California, the cost for each metric ton of concrete-grade aggregate ranges from USD 7–20 at the mine, plus USD 0.06–0.10 km^{-1} for site transportation. On the Mokelumne River, cost for in-basin river gravel (including triple-washing and transport) was USD 22.90 m^{-3} total. The cost for gravel placement equipment and labor was an additional USD 0.47 m^{-3}. As gravel is sold by weight, some volumetric change may be due to overestimates in mass to volume conversions.

1.1.2. Fluvial sediment recruitment

Fluvial sediment recruitment refers to the local sediment supply via fluvial erosion of upstream sources. Localized bank sloughing, tributaries, and upstream augmentation are potential sediment sources. Hydraulic structures are often intended to encourage gravel deposition (FISRWG, 1998). Depending on trap efficiency, reservoirs may pass sand at a reduced rate (Brune, 1953), detrimentally affecting developing salmonid embryos within the substrate (Kondolf, 1997). However, sand does not comprise a significant volumetric component of the sediment budget for a placement project.

1.1.3. Gravel losses before placement: operational losses

Depending on how gravel is imported to a site, staged at the site, and positioned in the stream, some material is lost prior to placement (Fig. 1). The larger the site and number of staging areas used, the greater the gravel loss from floodplain and channel bank imbedding. Overhandling during construction can cause gravel breakage and spawnable-material loss. Misconfiguration and loss from spillage during transport and placement may further decrease final volume. Unforeseen problems, such as loose banks or pools too deep to operate equipment, may require operators to use a gravel portion to create access.

1.1.4. Gravel losses after placement: fluvial erosion

The volume of the final configuration can be deflated by several mechanisms. Hydraulic drag and lift forces are foremost in conventional thinking (Paintal, 1971). Particle entrainment is generally assumed to be estimated by shear stress (Nelson et al., 2000). Lacking direct

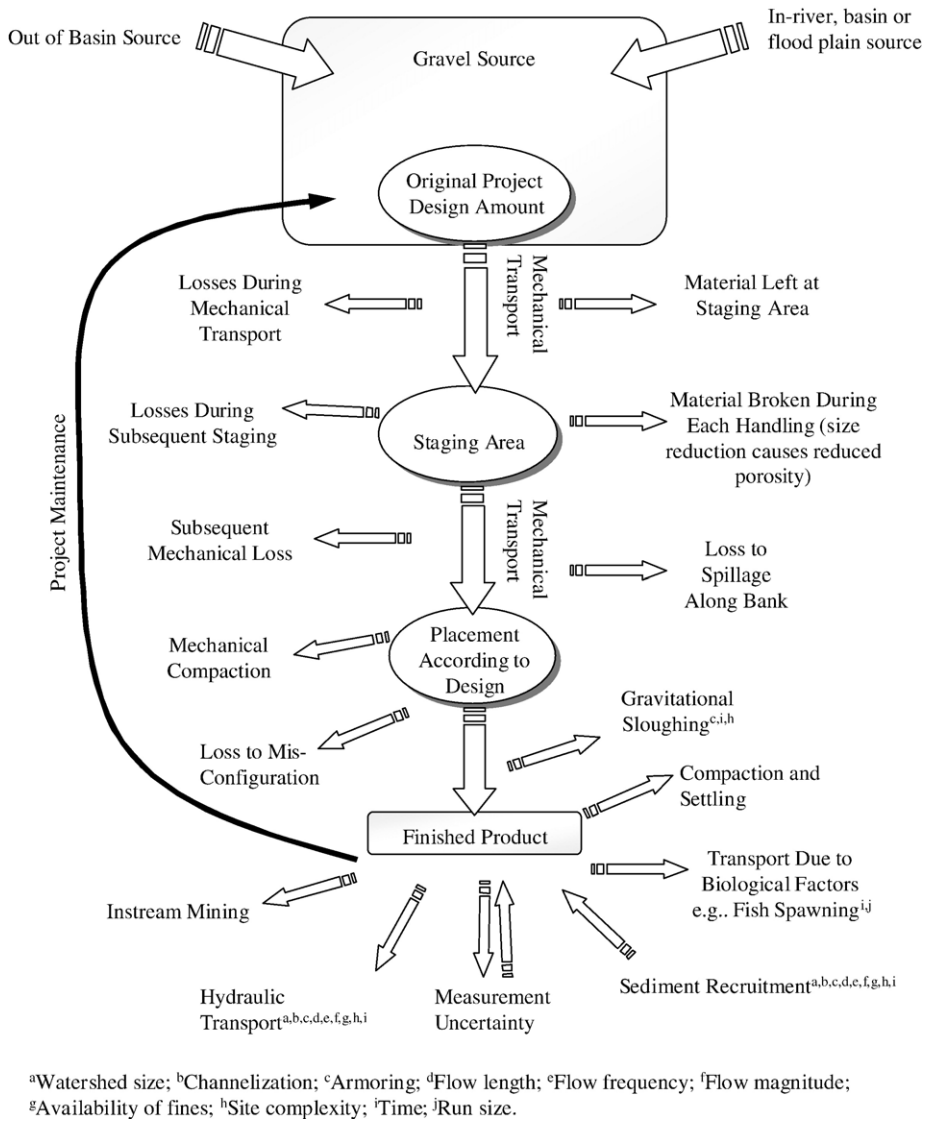

[a]Watershed size; [b]Channelization; [c]Armoring; [d]Flow length; [e]Flow frequency; [f]Flow magnitude; [g]Availability of fines; [h]Site complexity; [i]Time; [j]Run size.

Fig. 1. Factors influencing volumetric sediment budgets for salmonid spawning gravel enhancement. Arrows indicate direction and relative amount of gravel. Major effects on each mechanism for sediment loss[a–j].

measurements, shear stress is widely estimated based on flow field knowledge (Wilcock, 1996; Biron, 2004). Critical shear stress for sediment entrainment with particle diameter d_i can be estimated using the Shields (1936) equation:

$$\tau_c = \tau_c^*(\gamma_s - \gamma_f)d_i \quad (1)$$

where τ_c is critical shear stress (N/m^2), τ_c^* is dimensionless critical shear stress, γ_s is specific sediment weight (assumed to be 25 990 N/m^3), γ_f is specific water weight (9807 N/m^3), and d_i is the sediment size (m) of interest. Because placed gravel is well-mixed, an initially high relative exposure of smaller particles is likely, yielding a risk of partial transport of the finer fraction leaving behind the coarser fraction (Wilcock, 1997).

To estimate whether an individual grain is mobilized by flow, critical shear stress may be compared to shear stress induced by the flow (e.g., Pasternack et al., 2004). An individual grain's entrainment depends on its relative projection above the mean bed, its exposure relative to upstream grains, its shape, and its friction angle (Kirchner et al., 1990). Placed boulders, LWD, and man-made structures (such as deflector weirs) create local convective accelerations and secondary currents in the form of vortices that intermittently raise near-bed velocities, potentially increasing local scour (Smith and Beschta, 1994).

1.1.5. Gravel losses after placement: settling and compaction

In consideration of volumetric losses of placed gravels, erosion is not the only potential mechanism. Hole (1961) defined nine categories of pedoturbation, with faunal pedoturbation, gravipedoturbation (mixing by noncatastrophic mass-wasting), and seismipedoturbation (mixing by vibrations) applicable to aquatic volumetric changes. Fish, people, and wildlife can briefly increase local drag and lift, inducing local scour. Over time, this might add up to significant change where flow regulation precludes floods.

Unconsolidated materials that exhibit steep surface slopes are inherently unstable. Placed gravels will adjust oversteepend slopes through small, localized slope failures and in situ settling to achieve more stable configurations. These processes can be magnified when gravel piles are placed at steep angles (Buffington et al., 1992). Gravitational force and friction are in balance at the angle of repose, 23° for dry glass beads (Barabási et al., 1999). However, water lubricates grain motion, reducing intergranular friction and hence friction angles (Ingles and Grant, 1975). In practice, gravel injection along riverbanks yields steep-sided piles, that often mobilize easily. For in-stream placement, avoiding steep slopes may be limited by bathymetry and placement method—a front loader cannot construct a gentle riffle entrance or exit where the depth could flood it.

Deposit volume may change through time from natural settling and repacking enhanced by gravel vibration. Placed gravel may compact and subside preexisting substrate. Gravel can also spread laterally into the underlying alluvium. As gravel fill depths increase, so too does deposit mass and therefore its confining pressure. Similarly, the more equipment drives over the deposit, the more compaction. Finally, turbulent flow fluctuations exert forces causing settling and compaction. During low flows, a riffle is subjected to chaotic, turbulent flows that cause in situ particle vibration and sporadic particle motion (Sear, 1996).

Estimates of spherical packing density have been well discussed in the literature (Gauss, 1831; Rogers, 1958; Goldberg, 1971; Steinhaus, 1999). While the densest packing for uniform spheres is 77.836% of total volume (Muder, 1993), one must take into account shape/size variability and additional complications associated with natural stream sediments (Ingles and Grant, 1975). Measuring sediment packing directly over time as part of a sediment budget would help in understanding its contribution to the volumetric budget. Particle packing can significantly affect bulk density and natural particle assemblages are seldom unisized. Packing becomes denser with wider particle-size distribution, especially if the deposit becomes compacted. Packing can be described by calculating material bulk density or porosity. Bulk density (P_b) is calculated as

$$P_b = M_b / V_b \quad (2)$$

where M_b is bulk material weight and V_b is bulk volume (Bunte and Abt, 2001). Milhous (2001) observed bulk densities of 1.70–2.60 (g/cm^3) and porosities of 0.02–0.36 in several gravel-bed rivers. While it has not received significant study, grain-packing configuration and gravel-bar compaction could significantly impact site design, longevity, and future function of spawning gravel augmentation projects.

1.1.6. Detection uncertainties

Regardless of measurement technique, topographic surveying and DEM differencing contain uncertainties (Brasington et al., 2004; Holmes et al., 2000). In this study, we assume that detection uncertainties have equal influence on volumetric loss and gain and subsequently cancel each other out. These detection uncertainties are currently under further investigation to explore the validity of this assumption (Brasington et al., 2004; Wheaton et al., 2004a).

2. Regional setting

The snow-fed Mokelumne River, in California drains ~1624 km^2 of the central Sierra Nevada (Fig. 2). It presently has 16 major water impoundments, including Salt Springs (175 032 089 m^3), Pardee (258,909,341 m^3) and Camanche reservoirs (531,387,061 m^3), which have dramatically altered the late spring snowmelt flow regime (see Pasternack et al., 2004; Wheaton, 2003) (Fig. 3). The LMR bed slope ranges from 0.10% near Camanche Dam to 0.02% near the Cosumnes River confluence, with the active channel now half its former width (present average 30 m; range of 19–43 m) and overdeepened. In the upper ~9.5–14.5 km below Camanche Dam, the channel bed has limited amounts of compacted gravels and cobbles associated with higher bed slope and shallow riffle-run hydraulics. Camanche Dam blocks gravel delivery from upstream. Murphy Creek, a small tributary close to the dam, potentially contributes a small amount of gravel. Historic mining operations depleted instream gravel storage and yielded deep pits that are sediment transport barriers. Although isolated by berms and levees, mine tailings exist along the upper third of the LMR. Channel

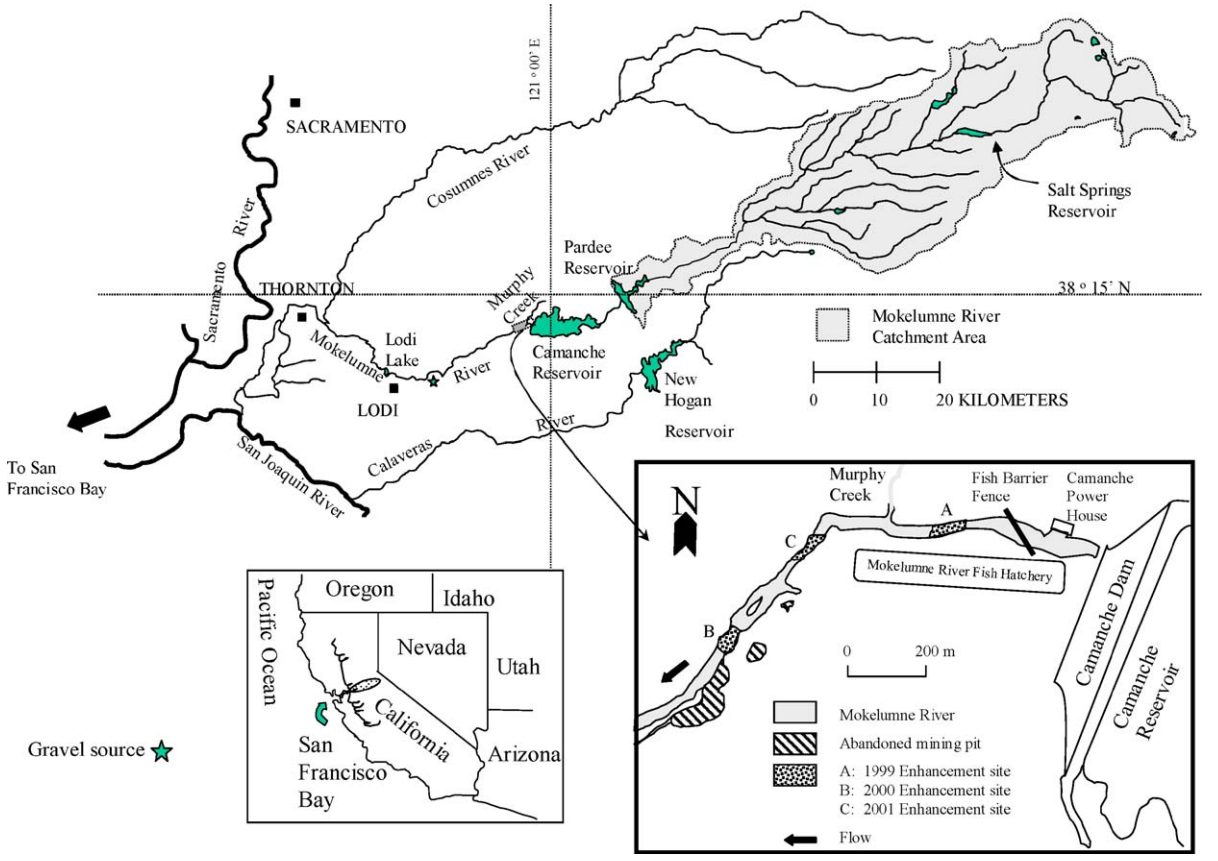

Fig. 2. Study location in relation to the Mokelumne River drainage, Sacramento–San Joaquin River system and the Southwestern United States.

and banks show little instability that could lead to gravel recruitment with a thin ribbon of riparian vegetation remaining along most of the stream, providing vegetative armoring of the bank. Presently, the LMR supports over 35 native and non-native fish species including native Chinook salmon (*Oncorhynchus tschawytscha*) and steelhead (*O. mykiss*) (Merz et al., 2004; Workman, 2003).

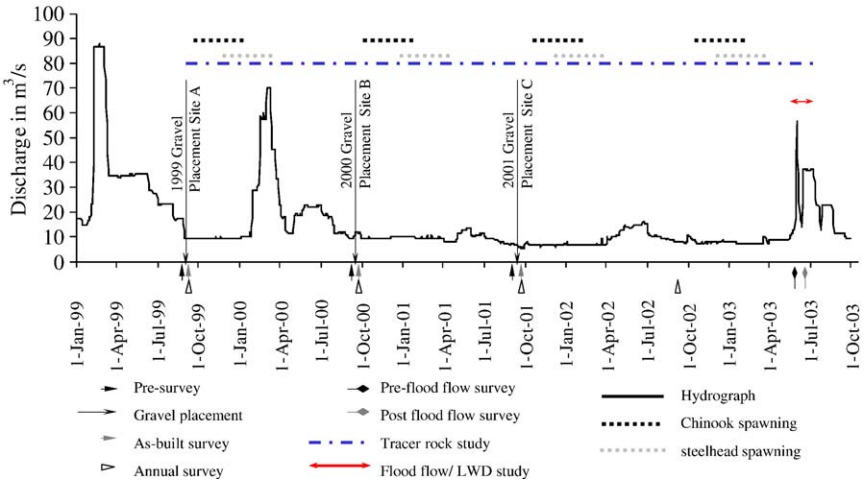

Fig. 3. Hydrograph of the lower Mokelumne River immediately below Camanche Dam, 1 January 1999 through 30 September 2003. Flood flow surveys not performed at site B. Only site B surveyed on 23 September 2003.

3. Material and methods

3.1. Site selection, enhancement procedures, and gravel input

The purpose of LMR SHR is to replenish suitable-sized gravel within the spawning reach (Fig. 2), provide immediate salmonid spawning habitat (recognizing that placed gravels will not be static), and serve as a controlled field experiment for river research.

In August of 1999, 2000 and 2001, three sites were augmented (Figs. 2–6; sites A–C). Degraded sites were selected based on depth and equipment access. Historic aerial photographs (1933–1963) were used to select sites of previously shallow gravel depths that had been mined between 1952 and 1964, and recent Chinook salmon and steelhead redd (nest) surveys to identify appropriate locations (Figs. 4–6) (Setka, 2002).

An estimated 1659, 1200, and 794 m^3 (sites A, B and C, respectively) of clean 25–150 mm diameter river gravel (CDFG, 1991; Kondolf and Wolman, 1993) from an open floodplain quarry located 0.5 km from the active channel (Fig. 2) was transported by dump truck and contoured by rubber-tire loader in berm, riffle, and staggered bar configurations. Configurations intended to enhance Chinook salmon and steelhead spawning conditions by reducing depth, increasing velocities, providing structure, and promoting exchanges of water between the stream and gravel interstices (Vronskiy, 1972; Chapman, 1988).

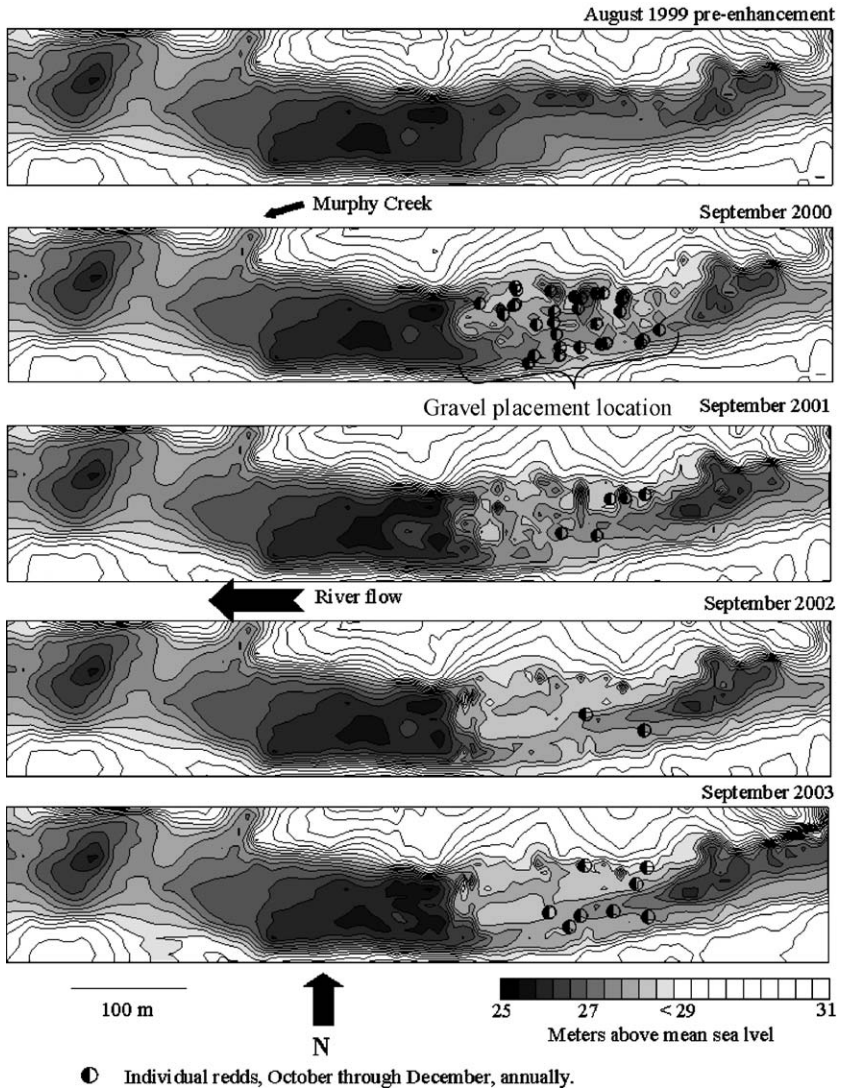

Fig. 4. Contour maps depicting streambed elevation before and after gravel placement at site A, lower Mokelumne River California.

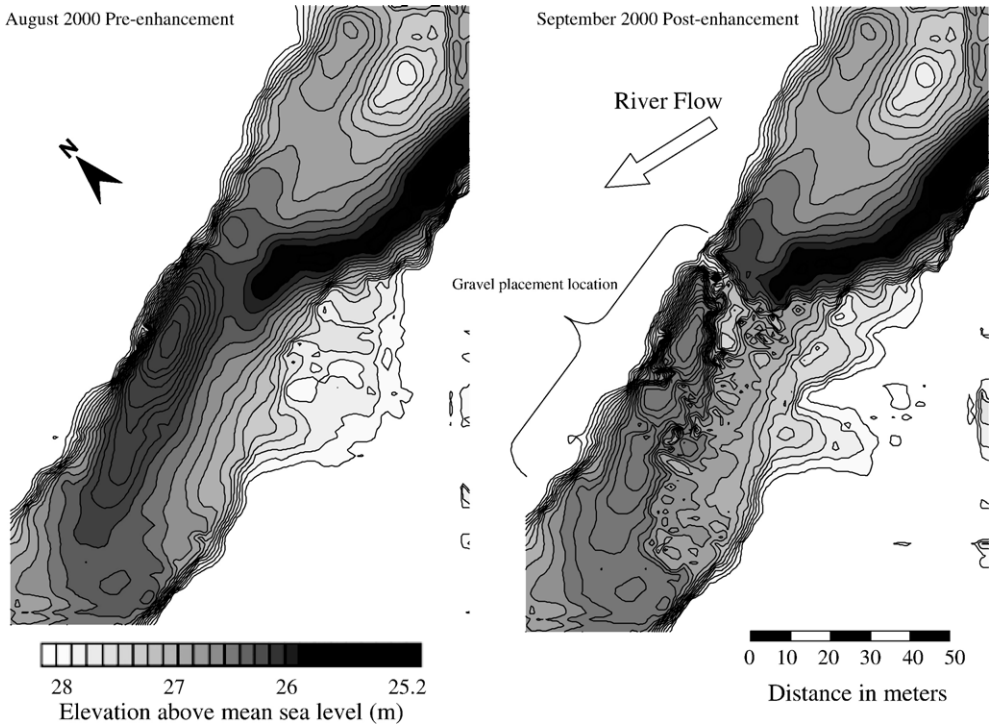

Fig. 5. Contour maps depicting streambed elevation before and after gravel placement at site B, lower Mokelumne River, California.

Boulders (0.6–1.2 m diameter) and LWD (trunks up to 0.6 m diameter) were placed throughout the sites to increase downwelling, channel complexity, and cover for spawning salmonids (House, 1996; Geist and Dauble, 1998; Merz, 2001). Gravel was placed under various configurations built on numerous modeling designs (Spawning Habitat Integrated Rehabilitation Approach–Adaptive Management Phase 5; see Wheaton et al. (2004b,c). Final design selection was based on model results, consideration of project constraints, and revisiting conceptual models (viewable on the web:http://www.shira.lawr.ucdavis.edu).

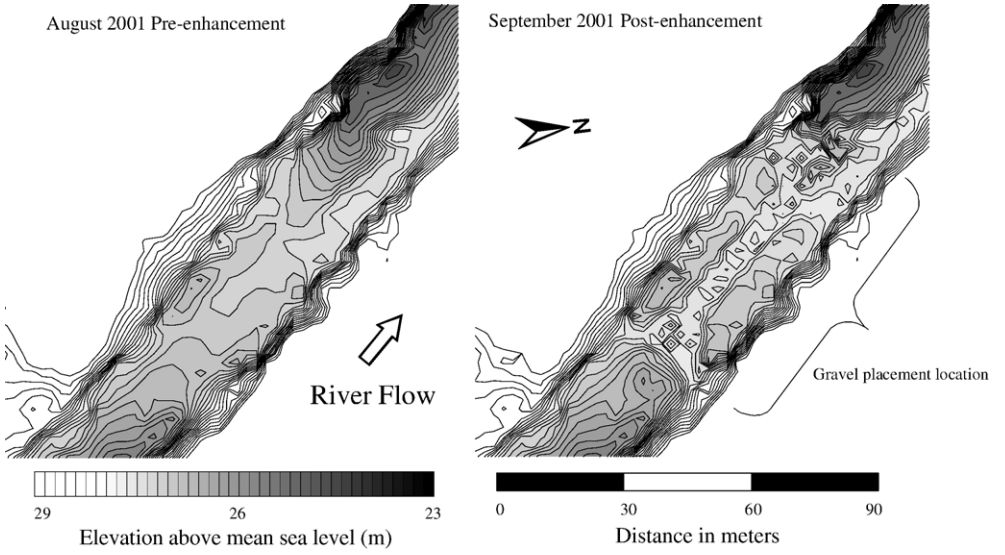

Fig. 6. Contour maps depicting streambed elevation before and after gravel placement at site C, lower Mokelumne River, California.

3.2. Sediment budget

3.2.1. Timing of monitoring program

Repeat surveys tracked morphometric change (Brasington et al., 2003) over two temporal scales: (i) annually with surveys each summer during low flows and (ii) event-based in response to a controlled flood release. Annual surveys were typically repeated during the first week of September (Fig. 3). This yielded six time steps during which surveys were conducted and five appraisal periods over which changes were analyzed.

3.2.2. Topographic channel surveys and DEM differencing

A Topcon GTS-802A total station (1 s angular accuracy) was used to record 1200–3400 bed points for each survey. Average point densities across all three sites (21 surveys) were 0.78 m^{-2} (min: 0.39; max: 2.41; SD: 0.32). This variation reflects higher density in complex areas and low point density in flat areas (Fuller et al., 2003).

Surfer® (Golden Software, Inc.) was used to build triangulated irregular networks (TINS) and interpolate survey data to 1.1-m resolution DEMs. Blanking files ensured that elevation and volumetric changes were only assessed where gravel, LWD, and boulders were specifically placed. Placed gravel volume and net cut/fill after specific time periods and flow events were calculated at each site using the Surfer Grid Volume Report (Golden Software Inc., 1999). Downstream tracking of exported sediment was not done; whereas placed gravels created easily discernable, localized features: exported grains may be only 1–2 D_{90} thick and spread over a large area, being impractical to resolve. Because of regulated flows, stable banks, and proximity to Camanche Dam, natural gravel recruitment was assumed negligible.

To estimate potential error from mapping and DEM analysis, two areas (13.28 and 8.55 m^2) were surveyed three times each, within a 15-min timespan (as to insure volumetric change was negligible) with a mean point density: 5.9 m^{-2} and analyzed as described above. Mean DEM error calculations were +0.01955 m^3/m^2 surveyed within the LMR channel.

3.2.3. Techniques to assess processes responsible for observed volumetric changes

3.2.3.1. Fluvial erosion estimates. Fluvial erosion potential based on recorded flows was estimated using the Shields (1936) equation for site-specific and 1-Φ grain sizes and for τ_c* of 0.03 and 0.045 (Table 1). The flow duration above each threshold was then calculated by comparing threshold values to actual Camanche Dam flow record. Spatially explicit predictions of mobilization at the 0.1–2 m scale for sites A and C pre- and post-project were previously published (Pasternack et al., 2004; Wheaton, 2003). As an alternative to process-based predictions, flow-based scour was also evaluated using statistical regressions between gravel volume changes and measures of flow magnitude and duration.

3.2.3.2. Fluvial erosion verification—tracer rocks. Bed material scour was verified with tracer rocks. Quarry stones (800 and 500 at sites A and B, respectively) were washed and painted for use as scour indicators and pathway tracers. Tracer rocks were clustered by grain size using a gravel template with 22, 32, 44, 64, and 89 mm round openings. One group of 100 sorted tracers was piled on the bed at a randomly located point along each of eight evenly spaced transects at site A (September 1999) and five at site B. A measuring tape was used to measure the distance each tracer had moved downstream of its release site, and grain size was measured using the template. This was repeated again 12 months later. Individual points were also recorded during channel bathymetry surveys for release and recovered tracer rock locations at site A on 8 September 1999 and 10 June 2003. The JMP linear regression model function with an analysis of variance (ANOVA) was used to compare distances tracer rocks moved with stream velocity at initial placement (Sall et al., 2001).

3.2.3.3. In situ slope settling. Slope analyses of as-built DEMs explored the influence of oversteepened (>23°) gravel piles on site adjustment. The terrain module of Land Desktop R3 was used to calculate the slope of each TIN triangular plane and add its area to predefined slope range bins. Although friction angles have been reported to vary from 10–110° in gravel streambeds (Kirchner et al., 1990; Buffington et al., 1992), Barabási et al. (1999) suggested that critical slope for stability is ~23° for spherical particles and Handin (1966) suggested 25–40° for filling angles of rock and sand. A maximum hypothetical gravel volume loss attributed to oversteep bedslopes was calculated by multiplying the area over 23° by the maximum observed scour depths. This yielded a conservative estimate of the maximum volume reasonably attributed to readjustment for these slopes.

3.2.3.4. Gravel porosity and potential compaction estimates. To assess possible volumetric change from compaction, dry bulk gravel density (kg/m^3) was measured prior to placement (six quarry samples collected in a 0.020-m^3 bucket) and empirically estimated after-

Table 1
Calculations for theoretical entrainment of site-specific grain sizes at three spawning gravel enhancement sites on the lower Mokelumne River, California

Variable	Values for site-specific grain sizes			Values for 1-Φ grain sizes					Values for site-specific grain sizes			Values for 1-Φ grain sizes					Units
	D_{10}	D_{50}	D_{90}	8 mm	16 mm	32 mm	64 mm	128 mm	D_{10}	D_{50}	D_{90}	8 mm	16 mm	32 mm	64 mm	128 mm	
$\gamma_{sediment}$	25945	25945	25945	25945	25945	25945	25945	25945	25945	25945	25945	25945	25945	25945	25945	25945	N m^{-3}
γ_{water}	9790	9790	9790	9790	9790	9790	9790	9790	9790	9790	9790	9790	9790	9790	9790	9790	N m^{-3}
f(Re)	0.045	0.045	0.03	0.045	0.045	0.045	0.045	0.045	0.03	0.03	0.03	0.03	0.03	0.03	0.03		
n	0.043	0.043	0.043	0.043	0.043	0.043	0.043	0.043	0.043	0.043	0.043	0.043	0.043	0.043	0.043		
Site A (1999)																	
D_s	24.9	48.0	80.6	8.0	16.0	32.0	64.0	128.0	24.9	48.0	80.6	8.0	16.0	32.0	64.0	128.0	mm
D_s	0.025	0.048	0.081	0.008	0.016	0.032	0.064	0.128	0.025	0.048	0.081	0.008	0.016	0.032	0.064	0.128	m
Q_crit	18.09	34.89	58.60	5.82	11.63	23.26	46.52	93.05	12.06	23.26	39.07	3.88	7.75	15.51	31.02	62.03	N m^{-2}
S	0.0016	0.0016	0.0016	0.0016	0.0016	0.0016	0.0016	0.0016	0.0016	0.0016	0.0016	0.0016	0.0016	0.0016	0.0016	0.0016	
R	1.124	2.169	3.644	0.362	0.723	1.446	2.893	5.785	0.750	1.446	2.429	0.241	0.482	0.964	1.928	3.857	m
V_crit	1.02	1.58	2.23	0.48	0.76	1.21	1.91	3.04	0.78	1.21	1.70	0.37	0.58	0.92	1.46	2.32	m/s
W	46	46	46	46	46	46	46	46	46	46	46	46	46	46	46	46	m
Q_crit	52.7	157.6	374.1	8.0	25.3	80.2	254.6	808.4	26.8	80.2	190.3	4.0	12.9	40.8	129.5	411.3	m^3/s
Site B (2000)																	
D_s	7.5	39.4	106.4	8.0	16.0	32.0	64.0	128.0	7.5	39.4	106.4	8.0	16.0	32.0	64.0	128.0	mm
D_s	0.007	0.039	0.106	0.008	0.016	0.032	0.064	0.128	0.007	0.039	0.106	0.008	0.016	0.032	0.064	0.128	m
Q_crit	5.45	28.66	77.31	5.82	11.63	23.26	46.52	93.05	3.63	19.11	51.54	3.88	7.75	15.51	31.02	62.03	N m^{-2}
S	0.0060	0.0060	0.0060	0.0060	0.0060	0.0060	0.0060	0.0060	0.0060	0.0060	0.0060	0.0060	0.0060	0.0060	0.0060	0.0060	
R	0.093	0.488	1.316	0.099	0.198	0.396	0.792	1.584	0.062	0.325	0.877	0.066	0.132	0.264	0.528	1.056	m
V_crit	0.37	1.12	2.16	0.39	0.61	0.97	1.54	2.45	0.28	0.85	1.65	0.29	0.47	0.74	1.18	1.87	m/s
W	41	41	41	41	41	41	41	41	41	41	41	41	41	41	41	41	m
Q_crit	1.4	22.3	116.7	1.6	5.0	15.8	50.1	159.0	0.7	11.4	59.4	0.8	2.5	8.0	25.5	80.9	m^3/s
Site C (2001)																	
D_s	26.4	40.5	60.0	8.0	16.0	32.0	64.0	128.0	26.4	40.5	60.0	8.0	16.0	32.0	64.0	128.0	mm
D_s	0.026	0.041	0.060	0.008	0.016	0.032	0.064	0.128	0.026	0.041	0.060	0.008	0.016	0.032	0.064	0.128	m
τ_crit	19.19	29.44	43.64	5.82	11.63	23.26	46.52	93.05	12.79	19.63	29.09	3.88	7.75	15.51	31.02	62.03	N m^{-2}
S	0.0013	0.0013	0.0013	0.0013	0.0013	0.0013	0.0013	0.0013	0.0013	0.0013	0.0013	0.0013	0.0013	0.0013	0.0013	0.0013	
R	1.470	2.256	3.344	0.446	0.891	1.782	3.565	7.130	0.980	1.504	2.229	0.297	0.594	1.188	2.377	4.753	m
V_crit	1.10	1.46	1.90	0.50	0.79	1.25	1.98	3.15	0.84	1.11	1.45	0.38	0.60	0.95	1.51	2.40	m/s
W	27	27	27	27	27	27	27	27	27	27	27	27	27	27	27	27	m
Q_crit	43.6	89.0	171.4	6.0	18.9	60.1	190.7	605.5	22.2	45.3	87.2	3.0	9.6	30.6	97.0	308.0	m^3/s

wards. Porosity of placed gravels was estimated with the Winterkorn formula ($\Phi = 0.385 - 0.08_{\log 10} d_{max}/d_{min}$), where d_{min} and d_{max} represent the smallest and largest particle sizes present, respectively (Ingles and Grant, 1975). The minimum and maximum porosity observed by Milhous (2001) in gravel and cobble rivers were used to calculate gravel porosity from the three SHR sites to estimate potential substrate deflation at various gravel placement depths.

3.2.3.5. Scour at boulders and LWD. In order to assess the extent to which structures placed to promote habitat heterogeneity caused local scour, the vicinity of such features was repeatedly surveyed. Placed boulder diameters, weights, and volumes ranged from 60–120 cm, 250–500 kg, and 0.01–0.25 m^3, respectively. Methods used to quantify boulder redistribution are described in Merz (2004). Briefly, sites A, B, and C boulders over the previously defined timesteps were surveyed by averaging ~20 elevation measurements on top of each boulder. We used a one-tailed *t*-test (Zar, 1996) to compare average boulder elevations at initial stream channel placement to elevations after selected time periods (e.g. every 12 months) and compared stream channel depth to boulders depth at each site after given time periods (typical time between surveys was 3–12 months).

During SHR site bathymetry surveys, at least 3 individual points were recorded on each piece of LWD to track its fate. After 12 months, points were recorded again to compare location and numerical change for LWD. High-density point surveys (8–14.3 points m^{-2}) were recorded around nine pieces of LWD at site A after initial construction (August 1999). These surveys were repeated in August 2000 to estimate scour volume using the Surfer Grid Volume Report.

3.2.3.6. Salmon pedoturbation. To measure Chinook salmon spawning effect on bed volume, bathymetry surveys were made to estimate channel morphology change caused by seven individual redds. Average point density per redd was 89.79 m^{-2} (min: 36.16; max: 132.45; SD: 39.60). Estimated volume differences were compared to estimated redd volumes calculated by lengths, widths, and depths of 98 Chinook salmon redds randomly measured between 1996 and 2002 to calculate an average volume of mobilized substrate by spawning salmon. Average estimated volumes were then multiplied by the number of redds observed each season to estimate total volume of bed material redistributed annually by spawning Chinook salmon at each enhancement site. Too few steelhead redds were observed during this study to provide an estimate.

4. Results

The LMR flow was largely unchanged at 10 m^3/s for most of the study period (Figs. 3 and 7). During its first snowmelt season, site A was subjected to a 77-day flow release with a peak of 70 m^3/s lasting 8 days. The peak flow corresponded to a 1.29-year event pre dam or a 2.5-year event post dam. In June 2003, all sites were

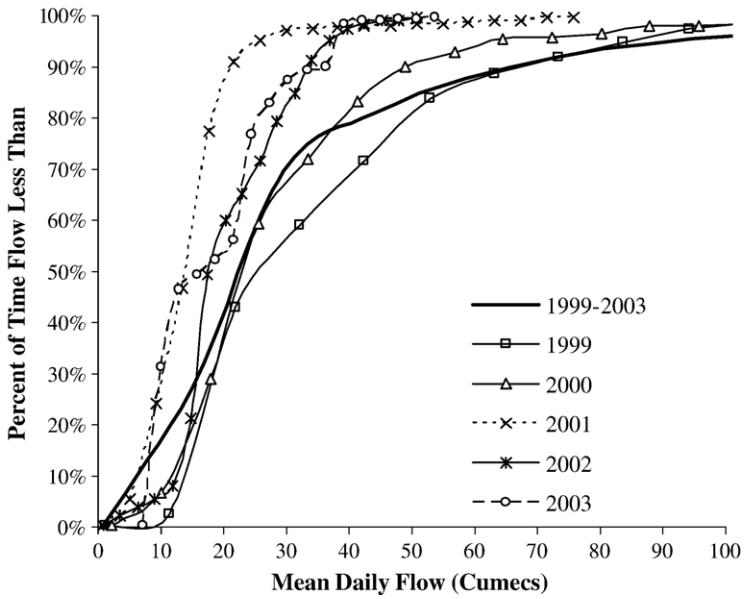

Fig. 7. Flow duration curves for the lower Mokelumne River, 1 January 1999 through 31 December 2003.

Table 2
Time periods, river discharge rates and gravel volumne calculations made at 3 spawning gravel enhancement sites on the lower Mokelumne River, California, 1 September 1999 through 23 September 2003

Flow period	Time period	Number of days	Site	River discharge rates									Gravel measurements				
				Total volume ($m^3 \times 10^5$)	Ave daily volume ($m^3 \times 10^5$)	Peak flow ($m^3\ s^{-1}$)	f(Re)=0.045 Number of days ≥ Q_crit for			f(Re)=0.03 Number of days ≥ Q_crit for			Volume remaining (m^3)	Volume lost (m^3)	Ave daily volume lost (m^3)	From previous period	
							D_{10}	D_{50}	D_{90}	D_{10}	D_{50}	D_{90}				Total percent lost	Daily percent lost
Flood release	23 May 2003 to 10 June 2003	19	1999 (A)	432.3	22.8	56.7	1 (5%)	0	0	8 (42%)	0	0	663.1	17.44	0.92	0.03	0.0013
4	1 Sept 2002 to 23 May 2003	266	1999 (A)	1841.8	6.9	12.5	0	0	0	22 (8%)	0	0	680.5	87.58	0.33	0.11	0.0004
3	1 Sept 2001 to 30 Aug 2002	364	1999 (A)	2751.1	7.5	15.9	1 (>1%)	0	0	92 (25%)	0	0	768.1	83.24	0.23	0.10	0.0003
2	1 Sept 2000 to 30 Aug 2001	364	1999 (A)	2990.3	8.1	13.4	6 (2%)	0	0	13 (4%)	0	0	851.4	207.00	0.56	0.20	0.0005
1	1 Sept 1999 to 30 Aug. 2000	364	1999 (A)	5830.9	16.0	70.0	30 (8%)	0	0	139 (38%)	126 (35%)	0	1058.4	264.90	0.73	0.20	0.0005
5	1 Sept 2002 to 23 Sept 2003	388	2000 (B)	4048.1	11.0	12.5	388 (100%)	127 (33%)	0	388 (100%)	282 (73%)	0	870.2	48.90	0.13	0.05	0.0001
3	1 Sept 2001 to 30 Aug 2002	364	2000 (B)	2751.1	7.5	15.9	362 (99%)	131 (36%)	0	364 (100%)	291 (80%)	0	919.1	56.54	0.15	0.06	0.0002
2	1 Sept 2000 to 30 Aug 2001	364	2000 (B)	2990.3	8.1	13.4	362 (99%)	26 (7%)	0	364 (100%)	268 (74%)	5 (1%)	947.6	224.00	0.61	0.19	0.0005
Flood release	23 May 2003 to 10 June 2003	19	2001 (C)	432.3	22.8	56.7	3 (16%)	0	0	9 (47%)	3 (16%)	0	524.9	13.75	0.72	0.03	0.0014
4	1 Sept 2002 to 23 May 2003	266	2001 (C)	1841.8	6.9	12.5	0	0	0	61 (23%)	0	0	538.6	17.57	0.07	0.03	0.0001
3	1 Sept 2001 to 30 Aug 2002	364	2001 (C)	2751.1	7.5	15.9	5 (1%)	0	0	135 (37%)	131 (36%)	0	556.2	93.21	0.25	0.14	0.0004

Flows are measured in m^3 /s and gravel volumes in m^3.

subjected to an 8-day release of 65 m^3/s, specifically designed for environmental purposes.

4.1. Volumetric budget results

DEM differencing of the 11 surveys performed over 4 years showed an overall decrease in placed gravel volume at all sites (Table 2). The total bed volume of 2948 m^3 created in the river among all sites was reduced by 28% by study end. Average site bed elevation change was 0.153 mm day^{-1} (range of 0.022–0.323 mm day^{-1}). Site A experienced a 50% volume reduction over the initial 45 months (September 1999 to June 2003). Site B experienced a 30% decrease over its initial 37 months, while site C experienced a 20% decrease over its initial 20 months.

Among annual surveys, normalized volumetric decreases ranged from 0.07–0.73 m^3/day (26–266 m^3/year) and trended downward over time (Table 2). For all three sites, the largest annual decreases occurred during the first year after placement. Site A showed gradual decreases in change rate until period 4, when it showed an increase. Sites B and C showed strong drops in change rate after the first year.

Sites A and C had higher event-based volumetric decreases than those observed on an annual basis. For site A, the 266-day period prior to the designed release had a 0.33 volumetric change. During the release, it increased to 0.92. For site C, the same numbers were 0.07 and 0.72, respectively. These changes are threefold and tenfold increases for sites A and C, respectively.

4.2. Fluvial erosion estimates

Based on predicted entrainment thresholds (Table 1), strong differences in flow-based scour were evident between sites and between periods (Table 2). Site B has ~4.5 times higher channel slope than either sites A or C, thus requiring a much lower sediment mobility discharge. The greatest overall flow-based scour was predicted at site B. Period 1 had the longest high flow durations, yielding the greatest overall potential for scour. This could only affect site A, as sites B and C were not yet built.

In terms of grain-size specific mobility, large particles were predicted to have rarely moved, while movement of smaller gravels was highly site and period dependent. For the substrate framework D_{90} particles, flows were never high enough to entrain them using $t_c^*=0.045$ for any site (just 5 days at site B for $t_c^*=0.03$). For the median substrate size (D_{50}), sites A and C were not predicted to ever experience scour using $t_c^*=0.045$; but for $t_c^*=0.03$ they would have both scoured ~35% of the time during the first year post-placement, though not in any subsequent periods. Median-sized material at site B was predicted to mobilize for a significant portion of time. Finally, for smaller bed particles (D_{10}), sites A and C were predicted to experience some mobility some of the time, while those at site B should have been susceptible to mobility all of the time.

From an empirical perspective, percent daily bed sediment volume cut was significantly related to average daily discharge (Fig. 8A) and total water volume released from Camanche Dam (Fig. 8B). SHR sites lost 0.05% of remaining material daily (range of 0.01–0.14%). We measured 17.4 m^3 of cut from site A during the 19-day flood increase.

4.3. Fluvial erosion verification—tracer rocks

Of the 800 tracer rocks released at site A in August 1999, 245 were recovered in August 2000 (31%). Of

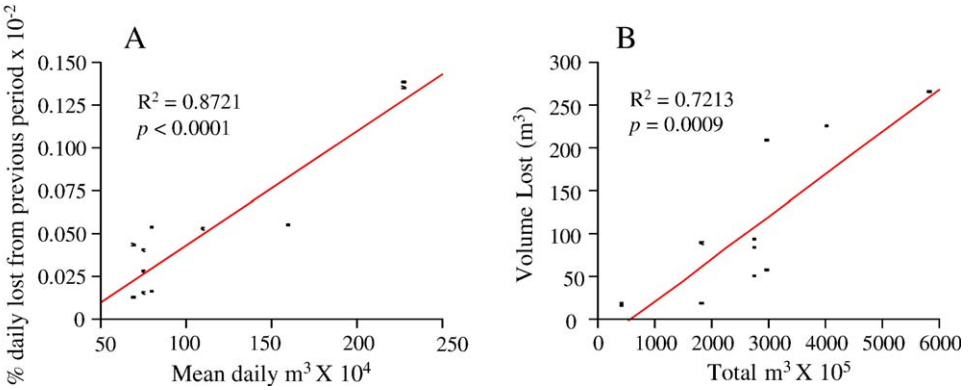

Fig. 8. Comparison of bed cut, as indicated by volume and percent, to river flow at 3 gravel enhancement sites over 5 various time periods, lower Mokelumne River, California. A: Percent daily gravel volume lost from previous period by mean daily m^3 of water released from Camanche Dam; B: Total gravel volume lost (m^3) by total m^3 of water released from Camanche Dam.

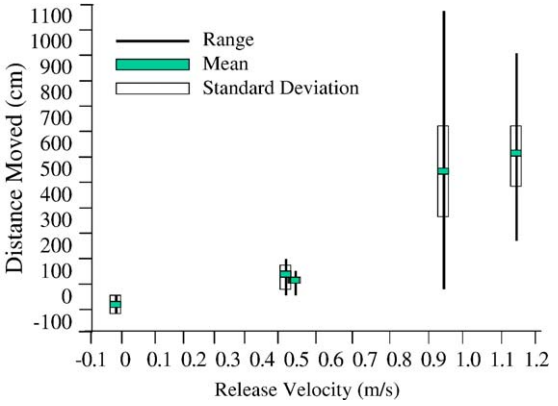

Fig. 9. Distance downstream tracer rocks were recorded after 12 months, compared to velocities recorded at initial release, site A, lower Mokelumne River, California.

those recovered 86% (211) did not move from initial placement locations. The mean distance downstream rocks were recovered after 12 months was 1.64 m (range of −0.38 to 25.81 m) (Fig. 9). Of those recovered that moved, four (12%) left the site. Piles 2, 6, 7, and 8 were completely scoured or buried by 10 June 2003 (Fig. 10). No tracers were recovered from these piles. Twenty-two (22%) of tracer rocks at release location 1 were mobilized upstream. Similarly, of the 500 tracer rocks released at site B in August 2000, 124 (20%) were recovered the following year. Three (2% of recovered, mobilized tracers) were recovered downstream of the site. Site B tracer rocks were disturbed by local visitors to the adjacent public park the following year and no further monitoring was performed. Tracer rocks had a higher propensity to move when placed in areas of higher velocities at low flow, typically near the channel center (Fig. 10). This was also observed for LWD (Fig. 11). By June 2003, four of the original eight tracer rock piles were completely scoured from site A. Maximum distance tracer rocks were recovered from original release locations was 121.9 m downstream in site A, 4 years after original placement.

4.4. In situ slope settling

Overall, as-built project areas with slopes over 23% were between 6 and 12% with the highest at site C (Fig. 12). This equates to 1405, 1393, and 2057 m^2 of area susceptible to slope failure at sites A–C, respectively, and expands to potentially 130, 26 and 19 m^3 of gravel scour at sites A–C, respectively. Greatest reduction in overall site slope (increase in area of slope 0–10°)

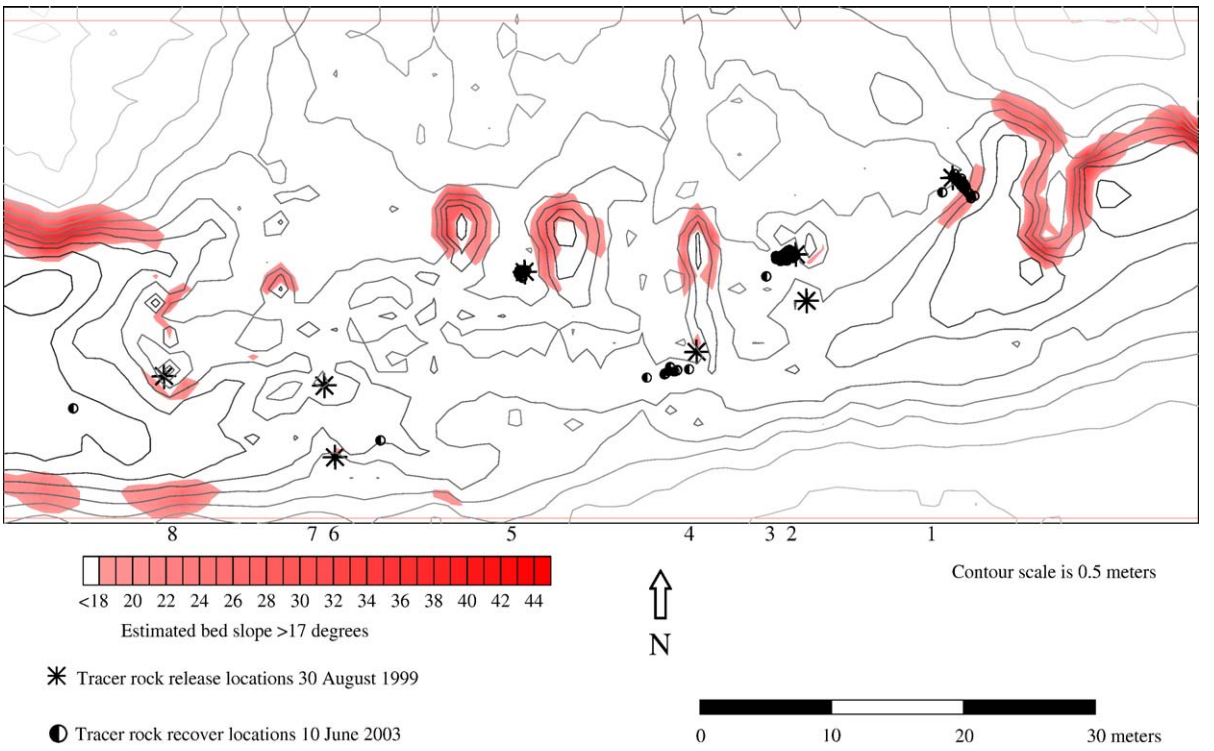

Fig. 10. Tracer rock release and recovery locations in relation to estimated bed areas where slope meets or exceeds the angle of repose. Base map is of as-built contours of site A, 30 August 1999. Numbers indicate tracer rock release pile designation.

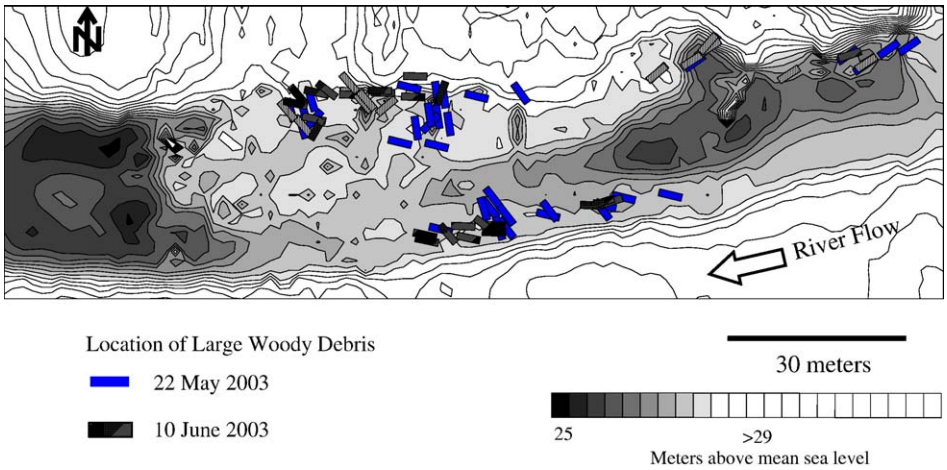

Fig. 11. Location of large woody debris before and after a 19-day flow increase at site A, lower Mokelumne River, California.

occurred after the first year at each site. Predicted areas of high failure potential corresponded well with tracer rock results (Fig. 9).

4.5. Gravel porosity and potential compaction

Estimated bulk density from our six enhancement gravel samples was 1.644 g cm^{-3} (SD: 0.054). Mean estimated gravel porosity was 0.281 (Tables 3 and 4). Likely porosity changes for sites A–C are 0.059, 0.107, and 0.072, respectively, with maximum plausible porosity change of 0.34 for all three sites. Based on porosity calculations, we estimate 28 to 41% of observed gravel volume reduction can be explained by deflation alone (max: 130–190%) (Table 4).

4.6. Scour at boulders and LWD

Site bed elevations lowered 0.022 to 0.323 mm day^{-1} (mean: 0.153). Mean boulder elevation change was 0.588 mm day^{-1} (range −0.053 to 2.054 mm day^{-1}). Average boulder elevational changes were significantly higher than average channel bed elevation between each monitoring period ($t=-1.825$; df=16; $p=0.043$).

SHR sites contained from 0.5 to 6.0 pieces of LWD/1000 m^2 of channel bed. While LWD was not captured in site C, we observed nearly a 300% LWD increase at sites A and B over a 4-year period. Some LWD was mobilized during the study, with individual pieces moving completely out of SHR sites within a year of placement. Distinct clumping and mobilization patterns were observed during a short-duration flow increase (Fig. 11). Seven of nine LWD pieces used in the high-density surveys were still intact in August 2000. Average cut around LWD was 0.58 m^3 (SD=0.231).

4.7. Salmon pedoturbation

Chinook salmon spawning use of three SHR sites was highly variable over several seasons (Table 5; Fig. 4). All three of the SHR sites had no documented spawning previous to gravel placement, although site C had an initial placement of gravel in 1996. Average substrate volume excavated during redd construction was 2.26 m^3 (min: 0; max: 10.37; SD: 2.16). Estimated annual bed material mobilization by spawning salmon within each site was 2.26–65.5 m^3 (mean: 19.13 m^3).

Estimated mean volume loss from mechanisms quantified in this study account for 86 to 113% of volume reductions observed with gravel deflation, faunal pedoturbation (salmon spawning), and surface scour explaining most of this loss (Fig. 13; Table 6).

5. Discussion

Our data show that SHR sites of 649–1323 m^3 of gravel lost from 11–24% of remaining volume annually during controlled flows of 8–70 m^3/s and 2.6% of placed material during short-duration (19 days) flow releases of 57 m^3/s. Site A lost 50% of gravel volume in a 4-year period. By using mean volume loss estimates from mechanisms quantified in this study, we can account for 86 to 113% of volume reductions observed. Overall, deflation appears to have the greatest influence, followed by spawning activity and surface scour. This is not surprising because of restricted flows in the system (Gilvear et al., 2002).

We observed significant bed material volume reductions (up to 20%) during the first year after gravel placement at all sites. Bement and Selby (1997) showed that although it took many minutes to fully reduce gran-

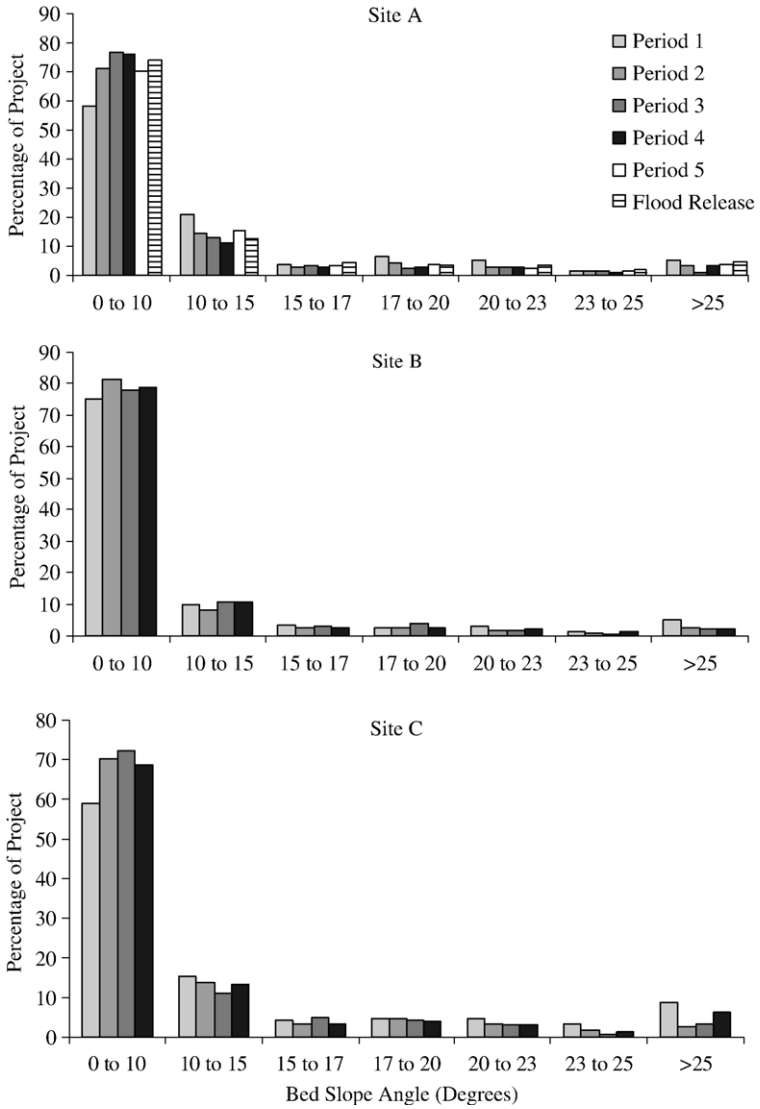

Fig. 12. Slope analysis distribution for sites A–C. Flow Period duration and magnitude are provided in Fig. 3 and Table 2.

ular soil volumes during a vibration test early response was more rapid. Similarly, we observed greater volumetric reduction in placed materials during the earliest surveys of individual sites. Because of selective screening and cleaning of placement gravels, porosity was higher and density was lower within placed gravels than what is typically observed in natural streambed conditions (Bunte and Abt, 2001). This suggests cleaned, placed material has a higher settling propensity. However, because in situ bed porosity and bulk density were not measured through time, we cannot quantify what proportion of volumetric change predicted by DEM differencing is due to settling. Measurement error must also be taken into consideration (Fuller et al., 2003).

Table 3
Estimated porosity compared to volume change of placed gravels at three spawning enhancement sites in the lower Mokelumne River, California

Site	D_{min}	D_{max}	Estimated Porosity (Φ)	Estimated percent volume lost 1st year	Total time monitored	Overall percent volume lost	Estimated percent volume lost day^{-1}
1999 (A)	16	178	0.301	25	1385	50	0.0360
2000 (B)	4	178	0.253	24	1104	25	0.0226
2001 (C)	8	127	0.289	17	651	18	0.0270

Table 4
Estimated gravel deflation at three spawning enhancement sites due porosity

Period	Volume loss (m^3)	Likely deflation		Plausible deflation	
		Volume (m^3)	Proportion	Volume (m^3)	Proportion
Site A:		Porosity: 0.301			
Calculated fill: 1323 m^3					
1	264.9	184.6	0.7	1063.5	4.0
2	207	184.6	0.9	1063.5	5.1
3	83.2	184.6	2.2	1063.5	12.8
4	87.6	184.6	2.1	1063.5	12.1
Flood flow	17.4	184.6	10.6	1063.5	61.0
Total lost:	660.2	184.6	0.3	1063.5	1.6
Site B		Porosity: 0.253			
Calculated fill: 1147 m^3					
2	224	136.6	0.6	434.2	1.9
3	56.5	136.6	2.4	434.2	7.7
5	48.9	136.6	2.8	434.2	8.9
Total Lost:	329.4	136.6	0.4	434.2	1.3
Site C		Porosity: 0.288			
Calculated fill: 649 m^3					
3	93.2	50.9	0.5	240.4	2.6
4	17.6	50.9	2.9	240.4	13.7
Flood flow	13.7	50.9	3.7	240.4	17.5
Total lost:	124.5	50.9	0.4	240.4	1.9

While our entrainment and compaction estimates indicate site B should have the highest volume loss potential, several site-specific aspects may explain why this did not occur. Because of a channel bend, site B was the only site receiving flow somewhat diagonally across the placed gravel, from the SE to the NW portion of the site. Flow actually cut into the site's north bank. Slower flow on the south bank, further protected by trees, actually settled fines (<8 mm diameter) out. These fines reduced the overall D_{10}–D_{90} of the site, yet were protected from the main force of channel flow.

According to Konrad et al. (2002), the probability of bed material transport is approximately uniform over a gravel bar during a flood, provided the bar has uniform sedimentologic and hydraulic conditions. Within our SHR sites, shallow berms, LWD, and boulders are used to attract spawning Chinook salmon. Such features specifically alter uniform gravel beds, adding complexity. Our data suggest that these features increase gravel scour within SHR sites, supported by Rosenfeld and Huato (1993).

LWD can also affect secondary morphological structures within a channel (Mutz, 2000). Over the monitoring period, we observed no net LWD loss. Surprisingly, all three sites entrained as much LWD as was lost over the study period even as close as they were to Camanche Dam, which does not pass upstream LWD. This suggests that adjacent riparian vegetation is gen-

Table 5
Number of Chinook salmon redds observed at each of three spawning gravel enhancment sites (A, B and C) in the lower Mokelumne River, California

Year	A				B				C			
	Number	Percent total[a]	Volume (m^3)[b]	Percent mobilized[c]	Number	Percent total	Volume (m^3)	Percent mobilized[c]	Number	Percent total	Volume (m^3)	Percent mobilized[c]
1999	1	0.2	2.3	0.2	0	0.0	0.0	0.0	3	0.5	6.8	1.0
2000	29	2.9	65.3	4.9	18	1.8	40.5	3.2	1	0.1	2.3	0.3
2001	5	0.6	11.3	0.1	11	1.3	24.8	1.9	7	0.8	15.8	2.2
2002	2	0.2	4.5	0.3	16	1.9	36.0	2.8	5	0.6	11.3	1.6
2003	8	1.1	18.0	1.4	17	2.1	38.3	3.0	4	0.5	9.0	1.3

[a] Percent of total lower Mokelumne River Chinook salmon redds observed at each site.
[b] Estimated total volume of gravel mobilized by spawning Chinook salmon.
[c] Percent volume of total placed gravel mobilized by spawning Chinook salmon.

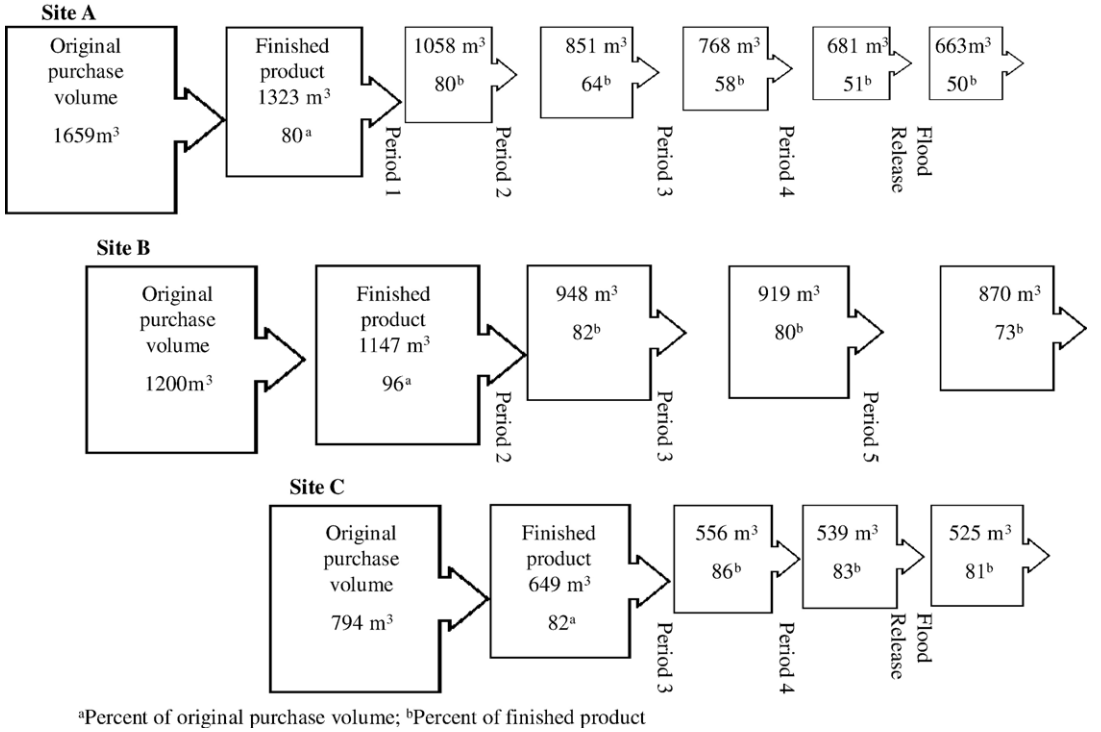

Fig. 13. Volumetric gravel budget for three Chinook salmon spawning enhancement projects in the lower Mokelumne River, California. Time periods are provided in Fig. 3 and Table 2.

erating enough material to compensate annual loss, at least during a period of relatively low and stable flows. LWD collected on the constructed gravel berms for periods of <12 months to >4 years. Merz (2001) concluded that such debris is important to spawning salmon, and these observations suggest that captured LWD may further benefit constructed spawning habitat. LWD budgets have been calculated for several northwestern coastal streams of the U.S. (Martin and Benda, 2001; Benda and Sias, 2003). The importance of this debris has been associated with maintenance of riverine gravel bars and structures (Everest and Meehan, 1981; Sedell et al., 1983). Surprisingly, we were not able to substantiate any LWD budget estimates for California Central Valley streams within the literature. To further benefit SHR sites, an LWD budget (including riparian woody vegetation regeneration) should be addressed (Gippel et al., 1996).

According to Gottesfeld et al. (2004), spawning salmon likely play an integral role in the sediment transport dynamics and annual sediment budget of stream reaches. Using tracer recovery experiments, they found that spawning salmon mobilized sediment only for short distances but were able to mobilize similar depths of bed material as annual floods did. This influence on sediment residence time and turnover frequency has important implications on the quality of the intra-gravel environment and subsequent survival of salmon embryos (Merz et al., 2004). Visible tailspill lengths for Chinook salmon redds in the LMR are typically 1 to 1.5 m in length, although tailspills have been reported as long as 6 m (Merz, unpublished data). This too suggests that while salmon may not necessarily mobilize material completely out of a site, they can have a significant impact on sediment turnover and potentially site morphology. It is possible for a site to have regular turnover and/or throughput of sediment while maintaining a consistent morphology. From a habitat sustainability perspective, the key is that some level of geomorphic dynamism is in place—not necessarily a static morphological habitat feature.

Considering the average gravel placement volume at each site was 1217 m^3, an average female Chinook salmon could rework ~0.2% of an LMR enhancement project. Therefore, 538 spawning female Chinook salmon could potentially rework an entire enhancement site. On average, annual construction at these SHR sites has been 11 redds. Assuming these averages persist, fall-run Chinook salmon might mobilize an entire enhancement site in about 49 years. Changes to the number of naturally spawning LMR salmonids may significantly affect this period. While over the short-term increased

Table 6
Observations of volumetric changes to the channel bed at three spawning gravel enhancment sites in the lower Mokelumne River, California

Site		Original purchase volume (m^3)	DEM error (m^3)	Operational losses (m^3)	Finished product		Duration of monitoring (Days)	Total volume loss	DEM error (m^3)	Mechanisms	Mechanism portion of total volume loss	Remaining volume (m^3)	DEM error (m^3)
					Volume (m^3)	DEM error (m^3)							
A	Actual	1659	±31.52	300 to 363	1323	±25.1	1380	659.9	±12.52			663.1	±12.6
	Percent									Deflation	30% to 160%		
			1.9%	18.1–21.9%	80%	1.9%		49%	2%	Faunal pedoturbation	0% to 15%	51%	1.9%
										Surface scour	8% to 33%		
										Local scour	1.5% to 3.5%		
										Slope angle (slippage)	3.1% to 9.8%		
										Total percent of observed volume loss:	42.1% to 221.3%		
B	Actual	1200	±22.8	25 to 71	1147	±21.79	1118	247.8	±4.71			870.2	±16.5
	Percent		1.9%	2.1–5.9%		1.9%		25%	1.90%	Faunal pedoturbation	0% to 42%	76%	1.9%
										Surface scour	4.5% to 27%		
										Local scour	0.8% to 2.0%		
										Slope angle (slippage)	0.4% to 2.3%		
										Total percent of observed volume loss:	45.7% to 203.3%		
C	Actual	794	±15.1	128 to 158	649	±12.33	650	125.1	±2.38			524.9	±9.9
	Percent									Deflation	40% to 190%		
			1.9%	16.1–19.9%		1.9%		19%	1.90%	Faunal pedoturbation	0% to 36%	81%	1.9%
										Surface scour	5.4% to 32.5%		
										Local scour	0.4% to 0.8%		
										Slope angle (slippage)	0.9% to 2.9%		
										Total percent of observed volume loss:	46.7% to 262.2%		

complexity attracts more spawning fish, shortened habitat lifespan from other forms of site degradation, lack of turnover and/or gravel loss may offset the relative importance of volumetric losses from spawners; may require some balancing between site attractiveness and longevity. In this context, if increased and continued salmon spawning is the goal of a specific spawning gravel enhancement project, is it better to have high spawning activity for a short period of time with short site longevity or low levels of spawning activity over a longer time period with long site longevity? Such a myopic management goal may be inappropriate, and ill-suited to providing habitat sustainability via geomorphic dynamism.

5.1. Management implications

While complexity is an extremely important aspect of ecological function, production of highly diverse and complex habitat features appears to come at a cost to site longevity. River restoration projects tend to provide little (if any) short-term monitoring and then declare success (Wheaton et al., 2004e). Particularly in the regulated river setting, the notion of self-sustainability may have little utility. Sustainability concepts would suggest that building and maintaining specific substrate features are less important than providing environmental processes necessary to rejuvenate new features as older features are destroyed. This includes insuring that mobilized enhancement gravels have the potential to be deposited to form future spawning sites instead of filling large gravel-mining pits downstream.

In highly managed systems with little natural coarse sediment recruitment, complex sites constructed with edges, high velocity chutes, and obstructions such as LWD and boulders will become less complex through time (scour, sinking of boulders, and even salmon erode and simplify site complexity) (Frissell and Nawa, 1992). Practically speaking, without disturbance, complex, organized systems tend to become simple and unorganized. Such disturbance, typically in the form of flood events, is receiving increasing attention as a mechanism for maintaining habitat and biota diversity in large, temperate streams (Huston, 1996; Townsend et al., 1997; Sparks and Spink, 1998). Our observations of tracer rock mobilization, channel cut at placed boulders, and constructed areas of high velocity suggest that complexity may actually reduce life-expectancy of a given enhancement site unless energy (in the form of additional gravel) is added to the site to maintain its complexity. While not a component of this study, Smith et al. (2004) observed an increase in rooted aquatic vegetation at sites A and C during the relatively stable flows of 2001 and 2002. This appeared to reduce spawning activity (Fig. 4). The 2003 study release removed a significant amount of rooted vegetation within the spawning gravel, which appeared to positively correlate with increased spawning use. In regulated systems with flow regimes incapable of supporting geomorphic dynamism, artificial intervention (e.g. gravel augmentation, SHR) may be necessary to prevent sites from returning to simple, degraded habitats over time (Wheaton et al., 2004b).

Numerous authors discuss the importance of habitat heterogeneity to restoration (Harper et al., 1999; Jungwirth et al., 1995). According to Ward and Tockner (2001), re-establishing functional diversity (e.g., hydrologic and successional processes) across the active corridor could serve as the focus of river conservation initiatives. Once functional processes have been reconstituted, habitat heterogeneity will increase, followed by corresponding increased diversity of aquatic and riparian species. Merz and Setka (2004) inferred that the addition of complexity to restoration sites within a highly regulated stream attracted spawning salmon to those sites. Wheaton et al. (2004d) proposed several habitat heterogeneity metrics relevant to spawning salmonids, which seemed to explain the utilization of heterogeneity elements by spawning salmonids. Increased benthic macroinvertebrate production and increased survival of Chinook salmon and steelhead embryos have also been observed (Merz et al., 2004; Merz and Chan, 2005). However, increased heterogeneity, especially in the way of structure and edge, increases erosive power within the site, not only through geomorphological principals (Buffington et al., 2002) but through increased substrate mobilization by increased numbers of spawning fish. For instance, our tracer rock and channel DEM modeling shows increased erosive force where greatest velocities are created or large structures have been placed.

This then begs the question as to whether form or function is the ultimate SHR goal. Unfortunately, creation or enhancement of specific habitats, such as spawning beds, has been interwoven into the false perception that natural aquatic systems are stable entities (Middleton, 1999). This misperception, coupled with the concept that habitat longevity equates to restoration success, may doom many projects to perceived failure. Restoration objectives are commonly based on value-laden societal choices (Davis and Slobodkin, 2004). Thus, if restoration science suggests that continued intervention is the cost of maintaining spawning habitat in a regulated river setting, is society willing to pay the price?

According to Middleton (1999), the perception of natural systems as stable entities may be rooted in human memory and cultural background. Importance of long-term maintenance of stream ecosystem processes should not be misconstrued as longevity of specific channel features, such as gravel berms and bars. In fact, Beechie and Bolton (1999) argued that attempts to build stable habitats may interrupt long-term processes that maintain habitat diversity. Our observations suggest that stable features in such regulated streams as the LMR may actually become less attractive and functional to spawning salmonids over time.

While this study provides some insight into the volumetric budget for site-specific spawning enhancement projects within the LMR spawning reach, it is important to note that our present method does not take into account the sediment deficit from historic mining and channel aggradation caused by flow regulation. Nor does it specifically take scale into account for DEM uncertainties (Wheaton et al., 2004a). According to Kondolf (1998), if changes in dammed rivers because of altered flow and sediment transport are not recognized, restoration designs are likely to be ineffective or inappropriate. Therefore, restoration may be driven by the desire to return to a historical condition, but it should be designed with contemporary processes and realities in mind. Perhaps then, this budget should be supplemented with an appropriate volume of material to restore acceptable channel geometry and to reduce the size and number of abandoned mining pits to satisfactory levels (Kondolf, 1997). This amount of material may be constrained more by fiscal budgets, gravel available, and the societal decisions of what is satisfactory than by geomorphic and hydrologic science. Once these factors are addressed, this volumetric budget might become a more meaningful component of a long-term restoration and management plan.

Acknowledgements

We thank Evan Buckland, Leigh Chan, Molly Cobleigh, Andrew Gilbert, James Jones, Warren Jung, Bert Mulchaey, Catalina Reyes, Matt Saldate, Jose Setka, Jason Shillam, Jim Smith, Brett Valle, Steve Winter, and Michelle Workman for numerous aspects of field data collection. Financial support was provided by East Bay Municipal Utility District, the California Department of Fish and Game, and the United States Fish and Wildlife Service through the Central Valley Project Improvement Act Restoration Funds and as a contracting entity for the CALFED Bay-Delta Ecosystem Restoration Program (Cooperative Agreement DCN# 113322G003).

References

Avery, E.L., 1996. Evaluations of sediment traps and artificial gravel riffles constructed to improve reproduction of trout in three Wisconsin streams. North American Journal of Fisheries Management 16 (2), 282–293.

Barabási, A.-L., Albert, R., Schiffer, P., 1999. The physics of sandcastles: maximum angle of stability in wet and dry granular media. Physica. A 266, 366–371.

Beechie, T.J., Bolton, S., 1999. An approach to restorin salmonid habitat-forming processes in Pacific Northwest watershed. Fisheries 24 (4), 6–15.

Bement, R.A.P., Selby, A.R., 1997. Compaction of granular soils by uniform vibration equivalent to vibrodriving of piles. Geotechnical and Geological Engineering 15, 121–143.

Benda, L., Sias, J., 2003. A quantitative framework for evaluating the wood budget. Journal of Forest Ecology and Management 172 (1), 1–16.

Biron, P.M., 2004. Comparing different methods of bed shear stress estimates in simple and complex flow fields. Earth Surface Processes and Landforms 29 (11), 1403–1415.

Brasington, J., Langham, J., Rumsby, B., 2003. Methodological sensitivity of morphometric estimates of coarse fluvial sediment transport. Geomorphology 53 (3-4), 299–316.

Brasington, J., Wheaton, J.M., Williams, R.D., 2004, Sub-reach scale morphological interpretations from DEM differencing: Accounting for DEM uncertainty. Eos Trans. AGU 85 (47): Fall Meeting Supplement, Abstract H43A-0352.

Brune, G.M., 1953. Trap efficiency of reservoirs. American Geophysical Union 34 (3), 407–418.

Buffington, J.M., Dietrich, W.E., Kirchner, J.W., 1992. Friction angle measurements on a naturally formed gravel streambed: implications for critical boundary shear stress. Water Resources Research 28, 411–425.

Buffington, J.M., Lisle, T.E., Woodsmith, R.D., Hilton, S., 2002. Controls on the size and occurrence of pools in coarse-grained forest rivers. River Research and Applications 18 (6), 507–531.

Bunte, K., Abt, S.R., 2001. Sampling surface and subsurface particle-size distributions in wadable gravel- and cobble-bed streams for analyses in sediment transport, hydraulics and stream bed monitoring. Gen. Tech. Rep. RMRS-GTR-74. RMRS-GTR, vol. 74. U.S. Department of Agriculture, Forest Service, Rocky Mountain Research Station, Fort Colins, CO.

CDFG, 1991. Lower Mokelumne River Fisheries Management Plan. California Department of Fish and Game. Resources Agency, Sacramento, CA.

Chapman, D.W., 1988. Critical review of variables used to define effects of fines in redds of large salmonids. Transactions of the American Fisheries Society 117, 1–21.

Chapman, D.W., 1995. Efficacy of structural manipulations of instream habitat in the Columbia River basin. Rivers 5 (4), 279–293.

Davis, M.A., Slobodkin, L.B., 2004. The science and values of restoration ecology. Restoration Ecology 12 (1), 1–3.

Dietrich, W.E., Dunne, T., Humphrey, N.F., Reid, L.M., 1982. Construction of sediment budgets for drainage basins. In: Swanson, F.J., Jan, R.J., Dunne, T., Swanston, D.N. (Eds.), Sediment Budgets in Forested Drainage Basins. Tech. Rep. PNW-141. United States Forest Service, Portland, OR.

Everest, F.H., Meehan, W.R., 1981. Forest management and anadromous fish habitat productivity. In: Sabol, K. (Ed.), Transactions of the 46th North American Wildlife and Natural Resources Conference, Washington, DC.

FISRWG, 1998. Stream Corridor Restoration: Principles, Processes, and Practices. GPO Item No. 0120-A. Federal Interagency Stream Restoration Working Group, Washington D.C.

Frissell, C.A., Nawa, R.K., 1992. Incidence and causes of physical failure of artificial habitat structures in streams of Western Oregon and Washington. North American Journal of Fisheries Management 12, 182–197.

Fuller, I.C., Large, A.R.G., Charlton, M.E., Heritage, G.L., Milan, D.J., 2003. Reach–Scale sediment transfers: an evaluation of two morphological budgeting approaches. Earth Surface Processes and Landforms 28, 889–903.

Gauss, C.F., 1831. Besprechung des Buchs von L. A. Seeber: intersuchungen über die Eigenschaften der positiven ternären quadratischen Formen usw. Göttingsche Gelehrte Anzeigen 2, 188–196.

Geist, D.R., Dauble, D.D., 1998. Redd site selection and spawning habitat use by fall chinook salmon: the importance of geomorphic features in large rivers. Environmental Management 22 (5), 655–669.

Gilvear, D.J., Bradley, S., 1997. Geomorphic adjustment of a newly engineered, ecologically sound upland gravel bed river diversion: Evan Water, Scotland. Regulated Rivers: Research and Management 13 (2), 1–13.

Gilvear, D.J., Heal, K.V., Stephen, A., 2002. Hydrology and the ecological quality of Scottish river ecosystems. Science of the Total Environment 294 (1-3), 131–159.

Gippel, C.J., O'Neill, I.C., Finlayson, B.L., Schnatz, I., 1996. Hydraulic guidelines for the reintroduction and management of large woody debris in lowland rivers. Regulated Rivers: Research and Management 12, 223–236.

Goldberg, M., 1971. On the densest packing of equal spheres in a cube. Mathematics Magazine 44, 199–208.

Gottesfeld, A.S., Hassan, M.A., Tunnicliffe, J.F., Poirer, R.W., 2004. Sediment dispersion in salmon spawning streams: the influence of floods and salmon redd construction. Journal of the American Water Resources Association 40 (4), 1071–1086.

Handin, J., 1966. Handbook of Physical Constants, Strength and Ductility. The Geological Society of America Memoir, vol. 97. New York, NY. 587 pp.

Harper, D.M., Ebrahimnezhad, M., Taylor, E., Dickinson, S., Decamp, O., Verniers, G., Balbi, T., 1999. A catchment-scale approach to the physical restoration of lowland UK rivers. Aquatic Conservation-Marine and Freshwater Ecosystems 9 (1), 141–157.

Hole, F.D., 1961. A classification of pedoturbation and some other processes and factors of soil formation in relation to isotropism and anisotropism. Soil Science 91, 375–377.

Holmes, K.W., Chadwick, O.A., Kiriakidis, P.C., 2000. Error in a USGS 30-meter digital elevation model and its impact on terrain modeling. Journal of Hydrology 233, 154–173.

House, R., 1996. An evaluation of stream restoration structures in a coastal Oregon Stream, 1981–1993. North American Journal of Fisheries Management 16 (2), 272–281.

Huston, M.A., 1996. Biological Diversity: The Coexistence Of Species on Changing Landscapes. Cambridge University Press, NY. 681 pp.

Ingles, O.G., Grant, K., 1975. The effects of compaction on various properties of coarse-grained sediments. In: Chilingarian, G.V., Wolf, K.H. (Eds.), Developments in Sedimentology 18A, Compaction of Coarse-Grained Sediments: I. Elsevier Scientific Publishing Company, New York, NY, pp. 293–348.

Jungwirth, M., Muhar, S., Schmutz, S., 1995. The effects of recreated instream and ecotone structures on the fish fauna of an epipotamal river. Hydrobiologia 303 (1–3), 195–206.

Kirchner, J.W., Dietrich, W.E., Iseya, F., Ikeda, H., 1990. The variability of critical shear stress, friction angle, and grain protrusion in water-worked sediments. Sedimentology 37, 647–672.

Kondolf, G.M., 1997. Hungry water: effects of dams and gravel mining on river channels. Environmental Management 21 (4), 533–551.

Kondolf, G.M., 1998. Lessons learned from river restoration projects in California. Aquatic Conservation-Marine and Freshwater Ecosystems 8 (1), 39–52.

Kondolf, G.M., 2000. Some suggested guidelines for geomorphic aspects of anadromous salmonid habitat restoration proposals. Restoration Ecology 8 (1), 48–56.

Kondolf, G.M., Wolman, M.G., 1993. The sizes of salmonid spawning gravels. Water Resources Research 29 (7), 2275–2285.

Kondolf, G.M., Vick, J.C., Ramirez, T.M., 1996. Salmon spawning habitat rehabilitation on the Merced River, California: an evaluation of project planning and performance. Transactions of the American Fisheries Society 125 (6), 899–912.

Konrad, C.P., Booth, D.B., Burges, S.J., Montgomery, D.R., 2002. Partial entrainment of gravel bars during floods. Water Resources Research 38 (7), 1–16.

Kuhnle, R.A., Alonso, C.V., Shields, F.D., 2002. Local scour associated with angled spur dikes. Journal of Hydraulic Engineering 128 (12), 1087–1093.

Lane, S.N., Chandler, J.H., 2003. Editorial: the generation of high quality topographic data for hydrology and geomorphology: new data sources, new applications and new problems. Earth Surface Processes and Landforms 28 (3), 229–230.

Martin, D., Benda, L., 2001. Patterns of in-stream wood recruitment and transport at the watershed scale. Transactions of the American Fisheries Society 130, 940–958.

Merz, J.E., 2001. Association of fall-run chinook salmon redds with woody debris in the lower Mokelumne River, California. California Fish and Game 87 (2), 51–60.

Merz, J.E., 2004, Spawning Habitat Enhancement For Pacific Salmon (*Oncorhynchus* spp.) In A Regulated River. PhD Dissertation Thesis, University of California at Davis, 190 pp.

Merz, J.E., Chan, L.K., 2005. Effects of gravel augmentation on macroinvertebrate assemblages in a regulated California river. River Research and Applications 21, 61–74.

Merz, J.E., Setka, J.D., 2004. Evaluation of a spawning habitat enhancement site for chinook salmon in a regulated California river. North American Journal of Fisheries Management 24, 397–407.

Merz, J.E., Setka, J.D., Pasternack, G.B., Wheaton, J.M., 2004. Predicting benefits of spawning-habitat rehabilitation to salmonid (*Oncorhynchus* spp.) fry production in a regulated California river. Canadian Journal of Fisheries and Aquatic Sciences 61 (8), 1433–1446.

Middleton, B., 1999. Wetland Restoration, Flood Pulsing, and Disturbance Dynamics. John Wiley and Sons, New York.

Milhous, R.T., 2001. Specific weight and median size of the bed material of gravel and cobble rivers. Proceedings of the Seventh Federal Interagency Sedimentation Conference, Reno, NV.7, vol. 1, pp. III70–III77.

Muder, D.J., 1993. A new bound on the local density of sphere packings. Discrete Computational Geometry 10, 351–375.

Mutz, M., 2000. Influences of woody debris on plow patterns and channel morphology in a low energy, sand-bed stream reach. International Review of Hydrobiology 85 (1), 107–121.

Nelson, J.M., Schmeeckle, M.W., Shreve, R.L., 2000. Turbulence and Particle Entrainment. In: Nolan, T.J., Thorne, C.R.(Eds.), Gravel-Bed Rivers 2000. A Special Publication of the New Zealand Hydrological Society. University of Canterbury.

Osmundson, D.B., Ryel, R.J., Lamarra, V.L., Pitlick, J., 2002. Flow–sediment–biota relations: implications for river regulation effects on native fish abundance. Ecological Applications 12 (6), 1719–1739.

Paintal, A.S., 1971. Concept of critical shear stress in loose boundary open channels. Journal of Hydraulic Research 9 (1), 91–113.

Pasternack, G.B., Wang, C.L., Merz, J.E., 2004. Application of a 2D hydrodynamic model to design of reach–scale spawning gravel replenishment on the Mokelumne River, California. River Research and Applications 20 (2), 202–225.

Reid, L.M., Dunne, T., 1996. Rapid evaluation of sediment budgets. Catena Supplement.. GeoEcology Paperbacks. Resikrchen, Germany.

Rogers, C.A., 1958. The packing of equal spheres. Proceedings of the London Mathematical Society 8, 609–620.

Rosenfeld, J.S., Huato, L., 1993. Relationship between large woody debris characteristics and pool formation in small coastal British Columbia streams. North American Journal of Fisheries Management 23 (3), 928–938.

Sall, J., Lehman, A., Creighton, L., 2001. JMP Start Statistics. A Guide to Statistics and Data Analysis. Duxbury, Pacific Grove, CA.

Scheeler, C.A., 1990. Umatilla river basin, anadromous fish habitat enhancement project. Annual report 1989. Report to the US. Department of Energy. Order Number: DE92003443/GAR, Confederated Tribes of the Umatilla Indian Reservation, Pendleton, OR.

Sear, D.A., 1996. Sediment transport processes in pool-riffle sequences. Earth Surface Processes and Landforms 21 (3), 241–262.

Sedell, J.R., Yuska, J., Speker, R., 1983. Study of westside fisheries in Olympic National Park, Washington. Final Report. CX-9000-0-E 081. National Park Service.

Setka, J.D., 2002. Fall-run chinook salmon and steelhead trout spawning survey, September 2001 through March 2002 Mokelumne River, California. Mimeo Report. East Bay Municipal Utility District, Orinda, CA.

Shields, A., 1936. Application of similarity principles and turbulence research to bedload movement, (translated from Anwendung der Achnlichkaitsmechanik und der Turbulenzforschung auf die Geschiebewegung: Mittei-lung Preussischen Versuchanstalt fur Wasserbau und Schiffbau, Berlin, No. 26, by W.P. Ott and J.C. von Uchelen). report no. 167. California Institute of Technology Hydro-dynamics, Pasadena.

Shields, F.D., Knight, S.S., Cooper, C.M., 2000. Cyclic perturbation of lowland river channels and ecological response. Regulated Rivers: Research and Management 16, 307–325.

Smith, R.D., Beschta, R.L., 1994. A mechanism of pool formation and maintenance in forest streams, Hydraulic engineering '94. Proceedings of the 1994 Conference. American Society of Civil Engineers, New York, NY, pp. 824–828.

Smith, J.R., Merz, J.E., Workman, M.L., 2004. Effect of a controlled flow release on rooted aquatic vegetation in Chinook salmon spawning habitat in the lower Mokelumne River, California. Mimeo Report, East Bay Municipal Utility District. Fisheries and Wildlife Division, Lodi, CA.

Sparks, R.E., Spink, A., 1998. Disturbance, succession and ecosystem processes in rivers and estuaries: effects of extreme hydrologic events. Regulated Rivers: Research and Management 14 (2), 155–159.

Steinhaus, H., 1999. Mathematical Snapshots, 3rd edition. Dover Publications, New York. 202 pp.

Townsend, C.R., Scarsbrook, M.R., Doledee, S., 1997. The intermediate disturbance hypothesis, Refugia, and biodiversity in streams. Limnology and Oceanography 42 (5), 938–949.

Vaithiyanathan, P., Ramanathan, A., Subramanian, V., 1992. Sediment transport in the Cauvery River basin: sediment characteristics and controlling factors. Journal of Hydrology 139, 197–210.

Vronskiy, B.B., 1972. Reproductive biology of the Kamchatka River chinook salmon. Journal of Ichthyology 12, 259–273.

Waldichuk, M., 1993. Fish habitat and the impact of human activity with particular reference to Pacific salmon. Perspectives on Canadian marine fisheries management. Canadian Bulletin of Fisheries and Aquatic Sciences, 295–337.

Ward, J.V., Tockner, K., 2001. Biodiversity: towards a unifying theme for river ecology. Freshwater Biology 46, 807–819.

Wheaton, J.M., 2003, Spawning Habitat Rehabilitation. M.S. Thesis Thesis, University of California at Davis, 223 pp.

Wheaton, J.M., Brasington, J., Williams, R.D., 2004a. Modeling fluvial sediment budgets under uncertainty, Eos Trans. AGU, 85 (47): Fall Meeting Supplement, Abstract H53C-1264.

Wheaton, J.M., Pasternack, G.B., Merz, J.E., 2004b. Spawning habitat rehabilitation:II. Using hypothesis testing and development in design, Mokelumne River, California, USA. International Journal of River Basin Management 2 (1), 21–37.

Wheaton, J.M., Pasternack, G.B., Merz, J.E., 2004c. Spawning habitat rehabilitation-I. Conceptual approach and methods. International Journal of River Basin Management 2 (1), 3–20.

Wheaton, J.M., Pasternack, G.B., Merz, J.E., 2004d. Use of habitat heterogeneity in salmonid spawning habitat rehabilitation design. In: Garcia, D., Martinez, P.V. (Eds.), Fifth International Symposium on Ecohydraulics: Aquatic Habitats: Analysis and Restoration. IAHR-AIRH, Madrid, Spain, pp. 791–796.

Wheaton, J.M., Sear, D.A., Darby, S.E., Milne, J.A., 2004e. The International River Restoration Survey. Internet URL. http: // www.geog.soton.ac.uk/ users/WheatonJ/ Restoration Survey Cover asp›.

Wilcock, P.R., 1996. Estimating local bed shear stress from velocity observations. Water Resources Research 32 (11), 3361–3366.

Wilcock, P.R., 1997. The components of fractional transport rate. Water Resources Research 33 (1), 247–258.

Workman, M.L., 2003. Lower Mokelumne River upstream fish migration monitoring Conducted at Woodbridge Irrigation District Dam. August 2002 through July 2003, East Bay Municipal Utility District, Lodi, CA.

Yoshiyama, R.M., Fisher, F.W., Moyle, P.B., 1998. Historical abundance and decline of chinook salmon in the Central Valley region of California. North American Journal of Fisheries Management 18, 487–521.

Zar, J.H., 1996. Biostatistical Analysis. Prentice Hall, Upper Saddle River, NJ.

Title: Backwater Control on Riffle-Pool Flow Pattern, Fish Habitat Quality, and Sediment Transport Regime

Authors: Michael K. Bounrisavong, Kaushal K. Parikh and Gregory B. Pasternack*

Address: Department of Land, Air, and Water Resources, University of California, One Shields Avenue, Davis, CA 95616.

Abstract

2D hydrodynamic models accurately predict patterns of physical habitat for spawning salmon at the 0.1-10 m scale. Using this capability, the effects of downstream water surface elevation (WSE), discharge, and riffle configuration on physical habitat quality and sediment transport regime were analyzed for 18 combinations of variables through numerical experimentation. Downstream WSEs mimicked backwater, uniform, and accelerating conditions normally controlled by downstream riffle morphology. Discharges included a fish-spawning flow, summer fish-attraction flow, and a snowmelt pulse. The key finding was that riffle-pool units require backwater conditions to have a significant area of high-quality spawning habitat. Backwater conditions also delay the onset of full bed mobility. The assumption of steady, uniform flow is inappropriate for gravel rivers whose non-uniformity controls spatial patterns of habitat and sediment transport. A "reverse domino" mechanism for catastrophic failure of sequences of riffles and pools that relies on downstream WSE effects on riffles is proposed.

Keywords: backwater effect; non-uniform flow; riffle-pool processes; river restoration; habitat enhancement; 2D modeling

1 Introduction

River restoration is one of the most rapidly growing professional practices in hydrology in the United States and worldwide today [*Bernhardt et al.*, 2005]. In arid and semi-arid regions where dams and channelization have degraded in-stream hydro-geomorphic functioning [*Kondolf*, 1997; *Brandt*, 2000], river restoration involves flow re-regulation to mimic the pre-dam hydrologic regime [*Webb et al.*, 1999; *Trush et al.*, 2000] and/or channel rehabilitation to naturalize hydraulic geometry [*Wheaton et al.*, 2004a]. Although pristine alluvial rivers show interdependence between flow regime and channel form [*Wolman and Miller*, 1960, *Leopold et al.*, 1964], the only major tests of the hypothesis that flow re-regulation alone can induce channel rehabilitation without direct intervention did not yield the predicted beneficial outcomes [*Melis et al.*, 2004; *Draut and Rubin*, 2005]. In many instances, channelization below dams, vegetation encroachment, excessive sedimentation at tributary junctions, or insufficient coarse sediment supply limit the potential effectiveness of re-regulated flows in producing significant channel change. Consequently, river rehabilitation methods capable of transforming a channelized reach lacking in ecosystem functions into a suitable channel form appears to be a necessary pre-cursor for flow re-regulation and coarse sediment augmentation on many regulated rivers. For example, levee removal was found to be an effective method for restoring floodplain topographic complexity, re-establishing stands of riparian vegetation, and expanding juvenile fish habitat by enabling floodplain access for even small floods [*Florshein and Mount*, 2003]. Further, significant ecological benefits of spawning habitat rehabilitation in gravel-bed reaches below dams without any flow re-regulation have been observed for benthic macro invertebrates [*Merz and Ochikubo Chan*, 2005], Chinook spawners [*Wheaton et al.*, 2004c], and Chinook fry [*Merz*

et al., 2004].

Three paradigms exist for designing and testing alternative channel forms for river rehabilitation projects prior to implementation. The most widely used method is the "applied river morphology" approach [*Rosgen*, 1997, *Shields et al.*, 2003] in which steady, uniform hydraulics equations are coupled with empirical equations from reference reaches to obtain channel cross-section shapes, reach slopes, and planform sinuosities as well as section-averaged sediment transport and habitat quality expectations. Recognizing the important role of channel non-uniformity common to natural gravel-bed river morphology, an alternative approach has been developed by coupling 3D digital elevation modeling, computer aided engineering design, and 2D depth-averaged hydrodynamic modeling together with analytical and empirical equations governing sediment transport regime and habitat quality [*Pasternack et al.*, 2004; *Wheaton et al.*, 2004a,b]. So far this approach has only been thoroughly evaluated for use in designing channel forms appropriate for Pacific salmon spawning in Central Valley, California, but exchanging spawning habitat functions for other ecosystem services or switching from a 2D to 3D model would be straightforward. Finally, physical modeling has been used to re-create scaled down versions of designs to observe 3D hydrodynamic and sediment transport processes in detail [*Loftin*, 1991; *Thompson*, 2005], providing the best conceptual insight of likely outcomes. Each of these approaches has its advantages and disadvantages, and it is too soon for a scientific consensus to emerge over their use.

In this study basic research was undertaken to further explore the significance of channel non-uniformity on physical habitat conditions and sediment transport regimes associated with

regulated gravel-bed riffle-pool units (Fig. 1). The objectives were to 1) assess the consequences of backwater, uniform, or accelerating hydrodynamics on physical habitat and sediment transport regimes in gravel-bed, riffle-pool channel units, 2) assess how the consequences of these hydrodynamics vary as a function of discharge, and 3) assess how the consequences from objectives 1 and 2 vary between a typical flat riffle with a notched crest and a steep diagonal riffle (Table 1). In river rehabilitation, the hydrodynamic regimes evaluated in objective 1 may be controlled by manipulating the crest elevation of the downstream riffle. The importance of this study is that it demonstrates the primacy of 3D channel non-uniformity in riffle-pool functionality and strongly questions the common practice of assuming uniform flow conditions in most gravel-bed river rehabilitation studies and basic scientific studies of sediment transport processes in gravel-bed rivers.

2 Experimental Design:

The overall approach used to assess riffle-pool response to downstream water surface elevation (WSE) was to conduct numerical modeling of a test reach manipulated to simulate 3 WSEs, 3 discharges, and 2 riffle-pool configurations (Tables 1,2). The selected test reach was a pool-riffle-pool sequence on the regulated Trinity River below Lewiston Dam, but its experimental configurations were artificially changed to provide the desired topography. System response was evaluated in terms of flow pattern, fish habitat, and sediment transport regime. Specific methods were previously well developed [*Pasternack et al.*, 2004; *Wheaton et al.*, 2004a, b], but in those cases, no attempt was made to evaluate multiple downstream WSEs or discharges. Downstream WSE was hypothesized to be very important for pool-riffle

functioning, because it is an intermediate variable that can be manipulated in rehabilitation or by natural processes, and in turn it controls channel hydraulics, fish habitat, and sediment transport regime. The three discharges assessed range from low-flow fish spawning conditions to the highest observed flow release during the study period at the test site.

2.1 Test Site

The 1,864-km^2 Trinity River basin above Lewiston is in the Klamath Mountain Province in Northwestern California. Trinity Dam was built in 1962, with Lewiston Dam built 13 km downstream shortly after to aid trans-basin diversions. Below Lewiston Dam, the channel-floodplain complex has been diminished to ~30% of its original width due to emplacement of a high terrace with a fish hatchery. The channel is pinned along the bedrock valley wall and its bed is heavily armored (Fig. 1). The river supports 18 fish species, including nine anadromous ones. By 1980, 80-90 % of salmonid habitat was lost [*USFWS*, 1999]. Chinook, coho, and steelhead salmon populations have been reduced to 67, 96, and 53% of pre-dam averages and consequently it is these species that are the focus of restoration efforts. The test reach has been altered multiple times over the decades by gravel augmentations and hydraulic structure placement.

As part of a river rehabilitation project using the Spawning Habitat Integrated Rehabilitation Approach (SHIRA) [*Wheaton et al.*, 2004a], the 760-m reach below Lewiston Dam was surveyed (point density of ~1.3 m^{-2}) and a baseline digital terrain model (DTM) developed. After a detailed pre-project characterization, 6 alternative channel configurations were designed and evaluated [details at http://shira.lawr.ucdavis.edu/trinity_designconcepts.htm] with the aid of Autodesk Land Desktop 3 using the approach of *Wheaton et al.* [2004b]. For this

study, design 4 was used as the starting template for developing 2 significantly different scientific test configurations of a single pool-riffle-pool sequence. Only one of the three riffles in the design-4 reach was used in order to limit the amount of data analysis necessary. One pool-riffle-pool sequence is sufficient to test the central hypothesis of this study, because any significant role for channel non-uniformity uncovered in this test case refutes the null hypothesis that riffle-pool rehabilitation can universally ignore channel non-uniformity. Other on-going studies are seeking to understand the interactions of longer sequences of rehabilitated channel units.

The first pool-riffle-pool configuration consisted of a transverse riffle with a 0.122 m high riffle crest above a notch and ~18 m across (Fig. 2a). Riffle notches are natural and useful features for bypassing flow to protect the riffle crest, but their design has yet to be fully evaluated. The upstream pool was in the middle of the channel with a riverbed elevation of 559.70 m (NAVD88 datum). The bed transitions to the riffle crest with a gradual slope of 0.00007 m m^{-1}. The riffle crest and notch were ~22-m long. The riffle exit had a steeper slope 0.0108 m m^{-1} from the riffle as it transitions into the downstream pool located in the middle of the channel at a bed elevation of 559.31 m. The overall bed slope was 0.0056 m m^{-1}, which is typical of good riffle conditions for salmon spawning habitat.

The second pool-riffle-pool configuration consisted of a slender, steep diagonal bar (Fig. 2b). The upstream pool bed elevation was 559.765 m. Then, the bed gradually slopes up the bar to a riffle crest elevation of 560.070 m with a riverbed slope estimated to be 0.0263 m m^{-1}. The length of the diagonal bar is about 57.2 m and 15.8 m across at the middle of the channel. Following the crest, there is a steep slope of 0.1407 m m^{-1} into a flat downstream pool at 559.308 m. The overall bed slope was 0.0059 m m^{-1}, which was very close to that of the notched,

transverse riffle, even though the two configurations were significantly different by any other measure.

2.2 Numerical Model

A 2-D hydrodynamic model, Finite Element Surface Water Modeling System 3.1.5 (FESWMS), was used to simulate the flow pattern and predict the fish habitat quality and sediment transport regime of the 2 test configurations [*Pasternack et al.*, 2004]. FESWMS solves the vertically integrated conservation of momentum and mass equations using a finite element method to acquire depth-averaged 2D velocity vectors and water depths at each node in a finite element mesh. The model is capable of simulating both steady and unsteady 2-D flow as well as subcritical and supercritical flows. The basic governing equations for vertically integrated momentum in the x- and y- directions under the hydrostatic assumption are given by

$$\frac{\partial}{\partial t}(HU)+\frac{\partial}{\partial x}(\beta_{uu}HUU)+\frac{\partial}{\partial y}(\beta_{uv}HUV)+gH\frac{\partial z_b}{\partial x}+\frac{1}{2}g\frac{\partial H^2}{\partial x} + \frac{1}{\rho}[\tau_x^b-\frac{\partial}{\partial x}(H\tau_{xx})-\frac{\partial}{\partial y}(H\tau_{xy})]=0 \quad (1a)$$

and

$$\frac{\partial}{\partial t}(HV)+\frac{\partial}{\partial x}(\beta_{vu}HVU)+\frac{\partial}{\partial y}(\beta_{vv}HVV)+gH\frac{\partial z_b}{\partial y}+\frac{1}{2}g\frac{\partial H^2}{\partial y} + \frac{1}{\rho}[\tau_y^b-\frac{\partial}{\partial x}(H\tau_{yx})-\frac{\partial}{\partial y}(H\tau_{yy})]=0, \quad (1b)$$

respectively, where H is the water depth, U and V are the depth-averaged velocity components in the horizontal x- and y- directions, z_b is the bed elevation, β_{uu}, β_{uv}, β_{vu}, and β_{vv} are the momentum correction coefficients that account for the variation of velocity in the vertical direction, τ^b_x and τ^b_y are the bottom shear stresses acting in the x- and y-directions, respectively,

and τ_{xx}, τ_{xy}, τ_{yx} are the τ_{yy} shear stresses caused by turbulence. Conservation of mass in two-dimensions is given by

$$\frac{\partial H}{\partial t} + \frac{\partial}{\partial x}(HU) + \frac{\partial}{\partial y}(HV) = 0. \quad (2)$$

Discretization and other details for solving the above equations using FESWMS is presented in *Froehlich* [1989], and is not reproduced here.

This model has previously been heavily validated for use in shallow gravel bed rivers, with poor predictions primarily occurring around large woody debris [*Pasternack et al.*, 2004; *Wheaton et al.*, 2004b, *Pasternack et al.*, in press]. FESWMS was implemented using Surface Water Modeling System v. 8.1 graphical user interface (EMS-I, South Jordan, UT). The computational meshes for the notched and diagonal riffle scenarios had a typical internodal distance of 1.37 m. To run the model, a discharge at the upstream boundary and water surface elevation at the downstream boundary are required. The flow release regime for Lewiston Dam was used to select appropriate discharges for spawning (8.5 cumecs), summer fish attraction (70.8 cumecs), and peak flood (170 cumecs) conditions. To reduce model instability associated with mesh-element wetting and drying at a threshold of 9-cm depth, meshes were iteratively trimmed to exclude dry areas, yielding slightly different final meshes for each discharge and each riffle configuration.

The two primary model parameters in FESWMS are bed roughness as approximated using Manning's n and eddy viscosity (E). A typical rehabilitated-riffle bed roughness for gravel with d_{50}~50 mm of n=0.043 was used in this study [*Pasternack et al.*, 2004]. Instead of using a constant E, the Boussinesq assumption was used to determine the eddy viscosity internally according to E=0.6·H·u^*, with an additional, minimized E_0 necessary for model stability [*Fisher et al.*, 1979]. The resulting range of E values was checked against field-based estimates using

depth and velocity measurements taken in the real reach at the spawning discharge and found to be similar (~0.02-0.1 $m^2 s^{-1}$).

In this study FESWMS was used primarily to obtain a conceptual understanding of how a gravel bed river would behave under the test conditions. Nevertheless, acceptance of the numerical experimentation approach requires reasonable confidence in the predictive utility of FESWMS for the conditions found at the test site. A baseline analysis of 2D model validity for this reach is available for 12.9 cumecs from the detailed pre-project characterization that was done prior to actual river rehabilitation design, but is beyond the scope of this study. Predictions at two cross-sections show the typical results, with depths accurately predicted and downstream velocities predicted less well (Fig. 3). Spatial gradients in downstream velocity were not predicted as strongly as they actually occurred, but at many spots velocity magnitude was very accurately predicted. This reasonable predictive capability illustrates the strengths and weaknesses of FESWMS along lines previously reported [*Pasternack et al.*, 2004]. Models such as FESWMS are best viewed as uncertain conceptual guides of likely outcomes, rather than literal truth.

2.3 Flow Experiments

To compare and contrast two different channel configurations with three different flow rates and three different downstream WSEs, a total of 18 simulations were performed (Table 2). The spawning flow was assessed for flow, habitat, and sediment transport patterns, while the fish-attraction and flood flows were assessed for those patterns excluding habitat. The model's downstream boundary was located in the pool upstream of the next riffle. Its WSE corresponds with the level that could be imposed by the design of that next riffle. The downstream WSE was

varied to achieve backwater, uniform and accelerating (subcritical) flow conditions. The WSE associated with backwater conditions was the same for both riffle configurations, and it was exactly the WSE predicted for that location in rehabilitation design 4 when the entire Lewiston Dam reach was modeled using the observed stage-discharge relation at the end of that long reach. In that design the next riffle crest had a bed elevation of 559.674 m. For both configurations, the uniform-flow WSE at the downstream cross-section was obtained using

$$Q = \frac{1.0}{n} A R_h^{2/3} S_0^{1/2} \quad (3)$$

where Q is discharge, n is Manning's coefficient for bed roughness, A is the downstream cross-sectional area, R_h is the hydraulic radius, and S_0 is the channel slope extracted from the DTM. The defining equation for the Froude number (Fr) was used to determine critical depth and from that the critical WSE. The downstream WSE associated with a subcritical accelerating flow was taken as the halfway WSE between those for uniform and critical flows, just as a representative case for this regime.

2.4 Fish Habitat Quality

Habitat quality predictions were made by extrapolating 2D model flow results through independent habitat suitability curves for depth and velocity that were developed locally for the Trinity River for Chinook, steelhead, and coho in the spawning and rearing life-stages [*USFWS* 1999]. No substrate quality curve was used, because in spawning habitat rehabilitation, ideal substrate sizes for spawning are placed everywhere, so that factor is not limiting. The final global habitat suitability index (GHSI) was calculated as the geometric mean of the depth and velocity indices [*Pasternack et al.*, 2004]. To account for model uncertainty, GHSI values were lumped into broad classes, with GHSI = 0 as non habitat, 0 < GHSI < 0.1 as very poor habitat, 0.1 <

GHSI < 0.4 as low quality, 0.4 < GHSI < 0.7 as medium quality, and 0.7 < GHSI < 1.0 as high quality [*Leclerc et al.*, 1995]. These broad classes help reduce the impact of velocity prediction error, since they are largely insensitive to ~0-25 % error, which is the typical accuracy observed for the 2D model of the test site.

2.5 Sediment Transport Regime

Shields stress was calculated at each node in the model to evaluate the sediment transport regime, which can be used to predict channel stability under different flow conditions. Previous validation of FESWMS for predicting shear velocity under similar simulation conditions found that ~60% of model predictions were within the 95% confidence limit of field-measured estimates [*Pasternack et al.*, in press]. The constant, narrow width imposed by the hatchery constriction precluded the likelihood of designing riffle-pool units that would be self-sustainable according to the new flow-convergence routing hypothesis of *McWilliams et al.* [submitted]. To obtain Shields stress, shear velocity and shear stress were first calculated using the model-predicted depth and depth-averaged velocity in the Prandtl - Karmen velocity distribution equation:

$$u^* = \frac{U}{5.75\log\left(\frac{12.2H}{2d_{90}}\right)} \text{ and } \tau^b_v = \rho_w \cdot u^{*2} \qquad (4,5)$$

where d_{90} is the size that 90% of the bed material is smaller than, τ^b_v is bed shear stress in the direction of the velocity vector, and ρ_w is water density. Shear stress was converted to non-dimensional Shields stress and used to predict the sediment transport according to

$$\tau^* = \frac{\tau_v^b}{(\gamma_s - \gamma_w)d_{50}} \quad (6)$$

where τ^* is Shields stress, d_{50} is median grain size, γ_s is sediment's specific weight, and γ_w is water's specific weight. *Lisle et al.* [2000] defined the sediment transport regimes relative to τ^* as $\tau^* < 0.01$ corresponds to no transport, $0.01 < \tau^* < 0.03$ corresponds to intermittent entrainment, $0.03 < \tau^* < 0.06$ corresponds to *Wilcock's* [1996] "partial transport", $0.06 < \tau^* < 0.10$ represent full transport, and greater than 0.10 is considered channel-altering conditions.

3 Results

The results are organized by test metric, with each subsection containing an overview paragraph and then detailed analyses by WSE, riffle configuration, and discharge. Model simulations showed significant differences in hydrodynamic, spawning habitat quality, and Shields stress distributions for the different flow conditions and topographies evaluated. The key finding is that different downstream water surface elevations controlled by the design crest elevation of the downstream riffle yielded significantly different habitat conditions and sediment transport regimes.

Key results are presented below to summarize the large amount of data generated in the 18 simulations and associated data analyses. For the sake of brevity, only the Chinook spawning habitat results are presented. Fry habitat for all species was limited to channel margins that were always present and showed little interesting variation. Steelhead spawning habitat results mimicked those of Chinook, but GHSI values were lower due to the preference of steelhead for lower velocities.

3.1 Downstream Water Surface Elevations

Iterative calculations for downstream WSEs associated with uniform and accelerating conditions differed greatly from those for backwater conditions (Table 2). For example, for the notched, transverse riffle at spawning flow, the estimated downstream WSE assuming uniform flow was 0.42 m lower than that for the expected backwater condition. The decrease in downstream WSE to get halfway to the critical value was only an additional 0.07 m. For the diagonal bar experiment, the corresponding values were 0.55 m and 0.06 m. At the highest discharge, the difference increased to 0.76 m and 0.23 m for the notched, transverse riffle and 0.88 and 0.22 m for the diagonal bar. The enhanced deviation from uniform flow at higher discharge indicates that channel non-uniformities exert more backwater effect at higher discharge. Since the bed is already underwater, the at-at-station hydraulic geometry changes at the next downstream riffle crest responsible for this must involve a channel width constriction.

3.2 Physical Habitat

Corresponding with a decrease in downstream WSEs, the spatial distribution of medium and high quality spawning habitat for Chinook salmon changed significantly. Habitat quality deterioration mainly occurred downstream of the riffle crest, indicating that the riffle crest elevation was controlling the hydrodynamics in the upstream pool, even with the downstream backwater condition imposed (Fig. 4). A similar response was observed in both riffle configurations, but with the notched, transverse riffle showing the more significant change. Overall, in the notched, transverse riffle configuration, the area of high- and medium-quality habitat decreased from 33 and 57 % of total area to 15 and 41 % of total area, respectively, as the flow conditions changed from backwater to uniform (Fig. 5). By further reducing the

downstream WSE to yield accelerating flow, an additional 1.4 and 3.6 % decrease in high- and medium-quality habitat area was observed, respectively. In contrast, for the diagonal bar riffle configuration, transition from backwater to uniform flow conditions yielded no change in the area of high (22 %) and medium (~50 %) quality habitat. There was a net decrease of 9 % in the area of medium-quality habitat when the downstream flow was accelerating. Although this change from uniform to accelerating conditions was more significant than for the notched, transverse riffle configuration, the difference in spatial distribution was more similar for accelerating and uniform than when compared with backwater flow conditions. As a result of overall decrease in high- to medium-quality habitat, low- to poor-quality habitat had substantially increased for both riffle configurations.

In the notched, transverse riffle configuration at spawning discharge with a downstream backwater condition, high-quality spawning habitat occurred in the channel margins and just downstream of the notch. These areas corresponded to depths of 0.23-0.61 m and velocities of 0.32-0.61 m s^{-1}. Depths and velocities with wider ranges of 0.21-0.91 m and 0.12-0.91 m s^{-1} yielded medium-quality habitat for most of the channel except for the region along the notch and the riffle crests, where excessive velocities of ~1 m s^{-1} yielded low-quality habitat conditions. Low-quality habitat was also observed further downstream on the lower bank after the notch, and this was attributed to the near stagnant velocities < 0.15 m s^{-1}.

When the downstream WSE at spawning discharge was decreased to uniform or accelerating flow, the similarities between the habitat distributions ended downstream of the riffle crest. The surface area of the flow decreased by 310 and 213 m^2 for uniform and accelerating flows, respectively, from the original 3330 m^2. The spawning-habitat quality deteriorated as water moved downstream from the notch with low-quality habitat extending itself

further downstream and covering a much larger area for uniform and accelerating flow conditions. In these areas, the water got faster and shallower as the maximum depth decreased to 0.610 m with increased velocities of 0.76-1.07 m s^{-1}. The areas of high-quality habitat were found to shrink in size with the bank and pool region practically fading into medium and low quality habitat. Caused by lower depths and faster velocities, low-quality habitat was also predicted along the downstream boundary.

The diagonal-bar riffle configuration had significantly different habitat distributions compared to the notch configuration at the spawning discharge. The area covered by water increased from 3330 m^2 to 3467 m^2. Upstream of the riffle, high-quality habitat was situated on the river-right channel margin and over the river-left half of the channel where it gradually sloped up. The rest of the upstream pool and riffle entrance had medium-quality habitat. As the water crested the diagonal bar, the river-right bank had mostly medium- and some high-quality habitat. Downstream of the riffle, with $0.09 < D < 0.24$ m, the water sped up to 1.83 m s^{-1} at the pool entrance, corresponding to low and very poor quality habitat. Some high-quality habitat was present along the back of the riffle where flow rapidly decelerated into the pool. The pool had a mix of medium and low quality habitat with higher depths of 0.76-0.91 m and wide ranging velocities between 0.06-0.76 m s^{-1}.

When the diagonal bar's downstream WSE was uniform or accelerating for the spawning discharge, the upstream habitat remained identical as for the backwater downstream WSE. Channel area decreased by 170 and 185 m^2 for uniform and accelerating flow conditions, respectively. A portion along the river-right bank of the riffle crest dried out causing a stagnant pool that had low and very poor quality habitat. Along the downstream side of the bar, depths were low and velocities were higher overall (up to 3.48 m s^{-1}) yielding low to very poor quality

habitat that covered the entire downstream side of the riffle crest. Flow deceleration into the downstream pool yielded a narrow zone of high-quality habitat. The downstream pool showed a mix of low- to medium-quality habitat. Besides the addition of more high-quality habitat under the accelerating downstream WSE, the river-right bank of the riffle remained nearly the same in habitat quality. Overall, accelerating conditions showed more deterioration of habitat quality in the downstream pool as the medium-quality habitat phased into low-quality habitat.

3.3 Channel Stability

Just as with habitat quality, the spatial τ^* distribution underwent major changes between backwater and uniform downstream WSE conditions, but only minor changes from uniform to accelerating downstream WSE conditions (Fig. 6). For both channel configurations, the backwater condition yielded the most area of stable bed ($\tau^* < 0.03$). For example, at 8.5 cumecs, 62.5 % of the surface area of the notched, transverse riffle configuration had $\tau^* < 0.01$. This area was reduced by 42.6 or 43.7 % in total area when the downstream WSE changed from backwater to uniform or accelerating, respectively. Similarly, τ^* indicating partial transport ($0.03 < \tau^* < 0.06$) increased from 4.8 % in total area by 17.3 or 20.3 % for the shift from backwater to uniform or accelerating, respectively. In the diagonal-bar riffle configuration, the same pattern emerged, with the total area of $\tau^* < 0.o1$ decreased from 73.6 % of total area by 34.4 or 33.2 % of total area for uniform or accelerating flow, respectively. In this scenario, the region of partial transport increased from 4.3 % of total area for the backwater condition to 0.7 or 3.6 % for uniform and accelerating conditions, respectively.

When the flow rate was 170 cumecs with a backwater condition imposed, τ^* intensity for both riffle configurations increased mainly to the partial transport domain under backwater

conditions (Fig. 6). When the downstream water condition was set to uniform, the region with τ^* indicating full bed mobility ($0.06 < \tau^* < 0.10$) surged in total area by 56 %. Going from backwater to accelerating conditions not only expanded the regional of full mobility, but also yielded $\tau^* > 0.1$ over 14.2 % of the total area. Similar to the notched, transverse riffle, under a backwater condition the diagonal riffle maintained ~ 30 % of its total area with $\tau^* < 0.03$, but had ~60 % experiencing partial transport. When the downstream WSE was dropped to uniform in this case, regions of partial transport shifted to a full bed mobility regime (Fig. 6b).

For the notched, transverse riffle at 8.5 cumecs and backwater flow conditions, the regions with the highest τ^* generally occurred over the riffle, which typically had the lowest depths and highest velocities (Fig. 7a). Most of the riffle had $0.01 < \tau^* < 0.03$ with $0.21 < D < 0.46$ m and $0.55 < U < 0.79$ m s^{-1}. Higher τ^* in the partial transport domain occurred on the back of the riffle crest and in the channel's center where $0.15 < D < 0.31$ m and $0.98 < U < 1.22$ m s^{-1}. In the pools, $\tau^* < 0.1$ occurred over the rest of the channel corresponding with $0 < D < 0.91$ m and $U < 0.64$ m s^{-1}.

When compared to backwater conditions, uniform conditions were remarkably different over most of the river, except for the upstream pool (Fig. 7b). The intensity of τ^* was higher throughout the channel. Regions of partial transport included much of the riffle crest, the whole notch, the riffle tail, and the downstream pool entrance. These areas had $0.15 < D < 0.40$ m and $1.07 < U < 1.22$ m s^{-1}. Over the riffle crest and along the river-left bank just downstream of it, a small region of full bed mobility corresponded with $0 < D < 0.15$ m and $0.55 < U < 1.22$ m s^{-1}. In the downstream pool, most of the channel had $0.01 < \tau^* < 0.03$ ($0.09 < D < 0.46$ m; $0.18 < U < 1.04$ m s^{-1}), except for narrow channel margins with $0 < D < 0.18$ m and $0 < U < 0.24$ m s^{-1}. Where there was a small rise in the bed of the pool on the river right, a zone of partial transport

occurred. With the decrease in WSE from uniform to accelerating conditions, minimal change was observed between the two.

The regions of highest stress remained the same for the diagonal bar riffle configuration, which had occurred over or just downstream of the riffle crest. For backwater flow conditions, the area of the upstream pool and channel margins had $\tau^* < 0.01$ (Fig. 7c) with $0 < D < 0.76$ m and $0 < U < 0.70$ m s^{-1}. Approaching the riffle entrance of the diagonal bar and including most of the river-right bank, the τ^* intensity increased to $0.01 < \tau^* < 0.03$ ($0.15 < D < 0.27$ m; $0.49 < U < 0.91$ m s^{-1}). Moving towards the downstream pool, τ^* increased rapidly from 0.03 to 1.0 (Fig. 7c) with $0.12 < D < 0.15$ m and $0.91 < U < 1.52$ m s^{-1}. Unlike the notched, transverse riffle, the diagonal bar had supercritical flow over a portion of the crest, even with backwater conditions. A hydraulic jump was predicted at the toe of the riffle exit. The FESWMS model did not crash with this present, but its predictive accuracy in the jump region is expected to be very poor. Downstream in the pool, τ^* dropped to < 0.01 corresponding with increased depth (~0.91 m) and decreased velocities (0.06-0.73 m s^{-1}).

In uniform or accelerating conditions, major changes occurred over the exiting half of the riffle and the second pool. Along the steep drop behind the riffle crest, supercritical flow expanded to cover the whole length of the bar, and it intensified τ^* (Fig. 7d). Channel-altering bed-load transport ($0.1 < \tau^* < 1.0$) was predicted here, where $0.03 < D < 0.31$ m and $1.22 < U < 2.44$ m s^{-1}. In the region where the dried out riffle crest created a stagnant pool, there was no transport predicted. At the base of the drop behind the bar, depths increased ($0.40 < D < 0.58$ m) and the water decelerated ($0.31 < U < 0.61$ m s^{-1}) to yield $\tau^* < 0.01$. The exception to this was in the horseshoe thalweg where flow convergence produced a narrow jet of high-velocity flow whose width expanded downstream. As it expanded, its sediment transport regime shifted from

full bed mobility to partial transport, to only intermittent transport (Fig. 7d). The only difference evident under the accelerating downstream WSE condition was an increased region of the riffle crest that dried out.

When the discharges were 70.8 and 170 cumecs, the spatial distribution and intensities of the stress changed again. At 70.8 cumecs for both configurations in backwater flow, the channel had τ^* between 0.01-0.03 for most of the channel. This area of intermittent transport occurred over the riffle tail, downstream pool, and part of the upstream pool for both riffle configurations. These regions typically had $0.09 < D < 1.92$ m and $0.61 < U < 1.52$ m s^{-1}. Partial transport occurred over the entrances of the riffle features corresponding with $1.28 < D < 1.49$ m and $1.52 < U < 1.71$ m s^{-1} for the notched, transverse riffle. While for the diagonal bar riffle, it had $0.21 < D < 1.16$ m and $1.16 < U < 1.66$ m s^{-1}. Channel-altering transport conditions found at 8.5 cumecs for the diagonal bar riffle were not at the higher discharges, because the hydraulic jumps drowned out. Similar to what occurred for 8.5 cumecs, in uniform conditions, the stability of the channel quickly deteriorated. For both riffle configurations, most of the channel away from the riffle and downstream boundary experienced partial transport. The notched, transverse riffle configuration had $0.61 < D < 1.37$ m and $1.07 < U < 1.98$ m s^{-1} while the diagonal bar riffle configuration had $1.52 < D < 2.13$ m and $1.52 < U < 2.13$ m s^{-1}. The peak transport regions, which shifted slightly downstream towards the exit of the riffle from backwater conditions, had stresses ranging from partial to channel-altering transport, which occurred over the notched and diagonal bar riffle crests. The notched, transverse riffle crest had $0.12 < D < 1.07$ m and $1.98 < U < 2.50$ m s^{-1}. While the diagonal bar configuration had $0.31 < D < 1.22$ m and $1.52 < U < 3.23$ m s^{-1}.

At 170 cumecs, in backwater conditions the stresses remained between 0.03-0.06

compared to 70.8 cumecs and expanded to include most of the channel for both riffle configurations (Fig. 8a,c). These regions had depths up to 2.71 m and velocities between 1.52-2.16 m s^{-1} for the notched, transverse riffle. While for the diagonal riffle, it had depths between 0.31-2.74 m and velocities between 1.65-2.90 m s^{-1}. When the WSE decreased to uniform or accelerating flow conditions, τ^* intensified over the entire channel with stresses mostly between 0.06-0.10 (Fig. 8b,d). In addition, stresses between 0.10-1.0 increased significantly throughout the channel and was found near the riffle crest for the notched, transverse riffle configuration and at the entrance of the diagonal bar for the other. Also, for the diagonal bar configuration, there was another region with channel-altering conditions further downstream at the river-right bank. Channel-altering transport was also found in only accelerating flow along the downstream boundaries for both riffles too. These regions had $0.31 < D < 1.65$ m and $0.49 < U < 3.05$ m s^{-1} occurred for the notched, transverse riffle configuration. While $0.31 < D < 1.74$ m and $1.83 < U < 3.14$ m s^{-1} occurred over the diagonal bar riffle configuration. Notably, neither riffle configuration showed a velocity or shear stress "reversal" from low to high discharges between riffles and pools. Peak shear stress always occurred on the riffles, regardless of discharge.

4 Discussion

Two different pool-riffle-pool configurations were simulated using FESWMS for varying discharges and downstream WSE conditions. These 18 simulations provided sufficient results to answer the three questions posed in this study (Table 1).

4.1 Role of Downstream WSE

Downstream WSE is a primary control on flow pattern, spawning habitat quality, and sediment transport regime. Significant differences in channel functionality were predicted by the 2D model for the different downstream WSEs. The most important finding was that backwater conditions are necessary for a pool-riffle-pool unit to have the highest quality salmon-spawning habitat (Fig. 4). Riffle-pool hydrodyanmics that yield backwater conditions also significantly enhance the morphological stability of high-quality habitat areas during all discharges (Fig. 5). During autumn low flows, scour does not naturally occur on non-uniform riffles and pools; hence Chinook salmon have evolved to establish egg pockets during that time. Even in subsequent months when Chinook embryos are incubating and Steelhead salmon are spawning, flows are primarily low. Infrequent early winter storms when basins are already saturated yield punctuated moderate flows for short durations. Backwater conditions stemming from riffle-pool non-uniformity were found to result in only partial transport under such discharges. Thus, embryos buried deeper than d_{90} would survive such events.

The extent of natural gravel riffles with accelerating downstream WSE conditions is not known, but *Grant's* [1997] hypothesized interdependence between near-critical flow conditions and bed material size limits their domain and sustainability under near-critical conditions. In contrast, their likelihood in construction of artificial riffles for spawning habitat rehabilitation and other forms of river restoration is apparently high. Most projects are designed using analytical or 1D numerical models that bias managers toward uniform channel morphologies. In this study, it was found that a riffle built to yield uniform conditions would be a major hazard to the next upstream riffle. Even at the spawning discharge, the relative area of the channel above the critical threshold for initiation of sediment transport (τ^*~0.03) was estimated to increase by 250-520 % when a uniform WSE was imposed instead of the backwater WSE. Concomitant

with this increased instability was a decrease in area of medium- and high-quality spawning habitat by 4-37 %. This decrease was significantly mitigated by the presence of another backwater condition imposed by the riffle in the middle of the study area, which acted as a weir maintaining higher depths and moderate velocities even as the downstream conditions deteriorated from a uniform to accelerating WSE.

4.2 Discharge Effects

Since most management schemes for regulated rivers call for low discharges during salmon spawning periods, the effect of higher discharge on spawning was not focused on here. Analysis showed that a small amount of spawning habitat was present under the 70 cumecs regime, but high depths and velocities were limiting. At 170 cumecs there was virtually none present except along narrow channel margins. More importantly, the area of channel bed subjected to partial or full bed mobility significantly increased as a function of discharge, with a mitigating effect provided by backwater downstream WSE, as described above. As discharge increased, the flow pattern became more homogeneous, with higher velocities in the channel center and lower velocities along the margins. The consequence of a riffle acting as an upward bed step under subcritical flow conditions is that flow decreases in depth and accelerates over the non-uniformity (Fig. 1), focusing scour at the point of maximum acceleration beyond the riffle crest. Higher discharges yield stronger scour regimes. As long as the flow width is nearly constant, as it was in this study, the location of maximum scour remains just downstream of the riffle crest, at least until the crest is destroyed.

4.3 Channel Configuration Control

In this study, only two simple channel geometries were investigated to exemplify the riffle-pool dynamics associated with varying downstream WSE. The notched, transverse riffle with backwater flow conditions was found to produce the maximum quantity of high-quality habitat. Higher quality habitat was found in both riffle entrance and exit, as flow over the crest was too fast. However, whereas the notch in the transverse riffle allowed water to bypass the crest, the physical habitat in the diagonal riffle configuration proved more resistant to changing flow conditions because the even crest elevation produced a weir effect that backed water up providing high-quality habitat in the convective acceleration zone between the pool and the riffle. When the flow conditions were uniform or accelerating, the diagonal bar riffle configuration yielded more medium- and high-quality habitat.

At 8.5 cumecs, the notched, transverse riffle configuration was more stable than the diagonal bar riffle configuration. Since the diagonal bar's riffle exit was so steep, supercritical conditions were predicted to occur and cause some instability. Further, even though it could not be accurately modeled, a hydraulic jump was predicted to be present, and this would induce local scour and knickpoint migration, eating away at the bar. Scour would be severe if the downstream riffle yielded uniform or accelerating WSE conditions. Had the diagonal bar been designed with a more gently sloped riffle tail, the deleterious hydraulic jump could have been avoided in favor of undular jump conditions, so this lesson served to aid improved diagonal riffle designs.

Once discharge was >70 cumecs, the hydrodynamic and sediment-transport-regime differences between the two riffle configurations diminished. The water flowed much faster over the same central region at the high flow rates for both channel types. Scour remained focused on the riffle crest. Neither configuration yielded a velocity or shear stress "reversal". The

significance of this finding is that this study provides further confirmation that equalization or reversal of water surface slopes between riffles and pools is not the mechanism for riffle-pool self-maintenance as proposed by *Keller* [1971]. Instead, pools must have a significantly lower expansion of cross-sectional area as a function of increasing discharge than riffles [*Carling et al.*, 1990; *MacWilliams et al.*, submitted]. Such a difference results in flow acceleration and scour through pools and deceleration over riffles. In straight reaches below dams, the primary means for initiating this difference through rehabilitation is by building riffles that are significantly wider and shallower than pools at low discharge. This conjecture has been incorporated into the Spawning Habitat Integrated Rehabilitation Approach [*Wheaton et al.*, 2004a,b].

4.4 At-a-station Design Analysis

Classic fluvial geomorphology and current river restoration practice place a primary focus on the role of a "dominant" discharge in the understanding and design of channel morphology [*Rosgen*, 1997]. An important outcome of this study is that the functionality of a riffle-pool morphology is not determined by the local discharge, but instead is determined by the downstream water surface elevation dictated by the non-uniform hydrodynamics induced by the next downstream riffle. This result has profound implications for river restoration design. At least on par with evaluating the dominant discharge, restoration practitioners should perform at-a-station hydraulic geometry cross-comparisons in which the stage-discharge rating curves for the riffle crest and adjacent pools are obtained by observation, not computed falsely assuming uniform flow. The impact of a change to in-channel morphology on at-a-station hydraulics is central to understanding the functionality of the riffle-pool channel unit. 2D modeling is a useful tool for evaluating the functionality, but it may also be possible to finesse this through other

means of at-a-station cross-comparison or using 1D modeling.

4.5 Reverse Domino Conjecture

Given that the sediment transport regime of riffles evaluated individually in this study showed a high sensitivity to downstream WSE, it is possible to conjecture on how this variable would affect broader channel morphodynamics. Specifically, gravel-bed rivers are currently thought to re-organize their riffles and pools when sufficient flow is present to induce widespread Shields stress to partially suspend whole features, at which point channel maintenance stemming from shear stress "reversal" between riffles and pools no longer functions. However, a detailed mechanism of riffle failure, including the sequence by which riffles fail does not exist. A "reverse domino" mechanism is proposed in which downstream WSE plays the critical role in determining the timing and sequence of riffle-pool re-organization (Fig. 9). Specifically, if one riffle were to catastrophically fail (Fig. 9b) for whatever reason to be discussed shortly, the water surface elevation would drop, sending a wave of flow acceleration upstream to the next riffle. A sudden shift in riffle tail conditions involving a dramatically increased local water surface slope would create a jump in Shields stress that could then cause that riffle to fail (Fig. 9c), according to *Grant's* [1997] critical flow threshold conjecture. This failure would send a wave with even greater acceleration upstream, causing further riffle failures (Fig. 9d).

The results of this study lend strong support to the idea that a rapid change in downstream WSE would destablize a riffle and cause it to catastrophically fail. For both riffle configurations, a shift from backwater to lower-than-uniform WSE was observed to transform the channel from ~40% of its area not experiencing even partial transport to >65 % of its area experiencing full

bed mobility. These results do not include the significant unsteady shear stress that would result from this failure scenario.

At the same time that a failed riffle would propagate a WSE depression upstream, it would also send increased discharge downstream. Under a competing conjecture, one might argue that this discharge could push the next downstream riffle beyond a key threshold and cause it to fail, yielding a downstream domino effect. A significant aid to such a mechanism would be a channel constriction at the riffle crest. However, the results of this study caution against this conjecture. The effect of increasing discharge on Shields stress is mitigated by riffle non-uniformity, such that each downstream riffle would work against the discharge pulse, slowing it down. This negative feedback contrasts with the positive feedback of an upstream propagating wave.

The primary question arises as to what causes the first riffle to fail in the first place. One possibility is that riffle failure occurs earlier at a particular site because that site has a valley constriction that is hydraulically activated at a threshold discharge governed by local at-a-station hydraulic geometry. The constriction would focus scour on the riffle and induce failure prior to failure at riffles lacking such a constriction. A second possibility is that large woody debris and hillslope-derived boulders that force riffles and pools [*Thompson et al.*, 1999] either become emplaced or fail, thereby causing the associated riffle to fail. A third possibility is that a riffle composed of finer bed material catastrophically fails first.

Although this “reverse domino” mechanism for riffle-pool channel re-organization is pure conjecture and cannot be evaluated solely on the basis of this study, this idea is new and warrants consideration and testing. As more restoration projects are built assuming uniform flow conditions, the opportunity for observing how such poorly designed structure fail increases,

which can be a benefit to advancing basic geomorphic theory. Determining the likely mechanism of riffle failure in a reach could significantly aid pulse-flow experiments that are trying to use flow re-regulation to change channel conditions downstream of dams.

5 Conclusions

This study evaluated the importance of considering the downstream water surface elevation to the functioning of riffle-pool units, whether natural or designed. In a pool-riffle-pool sequence, the influence of riffle crest elevation on flow patterns propagates upstream through the pool and to the next riffle. Sufficient backwater conditions are necessary to produce high-quality Chinook and steelhead spawning habitat. A higher backwater condition is needed for steelhead than for Chinook. Backwater conditions also help embryos survive moderate floods, by limiting mobility to partial transport, whereas uniform channel conditions would yield full bed mobility. A notched, transverse riffle was found to function better than a steep diagonal bar. From a design perspective, the downstream water surface elevation for a project site may be controlled by manipulating the crest of the next downstream riffle. One potential consequence of these results is that there may exist a “reverse domino” mechanism for the failure of a sequence of riffles and pools.

6. Acknowledgements

Financial support for this work was provided by the US Fish and Wildlife Service (contracting entity for CALFED Bay-Delta Ecosystem Restoration Program: Cooperative Agreement DCN#

113322G003), United States Bureau of Reclamation (Award #03FG230766), and University of California. We gratefully acknowledge Rocko Brown for his work on the Lewiston-Dam SHIRA project on the Trinity River that provided baseline data for this study. We also acknowledge Eve Elkins, Joseph Wheaton, Joseph Merz, and Marisa Escobar for their efforts as part of the UC Davis SHIRA group working on the Mokelumne River for sharing knowledge and discussions as they sought to incorporate our results into their real rehabilitation designs. We acknowledge Guillermo Jimenez aid with graphic arts.

7. List of Notations and Acronyms

2D	two dimensional
3D	three dimensional
A	cross-sectional area, m^2
β_{ij}	Momentum correction coefficients
d_{50}	median grain size, mm
d_{90}	size which 90% of the bed material is smaller than, mm
DTM	digital terrain model
E	eddy visocity, $m^2\ s^{-1}$
FESWMS	finite element surface water modeling system
Fr	Froude number
H	water depth, m
γ_s	specific weight of sediment
γ_w	specific weight of water

1	g	acceleration of gravity, m s^{-2}
2	GHSI	global habitat suitability index
3	n	Manning's coefficient for bed roughness
4	ρ_w	density of water, kg m^{-3}
5	Q	discharge, m^3 s^{-1}
6	R_h	hydraulic radius, m
7	S_o	channel slope, m/m
8	SHIRA	spawning habitat integrated rehabilitation approach
9	SMS	surface modeling software
10	τ^b_i	bottom shear stresses in direction i, N m^{-2}
11	τ^*	Shields stress
12	τ_{ij}	shear stresses caused by turbulence, N m^{-2}
13	u^*	shear velocity, m s^{-1}
14	U,	depth-average downstream velocity, m s^{-1}
15	V,	depth-average lateral velocity, m s^{-1}
16	WSE	water surface elevation, m
17	z_b	bed elevation , m

18

19 **8. References**

20

21 Bernhardt, E.S., M.A. Palmer, J.D. Allan, G. Alexander, K. Barnas, S. Brooks, J. Carr, S.
22 Clayton, C.N. Dahm, J. Follstad-Shah, D. Galat, S. Gloss, P. Goodwin, D. Hart, B. Hassett,
23 R. Jenkinson, S. Katz, G.M. Kondolf, P.S. Lake, R. Lave, J.L. Meyer, T.K. O'Donnell, L.

Pagano, B. Powell, and E. Sudduth (2005), Synthesizing US River Restoration Efforts, *Science, 308*, 636-63.

Brandt, S.A. (2000), Classification of geomorphological effects downstream of dams, *Catena*, *40*, 375–401.

Carling, P.A. (1990), An appraisal of the velocity-reversal hypothesis for stable pool-riffle sequences in the River Severn, England, *Earth Surf. Processes Landforms, 16*, 19-31.

Draut, A.E., and D.M. Rubin (2005), Investigating effects of the November 2004 high-flow release from Glen Canyon Dam on aeolian sand-transport rates in the Colorado River Corridor, Grand Canyon, Arizona., *Eos Trans. AGU*, *86*(52), Fall Meet. Suppl., H53D-0495.

Fischer H.B., E.J. List, R.C.Y. Koh, J. Imberger, and N.H. Brooks (1979), *Mixing in Inland and Coastal Waters,* Academic Press, Inc., New York.

Froehlich D.C. (1989), Finite element surface-water modeling system: two-dimensional flow in a horizontal plane user's manual, *U.S. Department of Transportation, Publication #FHWA-RD-88-177*, 285pp.

Grant, G. E. (1997), Critical flow constrains flow hydraulics in mobile-bed streams: A new hypothesis, *Water Resour. Res., 33*, 349-358.

Keller, E. A. (1971), Areal Sorting of Bed-Load Material: The Hypothesis of Velocity Reversal, *Geolog. Soc. Amer. Bull., 82*, 753-756.

Kondolf, G.M. (1997), Hungry water: effects of dams and gravel mining on river channels, *Environ. Man., 21*, 533–551.

Leclerc, M., A. Boudreault, J.A. Bechara, and G. Corfa (1995), Two-dimensional hydrodynamic modeling: a neglected tool in the instream flow incremental methodology, *Trans. Amer. Fish. Soc., 124*, 645-662.

Lisle, T. E., J.M. Nelson, J. Pitlick, M.A. Madej, and B.L. Barkett (2000), Variability of bed mobility in natural, gravel-bed channels and adjustments to sediment load at local and reach scales, *Water Resour. Res., 36*, 3743-3755.

Loftin, K (1991), Restoring the Kissimmee River, *Geotimes, 36*, 15-17.

MacWillians, M.L., J.M. Wheaton, G.B. Pasternack, P.K. Kitanidis, and R.L. Street, The Flow Convergence-Routing Hypothesis for Pool-Riffle Maintenance in Alluvial Rivers, *Water Resour. Res.*, submitted.

Melis, T.S., D. J. Topping, S.A. Wright, D.M. Rubin, J.C. Schmidt, J.E. Hazel, M.A. Kaplinski, and R.A. Parnell (2004), Sediment Studies Refute EIS Hypothesis, While Most Fundamental Process Questions Remain Unanswered: An Update on Experiments in Grand Canyon, *Eos Trans. AGU, 85*(47), Fall Meet. Suppl., H52A-03.

Merz, J.E., and L.K. Ochikubo Chan (2005), Effects of gravel augmentation on macroinvertebrate assemblages in a regulated California river, *River Res. Applic., 21*, 61-74.

Merz, J.E., J. Setka, G.B. Pasternack, and J.M. Wheaton (2004), Predicting benefits of spawning habitat rehabilitation to salmonid fry production in a regulated California river, *Can. J. Fish. Aquat. Sci., 61*, 1433-1446.

Munson, B.R., D.F. Young, and T.H. Okiishi (1998), *Fundamentals of Fluid Mechanics,* 3rd ed., 816pp., John Wiley and Sons, Inc., Hoboken, NJ.

Pasternack, G.B., C.L. Wang, and J.E. Merz (2004), Application of a 2D hydrodynamic model to design of reach-scale spawning gravel replenishment on the Mokelumne River, California *River Resear. Applic., 20*, 205 – 225.

Pasternack, G.B., A.T. Gilbert, J.M. Wheaton, and E.M. Buckland, 2D Model Fluid Mechanics Error Propagation for Velocity and Shear Stress Prediction, *J. Hydr.,* in press.

Rosgen, D. (1997), *Applied River Morphology*, Wildland Hydrology, Pagosa Springs, CO.

Thompson, D. M., E.E. Wohl, and R. D. Jarrett (1999), Velocity reversals and sediment sorting in pools and riffles controlled by channel constrictions, *Geomorphology, 27*, 229-241.

Thompson, J. (2005), Out, out, dam spot! The geomorphic response of rivers to dam removal, *Pacific Northwest Reseach Station, Science Findings 71*, 1-6.

Trush, W.J., S.M. McBain, and L.E. Leopold (2000), Attributes of an alluvial river and their relation to water policy and management, *Proc. Nat. Acad. Sci., 97,* 11858–11863.

U.S. Fish and Wildlife Service and Hoopa Valley Tribe (1999), Trinity River Flow Evaluation Final Report, U.S. Fish and Wildlife Service, Sacramento, California.

Webb, R.H., J.C. Schmidt, G.R. Marzolf, and R.A. Valdez (1999), The controlled flood in Grand Canyon, in *Geophys. Monogr. Ser.,* vol. 110, AGU, Washington, D.C.

Wheaton, J. M., G.B. Pasternack, and J.E. Merz (2004a), Spawning Habitat Rehabilitation - I. Conceptual Approach and Methods, *Int. J. River Basin Man., 2*, 3-20

Wheaton, J. M., G.B. Pasternack, and J.E. Merz (2004b), Spawning Habitat Rehabilitation - II. Using Hypothesis Testing and Development in Design, Mokelumne River, California, U.S.A., *Int. J. River Basin Man., 2*, 21-37.

Wheaton, J.M., G.B. Pasternack, and J.E. Merz (2004c), Use of habitat heterogeneity in salmonid spawning habitat rehabilitation design. Paper presented at 5*th International Symposium on Ecohydraulics. Aquatic Habitats: Analysis and Restoration, IAHR-AIRH*, Madrid, Spain, p. 791-796.

Wilcock, P. R., A. F. Barta, C.C. Shea, G.M. Kondolf, W.V.G. Matthews, and J. Pitlick (1996), Observations of flow and sediment entrainment on a large gravel-bed river, *Water Resourc. Res., 32*, 2897-2909.

Figure Captions:

Figure 1. Pool-Riffle sequence in the Lewiston Dam reach of the Trinity River (CA) illustrating a backwater effect causing convective flow acceleration into a riffle.

Figure 2. Oblique visualizations of the non-uniform channel morphologies of A) a notched, transverse riffle (44 m wide by 101 m long) and B) a diagonal bar riffle (49 m wide by 93 m long).

Figure 3. Comparisons of observed versus predicted depths (A,B) and velocities (C,D) at 2 cross-sections in the Lewiston Dam Reach from a baseline modeling study performed prior to the numerical experiments reported in this study. Field observations were fit with a curve using the locally weighted Least Squared error method to reduce measurement noise.

Figure 4. Spatial pattern of Chinook salmon spawning habitat quality. Habitat quality is illustrated as white for non-habitat in dry areas and deep pools, light grey for very poor quality, medium grey for low quality, dark grey for medium quality, black for high quality.

Figure 5. Comparison of relative areas of Chinook salmon spawning habitat quality for the two riffle configurations in three downstream WSEs. Shading is identical to that in Figure 4.

Figure 6. Comparison of discharge and downstream WSEs for their impact on bed stability ($\tau^* <$ 0.03) for A) a notched, transverse riffle and B) a diagonal bar riffle.

Figure 7. Spatial pattern of shields stress at 8.5 cumecs with superposed velocity vectors. Color legend is white = 0; lightest grey = 0-0.01, light grey = 0.01-0.03, medium grey = 0.03-0.06 (partial transport), dark grey = 0.06-0.10 (full bed mobility), black = 0.10-1.0.

Figure 8. Spatial pattern of shields stress at 170 cumecs with superposed velocity vectors. Color legend same as used in Figure 7.

Figure 9. Conceptual illustration of the mechanism of riffle-pool re-organization during a flood as proposed in the reverse domino conjecture.

Table 1. Study questions and test metrics used to evaluate the role of channel non-uniformity in gravel-bed pool-riffle-pool units.

Questions	Metrics used to evaluate questions
1) How does downstream water surface elevation affect salmon-spawning habitat quality and channel stability?	• Meter-scale predictions of Shields stress and habitat suitability indices for downstream backwater, uniform, and accelerating conditions.
2) How does increasing discharge affect the downstream water surface elevation control on channel stability?	• Meter-scale predictions of Shields stress for 8.5, 70.8, and 170 cumecs.
3) How does a diagonal riffle compare to a notched transverse riffle in habitat quality and channel stability?	• Comparison of Shields stress estimates and habitat quality indices between 2 pool-riffle-pool units designed with AutoCAD.

Table 2. Downstream water surface elevations* estimated for four different regimes.

	Q=8.5 $m^3 s^{-1}$	Q=70.8 $m^3 s^{-1}$	Q=170 $m^3 s^{-1}$
Notched, transverse riffle			
Backwater	560.19	561.17	561.99
Uniform	559.77	560.54	561.23
Accelerating	559.70	560.38	561.00
Critical	559.63	560.22	560.77
Diagonal Bar			
Backwater	560.19	561.17	561.99
Uniform	559.64	560.42	561.11
Accelerating	559.58	560.26	560.89
Critical	559.52	560.10	560.67

* All elevations in units of meters (NAVD88 datum).

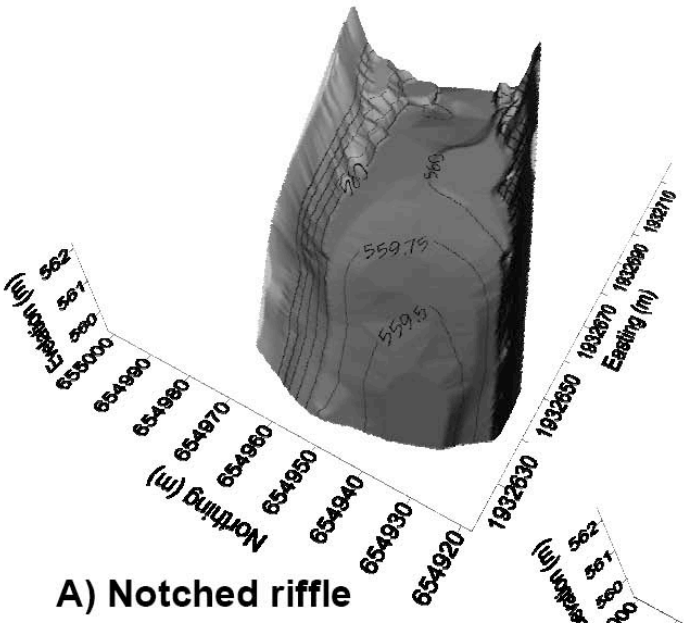

A) Notched riffle

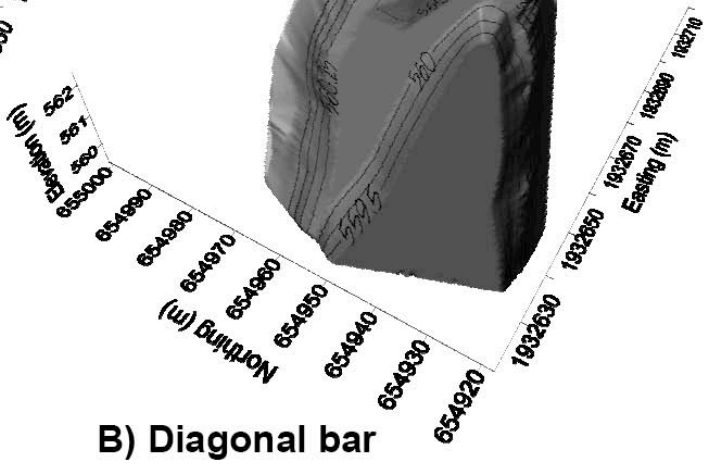

B) Diagonal bar

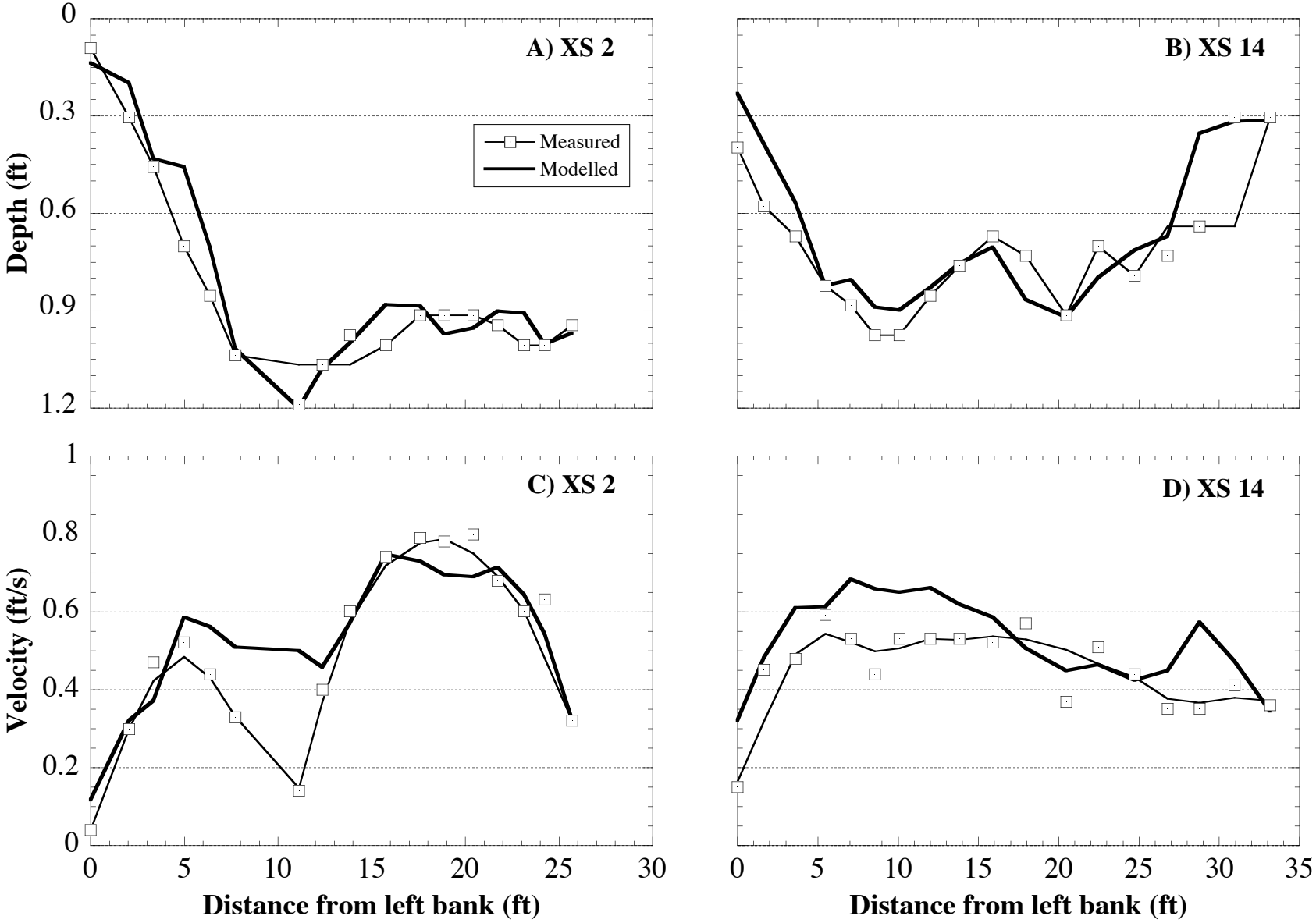
A) XS 2
B) XS 14
C) XS 2
D) XS 14
Measured
Modelled
Depth (ft)
Velocity (ft/s)
Distance from left bank (ft)
Distance from left bank (ft)
0
0.3
0.6
0.9
1.2
0.2
0.4
0.8
1
5
10
15
20
25
30
35

A) Notched, transverse riffle
Backwater WSE

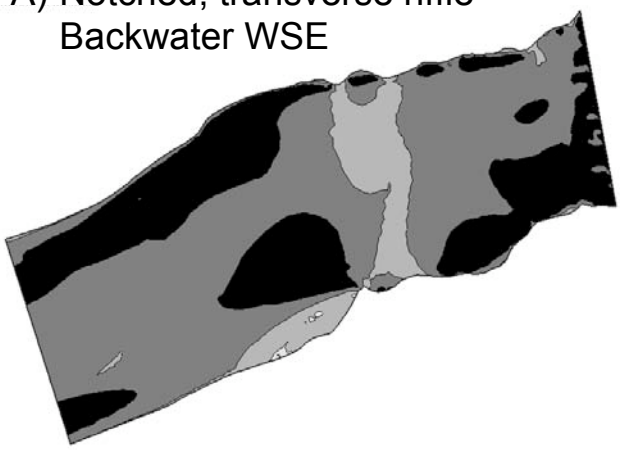

B) Notched, transverse riffle
Uniform WSE

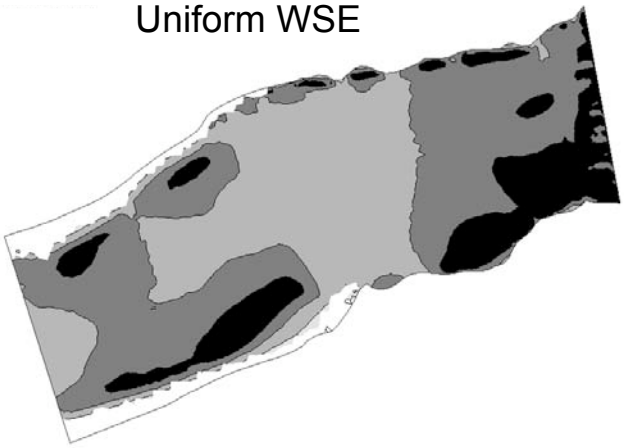

C) Diagonal riffle
Backwater WSE

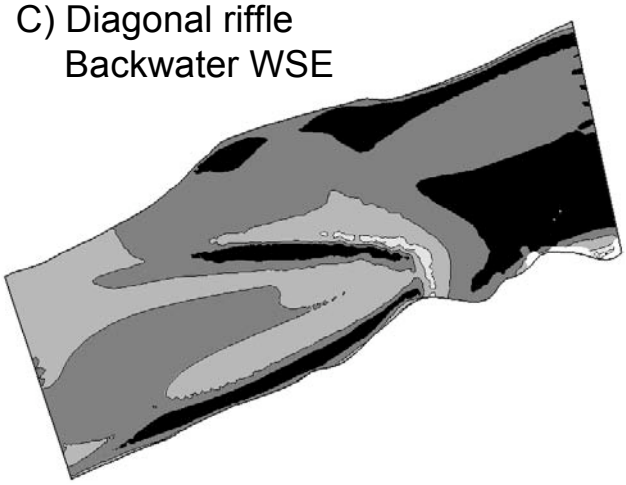

D) Diagonal riffle
Uniform WSE

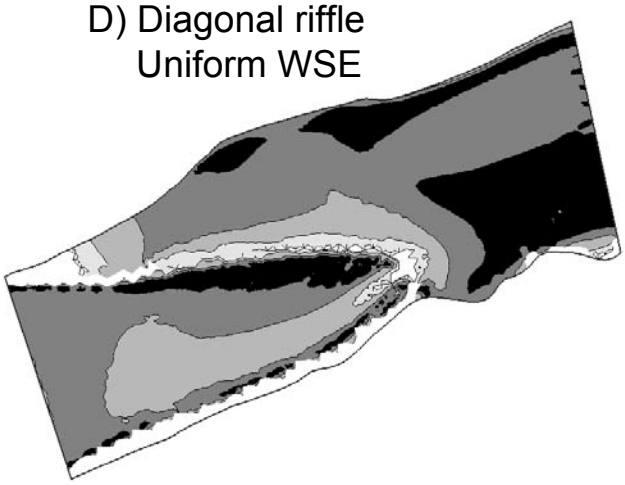

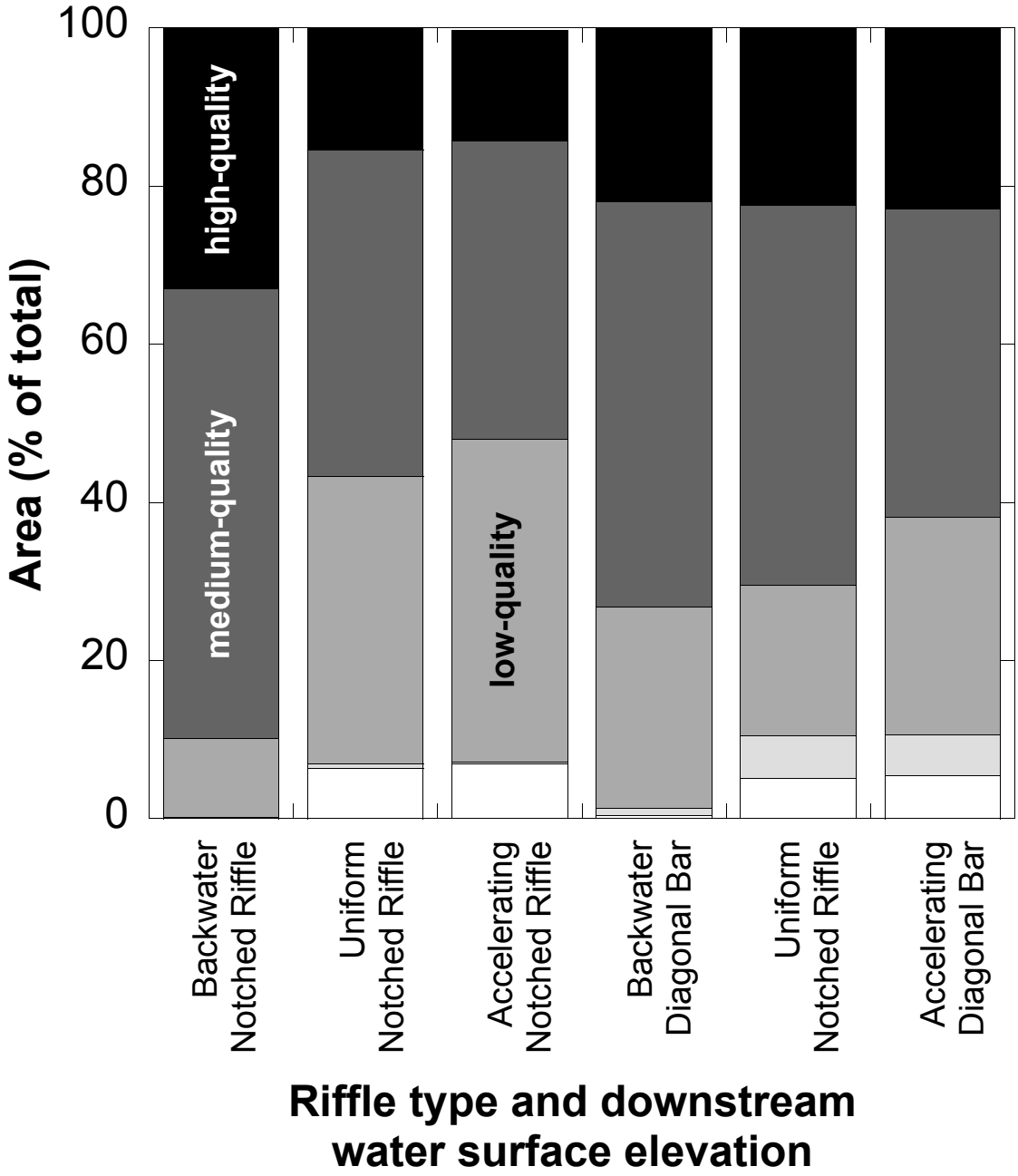
100
80
60
40
20
0
Area (% of total)
high-quality
medium-quality
low-quality
Backwater Notched Riffle
Uniform Notched Riffle
Accelerating Notched Riffle
Backwater Diagonal Bar
Uniform Notched Riffle
Accelerating Diagonal Bar
Riffle type and downstream water surface elevation

A) Notched Riffle

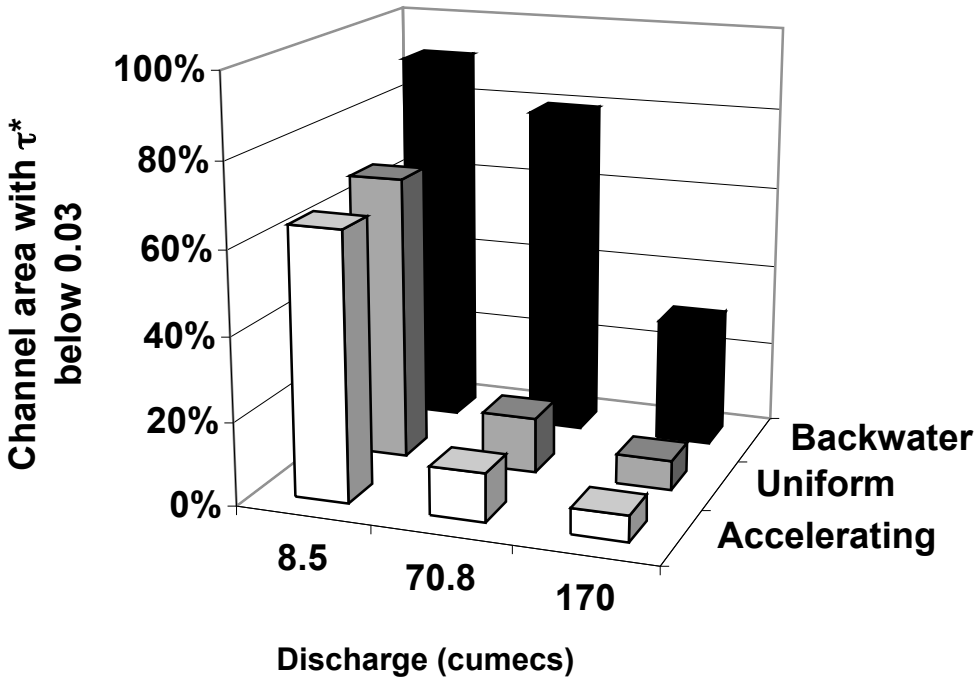

B) Diagonal Bar Riffle

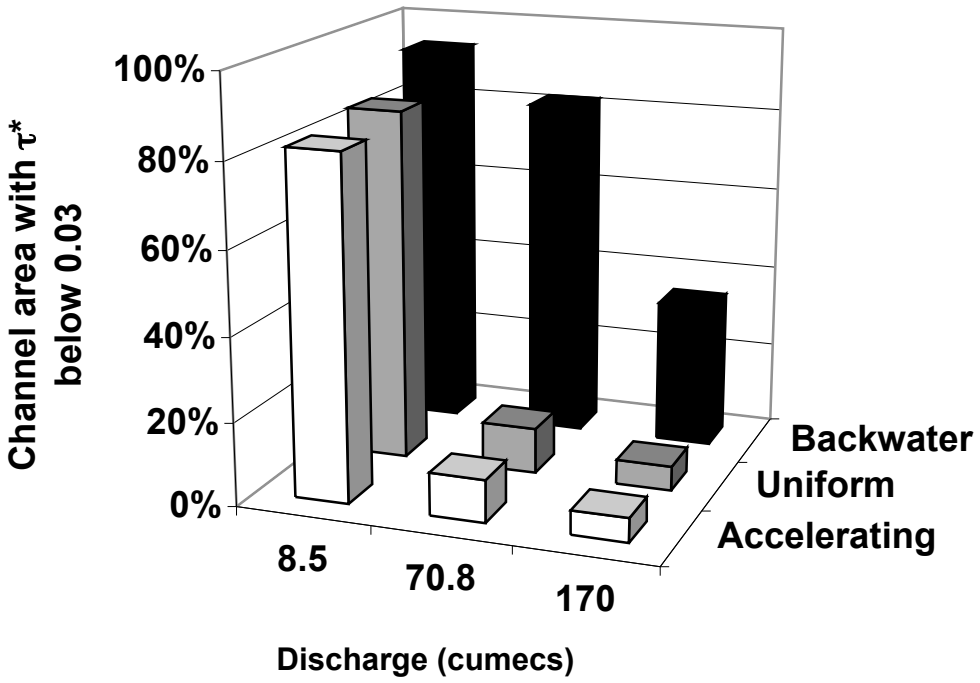

A) Notched, transverse riffle
Backwater WSE

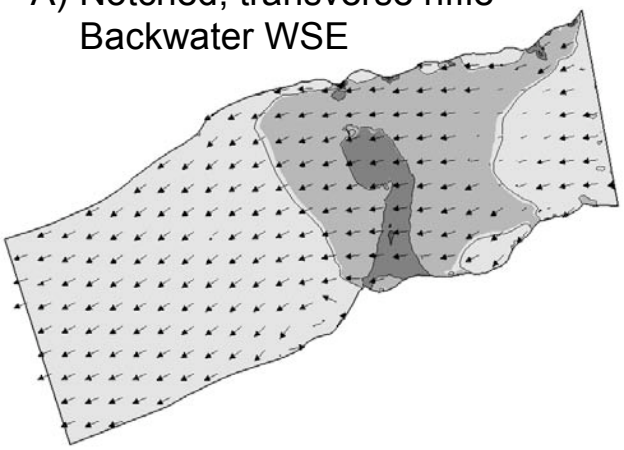

B) Notched, transverse riffle
Uniform WSE

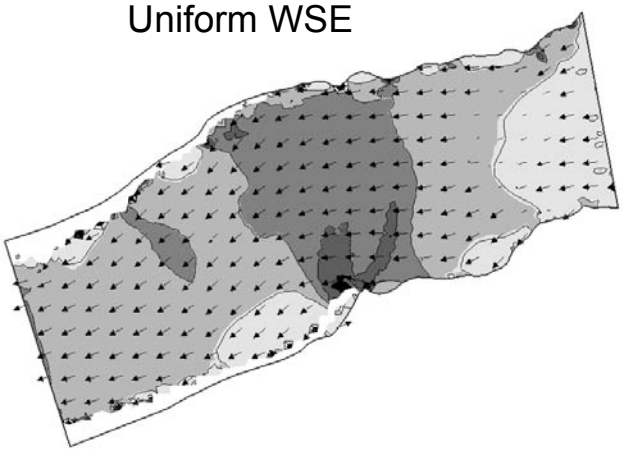

C) Diagonal riffle
Backwater WSE

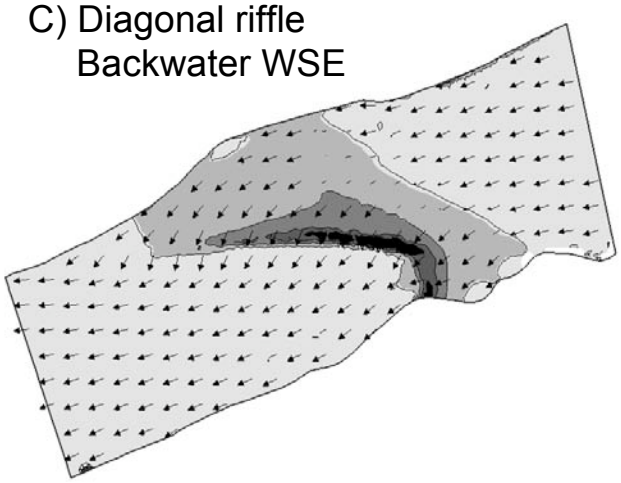

D) Diagonal riffle
Uniform WSE

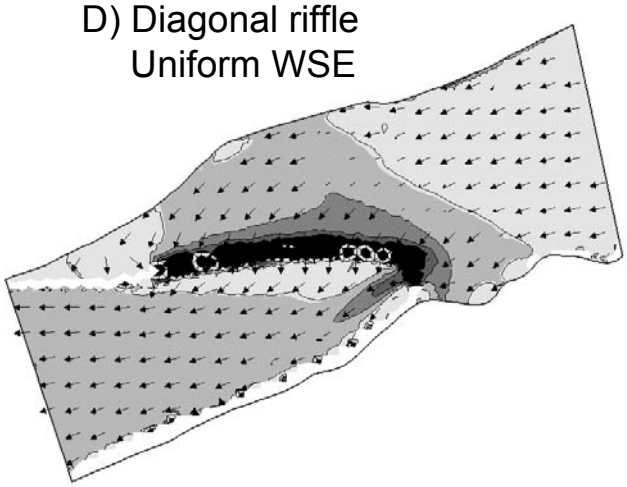

A) Notched, transverse riffle
Backwater WSE

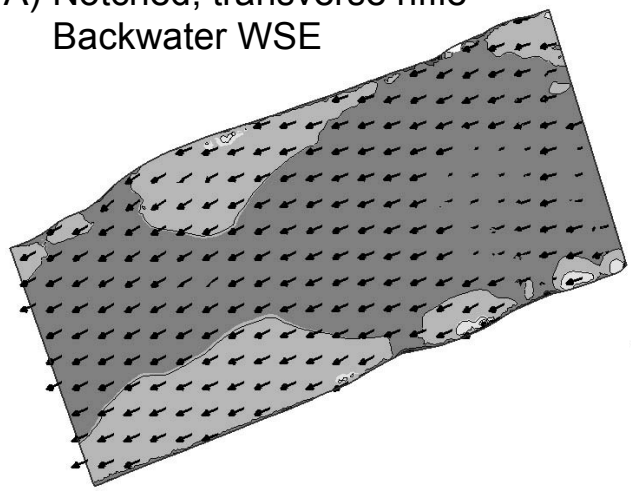

B) Notched, transverse riffle
Uniform WSE

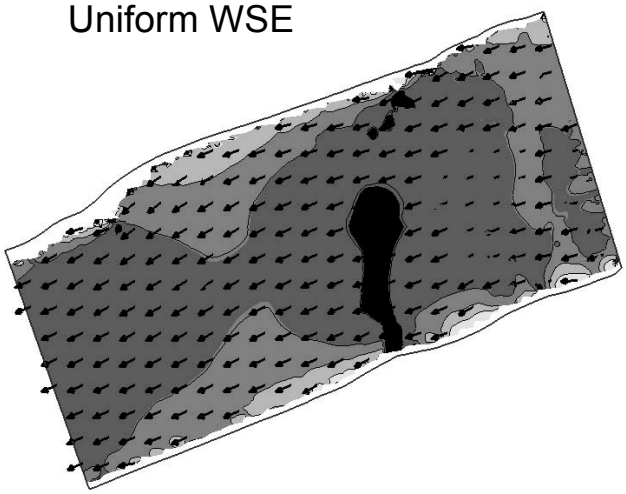

C) Diagonal riffle
Backwater WSE

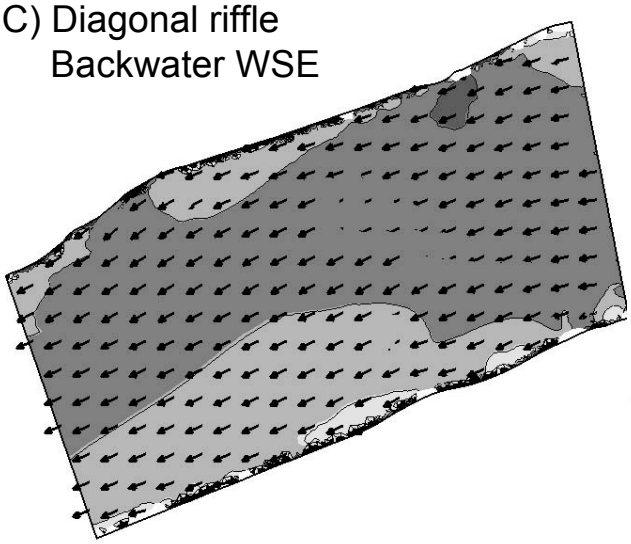

D) Diagonal riffle
Uniform WSE

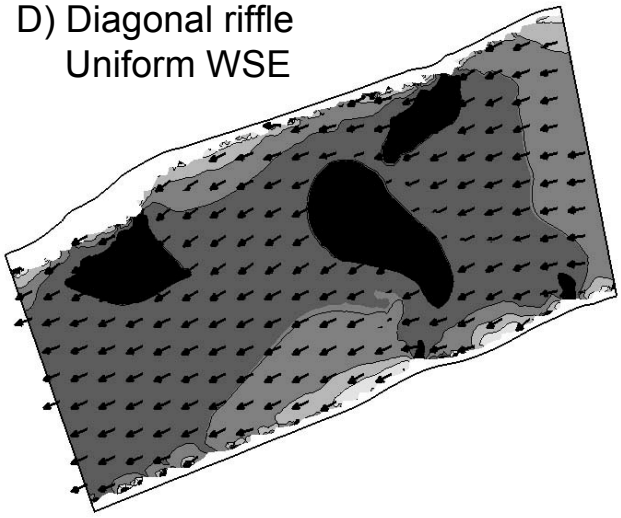

A
riffle scour
stage 1
B
riffle scour
stage 2
riffle scour
stage 1
C
riffle scour
stage 2
riffle scour
stage 1
D

Section 5

A Long Term Plan for Rehabilitating the Lower Mokelumne River

Background

Since 2001, East Bay Municipal Utility District (EBMUD) and University of California at Davis (UCD) have worked together on designing and implementing gravel placement projects on the lower Mokelumne River (LMR), primarily to rehabilitate salomind spawning habitat. Figure 1a shows the bathymetry of the LMR adjacent to the the Mokelumne River Day Use Area (MRDUA) where most of the gravel has been placed. The projects have been designed and monitored using the Spawning Habitat Integrated Rehabilitation Approach (SHIRA), which uses the status of salmonid spawning physical habitat conditions as an indicator of ecosystem health. Collaborative monitoring studies have shown that improving spawning habitat on the LMR also improves conditions for other salmon lifestages as well as macroinvertebrate species diversity. EBMUD intends to continue adding gravel to the LMR on an annual basis. To facilitate those future additions, this section provides guidance to EBMUD, and other interested parties in how those additions should be performed.

Phase 1 Rehabilitation

During 1999-2006 a total of 23,484 metric tons of coarse sediment was added to the LMR to achieve goals at hydraulic-unit, geomorphic-unit, and reach scales. Details on all design and as-built conditions for the 2001-2004 stages of SHR on the LMR are available at http://shira.lawr.ucdavis.edu. A comparison of the river's topography near the dam before 1999 and after 2006 shows that gravel and cobble in this section were primarily used to reconfigure

the river's longitudinal profile, thereby increasing bed slope and increasing floodplain connectivity (Fig. 1). Boulders, wood, and gravel bars were used to create diverse hydraulic structures throughout all project sites. The initial increase in bed elevation of 0.46 m at the upstream limit of spawning (i.e. at the fish-guidance fence at the base of the dam) in 2003 provided the energy necessary to sustain river rehabilitation from 2004-2006 through the top 0.5 km. The 0.46-m raise represented half of the rise necessary to get the whole 1-km reach back to pre-dam conditions with the desired riffle-to-riffle bed slope of 0.004. At present, the slope in the remaining area is ~0.0005, which is an order of magnitude too low.

Thorough monitoring has found that this effort improved physical habitat conditions for spawning over accelerated-flow regions, increased the area and frequency of juvenile rearing on the floodplain, and increased the area of adult holding habitat in enhanced pools. Whereas only 7 % of all salmon redds observed on the LMR were located in the main project zone prior to slope creation in 2003, by 2005 that fraction had increased to 22%, representing a population-scale impact helping sustain and possibly expand the existing population of naturally spawning salmon.

Phase 2 Rehabilitation

Based on an analysis of historical cross-sectional data, the amount of coarse sediment added from 1999-2006 is estimated to be roughly half of the coarse-sediment deficit in the top kilometer below the dam. This represents a relatively small deficit compared to that for adjacent rivers draining the Sierra Mountains (Kondolf 1997), making the LMR a good location for testing heirarchical SHR. With a sustained effort through the next 5-10 years comparable to that over the last 7 years, it is achievable to completely eliminate the historical deficit in the top 1-km

reach and re-initiate active bedload transport beyond that. Thus, addition of another ~25,000 metric tons is the reach-scale goal of Phase 2 rehabilitation.

As of October 2006 the best rehabilitation opportunities in the MRDUA require going back up to the fish-guidance fence and raising the bed there an additional 0.46m. This raise would provide the necessary elevation "head" to sustain gravel addition throughout the MRDUA reach to further rehabilitate the overall longitudinal profile. Consequently, the recommended plan for where to place coarse sediment in Phase 2 focuses on taking the existing SHIRA design surface for the top 0.7 km (i.e. from the 2001 and 2003-2006 projects as shown in Figure 2a) and raising it up 0.46m. Figure 2b shows the design bathymetry of the channel after the additional 0.46m increase in bed elevation. Note that the visual differences between Figures 2a and 2b are due to the coarse 0.3m contour interval used. Detailed bathymetric data for the phase 2 design was provided to EBMUD for construction planning on Feb 4, 2007. Each year that gravel and cobble is placed into the river, hydraulic-unit diversity may be promoted locally by adding boulders, wood, and doses of pea gravel.

After the rehabilitated area is raised to the elevation shown in Figure 2b, there will be enough energy available to sustain river rehabilitation for the final 0.3 km of the MRDUA reach. Because topographic data does not currently exist for ~60% of this final 0.3 km, it is not possible to provide a detailed gravel placement design for this area. However, it is recommended that EBMUD survey the missing area and consider alternatives for placing gravel there when that time comes.

Phase 3: MRDUA Reach Maintenance

After the gravel deficit in the MRDUA has been eliminated, it is estimated that an annual injection of 500-1000 metric tons per year just upstream of the fish-guidance fence would maintain the MRDUA reach (see section 4c). It is recommended that this maintenance injection estimate be revised periodically using two forms of measurement. First, once every 3-5 years the topography of the MRDUA reach should be re-surveyed so that a DEM difference can be made to determine the loss in sediment volume over time. Second, the sediment transport rate at the end of the MRDUA should be measured and a transport relation developed. These methods will enable adaptive management to provide the necessary channel maintenance. Once the sediment transport regime is underway, riffles and glides downstream of the MRDUA will begin to restore themselves as long as Camanche Dam periodically releases a diversity of flow rates. Specific key flows for achieving river management goals appear to be ~2000-2500 cfs to scour invasive aquatic weeds, ~2500-3500 cfs to remove organic fines, and ~3000-5000 cfs to transport gravels. The range in these values reflect local channel differences that enhance or impede the process at a given flow and the lack of data from specific discharges to clearly isolate the optimal discharge for each process at this time. Prior to Camanche Dam, a flow of >4,000 cfs occurred every 1-2 years, whereas since the dam was built it now recurs once every 5 years. Additional opportunities to accelerate restoration at individual sites downstream of the MRDUA may present themselves and should be considered.

Figure 1. Observed Channel Maps for the LMR MRDUA reach

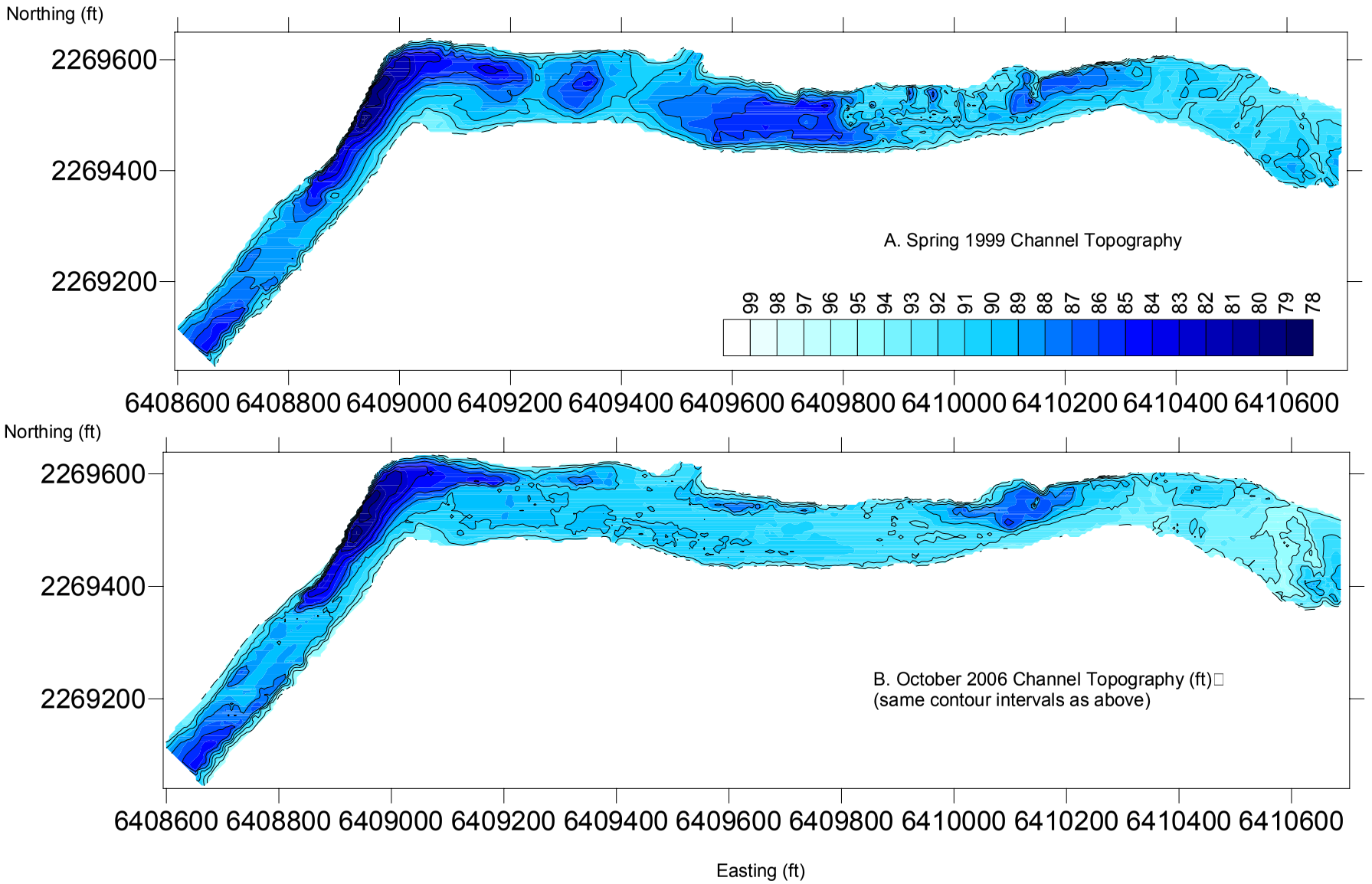

Figure 2. Designed Channel Maps for the LMR MRDUA reach